

Gels Horizons: From Science to Smart Materials

Vijay Kumar Thakur  
Manju Kumari Thakur *Editors*

# Polymer Gels

Synthesis and Characterization

 Springer

# **Gels Horizons: From Science to Smart Materials**

## **Series editor**

Vijay Kumar Thakur, School of Aerospace, Transport and Manufacturing,  
Cranfield University, Cranfield, Bedfordshire, UK

This series aims at providing a comprehensive collection of works on the recent advances and developments in the domain of *Gels*, particularly as applied to the various research fields of sciences and engineering disciplines. It covers a broad range of topics related to *Gels* ranging from *Polymer Gels*, *Protein Gels*, *Self-Healing Gels*, *Colloidal Gels*, *Composites/Nanocomposites Gels*, *Organogels*, *Aerogels*, *Metallogels & Hydrogels* to *Micro/Nano gels*. The series provides timely and detailed information on advanced synthesis methods, characterization and their application in a broad range of interrelated fields such as chemistry, physics, polymer science & engineering, biomedical & biochemical engineering, chemical engineering, molecular biology, mechanical engineering and materials science & engineering.

This Series accepts both edited and authored works, including textbooks, monographs, reference works, and professional books. The books in this series will provide a deep insight into the state-of-art of *Gels* and serve researchers and professionals, practitioners, and students alike.

More information about this series at <http://www.springer.com/series/15205>

Vijay Kumar Thakur · Manju Kumari Thakur  
Editors

# Polymer Gels

Synthesis and Characterization

 Springer

*Editors*

Vijay Kumar Thakur  
Faculty in Manufacturing, Enhanced  
Composites and Structures Centre,  
School of Aerospace, Transport  
and Manufacturing  
Cranfield University  
Cranfield  
UK

Manju Kumari Thakur  
Division of Chemistry  
Government Degree College Bhoranj,  
Himachal Pradesh University  
Shimla, Himachal Pradesh  
India

ISSN 2367-0061

ISSN 2367-007X (electronic)

Gels Horizons: From Science to Smart Materials

ISBN 978-981-10-6082-3

ISBN 978-981-10-6083-0 (eBook)

<https://doi.org/10.1007/978-981-10-6083-0>

Library of Congress Control Number: 2018939938

© Springer Nature Singapore Pte Ltd. 2018

This work is subject to copyright. All rights are reserved by the Publisher, whether the whole or part of the material is concerned, specifically the rights of translation, reprinting, reuse of illustrations, recitation, broadcasting, reproduction on microfilms or in any other physical way, and transmission or information storage and retrieval, electronic adaptation, computer software, or by similar or dissimilar methodology now known or hereafter developed.

The use of general descriptive names, registered names, trademarks, service marks, etc. in this publication does not imply, even in the absence of a specific statement, that such names are exempt from the relevant protective laws and regulations and therefore free for general use.

The publisher, the authors and the editors are safe to assume that the advice and information in this book are believed to be true and accurate at the date of publication. Neither the publisher nor the authors or the editors give a warranty, express or implied, with respect to the material contained herein or for any errors or omissions that may have been made. The publisher remains neutral with regard to jurisdictional claims in published maps and institutional affiliations.

This Springer imprint is published by the registered company Springer Nature Singapore Pte Ltd. The registered company address is: 152 Beach Road, #21-01/04 Gateway East, Singapore 189721, Singapore

# Preface

A gel is described as a soft, solid, or liquid-like unique condensed material that has a three-dimensional network composed of several components such as long polymers, species of small molecules, and a large amount of solvent. These 3D network condensed materials usually form through chemical, physical, or supramolecular crosslinking. The weight and size of gels are more like a liquid, but they are treated like a solid. Two important characteristics of gels are phase state and their rheological properties. On the other hand, a polymer is defined as a large molecule (macromolecules) composed of repeating structural units that comprise of multiple assemblies of simple structural units. In gels, the polymer network can be physically or chemically crosslinked. In case of physical gels, the network formation occurs due to various weak interactions, like the entanglement of the polymer chains, hydrogen bonds, or van der Waals interactions. Such structures are usually not permanent, and they dissolve over the time when immersed in their solvents. However, the polymer chains can also be crosslinked through chemical reactions, leading to strong covalent bonds. The chemically crosslinked network is much more stable and cannot be dissolved without the degradation of the polymer. Therefore, chemical gels are usually preferable in the majority of the application fields. Polymer gels comprise a great variety of different polymeric components that present innumerable industrial applications. Polymers can be naturally produced (sometimes referred as bio-based polymers), in which case the most representative group is polysaccharides. Natural polymers' demand is expected to grow 7.1% every year. Moreover, their low toxicity and excellent biodegradability have also attracted researchers to pay attention toward the widespread application of natural polymers. Polymer obtained from natural sources such as chitosan, alginate, dextran, starch, pectin, cellulose, lignin has shown excellent potential for biomedical and other applications in the form of microsphere, nanoparticles, crosslinked hydrogels, beads, membranes, and granules. On the other hand, a wide variety of synthetic polymers capable of forming gels presents different industrial applications, such as polyacrylamide and polyvinyl alcohol-based gels. Both synthetic and natural polymer-based gels find applications from health sciences such as agents for

controlled drug delivery, sustained drug delivery, targeted drug delivery, and various other types of novel drug delivery systems to water purification.

Polymer gels due to their several unique characteristics have become an indispensable part of new advanced and smart materials in the twenty-first century for numerous applications including but not limited to biological, biomedical, electronic, and environmental. Keeping in mind the immense advantages of polymer gel-based materials, *Polymer Gels: Synthesis and Characterization* provides a cutting-edge resource for researchers and scientists in different fields of science and technology as well as for specialists in polymers, biomaterials, bio-nanotechnology, and functional materials. It provides a comprehensive collection of works on the recent advances and developments in science and fundamentals of both synthetic and natural polymer-based gels particularly as applied to the various research fields of sciences and engineering disciplines. Some of the important topics include but not limited to structure and physico-mechanical properties of physically crosslinked polymer gels; polymer gels: molecular design and properties; clinical use and hemostatic application of gelatin; polysaccharide-based polymer gels: synthesis, characterization, and properties; modified polysaccharide gels: characterization and pharmaceutical applications; silica-based polymeric gels as platforms for delivery of pharmaceuticals; polymeric nanogel: a flexible nanocarrier for drug delivery; gel-based approaches in genomic and proteomic sciences; polymer gels in vaginal drug delivery systems: synthesis and properties; gel formation through non-covalent crosslinking from amylose formed by enzymatic polymerization; new aspects to physicochemical properties of polymer gels in particularly the coordination biopolymeric metal–alginate; smart polymer gels; neuro-evolutionary techniques applied for modeling processes involving polymer gels to name a few.

In editing and organizing this volume *Polymer Gels: Synthesis and Characterization* of the book series *Gels Horizons: From Science to Smart Materials*, we have made our best efforts to cover the growing field of polymer gels and related technologies. It reflects the recent theoretical advances and experimental results and opens new avenues for researchers as well as readers working in the field of polymer and functional materials. In addition, several critical issues and suggestions for future work are comprehensively discussed in this book with the hope that the book will provide a deep insight into the state of the art of “Polymer Gels.” We express our sincere thanks to all the authors, who have contributed their extensive experience through their work for the success of this book. We would also like to thank Swati Meherishi and the rest of the team at Springer for invaluable help in the organisation of the editing process.

Cranfield, UK  
Shimla, India

Vijay Kumar Thakur, Ph.D.  
Manju Kumari Thakur, M.Sc., M.Phil., Ph.D.

# Contents

<b>1</b>	<b>Physicomechanical Properties and Utilization of Hydrogels Prepared by Physical and Physicochemical Crosslinking</b> . . . . .	<b>1</b>
	Adriana Kovalcik	
<b>2</b>	<b>Polymer Gels: Molecular Design and Practical Application</b> . . . . .	<b>29</b>
	Vicente de Oliveira Sousa Neto, Raimundo Nonato Pereira Teixeira, Gilberto Dantas Saraiva and Ronaldo Ferreira do Nascimento	
<b>3</b>	<b>Clinical Use and Hemostatic Application of Gelatin</b> . . . . .	<b>53</b>
	Roberto Gazzeri, Marcelo Galarza, Marika Morabito and Alex Alfieri	
<b>4</b>	<b>Polysaccharide-Based Polymer Gels and Their Potential Applications</b> . . . . .	<b>97</b>
	Nabil A. Ibrahim, Ahmed A. Nada and Basma M. Eid	
<b>5</b>	<b>Silica-Based Polymeric Gels as Platforms for Delivery of Phosphonate Pharmaceutics</b> . . . . .	<b>127</b>
	Konstantinos E. Papathanasiou, Maria Vassaki, Argyro Spinthaki, Argyri Moschona and Konstantinos D. Demadis	
<b>6</b>	<b>Polymeric Hydrogel: A Flexible Carrier System for Drug Delivery</b> . . . . .	<b>141</b>
	Surbhi Dubey, Rajeev Sharma, Nishi Mody and S. P. Vyas	
<b>7</b>	<b>Gel-Based Approaches in Genomic and Proteomic Sciences</b> . . . . .	<b>185</b>
	Rafael A. Baraúna, Diego A. Graças, Joriane T. C. Alves, Ana Lúcia Q. Cavalcante and Artur Silva	
<b>8</b>	<b>Polymer Gels in Vaginal Drug Delivery Systems</b> . . . . .	<b>197</b>
	María-Dolores Veiga, Roberto Ruiz-Caro, Araceli Martín-Illana, Fernando Notario-Pérez and Raúl Cazorla-Luna	
<b>9</b>	<b>Gel Formation by Non-covalent Cross-Linking from Amylose Through Enzymatic Polymerization</b> . . . . .	<b>247</b>
	Tomonari Tanaka and Jun-ichi Kadokawa	



<b>10</b>	<b>New Aspects to Physicochemical Properties of Polymer Gels in Particularly the Coordination Biopolymeric Metal–Alginate Ionotropic Hydrogels</b> .....	275
	Refat M. Hassan (El-Moushy), Khalid S. Khairou and Aida M. Awad	
<b>11</b>	<b>Smart Polymer Gels</b> .....	355
	Waham Ashaier Laftah	
<b>12</b>	<b>Neuro-Evolutive Techniques Applied for Modeling Processes Involving Polymer Gels</b> .....	379
	Silvia Curteanu and Elena-Niculina Dragoi	

## About the Editors



**Dr. Vijay Kumar Thakur, Ph.D.** prior to commencing in the School of Aerospace, Transport and Manufacturing at Cranfield University, he was working as a Staff Scientist in the School of Mechanical and Materials Engineering at Washington State University, USA (2013–2016). Some of his other prior significant appointments include being a Research Scientist in Temasek Laboratories at Nanyang Technological University, Singapore (2009–2012), and a Visiting Research Fellow in the Department of Chemical and Materials Engineering at LHU, Taiwan. He did his postdoctoral study in Materials Science and Engineering at Iowa State University and received his Ph.D. in Polymer Chemistry (2009).

In his academic career, he has published more than 100 SCI journal research articles in the field of chemical sciences/materials science and holds one US patent. He has also published 33 books and 35 chapters on the advanced state of the art of polymer science/materials science/nanotechnology with numerous publishers. His research interests include the synthesis and processing of bio-based polymers, composites, nanostructured materials, hydrogels, polymer micro-/nanocomposites, nanoelectronic materials, novel high dielectric constant materials, engineering nanomaterials, electrochromic materials, green synthesis of nanomaterials, and surface functionalization of polymers/nanomaterials. Application aspects range from automotive to aerospace, energy storage, water purification, and biomedical fields.

He is an editorial board member of several international journals, as well as a member of scientific bodies around the globe. Some of his significant appointments include Associate Editor for *Materials Express* (SCI), Advisory Editor for *SpringerPlus* (SCI), Editor for *Energies* (SCI), Editor for *Cogent Chemistry* (SCI), Associate Editor for *Current Smart Materials*, Associate Editor for *Current Applied Polymer Science*, Regional Editor for *Recent Patents on Materials Science* (Scopus), and Regional Editor for *Current Biochemical Engineering* (CAS). He also serves on the Editorial Advisory Board of *Polymers for Advanced Technologies* (SCI) and is on the Editorial Board of *Journal of Macromolecular Science, Part A: Pure and Applied Chemistry* (SCI), *International Journal of Industrial Chemistry* (SCI), *Biointerface Research in Applied Chemistry* (SCI), and *Advances in Natural Sciences: Nanoscience and Nanotechnology* (SCI).  
e-mail: Vijay.Kumar@cranfield.ac.uk



**Dr. Manju Kumari Thakur, M.Sc., M.Phil., Ph.D.** has been working as an Assistant Professor of Chemistry at the Division of Chemistry, Government Degree College Sarkaghat, Himachal Pradesh University, Shimla, India, since June 2010. She received her B.Sc. in Chemistry, Botany, and Zoology; M.Sc. and M.Phil. in Organic Chemistry; and Ph.D. in Polymer Chemistry from the Chemistry Department at Himachal Pradesh University, Shimla, India. She has rich experience in the fields of organic chemistry, biopolymers, composites/nanocomposites, hydrogels, applications of hydrogels in the removal of toxic heavy metal ions, drug delivery, etc. She has published more than 30 research papers in several international journals, co-authored 5 books, and has also published 25 chapters in the field of polymeric materials.  
e-mail: chauhanmanjuchem@gmail.com

# Chapter 1

## Physicomechanical Properties and Utilization of Hydrogels Prepared by Physical and Physicochemical Crosslinking



Adriana Kovalcik 

### 1 Introduction

Hydrogels are viscoelastic polymer systems consisting of solid and liquid phases that are able to imbibe water without dissolution of polymer matrix (Fig. 1). Mohammed and Murphy (2009) described hydrogels as dynamic materials with alternating physical properties (e.g., degree of swelling, shape, pore size, mechanical properties, and optical properties) in dependence on ambient environmental factors (Mohammed and Murphy 2009). Hydrogels may be classified according to several criteria such as nature of polymer matrix (natural and synthetic hydrogels), kind of crosslinking (physical and chemical hydrogels), chemical structure and properties/reactivity (e.g., pH-sensitive, thermosensitive, light-sensitive, and electric charge-sensitive hydrogels), and processing/drying methodology (hydrogel, aerogel, cryogel, and xerogel). Attraction of water to hydrogels is connected with their hydrophilic nature. Among main factors, which determine swelling behavior of hydrogels in solvents, belong established balances between expanding and restoring forces. Expanding forces depend on osmotic pressure of polymer solvation, and restoring forces depend on character of chain segments between formed crosslinks (Mateescu et al. 2012).

Additionally, swelling kinetics of hydrogels in water or aqueous solvents as well as their mechanical properties are influenced by chemical nature of polymer matrix, molecular weight of polymer, character of applied crosslinking, and environmental conditions (e.g., temperature, solution pH) (De et al. 2002; Jaspers et al. 2014).

---

A. Kovalcik (✉)

Competence Centre for Wood Composites and Wood Chemistry (Wood K Plus),  
Kompetenzzentrum Holz GmbH, Altenberger Straße 69, 4040 Linz, Austria  
e-mail: adriana.kovalcik@gmail.com

A. Kovalcik

Faculty of Chemistry, Department of Food Chemistry and Biotechnology,  
Brno University of Technology, Purkynova 118, 612 00 Brno, Czech Republic

© Springer Nature Singapore Pte Ltd. 2018

V. K. Thakur and M. K. Thakur (eds.), *Polymer Gels*, Gels Horizons: From Science to Smart Materials, [https://doi.org/10.1007/978-981-10-6083-0\\_1](https://doi.org/10.1007/978-981-10-6083-0_1)

**Fig. 1** Simplified schema of hydrogel swelling in water



In recent years, there has been shown a renewed interest to apply crosslinking agent-free methods (known also as “eco-synthesis”) for the preparation of hydrogels to support their non-toxicity and biocompatibility (Abdel-Mohsen et al. 2011). The non-toxicity and biocompatibility of physical hydrogels can be further enhanced by using of natural water-soluble polymers (e.g., collagen, gelatin, alginate, agar, agarose, and guar gum) (Hago and Li 2013; Kamoun et al. 2015). Physical crosslinking comprises of linking of polymer chains by physical entanglements, formation of crystallites, electrostatic attraction forces, hydrogen bonding, hydrophobic effects, and van der Waals forces. Principal methods used for physical crosslinking of gel-forming polymers are: (1) freeze-thaw processing, (2) heat treatment, (3) ionic interactions, (4) hydrophobic interactions, (5) hydrogen bonding interactions, (6) self-assembly stereocomplexation, and (7) other non-covalent interactions. Physical hydrogels crosslinked by transient non-covalent bonds were also classified as supramolecular polymer networks which often have special behavior like stimuli-responsiveness, self-healing ability, and shape memory (Seiffert and Sprakel 2012).

It is generally accepted that physical crosslinks are reversible and their stability is controllable by changing the environmental conditions, such as solvent pH, temperature as well as type of solvent. Advantage of labile physical bond establishments in hydrogels is their controllable degradation. Another attribute important in medical applications (e.g., tissue engineering) is cytocompatibility of used materials (hydrogels must not be cytotoxic to living cells). The problem is that physical hydrogels compared to chemically crosslinked hydrogels possess much lower physical integrity and mechanical stability. Generally, both, swelling behavior and mechanical properties of hydrogels, depend on chemical and physical properties of polymer matrix and on the final crosslinking density. Higher crosslinking density practically means lower swelling degree and higher stiffness of hydrogels and usually higher mechanical stability. The present work summarizes the most frequent ways how to process physical hydrogels and how to modify their mechanical stability. It will be shown that some desired mechanical properties such as higher mechanical rigidity can be reached by blending of gel-producing polymers. It will be presented that the blending of polymers can increase the crosslinking density of physically crosslinked hydrogels as well as contribute to new special properties (e.g., antimicrobial activity or pH sensitivity). The blending of two polymers practically offers application of double crosslinking and thus

combining different types of crosslinking methods to produce physical hydrogels (Spoljaric et al. 2014). However, it must be said that applications of some crosslinking methods such as UV crosslinking may create permanent crosslinks and so hamper reversibility and biodegradability of hydrogels.

## 2 Physical and Physicochemical Crosslinking Methods Used for Hydrogels

### 2.1 Freeze-Thaw Cycling

Freeze-thaw cycling is a method based on formation of crystalline regions during freezing followed by an entanglement of hydrogen-bonded polymer chains in semicrystalline polymers. Basically, three events occurred during freeze-thaw cycling, namely formation of crystallites, hydrogen bonding, and liquid–liquid separation. Among the most investigated water-soluble polymers that are able to create hydrogels through the formation of crystallites belongs poly(vinyl alcohol) (PVA). The spread use of PVA hydrogels mainly in pharmaceutical and medical application is connected with its non-toxicity, good biocompatibility, and biodegradability (Tsujiyama et al. 2011). Zhang et al. (2012) announced that freeze-thawed PVA hydrogels are able for self-healing reaction at room temperature without using of any healing agent (Zhang et al. 2012). PVA can be predominantly synthesized through a free radical polymerization of vinyl acetate, followed by a hydrolysis of formed poly(vinyl acetate) (see Fig. 2) (Herrmann and Haehnel 1928). PVA is a semicrystalline polymer with a glass transition temperature ( $T_g$ ) about 80–85 °C and melting temperature ( $T_m$ ) about 180–240 °C. Final physical and chemical properties of PVA depend on a degree of hydrolysis.

The freeze-thaw physical crosslinking of PVA is based on densification of its original macromolecular structure in aqueous solutions (with the concentrations of 1–20 wt%). The densification is initiated by repeated application of freezing (at  $\sim -20$  °C) and thawing (at room temperature) cycles (Stauffer and Peppas 1992). The occurred crystallization of PVA can be described as a chain folding

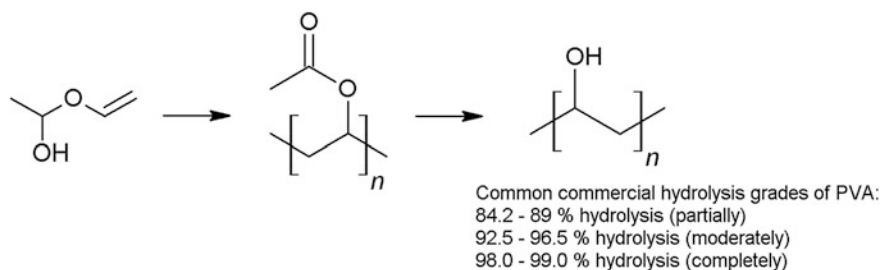


**Fig. 2** Synthesis of poly(vinyl alcohol)

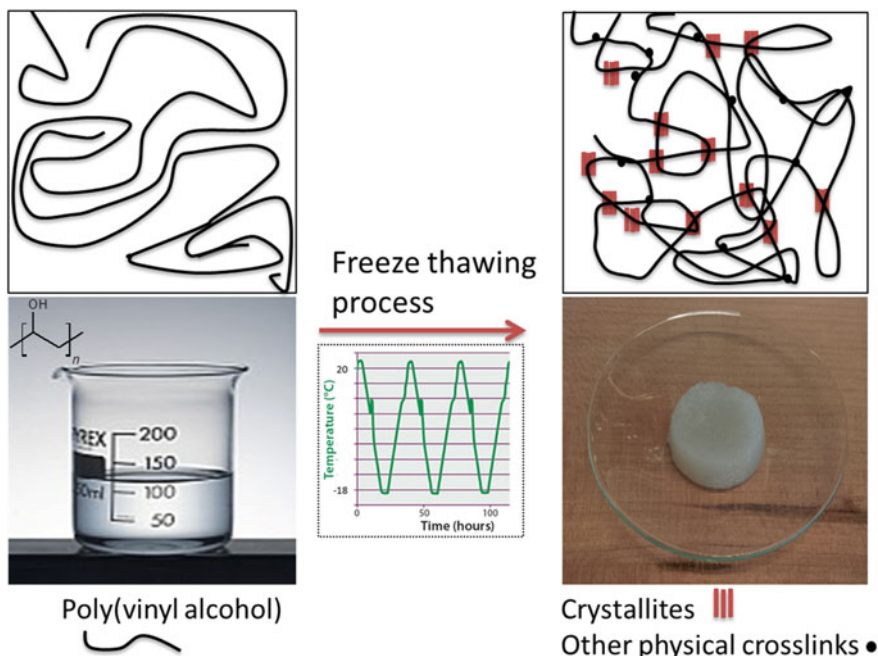


**Fig. 3** Freeze-thaw cycling method of poly(vinyl alcohol)

resulted in small ordered crystalline regions with layered structure, while molecules are held together by hydroxyl bonds and van der Waals forces (Hassan and Peppas 2000a). The solubility of PVA in water and its ability to crystallize depend on (a) chemical nature of PVA (molecular weight, molecular weight distribution, and degree of hydrolysis), and (b) applied freeze-thawing processing parameters (freeze-thaw time, freeze-thaw temperature, number of freeze-thaw cycles, and concentration of PVA in solution) (see Fig. 3).

Similarly, final physical properties of PVA hydrogels can be modified through a variation of its molecular weight, its initial concentration in the solution, and freeze-thaw cycling parameters. Among basic methods how to modify a formation and thickening of PVA belongs variation of the molecular weight of PVA, variation of the initial PVA concentration in solvent, and variation of number of applied freeze-thaw cycles. The degree of crystallinity and the thickness of crystals directly influence swelling and de-swelling behaviors of hydrogels as well as their mechanical properties (Gupta et al. 2012; Hassan and Peppas 2000b).

Another method influencing physical properties of PVA hydrogels is a modification of solute–solvent hydrogen bond dynamics by using a mixture of water with cosolvent, e.g., dimethyl sulfoxide (DMSO) (Kanaya et al. 1998). The mixing ratio of water/DMSO strongly influences kinetics of gelation process (gelation rate and phase separation rate), transparency of hydrogels, and mechanical properties of hydrogels (Kanaya et al. 1995; Ohkura et al. 1992; Takahashi et al. 2003;

Takeshita et al. 1999). Another modification method uses initiations of polar interactions in macromolecular network by the addition of electrolyte (e.g., NaOH, NaCl). Nugent et al. (2005) reported that van der Waals interactions and hydrogen bonding initiated through the addition of NaOH significantly influence crystallinity, melting behavior, swelling degree, and tensile strength of freeze-thaw-processed PVA hydrogels (Nugent et al. 2005). Latter method influencing physical properties of PVA hydrogels is a blending of PVA with various polymers or an addition of additives (see Table 1).

The addition of polymers or additives with different functionalities can support a formation of additional crosslinks, e.g., hydrogen bonds. As a result of formation of new additional physical junctions (entanglements) can be considered rate of

**Table 1** Possible effects induced by blending of PVA with second polymer and/or additives

Polymer/additive	Reached effect after blending with PVA	References
Poly(acrylic acid)	New functionality → condensation, increased pH sensitivity, and swelling ratio	Canillas et al. (2016), Gudeman and Peppas (1995), Hickey and Peppas (1997)
Poly(acrylic acid) and hydroxyapatite	New functionality → hydrogen bonding and increased stiffness	Goetten de Lima et al. (2015)
Chitosan	Antibacterial activity	Abdel-Mohsen et al. (2011)
Sodium carboxymethylcellulose	New functionality → hydrogen bonding and increased pH sensitivity	Xiao and Gao (2008)
Egg albumin	New functionality → hydrogen bonding and antibacterial activity	Bajpai and Saini (2006), Yadav and Kandasubramanian (2013)
Amine-terminated Polyamidoamine dendrimers	New functionality → hydrogen bonding, increased swelling ratio, and de-swelling rate	Wu et al. (2004)
Hemicelluloses and chitin nanowhiskers	New functionality → hydrogen bonding, improved thermal and mechanical properties, and reinforcing effect	Guan et al. (2014)
Starch	New functionality → hydrogen bonding, increased pH and thermal sensitivity, and improved mechanical properties	Bagri et al. (2009)
Alginate	New functionality → hydrogen bonding and improved biocompatibility	Kamoun et al. (2015)
Gelatin	New functionality → hydrogen bonding and improved biocompatibility	Hago and Li (2013)
Poly(vinyl pyrrolidone)	New functionality → hydrogen bonding	Jevne et al. (1986), Spiller et al. (2008)



gelation, enhanced crosslinking density and enhanced mechanical rigidity of hydrogels. One of the example materials that can be hydrogen bonded with PVA and thus supporting its gelation is poly(acrylic acid) (PAA) (Chen and Zhang 2010; Hickey and Peppas 1997). Newly established hydrogen bonds within PVA and PAA influence viscosity and swelling kinetics and impart pH sensitivity to hydrogels. The pH-sensitive hydrogels have found their applications, for example, as semipermeable membranes, drug carriers, and sensors (Hickey and Peppas 1997). Interactions between PVA and PAA can be accelerated by using of cosolvent. Better PVA/PAA interactions contribute to higher crosslinking density and enhanced mechanical stability of freeze-thawed PVA/PAA hydrogels (Nugent and Higginbotham 2006). Another polymer that supports crosslinking of PVA is poly(vinyl pyrrolidone) (PVP). PVP is a water-soluble synthetic biocompatible polymer used in cosmetic, pharmaceutical, and food industry as well as in tissue engineering (Jevne et al. 1986; Spiller et al. 2008).

Concerning freeze-thaw cycling methodology of crosslinking of PVA, it can be concluded that the size of crystallites and the degree of crystallinity significantly influence physical behavior of PVA hydrogels (Gupta et al. 2012). In summary, increase in mechanical strength and stiffness of PVA hydrogels can be reached by following modifications of freeze-thaw cycling method (Abdel-Mohsen et al. 2011; Bajpai and Saini 2006; Hassan and Peppas 2000a; Nugent and Higginbotham 2006; Ricciardi et al. 2003; Xiao and Gao 2008):

- increase in PVA content in the solution,
- increase in the number of freeze-thaw cycles,
- extension of the freezing time,
- increase in the drying temperature of a cryogel,
- promotion of the crystallization by nucleation,
- evocation of a phase separation (e.g., by an admixture of DMSO in water),
- blending of PVA with materials which support a formation of additional crosslinks (see Table 1).

## 2.2 Heat Treatment

Gelation of water-soluble polymers based on heat treatment can occur due to crosslinking upon temperature changes such as heating and cooling. The solubility of some polysaccharides, e.g., methylcellulose and chitosan in water, is temperature depended. The temperature-sensitive water-soluble polymers can often form, due to changes in conformation, thermally reversible gels. Methylcellulose and carboxymethylcellulose are typical inverse thermal gelling polymers that form hydrophobic junctions after breaking of hydrogen bonds upon heating (Ginzburg et al. 2016; Roy et al. 2010a, b, c). Different kinds of gelation upon heating shows poly(vinyl alcohol). Gelation of PVA upon heat treatment or annealing (holding polymer at temperature in the range of 150–200 °C for few minutes to hours) is

based on crystallization and formation of hydrogen bonds. Hydrogen bonds and crystallites reduce solubility and increase gel viscosity of PVA (McCrum et al. 1968). Heat treatment as a gelation method for PVA is effective only in the case of fully hydrolyzed PVA because the rest of acetate substituents inhibit changes in molecular orientation and crystallization of PVA (Drexler and Tesoro 1984). However, it must be said that heat treatment as crosslinking method for PVA is limited due to the thermal degradation that begins at about 200 °C. One possibility that how to inhibit the thermal degradation is a modification of thermal properties of PVA by plasticizing, for example, with glycerol or poly(ethylene glycol). Gelation of PVA during the heat treatment can be accelerated by an addition of additives with carboxyl functional groups such as poly(acrylic acid). The formation of physical junctions by heat treatment can be supported also by an admixture of second polymer that after cooling forms a phase separation (Nugent and Higginbotham 2006). An opaque appearance of gel can be taken as a certain indicator of a macroscopic phase separation (Takeshita et al. 1999). For a formation of hydrogels, it is also important to note that some combinations of polymers support a formation of hydrogen bonds upon drying, and therefore, final hydrogels reach higher strength properties and thermal stability (Gregorova et al. 2015). Dehydration and condensation are reactions that usually occur during mixing and heating of polymers bearing hydroxyl and carboxyl functional groups. PVA/PAA blends after esterification are crosslinked materials, and a degree of crosslinking depends on a degree of neutralization of poly(acrylic acid) (Kumeta et al. 2003). In conclusion, mechanical properties of heat-treated hydrogels highly depend on the following factors: molecular weight of polymers, concentration of additives, degree of neutralization of additives (e.g., PAA; see Fig. 4), and applied conditions during the thermal treatment (e.g., mixing temperature, drying temperature, time schedule, and solvent pH) (Chun et al. 2005; Kumeta et al. 2003).

Ruberti and Braithwaite (2004) developed another method, the so-called theta-gel method, for the processing of physically crosslinked PVA hydrogels with heat treatment (Ruberti and Braithwaite 2004). This method consists of two steps: (1) dissolving of PVA in the mixture of water with low-molecular weight cosolvent, e.g., poly(ethylene glycol) (PEG) at an elevated temperature, and (2) cooling of dissolved PVA to room temperature. It was found that densification and crystallization of PVA occur after interactions of PVA chains with each other as well as with PEG chains through hydrogen bonding (Choi et al. 2006).

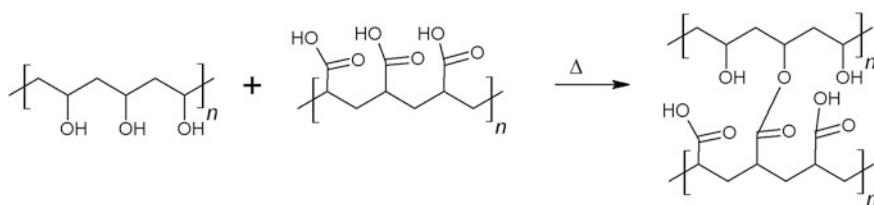


**Fig. 4** Schema of condensation of poly(vinyl alcohol) with poly(acrylic acid)

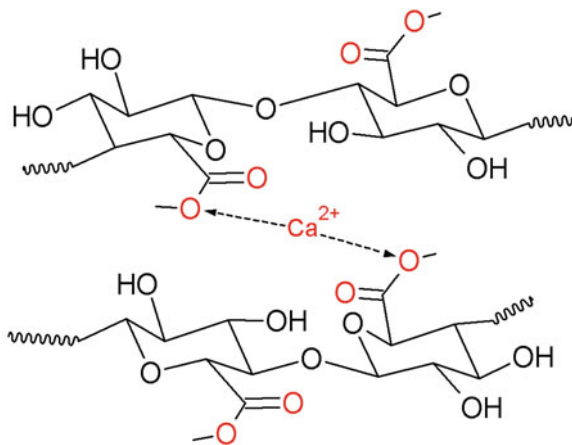
### 2.3 Ionic Interactions

The highly negatively charged anionic polymers such as alginate and carrageenan are able to form gel through ionic interactions with bivalent or trivalent ions. Hydrogels formed from polysaccharides in the presence of ions are often pH-sensitive, and their stability can be destroyed by an addition of chelating agent (Ebara et al. 2014).

Alginate (called also alginic acid) is an anionic polysaccharide, usually derived from cell walls of brown algae in the form of white or yellow fibrous powder. Alginate forms very easy gels in the presence of bivalent counter ions, e.g.,  $\text{Ca}^{2+}$ ,  $\text{Mg}^{2+}$ ,  $\text{Cu}^{2+}$  (Fig. 5). The gelation of alginate implies the interaction of its carboxylate groups and bivalent counter ions. Among often used techniques implying ionic interactions belongs a dripping technique consisting of dripping of solved polymer into a solution containing bivalent counter ions (e.g., calcium chloride solution) (Fundueanu et al. 1999). Hydrogels based on ionic interactions can be prepared in various forms, e.g., in the form of microspheres with high mechanical stability (Liu et al. 1997). Again, blending is a method often used for modification of physical properties of hydrogels prepared through ionic interaction. Many works have presented an enhancement of physical properties of alginate hydrogels by its blending with chitosan, carboxymethylcellulose, hyaluronic acid, and polyamines (poly-L-arginine, poly-L-lysine) (Ibrahim and El Salmawi 2013; Kilan and Warszynski 2014; Lawrie et al. 2007; Liu et al. 1997; Wang et al. 2013a, b).

In drug delivery applications, there are often required hydrogels with high pH sensitivity. The literature shows that pH sensitivity of hydrogels can be reached by blending of basic ionic crosslinkable polymer with thermally gelling polymer like methylcellulose or carboxymethylcellulose. An excellent pH sensitivity of methylcellulose/alginate hydrogel blended with NaCl was demonstrated, and these blended hydrogels were suggested to be a suitable carrier of bioactive proteins in

**Fig. 5** Scheme of ionic interactions of alginate with bivalent calcium ions



the intestine due to the high stability up to pH 7.4 (Liang et al. 2004). Swamy and Yun (2015) developed pH-sensitive hydrogels by blending of alginate with carboxymethylcellulose and crosslinking with ferric chloride solution (Swamy and Yun 2015).

Carrageenan is linear sulfated polysaccharide consisting of alternating 3-linked- $\beta$ -D-galactopyranose and 4-linked- $\alpha$ -D-galactopyranose units. This natural gelating polymer can be derived from edible seaweeds. There is a group of carrageenans that belong to natural hydrophilic polymers forming physical crosslinking network upon thermal treatment and ionic interactions. The initial gelation of carrageenans begins due to the changes of supermolecular structure after cooling of hot solutions, and the next gelation step is involved by ionic interactions in the presence of ions (e.g.,  $\text{Na}^+$  ionic solution) (Funami et al. 2007). Carrageenans are widely used in food industry as thickening agents. Carrageenans can be transferred to putty state by mixing with either calcium hydroxide or the mixture of calcium hydroxide with magnesium hydroxide through ionic interactions of intrinsic sulfate and hydroxyl groups with bivalent calcium and magnesium ions (Urano and Ina 2004).

As further gelation method through ionic interaction can be named a condensation occurred through ionic complexation of PVA with borax or boric acid or sulfuric acid (Fig. 6) (Khutoryanskiy et al. 2011; Pezron et al. 1989; Wang et al. 1999). The crosslinking reaction between two diols of PVA and one borate ion is the so-called di-diol complexation (Lin et al. 2002). It has to be mentioned that PVA–borate, PVA–boric acid, or PVA–sulfuric acid crosslinking is not any more physical crosslinking mechanisms but belongs to chemical crosslinking mechanisms (Zhang et al. 2015).

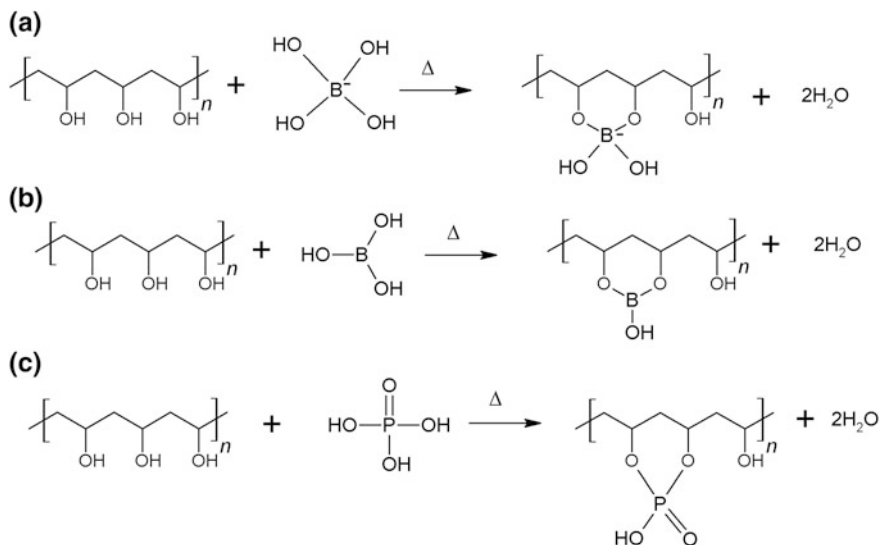


**Fig. 6** Reaction schemas of poly(vinyl alcohol) with **a** borax, **b** boric acid, and **c** sulfuric acid

## 2.4 *Hydrophobic Interactions*

Basically, the formation of hydrogels based on hydrophobic interactions requires an incorporation of monomers or polymers with low molecular weight with hydrophobic units usually linked with long alkyl side chains into hydrophilic polymers. The hydrophobic parts admixed in hydrophilic polymer chains create micelles which act as physical crosslinks within formed hydrogels (Okay 2015). Hydrophilic polymers can be chemically modified by grafting hydrophobic groups to receive structure which supports gelling through hydrophobic interactions. Structural organization and gelation of such hydrophilic–hydrophobic polymers occur at relatively high concentrations through associations of hydrophobic groups in aqueous solvents and formations of micelles up to a critical value (Alexandridis et al. 1994; Popa-Nita et al. 2010). A solgel transition of polymers or copolymers that are able to create micelles through hydrophobic interactions is a reversible process and depends on their concentration as well as external factors such as temperature, pH, or ionic strength.

The synthesis of hydrophilic–hydrophobic polymers can serve as a way to support biodegradability of polymers. Hydrophobicity and biodegradability of hydrophilic non-biodegradable polymers, such as poly(ethylene oxide) (PEO) or poly(ethylene glycol) (PEG), can be increased by copolymerization with hydrophobic and biodegradable blocks like poly(L-lactic acid) (PLLA), poly(DL-lactic acid-co-glycolic acid) (PLGA), or poly(caprolactone) (PCL) (Jeong et al. 2000; Jeong et al. 1997; Jeong et al. 1999). The synthesized biodegradable diblock (PEO-PLLA), triblock (PEO-PLLA-PEO or PEG-PLGA-PEG) or star-shaped copolymers are thermosensitive and can be used as drug carriers for controlled delivery of drugs with a low diffusion coefficient or low molecular mass. It was shown that a release kinetic can be easily controlled by loading, molecular weight and hydrophobicity of the drug and the initial concentration of hydrophilic–hydrophobic polymer matrix (Jeong et al. 1997).

Amphiphilic polysaccharides, such as chitosan, methylcellulose, and dextran, are thermal gelling polymers of which gelation kinetic is dependent on concentration of used amphiphilic polysaccharides and processing temperature. The gel formation polysaccharides have found their utilization mainly in drug delivery and tissue engineering applications (Hassani et al. 2012). Gelation kinetics of hydrogels based on amphiphilic polysaccharides can be modified by an admixture of second amphiphilic polysaccharide. As the successful combination of amphiphilic polysaccharides was found hyaluronan (HA) with methylcellulose (MC), where MC supports the formation of hydrophobic junctions and HA increases solution viscosity and enhances a strength of final hydrogel (Schupper et al. 2008). It was reported that the degradation of physical HA/MC hydrogels occurs within 4–7 days *in vivo* which is for some applications too short time (Kang et al. 2009). It was shown that an incorporation of polymeric hydrophobic particles, preferably based on biodegradable polymer, e.g., poly(lactic-co-glycolic acid), can enhance the stability of hydrogels (Shoichet et al. 2010).

Chitosan is another polysaccharide that is able to form hydrogels without external crosslinking agent. The mechanism of gelation of chitosan consists of modification of the hydrophilic–hydrophobic balance, allowing the formation of both hydrophobic interactions and hydrogen bonding. Montembault et al. (2004) highlighted several parameters that play a great role in gelation of chitosan such as apparent charge density of chitosan, dielectric constant of the solvent, degree of acetylation of chitosan, temperature applied during gelation, and viscosity of the medium (Montembault et al. 2004). Chenite et al. (2000) reported that thermogelation of chitosan can be improved by its mixing with beta glycerophosphate. Negatively charged polyol salt attracts positively charged amine groups of chitosan and therefore prevents its aggregation and precipitation at physiological environment (Chenite et al. 2000).

Cerchiara et al. (2002) crosslinked chitosan with lauric, myristic, palmitic, and stearic acids and studied their efficiency as drug delivery materials for topical use. This work reports that chitosan-laurate and chitosan-myristate hydrogels (see Fig. 7) have reached high transcutaneous permeation applicable for drug delivery (Cerchiara et al. 2002). Chitosan laurate was studied also as a lubricant for pharmaceutical tablet formulations. It was found that chitosan laurate compared to a common lubricant—magnesium stearate—supported better dissolution behavior, higher mechanical strength, and shorter disintegration time of acetaminophen tablets (Bani-Jaber et al. 2015).

Recent works showed that hydrogels formed by crosslinking of biopolymers or biodegradable copolymers via hydrophobic interactions can reach an extraordinary high mechanical strength, stretchability, and self-healing ability (Okay 2015; Zhang et al. 2008).

## 2.5 Hydrogen Bonding Interactions

The formation of hydrogen bonds can directly evocate process of the gelation of polymers or can contribute to a faster gelation in synergy with another type of the physical crosslinking, e.g., formation of gel-like structures by crystallization

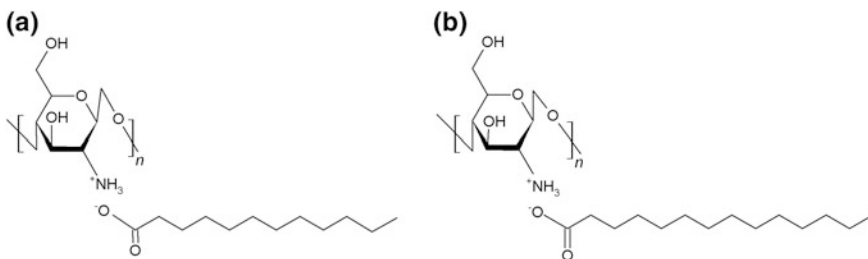


**Fig. 7** Chitosan crosslinked with fatty acids, **a** chitosan laurate and **b** chitosan myristate

(see Table 1) or gelation through hydrophobic interactions. It is evident that a formation of hydrogen bonds is often accompanied with a formation of other bonds, e.g., ester or peptide bonds (Saxena et al. 2011). The character of formed bonds directly influences rheological and physical properties of formed gels. Mechanical properties of physical hydrogels created by hydrogen bonding interactions highly depend on applied temperature and shear strain. The easy controllability of gelation and physical properties of natural polymers interacting through hydrogen bonds are often used in drug delivery (Gupta et al. 2006).

Hydrogels formed by hydrogen bonding interactions have found their applications in food, pharmaceutical, and medical industries mainly due to easy controllable gelation and low toxicity (Ebara et al. 2014; Saha and Bhattacharya 2010). Among typical examples of natural polymers creating crosslinking structure through hydrogen bonding belong carboxymethyl cellulose, methylcellulose, agar, gelatin, and hyaluronan (Gupta et al. 2006; Li et al. 2009; Saxena et al. 2011).

## 2.6 *Self-assembly Stereocomplexation*

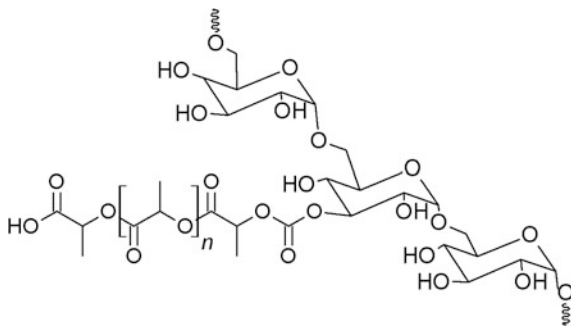
Formation of hydrogels through stereocomplexation of hydrophobic polymers belongs to the newest concept enlarging the group of physical hydrogels. The principle of the formation of stereocomplex hydrogels is based on the mixing of system A (water-soluble or water-dispersible polymer with grafts formed from monomers of certain chirality) with system B (water-soluble or water-dispersible polymer with groups formed from monomer of an opposite chirality compared to monomers used in system A), while physical crosslinking occurs through formation of racemic crystallites (Hennink and Van Nostrum 2005; Hennink et al. 2000).

It was found that physically crosslinked biocompatible and biodegradable hydrogels can be prepared based on the stereocomplex formation of a blend consisting of L-lactide oligomer and D-lactide oligomer (de Jong et al. 2000). Furthermore, thermoreversible lactide hydrogels can be prepared by grafting of dextran to lactide stereocomplex oligomers (see Fig. 8). Their viscoelastic properties depend on degree of polymerization of lactide oligomers, degree of substitution (number of lactide oligomers per 100 g glucopyranose units of dextran), and water content (de Jong et al. 2000).

## 2.7 *Other Non-covalent Interactions*

It has been found that in biological systems occur intermolecular non-covalent reversible interactions, leading to gelation of biopolymers. These interactions impart highly dynamics and permit relatively low energetically demanded processes of assembling and disassembling depending on environmental factors (Mohammed and Murphy 2009).

**Fig. 8** Lactide grafted to dextran



Proteins and peptides are typical natural polymers that form physical hydrogels crosslinked by intermolecular interactions. The ability of proteins and peptides to create polymer gel systems without any covalent bonds is often used as material for drug delivery. Gelation and physicochemical properties of gels as well as release kinetic of incorporated drugs can be modified through changes in amino acid sequences. Cappello et al. (1998) prepared hydrogels based on polymers consisting of silk-like and elastin-like blocks with variable amino acid sequences with the aim to confer properties similar to polyurethanes composed of hard and soft blocks and reported the controllable release of incorporated drugs depending on hydrogel composition (Cappello et al. 1998). Other works also showed that artificial proteins, e.g., proteins capping leucine zipper domains, can form self-assembling hydrogels with potential in bioengineering applications (Petka et al. 1998; Wang et al. 2013a).

It is known that peptides have an ability to form hydrogels by their conformation changing. Peptides under unfolding conditions have viscosity similar to water, but if they are in the  $\beta$ -hairpin conformation, they can form rigid hydrogels. This self-assembling ability initiated by external stimuli was explained by intermolecular hydrogen bonding between the strands of distinct hairpins and the hydrophobic interactions (Rajagopal et al. 2006).

### 3 Mechanical Stability of Physically Crosslinked Hydrogels

Hydrogels are soft materials with viscoelastic behavior; i.e., they show behavior like solid (storing of energy) as well as like liquid (dissipation of energy) materials. Viscoelastic properties of hydrogels and their response to environmental changes are important attributes limiting their applications. Viscoelastic properties of hydrogels depend mainly on chemical structure and molecular weight of polymer matrix, crosslinking degree, actual water content, and ambient conditions (e.g., pH, temperature, mechanical stresses).

It should be mentioned that mechanical properties of hydrogels are directly connected with a crosslinking density as well as water (or other solvent) content.



An increase in the crosslinking density of hydrogels causes increase in their stiffness. Generally, a value of crosslinking density can be indirectly determined through a degree of swelling. An increase in crosslinking density decreases a degree of swelling and increases a percentage of the gel fraction.

The degree of swelling ( $S$ ) can be determined gravimetrically:

$$S[g \cdot g^{-1}] = \frac{W_s - W_d}{W_d} \times 100 \quad (1)$$

where  $W_d$  is the weight of a sample in a dry state before swelling and  $W_s$  is the weight of a wet sample after swelling for the chosen time (hydrogels usually swell to equilibrium within a few hours).

Generally, mechanical properties of hydrogels are quite poor in relation to their mechanical strength and geometrical stability. Generally, chemically crosslinked hydrogels with permanent crosslinking network are more stable and stiffer compared to physically crosslinked hydrogels with a reversible crosslinking network. Basically, mechanical properties of physically crosslinked hydrogels can be modified by composition of hydrogels or by modification of processing parameters. The blending of hydrogel forming hydrogel with the second water-soluble polymer is a common method to modify properties of physically crosslinked hydrogels. Furthermore, crosslinking methods as well as admixed additives have a direct influence on the formation of morphology and a degree of swelling of hydrogels. The purpose of this subchapter is to provide information on ways how to control and/or modify mechanical and dimensional stability of physically crosslinked hydrogels. Creep compliance and creep recovery measurements are useful methods that are often used to assess time-dependent mechanical stability of hydrogels (Ahearne et al. 2005; Mahanta et al. 2013; Yan and Pochan 2010). The especial importance of this review is creep behavior of PVA-based hydrogels in dependence on equilibrium water content and crosslinking degree.

### ***3.1 Dependence of Creep Behavior of Hydrogels on Equilibrium Water Content***

As already mentioned, hydrogels are special materials consisting of crosslinked polymer and water or other solvent. Their mechanical properties including a mechanical stability under mechanical stress depend highly on equilibrium water content. A number of theories including linear poro-elasticity as well as various nonlinear approaches have been proposed for the prediction and description of mechanical properties of hydrogels. Based on a nonlinear continuum theory, it can be concluded that mechanical properties of hydrogels strongly depend on type of the solvent and stage of swelling (initial or equilibrium state of swelling) (Bouklas et al. 2015). The value of the equilibrium water content of PVA hydrogels can be decreased by dehydration initiated by a soaking step and a rehydration step in

different solvents. Choi et al. (2006) modified chain mobility and increased final density of PVA hydrogels by solvent dehydration of theta-gel PVA hydrogels prepared with PEG as a cosolvent. As a consequence of the increased density, dehydrated hydrogels reached much lower creep compliance compared to original theta-gel hydrogels with PEG traces (Choi et al. 2006).

### ***3.2 Dependence of Creep Behavior of Hydrogels on a Crosslinking Density***

Based on a number of research works, it can be suggested that a higher mechanical stability of hydrogels, namely lower creep compliance and higher elastic recovery, might be reached by increase in crosslinking density (Mahanta et al. 2013). However, their final porosity plays also a great role in mechanical behavior of hydrogels (Spiller et al. 2008). Generally, the value of crosslinking density of hydrogels can be increased by an addition of additives which support a formation of hydrogen bonds. This subchapter gives examples how a mechanical stability of physically crosslinked hydrogels can be modified by (1) an addition of hydrophilic nanofiller and (2) an addition of hydrophilic polymer.

#### **3.2.1 Effect of Hydrophilic Nanofiller on Mechanical Properties of PVA Hydrogels**

Generally, it is accepted that rheological and mechanical properties of hydrogels can be altered by an addition of low concentration of nanofiller. Qiao et al. (2015) enhanced physical crosslinking degree of PVA hydrogels through a formation of additional hydrogen by an addition of hydrophilic nanofiber bacterial cellulose (nf-BC). In this work, it was reported that the addition of nf-BC improved the mechanical rigidity of PVA hydrogels. It was detected by a decrease in final creep compliance under mechanical loading. The ratio 1/20 of nf-BC/PVA was found as an optimum concentration of nf-BC admixed in PVA. Filled hydrogels reached a compact porous structure and enhanced mechanical stiffness compared to neat PVA hydrogels (Qiao et al. 2015). Spoljaric et al. (2014) prepared self-healing PVA hydrogels with reversible crosslinking and low creep compliance by filling of PVA with nanofibrillated cellulose (NFC) and by crosslinking with borax. Self-healing ability of PVA/NFC hydrogels was reached due to the ability of NFC to de-bond and re-bond hydrogen bonds. Additionally, interactions of PVA with borax and nanofibrillated cellulose induced the crosslinking density and contributed to improve mechanical performance of PVA hydrogels. PVA–borax crosslinking directly influences value of the tensile modulus of PVA/NFC hydrogels, and PVA/NFC intermolecular hydrogen bonding has an effect on tensile strength. The 40 wt % of NFC was found to be maximal effective concentration able to decrease creep

compliance without deterioration of tensile strength and tensile moduli of hydrogels (Spoljaric et al. 2014).

### 3.2.2 Effect of an Addition of PVA on Mechanical Properties of Hydrogels Based on Polyanionic Polysaccharides

The objective of the following investigation was to demonstrate an effect of PVA addition on mechanical and viscoelastic properties of hydrogels based on sodium carboxymethylcellulose or sodium alginate. CMC and SA are polyanionic water-soluble polysaccharides able to create physically crosslinked hydrogels by using the ionic interactions of carboxylate groups with divalent or trivalent ions (e.g.,  $\text{Ca}^{2+}$ ,  $\text{Fe}^{3+}$ ). Among advantages of these polyanionic polymers, we can count their large commercial accessibility, relatively low price, biocompatibility, and biodegradability. Their utilization covers a large scale of applications predominantly in food, pharmaceutical, and cosmetic industry.

Many works showed that a blending of water-soluble polymers and a combination of several crosslinking methods allow formation of hydrogels with new structure, modified crosslinking density, and modified mechanical properties. New properties of hydrogels can enlarge their usability as smart hydrogels in pharmaceutical, medical, dental, cosmetic, and agriculture applications. Oniki and Ishiguro (2000) announced that the combination of CMC and PVA enable forming hydrogels with mechanical stiffness suitable for the production of dentifrices for cleaning of the buccal cavity (Oniki and Ishiguro 2000). El Salmawi (2007) prepared hydrogels with enhanced water retention ability in the soil by blending of CMC with PVA in the ratio of 80:20 vol.% and by combination of freeze thawing with electron-beam irradiation (El Salmawi 2007). Another work showed that pH-sensitive hydrogels can be prepared by blending of CMC with PVA blend and their double crosslinking with interaction with  $\text{Fe}^{3+}$  ions and freeze thawing. The pH sensitivity of physically crosslinked hydrogels is one of the attributes applicable in drug delivery systems for bioactive agents (Wang et al. 2011). Another work showed that biocompatible CMC/PVA hydrogels can be used as active adhesion barriers reducing an adhesion formation after abdominal and gynaecological surgeries (Mueller et al. 2011).

The positive effect of double crosslinking on mechanical stability of sodium alginate/poly(vinyl alcohol) blend hydrogels was reported in the case of combination of freeze thawing with ionic interaction with  $\text{Ca}^{2+}$  ions (Mahdavinia et al. 2016; Zou et al. 2015).

As already mentioned, the blending of two gel-forming polymers can admit the application of double crosslinking. The following data will show that the blending of poly(vinyl alcohol) (PVA) with sodium carboxymethyl cellulose (CMC) or with sodium alginate (SA) polymers permits the double crosslinked, namely freeze thawing and ionic interaction with calcium divalent ions (Fig. 9).

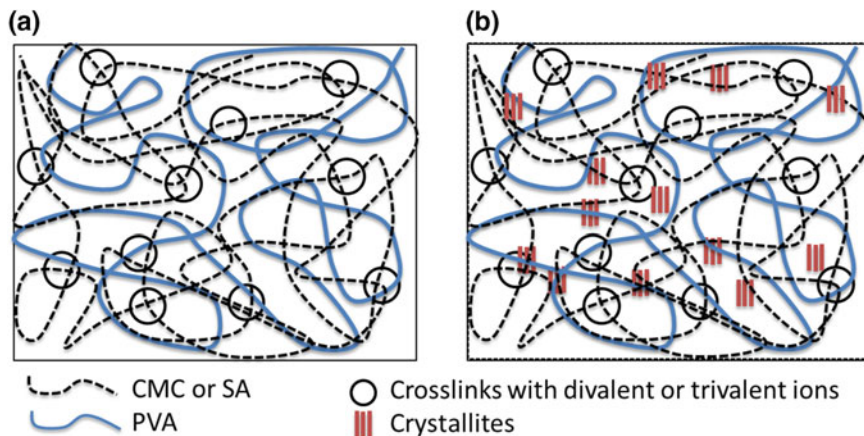
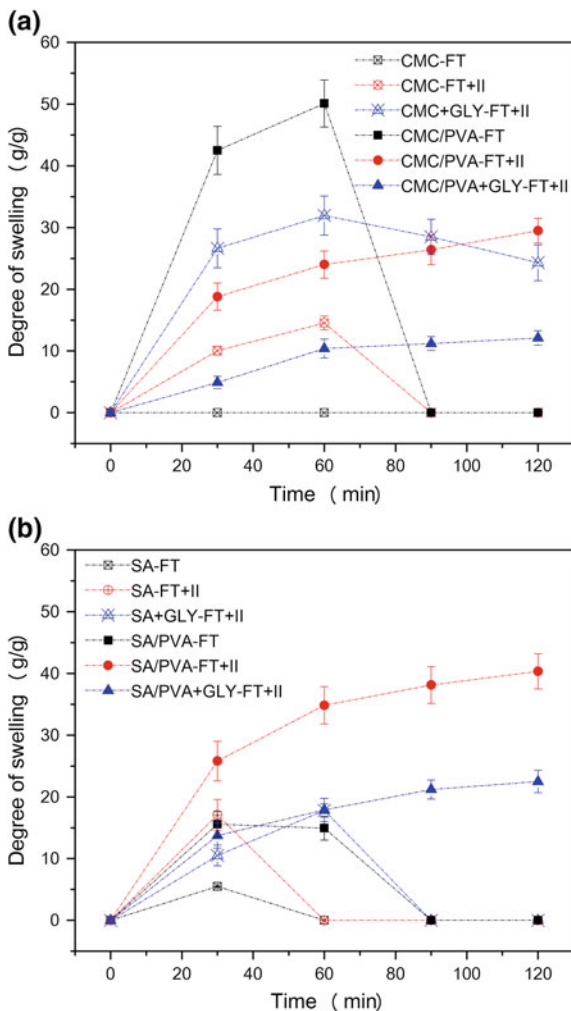


**Fig. 9** Physically crosslinked hydrogels based on sodium carboxymethylcellulose or sodium alginate hydrogels blended with poly(vinyl alcohol) after ionic interaction with divalent or trivalent ions, **a** before freeze thawing and **b** after freeze thawing

Figure 10 shows the swelling behavior of CMC, SA, CMC/PVA (1:1), and SA/PVA (1:1) hydrogels that were physically crosslinked by freeze thawing (FT) or freeze thawing and ionic interaction with divalent calcium ions (FT +  $\text{Ca}^{2+}$ ). Additionally, an effect of 2 wt% of glycerol (GLY) used as plasticizer was investigated (Kovalcik 2015). Plasticizers such as glycerol are often used as additives for hydrogels to overcome their brittleness and improve their elasticity. The determined swelling behavior showed that freeze thawing is not an effective crosslinking method for neat CMS or SA. The combined freeze thawing method with the ionic interaction was only partially effective. The addition of glycerol into CMC and SA had plasticizing effect on hydrogels. The highest degree of swelling reached freeze-thawed CMC/PVA hydrogel ( $S = 50.1 \text{ g/g}$ ), but these hydrogels were stable in water only up to 60 min. The formation of hydrogels from CMC and PVA or SA and PVA blends requested an application of combined crosslinking with calcium ions and freeze thawing. CMC/PVA-FT+II and SA/PVA-FT+II hydrogels reached the degree of swelling of 29.2 and 40.3 g/g, respectively. Both hydrogels, CMC/PVA-FT+II and SA/PVA-FT+II, were mechanically stable in water even after 24 h (data not shown). Similarly, double crosslinked plasticized CMC/PVA+GLY-FT+II and SA/PVA+GLY-FT+II hydrogels reached a high stability in water, but the swelling degree decreased about 40–50% due to the modified crosslinking density after the addition of hydrogels.

In addition to crosslinking density, the swelling behavior of hydrogels depends also on their morphology. The morphology of freeze-thawed hydrogels CMC/PVA-FT and SA/PVA-FT hydrogels is shown in Fig. 11a, b. An effect of the combined crosslinking with two methods (FT and II) on morphology of hydrogels is depicted in Fig. 11c, d. The SEM images of cross sections of hydrogels show clear differences in texture among hydrogels depending on kind of polymer

**Fig. 10** Degree of swelling of hydrogels crosslinked by freeze thawing (FT) or by freeze thawing and ionic interaction with calcium ions (FT+II) of **a** sodium carboxymethylcellulose (CMC), plasticized CMC (CMC+GLY), blend of sodium carboxymethylcellulose with poly(vinyl alcohol) (CMC/PVA), and plasticized blend CMC/PVA+Gly; **b** sodium alginate (SA), plasticized SA (SA+Gly), blend of sodium alginate with poly(vinyl alcohol) (SA/PVA), and plasticized blend SA/PVA+GLY (Kovalcik 2015)



(CMC or SA) as well as on crosslinking method. CMC/PVA and SA/PVA hydrogels crosslinked by combined FT+II methodology were capable to absorb water without dissolution. The highest swelling capacity detected by SA/PVA-FT+II hydrogel was supported probably due to the developed highly porous structure (see Fig. 11d).

The developed morphology as well as crosslinking density influenced mechanical and viscoelastic properties of hydrogels. The following results show that an admixture PVA as well as kind of applied crosslinking methodology influenced viscoelastic properties of CMC- and SA-based hydrogels. It is generally accepted that the mechanical strength of physically crosslinked hydrogels is much lower than that of chemically crosslinked. Furthermore, environmental conditions

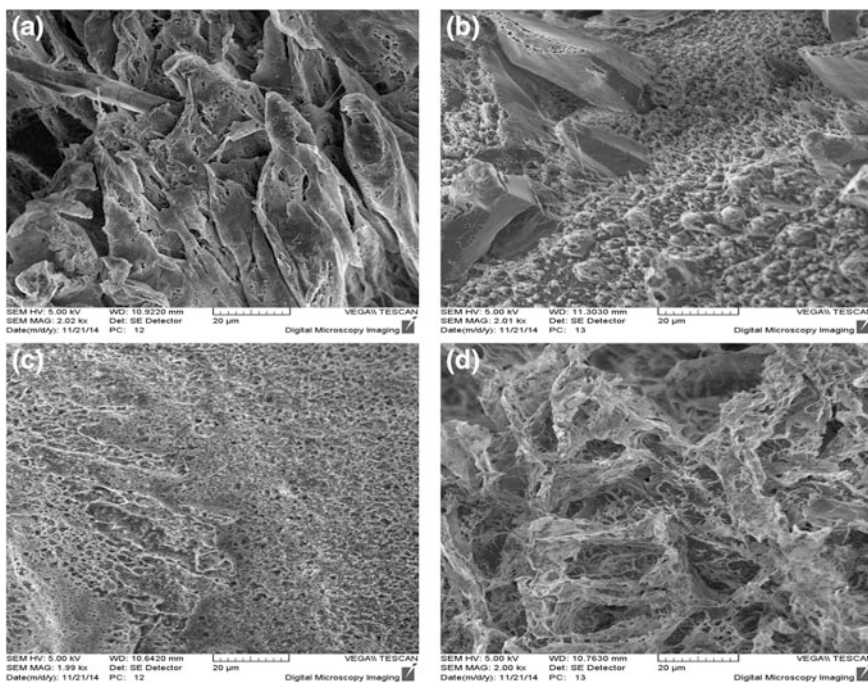


**Fig. 11** SEM images of lyophilized hydrogels: **a** CMC/PVA-FT, **b** SA/PVA-FT, **c** CMC/PVA-FT+II, and **d** SA/PVA-FT+II (Kovalcik 2015)

such as air humidity and temperature substantially affect mechanical strength of hydrogels due to their high compliance to adsorb water from the air. Many products based on hydrogels, for example, materials used as wound dressing, are exposed to mechanical stresses during their service life as well as during storing. Their ability to withstand these mechanical stresses can depend on temperature or humidity changes. Mechanical and hygrothermal stresses can be simulated and determined by dynamic mechanical analysis with adjustment of relative humidity concentration (DMA-RH-dynamic mechanical analyzer with relative humidity accessory) (Gregorova et al. 2013, 2015; Grundelova et al. 2015). CMC, SA, CMC/PVA, and SA/PVA hydrogels were subjected under tensile mode to a constant load of 10 MPa for 5 min, and the occurred dimensional changes (strain) were determined. Consequently, the load was released and an elastic recovery after 10 min was determined. Figure 12 and Tables 2 and 3 show creep and creep recovery data depending on a kind hydrogel and environmental conditions (temperature of 25 °C and relative humidity of 0% RH or 50% RH). The determined stress–strain–time data show that CMC-FT and SA-FT hydrogels have high stiffness and respond to loaded stress of 10 MPa at dry atmosphere with strain of 0.16 and 0.28%, respectively. In spite of high stiffness, CMC-FT and SA-FT hydrogels reached 100% recovery at the end of creep zone. CMC-FT+II and SA-FT+II hydrogels were

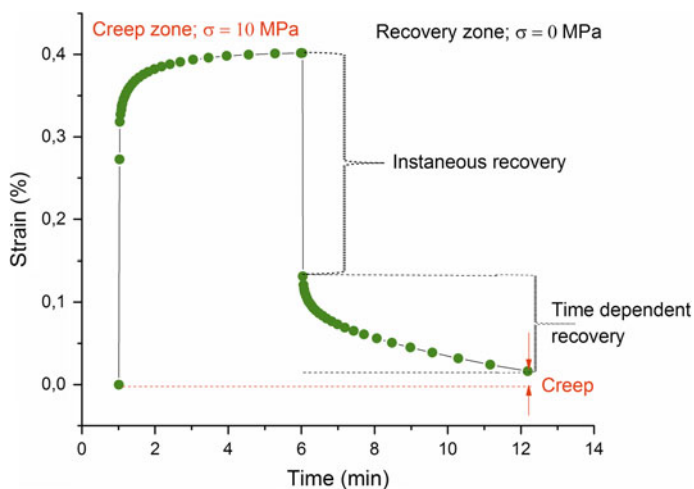


**Fig. 12** Strain response of CMC-FT hydrogel during creep and creep recovery experiment under stress of 10 MPa at 25 °C and 0% RH

**Table 2** Creep and creep recovery data of CMC and SA hydrogels at 25 °C and 0% RH (Kovalcik 2015)

Sample	Maximal strain (%) in creep zone (%)	Strain recovery (%) in recovery zone (%)	Jer (Pa <sup>-1</sup> )
CMC-FT	0.16	100	$1.00 \times 10^{-12}$
CMC-FT+II	Hydrogel ruptured		
CMC+GLY-FT+II	3.2	76.2	$7.59 \times 10^{-8}$
CMC/PVA-FT	0.40	100.0	$1.00 \times 10^{-12}$
CMC/PVA-FT+II	0.54	96.2	$2.09 \times 10^{-9}$
CMC/PVA+GLY-FT+II	131.8	50.0	$6.59 \times 10^{-6}$
SA-FT	0.28	100	$1.00 \times 10^{-12}$
SA-FT+II	Hydrogel ruptured		
SA+GLY-FT+II	3.7	97.0	$7.30 \times 10^{-9}$
SA/PVA-FT	0.41	95.6	$1.81 \times 10^{-9}$
SA/PVA-FT+II	0.44	100	$1.00 \times 10^{-12}$
SA/PVA+GLY-FT+II	107.4	49.2	$5.46 \times 10^{-6}$

CMC sodium carboxymethylcellulose, SA sodium alginate, PVA poly(vinyl alcohol), GLY glycerol, FT freeze thawing, II ionic crosslinking with Ca<sup>2+</sup> ions

**Table 3** Creep and creep recovery data of CMC and SA hydrogels at 25 °C and 50% RH (Kovalcik 2015)

Sample	Maximal strain (%) in creep zone (%)	Strain recovery (%) in recovery zone (%)	Jer ( $\text{Pa}^{-1}$ )
CMC-FT	0.67	60.1	$2.67 \times 10^{-8}$
CMC-FT+II	Hydrogel ruptured		
CMC+GLY-FT+II	54.9	58.0	$2.31 \times 10^{-6}$
CMC/PVA-FT	0.43	67.5	$1.40 \times 10^{-8}$
CMC/PVA-FT+II	0.85	60.2	$3.39 \times 10^{-8}$
CMC/PVA+GLY-FT+II	Hydrogel ruptured		
SA-FT	1.1	50.3	$5.26 \times 10^{-8}$
SA-FT+II	Hydrogel ruptured		
SA+GLY-FT+II	5.9	77.5	$1.13 \times 10^{-8}$
SA/PVA-FT	0.78	82.7	$1.35 \times 10^{-8}$
SA/PVA-FT+II	0.71	72.8	$1.35 \times 10^{-8}$
SA/PVA+GLY-FT+II	Hydrogel ruptured		

CMC sodium carboxymethylcellulose, SA sodium alginate, PVA poly(vinyl alcohol), GLY glycerol, FT freeze thawing, II ionic crosslinking with  $\text{Ca}^{2+}$  ions

too brittle and ruptured immediately after stretching in tensile clamp before the creep test could begin. Plastizing of these hydrogels decreased their brittleness and promoted their strain response on the loaded stress. The strain recovery of SA +GLY-FT+II was comparable with the hydrogel without plasticizer, but the strain recovery of CMC+GLY-FT+II decreased to 56%. Blending of CMC and SA with PVA slightly decreased their stiffness, and hydrogels crosslinked with both methods (freeze thawing or freeze thawing combined with ionic interactions) reached high elasticity with strain recovery of 95.6–100%. Plasticized blended hydrogels (CMC/PVA+GLY-FT+II and SA/PVA+GLY-FT+II) were very soft with the strain in the creep zone about 107.4–131.8 and creep recovery only about 49.2–50%. Hydrogels are materials with function to adsorb and retain high volumes of water; however, it must be noted that the retained water changes their mechanical strength and viscoelastic behavior. Table 3 shows that an increase in relative humidity on 50% RH had plasticizing effect on all tested hydrogels and markedly decreased their elasticity. Hydrogels primary plasticized hydrogels with glycerol responded on humid conditions with the essential loss in mechanical stability, and they ruptured already at conditioning phase before creep testing.

## 4 Conclusion and Future Perspective

Mechanical properties of physical hydrogels are highly dependent on environmental factors (e.g., pH, temperature, solvent). At one side, the mechanical stability under mechanical stresses (creep behavior) and toughness of physically crosslinked



hydrogels are usually much lower than those of chemically crosslinked hydrogels. At the second time, degradation of physically crosslinked hydrogels can be managed by an application of special conditions. However, establishment of covalent linkages inhibits the so-called degradation upon request or under special environmental conditions. The biocompatibility and controllable degradation of hydrogels are predominantly required in biomedical applications such as tissue engineering and drug delivery. Another advantage of physical crosslinking is that physical crosslinking methods do not require the use of chemical crosslinking agents that are often harmful to living cells and environment. Next, the rheological behavior of physical crosslinked hydrogels such as shear-thinning is easily manageable by physical crosslinking. The literature shows that new designed physical hydrogels with improved mechanical rigidity have a perspective to be usable in addition to cosmetic, pharmaceutical, and medical areas also in technical applications, for example, in water treatment, agriculture, and packaging. However, these hydrogels should be rapidly and easily formed in large processing scale and their dependence of mechanical behavior on environmental factors should be adjustable according to service requirements.

## References

- Abdel-Mohsen AM, Aly AS, Hrdina R, Montaser AS, Hebeish A (2011) Eco-synthesis of PVA/Chitosan hydrogels for biomedical application. *J Polym Environ* 19(4):1005–1012
- Ahearne M, Yang Y, El Haj AJ, Then KY, Liu K-K (2005) Characterizing the viscoelastic properties of thin hydrogel-based constructs for tissue engineering applications. *J R Soc Interface* 2(5):455–463
- Alexandridis P, Holzwarth JF, Hatton TA (1994) Micellization of poly(ethylene oxide)-poly(propylene oxide)-poly(ethylene oxide) triblock copolymers in aqueous solutions: thermodynamics of copolymer association. *Macromolecules* 27(9):2414–2425
- Bagri LP, Bajpai J, Bajpai AK (2009) Cryogenic designing of biocompatible blends of polyvinyl alcohol and starch with macroporous architecture. *J Macromol Sci Part A: Pure Appl Chem* 46(11):1060–1068
- Bajpai AK, Saini R (2006) Preparation and characterization of novel biocompatible cryogels of poly(vinyl alcohol) and egg-albumin and their water sorption study. *J Mater Sci: Mater Med* 17(1):49–61
- Bani-Jaber A, Kobayashi A, Yamada K, Haj-Ali D, Uchimoto T, Iwao Y, Noguchi S, Itai S (2015) A newly developed lubricant, chitosan laurate, in the manufacture of acetaminophen tablets. *Int J Pharm (Amsterdam Neth)* 483(1–2):49–56
- Bouklas N, Landis CM, Huang R (2015) A nonlinear, transient finite element method for coupled solvent diffusion and large deformation of hydrogels. *J Mech Phys Solids* 79:21–43
- Canillas M, de Lima GG, Rodriguez MA, Nugent MJD, Devine DM (2016) Bioactive composites fabricated by freezing-thawing method for bone regeneration applications. *J Polym Sci Part B: Polym Phys* 54(7):761–773
- Cappello J, Crissman JW, Crissman M, Ferrari FA, Textor G, Wallis O, Whitley JR, Zhou X, Burman D, Aukerman L, Stedronsky ER (1998) In-situ self-assembling protein polymer gel systems for administration, delivery, and release of drugs. *J Control Release* 53(1–3):105–117
- Cerchiara T, Luppi B, Bigucci F, Orienti I, Zecchi V (2002) Physically cross-linked chitosan hydrogels as topical vehicles for hydrophilic drugs. *J Pharm Pharmacol* 54(11):1453–1459

- Chen N-X, Zhang J-H (2010) The role of hydrogen-bonding interaction in poly(vinyl alcohol)/poly(acrylic acid) blending solutions and their films. *Chin J Polym Sci* 28(6):903–911
- Chenite A, Chaput C, Wang D, Combes C, Buschmann MD, Hoemann CD, Leroux JC, Atkinson BL, Binette F, Selmani A (2000) Novel injectable neutral solutions of chitosan form biodegradable gels in situ. *Biomaterials* 21(21):2155–2161
- Choi J, Bodugoz-Senturk H, Kung HJ, Malhi AS, Muratoglu OK (2006) Effects of solvent dehydration on creep resistance of poly(vinyl alcohol) hydrogel. *Biomaterials* 28(5):772–780
- Chun HJ, Lee SB, Nam SY, Ryu SH, Jung SY, Shin SH, Cheong SI, Rhim JW (2005) Preparation and swelling behavior of thermally cross-linked poly(vinyl alcohol) and poly(acrylic acid) hydrogel. *J Ind Eng Chem (Seoul Repub Korea)* 11(4):556–560
- de Jong SJ, De Smedt SC, Wahls MWC, Demeester J, Kettenes-van den Bosch JJ, Hennink WE (2000) Novel self-assembled hydrogels by stereocomplex formation in aqueous solution of enantiomeric lactic acid oligomers grafted to dextran. *Macromolecules* 33(10):3680–3686
- De SK, Aluru NR, Johnson B, Crone WC, Beebe DJ, Moore J (2002) Equilibrium swelling and kinetics of pH-responsive hydrogels: models, experiments, and simulations. *J Microelectromech Syst* 11(5):544–555
- Drexler PG, Tesoro G (1984) *Materials and processes for textile warp sizing*. CRC Press
- Ebara M, Kotsuchibashi Y, Uto K, Aoyagi T, Kim Y-J, Narain R, Idota N, Hoffman JM (2014) *Smart biomaterials*. Springer, p 9
- El Salmawi KM (2007) Application of polyvinyl alcohol (PVA)/carboxymethyl cellulose (CMC) hydrogel produced by conventional crosslinking or by freezing and thawing. *J Macromol Sci Part A Pure Appl Chem* 44(6):619–624
- Funami T, Hiroe M, Noda S, Asai I, Ikeda S, Nishinari K (2007) Influence of molecular structure imaged with atomic force microscopy on the rheological behavior of carrageenan aqueous systems in the presence or absence of cations. *Food Hydrocoll* 21(4):617–629
- Fundueanu G, Nastruzzi C, Carpov A, Desbrieres J, Rinaudo M (1999) Physico-chemical characterization of Ca-alginate microparticles produced with different methods. *Biomaterials* 20(15):1427–1435
- Ginzburg VV, Sammler RL, Huang W, Larson RG (2016) Anisotropic self-assembly and gelation in aqueous methylcellulose-theory and modeling. *J Polym Sci Part B: Polym Phys (Ahead of Print)*
- Goetten de Lima G, Campos L, Junqueira A, Devine DM, Nugent MJD (2015) A novel pH-sensitive ceramic-hydrogel for biomedical applications. *Polym Adv Technol* 26(12):1439–1446
- Gregorova A, Lahti J, Schennach R, Stelze F (2013) Humidity response of Kraft papers determined by dynamic mechanical analysis. *Thermochim Acta* 570:33–40
- Gregorova A, Saha N, Kitano T, Saha P (2015) Hydrothermal effect and mechanical stress properties of carboxymethylcellulose based hydrogel food packaging. *Carbohydr Polym* 117:559–568
- Grundelova L, Gregorova A, Mracek A, Vicha R, Smolka P, Minarik A (2015) Viscoelastic and mechanical properties of hyaluronan films and hydrogels modified by carbodiimide. *Carbohydr Polym* 119:142–148
- Guan Y, Zhang B, Bian J, Peng F, Sun R-C (2014) Nanoreinforced hemicellulose-based hydrogels prepared by freeze-thaw treatment. *Cellulose (Dordrecht Neth)* 21(3):1709–1721
- Gudeman LF, Peppas NA (1995) pH-Sensitive membranes from poly(vinyl alcohol)/poly(acrylic acid) interpenetrating networks. *J Membr Sci* 107(3):239–248
- Gupta D, Tator CH, Shoichet MS (2006) Fast-gelling injectable blend of hyaluronan and methylcellulose for intrathecal, localized delivery to the injured spinal cord. *Biomaterials* 27(11):2370–2379
- Gupta S, Goswami S, Sinha A (2012) A combined effect of freeze-thaw cycles and polymer concentration on the structure and mechanical properties of transparent PVA gels. *Biomed Mater (Bristol UK)* 7(1):015006/015001–015006/015008

- Hago E-E, Li X (2013) Interpenetrating polymer network hydrogels based on gelatin and PVA by biocompatible approaches: synthesis and characterization. *Adv Mater Sci Eng* 328763, 328769 pp
- Hassan CM, Peppas NA (2000a) Structure and applications of Poly(vinyl alcohol) hydrogels produced by conventional crosslinking or by freezing/thawing methods. *Adv Polym Sci* 153 (Biopolymers, PVA Hydrogels Anionic Polymerisation Nanocomposites):37–65
- Hassan CM, Peppas NA (2000b) Structure and morphology of freeze/thawed PVA hydrogels. *Macromolecules* 33(7):2472–2479
- Hassani LN, Hendra F, Bouchemal K (2012) Auto-associative amphiphilic polysaccharides as drug delivery systems. *Drug Discov Today* 17(11–12):608–614
- Hennink WE, Van Nostrum CF (2005) Stereocomplex hydrogels with tunable degradation times. Universiteit Utrecht, Neth. WO2005054318A1, p 30
- Hennink WE, Van Nostrum CF, De Jong SJ (2000) Stereocomplex hydrogels. Universiteit Utrecht, Neth. WO2000048576A1, p 65
- Herrmann WO, Haehnel W (1928) Polymerized vinyl alcohol. Consortium fur elektrochemische Industrie, US1672156
- Hickey AS, Peppas N (1997) Solute diffusion in poly(vinyl alcohol)/poly(acrylic acid) composite membranes prepared by freezing/thawing techniques. *Polymer* 38(24):5931–5936
- Ibrahim SM, El Salmawi KM (2013) Preparation and properties of carboxymethyl cellulose (CMC)/sodium alginate (SA) blends induced by gamma irradiation. *J Polym Environ* 21(2): 520–527
- Jaspers M, Dennison M, Mabesoone MFJ, MacKintosh FC, Rowan AE, Kouwer PHJ (2014) Ultra-responsive soft matter from strain-stiffening hydrogels. *Nat Commun* 5:5808
- Jeong B, Bae YH, Lee DS, Kim SW (1997) Biodegradable block copolymers as injectable drug-delivery systems. *Nature (London)* 388(6645):860–862
- Jeong B, Choi YK, Bae YH, Zentner G, Kim SW (1999) New biodegradable polymers for injectable drug delivery systems. *J Control Release* 62(1–2):109–114
- Jeong B, Bae YH, Kim SW (2000) Drug release from biodegradable injectable thermosensitive hydrogel of PEG-PLGA-PEG triblock copolymers. *J Control Release* 63(1–2):155–163
- Jevne AH, Vegoe BR, Holmblad CM, Cahalan PT (1986) Hydrophilic pressure sensitive biomedical adhesive composition. Medtronic, Inc., USA, p 5 (US4593053A)
- Kamoun EA, Kenawy E-RS, Tamer TM, El-Meligy MA, Mohy Eldin MS (2015) Poly (vinyl alcohol)-alginate physically crosslinked hydrogel membranes for wound dressing applications: characterization and bio-evaluation. *Arabian J Chem* 8(1):38–47
- Kanaya T, Ohkura M, Takeshita H, Kaji K, Furusaka M, Yamaoka H, Wignall GD (1995) Gelation process of poly(vinyl alcohol) as studied by small-angle neutron and light scattering. *Macromolecules* 28(9):3168–3174
- Kanaya T, Takeshita H, Nishikoji Y, Ohkura M, Nishida K, Kaji K (1998) Micro- and mesoscopic structure of poly(vinyl alcohol) gels determined by neutron and light scattering. *Supramol Sci* 5(3–4):215–221
- Kang CE, Poon PC, Tator CH, Shoichet MS (2009) A new paradigm for local and sustained release of therapeutic molecules to the injured spinal cord for neuroprotection and tissue repair. *Tissue Eng Part A* 15(3):595–604
- Khutoryanskiy V, Khutoryanskaya O, Cook JP, Goodall GW (2011) Hydrogel synthesis by crosslinking of hydrophilic polymers. The University of Reading, UK, p 33 (WO2011089432A1)
- Kilan K, Warszynski P (2014) Thickness and permeability of multilayers containing alginate cross-linked by calcium ions. *Electrochim Acta* 144:254–262
- Kovalcik A (2015) Project report for the project: F-AF2-638-0. Hydrogels based on microbially treated lignin. Initial Funding Programm of Graz University of Technology
- Kumeta K, Nagashima I, Matsui S, Mizoguchi K (2003) Crosslinking reaction of poly(vinyl alcohol) with poly(acrylic acid) (PAA) by heat treatment: effect of neutralization of PAA. *J Appl Polym Sci* 90(9):2420–2427

- Lawrie G, Keen I, Drew B, Chandler-Temple A, Rintoul L, Fredericks P, Grondahl L (2007) Interactions between alginate and chitosan biopolymers characterized using FTIR and XPS. *Biomacromol* 8(8):2533–2541
- Li W, Sun B, Wu P (2009) Study on hydrogen bonds of carboxymethyl cellulose sodium film with two-dimensional correlation infrared spectroscopy. *Carbohydr Polym* 78(3):454–461
- Liang H-F, Hong M-H, Ho R-M, Chung C-K, Lin Y-H, Chen C-H, Sung H-W (2004) Novel method using a temperature-sensitive polymer (methylcellulose) to thermally gel aqueous alginate as a pH-sensitive hydrogel. *Biomacromol* 5(5):1917–1925
- Lin H-L, Liu W-H, Liu Y-F, Cheng C-H (2002) Complexation equilibrium constants of poly(vinyl alcohol)-borax dilute aqueous solutions—consideration of electrostatic charge repulsion and free ions charge shielding effect. *J Polym Res* 9(4):233–238
- Liu L-S, Liu S-Q, Ng SY, Froix M, Ohno T, Heller J (1997) Controlled release of interleukin-2 for tumor immunotherapy using alginate/chitosan porous microspheres. *J Control Release* 43(1): 65–74
- Mahanta N, Teow Y, Valiyaveetil S (2013) Viscoelastic hydrogels from poly(vinyl alcohol)-Fe (iii) complex. *Biomater Sci* 1(5):519–527
- Mahdavinia GR, Mousanezhad S, Hosseinzadeh H, Darvishi F, Sabzi M (2016) Magnetic hydrogel beads based on PVA/sodium alginate/laponite RD and studying their BSA adsorption. *Carbohydr Polym* 147:379–391
- Mateescu A, Wang Y, Dostalek J, Jonas U (2012) Thin hydrogel films for optical biosensor applications. *Membranes (Basel Switz)* 2:40–69
- McCrum NG, Read BE, Williams G (1968) Anelastic and dielectric effects in polymeric solids. Wiley, New York
- Mohammed JS, Murphy WL (2009) Bioinspired design of dynamic materials. *Adv Mater (Weinheim Ger)* 21(23):2361–2374
- Montebault A, Viton C, Domard A (2004) Physico-chemical studies of the gelation of chitosan in a hydroalcoholic medium. *Biomaterials* 26(8):933–943
- Mueller SA, Weis C, Odermatt EK, Knaebel H-P, Wente MN (2011) A hydrogel for adhesion prevention: characterization and efficacy study in a rabbit uterus model. *Eur J Obstet Gynecol Reprod Biol* 158(1):67–71
- Nugent MJD, Higginbotham CL (2006) Investigation of the influence of freeze-thaw processing on the properties of polyvinyl alcohol/polyacrylic acid complexes. *J Mater Sci* 41(8):2393–2404
- Nugent MJD, Hanley A, Tomkins PT, Higginbotham CL (2005) Investigation of a novel freeze-thaw process for the production of drug delivery hydrogels. *J Mater Sci: Mater Med* 16 (12):1149–1158
- Ohkura M, Kanaya T, Kaji K (1992) Gelation rates of poly(vinyl alcohol) solution. *Polymer* 33 (23):5044–5048
- Okay O (2015) Self-Healing Hydrogels Formed via Hydrophobic Interactions. *Adv Polym Sci* 268 (Supramolecular Polymer Networks and Gels):101–142
- Oniki T, Ishiguro K (2000) Dentifrices containing polyvinyl alcohol hydrogels. Lion Corp., Japan, p 8 (JP2000159646A)
- Petka WA, Hardin JL, McGrath KP, Wirtz D, Tirrell DA (1998) Reversible hydrogels from self-assembling artificial proteins. *Science (Washington DC)* 281(5375):389–392
- Pezron E, Leibler L, Lafuma F (1989) Complex formation in polymer-ion solutions. 2. Polyelectrolyte effects. *Macromolecules* 22(6):2656–2662
- Popa-Nita S, Alcouffe P, Rochas C, David L, Domard A (2010) Continuum of structural organization from chitosan solutions to derived physical forms. *Biomacromol* 11(1):6–12
- Qiao K, Zheng Y, Guo S, Tan J, Chen X, Li J, Xu D, Wang J (2015) Hydrophilic nanofiber of bacterial cellulose guided the changes in the micro-structure and mechanical properties of nf-BC/PVA composites hydrogels. *Compos Sci Technol* 118:47–54
- Rajagopal K, Ozbas B, Pochan DJ, Schneider JP (2006) Probing the importance of lateral hydrophobic association in self-assembling peptide hydrogelators. *Eur Biophys J* 35(2): 162–169

- Ricciardi R, Gaillet C, Ducouret G, Lafuma F, Laupretre F (2003) Investigation of the relationships between the chain organization and rheological properties of atactic poly(vinyl alcohol) hydrogels. *Polymer* 44(11):3375–3380
- Roy N, Saha N, Humpolicek P, Saha P (2010a) Permeability and biocompatibility of novel medicated hydrogel wound dressings. *Soft Mater* 8(4):338–357
- Roy N, Saha N, Kitano T, Saha P (2010b) Development and characterization of novel medicated hydrogels for wound dressing. *Soft Mater* 8(2):130–148
- Roy N, Saha N, Kitano T, Saha P (2010c) Novel hydrogels of PVP-CMC and their swelling effect on viscoelastic properties. *J Appl Polym Sci* 117(3):1703–1710
- Ruberti JW, Braithwaite GJC (2004) Methods for controlling gel properties, articles, and forming physically crosslinked vinyl polymer gels. Cambridge Polymer Group, Inc., USA, p 26 (US20040092653A1)
- Saha D, Bhattacharya S (2010) Hydrocolloids as thickening and gelling agents in food: a critical review. *J Food Sci Technol* 47(6):587–597
- Saxena A, Tahir A, Kaloti M, Ali J, Bohidar HB (2011) Effect of agar-gelatin compositions on the release of salbutamol tablets. *Int J Pharm Invest* 1(2):93–98
- Schupper N, Rabin Y, Rosenbluh M (2008) Multiple stages in the aging of a physical polymer gel. *Macromolecules* (Washington DC, US) 41(11):3983–3994
- Seiffert S, Sprakel J (2012) Physical chemistry of supramolecular polymer networks. *Chem Soc Rev* 41(2):909–930
- Shoichet MS, Baumann MD, Kang CE (2010) Enhanced stability of inverse thermal gelling composite hydrogels. University of Toronto, Can., p 26 (Cont.-in-part of U.S. Ser. No. 410,831.) (US20100285113A1)
- Spiller KL, Laurencin SJ, Charlton D, Maher SA, Lowman AM (2008) Superporous hydrogels for cartilage repair: evaluation of the morphological and mechanical properties. *Acta Biomater* 4(1):17–25
- Spoljaric S, Salminen A, Luong ND, Seppala J (2014) Stable, self-healing hydrogels from nanofibrillated cellulose, poly(vinyl alcohol) and borax via reversible crosslinking. *Eur Polym J* 56:105–117
- Stauffer SR, Peppas NA (1992) Poly (vinyl alcohol) hydrogels prepared by freezing-thawing cyclic processing. *Polymer* 33(18):3932–3936
- Swamy BY, Yun Y-S (2015) In vitro release of metformin from iron (III) cross-linked alginate-carboxymethyl cellulose hydrogel beads. *Int J Biol Macromol* 77:114–119
- Takahashi N, Kanaya T, Nishida K, Kaji K (2003) Effects of cononsolvency on gelation of poly (vinyl alcohol) in mixed solvents of dimethyl sulfoxide and water. *Polymer* 44(15):4075–4078
- Takeshita H, Kanaya T, Nishida K, Kaji K (1999) Gelation process and phase separation of PVA solutions as studied by a light scattering technique. *Macromolecules* 32(23):7815–7819
- Tsujiyama S-I, Nitta T, Maoka T (2011) Biodegradation of polyvinyl alcohol by *Flammulina velutipes* in an un submerged culture. *J Biosci Bioeng* 112(1):58–62
- Urano T, Ina S (2004) Lime-based coating material compositions containing carrageenan for plastering. Murakashi Lime Industry Co., Ltd., Japan, p 26 (WO2004031098A1)
- Wang H-H, Shyr T-W, Hu M-S (1999) The elastic property of polyvinyl alcohol gel with boric acid as a crosslinking agent. *J Appl Polym Sci* 74(13):3046–3052
- Wang S, Zhang Q, Tan B, Liu L, Shi L (2011) pH-Sensitive poly(Vinyl alcohol)/sodium carboxymethylcellulose hydrogel beads for drug delivery. *J Macromol Sci Part B Phys* 50(12): 2307–2317
- Wang H, Shi Y, Wang L, Yang Z (2013a) Recombinant proteins as cross-linkers for hydrogelations. *Chem Soc Rev* 42(3):891–901
- Wang M-D, Zhai P, Schreyer DJ, Zheng R-S, Sun X-D, Cui F-Z, Chen X-B (2013b) Novel crosslinked alginate/hyaluronic acid hydrogels for nerve tissue engineering. *Front Mater Sci* 7(3):269–284
- Wu X-Y, Huang S-W, Zhang J-T, Zhuo R-X (2004) Preparation and characterization of novel physically cross-linked hydrogels composed of poly(vinyl alcohol) and amine-terminated polyamidoamine dendrimer. *Macromol Biosci* 4(2):71–75

- Xiao C, Gao Y (2008) Preparation and properties of physically crosslinked sodium carboxymethylcellulose/poly(vinyl alcohol) complex hydrogels. *J Appl Polym Sci* 107(3): 1568–1572
- Yadav R, Kandasubramanian B (2013) Egg albumin PVA hybrid membranes for antibacterial application. *Mater Lett* 110:130–133
- Yan C-Q, Pochan DJ (2010) Rheological properties of peptide-based hydrogels for biomedical and other applications. *Chem Soc Rev* 39(9):3528–3540
- Zhang H, Yu L, Ding J (2008) Roles of hydrophilic homopolymers on the hydrophobic-association-induced physical gelling of amphiphilic block copolymers in water. *Macromolecules (Washington DC US)* 41(17):6493–6499
- Zhang H, Xia H, Zhao Y (2012) Poly(vinyl alcohol) hydrogel can autonomously self-heal. *ACS Macro Lett* 1(11):1233–1236
- Zhang Y, Hui B, Ye L (2015) Reactive toughening of polyvinyl alcohol hydrogel and its wastewater treatment performance by immobilization of microorganisms. *RSC Adv* 5(111): 91414–91422
- Zou X, Zheng D, Yu G, Wang H, Yang L, Shan J (2015) Preparation of poly(vinyl alcohol)/calcium alginate hydrogel and the study on mechanical property. *Huagong Xinxing Cailiao* 43(6):118–120, 123

# Chapter 2

## Polymer Gels: Molecular Design and Practical Application



Vicente de Oliveira Sousa Neto, Raimundo Nonato Pereira Teixeira,  
Gilberto Dantas Saraiva and Ronaldo Ferreira do Nascimento

### 1 Introduction

A polymer gel comprises a malleable cross-linked organize and a fluid stuffing the interstitial spaces of the system (Yoshihito and Jian-Ping 1998). The system of long polymer chain holds the it organized and thus gives the gel texture. The gels are wet and moldable and resemble a strong material yet are set up for experiencing considerable distortion.

It is known that polymer typically contains a large amount of solvent (Paul and John 1943). Solvents give them a characteristic softness originated from a liquid nature. Additionally, they can keep up shape like strong materials, unless extra stress is applied. As a result, the mix of flexibility and shape maintenance capacity gives special properties, especially mechanical properties. They demonstrate different qualities and performance; however, they are not quite the same as would be expected solids and fluids. The properties of a polymer gel depend generally on the structure of the polymer arrange that makes up the gel and the interaction of the system and the solvent. The polymeric system's mobility is limited by its crosslink

---

V. de Oliveira Sousa Neto (✉)

Department of Chemistry, State University of Ceará (UECE-FECLESC), Quixadá, Brazil  
e-mail: vicente.neto@uece.br

R. N. P. Teixeira

Department of Biological Chemistry, Regional University of Cariri (URCA), Crato, Brazil

G. D. Saraiva

Department of Physical, State University of Ceará (UECE-FECLESC), Quixadá, Brazil  
e-mail: gilberto.saraiva@uece.be

R. F. do Nascimento (✉)

Department of Analytical Chemistry and Physical-Chemistry, Federal University of Ceara, Ceara, Brazil  
e-mail: ronaldo@ufc.br

**Fig. 1** Chemical gels. The figure shows the chemical cross-linking in the polymeric chain. Printed with permission from Ahn et al. (2008)

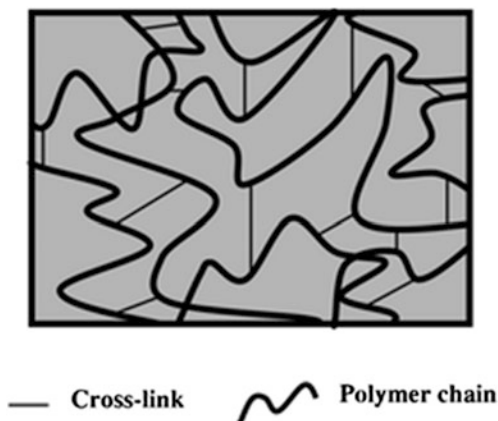
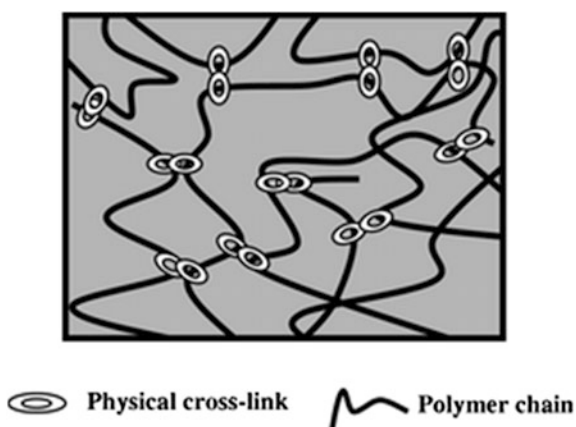


**Fig. 2** Physical gels obtained by non-covalent bonding of polymer chains. Printed with permission from Ahn et al. (2008)



structure. In general, polymer gels are classified as to the nature of their chemical binding, i.e., chemical gels and physical gels (Figs. 1 and 2, respectively). In chemical gels, it is predominantly formed by covalent bonds resulting in a three-dimensional mesh obtained through cross-links between molecularly close groups. Such polymers are readily obtainable by cross-linking, as set out in Fig. 1. Unlike the chemical gels, the physical gels do not involve the formation of chemical bonds but simply involve the growth of physically combined molecular aggregates as set out in Fig. 2 (Ahn et al. 2008). In a physical gel, considering the constitution of each gelation framework, the joints may be hydrogen bonds, crystalline regions, ionic clusters, etc. (Knoben et al. 2007; Li and Aoki 1997; Guenet 2000).



## 2 Thermoresponsive Polymers

Thermoresponsive polymers are compounds whose properties are sensitive to small (or modest) temperature changes. This characteristic stimulated the development of new materials that could be used directly in biological systems involving drugs and their dosage in the region that should act. The expectation is that such compounds may mimic biological behavior up to a certain level. In this way, such materials are potential candidates in the development of a wide variety of applications, such as pharmaceuticals, tissue engineering scaffolds, and gene delivery. As it is vital for the use of these gels to have the ability to control and adapt the gelation temperature and fixation, this was the main focus and purpose of this theme. Accordingly, it is examined in detail how by fluctuating the molar mass, composition, and stereochemistry affect the thermoresponsive properties of these gels are modified. In Fig. 3 are illustrated the thermoresponsive polymers gels synthesis.

Thermoresponsive polymers are characterized as polymers that show an brusque change in their physical properties when temperature is changed. In solution, this irregular change in physical properties appears as a decrease in solubility of the polymer, and with a temperature adjustment, the polymer begins to be distinctly insoluble. Polymers that become clearly hydrophobic while the temperature is raised show a property called lower critical solution temperature (LCST) that can be clearly observed externally, since the polymer solution is clearly turbid (Constantinou and Georgiou 2016). The Fig. 4 shows the illustration of this effect. The base of the curve is related to the LCST. Cloud point (or LCST) is also affected by the molar mass (MM) and the molar mass distribution (MMD, dispersion,  $\bar{D}$ ) of the polymer (Halperin et al. 2015; Bütün et al. 2001; Saeki et al. 1977). Upon specific conditions and typically when the thermoresponsive polymers are blended with other polymers, their watery solutions can shape physical gels while raising the temperature. A physical gel is a three-dimensional (3-D) polymer organize that is

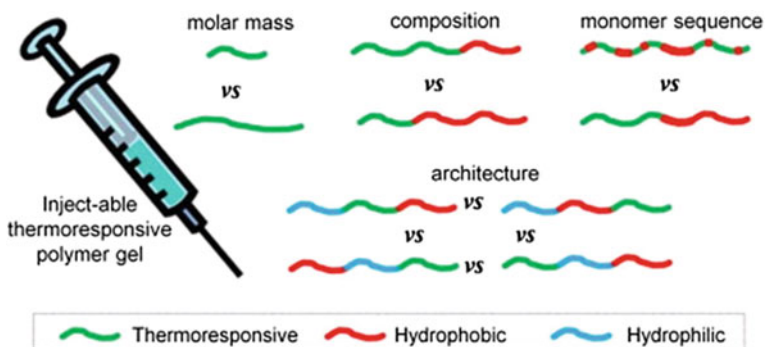


**Fig. 3** Scheme showing thermoresponsive polymers gels synthesis. Printed with permission from Constantinou and Georgiou (2016)

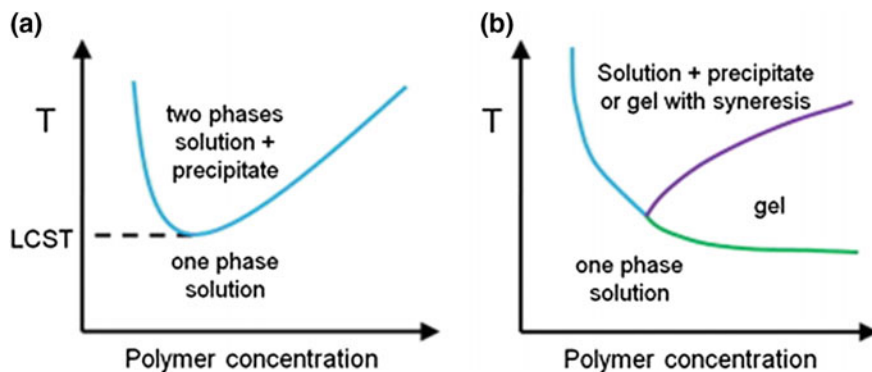


**Fig. 4** Phase diagram, **a** the polymer exhibits LCST point and **b** the polymer form a reversible gel. Printed with permission from Constantinou and Georgiou (2016)

held together through physical tangle, hydrogen bonds, and additionally hydrophobic interactions (Buwalda et al. 2014; Yu and Ding 2008). Physical gels are affected by environmental factors. This polymer gels are known by capacity to form dynamic cross-links that are always build and broken, changing its state between fluid and solid (An et al. 2010). The figure of this watery system-based framework of thermoresponsive gels is set out in Fig. 4b.

## 2.1 UCST and LCST Behavior

Temperature-responsive polymers show a volume phase transition at a specific temperature, which promotes a abrupt modification in the solvation state. The systems which get to be distinctly soluble after warming have an experimental condition called upper critical solution temperature (UCST). It should be emphasized that both the LCST system and the UCST system are not limited to aqueous conditions, but they are limited to conditions that are essential for its application in biomedicine. The modification in the hydration state, which promotes the volume phase transition, suggests the presence of intra- and intermolecular hydrogen bonds competing with each other, where both the intramolecular hydrogen bonds and the intermolecular hydrogen bonds present in the polymer are completely favored compared to a water solubilization (Feil et al. 1993; Vihola et al. 2008; Liu and Urban 2010). The solubility of a polymer in watery medium is reliant on different variables, for example molecular weight, temperature or adding of a co-solvent or additive component. In Fig. 5 is shown a Temperature-responsive graphic is possible identify both UCST and LCST. When polymer/solvent mixture versus temperature is plotted, the phase diagram will show one-phase region (UCST) or two-phase region (LCST). In Fig. 5 is set out this event. It is common to find in scientific literature the terms UCST and LCST. However, most of the time they are

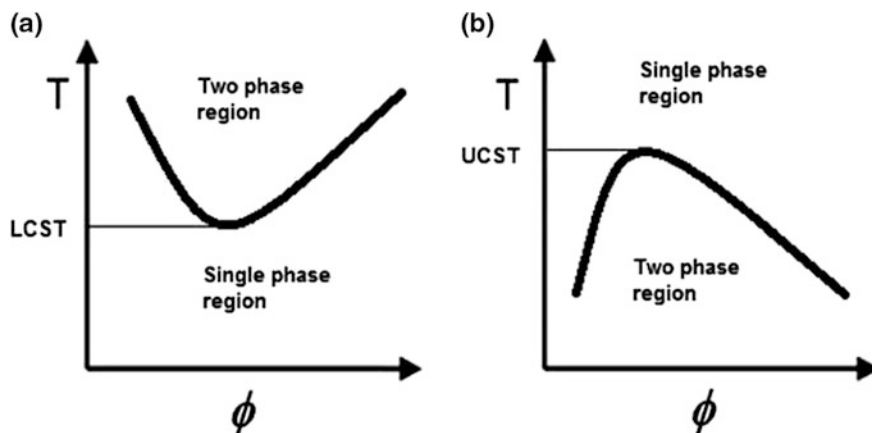


**Fig. 5** Phase diagrams for polymer solution showing, **a** single-phase region and **b** two-phase region. Printed with permission from Gandhi et al. (2015)

used incorrectly; therefore, it must be noticed that they ought to just be utilized, if the phase diagram has been experimentally determined. Then, it is the UCST or the LCST, respectively, of the phase diagram. In general, it is possible to observe any transition from soluble to insoluble or the other way around (at a given focus) ought to be indicated as transition temperature ( $T_{tr}$ ). Be that as it may, only a few polymers are similar to PNIPAM and exhibit a phase transition almost independent of molecular weight or concentration. At that point, the  $T_{tr}$  at any given concentration is practically indistinguishable to the LCST.

## 2.2 Thermoresponsive Polymer Systems

Poly(*N*-alkyl (meth)acrylamide)s are possibly the polymers with thermosensitive properties in which more attention has been given in the development of new technologies (Roy et al. 2013). It is no surprise that, specifically, homopolymers and copolymers of poly(*N*-isopropylacrylamide) (PNIPAM) (L1) have gained so much attention from the scientific community (Dai et al. 2009; Schild 1992; Schmaljohann 2006; Vogt and Sumerlin 2009). The sharp phase transition around 32 °C and the relatively easy ability to fit close to the temperature of the human body make PNIPAM (co)polymers a potential candidate in biomedical applications. These characteristics of work at low temperature favor the incorporation of comonomers or hydro-philic groups into PNIPAM (Schild 1992; Fujishige et al. 1989). However, it is necessary to ponder the use of PNIPAM because it has some objections. Among them, its controversial biocompatibility, phase transition hysteresis, and a significant end group influence on thermal behavior (Wang et al. 1998; Kujawa et al. 2006; Xia et al. 2006).

### 2.2.1 Poly(*N*-alkylacrylamide)s

Currently, the most promised candidate as a thermoresponsive polymer is the PNIPAM, even though the PDEAM polymer belonging to a class of compound that has a nearly identical transition temperature (Schild 1992) depends on the tacticity of the polymer, which is in contrast to the PNIPAM. The PNIPAM is a very interesting material due to the important biocompatibility and the position of the LCST at 32–33 °C, which makes this compound applicable for the controlled release application. The LCST of PNIPAM is well known by the changing upon shifting the hydrophilic and or hydrophobic balance as well as being independent from the molecular weight and the concentration (Fujishige et al. 1989). The aforementioned copolymers were developed and studied for purposes directly applied to the oral administration of calcitonin and insulin. This objective can be achieved because the peptide (or hormone) when immobilized on the polymer beads remains stable as it passes through the stomach. Then, reaching the intestine whose conditions are alkaline, the beads easily disintegrate, allowing the planned release of the drug.

### 2.2.2 Poly(*N*-vinyl caprolactam) [PNVLC]

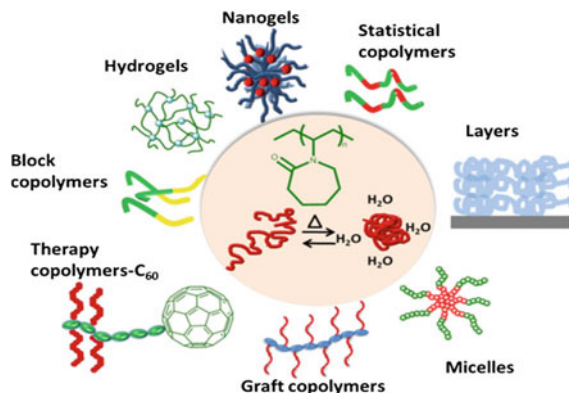
Poly(*N*-vinyl caprolactam) shows good interaction with both organic and water solvents. This property promotes good biocompatibility of this polymer as a result of its large absorption capacity and a transition temperature (in the range of 33 °C) that is within the conditions of its application as biomaterial (Makhaeva et al. 1998). Despite this potential, PNVLC has not been studied as intensively as the PNIPAM. The PNVCL (Fig. 6) has only been synthesized by the free radical polymerization (Cortez-Lemus and Licea-Claverie 2016; Shostakovsky et al. 1952).

The PNVCL is an organo-soluble amphiphilic substance. It is obtained by free radical synthesis which has been performed in different media, as follows: bulk (Solomon et al. 1968) and (Lau and Wu 1999), toluene (Solomon et al. 1968), benzene (Eisele and Burchard 1990; Makhaeva et al. 1998), isopropanol (Kirsh et al. 1999), dimethylsulfoxide (DMSO)/water (Lozinsky et al. 2000), water (Eisele and Burchard 1990).

### 2.2.3 Application

One of the most important applications for the thermally responsive polymers is presented in the field regarding biomedical, since these compounds are widely investigated for their usage in the biomedical applications. The PNVCL is well known for containing an hydrophilic amide group and repeating a unit consisting of a cyclic amide. The nitrogen of the amide group is attached to the backbone of the polymer, thereby composing its hydrophobic region (Fig. 6). Vihola et al. (2005) studied various molecular weights in order to investigate the “in vitro” cytotoxicity

**Fig. 6** PNVCL in various arrangements for different applications. Printed with permission from Cortez-Lemus and Licea-Claverie (2016)



of the PVCL and PVCL grafted with amphiphilic chains containing the PEO segments (PVCL-graft-C11EO42). The putative cytotoxicities of the monomers were compared with those from the corresponding polymers. The tests were conducted at about 23 and 37 °C, below and above the LCST values of above-stated polymers. The study herein shows the cytotoxicity assays of two different cell cultures being carried out. The first was intestinal Caco-2, and the second was the pulmonary Calu-3, which acted as a model epithelia for the oral and pulmonary drug deliveries, respectively. The evaluation of the cytotoxicity of the polymers was done by two methods: The 3-(4,5-Dimethylthiazol-2-yl)-2,5-diphenyltetrazolium bromide (MTT) and the lactate dehydrogenase (LDH) tests that indicated the cell survival and in the damage of cell membranes, respectively. The said tests were performed as a function of the incubation time and polymer concentration. The macromonomer polymer is composed of a hydrophilic PEO chain (42 ethylene oxide units) and a short hydrophobic alkyl chain (11 methylene units), being the reactive methacrylate located in the hydrophobic end of the molecule (Fig. 7). Furthermore, the influence of the chain end functionality on toxicity was also examined. The viability of the MTT and the cellular damage (LDH) of the cells were shown to be dependent on the surface properties of the polymers, hydrophilicity, or the hydrophobicity. According to authors, the concentration, temperature, and incubation time are an important factor that influences directly into the cell damage (Vihola et al. 2005). The chemical structures of the monomers and polymers are presented in Fig. 7.

The procedure preparation of the polymer samples was done with a solution of monomers in the selected solvents (Table 1) that was degassed with nitrogen for 30 min. This particular process leads the isolation by precipitation of the polymer occurring at the end of the polymerization. The PVCL polymers (PVCL-330, PVCL-1300, and PVCL-1500 indicated the molecular weight of the polymers as shown on Table 2) were precipitated in hexane, and PNIPAM was precipitated in diethyl ether. Both polymers were purified further by two reprecipitations. In the case of the PVCL-1500, it was necessary to dry the polymer in vacuum prior to the

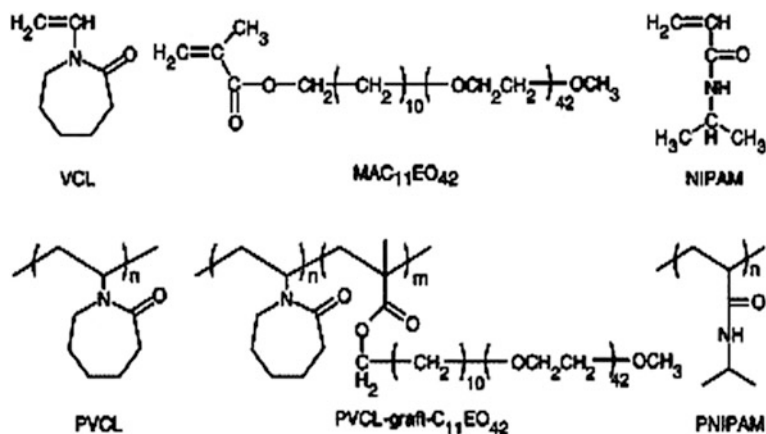


**Fig. 7** Chemical structures of monomers VCL, MAC11EO42, NIPAM, and their respective polymers. Printed with permission from Vihola et al. (2005)

**Table 1** Summary of the reaction conditions during the polymerizations

Sample	Solvent	[VCL] (mol/l)	[NIPAM] (mol/l)	[MAC11EO42] (mmol/l)	[Initiator] (mmol/l)	T (°C)
PVCL-1500	water	1.08	–		7.28 <sup>a</sup>	20
PVCL-1300	Benzene	1.08	–		7.03 <sup>b</sup>	68
PVCL-330	Benzene	1.08	–		2.56 <sup>b</sup>	20
PVCL-graft-C11EO40	Benzene	1.08	–	14.5	2.56 <sup>b</sup>	20
PANIPAM	Dioxane	–	1.47		2.56 <sup>b</sup>	7

<sup>a</sup>Initiator VA-(086)

<sup>b</sup>Initiator AIBN

reprecipitation. It is worthwhile to mention that by the extensive dialysis against water (5 days) and isolation by freeze-drying, all the polymers were purified. The exact reaction conditions of the polymerizations are given on Table 1.

### 2.3 Poly(N-ethyl oxazoline) [PEtOx]

The PEtOx is a polymer interesting to diverse and large range biomedical applications. An example of this is that your blood clearance is much faster than that of PEO poly(ethylene oxide) (Hoogenboom 2009; Adams and Schuber 2007). Hence, a cloud-pointing temperature at about 61–64 °C could be tuned to vary the degree of polymerization, polymer composition, and concentration. This behavior was only exhibited by the PEtOx polymers whose average molar weights were in the range from 20 to 500 kDa (Hoogenboom 2009). It was also observed that PEtOX

**Table 2** A list of some techniques used to monitor morphology and property changes due to photo-irradiation

Technique	Property	References
UV spectroscopy	Isomerization	Han et al. (2010)
Ellipsometry	Variation of average thickness of sample in fair agreement with the calculated geometries of the molecules	Takamatsu et al. (2010)
Surface plasmon resonance spectroscopy	Switching in real time under ambient conditions	Tamada et al. (2003)
Contact angle measurement	Switching wetting of surfaces	Klajn (2010)
Adsorption of molecules/particles from solution	Control of adsorption on surfaces	Klajn (2010)
Atomic force microscopy	Switching in individual molecule	Takamatsu et al. (2010)

polymers as molar weight <10 KDa do not exhibit a cloud point (Hoogenboom et al. 2008; Weber et al. 2009). Polar groups exhibit a strong affinity for an aqueous solvent. Therefore, it is natural that they interact easily with water, facilitating the entire process of solvation. This explains the great water solubility of polyoxazolines as the poly(2-methyl-2-oxazoline) (polyMeOxa) and poly(2-ethyl-2-oxazoline). Unlike polar groups, apolar groups have the ability to interact and be solubilized by organic solvents. The acyl group, in this case, is formed at their greatest by extensive aliphatic chains, aromatic chain, and fluorinated groups. The importance of the nature of the acyl group in polyoxazolines can be better understood when it is possible to easily verify (over a wide temperature range) the increase in the degree of hydrophobicity through the LCST study. Experimental evidence using the phase transition study shows that poly(2-ethyl-2-oxazoline) has a more pronounced hydrophobic behavior than the poly(2-methyl-2-oxazoline) polymer. In fact, the poly(2-ethyl-2-oxazoline)-containing hydrogels have also been suggested as temperature-sensitive biomaterials (Wang and Hsiue 2002).

A transition temperature at about 62 °C was observed for the poly(*N*-ethyl oxazoline)s, which is too high for any drug-delivery application. Recently, a double thermoresponsive system was prepared by graft polymerization of the EtOx into a modified PNIPAM backbone (Rueda et al. 2005), being explored for their potential application in drug delivery.

### 2.3.1 Application

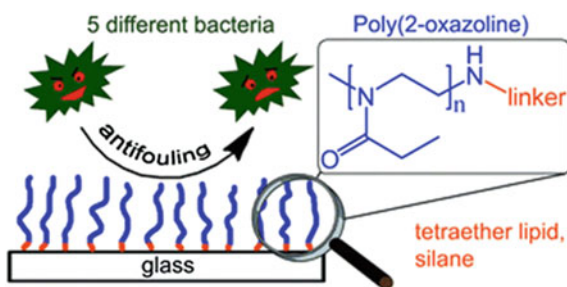
Tauhardt et al. (2014) developed five different PEtOx coatings from poly(2-ethyl-2-oxazoline). All experiment it was studied under “real-life” conditions (set out in Fig. 8). In this work, authors functionalized PEtOx with amine end of different molar weights. The synthesis employed is simple, unprecedented, and

involved two steps. Then, the PEtOx was linked to glass surfaces through a tetraether lipid and a common silane, respectively.

The authors employed  $^1\text{H}$  NMR spectroscopy and MALDI-TOF-MS as well as XPS to characterize both polymers and coatings. According to Tauhardt et al. (2014) when the coatings were exposed to five different bacteria in synthetic medium, it was observed a marked decrease of the bacterial colony (biofilm). The authors mention the fact that Lin et al. (2012) had already proposed the synthesis of an amine end-functionalized poly(2-oxazoline) (POx). They terminated the living oxazolinium species directly with ammonia in acetonitrile. It is necessary to consider that in this work the authors obtained a low degree of functionalization that reached approximately 80%. As an alternative, Park et al. (2004) suggested three-step method in which it promotes the interruption of the reaction mixture employing a solution of NaOH. The hydroxyl end group obtained in this step was reacted with phthalimide in medium containing both triphenylphosphine ( $\text{PPh}_3$ ) and diethyl azodicarboxylate to yield POx with a phthalimide end group. In a final step, by treatment with hydrazine monohydrate, the amine end group was produced. However, this procedure has a poor yield. It was obtained only to an amine end group functionalization efficiency of 62%. A problem that frequently affects the yield of the reaction is associated with possible secondary reactions leading to the formation of ester end groups rather than hydroxyl end groups when the reaction is terminated (Baumgaertel et al. 2010, 2011; Kobayashi et al. 1989). If there are ethers by secondary reaction, they need to be hydrolyzed to hydroxyl groups before the polymer can be finally functionalized. To overcome the drawbacks of these methods, a new synthesis route to synthesize amine end-functionalized PEtOx was developed (Fig. 9). In this new procedure, an excess of potassium phthalimide is directly added to the living cationic species. In this way, it is easily eliminated. This simple modification suppressed a step of the method originally proposed by Park et al. (2004).

In the same work, Tauhardt et al. (2014) related that to prove the suitability of the attachment methods and to investigate the stability of the obtained PEtOx layers against different types of stress, a fluorescein-labeled PEtOx (Fluo-PEtOx, 5) was used.

**Fig. 8** Antifouling on glass.  
Printed with permission from  
Tauhardt et al. (2014)





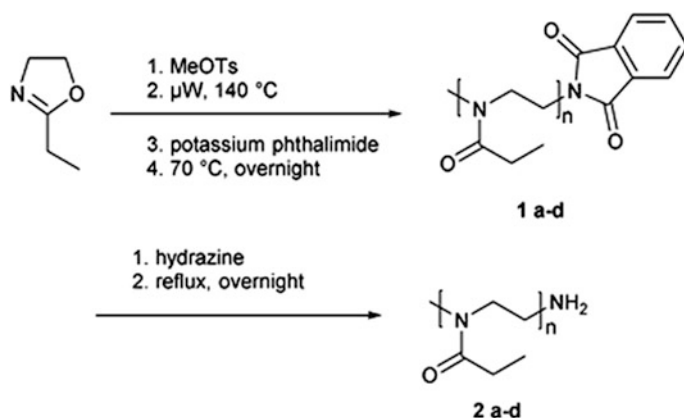


**Fig. 9** Synthetic route proposed to obtain amine end-functionalized PEtOx. Printed with permission from Tauhardt et al. (2014)

In this way, by opting to synthesize a copolymer with polymerization degree (DP) of 40 (P (EtOx<sub>36</sub>-stat-AmOx<sub>4</sub>)) and with an amine monomer content of 10%, substance (4) was synthesized by copolymerization of EtOx and a tert-butyloxycarbonyl (Boc)-protected amine group containing 2-oxazoline followed by deprotection (Fig. 10) (Hartlieb et al. 2013). In the subsequent step, an amino group was tagged employing a fluorescein-NHS ester derivative. It is not surprising that the reaction of this activated acid with amine groups is extremely efficient in basic medium. Therefore, triethylamine (TEA) was used as the base. Repeated precipitations in diethyl ether were used in the purification in order to remove traces of unreacted fluorescein.

Tauhardt et al. (2014) also studied the potential use of them for prevention of bioadhesion, the PEtOx polymers (2a–d) were immobilized on borofloat<sup>®</sup> 33 glass employing either (1) a silane-based linker or (2) a TEL linker (Fig. 11). In the case where the coupling occurs through a silane-based binder, the glass slides were initially treated with (3-glycidyloxypropyl) trimethoxysilane (GOPTMS). Then, PEtOx was prepared from different molar masses and linked by reaction of the epoxide unit of GOPTMS with the end group of the polymer (Fig. 11a route 1). For the coupling by means of a TEL linker (Fig. 11b), the hydroxyl end groups of the lipid were altered with cyanuric chloride to allow the covalent coupling to the glass surfaces and in addition the covalent binding of PEtOx on top of the lipid layer (Fig. 11a route 2). The TEL-functionalized glass slides were covered with PEtOx with an indistinguishable molar masses from for route 1. The TEL-functionalized glass slides were coated with PEtOx with the same molar masses as for route 1.

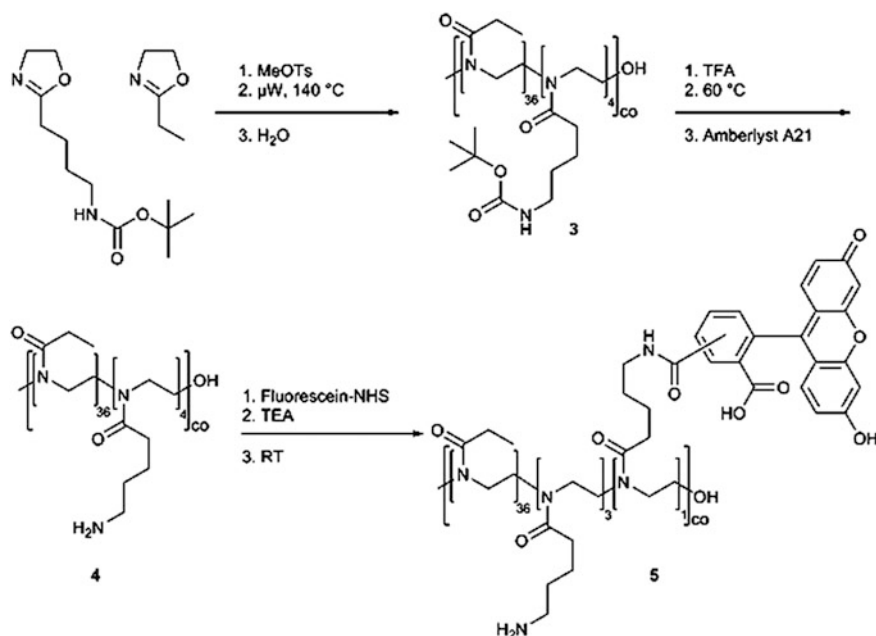


**Fig. 10** Synthetic route to obtain POX containing amine and labeling of the polymer with fluorescein. Printed with permission from Tauhardt et al. (2014)

### 3 Smart Polymer Gels

Another idea broadly utilized as a part of materials science involves the concept of smart polymeric gels. They belong to a new technological era of biomaterials that are presently being created at an intense productive pace for use in a large range of application including templates for nanoscale and other biomedical devices, scaffolds for tissue engineered prostheses, and biosensors and actuators.

#### 3.1 Some Types of Smart Polymers

**pH-sensitive smart polymers**—They are polymeric species that can be proton acceptor (or donor) depending on pH variation. This ability is associated with the structure of these materials. Their structure contains acid groups such as carboxylic or sulphonic groups, while the basic groups generally are amine salts (You et al. 2010a). This kind of smart polymer is polyelectrolytes that have in their structure acid or basic groups that can accept or release protons in response to pH changes in the surrounding environment. The human body is very sensitive to changes in pH. Thus, the system has the ability to strictly control this parameter. Changes in pH

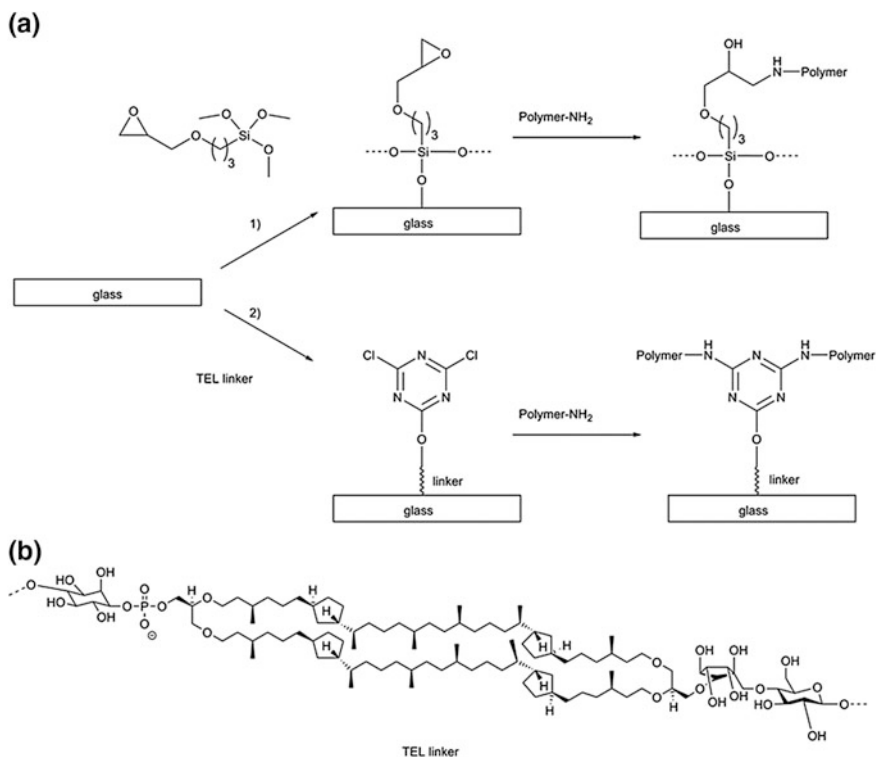


**Fig. 11** **a** Schematic representation of the PETox coating process using GOPTMS (route 1) and a TEL (route 2) linker, respectively, and **b** of the TEL linker structure. Printed with permission from Tauhardt et al. (2014)

made in an appropriate manner and respecting the conditions of the human body may allow the use of therapeutic agents in a targeted manner to areas of the human body such as tissues, organs, cell compartment, and other well-defined areas of the body. Such conditions allow the use of the so-called pH-sensitive polymers. They are ideal pharmaceutical systems to the specific delivery of therapeutic agents. Chitosan is an interesting natural polymer. It is a polycationic biopolymer soluble in acidic solution and undergoes phase separation at a pH range close to neutrality through deprotonation of the primary amino group by inorganic ions. The gelation mechanism of chitosan occurs through the following interactions which involve electrostatic attraction between the ammonium group of the chitosan and an inorganic ion, hydrogen bonding between the chitosan chains, and chitosan–chitosan hydrophobic interactions. However, the formed gel is in further need of cross linking agents to produce a gel with sufficient mechanical stability and to release the low molecular weight drug in a controlled manner. Several studies reported that the structural strength of chitosan depends on the porosity of the chitosan gel which in turn is a function of the crystallinity of the polymer. The structural strength of the

polymer can be improved either by blending with the polymers or by hydrophobic modification of the polymer. One example includes the cross-linking of chitosan—polyvinylpyrrolidone with glutaraldehyde to form a semi-interpenetrating polymeric network that gells in situ at physiological pH. Su et al (2016) has produced smart polymers from chitosan. According to the authors, it is possible to highlight their potential use as oral drug delivery systems, such as antibacterial and mucoadhesive properties. Su and co-workers developed a pH-sensitive nanocarrier whose pH determined the release rate of drug amoxicillin. These results showed that at pH 2.5 (fasted state), the drug amoxicillin is released slowly and continuously in the gastric juice. However, the release of the same drug into the gastric mucosa, infected with *Helicobacter pylori* (pH between 5.0 and 7.0) is rapid. Both Lu et al. (2014) and Jheng et al. (2015) showed that CS-N-Arg conjugate has a potential to be applied in medical procedure. This cationic polymer could be used for delivery of protein and a near-infrared fluorescence imaging dye. Furthermore, positively charged, CS-based NPs can interact with the cell wall of *H. pylori*, and then target the site of *H. pylori* infection (Lin et al. 2013). The effects of electric field (electrostatic interaction) between  $\gamma$ -PGA-g-Arg polypeptide and CS-N-Arg conjugate promote additional stability of the self-assembled nanoparticles to a higher pH (pH > 6.0). In this work, antimicrobial activity of amoxicillin-loaded nanoparticles prepared from  $\gamma$ -PGA-g-Arg polypeptide and CS-N-Arg was evaluated. The pH-triggered disassembly of the colloidal nanoparticles and their corresponding amoxicillin releases from the nanocarriers are shown in Fig. 12.

According to the authors, the development of  $\gamma$ -PGA-g-Arg nanoparticles contributed to the oral administration of amoxicillin dosages at controlled pH. In addition, it was found that at a pH lower than 3.5, there was a reversible reversal of the CS-N-Arg/ $\gamma$ -PGA-g-Arg complex. At this pH, there would therefore be a better control on drug release, i.e., a decrease in this release. However, when the pH is raised to 7.0, an increase in drug release occurs. It was therefore realized that the drug-bearing nanoparticles could contribute intelligently to the administration of the antibiotic for the eradication of *H. pylori*. According to the authors, the development of  $\gamma$ -PGA-g-Arg nanoparticles contributed to the oral administration of amoxicillin dosages at controlled pH. In addition, it was found that at a pH lower than 3.5, this polymer could self-assemble into nanoparticles, and reversibly disassemble as the pH was increased to higher than 3.5. At this pH, there would therefore be a better control on drug release, i.e., a decrease in this release. However, when the pH is raised to 7.0 an increase in drug release occurs. It was therefore realized that the drug-bearing nanoparticles could contribute intelligently to the administration of the antibiotic for the eradication of *H. pylori*.

### 3.1.1 Light-Sensitive Smart Polymers

Light is a clean stimulus that allows remote control without physical contact. It becomes attractive because it interacts easily with molecules modifying their geometry and consequently also affecting their dipole. This interaction of the light

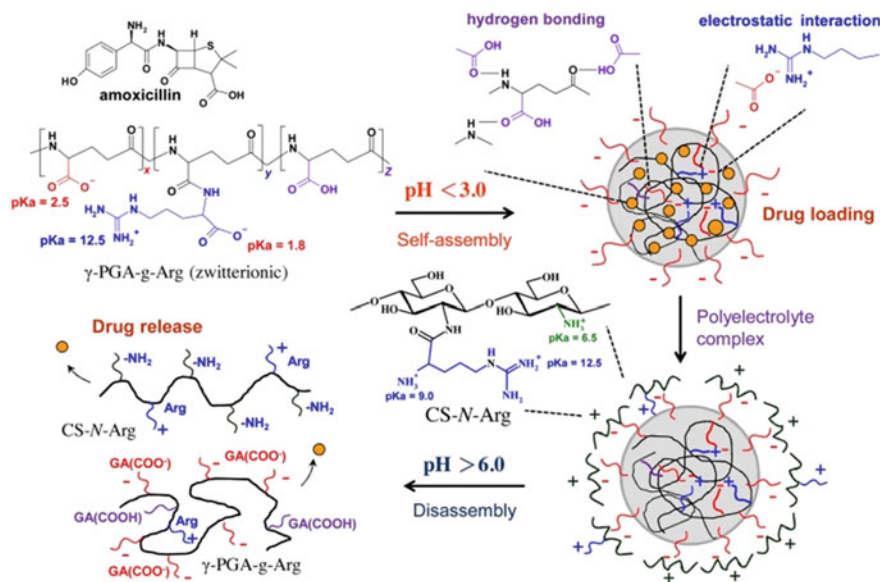


**Fig. 12** Diagram of assembly and disassembly of self-assembled  $\gamma$ -PGA-g-Arg nanoparticles and CS-N-Arg/ $\gamma$ -PGA-g-Arg complex nanoparticles. Printed with permission from Su et al. (2016)

photon with the molecule causes significant macroscopic variations of molecularly organized structures, resulting in minor perturbations. These changes can affect the final properties, such as wettability, permeability, load, color, bonding, among others. A fine-tuning of these can be done through a series of sophisticated techniques listed on Table 2.

Polymers which are sensitive to visible light are called as light-sensitive polymers. The major advantages of light-sensitive polymers are that they are water soluble, biocompatible, and biodegradable. Another one is their capacity for instantaneous delivery of the sol–gel stimulus, making light-responsive polymers important for various engineering and biomedical applications. For example, photodynamic therapy (Arguinzoniz et al. 2014; Lim et al. 2013) is widely studied and used for treatment of especially skin cancer and consists in an application of photosensitizer followed by laser irradiation of tumor lesion. Another potential medical application may be laser-triggered drug release from photoresponsive delivery system in the target tissue. For polymers, light responsivity may be achieved (Jochum and Theato 2013; Liu et al. 2013; Shibu et al. 2013), with photochemical reaction or photoinduced conformational change. The photochemical reaction includes spiropyran isomerization leading to polarity change (Son et al. 2014; Wang et al. 2014), cross-linking by photocyclodimerization of cinnamic acid derivatives (Matsusaki et al. 2001) or of thymine (Kuang et al. 2013), photohydrolysis of 2-nitrobenzyl ethers and esters (Jiang et al. 2006) and coumarin-based (Kumar et al. 2012), esters and ethers or 2-diazo-1,2-naphthoquinone moieties

(Chen et al. 2011; Yu et al. 2009). The photoinduced conformational changes include, e.g., a synthetic case—the cis–trans photoisomerization of azobenzene (Feng et al. 2014; Tang et al. 2010), and a natural case—the photoinduced cis–trans isomerization of 11-cis-retinal, the principle of vision in eye retina (Palczewski 2012).

### 3.1.2 Application

The investigation on temperature- and light-responsive copolymer systems has inspired also the work of Jochum and Theato (2009). In this paper was reported the synthesis of several copolymers based on the PNIPAM, poly(*N*-cyclopropylacrylamide) (Maeda et al. 2001), poly(*N*-ethyl-*N*-methylacrylamide) (Plate et al. 1999) and poly(*N,N*-dimethylacrylamide) (El-Ejmi and Huglin 1996) each with various amounts of azobenzene moieties incorporated. The aim of their study was to investigate the different thermoresponsive polyacrylamide systems with regard to the ability to photo-control the LCST by the attachment of azobenzene. As a synthetic tool, activated ester polymers were utilized as polymeric precursors that were synthesized in a defined molecular weight by RAFT-polymerization. The temperature- and light-responsive copolymers were then obtained via a polymer-analogous reaction of the polymeric precursor with functional amines (see Fig. 13).

**Limitation:** Limitations of light-sensitive polymers include inconsistent response due to the leaching of non-covalently bound chromophores during swelling or contraction of the system and a slow response of hydrogel toward the stimulus. Dark toxicity is also one of the drawbacks of light-responsive polymeric systems. These polymers can be classified into UV-sensitive and visible-sensitive systems on the basis of the wavelength of light that triggers the phase transition. Visible light-sensitive polymers are comparatively preferred over UV-sensitive polymers

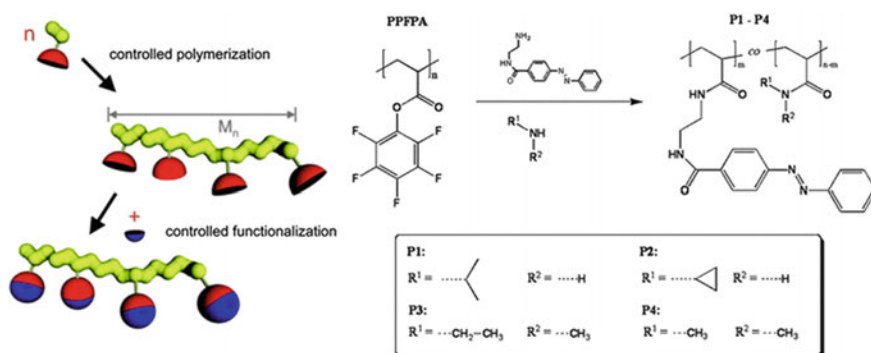


**Fig. 13** Synthetic concept (left illustration) of a polymer-analogous reaction of activated ester polymers to synthesize well-defined polymers. Printed with permission from Theato (2008)

because of their availability, safety, and ease of use (Qiu and Park 2001; You et al. 2010b).

### 3.1.3 Glucose-Sensitive Polymer Gel

In the scientific community, glucose-sensitive polymer gel is recognized as an ideal system for controlled administration of drugs. Its self-regulating function allows it to reach specific targets (Qiu and Park 2012).

In theory, it would be possible to build a “smart sensor” inside this material. Once these sensors were installed, they would be able to detect, measure, and collect the stimuli caused by the change of diabetics’ glycemic concentration. It would also be able to activate the 3D structure of the hydrogel’s cross-linked network to control drug release at predetermined rates and predefined time. In addition, this kind of hydrogels also plays a key role to separate the drug from ambient hostile medium before its release (Siegel 2014).

**Limitation:** their application has been limited largely due to some inherent drawbacks such as poor mechanical conformability, unfavorable biocompatibility, and low-controlled drug-release ability (Podual et al. 2000).

#### Application

Xiao et al. (2016) have developed a glucose-sensitive chitosan–polyethylene oxide (CS–PEO) hydrogel with controlled release of metronidazole (MNZ)—a highly effective antibiotic to treat periodontitis (EI-Kamel et al. 2007). According to authors, chitosan (CS) was employed because it is an extremely versatile biopolymer that exhibits good biocompatibility and recognized antibacterial properties (Bhattarai et al. 2010; Anitha et al. 2014). The PEO was also employed because of its biocompatibility and to be able to improve both the mechanical properties and the biological properties of the hydrogel composites (Feng et al. 2015). In this study, the hydrogel was tested for its physicochemical and mechanical properties, biocompatibility, drug-release ability in response to different glucose concentrations (GC) and antibacterial activity against *Porphyromonas gingivalis* (*P. gingivalis*), which is regarded as one of the major bacteria to be associated with human periodontitis. In Fig. 14 is shown the mechanism of chitosan–PEO hydrogel’s glucose sensitivity. Below is the procedure adopted by the authors to prepare CS–PEO films.

**Preparation of CS–PEO film:** Prewighted CS was dissolved in 0.5 M acetic acid aqueous solution to prepare 1.5% weight/volume (w/v) CS solution. After 2 h stirring, PEO was added to form the blend with predetermined weight ratio (CS/PEO = 1:0.5–1:2.5). Then, the mixture was stirred constantly until these two components completely dissolved and formed homogeneous solution. After that,

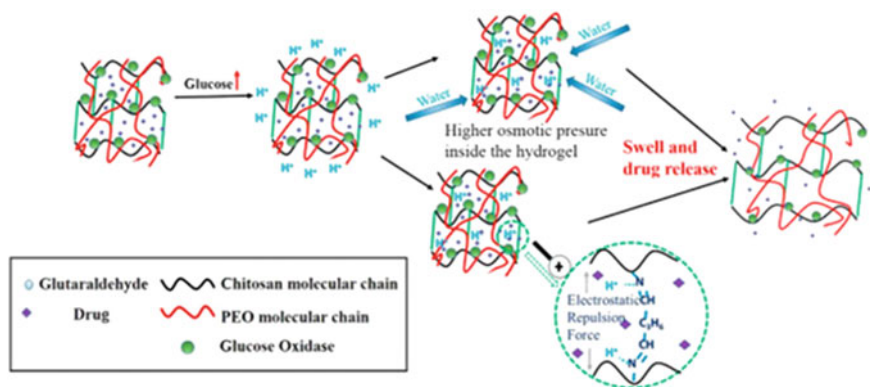


**Fig. 14** Mechanism of chitosan-PEO hydrogel's glucose sensitivity and controlled drug-release process. Printed with permission from Xio et al. (2016)

the solution was poured onto glass surface and dried in vacuum oven at 60 °C. The CS-PEO films with thickness of 0.8–1.0 mm were obtained after 24 h drying.

**Preparation of cross-linked CS-PEO hydrogel film:** The preparation of cross-linked CS-PEO hydrogel film was carried out similarly as described above. The only difference was that after obtaining the homogeneous CS-PEO blend, a certain amount of cross-linking agent (GA) was slowly dripped into this solution under constant stirring. Then, the solution was transferred onto a glass surface to form the CS-PEO hydrogel at room temperature. The resulting product was obtained by putting the hydrogel into the vacuum oven at 60 °C overnight.

**Preparation of glucose-sensitive CS-PEO hydrogel loaded with MNZ:** First, the CS-PEO blend was obtained using the method already mentioned above. Then, 0.5% (w/v) MNZ was added into this solution. After the drug was completely dissolved, cross-linking agent GA (0.5–2.5%, v/v) was slowly added into this mixture under constant stirring. Next, the solution was poured into a homemade cylinder mode (diameter: 25 mm, height: 20 mm) to form the hydrogel at room temperature. The hydrogel was washed three times with deionized water to remove extra GA and acetic acid. Finally, the samples were immersed in GOx solution (phosphate buffer pH = 5) for 24 h and kept at -40 °C (Susanto et al. 2013).

According to Xiao et al. (2016), the results suggest that this kind of composite hydrogel possessed better mechanical properties and biocompatibility than “single-component” CS hydrogel. Meanwhile, it can self-regulate the metronidazole release according to the ambient glucose stimulus, thus achieving optimal antibacterial activity (*P. gingivalis* as subject) at high glucose concentration. According to the authors, hydrogels are not only a simple controlled drug release system, but also a potential scaffold to repair and regenerate periodontal tissues.



## 4 Considerations

Concurrent developments in design of new responsive polymers along with structure–property evaluation, fabrication of materials, and modeling of materials are vital for the applications of polymer gels. Polymer gels are important for biotechnological applications of shape-memory including modulated drug-release studies, biosensors, diagnostics, tissue regeneration/wound healing, cell-encapsulation membranes, and hybrid organ development. Major considerations for the usage of these materials include biocompatibility, biodegradability, mechanical strength, response time under physiological conditions, and good correlation between *in vitro* and *in vivo* studies.

In this chapter, it was commented about polymer gels in terms of thermoresponsive polymer systems, design and properties. The studies shown in this chapter depended on the preparation. In particular, many basic properties have been revealed about smart polymer as pH sensitive, light sensitive, and glucose sensitive.

## References

- Adams N, Schuber US (2007) Poly(2-oxazolines) in biological and biomedical application contexts. *Adv Drug Deliv Rev* 59:1504–1520
- Ahn SK, Kasi RM, Kim S-C, Sharma N, Zhou Y (2008) Stimuli-responsive polymer gels. *Soft Matter* 4:1151–1157
- An Y, Solis FJ, Jiang H (2010) A thermodynamic model of physical gels. *J Mech Phys Solids* 58:2083–2099
- Anitha A, Sowmya S, Sudheesh Kumar PT, Deepthi S, Chennazhi KP, Ehrlich H, Tsurkan M, Jayakumar R (2014) Chitin and chitosan in selected biomedical application. *Prog Polym Sci* 39 (9):1644–1667
- Arguinoniz AG, Ruggiero E, Habtemariam A, Hernandez-Gil J, Salassa L, Mareque-Rivas JC (2014) Light harvesting and photoemission by nanoparticles for photodynamic therapy. *Part Part Syst Charact* 31(1):46–75
- Baumgaertel A, Altuntaş E, Kempe K, Crecelius A, Schubert US (2010) Characterization of different poly (2-oxazoline) block copolymers by MALDI-TOF MS/MS and ESI-Q-TOF MS/MS. *J Polym Sci Part A: Polym Chem* 48:5533–5540
- Baumgaertel A, Weber C, Fritz N, Festag G, Altuntaş E, Kempe K, Hoogenboom R, Schubert U S (2011) Characterization of poly (2-oxazoline) homo- and copolymers by liquid chromatography at critical conditions. *J Chromatogr A* 1218:8370–8378
- Bhattarai N, Gunn J, Zhang MQ (2010) Chitosan-based hydrogels for controlled localized drug delivery. *Adv Drug Deliv Rev* 62:83–99
- Bütün V, Armes SP, Billingham NC (2001) Synthesis and aqueous solution properties of near-monodisperse tertiary amine methacrylate homopolymers and diblock copolymers. *Polymer* 42:5993–6008
- Buwalda SJ, Boere KWM, Dijkstra PJD, Feijen J, Vermonden T, Hennink WE (2014) Hydrogels in a historical perspective: from simple networks to smart materials. *J Control Release* 190:254–273
- Chen CJ, Liu GY, Liu XS, Pang SP, Zhu CS, Lv LP et al (2011) Photo-responsive, biocompatible polymeric micelles self-assembled from hyperbranched polyphosphate-based polymers. *Polym Chem* 2(6):1389–1397

- Constantinou AP, Georgiou TK (2016) Tuning the gelation of thermoresponsive gels. *Eur Polymer J* 78:366–375
- Cortez-Lemus NA, Licea-Claverie A (2016) Poly(N-vinylcaprolactam), a comprehensive review on a thermoresponsive polymer becoming popular. *Prog Polym Sci* 53:1–51
- Dai S, Ravi P, Tam KC (2009) Thermo- and photo-responsive polymeric systems. *Soft Matter* 5:2513–2533
- EI-Kamel AH, Ashri LY, Alsarra LA (2007) Micromatrical metronidazole benzoate film as a local mucoadhesive delivery system for treatment of periodontal diseases. *AAPS PharmSciTech* 8 (3):184–194
- Eisele M, Burchard W (1990) Hydrophobic water-soluble polymers, 1. Dilute solution properties of poly(1-vinyl-2-piperidone) and poly(N-vinylcaprolactam). *Makromol Chem* 191:169–184
- El-Ejmi AAS, Huglin MB (1996) Characterization of N, N-dimethylacrylamide/2-methoxyethylacrylate copolymers and phase behaviour of their thermotropic aqueous solutions. *Polym Int* 39:113–119
- Feil H, Bae YH, Feijen J et al (1993) Effect of comonomer hydrophilicity and ionization on the lower critical solution temperature of N-isopropylacrylamide copolymers. *Macromolecules* 26:2496–2500
- Feng N, Han GX, Dong J, Wu H, Zheng YD, Wang GJ (2014) Nanoparticle assembly of a photo- and pH-responsive random azobenzene copolymer. *J Colloid Interface Sci* 421:15–21
- Feng M, Tian Y, Chang SY, Xu DQ, Shi HJ (2015) Polyethylene-oxide improves microcirculatory blood flow in a murine hemorrhagic shock model. *Int J Clin Exp Med* 8(4):5931–5936
- Fujishige S, Kubota K, Ando I (1989) Phase transition of aqueous solutions of poly(N-isopropylacrylamide) and poly(N-isopropylmethacrylamide). *J Phys Chem* 93:3311–3313
- Gandhi A, Paul A, Sen Q, Sen KK (2015) Studies on thermoresponsive polymers: phase behaviour, drug delivery and biomedical applications. *Asian J Pharm Sci* 10:99–107
- Guenet JM (2000) Structure versus rheological properties in fibrillar thermoreversible gels from polymers and biopolymers. *J Rheol* 44:947–960
- Halperin A, Kröger M, Winnik FM (2015) Poly(N-isopropylacrylamide) phase diagrams: fifty years of research. *Angew Chem Int Ed* 54:15342–15367
- Han M, Ishikawa D, Honda T, Ito E, Hara M (2010) Light-driven molecular switches in azobenzene self-assembled monolayers: effect of molecular structure on reversible photoisomerization and stable cis state. *Chem Commun* 46:3598–3600
- Hartlieb M, Pretzel D, Kempe K, Fritzsche C, Paulus RM, Gottschaldt M, Schubert US (2013) Cationic poly(2-oxazoline) hydrogels for reversible DNA binding. *Soft Matter* 9:4693–4704
- Hoogenboom R (2009) Poly(2-oxazoline)s: a polymer class with numerous potential applications. *Angew Chem Int Ed* 48:7978–7994
- Hoogenboom R, Thijs HML, Jochems MJHC, van Lankvelt BM, Fijten MWM, Schuber US (2008) Tuning the LCST of poly(2-oxazolines) by varying composition and molecular weight: alternatives to poly(N-isopropylacrylamide). *Chem Commun* 5758–5760
- Jheng PR, Lu KY, Yu SH, Mi FL (2015) Free DOX and chitosan-N-arginine conjugate stabilized indocyanine green nanoparticles for combined chemophotothermal therapy. *Colloids Surf B: Biointerfaces* 136:402–412
- Jiang JQ, Tong X, Morris D, Zhao Y (2006) Toward photocontrolled release using light-dissociable block copolymer micelles. *Macromolecules* 39(13):4633–4640
- Jochum FD, Theato P (2009) Temperature and light sensitive copolymers containing azobenzene moieties prepared via a polymer analogous reaction. *Polymer* 50:3079–3085
- Jochum FD, Theato P (2013) Temperature- and light-responsive smart polymer materials. *Chem Soc Rev* 42(17):7468–7483
- Kirsh YE, Yanul NA, Kalninh KK (1999) Structural transformation of water associate interactions in poly-N-vinylcaprolactam-water system. *Eur Polym J* 35:305–316
- Klajn R (2010) Immobilized azobenzenes for the construction of photoresponsive materials. *Pure Appl Chem* 82:2247–2279

- Knoben W, Besseling NAM, Stuart MAC (2007) Rheology of a reversible supramolecular polymer studied by comparison of the effects of temperature and chain stoppers. *J Chem Phys* 126:024907
- Kobayashi S, Masuda E, Shoda S, Shimano Y (1989) Synthesis of acryl- and methacryl-type macromonomers and telechelics by utilizing living polymerization of 2-oxazolines. *Macromolecules* 22:2878–2884
- Kuang HH, He HY, Hou J, Xie ZG, Jing XB, Huang YB (2013) Thymine modified amphiphilic biodegradable copolymers for photo-cross-linked micelles as stable drug carriers. *Macromol Biosci* 13(11):1593–1600
- Kujawa P, Segui F, Shaban S, Diab C, Okada Y, Tanaka F, Winnik FM (2006) Impact of end-group association and main-chain hydration on the thermosensitive properties of hydrophobically modified telechelic poly(N-isopropylacrylamides) in water. *Macromolecules* 39:341–348
- Kumar S, Allard JF, Morris D, Dory YL, Lepage M, Zhao Y (2012) Near-infrared light sensitive polypeptide block copolymer micelles for drug delivery. *J Mater Chem* 22(15):7252–7257
- Lau ACW, Wu C (1999) Thermally sensitive and biocompatible poly(N-vinylcaprolactam): synthesis and characterization of high molar mass linear chains. *Macromolecules* 32:581–584
- Li L, Aoki Y (1997) Rheological images of poly(vinyl chloride) Gels. 1. The dependence of Sol–Gel transition on concentration. *Macromolecules* 30:7835–7841
- Lim CK, Heo J, Shin S, Jeong K, Seo YH, Jang HD (2013) Nanophotosensitizers toward advanced photodynamic therapy of cancer. *Cancer Lett* 334(2):176–187
- Lin CP, Sung YC, Hsiue GH (2012) Non-viral pH-sensitive gene carriers based on poly((2-ethyl-2-oxazoline)-co-ethylenimine)-block-Poly(2-ethyl -2-oxazoline): a study of gene release behavior. *J Med Biol Eng* 32:365–372
- Lin YH, Tsai SC, Lai CH, Lee CH, He ZS, Tseng GC (2013) Genipin-cross-linked fucose-chitosan/heparin nanoparticles for the eradication of *Helicobacter pylori*. *Biomaterials* 34:4466–4479
- Liu F, Urban MW (2010) Recent advances and challenges in designing stimuli-responsive polymers. *Prog Polym Sci* 35:3–23
- Liu G, Liu W, Dong CM (2013) UV- and NIR-responsive polymeric nanomedicines for on-demand drug delivery. *Polym Chem* 4(12):3431–3443
- Lozinsky VI, Simenel IA, Kurskaya EA, Kulakova VK, Galaev IY, Mattiasson B, Grinberg VY, Gimberg NV, Khokhlov AR (2000) Synthesis of N-vinylcaprolactam polymers in water containing media. *Polymer* 41:6507–6518
- Lu KY, Lin CW, Hsu CH, Ho YC, Chuang EY, Sung HW, Mi FL (2014) FRET-based dual-emission and pH-responsive nanocarriers for enhanced delivery of protein across intestinal epithelial cell barrier. *ACS Appl Mater Interfaces* 6:18275–18289
- Maeda Y, Nakamura T, Ikeda I (2001) Changes in the hydration states of poly(N-alkylacrylamide)s during their phase transitions in water observed by FTIR spectroscopy. *Macromolecules* 34:1391–1399
- Makhaeva EE, Tenhu H, Khokhlov AR (1998) Conformational changes of poly(N-vinylcaprolactam) macromolecules and their complexes with ionic surfactants in aqueous solution. *Macromolecules* 31:6112–6118
- Matsusaki M, Kishida A, Stainton N, Ansell CWG, Akashi M (2001) Synthesis and characterization of novel biodegradable polymers composed of hydroxycinnamic acid and D, L-lactic acid. *J Appl Polym Sci* 82(10):2357–2364
- Palczewski K (2012) Chemistry and biology of vision. *J Biol Chem* 287(3):1612–1619
- Park JS, Akiyama Y, Winnik FM, Kataoka K (2004) Versatile synthesis of end-functionalized thermosensitive poly(2-isopropyl-2-oxazolines). *Macromolecules* 37:6786–6792
- Paul JF, John RJ (1943) Statistical mechanics of cross-linked polymer networks II. Swelling *J Chem Phys* 11:521–526
- Plate NA, Lebedeva TL, Valuev LI (1999) Lower critical solution temperature in aqueous solutions of N-Alkyl-substituted polyacrylamides. *Polym J* 31:21–27

- Podual K, Doyle FJ, Peppas NA (2000) Glucose-sensitivity of glucose oxidase-containing cationic copolymer hydrogels having poly (ethylene glycol) grafts. *J Control Release* 67:9–17
- Qiu Y, Park K (2001) Environment-sensitive hydrogels for drug delivery. *Adv Drug Deliv Rev* 53:321–339
- Qiu Y, Park K (2012) Environment-sensitive hydrogels for drug delivery. *Adv Drug Deliv Rev* 64:49–60
- Roy D, Brooks WLA, Sumerlin BS (2013) New directions in thermoresponsive polymers. *Chem Soc Rev* 42:7214–7243
- Rueda J, Zschoche S, Komber H, Schmaljohann D, Voit B (2005) Synthesis and characterization of thermoresponsive graft copolymers of NIPAA and 2-alkyl-2-oxazolines by the “grafting from” method. *Macromolecules* 8:7330–7336
- Saeki S, Kuwahara N, Nakata M, Kaneko M (1977) Phase separation of poly(ethylene glycol)-water-salt systems. *Polymer* 18:1027–1031
- Schild HG (1992) Poly(N-isopropylacrylamide): experiment, theory and application. *Prog Polym Sci* 17:163–249
- Schmaljohann D (2006) Thermo- and pH-responsive polymers in drug delivery. *Adv Drug Deliv Rev* 58:1655–1670
- Shibu ES, Hamada M, Murase N, Biju V (2013) Nanomaterials formulations for photothermal and photodynamic therapy of cancer. *J Photochem Photobiol C-Photochem Rev* 15:53–72
- Shostakovskiy MF, Sidelkovskaya FP, Zelenskaya MG (1952) Synthesis and transformations of N-Vinylcaprolactam. Part 1: polymerization in presence of hydrogen peroxide. *Bull Acad Sci USSR Div Chem Sci* 4:633–636
- Siegel RA (2014) Stimuli sensitive polymers and self regulated drug delivery systems: a very partial review. *J Control Release* 190:337–351
- Solomon OF, Corciovei M, Ciuta I, Boghina C (1968) Properties of solutions of poly (N-vinylcaprolactam). *J Appl Polym Sci* 12:1835–1842
- Son S, Shin E, Kim BS (2014) Light-responsive micelles of spiropyran initiated hyperbranched polyglycerol for smart drug delivery. *Biomacromolecules* 15(2):628–634
- Su Y-R, Yu S-H, Chao A-C, Wu J-Y, Lin Y-F, Lu K-Y, Mi F-L (2016) Preparation and properties of pH-responsive, self-assembled colloidal nanoparticles from guanidine-containing polypeptide and chitosan for antibiotic delivery. *Colloids Surf A* 494:9–20
- Susanto H, Samsudin AM, Rokhati N, Widiasta IN (2013) Immobilization of glucose oxidase on chitosan-based porous composite membranes and their potential use in biosensors. *Enzyme Microb Technol* 52:386–392
- Takamatsu D, Fukui K, Aroua S, Yamakoshi Y (2010) Photoswitching tripodal single molecular tip for noncovalent AFM measurement: synthesis, immobilization and reversible configurational change on gold surface. *Org Biomol Chem* 8:3655–3664
- Tamada K, Akiyama H, Wei TX, Kim SA (2003) Photoisomerization reaction of unsymmetrical azobenzene disulphide self-assembled monolayers: modification of azobenzene dyes to improve thermal endurance for photoreaction. *Langmuir* 19:2306–2312
- Tang XD, Liang XC, Gao LC, Fan XH, Zhou QF (2010) Water-soluble triply-responsive homopolymers of N, N-dimethylaminoethyl methacrylate with a terminal azobenzene moiety. *J Polym Sci Part A-Polym Chem* 48(12):2564–2570
- Tauhardt L, Frant M, Pretzel D, Hartlieb M, Bücher C, Hildebrand G, Schröter B, Weber C, Kempe K, Gottschaldt M, Liefelth K, Schubert US (2014) Amine end-functionalized poly (2-ethyl-2-oxazoline) as promising coating material for antifouling applications. *J Mater Chem B* 2:4883–4893
- Theato P (2008) Synthesis of well-defined polymeric activated esters. *J Polym Sci A: Polym Chem* 46:6677–6687
- Vihola H, Laukkanen A, Vihola L, Tenhu H, Hirvonen J (2005) Cytotoxicity of thermosensitive polymers poly(N-isopropylacrylamide), poly(N-vinylcaprolactam) and amphiphilically modified poly(N-vinylcaprolactam). *Biomaterials* 26(2005):3055–3064

- Vihola H, Laukkanen A, Tenhu H, Hirvonen J (2008) Drug release characteristics of physically cross-linked thermosensitive poly(N-vinylcaprolactam) hydrogel particles. *J Pharm Sci* 97:4783–4793
- Vogt AP, Sumerlin BS (2009) Temperature and redox responsive hydrogels from ABA triblock copolymers prepared by RAFT polymerization. *Soft Matter* 5:2347–2351
- Wang CH, Hsiue GH (2002) Synthesis and characterization of temperature- and pH-sensitive hydrogels based on poly(2-ethyl-2-oxazoline) and poly(D, L-lactide). *J Polym Sci Part A: Polym Chem* 40:1112–1121
- Wang X, Qiu X, Wu C (1998) Comparison of the coil-to-globule and the globule-to-coil transitions of a single poly(N-isopropylacrylamide) homopolymer chain in water. *Macromolecules* 31:2972–2976
- Wang B, Chen KF, Yang RD, Yang F, Liu J (2014) Stimulus-responsive polymeric micelles for the light-triggered release of drugs. *Carbohydr Polym* 103:510–519
- Weber C, Becer CR, Hoogenboom R, Schubert UC (2009) Lower critical solution temperature behavior of comb and graft shaped poly[oligo(2-ethyl-2-oxazoline)methacrylates]. *Macromolecules* 42:2965–2971
- Xia Y, Burke NAD, Stoeber DH (2006) End group effect on the thermal response of narrow-disperse poly(N-isopropylacrylamide) prepared by atom transfer radical polymerization. *Macromolecules* 39:2275–2283
- Xiao Y, Gong T, Jiang Y, Wang Y, Wen ZT, Zhou S, Bao C, Xu X (2016) Fabrication and characterization of a glucose-sensitive antibacterial chitosan–polyethylene oxide hydrogel. *Polymer* 82:1–10
- Yoshihito O, Jian-Ping G (1998) Soft and wet materials: polymer gels. *Adv Mater* 10:827–837
- You J, Almeda D, Ye GJC, Auguste DT (2010a) Bioresponsive matrices in drug delivery. *J Biol Eng* 4(5):1–12
- You J, Shao RP, Wei X, Gupta S, Li A (2010b) Near-infrared light triggers release of paclitaxel from biodegradable microspheres: photothermal effect and enhanced antitumor activity. *Small* 6:1022–1031
- Yu L, Ding J (2008) Injectable hydrogels as unique biomedical materials. *Chem Soc Rev* 37:1473–1481
- Yu YY, Tian F, Wei C, Wang CC (2009) Facile synthesis of triple-stimuli (photo/pH/thermo) responsive copolymers of 2-diazo-1,2-naphthoquinone-mediated poly(N-isopropylacrylamide-co-N-hydroxymethylacrylamide). *J Polym Sci Part A-P*

# Chapter 3

## Clinical Use and Hemostatic Application of Gelatin



Roberto Gazzeri, Marcelo Galarza, Marika Morabito and Alex Alfieri

### 1 Background

Although each surgical procedure shows distinctive features that characterize itself, most surgeries follow well-defined operatory steps, which can be identified in: incision, dissection, exposure, resection, hemostasis, restoring anatomy, and closure. Although diversified by anatomical district and relative approach difficulties, fundamental challenges that any surgeon has to deal with are almost the same: bleeding, delayed healing or healing complications, effusion, and adherence development. Any of these, if treated improperly, can influence patient's outcome such as hemorrhagic shock, hemoglobin replacement, transfusion, and extended postoperative hospitalization. This affects the patients and the health care system, which register an increase in health care costs, among other negative consequences. Therefore, it is clear that how to reduce blood loss is an argument of major interest for any surgical specialty. An adequate hemostasis can be ordinarily achieved by conventional methods, like manual compression and ligatures, that maybe laborious and less-effective techniques for control bleeding, particularly in complex injuries and areas with difficult anatomical access. Thermal methods can also be used, such as electrical or laser cauterization, although in such cases it is necessary to take note about the increased possibility of infection and damaging wound borders, sec-

---

R. Gazzeri (✉) · M. Morabito  
Department of Neurosurgery, San Giovanni Addolorata Hospital, Rome, Italy  
e-mail: robertogazzeri@gmail.com

M. Galarza  
Department of Neurosurgery, Hospital Universitario Virgen de la Arrixaca,  
Murcia, Spain

A. Alfieri  
Department of Neurosurgery and Spinal Surgery, Ruppiner Kliniken GmbH,  
Neuruppin, Germany

ondary to the areas of char and necrosis arose by the physical principle of the cauterization. Hemostatic agents like fibrin sealant are a valid option, which maybe useful in the various hemorrhagic circumstances. During last years, a lot of topical hemostatic agents were created, currently available, which perform their action in different ways and can be used both as unique solution in situation without alternative or as suture reinforcement. Although routinely used during surgical procedures, there is still big confusion concerning recommendation and optimal use of these products, because of the wide range of products, as absorbable topical agents, antifibrinolytic agents, fibrin sealants, and hemostatic matrix. Great results with topical hemostatic agents based on a gelatin matrix and thrombin compound have been shown in many surgical branches. These systemic review aims to analyze Floseal<sup>®</sup> (Baxter HealthCare Corporation, Deerfield, IL, USA) and Surgiflo<sup>®</sup> (Ethicon, Sommerville, NJ, USA) pharmacodynamics and pharmacokinetic properties, its therapeutic effects, tolerability, and complication of its use. The analysis included all the references discovered by Medline, NILDE and PubMed in Floseal<sup>®</sup> and Surgiflo<sup>®</sup> literature, for an amount of 111 articles (case report, letters for the editors, laboratory models were all included) draw up in English: 33 from urology, 25 from otolaryngology, 16 from gynecology, 13 from neurosurgery (specifically: 1 from animal model, 7 from neurosurgery, 3 from spine surgery, and 2 from both subtypes of procedures), 11 from cardiovascular surgery, 5 from general surgery, 4 from orthopedic surgery, 4 from traumatology, and 1 from ophthalmology. Out of which, 10 reported studies on Surgiflo<sup>®</sup>: 4 from neurosurgery (specifically: 2 from spine surgery and 2 from both subtypes of procedures), 2 from otolaryngology, 1 from general surgery, 1 from cardiovascular surgery and 1 from urology.

## 2 Pharmacodynamics Properties

Floseal<sup>®</sup> (Baxter Health Care Corporation, Fremont, CA) was approved by the Food and Drug Administration in 1999: it is a reabsorbable matrix hemostatic sealant obtained of flowable bovine gelatin granules (obtained by the extraction of collagen from corneal tissue which undergoes gelatinization and crosslinking/stabilization with glutaraldehyde) coated in human-derived thrombin, which works through a combination of various pharmacological and mechanical effects. Gelatin matrix is ground into 500–600  $\mu\text{m}$  particles. Thrombin compound is from bovine derivation and is provided as a sterilize freeze-dried powder which is reorganized in a 0.9% sodium chloride solution and immediately added to the Gelatin before being directly injected into the bleeding site. The matrix is applied to the bleeding source and kept in place for approximately 2 min. Excess of Floseal<sup>®</sup> should be removed by gentle irrigation. It is a biocompatible matrix that is resorbed in 6 or 8 weeks, following the natural wound healing process. It works on moistened tissues, active bleeding and conforms itself to non-regular surfaces.

Surgiflo<sup>®</sup> (Ethicon, Sommerville, NJ, USA), as Floseal<sup>®</sup>, is a topical hemostatic agent made from a gelatin matrix, that consist of crosslinked porcine gelatin

granules, and human thrombin. Surgiflo<sup>®</sup> is completely absorbed within 4–6 weeks. Spongostan absorbable gelatin sponge (Johnson & Johnson) is crosslinked and hardened by treatment with dry heat rendering it insoluble in water. The gelatin sponges are then granulated into a powder that is mixed and foamed with a liquid component: this procedure allows to put the resultant gelatin paste in a syringe (that must be capped immediately). Time for preparation (ready to use) of Surgiflo<sup>®</sup> is 81 s, about half the time that it takes to prepare Floseal<sup>®</sup>, 168 s (Gazzeri et al. 2013).

## 2.1 Mechanism of Actions

The mechanism of action of gelatin-based hemostats, such as Floseal<sup>®</sup> and Surgiflo<sup>®</sup>, works through mechanical effects that involve physical area instead of any other pharmacological effects on the hemostatic mechanism. First of all, the gelatin acts with a buffer effect to reduce blood flux. Moreover, Floseal<sup>®</sup> acts by mimicry blood coagulation process: The thrombin component directly activates fibrinogen and cleaves this one into fibrin monomers, bypassing the intrinsic and the extrinsic systems. It also activates factor XIII to factor XIIIa, which covalently crosslinks the soluble mesh given by polymerization of fibrin to form a stable clot. Both the steps require the presence of calcium ions.

## 2.2 Mechanism Properties of Fibrin Coat

Because Floseal<sup>®</sup> does not contain fibrinogen—so that the endogenous fibrinogen must be turned into fibrin—it is necessary for the thrombin compound to enter in contact with blood. When bleeding occurs and the blood filter across the granules of the matrix, the gel has roughly 20% in 10 min, making fibrin polymers that perfectly adapt to the wound's profile. These clots have higher resistance to stretching and more tensile strength, indicating that gelatin matrix hemostatics clots are able to maintain their primary structure even under pressure. In specialties as cardiovascular surgery, the mechanical properties of sealants maybe important for determining the choice of agents to use for hemostasis at sutures lines, because of compliance: sealants with better stiffness than aortic root placement material may constrict normal physiological expansion and produce anastomotic narrowings.

Surgiflo<sup>®</sup> gelatin matrix neither contains fibrinogen. Its flowable gelatin matrix creates the perfect situation for the platelets (based on the human's physiological coagulation cascade) to adhere and aggregate. Surgiflo<sup>®</sup> is distributed to the patient at a hydration level that is under its equilibrium swell. When the granulomatous matrix touches blood, or body fluids, they swell by 7–20% (Gazzeri et al. 2014).



### **2.3 Hemostatic Effects**

Gelatin hemostatic matrix is hydrophilic so it is not necessary to have a dry surface, as other agent as fibrin glue: It adheres perfectly to wet tissue and irregular surfaces. Floseal<sup>®</sup> and Surgiflo<sup>®</sup> matrix were compared in many studies with Gelfoam<sup>®</sup> (Pharmacia & Upjohn) a porcine gelatin, in combination with thrombin. Gelatin matrix hemostatic provided a rapid and efficacious hemostasis in all the patients underwent surgical procedures in several specialties, particularly in the site of active bleeding.

### **2.4 Other Effects**

By now, differently from other fibrin sealants, no histopathological changes or neurotoxicity have been reported.

### **2.5 Animal Model**

In every medical and surgery procedures, it is fundamental to evaluate biocompatibility and safety of the materials that we are going to use on humans, first in animal model. In a rat neurosurgical model, the authors created a lesion in the brain tissue of 228 Wistar outbred rats, and either no agent (negative control), Arista (microporous polysaccharide hemosphere), Avitene (microfibrillar collagen), Surgicel (oxidized cellulose), Floseal (gelatin matrix thrombin sealant) or kaolin (positive control) was delivered. The same authors documented time to hemostasis and determined presence of foreign body reaction and residual material, after sacrificed the animals at different intervals up to 4 weeks. As results, Floseal<sup>®</sup> and the other hemostatic agents perform better (i.e., in one minute they obtained a complete hemostasis) than control group. Remaining materials was visible in all the lesion in Floseal<sup>®</sup>, Avitene, and Surgicel groups on second week. Floseal<sup>®</sup> and Avitene showed a propensity to cause granuloma aggregation (Ereth et al. 2008).

The unintentional injury of the ICA (internal carotid artery)—and the consecutive massive bleeding—is the most dramatic complication during endonasal surgeries. We found an animal model study in which aim was to compare the efficacy of application of hemostatics using endoscopic techniques to maintain vascular flow in carotid artery injury. Twenty sheep were referred to internal carotid artery dissection and/or isolation; subsequently a modified SIMONT model (Sinus Model Otorhino Neuro Trainer) replaced the artery. A 4 mm injury of carotid artery was endoscopically created. One of the five disposable hemostatic techniques (oxidized regenerated cellulose, Floseal, Chitosan gel, muscle patch or the U-Clip device for anastomosis) was randomly assigned to each sheep. The significant

parameters of this trial were respectively time to hemostasis, length of time in which mean arterial pressure (MAP) was more than 55 mmHg, total blood loss and total survival time. The outcomes suggest that the hemostasis with muscle patch and the U-Clip were considerably more efficient in achieving a shorter time to hemostasis, allowing lower loss of blood, a longer survival time, and a longer mean arterial pressure >55 mmHg time than Chitosan gel, oxidized regenerated cellulose, and Floseal. In none of the case Floseal nor oxidized regenerated cellulose were sufficient to achieve hemostasis, causing all the animals to extinguish prematurely (Valentine et al. 2011).

The use of free flaps is, in related manner, the (so-called) golden standards for the treatment of damages resulting from the invasive treatment of malignant head and neck tumors. Many procedure-related factors, from mere technicalities to specific matters regarding the several techniques more used to apply the different agents can influence the outcomes in free microsurgical tissue transfers. We found a study in which the researchers had divided Sprague-Dawley rats into three different groups: control (group I), Floseal® (group II), Tisseel (group III). For every group, the researchers elevated a 3 × 6 cm ventral fascio-cutaneous groin flap based on the left superficial epigastric artery and applied the experimental trial material (0.2 mL saline in the control group, 0.5 mL Floseal® and 0.2 mL Tisseel) beneath the flap and around the flap pedicle prior to suture the flap back to the wound area. The researchers exposed five rats of each study group to four ischemic times (6-8-10-12 h). Flap survival was controlled 1 week after reversal of the ischemia. Flap survival from Control, Floseal®, and Tisseel groups was, respectively, (in percentage): at 6 h, 80 (no differences between the groups); at 8 h, 80-80-60; at 10 h, 60-33-40; at 12 h, 20-20-0. Probit curves and critical ischemic times were considered: 9.4 (Control), 9 (Floseal®), and 7 (Tisseel) hours, respectively. In this experiment, Floseal® and Tisseel does not demonstrate adverse effect on flap survival (Partsafas et al. 2004).

The purpose of a rabbit aortic anastomosis model study was to compare the common surgical hemostatic agents' cogency to achieve hemostasis using fibrin sealant (FS) and to compare their functional power to obtain hemostasis instead of the placement of additional sutures. The researchers performed an end-to-end anastomosis of transected abdominal aorta in mildly anticoagulated rabbits using four or six interrupted sutures. The suture line was covered with gauze alone, or adding Surgicel, Avitene, Gelfoam, Fibrin Sealant or Floseal to the gauze, following which blood flow was restored. The loss of blood-soaked by the gauze was eventually calculated. The rabbits who survived were rehabilitated and their treated vessels underwent histological examination four weeks after the procedure. The above-mentioned treatment groups were part of a blind study. In the untreated group, aortic anastomosis was also achieved by mean of 8 or 12 stitches. An 100% mortality ( $n = 4$ ) rate with an average around 108 mL blood loss (profuse hemorrhage) outcome for untreated 4 stitches anastomosis of the aorta. Floseal® ( $44.2 \pm 8.5$  mL blood loss) and other hemostatic agents reduced the bleeding in several ways in comparison with the animals that were not treated, but the results were not statistically relevant. One to three rabbits in each group survived the

surgery. Six out of six sutures aortic anastomoses that, were untreated, result in  $67.7 \pm 21.8$  mL blood loss and 100% survival. Floseal<sup>®</sup> ( $33.9 \pm 5.4$  mL blood loss) and other hemostatic agents decreased bleeding, but these results were not statistically significant. The 8 and 12 sutures aorta repairs resulted in a moderate loss of blood ( $43.9 \pm 19$  and  $21.3 \pm 14.9$  mL, respectively), with a stable hemostasis that did not require any hemostatic agent. (Kheirabadi et al. 2002). 5–30% of fetoscopic approaches are complicated by the occurrence of premature rupture of membranes (PROM). We found a study which proposes an approach called Amnioseal that of presealing the chorioamniotic membrane prior the rupture of the membrane. To test this proposal the authors designed a set of experiments using two models based on unfertilized chicken eggs. The first model simulated the amniotic cavity and the chorioamniotic membrane. The second one simulated the amniotic cavity and the uterine muscle and chorioamniotic membrane interface. Untreated controls were tested with four different biomaterials (100% petroleum jelly, Bioglue Surgical Adhesive, Coseal, and Floseal<sup>®</sup>). The sealants were applied by the researchers directly to the egg membranes and then the membrane was furtherly manipulated and biopsied by needle. Floseal<sup>®</sup> resulted to adhere weakly and this was correlated with a bigger defect area and higher amount of leakage (Carnaghan and Harrison 2009).

To investigate the influence of hemostatic agents on the origination of adhesion, excisions of a portions of peritoneum were performed on 70 Wister outbred rats by laparotomy to initiate a process of adhesion formation. The area of peritoneal defect was treated with one of the six different hemostatic agents (Arista, BioGlue, Floseal<sup>®</sup>, Tisseel, Coseal, or Surgicel). The model system showed complete formation of adhesion in the control group with a mean adhesion total score of 6.0. Adhesion scores of Floseal<sup>®</sup>, Tisseel, and Surgicel were not statistically different from control rats (Hoffmann et al. 2009). The potential use of intraoperative Floseal<sup>®</sup> (GMHS) embedded with macrophages transduced with murine interleukin (IL)-12 recombinant adenoviral vector (G/M $\phi$ /AdmIL-12) was evaluated for the prevention of recurrence of prostate cancer after total prostatectomy. Analyzing the controls in a preclinical mouse study of residual prostate cancer, injection of G/M $\phi$ /AdmIL-12 resulted in major suppression of tumor development and spontaneous lung metastases, a critical survival superiority of the G/M $\phi$ /AdmIL-12 treated mice, more efficient trafficking of M $\phi$  to lymph nodes draining from the prostate and production of systemic natural killer cell activity and neoplastic specific cytolytic T lymphocyte response (Tabata et al. 2009). The efficacy of Floseal<sup>®</sup> and Surgiflo<sup>®</sup> in urology has been proved on other several studies specifically analyzed in Sect. 4.7. In addition, animal model for trauma surgery is specifically analyzed in Sect. 4.4.3. All of these studies rely on animal model to mimic the patient; nonetheless, the analogies of animal and patient coagulation characterization are still unknown. Floseal<sup>®</sup> and Surgiflo<sup>®</sup> were also compared with other common topical hemostatic agents and they demonstrated to be the most effective, superior to the others tested. When it is injected prophylactically, the clot is capable to prevent hemorrhage independently to the hemostatic capacity of the host. The results obtained suggest

that Floseal<sup>®</sup> and Surgiflo<sup>®</sup> can be safely used to achieve hemostasis in major surgery procedures.

### 3 Pharmacokinetic Properties

Floseal<sup>®</sup> and Surgiflo are intended only for topical use, as pure hemostatic agent, and not as tissue glue, urinary tract sealant or for adhesion prevention.

### 4 Therapeutic Efficacy

In this section, we want to estimate the hemostatic efficiency of FloSeal<sup>®</sup> and Surgiflo<sup>®</sup> as treatment of bleeding in patients undergoing neurosurgical procedure (Sects. 4.1 and 4.2), cardiovascular surgery (Sect. 4.3), liver (Sect. 4.4.1) and thyroid surgery (Sect. 4.4.2), orthopedic surgery (Sect. 4.5), head and neck surgery (Sect. 4.6), urological surgery (Sect. 4.7), gynecologic surgery (Sect. 4.8), and ophthalmologic surgery (Sect. 4.9).

#### 4.1 Neurosurgery

We found nine articles evaluating efficacy of Floseal<sup>®</sup> in neurosurgical procedures (Table 1). Obtaining an adequate hemostasis during cranial surgery is fundamental in any neurosurgeon's daily practice. Bleeding from dura mater or nervous tissue can limit the ability to have a good view of the operatory field, which is critical especially in minimally invasive surgery. Floseal has been manifested to be bio-compatible and safe in comparison with other topical hemostatic agents. Its efficacy has been proved in the surgical management of spontaneous intracerebral hemorrhage. Numerous approaches to evacuating the intracerebral spontaneous hemorrhage have been described: mini-invasive approaches associate the advantages of surgical clot removal with minimal addition cerebral tissue damage. The most common technique see three passages: fast decompression, removal of the hematoma without use of brain retractors and total evacuation. After the last step, gelatin hemostatic matrix, injected directly into the operative cavity, adapts to the cavity walls, and conforms to any irregular geometry. There is a theoretical peril of aggravating brain edema around the hematoma and thereby augmenting local thrombin concentrations, although with irrigation and suction it is possible to decrease the concentration of intracerebral thrombin, leaving a clean surgical area (Gazzeri et al. 2013). In a retrospective review of cases undergoing craniotomy for meningioma resection, the primary outcome was the presence of a new thromboembolic event (deep vein thrombosis or pulmonary embolism), a life-threatening

and potentially preventable complication, within 14 days of the operation. The association between hemostatic agents and development of systemic thromboembolic events remains poorly understood. In this study was presented the first evidence of possible association, maybe due to direct intravascular injection of the agent. Furthermore, patient BMI was found to be significantly associated with DVT/PE confirming that overweight is an important risk factor for thromboembolic events in patients undergoing any surgical procedure. These findings suggest that overweight patients and patients who receive incrementally higher volumes of hemostatic agents intraoperatively should be closely monitored for postoperative thromboembolic events (Safaei et al. 2014). During transsphenoidal surgery, prodigious and persistent bleeding may occur from the cavernous sinuses or the tumoral bed. For transsphenoidal surgery, a longer directional tip that holds shape and retains bend at multiple angles for access to difficult-to-reach surgical sites, must be used. Gelatin hemostatic matrix is an inestimable technical adjunct in reaching complete hemostasis with this restricted approach which frequently inhibits the use of bipolar cautery forceps (Gazzeri et al. 2013). In an accurate study, all the operative data of the cases who underwent transsphenoidal approach since January 2000 were reviewed for an 18-month period. During this time of observation, 293 transsphenoidal operations were carried out for pituitary lesion. Of these, 20 procedures were affected by extreme or continuous bleeding. Floseal<sup>®</sup> was injected into the area of hemorrhage by use of a 14-gauge angiocatheter to arrive to the sella. Total hemostasis was obtained immediately in all patients except one, which required a second injection of the product. This second application guaranteed an immediate complete hemostasis (Ellegala et al. 2002). In a most recent study, in a 4 years period, 65 patients underwent extended endoscopic endonasal transsphenoidal approaches. Of these, 29 surgeries required the use of a gelatin hemostatic matrix. Bleedings from the major venous sinuses, arteries, tumoural bed, and internal carotid artery were analyzed by the authors, which reported complete hemostasis furtherly following injection of Floseal. The gelatin hemostatic was useful for both focal hemorrhage and oozing and was effective also for high-flow bleeding. A second application was required only in the hemorrhages from an internal carotid artery tear (Cappabianca et al. 2009).

## 4.2 *Spine Surgery*

We found 5 and 4 articles, respectively, evaluating use of Floseal<sup>®</sup> and Surgiflo in spinal surgery, in which the loss of blood can be significant and become life-threatening. Any minimal bleeding may cause disastrous neurological damage. Microsurgical approaches to intra-spinal nervous structures depend strictly on a clear vision of those delicate anatomical elements: continuous bleeding may pose an impediment to the identification of pathological components or cleavage planes. In this major type of surgery, bipolar cautery is commonly used but it has serious disadvantages. Dissipation of the heat from bipolar forceps can cause thermal injury

**Table 1** Neurosurgery and Spine surgery

Author	Year	Multicenter/ Single center	Prospective/ Retrospective	Gender and number of patients	Age (median of years)	Hemostatic	Type of bleeding	Time to hemostasis (MIN)	Procedure time (MIN)	Pathology/ Procedure	Complications
Renkens KL, et al.	2001	Multicenter	Prospective	127	21	Proceed™ Gelfoam	Oozing, Flowing, Pulsatile	1.5 (median time)	NA	Discectomy, Laminectomy with/ without fusion	Anemia, redness, drainage, swelling (Proceed), wound infection (Gelfoam)
Ellegala DB, et al.	2002	Single center	Retrospective	14 M + 6 F (20)	9 to 69 (46)	FloSeal®	Venous, bony margins, generalized ooze, tumor bed	NA	NA	Macroadenoma (11), meningioma (2), chordoma (2), germinoma (1), craniopharyngioma (4)	NA
Fiss I, et al.	2007	Single center	Retrospective	7	25 to 85 (57)	FloSeal® Tissuco® Spongostan®	Arterial (2), generalized venous oozing (3), venous bleeding from superior sagittal sinus (2)	< 4	NA	Pituitary macroadenoma (2), falx meningioma, cerebellar hemangioblastoma, glioblastoma (2), convexity meningioma	None
Cappabianca P, et al.	2008	Single centre	Retrospective	15 W + 14 M (29)	33 to 68 (52)	FloSeal®	Oozing and focal Dural and intradural Venous, arterious site and tumor bed haemorrhage	NA	NA	Anterior skull base meningioma (8) Middle cranial fossa meningioma (1) Intra-supra-sellar non functioning giant macro- adenoma (5) Suprasellar craniopharyngioma (11)	None

(continued)

Table 1 (continued)

Author	Year	Multicenter/ Single center	Prospective/ Retrospective	Gender and number of patients	Age (median of years)	Hemostatic	Type of bleeding	Time to hemostasis (MIN)	Procedure time (MIN)	Pathology/ Procedure	Complications
Gazzeri R, et al.	2009	Multicenter	Retrospective	31	NA	FloSeal®	Generalized and Capillary oozing	NA	NA	Cavernous sinus chordoma (1) Clivus chordoma (1) Optic glioma (1) Intra-suprasellar Rathke cleft cyst (1)	NA
Gazzeri R, et al.	2010	Multicenter	Prospective	127 W + 87 M (214)	NA	FloSeal®	Generalized venous oozing (128), epidural venous plexus bleeding (61), venous sinuses bleeding (16), arterial capillary bleeding (9)	< 3	NA	Glioma (37), spontaneous ICH (35), traumatic ICH (26), meningioma (25), extra-axial hematoma/ cranial base fracture (16), metastasis (11) schwannoma (2), pituitary adenoma (1), anterior cervical discectomy (6), cervical laminoplasty (7)/ laminectomy (5), cervicothoracic (1)/ thoracic (3) laminectomy , posterior lumbar fusion (9), microdiscectomy (2)	Rebleeding (4 cases: 1 traumatic ICH, 1 spontaneous ICH, 2 malignant gliomas), abscess (1), status epilepticus (1)

(continued)

Table 1 (continued)

Author	Year	Multicenter/ Single center	Prospective/ Retrospective	Gender and number of patients	Age (median of years)	Hemostatic	Type of bleeding	Time to hemostasis (MIN)	Procedure time (MIN)	Pathology/ Procedure	Complications
Bedi AD, Toms SA, et al.	2011	Single center	Retrospective	39	NA	Floseal®	Venous	NA	NA	Pituitary adenoma (33), craniopharyngioma (4), clival plasmacytoma (1), planum meningioma (1)	None related to hemostatic agent
Gazzeri R, Galarza M, Alfieri A	2012	Multicenter	Retrospective	170 W + 139 M (318)	18 to 80 (58.8 ± 16.6)	Floseal® (264 cases) Surgiflo (54 cases, only brain surgery)	Generalized oozing	< 5	NA	Cranial neurosurgery (194 supratentorial + 33 posterior fossa surgeries), craniocervical junction (4), spinal procedures (78 posterior + 9 anterior approaches) most common: lumbar laminectomy (35) + lumbar fixation (15)]	Delayed hemorrhage (8 cases), epidural abscess (6 cases; 5 with Floseal, 1 with Surgiflo)
Gazzeri R, Galarza M, Alfieri A	2013	Multicenter	Retrospective	NA	NA	Floseal® Surgiflo Gelfoam Surgifoam	Generalized oozing	3 (Floseal)	NA	Spontaneous ICH, Cerebral tumors, transphenoidal surgery and degenerative spinal disease	Re-bleeding and inflammatory reaction (1 case)
Gazzeri R, De Bonis C, et al	2014	Multicenter	Retrospective	41 W + 26 M (67)	25 to 74 (57.8)	Surgiflo	Venous bleeding from spine epidural space	<3	136 (range 56-284)	Lumbar stenosis with (25)/without (18) instability, herniated cervical (6)/ lumbar(9) disc, tumor (9)	Delayed hemorrhage (1 case)

(continued)



Table 1 (continued)

Author	Year	Multicenter/ Single center	Prospective/ Retrospective	Gender and number of patients	Age (median of years)	Hemostatic	Type of bleeding	Time to hemostasis (MIN)	Procedure time (MIN)	Pathology/ Procedure	Complications
Safae M, Sun MZ, et al.	2014	Single center	Retrospective	331 W + 136 M (467)	18 to 92 (58±14)	Floseal®	NA	NA	348±142	Cranial Meningioma	DVT/PE (12)
Landi A, Gregori F, et al.	2016	Single center	Prospective	98 M + 51 W (149)	25 to 80 (52.5)	Floseal® Surgiflo	Massive epidural venous plexus bleeding	< 7 (Floseal 5 min 35 sec ± 52 sec; Surgiflo 5 min 32 sec ± 54 sec)	NA	Arthrosis (92) or and traumatic (57) pathology of lumbar and thoracolumbar spine	None

W : women; M: men; NA: not available ; DVT/PE: deep venous thrombosis/ pulmonary emboli; ICH: intracerebral hematoma

to vascular and neural tissue nearby the site of application, while the occlusion of the artery may compromise the perfusion of nervous structures. For both of these reasons, hemostatic agents are a better choice for intra-spinal procedures, whereas bipolar cautery has minimal effects in controlling copious capillary bleeding that characterize this type of surgery. Critical is the manipulation of the epidural veins plexus that surround the spinal cord and the spinal nerves: Bleeding from these vessels can be hard to control due to their anatomical position next to the nerves and their intra-foraminal courses. In these cases, even mild hemorrhage can reduce the accuracy and safety of the surgical technique, with increased procedure time and higher risk for infection for the patients (Gazzeri et al. 2012). In one study which lasted six months, the authors accomplished more than 170 major spinal surgeries: in 67 of these surgeries, they injected Surgiflo into vertebral epidural space to achieve hemostasis. When the venous hemorrhage continued from the epidural space in the spinal canal after packing with hemostatic agents as oxidized regenerated cellulose and fibrillary collagen, the use of gelatin matrix was required. In all patients, the results were evaluated to be superlative, with immediate halt of venous epidural bleeding, or great. The authors did not observe any complication related to the thrombin-gelatin hemostatic matrix (Gazzeri et al 2014). In a most recent study, 149 patients (98 men and 51 women) were recruited for a prospective study aimed to comparatively evaluate Floseal<sup>®</sup> and Surgiflo in hemostatic control during spinal surgery. All patients required laminectomy or lamino-artrectomy, exposing the perivertebral venous plexus. 92 patients were affected by a degenerative spinal disease, 57 by vertebral trauma. 42 patients assumed antiaggregant and/or anticoagulant therapy before surgery. In all patients, an important bleeding originated from the intracanalicular epidural venous plexus. Floseal<sup>®</sup> was applied in 86 cases, while Surgiflo in 63 cases, a perfect hemostasis was achieved in all cases in a period of time between 3 min 30 s and 7 min (Floseal<sup>®</sup> 5 min 35 s  $\pm$  52 s, Surgiflo 5 min 32 s  $\pm$  54 s). There was no statistical association between coagulation time and hemostatic, age of the patient, gender, pathology surgically treated. The clinical and radiological follow-up demonstrated no evidence of postsurgical hematomas (Landi et al. 2016).

### 4.3 Cardiovascular Surgery

Hemostasis is a key tenet of any surgical procedure, even more crucial in cardiac surgery practice. We found 11 studies evaluating efficacy of Floseal<sup>®</sup> in cardiovascular surgery (Table 2). The suture lines within the cardiac chamber or the great vessels and the various high-pressure anastomoses performed during cardiac surgery often results in hemorrhage, which is more efficiently controlled with modern topical hemostatic agents than by conventional approaches such as manual pressure, electrocoagulation or sutures. Further, heparinization for cardiopulmonary bypass, blood contact with extracorporeal tubing-oxygenator and systemic hypothermia, contribute to a various degree of coagulopathy in most cardiac surgical patients

(Nasso et al. 2009). A very important factor to considerate in the choice of the hemostatic agent is the history of the cardiovascular patients: Most of them assume aspirin at home and this change the reaction of their coagulation systems at some hemostatic, not Floseal<sup>®</sup> that has demonstrated an optimal function in these patients too. Perioperative hemorrhage leads to increase operating room time, blood bank product transfusion, pulmonary hypertension, and probably to mortality. Further, postoperative bleeding is a feared complication associated with prolonged intensive care unit stay, need for surgical revision of hemostasis, and even increased mortality. In a prospective randomized study, 209 cases were treated using Floseal<sup>®</sup> and 206 patients were assigned to the comparison group that received alternative agents as topical hemostatic materials, including hemostatic patches or sponges composed of oxidized regenerated cellulose or derived porcine gelatin. Higher rates of successful hemostasis and shorter time to hemostasis were observed in the Floseal<sup>®</sup> group. Difference of statistical importance was observed in time to event analysis. A statistically important reduction was appreciated in postoperative bleeding and rate of transfusion of blood products in the Floseal<sup>®</sup> group. There were no statistical differences among groups in terms of rates of revision for bleeding and of minor complications in the overhaul cohort, but considering only patients with overt intraoperative bleeding were significantly lesser in the Floseal<sup>®</sup> group. The advantages observed in the Floseal<sup>®</sup> group were not offset in case who underwent systemic hypothermia (Nasso et al. 2009). A most recent study examined clinical outcomes of flowable hemostatic agents in a cardiac surgical population, analyzing the retrospective database of cardiac surgical cases for a period of 6 years. Three different groups were formed, based on the use of hemostatic matrices: (1) Floseal<sup>®</sup> or Surgiflo, exclusively; (2) Floseal<sup>®</sup> or Surgiflo, associated with fibrin sealants, sealants, or powder hemostat; (3) Floseal<sup>®</sup> or Surgiflo, with non-flowable hemostats with or without thrombin. Group 1 included 4,480 Floseal<sup>®</sup> and 326 Surgiflo cases. Participants underwent coronary artery bypass grafting (CABG), aortic valve or valvular with CABG surgery. Clinical outcomes included surgical complications, transfusion, surgical revision, mortality, length of stay, and surgical time. Results suggest Surgiflo cases were associated with significantly higher risk of multiple adverse outcomes, including major and minor complications, surgical revisions, transfusion for any blood products and longer surgery times than the Floseal<sup>®</sup> group. There were no significant differences in mortality and LOS. Results were similar in group 2 and 3. But this study has an important bias, because the first and corresponding author has a conflict of interest, while he is an employee of Baxter Healthcare Corporation (Tackett et al. 2014).

#### **4.4 General Surgery**

Despite all recent developments in surgical techniques, hemorrhage is an expected complication. If untreated, bleeding can lead to dehiscence, hemorrhage or post-operative infection resulting in surgical failure. Unlike adhesive and sealants,

**Table 2** Cardiovascular surgery

Author	Year	Multicenter/ Single center	Prospective/ Retrospective	Gender and number of patients	Age (years)	Hemostatic	Type of bleeding	Time to hemostasis (MIN)	Procedure time (MIN)	Pathology/ Procedure	Complications
Oz MC, Cosgrove III DM, et al.	2000	Multicenter	Prospective	32 M + 16 W 33 M + 12 W	63.7±9.3 (M), 66.5±15.1 (W) 61.9±11.5 (M), 70.3±11.7 (W)	Floseal® Control	Oozing and heavy bleeding	3 (72%) to 10 (94%) 3 (29%) to 10 (66%)	NA	Valve repair/ replacement, CABG, Redo CABG, orthotopic heart transplant, miscellaneous	None atypical for cardiac surgery; mediastinal bleeding and cough possibly related to Floseal
Reuthenbuch O, Lachat ML, et al.	2000	Single center	Prospective	12 M + 5 W (17)	NA	Floseal®	Pulsatile, severe and profuse	5.29 ± 2.7	NA	Peripheral vascular surgery	None
Weaver FA, Hood DB, et al.	2002	Multicenter	Prospective	89 (43 Floseal® + 46 GT; 51 M + 39 W)	21	Floseal® Gelfoam plus thrombin (GT)	Oozing, flowing, pulsatile	2.5 (median time) 6.5 (median time)	NA	Femoral bypass, carotid endarterectomy, AV fistula, aortic-femoral bypass, abdominal aortic aneurysm, aortic-renal bypass, aortic endarterectomy, carotid bypass, thrombectomy, femoral artery repair, visceral endarterectomy	None related to hemostatic agents
Nasso G, Piancone F, et al.	2009	NA	Prospective	209 (127 M + 82 W) 206 (132 M + 74 W)	68.5 ± 4.3 69.1 ± 4.1	Floseal® Topical hemostatic agent (control)	NA	3.8 ± 2.4 6.8 ± 3.1		Isolated coronary surgery, isolated valvular surgery, combined coronary/ valvular surgery, aortic surgery	None related to hemostatic agents

(continued)

Table 2 (continued)

Author	Year	Multicenter/ Single center	Prospective/ Retrospective	Gender and number of patients	Age (years)	Hemostatic	Type of bleeding	Time to hemostasis (MIN)	Procedure time (MIN)	Pathology/ Procedure	Complications
Benedetto F, Passari G, et al.	2010	Single center	Case report	1 (W)	70	Floseal®	NA	NA	NA	Voluminous aneurysm of a lower gluteus artery	None
Martinez CA, Rosen R, et al.	2010	Single center	Case report	1 (W)	53	Surgiflo				Symptomatic mitral paravalvular leak	
Borges Santos M, Silva S, et al.	2012	Single center	Cohort study	13	64 ± 9.46	Floseal®	NA	NA	10	Iatrogenic femoral artery pseudoaneurysms	None
Lee L, Henderson R, et al.	2012	Single center	Case report	1 (W)	84	Floseal®	NA	NA	2 hours	Aortic root rupture during TAVI	None
Tackett SM, Calcaterra D, et al.	2014	Multicenter (Premier's US Perspective Hospital Databases)	Retrospective	24,098	NA	Floseal® and Surgiflo, alone or combined ± other commonly hemostats	NA	NA	NA	CABG, aortic surgery, valve surgery	Major and minor complications (not specified)

W: women; M: men; CABG: cardiopulmonary bypass grafting; TAVI: transcatheter aortic valve implantation

gelatin matrix hemostatics are intraoperative tools that treat bleeding increasing the likelihood of successful surgical outcomes. Data from use of Floseal<sup>®</sup> and Surgiflo from general surgery are reported in Table 3.

#### 4.4.1 Liver

Recent advances in operative techniques have diminished the occurrence of post-surgical complications after hepatic resection. Despite these improvements, liver resection might still be associated with significant intraoperative blood loss. The predisposition of the liver to diffuse bleeding is directly related to its major vascularity, especially because of the presence of hepatic sinusoidal structure, with the absence of smooth muscle capable of contraction to induce vasoconstriction. As a consequence, traumatic injury (as hepatic parenchymal lacerations and fractures) and surgical incisions both tend to expose large, raw surfaces with multiple various bleeding areas that are not manageable to suturing and ligation. Accomplishing and maintaining hemostasis is mainly dependent on various key factors, including anesthetic and surgical techniques, the quality of the hepatic tissue, extrinsic, and intrinsic clotting factors. To accomplish not only the final control of the bleeding at the resection surface of the liver but also to prevent intraperitoneal complications secondary to bile leakage and fluid accumulation, the use of topical hemostatic agents has now gained wide acceptance. Gelatin matrix hemostatic agents have been tested in several clinical trials and small prospective randomized clinical studies have been documented with positive results. In a recent randomized trial with patients who underwent hepatic resection, the mixture of bovine collagen and thrombin associated with autologous plasma during surgery demonstrated to be more effectively able of controlling and halting diffuse bleeding from the liver tissue than a collagen sponge alone. To prevent bile leakage, perioperative treatment of the remnant hepatic tissue after resection is extremely important and use of topical hemostatic agent fleeces maybe helpful, although accurate preparation during removal of liver tissue remains the principal factor with meticulous placement of clips and sutures.

#### 4.4.2 Thyroid

Percentage of morbidity with surgery of the thyroid gland diminished greatly after standardization of the Thompson's technique of capsular dissection. Nowadays, the most frequent complications associated with thyroid surgery are recurrent laryngeal nerve palsy and hypoparathyroidism. Intraoperative hemorrhage may obscure important anatomical structures, thus complicating operative dissection, and causing indirect morbidity linked to lesion of laryngeal nerves and parathyroid glands due to blind procedures. Hence, the need for safer and more effective hemostatic procedures than the conventional hemostatic thermal methods to stop bleeding. Before Testini et al. (2009) randomized study, only one study uncontrolled study

**Table 3** General surgery

Author	Year	Multicenter/ Single center	Prospective/ Retrospective	Gender and number of patients	Age (years)	Hemostatic	Type of bleeding	Time to hemostasis	Procedure time (MIN)	Pathology/ Procedure	Complications
Henkel A, Cooper RA, et al.	2008	Single center	Retrospective	7 W	NA	Floseal®	NA	NA	NA	Breast cancer	Microcalcifications on mammography
Testini M, Marzatoli R, et al.	2009	Single center	Retrospective	35 M + 19 W (54) 38 W + 14 M (52) 39 W + 10 M (49)	16 to 75 (53) 19 to 79 (52) 18 to 82 (56)	Floseal® Tabotamp® None	NA	NA	105 122 133	Benign nodular goiter, thyroiditis, malignancy	Transient postoperative hypoparathyroidism (overall: 40), transient recurrent laryngeal nerve palsy (overall: 5), postoperative hemorrhage (Tabotamp®)

NA: not available; W: women; M: man

about use of Floseal<sup>®</sup> matrix in thyroid surgery was published (Tonante et al. 2006). The patients were randomized into three different groups, each using a different hemostatic maneuver: (1) use of classical surgical procedures to achieve hemostasis, such as ligature and bipolar electrocauterization alone, (2) use of Fibrillar oxidized regenerated cellulose (Tabotamp), and (3) use of Floseal<sup>®</sup> matrix hemostatic agent; in both group 2 and 3 hemostatic agents were used in addition to classical methods. Outcomes' measures were surgical time, time to removal of wound drain, length of postoperative stay, and incidence of morbidity after surgery. Morbidity measures included blood loss, hypoparathyroidism, and recurrent laryngeal nerve palsy. Mean surgical time was 133 min in the surgical hemostasis group versus 122 min in the Tabotamp group and 105 min in Floseal<sup>®</sup> group. Removal of the surgical drainage occurred earlier in the Floseal<sup>®</sup> group; also the length of hospital stay after surgery was shorter in the Floseal<sup>®</sup> group in comparison with the surgical hemostasis and Tabotamp group; in both of the parameters there was no statistical difference between the two groups. Regarding the morbidity, no statistical difference was distinguished among the three groups, confirming the observation that morbidity in thyroid surgery is not very dependent on intraoperative method performed to achieve hemostasis. By these results, gelatin hemostatic matrix agents seem to be an efficacious hemostatic agent for stopping bleeding during thyroid surgery.

#### 4.4.3 Trauma Surgery

Hemorrhage is the second cause of mortality in civilian trauma. Approximately, 80% of death are from wound that are not accessible from manual pressure and by that are treatable only with surgical procedures. The current damage control practice is formed of three different phases: (1) resuscitative surgery for management of hemorrhage and contamination; (2) intensive care unit admission concentrated on the correction of hypothermia, coagulopathy, and acidosis, called the "lethal triad"; (3) re-exploration for definitive control of injuries after the recovery of normal physiology (Pursifull et al. 2006). Four studies on animal model evaluate Floseal<sup>®</sup> as hemostatic agent in trauma, respectively, one on rat liver model, two on porcine renal model, and one on rat renal model. The first controlled trial was performed to assess the use of Floseal<sup>®</sup> as intracavitary hemostatic agent testing its ability to decrease hemorrhage and prolong life after direct injection to a liver lesion with open abdomen during application and with no supplementary compression. Immediate injection of Floseal<sup>®</sup> directly on to the injured liver surface without any compression reduced, but did not halt, hemorrhage. Contrary to the use of clamps and ligation, reduction of hemorrhage with Floseal<sup>®</sup> did not increase survival time nor survival rate. This dichotomy is not uncommon. These results, however, demonstrate the efficacy of Floseal<sup>®</sup> to transiently enhance mean arterial pressure and to decrease hemorrhage from damaged liver tissue with mixed venous, arterial, capillary, and sinusoidal hemorrhage without additional compression. Preliminary data indicate that a 5-min delay is excessive for a useful application as intracavitary



agent in a closed cavity (Klemcke 2006). The second study reported a porcine renal laceration model: 21 swine underwent celiotomy creating a complex superior pole injury of the kidney using a 4 × 4 cm cruciate press instrument. Cases were prospectively divided into three different treatment groups. The animals used in this experiment were treated with the application of gelatin matrix with (7 in group 1) or without (7 in group 2) preliminary renal artery occlusion. Control subjects (7 in control 3) were treated with conventional horizontal mattress sutured gelatin sponge bolster over the capsular injury. Gelatin matrix hemostatic use resulted in significantly less mean blood loss (80.7 and 99.0 mL in groups 1 and 2) versus classical suture treatment (191.8 mL in group 3). Time to hemostasis was similarly decreased (1.1, 2–2.5, and 5.8 min in groups 1–3, respectively). Follow-up abdominal computerized tomography with contrast medium showed no clinically significant perinephric fluid collections/larger than 2 cm). Floseal<sup>®</sup> appeared to provide effective hemostasis with and without preliminary vascular control (Hick et al. 2005). The third trial assessed the hemostatic efficacy of Floseal<sup>®</sup> in a porcine grade 5 renal injury. The gelatin matrix performed very well as a rapidly deployable effective hemostatic agent (hemostasis was complete after 2 min), without post-operative bleeding or significant hematoma in the perirenal area: no nephrotoxic effects were appreciated since renal function approached preoperative baseline within one week. Gelatin matrix is secure to apply near the collecting system because it remains a colloidal suspension in the presence of urine. Data suggest an increased role of Floseal<sup>®</sup> as an alternative to nephrectomy or renal fossa packing in injury control surgery with high-grade renal damage (Pursifull et al. 2006). In the last study, we found the authors performed a standardized heminephrectomy in 180 heparinized and normotensive Sprague-Dawley rats. Four different hemostatic agents were randomized compared (separate and in combination): microporous polysaccharide hemospheres, gelatin sponge and matrix, bovine thrombin, and freeze-dried recombinant factor VIIa (rFVIIa). Eight different treatment groups were studied, and the primary endpoint was stop of hemorrhage within 20 min. Hemostasis was obtained in all those animals treated with gelatin, with and without thrombin or rFVIIa. The groups with an effective treatment were subsequently evaluated for 60 min after hemostasis to check the stability of the clot, in which gelatin alone and in association with thrombin or rFVIIa was studied. 34% of the animals had a new hemorrhage with no significant difference between the various treatment groups (Björse and Holst 2009).

#### **4.5 Orthopedic Surgery**

Total knee arthroplasty is a popular surgical technique with really good results in the treatment of severe osteoarthritis (a degenerative disease). It is not free from complication, first of all an exaggerated blood loss, which may cause general complications and increased morbidity. Although techniques such as hypotensive or regional anesthesia and intra- or postoperative salvage of blood maybe used, the

appropriate use of intraoperative topical hemostatic agents is a better approach to minimize blood loss by enhancing local hemostasis perioperatively, potentially reducing necessity of concentrated red blood cells transfusion and related complications, as transfusion reactions (immunological rejection, anaphylactic reaction, hemolytic reaction), metabolic disorders and infectious disease. All the four clinical studies we found (Table 4) suggest that the use of gelatin hemostatic matrix in total knee arthroplasty provided secure, major control of hemorrhage and may decrease after surgery extravasation of blood into the tissue preventing the formation of hematoma. No differences between the incidences of infections were found, but an assessment after a protracted follow-up period is needed because infections may also occur later. Thromboembolic events are also an important concern: neither about this complication there were significant differences between the Floseal<sup>®</sup> and the control groups. In one of the most recent prospective study, 157 consecutive cases who underwent primary total knee arthroplasty received Floseal<sup>®</sup>: 5 mL was applied in 74 patients, while 10 mL in 83 patients. All cases received warfarin as thromboprophylaxis the first postoperative day. The review of the hospital chart of 100 consecutive patients who underwent total knee arthroplasty and immediately preceded the Floseal<sup>®</sup> groups and did not receive Floseal<sup>®</sup> (control group) was performed. After surgery, blood drainage was significantly lower in the Floseal<sup>®</sup> 5 mL (236.9 mL) and 10 mL (120.5 mL) groups compared with the control group (430.8 mL;  $p < 0.001$ ). The Floseal<sup>®</sup> 10 mL group had significantly less blood drainage than Floseal<sup>®</sup> 5 mL group ( $p < 0.001$ ), but the predicted probability of transfusion in the Floseal<sup>®</sup> 5 mL group was not significantly different compared with the control group (6% vs. 7.6%,  $p = 0.650$ ), while it was lower in the Floseal<sup>®</sup> 10 mL group (0.5% vs. 5.5%,  $p = 0.004$ ). In the 10 mL Floseal<sup>®</sup> group, application of gelatin matrix either ante or posttourniquet removal had a similarly significant effect on blood drainage percentage and anticipated the probability of blood transfusion. No real adverse events occurred related to gelatin matrix application (Velyvis 2015).

## 4.6 Otolaryngology

Absorbable hemostatic agents are used routinely in ear, nose and throat (ENT) surgeries. We found 25 articles evaluating use of Floseal<sup>®</sup>, and 2 evaluating use of Surgiflo, in otolaryngologic procedures (Table 5). Epistaxis is one of the most frequent emergencies for general practitioners. The management of this condition required first application of proper aid: patients rarely need to be treated by an ENT specialist. Epistaxis is commonly classified in anterior and posterior bleeds: this division lies at the piriform aperture anatomically. Most techniques used nasal package to tamponade the hemorrhage from the nasal vessels, which cause discomfort and pain to the patients, besides being cause of severe complications as nasal mucosal atrophy, alar necrosis, toxic shock syndrome, sleep apnea, and cardiovascular failure secondary to nasal-pulmonary reflex. As a result of their

**Table 4** Use of Gelatin matrix in Orthopedic surgery

Author	Year	Multicenter/ Single center	Number of patients and gender	Age (years)	Pathology/ Procedure	Hemostatic	Type of bleeding	Time to hemostasis	Procedure time	Complications
Kim Han Jo, Frasen MR, et al.	2012	Single center (Prospective)	10 (7 W + 3 M) 10 (6 W + 4 M)	54 to 81 (67.8) 59 to 77 (66.6)	Primary arthrosis/ Total Knee Arthroplasty	Floseal® Electrocautery	N/A	N/A	N/A	Postoperative hemoglobin level drop (lesser in Floseal® group)
Partezani Helito C, Gomes Gobbi R, et al.	2013	Single center (Prospective)	196 (97 Floseal® group + 99 control group)	Average: 72.7 Floseal® group, 70.1 control group	Degenerative joint disease (98%), osteonecrosis (2%) / Total knee arthroplasty	Floseal®	N/A	N/A	N/A	None related to use of Floseal®
Wang C, Han Z, et al.	2014	Meta-analysis (3 RCTs, 1 PCTs, 1 CCTs)	766	65.9 to 72.7 (mean)	Severe osteoarthritis / Total knee arthroplasty	Floseal®	N/A	N/A	N/A	Hemoglobin decline, infections
Velysis John H	2015	Single center (Prospective)	157 74 83	72 73	Total knee arthroplasty	Floseal® 5 mL Floseal® 10 mL	N/A	N/A	N/A	None

NA, not available, W: women, M: man; RCTs: randomized controlled trials, PTCs: prospective control trials, CCTs: case controlled trials

**Table 5** Use of Surgiflo and Floseal in Otolaryngology

Author	Year	Multicenter/ Single center Prospective/ Retrospective	Gender and number of patients	Age (years)	Pathology/ Procedure	Hemostatic	Type of bleeding	Time to hemostasis (MIN)	Procedure time (MIN)	Complications
Chandra RK, Conley DB, Kern RC	2002	Single center (Prospective)	20	N/A	ESS	Floseal® Thrombin-soaked Gelatin Foam	N/A	N/A	N/A	Granulation tissue and adhesion formation
Gall RM, Witterick JJ, et al.	2002	Single center (Prospective)	(18) 14 M + 4 F	25 to 65 (41.4 ± 11.1)	INE, INA, INP, septoplasty, intrasal partial turbinectomy, bilateral frontal sinusotomy	Floseal®	1.93 on a 5-point scale severity	<2 (1 to 5)	N/A	1 patient develop bleeding 6 hours after surgery, treated with Gelfoam
Baumman A, Caversaccio M	2003	Single center (Prospective)	(50) 31 M + 19 F	14 to 76 (46)	Endoscopic anterior ethmoidectomy	Floseal® vs Merocel™	N/A	3	N/A	1 case of postoperative bleeding on the 6 <sup>th</sup> day
Mathiansen RA, Cruz RM	2005	Single center (Prospective)	(35) 21 M + 14 F (35) 11 M + 24 F	6.8 ± 3.5 7.2 ± 3.8	Obstructive sleep apnea/ Adenoidectomy	Floseal® Cautery	N/A	0.6 ± 1.3 9.5 ± 5.4	N/A	3 patients in the cautery group were crossed over the Floseal® group
Chandra RK, Conley DB, et al.	2005	Single center (Retrospective)	18		ESS	Floseal®				Symptomatic adhesion
Jameson M, Gross CW, et al.	2006	Single center (Prospective)	(45) 21 M + 24 F	50.4 (M) 43.2 (F)	Bilateral FESS	Floseal®	N/A	16.4 (vs. 30.8 control group) after arrival in PACU	N/A	Nasal-drip/bleeding, not significant; crusting and scarring
Jo SH, Mathiansen RA, Gurushanthaiah D	2007	Single center (Prospective)	68	7 7.2 (2 to 16)	Adenotonsillectomy for adenotonsillar hypertrophy, obstructive sleep apnea, chronic tonsillitis	Floseal® (34) Electrocautery (34)	4-point VAS	NA	16 31.2	None
Shrime MG, Tabaei A, et al.	2007	Single center (Retrospective)	(172) 93 F + 79 M	46.1	Chronic rhinosinusitis / ESS with middle turbinate medialization	Floseal® (37: 21 F + 16 M)	N/A	N/A	N/A	Higher incidence of synchia formation (7), epistaxis (1) in Floseal® group

(continued)

Table 5 (continued)

Author	Year	Multicenter/ Single center Prospective/ Retrospective	Gender and number of patients	Age (years)	Pathology/ Procedure	Hemostatic	Type of bleeding	Time to hemostasis (MIN)	Procedure time (MIN)	Complications
Blackmore KJ, O'Hara J, et al.	2008	Single center (Retrospective)	30	>16	Tonsillectomy for recurrent tonsillitis	Floseal®	N/A	N/A	N/A	2 patients had a reactionary haemorrhage
Woodworth BA, Chandra RK, et al.	2009	Multicenter (Prospective)	(30) 17 M + 13 F	48.2 ± 15.1	Chronic sinusitis	Surgiflo	N/A	61 seconds (10 minutes products application)	N/A	None
Côté D, Barber B, et al.	2010	Single center (Prospective)	(10) 8 M + 2 F	21 to 88	Persistent epistaxis	Floseal®	N/A	N/A	N/A	None related to hemostatic agent
Beyea JA, Rotenberg BW, et al.	2011	Single center (Prospective)	10 (6 M + 4 F) 8 (4 M + 4 F)	38 to 69 (55.7) 35 to 72 (57)	FESS	Floseal® HemoStase	N/A	3 to 5	N/A	N/A
Mozet C, Pretin C, et al.	2011	Single center (Prospective)	176	>18	Cold-knife tonsillectomy because of recurrent tonsillitis, tonsillar hypertrophy or peritonsillar abscess	Floseal® (89) Bipolar electrocautery (87)	N/A	<2	N/A	None related to hemostatic agent
Soyka MB, Nikolaou G, et al.	2011	Single center (Retrospective study)	537 (M to F ratio 5:4)	11 to 96 (70)	Epistaxis	Floseal®	N/A	N/A	N/A	None related to hemostatic agent
Ujam A, Awad Z, et al.	2012	Single Center (Prospective)	(42) 28 F + 14 M	13 to 82 (54)	Head and neck surgery	Floseal®	N/A	N/A	111 (30 to 240)	Hematoma (2 patients)
Burret G, Pavic M, et al.	2013	Single center (Retrospective)	2 (M)	58 and 89	Recurrent epistaxis in hematology units	Surgiflo	N/A	N/A	N/A	N/A

M: male; F: female; N/A: not available; FESS: functional endoscopic sinus surgery, PACU: post-anesthesia care unit; VAS: visual analogue scale, ESS: endoscopic sinus surgery, INE: intranasal ethmoidectomy, INA: intranasal antrostomy, INP: intranasal polypectomy, ESS: endoscopic sinus surgery

particular nature, Floseal<sup>®</sup> and Surgiflo<sup>®</sup> can be well applied topically at the bleeding area; the gelatin granules conform to irregular surfaces and adhere hard to wet tissue as mucosal. Floseal<sup>®</sup> is more efficient at early control of epistaxis than nasal packing and easier to use to achieve hemostasis. Furthermore, patients experience minor discomfort at initial epistaxis control and at the follow-up visit, with more final satisfaction. Floseal<sup>®</sup> and Surgiflo<sup>®</sup> also demonstrated to be effective in recovering patients in whom hemostasis was not achieved using packing. Gelatin matrix hemostatic agents are also commonly used to obtain hemostasis during endoscopic sinus surgery, in which postoperative bleeding is commonly treated with packing or stents. The main drawbacks are the same of the previously listed, in addition to sensation of intranasal and periorbital pressure, Eustachian tube obstruction or dislocation of the packing with possible aspiration and septal perforation. The postoperative synechia formation after endoscopic sinus surgery has been linked to poor postoperative outcomes and higher rates of revision surgery. Multiple methods of middle turbinate medialization have been described in an attempt to decrease its occurrence. In a retrospective chart review, the use of Floseal<sup>®</sup> significantly increases the risk of synechia formation, data that may argue against its routine use. A more recent prospective controlled study using rabbit model demonstrated how topical hemostatic agents have completely different effects on healing of the mucosa. Floseal<sup>®</sup> significantly obstructed the re-epithelialization process and were directly included into sinus mucosa that healed. Evaluation with hematoxylin and eosin staining consented to identify the prominent eosinophilia as a part of the inflammatory reaction. This finding suggests that there maybe an allergic reaction in addition to foreign body response in the animal model. The fact that Floseal<sup>®</sup> is a product derivate from animal, it maybe possible that an allergic reaction could occur also in human subjects. The capacity of Floseal<sup>®</sup> to promote an intense inflammatory reaction in the face of an intact mucosal barrier maybe less related to its absorption kinetics and more related to a congenital irritating effect of this material on the host tissue. If topical hemostatic materials with slow resorption kinetics as Floseal<sup>®</sup> are used following endoscopic sinus surgery, it could be more prudent to frequently irrigate surgical field with saline solution to decrease the amount and duration of exposure of foreign hemostatic agents to healing sinus mucosa. Another common procedure performed in otolaryngology is adenotonsillectomy. Floseal<sup>®</sup> has been reported to control bleeding ranging from capillary oozing to arterial spurting, decreasing intraoperative blood loss, surgical time and postoperative morbidity with lower pain scores, less postoperative pain medication and rapid return to regular activity when compared to classical electrocoagulation hemostasis. A recent study evaluated the effectiveness of Floseal<sup>®</sup> compared to bipolar electrocoagulation after tonsillectomy. 176 adult patients underwent cold-knife tonsillectomy due to tonsillar hypertrophy, recurrent tonsillitis, or tonsillar abscess. Patients were randomly allocated to either Floseal<sup>®</sup> or electrocoagulation for hemostasis during surgical cold-knife tonsillectomy. Five different surgeons judged the handling of Floseal<sup>®</sup> application using a five-point scale, from very good to very poor. Pain scores after surgery were classified with a scale for 20 days; the duration and consumption of

pain were compared. Wound healing was evaluated on days 1–5, 10 and 20. Overall 98.7% of surgeon evaluations of Floseal<sup>®</sup> handling were evaluated at least “good.” Patients treated using gelatin matrix showed improved wound healing, with less thickness of wound plaques, in the postoperative observation period, with a trend for diminished postoperative pain, and a shorter duration of pain medication use (mean 2.1 days) and also less pain medication use. There were no differences in the rate of surgical blood loss between the two groups, with 4.9% for Floseal<sup>®</sup> and 6.0% for electrocautery patients. This study demonstrated the easy handling of Floseal application and showed the beneficial effects of its use on mucosal recovery. Furthermore, Floseal<sup>®</sup> was associated with a significantly diminished time of pain medication use and decrease in consumption (Mozet et al. 2012). At least, Floseal<sup>®</sup> has been used in bleeding control during dermabrasion, cryosurgery, free-hand surgical scalped shaving and laser for the treatment of rhinophyma, a rare condition due to hyperplasia of sebaceous and fibrous tissue of the nose.

#### ***4.7 Urology and Andrology***

Achieving hemostasis has always been demanding in the surgical theater. The modern surgeon is faced with several tools to perform hemostasis. The explosion in the use of hemostatic agents and sealants has been reported also in the recent urological literature: we found 33 articles evaluating use of Floseal<sup>®</sup> and Surgiflo during urological surgeries (Table 6). As the indication for biosurgical hemostatic agents increases, there is a question about what happens to these materials as they get in the urinary collecting system. Oxidized regenerated cellulose and fibrin glue initially maintain a solid form when applied directly in contact with urine and later form a gelatinous state, while polyethylene glycol assumes a solid clot that does not change for the next 5 days. However, hemostatic gelatin sealant matrix remains as fine particulate suspension in both normal and bloody urine so that the signification of these findings regarding the sealing of the renal parenchyma or the collecting system must be controlled. Online library is plenty of urological procedures in which surgeons use Floseal<sup>®</sup> and Surgiflo<sup>®</sup> to achieve hemostasis. Particularly there are numerous reports about gelatin matrix hemostatic use during laparoscopic partial nephrectomy, a conservative technique that improves the postoperative outcomes compared with open partial nephrectomy in the treatment of small renal cancer. Efficacy to obtain hemostasis with Floseal<sup>®</sup> has been evaluated also in prostatectomy procedures, enucleoresection, tubeless percutaneous nephrolithotomy, nephrostomy, percutaneous renal cryoablation, heminephrectomy, and laparoscopic nephron-sparing surgery. Conservative renal surgery is usually the surgical treatment of choice in cases of small renal cancer. Laparoscopic partial nephrectomy (LPN) has been described to improve clinical outcomes after surgery compared with open partial nephrectomy. We found various animal studies evaluating the effectiveness of Floseal<sup>®</sup> during laparoscopic partial nephrectomy. In the first study, an open right lower-pole partial nephrectomy was performed by the

**Table 6** Urology and andrology

Author	Year	Multicenter/ Single center	Prospective/ Retrospective	Gender and number of patients	Age (years)	Hemostatic	Type of bleeding	Time to hemostasis	Procedure time	Pathology/ Procedure	Complications
Bhayani SB, Grubb III RL, et al.	2002	Single center	Case report	1	55 (M)	Floseal®	NA	NA	NA	Repair of diaphragmatic injury during laparoscopy for renal cell carcinoma	None
Richter F, Schnorr D, et al.	2003	Single center	Retrospective	25	NA	Floseal®	NA	116 sec	NA	Renal cell carcinoma (partial nephrectomy)	None
Lee DJ, Uribe C, et al.	2004	Single center	Case report	2 (W)	46 and 56	Floseal®	NA	NA	180 and 75	PCNL	None
Ahlering TE, Eichel I, et al.	2005	Single center	Retrospective	150 (M)	NA	Floseal® Gelfoam Bipolar electrocautery	Pulsatile	NA	NA	Radical prostatectomy cautery-free neurovascular bundle preservation	None related to hemostatic agents
Borin JF, Sala LG, et al.	2005	Single center	Prospective	10	NA	Floseal®	NA	NA	NA	PCNL	NA
Triaca V, Zagha RM, Libertino JA	2005	Single center	Prospective	23 M + 20 W (43)	32 to 75 (58.5)	Floseal®	NA	NA	256.4 (mean time)	Nephron sparing surgery for renal tumors	None related to hemostatic agents
Wille AH, Tüllmann M, et al.	2005	Single center	Retrospective	44	33 to 79 (61)	Floseal®	NA	NA	210 min	Laparoscopic partial nephrectomy in renal cell cancer	None related to hemostatic agents
Kaul S, Laungian R, et al.	2006	Single center	Prospective	7 M + 3 W (10)	59 (mean age)	Floseal®	NA	NA	155 min	Partial nephrectomy for small exophytic renal masses	Urinary leak (1 patient), persistent bleeding (1 patient)
Breda A, Stepanian SV, et al.	2007	Multicenter	Retrospective	1347	NA	Floseal® Tissel BioGlue Glubran Surgicel	NA	NA	NA	Laparoscopic partial nephrectomy (renal tumors)	Postoperative bleeding requiring transfusion (28 patients), urinary leakage (20 patients)

(continued)



Table 6 (continued)

Author	Year	Multicenter/ Single center	Prospective/ Retrospective	Gender and number of patients	Age (years)	Hemostatic	Type of bleeding	Time to hemostasis	Procedure time	Pathology/ Procedure	Complications
Gong EM, Zorn KC, et al.	2007	Single center	Case report	3 (M)	62 and 73 (same procedure), 69	Floseal®	NA	NA	NA	Laparoscopic radical nephrectomy (1), RLRP (2)	None
Zorn KC, Gong EM, et al.	2007	Single center	Prospective	84 (52 requiring CSR)	35 to 83 (61, requiring CSR) and 23 to 82 (59.2 not requiring repair)	Floseal®	NA	NA	238 (with CSR) vs 207 (without CSR)	CSR during laparoscopic partial nephrectomy (T1 renal tumors)	None related to hemostatic agent
Celia A, Zeccolini G, et al.	2008	Multicenter	Retrospective	592	NA	Floseal® Tissucol BioGlue Glubran	NA	NA	NA	Laparoscopic nephron sparing surgery	None
Abraham JBA, Gambao AJR, et al.	2009	Single center	Prospective	8 M + 4 F (12; 2 masses in one patients)	45 to 77 (59)	Floseal®	NA	NA	2.9 hours	Percutaneous renal tumor cryoablation	None
Guzzo TJ, Pallock RA, et al.	2009	Multicenter (single surgeon, two institutes)	Prospective	19 21	23 to 66 (50.7) 34 to 72 (56)	Floseal® Cellfoam	NA	NA	150 min	Laparoscopic partial nephrectomy	Postoperative urine leak (1 for group), postoperative pseudoneurysms (2, Floseal® group)
Kaufmann OG, Sountoulides P, et al.	2009	Single center	Prospective	10	NA	Floseal®	NA	NA	NA	PCNL	None

(continued)

Table 6 (continued)

Author	Year	Multicenter/ Single center	Prospective/ Retrospective	Gender and number of patients	Age (years)	Hemostatic	Type of bleeding	Time to hemostasis	Procedure time	Pathology/ Procedure	Complications
Madi R, Wolf S Jr	2009	Single center	Retrospective	2 M + 1 W (3)	59 and 76 (M), 55 (W)	Floseal®	NA	NA	246 min (mean time)	Laparoscopic partial nephrectomy	Slight elevation in serum creatinine level on postoperative day 1
Nadler RB, Perry KT, et al.	2009	Single center	Prospective	16	NA	Floseal® BioGlue	NA	NA	435 min (mean time)	Clampless partial nephrectomy	None
Wille AH, Johannsen M, et al.	2009	Single center	Prospective	102	26 to 79 (58)	Floseal®	NA	NA	201 min (mean time)	Laparoscopic partial nephrectomy	None related to hemostatic agent
Li R, Louie MK, et al.	2010	Single center	Prospective	31	57 50.2 59.8 (mean age)	Floseal® (10 patients) Fascial sitch (10 patients) Cope loop (11 patients)	NA	NA	NA	PCNL	1 patient with multiple sclerosis had an exacerbation of symptoms (Floseal® group), 2 patients had postoperative hospital stays complicated by low-grade fevers (Cope loop and fascial sitch groups)
Pace G, Saldutto P, et al.	2010	Multicenter	Prospective	17 M + 13 W (30)	52.5 (median group 1 vs 2)	Floseal® ISC	NA	8.1 12.9	58.7 ± 12 62.4 ± 15	T1 Renal cell carcinoma	None
Waldert M, Remzi M, et al.	2011	Single center	Prospective	142 (32 with Floseal®)	61.6 ± 6.3 (Floseal® group)	Floseal®	NA	NA	NA	Lymphadenectomy in radical prostatectomy	None

(continued)

Table 6 (continued)

Author	Year	Multicenter/ Single center	Prospective/ Retrospective	Gender and number of patients	Age (years)	Hemostatic	Type of bleeding	Time to hemostasis	Procedure time	Pathology/ Procedure	Complications
Palacios DA, McDonald M, et al.	2013	Single center	Retrospective	13 M + 10 W (23)	57.9 ± 10.4	Floseal® (11) Aristar® (12)	NA	NA	NA	Partial nephrectomy for renal tumor (renal cell carcinoma and oncocytomas)	2 intraoperative; transfusion for blood loss, small ipsilateral pneumothorax; 5 post-operative; prolonged urinary leak, readmission for chest pain, ileus; reduction >25% GFR
Antonelli A, Minervini A, et al.	2015	Multicenter	Prospective	820	61.7 62 64.3 (mean age)	Floseal® (489) TachoSil (200) No hemostatic agent (131)	NA	NA	130 127.5 132.5 (mean time)	Partial nephrectomy for renal tumor	None related to hemostatic agent

W: women, M: men; ISC: infrared-sapphire coagulator, PCNL: percutaneous nephrolithotomy, NA: not available, CSR: Collecting system-repair, RLRP: laparoscopic radical prostatectomy

authors on 15 female pigs. In 5 cases (control group) the defect was repaired using standard open techniques, Tisseel alone (group 1) was used in 6 and Floseal<sup>®</sup> followed by Tisseel was used in 4 cases (group 2). Operative times were decreased in groups 1 and 2, achieving statistical significance in the first study group. In both study groups warm ischemia times were significantly improved, while time to bleeding control was significantly shorter in group 2. Estimated blood loss did not differ significantly in the three groups. After hilar control, in study group 1 where Tisseel was applied alone, hemorrhage under the Tisseel was noted after releasing the hilar clamp. 7 days after surgery, one urinoma and three urine leaks were appreciated in the control group; in Tisseel alone group, one urinoma and four urine leaks were discovered, while in group 2 there was no urinomas and only one urine leak. As results, Tisseel applied over Floseal<sup>®</sup> had a better control in major vascular and collecting system injuries without other surgical procedures (L'Esperance et al. 2005). In the second study, the authors compared the effectiveness of three biologic hemostatic devices with the conventional suture during laparoscopic partial nephrectomy in a hypertensive porcine model. 40 pigs undergoing bilateral LPN were randomly divided into 4 groups. Right LPN involved 30% of the renal parenchyma without a urinary tract opening, while left LPN involved 40% of the renal parenchyma with a urinary tract opening. Fibrin/thrombin sealant (Quixil), was applied on the section of the kidney in group 1, fibrin glue (Tissucol) in group 2, while in group 3 gelatin matrix with thrombin (Floseal<sup>®</sup>) was used, and in group 4 only conventional sutures. Left retrograde pyelography was performed 10 days after surgery. Data revealed that the estimated blood loss was significantly lower in the pigs treated with suture or Floseal<sup>®</sup>. Furthermore, the application of Floseal<sup>®</sup> reduced the warm ischemia time compared with use of suture, but in the pigs treated with suture the leaking pressure was better. The mean area of necrosis around the renal section was shorter when using the biosurgical hemostatics and not the sutures. Use of Floseal<sup>®</sup> resulted significantly efficient for improving hemostasis and warm ischemia (Rouach et al. 2009). The treatment of choice for large kidney stones is the percutaneous nephrolithotomy (PCNL). We found a study where the authors examined the effect of topical hemostatic materials in the urinary collecting system of pigs after injection through a percutaneous nephrostomy (PCN) tract: the animal model study was performed in 40 kidneys of domestic pigs. The pigs were divided into four groups of six animals: Floseal<sup>®</sup> (group 1), Tisseel (group 2), Coseal (group 3), and BioGlue (group 4). The contralateral kidney was used as control in only 16 pigs that tolerated the surgical procedure. Urinary tracts were dilated to 30 F and 2 mL of the hemostatic agent was applied to the urinary collecting system of pigs. After 5 days, no obstruction was detected among the control PCN kidneys. But, four of six kidneys injected with BioGlue and also half of six kidneys injected with Floseal<sup>®</sup>, Tisseel, or Coseal were obstructed. In all of these obstructive cases, a retroperitoneal urinoma was associated (Kim et al. 2007). Another study examined the efficacy and feasibility of a streamlined sutureless system to repair defects of the renal parenchyma and collecting system. Ten kidneys of five pigs were used for a left-side transperitoneal laparoscopic heminephrectomy, followed 14 days later by right-side heminephrectomy with complete ureteral

transaction to provide a mechanical stressor on the repair, followed 14 days later by euthanasia: in all the pigs, after hilar clamping, the lower pole of the kidney was resected with a bipolar electrocautery. Hemostasis was achieved with argon beam coagulator and Floseal<sup>®</sup>, followed by ProPatch-BioGlue “sandwich,” a sutureless repair. Mean operative time was 77.8 min and estimated blood loss was 49.5 mL. Immediate hemostasis was appreciated in all animals demonstrated after hilar clamp release. At euthanasia, there was not any collecting system leakage at pyelography, and in all case,s closure and healing were confirmed. At euthanasia, four out of five pigs had intact renal function. The principle that sutureless laparoscopic heminephrectomy is effective in chronic and physiological obstruction in the porcine model was thus provided by this study (Derweesh et al. 2008). In addition, a specific in vitro study of what occurs at hemostatic material when entering in contact with urine was found. Because the indication for use of biosurgical hemostatic agents enlarges in urology, the authors produced various in vitro experiments mixing three hemostatic agents with normal and bloody urine to discover what occurs to these agents when in contact with the urinary collecting system. Four commercial products were studied: Surgicel<sup>®</sup> (an oxidized regenerated cellulose), Tisseel<sup>®</sup> (a fibrin sealant), Floseal<sup>®</sup> (the gelatin matrix hemostatic we are focusing on in these review), and CoSeal<sup>®</sup> (as polyethylene glycol). They made three samples for each substance, in which 10 mL of human urine was added. The 12 samples tubes were then capped and placed at 37 °C on a tube shaker at slow speed. The material’s consistency observation were made at various hours, from 6 to 120 h. Floseal<sup>®</sup> was tested in different tubes with urine with various amounts of blood. They observed that gelatin matrix was immediately transformed by urine into a fine colloidal suspension that did not change over the 5 days of the study. When in contact with blood clot, Floseal<sup>®</sup> appeared to be part of a clot or remained in a colloidal suspension. After 5 days, all blood clots and gelatin matrix had dissolved and appeared as fine particulate suspension. By the results of this study, the conclusions were that fibrin glue and oxidized regenerated cellulose assume a semisolid gelatinous state, which is still present at 5 days, while polyethylene glycol forms a solid clot initially and do not change after 5 days. Only hemostatic gelatin matrix remained a fine particulate suspension in both normal and sanguineous urine. Obviously, the implications of these conclusions in repair of urinary collecting system after laparoscopic or percutaneous approach need further in vivo study (Uribe et al. 2005).

#### ***4.8 Gynecological and Obstetrics Surgery***

Hemostatic sealants are frequently used in gynecological surgery. We found 16 articles evaluating use of Floseal<sup>®</sup> and Surgiflo in this kind of surgery (Table 7). Application of Floseal<sup>®</sup> gelatin matrix in laparoscopy and inguinal lymphadenectomy has been reported. Similarly, use of Floseal<sup>®</sup> in obstetric cases of re-laparotomy after cesarean delivery and postcesarean hysterectomy for persistent

postpartum hemorrhage have been described. Although hemostasis has been achieved with great results in all the reports, few postoperative adverse reactions have been notified too: small bowel obstructions (Hobday et al. 2009; Suzuki et al. 2010), caseating granulomata (Shashoua et al. 2009), and eosinophil-rich inflammatory response with postoperative pelvic pain (Thomas and Trawfic 2009). Worldwide, early postoperative adhesion defined as small bowel obstruction is a relatively common complication in women undergoing a major gynecologic procedure that occurs within the first 30 postoperative days. Immediate postoperative stasis in the presence of prothrombotic agents on cellulose matrix is a reasonable and likely cause of adhesion formation that should be considered in differential diagnosis of a patient with early postoperative small bowel obstruction. In one case, giant cell granulomas secondary to the use of Floseal<sup>®</sup> were mistaken for metastatic leiomyosarcoma. The patient underwent a laparoscopic supracervical hysterectomy and bilateral salpingo-oophorectomy. According to the operative report, Floseal<sup>®</sup> was applied to the cervical stump for adhesion prevention. Gelatin matrix should be used only as pure hemostatic agent when control of bleeding is needed, not as a prophylactic measure or for adhesion prevention. Besides, excess of gelatin granules not incorporated in the clot should be removed to prevent foreign body reaction. A pilot study was performed to evaluate the use of Floseal<sup>®</sup> for minor bleeding control of the ovarian wall after the laparoscopic stripping procedure for endometriomas removal. The study included 20 consecutive patients who underwent laparoscopic excision of endometriomas. 8 patients were allocated to Floseal<sup>®</sup> group, whereas the remaining 12 patients were allocated to the control group. At the end of the laparoscopic stripping procedure for the treatment of ovarian cysts, with a diameter from 3 to 6 cm, to detect the exact localization of bleeding spots, the ovarian cortex was carefully everted and entirely flushed. In the Floseal<sup>®</sup> group the areas of hemorrhage were covered with gelatin matrix using a laparoscopic applicator under direct vision. Gentle pressure of the ovary was applied for five consecutive minutes and subsequently the areas of bleeding were reexamined. In the control group, hemostasis was obtained with conventional methods. Hemostasis was obtained in all cases by 3 min from Floseal<sup>®</sup> application in both study arms. The time of hemostasis was similar in control and Floseal<sup>®</sup> groups with a median time of 172 and 182 s, respectively (Angioli et al. 2009).

#### **4.9 Ophthalmology**

In the entire literature on gelatin matrix use, we found only one prospective comparative study evaluating the efficacy of Floseal<sup>®</sup> in ophthalmological patients, all of them undergoing external dacryocystorhinostomy (DCR) surgery with a large bony rhinostomy and sutured mucosal flaps (Table 8). Use of Floseal<sup>®</sup> was compared with nasal packing performed using ribbon gauze. In the gelatin matrix group, one patient was excluded from analysis because of non-correct use of Floseal<sup>®</sup>; of the other 9 patients, only 2 presents minimal bleeding immediately and 12 h after

**Table 7** Gynecology and obstetric surgery

Author	Year	Multicenter/ Single center	Prospective/ Retrospective	Number of Patients	Age (years)	Hemostatic	Type of bleeding	Time to hemostasis	Procedure time	Pathology/ Procedure	Complications
Han LY, Schimp V, et al.	2004	Single center	Case report	1	86	Floseal®	Lymphatic drainage	NA	NA	Groin breakdown after inguinal lymphadenectomy for vulvar cancer	None
Moriarty KT, Premila S, Bulmer PJ	2008	Single center	Case report	1	35	Floseal®	Oozing, several hemorrhage	NA	NA	Massive obstetric hemorrhage (postpartum)	None related to hemostatic agent
Angioli R, Muzii L, et al.	2009	Single center	Prospective	20 ( 8 Floseal® + 12 control)	23 to 43 (32 ± 6)	Floseal®	NA	3 min (Floseal®) 172 sec; 182 sec control group)	52.7 ± 12 min (Floseal®) vs 49.1 ± 8 (control group)	Endometrioma, Pelvic pain, primary infertility	None
Ebert AD, Hollauer A, et al.	2009	Single center	Case report	1	36	Floseal®	NA	35 s	NA	Laparoscopic ovarian cystectomy	None
Hobday CD, Miliam MR, et al.	2009	Single center	Case report	1	46	Floseal®	NA	NA	NA	Laparoscopic staging for endometrial cancer	Postoperative small bowel obstruction
Shashoua AR, Gill D, et al.	2009	Single center	Case report	1	61	Floseal®	NA	NA	NA	Previous laparoscopic supracervical hysterectomy	Caseating granulomata
Thomas PJ, Tawfic SN	2009	Single center	Case report	3	38 35 30	Floseal®	NA	NA	NA	Complex eft ovarian cyst Right adnexal enlargement and cul-de-sac nodularity Tubal ligation and vaginal hysterectomy	Eosinophil-rich inflammatory response

(continued)

Table 7 (continued)

Author	Year	Multicenter/ Single center	Prospective/ Retrospective	Number of Patients	Age (years)	Hemostatic	Type of bleeding	Time to hemostasis	Procedure time	Pathology/ Procedure	Complications
Law LW, Chor CM, Leung TY	2010	Single center	Case report	1	35	Floseal®	Postpartum hemorrhage	NA	NA	Placenta previa type III	None
Madhuri TK, Tailor A, Butler-Mannuel S	2010	Single center	Case report	1	75	Floseal®	NA	< 4 min	NA	Debulking surgery for advanced ovarian carcinoma	None
Suzuki Y, Vellinga TT, et al.	2010	Single center	Case report	2	44 and 47	Floseal®	Persistent oozing			Previous laparoscopic surgery	Small bowel obstruction
Gorry A, Morelli ML, et al.	2011	Single center	Case report	1	32	Floseal®	NA	NA	NA	Laparoscopic management of abdominal ectopic pregnancy	None
Wohlmueth CT, Merced JD	2011	Single center	Case report	1	28	Floseal®	Profuse bleeding	NA	NA	Tertiary repeat cesarean delivery for complete placenta previa	None
Lemma R, Albrech M, Bauer G	2012	Single center	Case report	1	30	Floseal®	Postpartum hemorrhage	NA	NA	Hypofibrinemia due to primary acute fatty liver of pregnancy	None
Clapp M, Huang JC	2013	Single center	Case report	1	33	Floseal®	active	NA	NA	Tubal ectopic pregnancy	None



**Table 8** Ophthalmology

Author	Year	Multicenter/ Single center	Prospective/ Retrospective	Gender and number of patients	Age (years)	Hemostatic	Type of bleeding	Time to hemostasis (MIN)	Procedure time	Pathology	Complications
Duranni OM, Fernando AI, Reuser TQ	2007	Single center	Prospective	10 (3 using Aspirin) gender NA 10, gender NA	NA	Floseal Nasal packing		2 NA	NA NA	Tearing (ephipora) Tearing (ephipora)	Minimal bleeding in a patient taking aspirin Mild to moderate postoperative bleeding, discomfort pain, alar necrosis, sleep apnea, toxic shock syndrome, nasal mucosal atrophy, cardiovascular shock

operation, no one at 24 h after surgery. Instead, all the patients in comparative group had mild to moderate postoperative bleeding until 12 h after the operation and 5 of them up to 24 h after surgery too. These data were statistically significant. The average time to accomplish hemostasis was 120 s and a more comfortable postoperative time was reported in the group in which Floseal<sup>®</sup> was applied. There are some consideration about the limitation of this pilot study: the nasal packing technique differences from non-nasal packing so the patients underwent that surgical procedure were not a real control group; the sample size was fairly small and there was potential biases in the subjective data collection. However, no complication in the use of Floseal<sup>®</sup> was reported (Duranni et al. 2007).

## 5 Tolerability and Complications

The tolerability and a summary of the most frequent complications of Floseal<sup>®</sup> were obtained from the studies discussed in Sect. 3. Adverse events that theoretically may occur with the use of fibrin sealants include hypersensitivity or allergy reactions and the maturation of antibodies against component of fibrin sealant or hemostatic products. There is also a risk, which has not been observed in clinical studies, of thromboembolic events (only two retrospective studies have evaluated the possibility of association between the use of hemostatic matrix and thromboembolic complications as deep vein thrombosis and/or pulmonary embolism) or disseminated intravascular coagulation, because of inadvertent intravascular injection, or anaphylaxis with the use of fibrin sealants.

## 6 Dosage and Somministration

In USS and EU, Floseal<sup>®</sup> and Surgiflo<sup>®</sup> are indicated as supportive treatment in patients undergoing surgery when control of hemorrhage (ranging from oozing to spurting) using classical surgical techniques (ligatures, suture, or cautery) is inadequate or not effective. Floseal<sup>®</sup> and Surgiflo<sup>®</sup> are indicated for topical used and should be applied on the surface of bleeding tissue only.

Floseal<sup>®</sup> has to be reconstructed before use: lyophilized bovine gelatin has to be assembled with human thrombin stored in the hemostatic kit; thrombin compound has to be reconstituted with calcium chloride (40  $\mu\text{mol/mL}$  with a concentration of thrombin of approximately 500 IU/mL). Floseal<sup>®</sup> gelatin from a 10 mL kit, when hydrated with 8 mL of the thrombin solution yielding approximately 10 mL of final product with about 400 IU/mL of thrombin. The amount of product used depends on the surgical bleeding site to be treated and the method of application should be individualized by the treating physician. One dose of 5 mL application approximately cost from \$160 to \$340 per case. Prescribing information should be

consulted to comprehend the dosage and administration, and the precautions of use, contraindications, and warning.

Surgiflo<sup>®</sup> also has to be prepared before injection: when the original hemostatic property of the flowable gelatin matrix is not sufficient, a subsidiary effect can be obtained by adding exogenous thrombin.

## 7 Conclusions: Place of Fibrin Sealant in the Management of Hemostasis in Surgery

Whatever is the surgical specialty, speaking of an ideal hemostatic agent means referring to something that answers to determinate characteristics: easily use, effectiveness, safety, and low price. Nowadays many topical hemostatic agents are available to control bleeding during surgical procedures: fibrin sealants, tissue glues, gelatin matrix. Any of these shows a series of advantages and disadvantages. In the end, no one embodies all the criteria to define itself “ideal.” Therefore, surgeon choice leads on other factors, such as severity, location and type of bleeding, hemostatic agent’s mechanism of action, possible interactions, costs and patient’ singularity on coagulation system. For example, collagen-, cellulose- and gelatin-based hemostats depend on intact clotting mechanism and are less efficacious in coagulopathic patients; therefore, agents such as fibrin sealants, which are independent of the patient’s clotting mechanism, maybe more appropriate for these patients.

## 8 Conflict of Interest

The authors declare that they have no conflict of interest.

## References

- Aguilar Palacios D, Mcdonald M, Miyake M, Rosser CJ (2013) Pilot study comparing the two hemostatic agents in patients undergoing partial nephrectomy. *BMC Res Notes* 6:399–403
- Ahlering TE, Eichel L, Chou D, Skarecky DW (2005) feasibility study for robotic radical prostatectomy cautery-free neurovascular bundle preservation. *Urology* 65(5):994–997
- Angioli R, Muzii L, Montera R, Damiani P, Bellati F, Plotti F, Zullo MA, Ortoni I, Terranova C, Benedetti Pacini P (2009) Feasibility of the use of novel matrix hemostatic sealant (FloSeal) to achieve hemostasis during laparoscopic excision of endometrioma. *J Minim Invasive Gynecol* 16(2):153–156
- Antisdel JL, Janney CG, Long JP, Sindwani R (2008) Hemostatic agent microporous polysaccharide hemospheres (MPH) does not affect healing or Intact sinus mucosa. *Laryngoscope* 118:1265–1269

- Antonelli A, Minervini A, Mari A, Bertolo R, Bianchi G, Lapini A, Longo N, Martorana G, Mirone V, Morgia G, Novara G, Porpiglia F, Rocco B, Rovereto B, Schiavina R, Simeone C, Sodano M, Terrone C, Ficarra V, Carini M, Serni S, members of the RECORD project-LUNA foundation (2015) TriMatch comparison of the efficacy of Floseal versus Tachosil versus no hemostatic agents for partial nephrectomy: results from a large multicenter dataset. *International J Urol* 22:47–52
- Baumann A, Caversaccio M (2003) Hemostasis in endoscopic sinus surgery using a specific gelatin-thrombin based agent (FloSeal™). *Rhinology* 41:244–249
- Bedi DA, Toms SA, Dehdashti AR (2011) Use of hemostatic matrix for hemostasis of the cavernous sinus during endoscopic endonasal pituitary and suprasellar tumor surgery. *Skull Base* 21(3):189–192
- Benedetto F, Passari G, Stilo F, La Spada M, Cotroneo A, Lentini S, Spinelli F (2010) Use of FloSeal in the endovascular treatment of voluminous aneurysm of a lower gluteus artery. *Minerva Chir* 65(1):117–121
- Benito J, Abraham A, Gamboa AJR, Finley DS, Beck SM, Lee HJ, Santos RJS, Box GN, Deane LA, Vajgrt DJ, McDougall EM, Clayman RV (2009) The UCI Seldinger technique for percutaneous renal cryoablation: protecting the tract and achieving hemostasis. *J Endourol* 23(1):43–49
- Berreoet F, De Hemptinne B (2007) Use of topical hemostatic agents during liver resection. *Dige Surg* 24:288–293
- Beyea JA, Rotenberg BW (2011) Comparison of purified plant polysaccharide (HemoStase) versus Gelatin-Thrombin matrix (FloSeal) in controlling bleeding during sinus surgery: a randomized controlled trial. *Ann Otol Rhinol Laryngol* 120(8):495–498
- Bhayani SB, Grubb RL III, Andriole GL (2002) Use of gelatin matrix to rapidly repair diaphragmatic injury during laparoscopy. *Urology* 60(3):514i–514ii
- Björkses K, Holst J (2009) Topical haemostatics in renal trauma—an evaluation of four different substances in an experimental setting. *J Trauma* 66:602–611
- Blackmore KJ, O'Hara J, Flood LM, Martin FW (2008) The effect of Floseal on post-tonsillectomy pain: a randomized controlled pilot study. *Clin Otolaryngol* 33:265–284
- Borges Santos M, Silva S, Bettencourt V, Campante Teles R, Souse Almeida M, Medeiros D, Aniceto Silva J (2012) Ultrasound-guided- thrombin-gelatin injection is effective for the treatment of iatrogenic femoral artery pseudoaneurysms: initial results. *Catheter Cardiovasc Interv*
- Borin JF, Sala LG, Eichel L, McDougall EM, Clayman RV (2005) Tubeless percutaneous nephrolithotomy using hemostatic gelatin matrix. *J Endourol* 19(6):614–617
- Brandes SB (2006) Editorial comment: “damage control management of experimental grade 5 renal injuries: further evaluation of Floseal gelatin matrix”. *J Trauma* 60:346–350
- Breda A, Stepanian SV, Lam JS, Liao JC, Gill IS, Colombo JR, Guazzoni G, Stifelman MD, Perry KT, Celia A, Breda G, Fornara P, Jackman SV, Rosales A, Palou J, Grasso M, Pansadoro V, Disanto V, Porpiglia F, Milani C, Abbou CC, Gaston R, Janetschek G, Soomro NA, De la Rosette JJ, Laguna PM, Schulam PG (2007) Use of hemostatic agents and glues during laparoscopic partial nephrectomy: a multi-institutional survey from the united States and Europe of 1347 cases. *Eur Urol* 52:798–803
- Buiret G, Pavic M, Pignat JC, Pasquet F (2013) Case Rep *Otolaryngol*
- Cappabianca P, Esposito F, Esposito I, Cavallo LM, Leone CA (2009) Use of a thrombin-gelatin haemostatic matrix in endoscopic endonasal extended approaches: technical note. *Acta Neurochir* 151(1):69–77
- Carnaghan HK, Harrison MR (2009) Presealing of the chorioamniotic membranes prior to fetoscopic surgery: preliminary study with unfertilized chicken egg models. *Eur J Obstet Gynecol Reprod Biol* 144:142–145
- Celia A, Zeccolini G, Guazzoni G, Pansadoro V, Disanto V, Porpiglia F, Milani C, Abou C, Gaston R, Janetschek G, Soomro NA, Fornara P, Breda A, Schulam PG, De La Rosette J, Laguna MP, Palou J, Breda G (2008) laparoscopic nephron sparing surgery: a multi-institutional European survey of 592 cases. *Archivio Italiano di urologia e andrologia* 80(3):85–91

- Chandra RK, Conley DB, Kern RC (2003) The effect of Floseal on mucosal healing after endoscopic sinus surgery: a comparison with Thrombin-soaked gelatin foam. *Am J Rhinol* 17(1):51–55
- Chandra RK, Conley DB, Haines GK III, Kern RC (2005) Long-term effects of FloSeal™ packing after endoscopic sinus surgery. *Am J Rhinol* 19(3):240–243
- Clapp M, Huang JC (2013) Use of floseal sealant in the surgical management of tubal ectopic pregnancy. *Case Rep Obstet Gynecol*
- Côté D, Barber B, Diamond C, Wright E (2010) FloSeal hemostatic matrix in persistent epistaxis: prospective clinical trial. *J Otolaryngol-Head Neck Surg* 39(3):304–308
- Derweesh IH, Malcolm JB, Diblasio CJ, Mehrazin R, Jackson S (2008) Sutureless laparoscopic heminephrectomy: safety and efficacy in physiologic and chronically obstructed porcine kidney. *Surg Innov* 15(3):194–202
- Dhillon S (2011) Fibrin Sealant (Evicel® [Quixil®/Crosseal™]) A review of its use as supportive treatment for hemostasis in surgery. *Drugs* 71(14):1893–1915
- Duranni OM, Fernando AI, Reuser TQ (2007) Use of a novel topical hemostatic sealant in lacrimal surgery: a prospective, comparative study. *Ophthalmic Plast Reconstr Surg* 23(1):25–27
- Ebert AD, Hollauer A, Fuhr N, Langolf O, Papadopoulos T (2009) Laparoscopic ovarian cystectomy without bipolar coagulation or sutures using a gelatin-thrombin matrix sealant (FloSeal©): first support of a promising technique. *Arch Gynecol Obstet* 280:161–165
- Echave M, Oyagüez I, Casado MA (2014) Use of Floseal®, a human gelatin-thrombin matrix sealant, in surgery: a systematic review. *BMC Surg* 14:111–123
- Ellegala DB, Maartens NF, Laws ER (2002) Use of Floseal hemostatic sealant in transphenoidal pituitary surgery: technical note. *Neurosurgery* 51(2):513–516
- Ereth MH, Shaff M, Ericson EF, Wetjen NM, Nuttall GA, Oliver WC (2008) Comparative safety and efficacy of topical hemostatic agents in a rat neurosurgical model. *Neurosurgery* 63:369–372
- Fiss I, Danne M, Stendel R (2007) Use of gelatin-thrombin matrix hemostatic sealant in cranial neurosurgery. *Neurol Med Chir (Tokyo)* 47:462–467
- Gall RM, Witterick IJ, Shargill NS, Hawke M (2002) Control of bleeding in endoscopic sinus surgery: use of a novel gelatin-based hemostatic agent. *J Otolaryngol* 31(5):271–274
- Gazzeri R (2016) Commentary on: efficacy, security and manageability of gelified hemostatic matrix in bleeding control during thoracic and lumbar spine surgery; Floseal versus Surgiflo. *J Neurol Surg Part A Cent Eur Neurosurg* 77:143–145
- Gazzeri R, Galarza M, Neroni M, Alfieri A, Esposito S (2009) Minimal craniotomy And matrix hemostatic sealant for the treatment of spontaneous supratentorial intracerebral hemorrhage. *J Neurosurg* 110:939–942
- Gazzeri R, Galarza M, Neroni M, Alfieri A, Giordano M (2011) Hemostatic matrix sealant in neurosurgery: a clinical and imaging study. *Acta Neurochir* 153:148–154
- Gazzeri R, Galarza M, Alfieri A (2012) The safety and biocompatibility of gelatin hemostatic matrix [FloSeal and Surgiflo] in neurosurgical procedures. *Surg Technol Int* 22:49–54
- Gazzeri R, Galarza M, Alfieri A (2013) Use of gelatin sponge and matrix hemostatics sealant in neurosurgery. *Gelatin: production, applications and health implications* (Chap. 7), pp 123–136
- Gazzeri R, De Bonis C, Galarza M (2014) Use of a thrombin-gelatin hemostatic matrix [Surgiflo] in spinal surgery. *Surg Technol Int* 25:280–285
- Gazzeri R, Galarza M, Conti C, De Bonis C (2017) Incidence of thromboembolic events after use of gelatin-thrombin-based hemostatic matrix during intracranial tumor surgery. *Neurosurg Rev*
- Gong EM, Zorn KC, Gofrit ON, Lucioni A, Orvieto MA, Zagaja GP, Shalhav AL (2007) Early laparoscopic management of acute postoperative hemorrhage after initial laparoscopic surgery. *J Endourol* 21(8):872–878
- Gorry A, Morelli ML, Olowu O, Shahid A, Odejinmi F (2011) Laparoscopic management of abdominal ectopic pregnancy using Floseal hemostatic matrix. *Int Fed Gynecol Obstet*
- Guzzo TJ, Pollock RA, Forney A, Aggarwal P, Matlaga BR, Allaf ME (2009) Safety and efficacy of a surgeon-prepared gelatin hemostatic agent compared with Floseal for hemostasis in laparoscopic partial nephrectomy. *J Endourol* 23(2):279–282

- Han LY, Schimp V, Oh C, Ramirez PT (2004) A gelatin matrix-thrombin tissue sealant (FloSeal®) application in the management of groin breakdown after inguinal lymphadenectomy for vulvar cancer. *Int J Gynecol Cancer* 14:621–624
- Henkel A, Cooper RA, Ward KA, Bova D, Yao K (2008) Malignant-appearing microcalcifications at the lumpectomy site with the use of Floseal Hemostatic sealant. *AJR* 191:1371–1373
- Hick EJ, Morey AF, Harris RA, Morris MS (2005) Gelatin matrix treatment of complex renal injuries in a porcine model. *J Urol* 173:1801–1804
- Hobday CD, Milam MR, Milam RA, Eusher E, Brown J (2009) Postoperative Small Bowel Obstruction associated with use of hemostatic agents. *J Minim Invasive Gynecol* 16(2):224–226
- Hoffmann NE, Siddiqui SA, Agarwal S, McKellar SH, Kurtz HJ, Gettman MT, Ereth MH (2009) Choice of hemostatic agent influences adhesion formation in a rat cecal adhesion model. *J Surg Res* 155:77–81
- Hong YM, Loughlin KR (2006) The use of hemostatic agents and sealants in urology. *J Urol* 176:2367–2374
- Jameson M, Gross CW, Kountakis SE (2006) Floseal use in endoscopic sinus surgery: effect on postoperative bleeding and synechia formation. *Am J Otolaryngol-Head Neck Med Surg* 27:86–90
- Jo SH, Mathiasen RA, Gurushanthaiah D (2007) Prospective, randomized, controlled trial of a hemostatic sealant in children undergoing adenotonsillectomy. *Otolaryngol-Head Neck Surg* 137(454):458
- Jorgensen S, Bascom DA, Partsafas A, Wax MK (2003) The effect of 2 sealants (FloSeal and Tisseel) on fasciocutaneous flap revascularization. *Arch Facial Plast Surg* 5:399–402
- Kaufmann OG, Sountoulides P, Kaplan A, Louie M, McDougall E, Clayman R (2009) Skin treatment and tract closure for tubeless percutaneous nephrolithotomy: university of California, Irvine, technique. *J Endourol* 23(10):1739–1741
- Kaul S, Laungani R, Sarle R, Stricker H, Peabody J, Littleton R, Menon M (2007) Da Vinci-assisted robotic partial nephrectomy: technique and results at a mean of 15 months of follow up. *Eur Urol* 51:186–192
- Kaushik V, Tahery J, Malik TH, Jones PH (2003) new surgical adjuncts in the treatment of rhinophyma: the microdebrider and Floseal®. *J Laryngol Otol* 117:551–552
- Kheirabadi BS, Field-Ridley A, Pearson R, MacPhee M, Drohan W, Tuthill D (2002) Comparative study of the efficacy of the common topical hemostatic agents with fibrin sealant in a rabbit aortic anastomosis model. *J Surg Res* 106:99–107
- Kim IY, Eichel L, Edwards R, Uribe C, Chou DS, Abdelshehid C, Ahlering M, White S, Woo E, McDougall E, Clayman RV (2007) Effects of commonly used hemostatic agents on the porcine collecting system. *J Endourol* 21(6):652–654
- Kim HJ, Fraser MR, Kahn B, Lyman S, Figgie MP (2012) The efficacy of a thrombin-based hemostatic agent in unilateral total knee arthroplasty: a randomized controlled trial. *J Bone Joint Surg* 94(13):1160–1165
- Klemcke HG (2006) Evaluation of FloSeal as a potential intracavitary hemostatic agent. *J TRAUMA® Inj Infect Crit Care* 60(2):385–389
- L'Esperance JO, Sung JC, Marguet CG, Maloney ME, Springhart WP, Preminger GM, Alabala DM (2005) Controlled survival study of the effects of Tisseel or a combination of Floseal and Tisseel on major vascular injury and major collecting-system injury during partial nephrectomy in a porcine model. *J Endourol* 19(9):114–1121
- Landi A, Gregori F, Marotta N, Delfini R (2016) Comparative analysis about efficacy, security and manageability of gelified hemostatic matrix in bleeding control during thoracic and lumbar spine surgery: Floseal versus Surgiflo. *J Neurosurg Surg Part A Cent Eur Neurosurg* 77(2):139–143
- Law LW, Chor CM, Leung TY (2010) Use of hemostatic gel in postpartum hemorrhage due to placenta previa. *Obstet Gynecol* 116(2):528–530
- Lee DI, Clayman RV (2004) Use of gelatin matrix to rapidly repair diaphragmatic injury during laparoscopy. *Urology* 63:419

- Lee DI, Uribe C, Eichel L, Khonsari S, Basilote J, Park HK, Li CC, McDougall EM, Clayman RV (2004) Sealing percutaneous nephrolithotomy tracts with gelatin matrix hemostatic sealant: initial clinical use. *J Urol* 171:575–578
- Lee L, Henderson R, Baig K (2014) Successful treatment of aortic root rupture following transcatheter aortic valve implantation in a heavily calcified aorta: a novel approach to a serious complication. *Catheter Cardiovasc Interv* 84:303–305
- Lemmer R, Albrech M, Bauer G (2012) Use of Floseal hemostatic matrix in a patient with severe postpartum hemorrhage. *J Obstet Gynaecol Res* 38(2):435–437
- Lewis KM, Atlee HD, Mannone AJ, Dwyer J, Lin L, Goppelt A, Redl H (2013) Comparison of two gelatin and thrombin combination hemostats in a porcine liver abrasion model. *J Invest Surg* 26:141–148
- Lewis KM, Atlee H, Mannone A, Lin L, Goppelt A (2015) Efficacy of hemostatic matrix and microporous polysaccharide hemospheres. *J Surg Res* 193:825–830
- Li R, Louie MK, Lee HJ, Osann K, Pick DL, Santos R, Mc Dougall EM, Clayman RV (2010) Prospective randomized trial of three different methods of nephrostomy tract closure after percutaneous nephrolithotripsy. *BJU Int* 107:1660–1665
- Maccabee MS, Trune DR, Hwang PH (2003) Effects of topically applied biomaterials on paranasal sinus mucosal healing. *Am J Rhinol* 17(4):203–207
- Madhuri TK, Tailor A, Butler-Manuel S (2010) Use of surgical sealant in debulking surgery for advanced ovarian carcinoma—case report. *Eur J Gynecol Oncol* 31(5):582–583
- Madi R, Wolf JS (2009) Single-setting bilateral hand-assisted laparoscopic partial nephrectomy. *J Endourol* 23(6):929–932
- Martinez C, Rosen R, Cohen H, Ruiz CE (2010) A novel method for closing the percutaneous transapical access tract using coils and gelatin matrix. *J Invasive Cardiol* 22:107–109
- Mathiasen RA, Cruz RM (2004) Prospective, randomized, controlled clinical trial of a novel matrix hemostatic sealant in children undergoing adenoidectomy. *Otolaryngol-Head Neck Surg* 131(5):601–605
- Mathiasen RA, Cruz RM (2005) Prospective, randomized, controlled clinical trial of a novel matrix hemostatic sealant in patients with acute anterior epistaxis. *Laryngoscope* 115:899–902
- Moriarty KT, Premila S, Bulmer PJ (2008) Use of FloSeal™ hemostatic gel in massive obstetric haemorrhage: a casa report. *BJOG* 115:793–795
- Mozet C, Prettin C, Dietze M, Fickweiler U, Dietz A (2012) Use of Floseal and effects on wound healing and pain in adults undergoing tonsillectomy: randomised comparison versus electrocautery. *Eur Arch Otorhinolaryngol* 269:2247–2254
- Nadler RB, Perry KT, Smith ND (2009) Hybrid laparoscopic and robotic ultrasound-guided radiofrequency ablation-assisted clampless partial nephrectomy. *Urology* 74(1):202–205
- Nasso G, Piancone F, Bonifazi R, Romano V, Visicchio G, De Filippo CM, Impiombato B, Fiore F, Bartolomucci F, Alessandrini F, Speziale G (2009) Prospective, randomized clinical trial of the FloSeal Matrix sealant in cardiac surgery. *Ann Thorac Surg* 88:1520–1526
- Oz MC, Cosgrove III DM, Badduke BR, Hill JD, Flannery MR, Palumbo R, Nina Topic for The Fusion Matrix Study Group (2000) Controlled clinical trial of a novel hemostatic agent in cardiac surgery. *Ann Thorac Surg* 69:1376–1382
- Pace G, Saldutto P, Vincentini C, Miano L (2010) Haemostatic in surgery and our experience in the enucleoresection of renal cell carcinoma. *World J Oncol* 8:37
- Partezani Helito C, Gomes Gobbi R, Machado Castrillon L, Bremer Hinkel B, Pécora JR, Camanho GL (2013) Comparison of Floseal® and electrocautery in hemostasis after total knee arthroplasty. *Acta Orthopaedica Bras* 21(6):320–322
- Partsafas AW, Bascom DA, Jorgensen SA, Wax MK (2004) Effects of Tisseel and Floseal on primary ischemic time in a rat fasciocutaneous free flap model. *Laryngoscope* 114:301–304
- Prowse S, Kelly G (2010) The oozing tracheostomy—a novel application for FloSeal™
- Pursifull NF, Morris MS, Harris RA, Morey AF (2006) Damage control management of experimental grade 5 renal injuries: further evaluation of FloSeal gelatin matrix. *J TRAUMA® Inj Infect Crit Care* 60(2):346–350

- Renkens KL Jr, Payner TD, Leipzig TJ, Feuer H, Morone MA, Koers JM, Lawson KJ, Lentz R, Shuey H Jr, Conaway GL, Anderson GBJ, Hs An, Hickey M, Rondonone JF, Shargill NF (2001) A multicenter, prospective, randomized trial evaluating a new hemostatic agent for spinal surgery. *SPINE* 26(15):1645–1650
- Reuthenbuch O, Lachat ML, Vogt P, Schurr U, Turina M (2000) Floseal®: a new hemostyptic agent in peripheral vascular surgery. *VASA* 29:204–206
- Richter F, Schnorr D, Deger S, Türk I, Roigas J, Wille A, Loening SA (2003) Improvement of hemostasis in open and laparoscopically performed partial nephrectomy using a gelatin matrix-thrombin tissue sealant. *Urology* 61(1):73–77
- Rouach Y, Delongchamps NB, Patey N, Fontaine E, Timsit MO, Thiounn N, Méjean A (2009) Suture or hemostatic agent during laparoscopic partial nephrectomy? A randomized study using a hypertensive porcine model. *Urology* 73(1):172–177
- Safaei M, Sun MZ, Oh T, Aghi MK, Berger MS, McDermott MW, Parsa AT, Bloch O (2014) Use of thrombin-based hemostatic matrix during meningioma resection: a potential risk factor for perioperative thromboembolic events. *Clin Neurol Neurosurg* 119:116–120
- Seyednejad H, Imani M, Jamieson T, Seifalian M (2008) Topical hemostatic agents. *Br J Surg* 95:1197–1225
- Shashoua AR, Gill D, Barajas R, Dini M, August C, Kirshenbaum GL, Escuardo L (2009) Caseating granulomata caused by hemostatic agent posing as metastatic leiomyosarcoma. *J Soc Laparoendosc Surg* 13:226–228
- Shire MG, Tabaei A, Hsu AK, Rickert S, Close LG (2007) Synechia formation after endoscopic sinus surgery and middle turbinate medialization with and without Floseal. *Am J Rhinol* 21(2):174–179
- Soyka MB, Nikolaou G, Rufibach K, Holzmann D (2011) On the effectiveness of treatment options in epistaxis: an analysis of 678 interventions. *Rhinology* 49:474–478
- Stevens AC, Stevens D (2009) Robotic-assisted laparoscopic partial nephrectomy: surgical technique and clinical outcomes at 1 year. *BJU Int* 103:994–995
- Suzuki Y, Vellinga TT, Istre O, Einarsson JI (2010) Small Bowel Obstruction associated with use of a gelatin-thrombin matrix sealant (FloSeal) after laparoscopic gynecologic surgery. *J Minim Invasive Gynecol* 17(5):641–645
- Tabata K, Watanabe M, Naruishi K, Edamura K, Satoh T, Yang G, Fattah EA, Wang J, Goltsov A, Floryk D, Soni SD, Kadmon D, Thompson TC (2009) Therapeutic effects of gelatin matrix-embedded IL-12 gene-modified macrophages in a mouse model of residual prostate cancer. *Prostate Cancer Prostatic Dis* 12:301–309
- Tackett SM, Calcaterra D, Magee G, Lattouf OM (2014) Real-world outcomes of hemostatic matrices in cardiac surgery. *J Cardiothorac Vasc Anesth* 28(6):1558–1565
- Tan BK, Chandra RK (2010) Postoperative prevention and treatment of complications after sinus surgery. *Otolaryngology* 43:769–779
- Testini M, Marzaioli R, Lissidini R, Lippolis A, Logoluso F, Gurrado A, Lardo D, Poli E, Piccinni G (2009) The effectiveness of Floseal® matrix hemostatic agent in thyroid surgery: a prospective, randomized, control study. *Langenbecks Arch Surg* 394:837–842
- Thomas PJ, Trawfic SN (2009) Eosinophil-rich inflammatory response to FloSeal hemostatic matrix presenting as postoperative pelvic pain. *Am J Obstet Gynecol* 11–12
- Tonante A, Lo Schiavo MG, Bonanno L et al (2006) Hemorrhagic complications in thyroid surgery. Control of bleeding from retronural vessels using collagen and thrombine gelatin granules. *Chir Ital* 58:61–68
- Triaca V, Zaghera RM, Libertino JA (2005) Does Thrombin sealant allow nephron-sparing surgery with no renal artery occlusion? A description of technique and initial results. *BJU Int* 95:1273–1275
- Ujam A, Awad Z, Wong G, Tatla T, Farrell R (2011) Safety trial of Floseal® hemostatic agent in head and neck surgery. *Ann R Coll Surg Engl* 94:336–339
- Uribe CA, Eichel L, Khonsari S, Finley DS, Basillote J, Park HK, Li CC, Abdelshehid C, Lee DI, McDougall EM, Clayman RV (2005) What happens to hemostatic agents in contact with urine? An in vitro study. *J Endourol* 19(3):312–317



- Valentine R, Wormald PJ, Sindwani R (2009) Advances in absorbable biomaterials and nasal packing. *Otolaryngology* 42:813–828
- Valentine R, Boase S, Jervis-Bardy J, Dones Cabral JD, Robinson S, Wormald PJ (2011) The efficacy of hemostatic techniques in the sheep model of carotid artery injury. *Int Forum Allergy Rhinol* 1(2):118–122
- Velyvis JH (2015) Gelatin matrix use reduces postoperative bleeding after total knee arthroplasty. *Orthopedics* 38(2):118–123
- Waldert M, Remzi M, Klatte T, Klinger HC (2011) Floseal reduces the incidence of lymphoceles after lymphadenectomies in laparoscopic and robot-assisted extraperitoneal radical prostatectomy. *J Endourol* 25(6):969–973
- Wang C, Han Z, Zhang T, Ma JX, Jiang X, Wang Y, Ma XI (2014) The efficacy of a thrombin-based hemostatic agent in primary total knee arthroplasty: a meta-analysis. *J Orthop Surg Res* 9:90
- Weaver FA, Hood DB, Zatina M, Messina L, Badduke B, Francisco San, Fremont California, Baltimore Maryland (2002) gelatin-thrombin-based hemostatic sealant for intraoperative bleeding in vascular surgery. *Ann Vasc Surg* 16(3):286–293
- Wille AH, Tüllmann M, Roigas J, Loening SA, Deger S (2006) Laparoscopic partial nephrectomy in renal cell cancer—results and reproducibility by different surgeons in a high volume laparoscopic center. *Eur Urol* 49:337–343
- Wille AH, Johannsen M, Miller K, Deger S (2009) Laparoscopic partial nephrectomy using Floseal for hemostasis: technique and experiences in 102 patients. *Surg Innov* 14(4):306–312
- Williams MR, D'Ambra AB, Beck JR, Spanier TB, Morales DLS, Helman DN, Oz MC (2000) A randomized trial of antithrombin concentrate for treatment of heparine resistance. *Ann Thorac Surg* 70:873–877
- Wohlmuth CT, Merced JD (2011) Gelatin-thrombin hemostatic matrix in the management of placenta site postpartum hemorrhage. *J Reprod Med* 56(5–6):271–273
- Zeltser I, Dugi D, Gupta A, Park S, Kabbani W, Cadeddu J (2008) Does topical hemostatic agent have an adverse effect on the function of the prostatic neurovascular bundle? *BJU Int* 102:1005–1007
- Zorn KC, Gong EM, Orvieto MA, Gofrit ON, Mikhail AA, Shalhav AL (2007) Impact of collecting-system repair during laparoscopic partial nephrectomy. *J Endourol* 31(3):315–320

# Chapter 4

## Polysaccharide-Based Polymer Gels and Their Potential Applications



Nabil A. Ibrahim, Ahmed A. Nada and Basma M. Eid

### 1 Introduction

#### 1.1 Polymer Gel Definition

Although gel is very popular and can be found everywhere, it is difficult to define polymer gels as a type of materials. Gel can be described as a state of matter intermediate between solid and liquid. It is a diluted matrix of cross-linked system which contains fluids and shows no flow at its steady-state condition (Jen et al. 1996). Such systems can be cross-linked through physical or chemical bonds in the presence of an extender (medium) which fills the pores of this network such as water (hydrogel) (Kabiri et al. 2011; Wakheth et al. 2015), oil (oil-gel) (Lee et al. 2008b), or air (aerogel) (Soleimani Dorcheh and Abbasi 2008). Technically, gel network swells to the equilibrium state (Fig. 1) that is established between osmotic forces and the capability of polymer chains to extend (Hong et al. 2009).

Such polymer extension leads to a large swelling ability and medium absorption to reach as much as 10–20 times its molecular weight (Singh et al. 2010). It is worth to mention that gel swells but does not dissolve and this ability of swelling arises from hydrophilic functional groups attached to the polymeric chains, while the resistance of dissolution arises from the cross-links between polymer chains. This promotes gel to be considered as an ideal substance for absorbing materials employed in numerous applications such as baby diaper and plant soil (Singh et al. 2010; Ahmed 2015).

---

N. A. Ibrahim (✉) · A. A. Nada · B. M. Eid  
Textile Research Division, National Research Center, Giza, Egypt  
e-mail: nabibrahim@hotmail.com; nabibrahim49@yahoo.co.uk

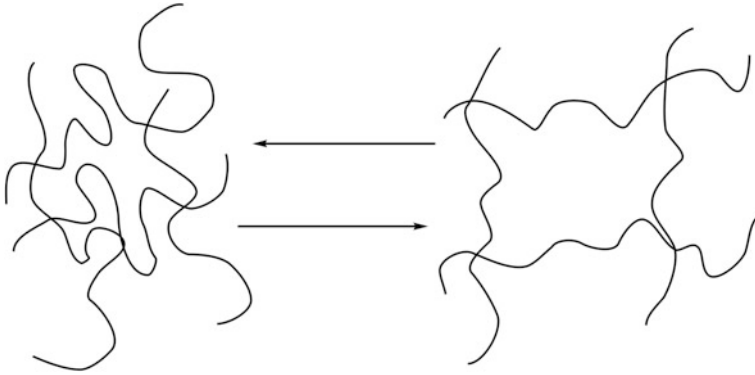


**Fig. 1** Gel equilibrium

## ***1.2 General Features***

Generally speaking, gels possess characteristics of both liquid and solid; high diffusion coefficients for small molecules; and mechanical properties of soft solids (Singh et al. 2010). Gel properties depend on polymer constituents; cross-links in terms of cross-linking mechanisms and density; and interactions between the polymer and solvent (Pal et al. 2013).

## ***1.3 Mechanism of Gel Formation***

The mechanism of gel formation is divided into two types: chemical cross-linking and physical cross-linking (Park et al. 2010).

The chemical cross-linking mechanism provides permanent bonding between chains due to the formation of covalent bonds. Such cross-linked gels are not processed after formation so that is called irreversible gels.

Irreversible gels can technically be fabricated by two different methods, namely cross-linking during polymerization and cross-linking polymer chains. Cross-linking during polymerization can be formed via different routes of polymerizations such as condensation polymerization; free radical polymerization (Thakur et al. 2014; Thakur and Thakur 2014a); photo-polymerization; and plasma polymerization. However, in the cross-linking polymer chain method, gel network cross-links by reaction of substituents, attached to polymer chains, also via either radiation cross-linking, photo-cross-linking, or plasma cross-linking (Ito 2007).

The physical cross-linking mechanism provides reversible gel with temporary bonding between chains, and it occurs as a result of changes in temperature, pH,

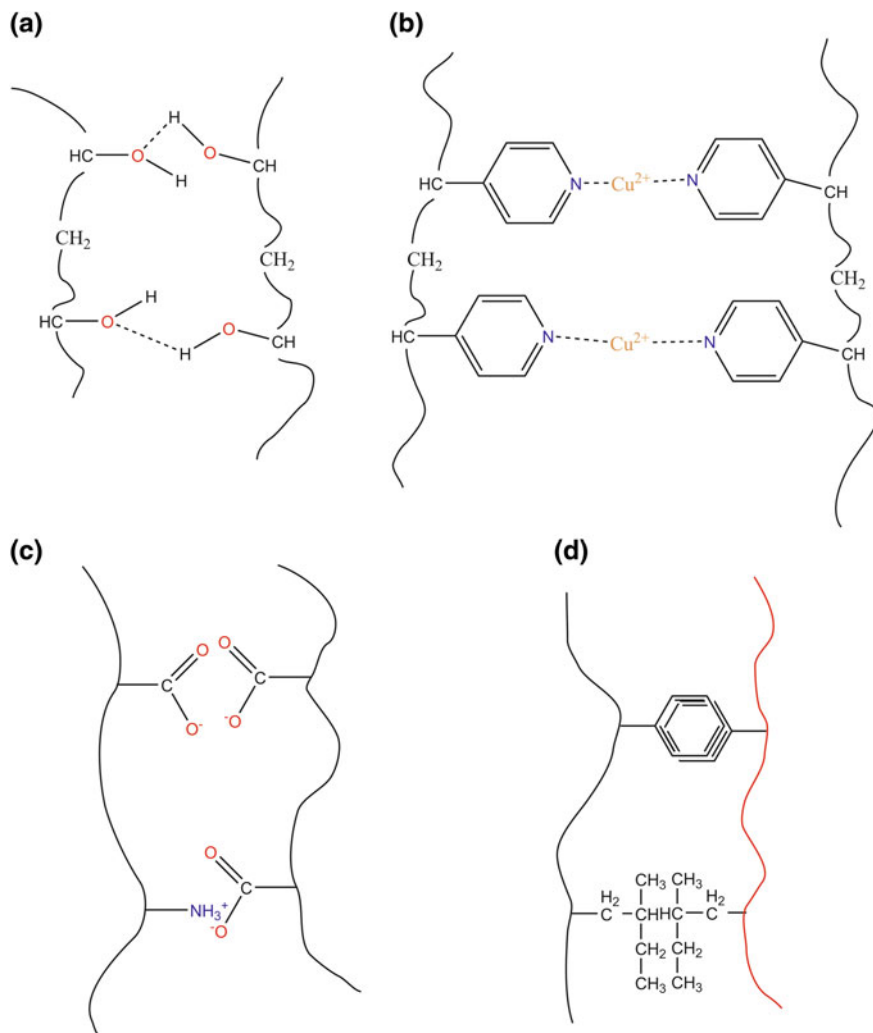


**Fig. 2** Forces controlling gel behavior; **a** hydrogen bonding; **b** coordination bonding; **c** ionic interactions; **d** hydrophobic interactions

and solvent composition. Reversible gels typically formed as mentioned before via temporary bonds through different mechanisms such as hydrogen bonding, ionic bond, coordination bonding, helix formation, and hydrophobic association (Fig. 2) (Hurtado et al. 2007).

## 2 Hydrogels

Hydrogels are polymeric network with chains containing hydrophilic functional groups which absorb large amount of water. Hydrogel can be created either from natural polymers (Thakur and Thakur 2015) or from synthetic polymers. In this review, there is no intention to provide further details of the synthetic polymers.

Natural polymers include collagen, hyaluronate, fibrin, alginate, agarose, chitosan, and cellulose have a number of advantages over synthetic polymers (Thakur and Thakur 2014b). Basically, natural polymers are not toxic, biologically compatible, biodegradable, and abundant.

The second part of this review will provide more details about polysaccharides, their chemical structures, physical properties, chemical modifications, polysaccharide derivatives, their reactions to fabricate hydrogels, their characterization, and potential utilizations.

### 2.1 Alginate

#### 2.1.1 General Features

Alginate, water-soluble sodium salt of alginic acid, is an anionic natural polymer that can be extracted from affordable resources such as brown seaweed. Alginate has been used in medical applications due to its biocompatibility, low toxicity, and rapid gelation in the presence of divalent cations commonly such as calcium cation ( $\text{Ca}^{2+}$ ). Chemical structure of alginate is composed of blocks of mannuronic acid units (M) and guluronic acid units (G) to form linear copolymer of different and long sequences of Ms and/or Gs (Fig. 3) (Augst et al. 2006). It has been reported that differences in M and G contents and alternation depend on the extracted sources (Pawar and Edgar 2012). Also, it is believed that G sequences in alginate copolymer are responsible for gel formation of alginate in the presence of calcium cations (Lee and Mooney 2012).

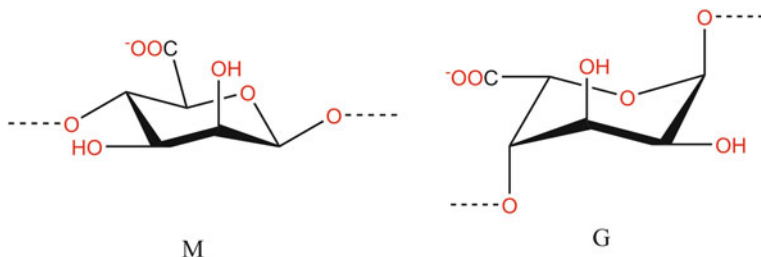


**Fig. 3** Chemical structures of mannuronic acid units (M) and guluronic acid units (G) of alginate

The commercial alginate has an average molecular weight between 32,000 and 400,000 g/mol. to provide wide broad viscosity value applicable to varied applications. Alginate viscosity depends mainly on pH to reach maximum at pH 3 at which carboxylic groups are converted to acid form and form hydrogen bonds. Regarding alginate biocompatibility, highly pure alginate that is heavy metal-free did not show any reaction or significant inflammation when tested in vivo models (Augst et al. 2006).

Chemical structure of alginate containing hydroxyl groups and carboxylic groups can share in multiple chemical reactions to modify the final characteristics of the modified derivatives. Alginate can be modified through the hydroxyl groups by oxidation, reductive amination, sulfation, copolymerization reactions and coupling of cyclodextrin units. However, it can be modified through the carboxylic groups by esterification and amidation reactions (Yang et al. 2011).

In the following section, related alginate derivatives contributed to gel formation will be summarized.

### 2.1.2 Alginate Hydrogel Formation

#### Reversible Hydrogel of Alginate

Generally speaking, alginate readily can form reversible hydrogel when sodium alginate solution combines with calcium chloride solution to form physical hydrogel through ionic cross-linking (Fig. 2c). It is worth to mention that such ionic bonds take place mainly with guluronic acid units (G) where the coordination between the divalent ions and carboxylic groups reaches the highest degree (Fig. 4). Different ionic cross-linkers have been reported (Lee and Mooney 2012) for the alginate gelation such as calcium chloride, sodium hexametaphosphate, calcium sulfate, and calcium carbonate. Preferred agent is the one that allows slower gelation process to facilitate the way to control the hydrogel properties. For instance, alginate has been mixed with calcium carbonate which is very poor soluble in water at pH7 and by lowering the pH value using Glucono-alpha-lactone,  $\text{Ca}^{2+}$  starts to be released and performs alginate hydrogel in a controlled manner (Lee and Mooney 2012). Also, polyols have been reported to slow down the gelation process which hinders the immediate complexation of the divalent ions and alginate (Van Vlierberghe et al. 2011).

One of the most important drawbacks of the ionic cross-linking of alginate is the short-term stability due to loss of divalent ions in the surrounding medium.

#### Irreversible Hydrogel of Alginate

Alginate can form irreversible hydrogel via creating permanent bonds between alginate chains either by chemical cross-linking agents or by photo-cross-linking

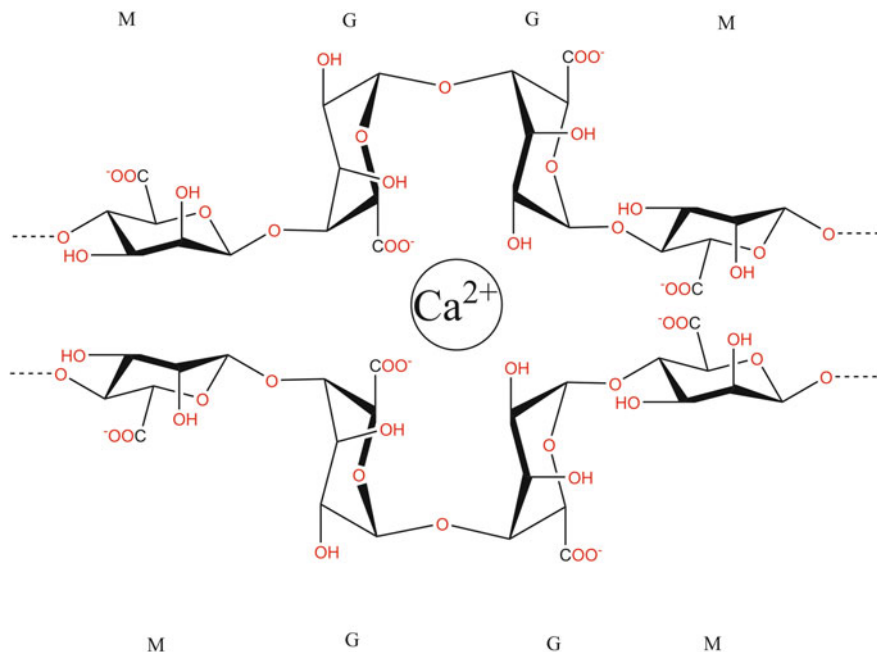


**Fig. 4** Physical cross-linking of guluronic acid units (G) with calcium cations

using photo-initiators. In chemical cross-linking hydrogel, network can be performed in the presence of either bifunctional or multifunctional cross-linkers.

In case of bifunctional cross-linker, adipic dihydrazide was used to cross-link the oxidized alginate which possesses dialdehyde groups along with their chains. Oxidation has been carried out via sodium periodate in mild and controlled condition to monitor the oxidation process (Augst et al. 2006). Figure 5 shows hydrogel formation of alginate in the presence of poly(ethylene glycol) diamine by which reductive amination reaction takes place by reacting with the amino groups of the cross-linker and aldehyde groups groups of oxidized alginate (Yang et al. 2011). In Fig. 6, glutaraldehyde was used as bifunctional chemical cross-linker for alginate performing an acetal link with alginate hydroxyl groups (Chan et al. 2009).

Such bifunctional cross-linkers have shown higher capacity in absorbing water than other networks performed in the presence of multifunctional cross-linkers (West et al. 2007). Poly(acrylamide-co-hydrazide) has been reported for alginate irreversible hydrogel which showed higher mechanical properties and longer degradation than those treated with bifunctional cross-linkers (Lee et al. 2004).

Photo-cross-linked alginate hydrogel has been studied to perform irreversible hydrogel applicable for medical purposes (Jeon et al. 2009). It requires modifying alginate with photo-active groups such as methyl acrylate, in the first place, and then initiates via energy source for few seconds. The advantage of such route is to produce hydrogel in mild conditions even with direct contact with bioactive materials.

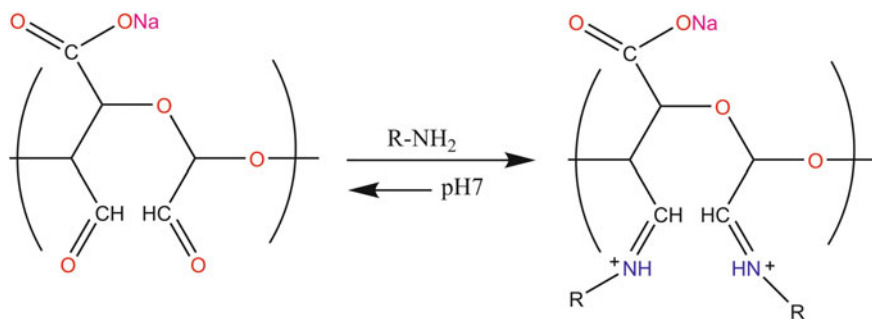


**Fig. 5** Reductive amination of dialdehyde alginate

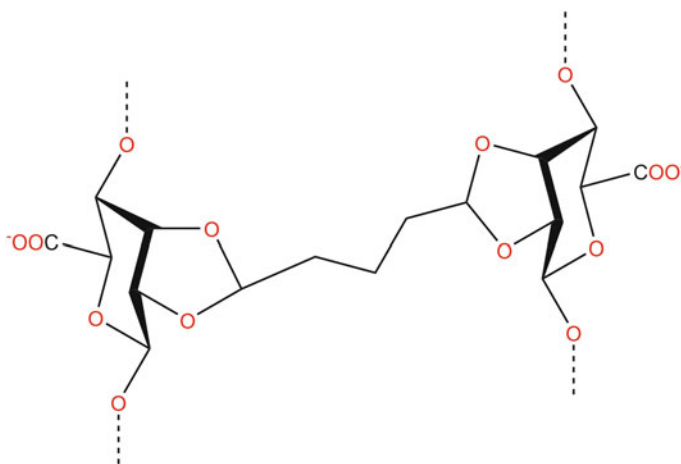


**Fig. 6** Glutaraldehyde chemical cross-linking of alginate

## 2.2 Chitosan

### 2.2.1 General Features

Chitosan is regarded as the most valuable biopolymer in polysaccharides in terms of the tremendous involved medical applications: high biocompatibility; non-toxicity; biodegradability; etc. It has been reported (Nada et al. 2014) that chitosan showed multiple bioactive potentials such as hemostatic, bacteriostatic, fungistatic, and even anticancer agent. Chitosan applications are not limited to medical purposes but also include textile treatments (Ibrahim et al. 2013a, b, c, e, 2017), food industry, and cosmetics (Thakur and Thakur 2014a).

In general, chitosan is produced from chemical treatments of chitin that is extracted and purified from shrimp shells, oysters, and squid pens. Chitosan



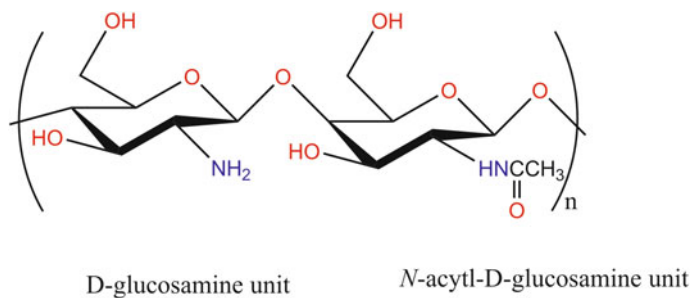


**Fig. 7** Chitosan chemical structure

polymeric structure is composed of linear sequence of D-glucosamine and N-acetyl-D-glucosamine (Fig. 7). Therefore, chitosan family consists of different series that differ in percentage of those units in linear chains and the term of degree of deacetylation (DD) which is defined as the percentage of the amino groups compared to the molecular weight of the polymer. The average molecular weight of chitosan spans from 50,000 to 300,000 g/mol. depending upon the source of extraction.

Chitosan is water-insoluble and dissolved in acidic medium to provide very viscous solution (depending upon the molecular weight) in low concentrations (2–3% wt/v) due to the rigidity of its crystalline structure. Therefore, much has been done to modify chitosan chemical structure by blocking the amino groups in order to reduce such rigidity and obtain moderate viscosity for higher concentrations (12–15% wt/v) (Nada et al. 2014). Chitosan possesses two reactive types of functional groups: first, the free amino groups existing in the D-glucosamine units and second, the free hydroxyl groups attached to both the N-acetyl-D-glucosamine units and D-glucosamine units. Many studies have been conducted to impart superior functionalities to chitosan backbone via chemical modifications or grafting through such active functional groups. For example, chitosan has been covalently bonded with tertiary amine in order to impart and broaden its antimicrobial activities (Lim and Hudson 2004).

In the following section, related chitosan derivatives contributed to gel formation will be summarized.

### 2.2.2 Chitosan-Based Hydrogel Formation

Chitosan has served for hydrogels in different forms such as liquid gel, microspheres, nanospheres, impregnated films, capsules, and beads. In each type of chitosan hydrogels, networks can be achieved either by physical or by chemical cross-linking process.

## Reversible Hydrogel of Chitosan

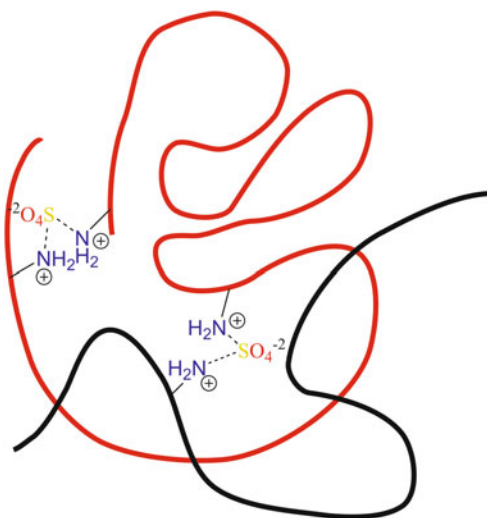
As mentioned above, the physical cross-linking hydrogel can be created under different types of forces controlling the gel behavior. Our discussion will focus on each approach in preparation for chitosan reversible hydrogel and its characteristics (George and Abraham 2006; Ishihara et al. 2006; Chang et al. 2007; Hong et al. 2007; Lawrie et al. 2007; Alves and Mano 2008; Prabakaran 2008; Chatterjee et al. 2009a, b, 2010a, b; Ribeiro et al. 2009; Bhattarai et al. 2010; Rickett et al. 2011; Van Vlierbergh et al. 2011; Sudheesh Kumar et al. 2012).

Non-covalent cross-linked chitosan networks can occur by the ionic complex between the cationic amino groups of chitosan and negatively charged molecules or anions such as sodium sulfate ions (Fig. 8) (Bacaita et al. 2014), metal ions like platinum (Bhattarai et al. 2010), pentasodium tripolyphosphate (Csaba et al. 2009), and many other anions. The preformed hydrogel from those ionic interactions provides reversible, unstable, hydrogel toward processing conditions such as temperature and pH with short lifetime.

However, such ionic interactions can be enhanced by using polyelectrolyte complexes instead such as alginate (George and Abraham 2006). The advantage of this approach is that hydrogel networks cross-linked without organic precursors, catalyst, or reactive agents. Plus, because in such system there are only chitosan and the other polyelectrolyte polymer, their complexions are straightforward and reversible.

Hydrogen bonding is considered as an important approach of the physical cross-linking chitosan hydrogel when chitosan chains are mixed with polyvinyl alcohol (PVA) solution in which polymer chains form junction points that act like cross-linking sites. In this case, hydrogel network is taking place after a series of freeze–thaw cycles in order to affect the formation of the PVA crystallites resulting

**Fig. 8** Ionic complex between chitosan amino groups and sodium sulfate



in hydrogel with less ordered structure (Bhattacharai et al. 2010). Interestingly, hydrogen bonding forces can be employed in very amazing manner to provide hydrogel status at a certain temperature degree. The latter phenomenon is called thermoreversible hydrogel that occurs when chitosan solution mixed with glycerol phosphate disodium salt at 37 °C hydrogen bonding increases to create the physical cross-linking networks. It is believed that glycerol phosphate disodium salt neutralizes the amino groups of chitosan and increases the hydrogen bonding between chitosan chains. Such special characteristic can be employed in performing injectable hydrogel that is in liquid state at room temperature and turns into gel at body temperature (Cheng et al. 2010).

### Irreversible Hydrogel of Chitosan

Irreversible chitosan hydrogel has been investigated in order to overcome the physical cross-linking limitations such as instability for temperature and pH. Chemical cross-linking can provide precise pore size of hydrogel, controllable functionalities, governed degradation rate, and dissolution (Hong et al. 2007; Alves and Mano 2008; Muzzarelli 2009; Azlan et al. 2009; Cheng et al. 2010; Rickett et al. 2011; Mirzaei et al. 2013). On the other hand, this type of cross-linking requires multiple steps of preparations and purifications with serious concerns about the cross-linker cytotoxicity.

Chemical cross-linking can be achieved via different routes such as using small bifunctional cross-linkers and photo-reactive and enzymatic molecules. Much has been reported for chitosan chemical cross-linking via small molecules such as glutaraldehyde (Mirzaei et al. 2013). The latter molecule is very reactive cross-linker toward polymeric materials with amino groups. It reacts with chitosan through the primary amino groups resulting imine bond (Schiff's base reaction) that requires a reduction step to convert it to stable bond (Fig. 9). The mechanical properties of the prepared network depend on the glutaraldehyde amount and chitosan concentration.

Similar to glutaraldehyde, different bifunctional molecules such as diglycidyl ether (Azlan et al. 2009), diisocyanate, epichlorohydrin (Xu et al. 2015) (Fig. 10), and diacrylate (Bhattacharai et al. 2010) react with chitosan mainly through the amino groups and provide chitosan hydrogel with different spacers that possesses different pore size and mechanical properties.

Unlike the previous small cross-linkers, genipin has been used as chemical cross-linker with higher biocompatibility and unremarkable cytotoxicity than others (Fig. 11) (Xu et al. 2015). Genipin showed slower degradation than glutaraldehyde which results in longer duration to release the encapsulated drugs (Muzzarelli 2009).

Instead of using small molecules for chemical cross-linking, some studies have been concerned to use polymeric materials possessing multiple functional groups that are capable of reacting with chitosan amino and/or hydroxyl functional groups. Oxidized dextran has been employed as chemical cross-linker to chitosan in which carbon-carbon sigma bond between carbon 2 and carbon 3 cleaved into dialdehyde

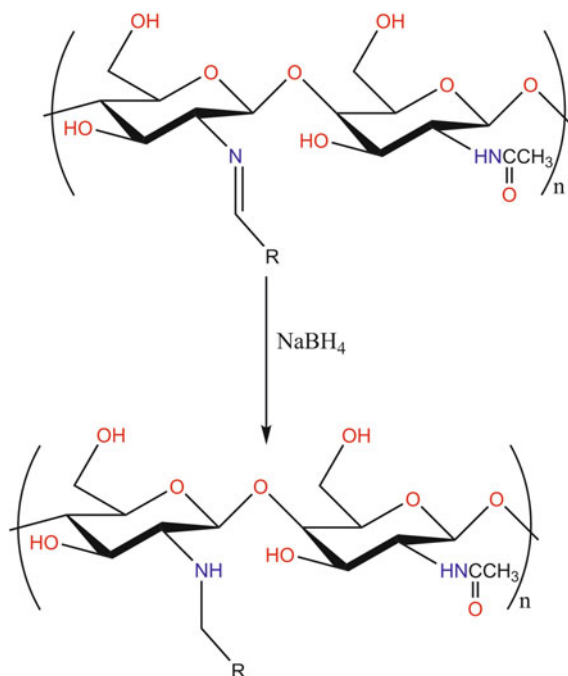


**Fig. 9** Glutaraldehyde cross-links with chitosan (Schiff's base reaction), R = glutaraldehyde

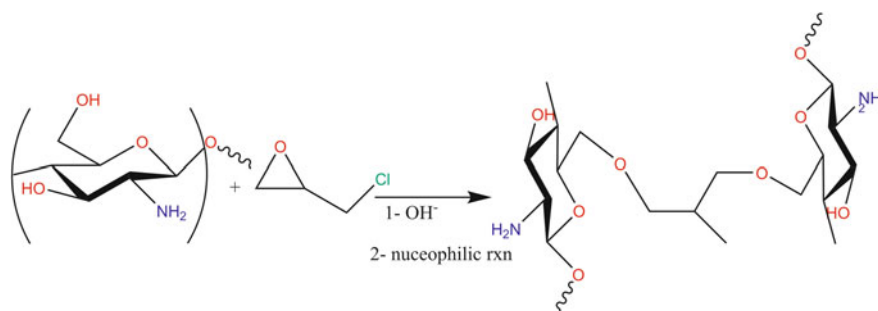


**Fig. 10** Proposed reaction mechanism of chitosan and epichlorohydrin (Xu et al. 2015)

groups along the polymeric chains providing hydrogel with good mechanical properties with limited biological toxicity (Cheng et al. 2014).

Other studies have been conducted to investigate the reaction of acrylated chitosan derivatives with thiolated polyethylene glycol (Kim et al. 2007) to achieve the hydrogel networks and avoid the small cross-linking molecule cytotoxicity. In vice versa, thiolated chitosan was reacted with acrylated chitosan to achieve the same results (Teng et al. 2010).

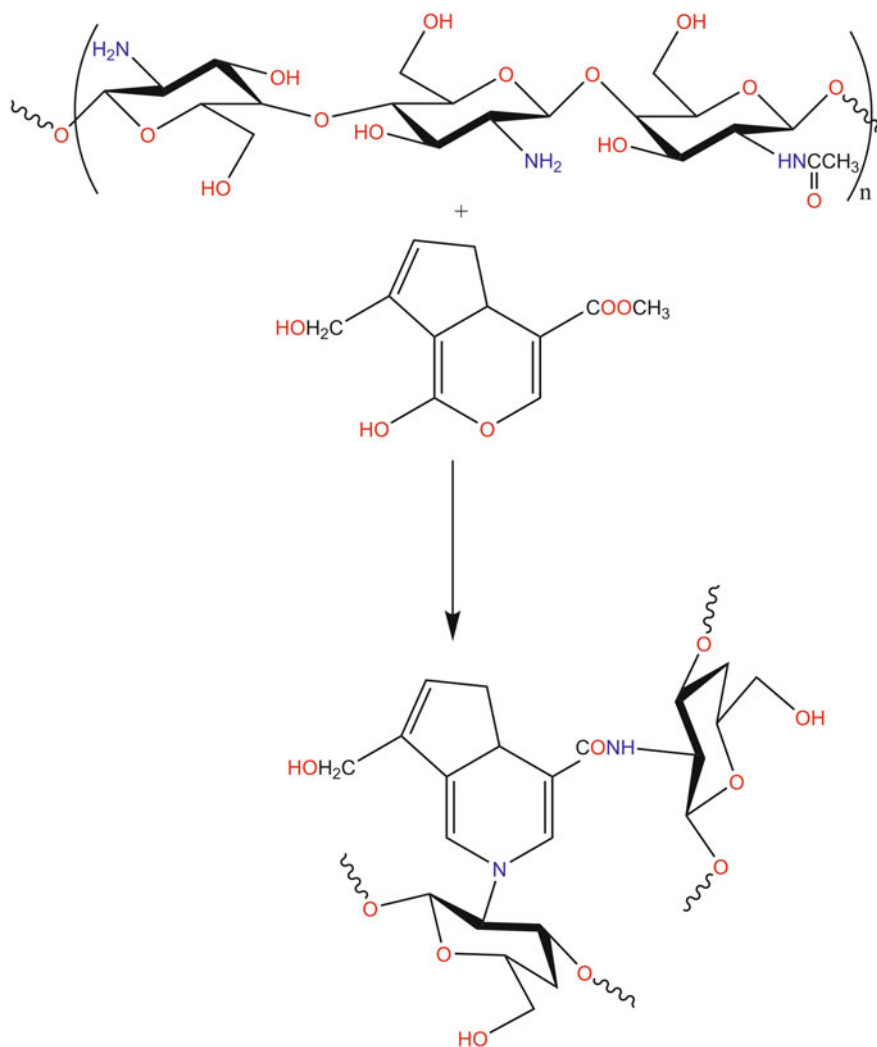


**Fig. 11** Proposed mechanism of chitosan cross-linked by genipin (Xu et al. 2015)

In general, thiol-ene reaction (Fig. 12) is considered as a promising method to achieve cross-linked chitosan in mild conditions with less purification steps and high yield in which thiol groups react with alkene groups to form alkyl sulfide.

Photo-cross-linkable chitosan derivatives have widely employed to produce in situ hydrogel network that is suitable for tissue engineering, wound dressing, and drug delivery applications (Jameela et al. 2002). The typical approach of the photo-cross-linkable chitosan derivatives relies on grafting acrylate monomers onto chitosan backbone and in the presence of photo-initiator associated with UV light radiation, the cross-linking process starts up. However, new approach has been

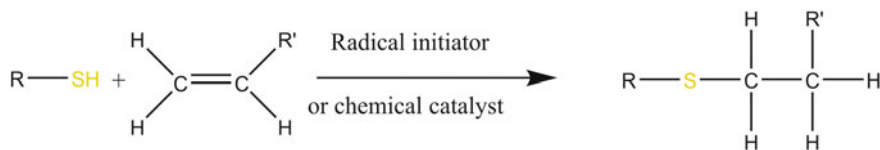


**Fig. 12** Thiol-ene prototype reaction

discovered in which chitosan backbone grafted with 4-azidobenzamide results in a water-soluble chitosan derivative with viscous solution that turns into hydrogel instantaneously upon UV curing (Rickett et al. 2011).

Although photo-crosslinking procedures for producing irreversible chitosan hydrogel have many advantages over conventional methods, photo-processing requires photo-initiators and prolonged radiation that result in an increase in local temperature and ruin the encapsulated bioactive materials.

Enzymatic cross-linking approach has been recently reported as a mild process for in situ hydrogel formation. The main representative for this category is horseradish peroxidase, metalloenzyme, which catalyzes the phenolic or aniline hydroxyl groups, introduced to chitosan backbone and amino groups of chitosan to create hydrogel network. The main idea of such enzyme applies on the decomposition of hydrogen peroxide resulting in active species capable of initiating the cross-linking process in the presence of either phenolic or aniline groups on chitosan backbone (Jin et al. 2009).

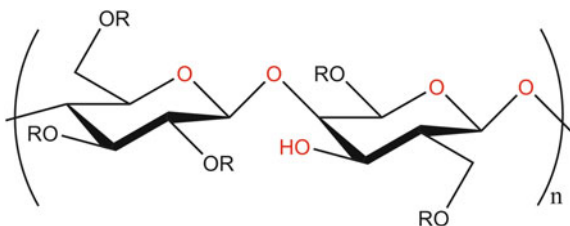
## 2.3 Cellulose

### 2.3.1 General Features

Cellulose is the most abundant natural polymer that is found as the main component of cotton linen and other plants. The chemical structure of cellulose depends on glucose units that are connected to each other through 1, 4-beta-glucosidic linkages (Fig. 13). Cellulose can be also biosynthesized via certain types of bacteria (for instance, *Acetobacter xylinum*) with slightly different physical and macromolecular properties. Cellulose is obtained either from plant or from bacterial source that shows high degree of crystallinity usually 40–60% in plant cellulose and 61–72% for bacterial cellulose. Such high crystallinity is due to the extended hydrogen bonding along the cellulose chains resulting in very tight and well-packed chains hindering cellulose dissolution in common solvents (Sannino et al. 2006, 2009).

Glucose unit, repeating unit of cellulose, has three hydroxyl functional groups in carbon atoms 6 (primary) and 2 and 3 (secondary) that open wide possibilities of chemical modifications in order to produce cellulose derivatives with distinguished characteristics. Nowadays, a great attention has been focused on environmental,

**Fig. 13** Repeating unit of cellulose and cellulose derivatives



ecofriendly, and biocompatible products, thus, cellulose-based substrates have been used in numerous new applications in diverse fields. In the following sections, cellulose-based hydrogel formation and applications will be covered in more details.

### 2.3.2 Cellulose-Based Hydrogel Formation

In this subsection, recent literature was cited to summarize the hydrogel formation of cellulose-based substrates including pure cellulose, modified cellulose, and cellulose composites (Sannino et al. 2006, 2009; El-Hag Ali et al. 2008; Chang and Zhang 2011; Koschella et al. 2011).

As mentioned above, hydrogel forms when hydrophilic polymer chains cross-link by either physical or chemical bonds to create a three-dimensional network. Such mechanism requires water- or solvent-soluble polymers in order to facilitate the physical or chemical interactions with cross-linkers. Due to the difficulties to dissolve cellulose, some studies have been done on native cellulose through chemical or even physical cross-linking (Farag and Al-Afaleq 2002; Zhou et al. 2002, 2005, 2007; Song et al. 2008a, b; Qi et al. 2009; Dahou et al. 2010). Studies concerned mainly about developing the dissolution methods of native cellulose and then using cross-linkers matching the solvent system condition. Special solvent systems have been used for such task such as *N*-methylmorpholine-*N*-oxide (NMMO), ionic liquids (ILs), and alkali/urea (Zhou et al. 2004; Qin et al. 2013). Those new solvent systems have opened new horizon of native cellulose for chemical modifications such as reversible and irreversible cellulose-based hydrogels (Chang and Zhang 2011).

On the other side, cellulose derivatives such as carboxymethylcellulose and hydroxyethyl cellulose (Marci et al. 2006; Sannino et al. 2006, 2009; El-Hag Ali et al. 2008; Kulkarni and Sa 2008; Vinatier et al. 2009; Chang et al. 2010, 2011) have been widely utilized in hydrogel preparation.

### 2.3.3 Reversible Hydrogel Based on Cellulose

Reversible cellulose-based hydrogel can be obtained using either native cellulose or cellulose derivatives.

Native cellulose solution which is dissolved in lithium chloride/dimethyl acetamide (LiCl/DMAc) system leads to 3D network hydrogel upon dropping into non-solvent systems such as azeotropic methanol and isopropanol (Müller et al. 2006). Same technique of hydrogel formation has been reported by using different dissolution systems such as paraformaldehyde/dimethylsulfoxide (DMSO), triethylammonium chloride/DMSO, and tetrabutylammonium chloride/DMSO (Müller et al. 2006).

However, NMMO solvent system for cellulose dissolution can form physical cross-linking hydrogel when cellulose/NMMO solution is heated up to 150 °C at which water molecules replace NMMO solvent between chains to create regenerated cellulose in the form of hydrogel (Müller et al. 2006).

The replacement of the dissolving system by water molecules has been reported (Ruel-Gariépy and Leroux 2004), once again, when cellulose solution, dissolved in 1-butyl-3-methylimidazolium chloride and 1-allyl-3-methylimidazolium chloride, was mixed with water, ethanol, or acetone to end up with regenerated cellulose hydrogel.

Other regenerated cellulose hydrogel has been prepared by dissolving cellulose in sodium hydroxide/urea system (Zhou et al. 2002, 2004; Song et al. 2008a, b; Qi et al. 2009; Qin et al. 2013).

Reversible cellulose-based hydrogels have been made by using water-soluble cellulose derivatives. Partially substitution of the hydroxyl groups of the glucose units by methyl, hydroxyethyl, hydroxypropyl, and many other functional groups, resulting in decreases the hydrogen bonding between cellulose chains and provides water-soluble cellulose derivatives.

Interestingly, methylcellulose (MC) has thermoreversible characteristic. MC solution turns into hydrogel as a result of hydrophobic interactions at particular temperature. Such unusual characteristic promotes MC for special use in medical-related applications (Ruel-Gariépy and Leroux 2004). Similar to MC, hydroxypropyl methylcellulose shows thermoreversible hydrogel with higher gelation temperature than that of MC (Müller et al. 2006).

### Irreversible Cellulose-Based Hydrogel

Chemical cross-linking of cellulose and mainly cellulose derivatives depends on few small molecules that react with the free hydroxyl functional groups of the glucose units such as citric acid, divinyl sulfone (Marci et al. 2006; Chang et al. 2010; Guo et al. 2013), diglycidyl ether (Mathur et al. 1996), epichlorohydrin (Zhou et al. 2007; Chang et al. 2010, 2011), and water-soluble carbodiimide (Sannino et al. 2006, 2009; Guo et al. 2013). For example, divinyl sulfone (Kriegel 2004) was reported for cross-linking carboxymethylcellulose (CMC) and hydroxyethyl cellulose to create superabsorbent hydrogel (Fig. 14).

Another chemical cross-linking hydrogel of cellulose was investigated by using diglycidyl ether with hydroxypropylcellulose (Marsano et al. 2003) to end up with thermosensitive hydrogel (Fig. 15).



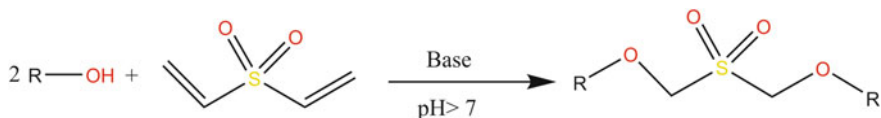


**Fig. 14** Prototype reaction between water-soluble cellulose derivatives and divinyl sulfone



**Fig. 15** Prototype reaction between diglycidyl ether and water-soluble cellulose derivatives

In general, the swelling and mechanical properties are manipulated by changing the cross-linker concentrations where stiffer hydrogel comes from intense cross-linking between cellulose derivatives chains (Sannino et al. 2009; Chang et al. 2010, 2011; Chang and Zhang 2011).

Radical cross-linking is another type of the chemical cross-linking to cellulose derivatives. CMC was cross-linked via gamma ray treatment to perform stable and non-toxic hydrogel (El-Hag Ali et al. 2008).

Accordingly, cellulose and cellulose derivative-based hydrogel showed a low toxic final product that is biodegradable, biocompatible, and stable. Therefore, cellulose-based hydrogels are used in numerous applications in diverse fields as well as those produced from alginate or chitosan.

## 2.4 Hyaluronic Acid

### 2.4.1 General Features

Hyaluronic acid (HA) is a linear copolymer of an alternative repeating disaccharide units, namely beta-1',4'-D-glucuronic acid and beta-1,3-N-acetyl-D-glucosamine (Fig. 16).

Hyaluronic acid is naturally found in the extracellular tissue in many parts of the human body. HA is playing an important role in many biological processes due to its excellent water-holding capacity that retains moisture in joints, eyes, and skin tissue. Plus, HA degrades readily by body enzymes resulting in non-toxic by-products. Therefore, HA shows better biocompatibility to tissue-related applications and is considered as a promising biopolymer among many other polysaccharides (Bhattacharyya et al. 2008; Tan et al. 2009; Burdick and Prestwich 2011; Collins and Birkinshaw 2013). It is notable that according to the poor mechanical

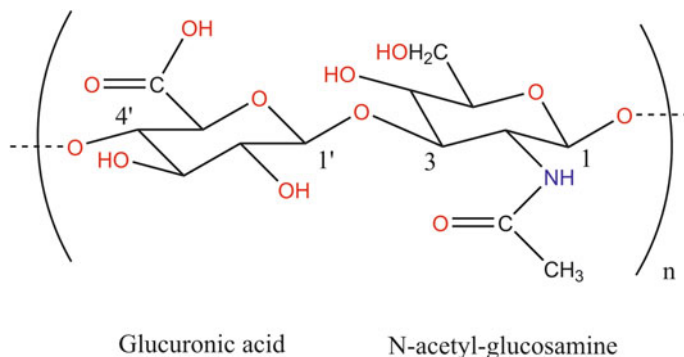


**Fig. 16** Chemical structure of hyaluronic acid

properties and rapid degradation of HA hydrogel, some studies are done to improve its performance.

#### 2.4.2 Hyaluronic Acid Hydrogel Formation

Chemical structure of native HA possesses different accessible functional groups, namely hydroxyl and carboxyl groups which are responsible for its solubility in water and fast degradation. These functional groups have contributed to either physical or chemical cross-linking of HA to create 3D network hydrogel.

#### 2.4.3 Reversible Hydrogel of Hyaluronic Acid

Few studies have been published on the physical cross-linking of HA, and only phosphatidylethanolamine was reported to form reversible HA hydrogel by making hydrogen bonding or hydrophobic interactions between HA chains (Kitazono and Kaneko 2012).

#### Irreversible Hydrogel of Hyaluronic Acid

On the other hand, few studies have been focused on the chemical crosslinking of HA in which cross-linking molecules react with the accessible functional groups in HA. It is believed that HA reacts with divinyl sulfone via the hydroxyl groups creating ether bonds. Also, glutaraldehyde cross-links with HA chains through reaction with the hydroxyl groups creating hemiacetal or ether bonds in acidic medium.

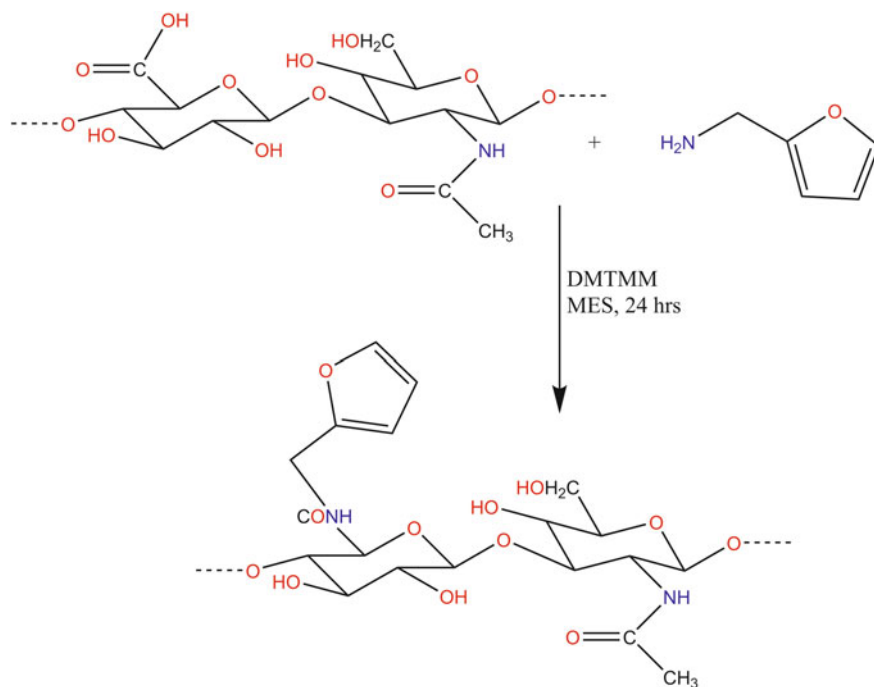


**Fig. 17** Synthesis of furan-HA in the presence of 4-(4,6-dimethoxy-1,3,5-triazin-2-yl)-4-methylmorpholinium chloride (DMTMM) and 2-(*N*-Morpholino)-ethanesulfonic acid (MES) (Nimmo et al. 2011)

On the other side, new techniques have been emerged by starting with modified HA and then crosslinking with the suitable cross-linkers. Furan-modified HA (Fig. 17) was synthesized and reacted with dimaleimide poly(ethylene glycol) (Fig. 18) (Nimmo et al. 2011). Also, HA hydrogel was done by using photo-polymerization of methacrylated-HA and *N*-vinylpyrrolidone. Such HA hydrogel is potentially applicable in injectable cell delivery for tissue engineering (Ki et al. 2006).

Like chitosan enzymatic crosslinking, horseradish peroxidase (HRP) was used with modified HA (HA-tyramine conjugate) to perform controllable mechanical strength and gelation rate as injectable hydrogel (Lee et al. 2008a).

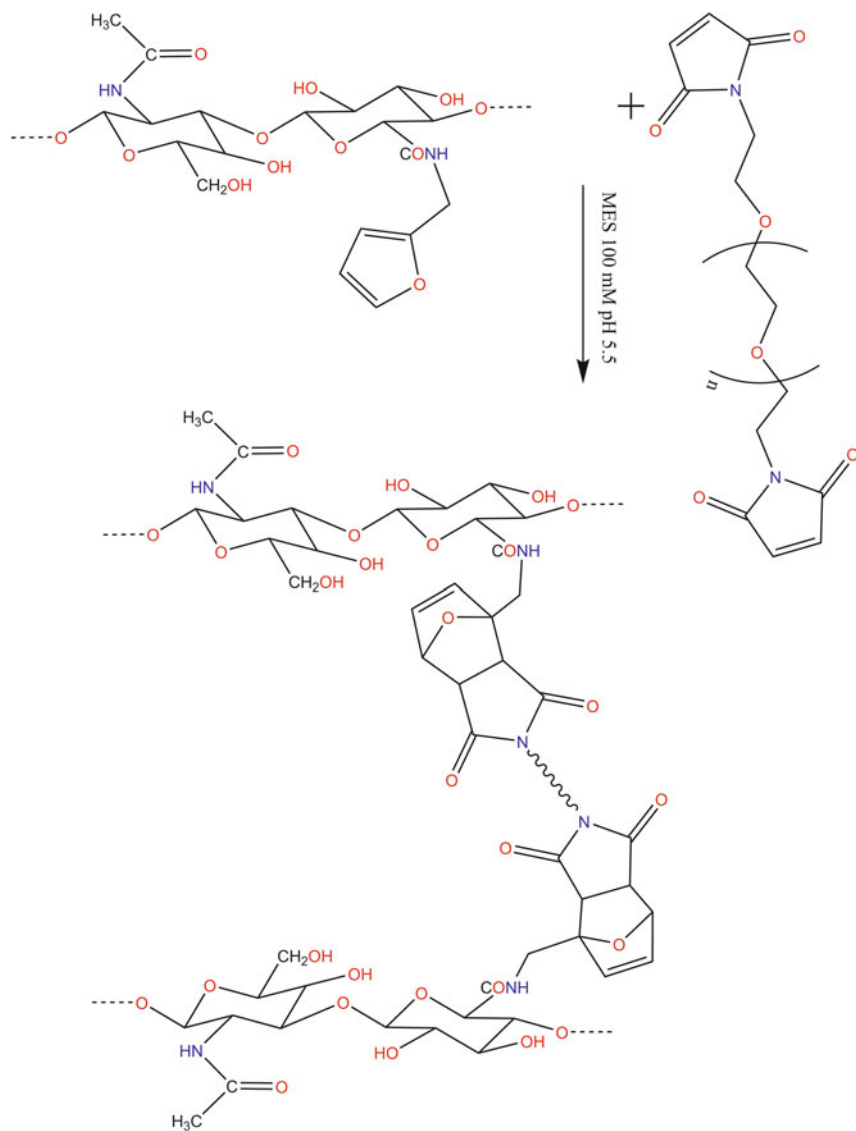


**Fig. 18** Chemical crosslinking of furan-HA with dimaleimide poly(ethylene glycol) (Nimmo et al. 2011)

## **2.5 Starch**

### **2.5.1 General Features**

Starch is a renewable polysaccharide produced from potatoes, rice, and other locally available resources. Starch is consisting of glucose repeating units in two different types, namely linear and helical amylose and branched amylopectin. Starch is insoluble in cold water and has been described by some limitations such as poor processability (Reis et al. 2008).

### **2.5.2 Starch-Based Hydrogel**

#### Reversible Hydrogel of Starch

Several studies have been done on starch grafting with acrylic acid and glycidyl methacrylate (Fig. 19) (Reis et al. 2008) in order to obtain higher capability of water absorbance and retention. Also, acrylonitrile has been grafted on starch by free radical polymerization using ceric ions. The resultant starch derivatives were used to prepare superabsorbance hydrogels.

Chemical cross-linking of native starch to form hydrogel shows exceptional properties. Thus, these produced starch-based hydrogels can be used for drug delivery, agriculture, and filtrations (Reis et al. 2008; Li et al. 2009; Laftah et al. 2011; Ahmed 2015).

## **3 Hydrogel Characterization**

### **3.1 Spectral Analysis**

The chemical structure of produced hydrogel, in most cases, has been characterized via infrared (IR) by which new covalent bonds can be detected. Also,  $C^{13}$  and  $H^1$  nuclear magnetic resonance (NMR) spectroscopes for solid materials have been used to detect the physical and the chemical properties of atoms in hydrogel matrices.

### **3.2 Gelation Time**

Gelation time of the polysaccharide-based hydrogel represents the time at which the polymer status changes from fluid-like to solid-like matrix. Typically, polymer-producing hydrogel is incubated into the conditions of crosslinking, and time for complete gelation will be reported.

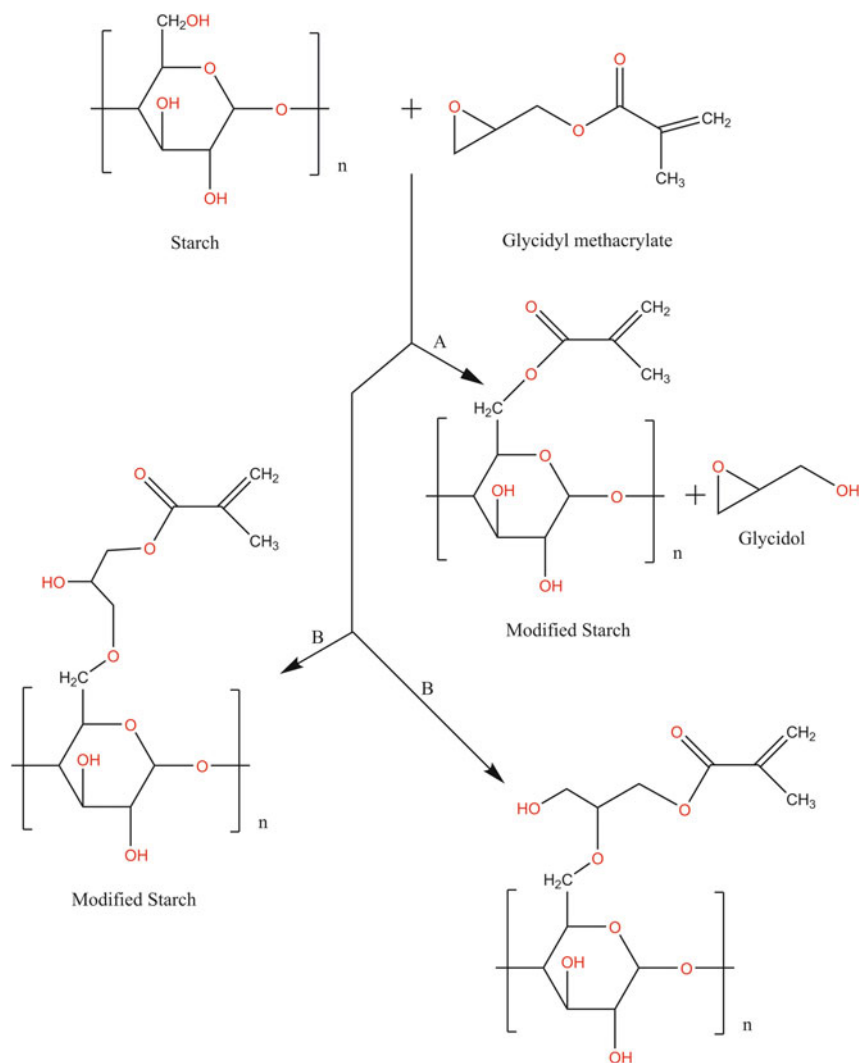


**Fig. 19** Reaction mechanism of starch with glycidyl methacrylate, **A**: via trans-esterification, **B**: via opening the epoxy ring (Reis et al. 2008)

### 3.3 Mechanical Properties

Mechanical properties and hydrogel stiffness can be demonstrated by using oscillatory shear measurements of elastic ( $G'$ ) and viscous modulus ( $G''$ ) of hydrogel matrices that have been measured at varied temperatures using constant stress rheometer.

### 3.4 *Swelling Test*

Swelling characteristic of prepared hydrogels is one of the most important properties that give hydrogel-wide applications. Basically, swelling behavior depends mainly on the presence of the hydrophilic functional groups in the matrices. The extent of water absorption by the freeze-dried composite hydrogels is evaluated by incubating the hydrogels in phosphate buffered saline (PBS) solution at 37 °C. Typically, the initial weights ( $W_a$ ) of the freeze-dried samples of hydrogel were determined before incubation while the weights of the wet hydrogel ( $W_b$ ) are reported after 7 days of incubation (Laftah et al. 2011). The swelling percentage was calculated by:

$$\% \text{ Swelling percentage} = (W_b - W_a)/W_a \times 100$$

### 3.5 *Scan Electron Microscope for Morphology*

The surface and cross-sectional morphology are very crucial parameter that will provide the porous structure of the produced hydrogel to confirm their applications accordingly. Typically, hydrogel morphology has been examined by scan electron microscopy (SEM).

### 3.6 *Encapsulation Efficiency*

The encapsulation efficiency is defined as the measurement of the remaining content of the core material which is encapsulated in the wall material compared to the starting core material content:

$$EE\% = [\text{Practical loading drug}]/[\text{Theoretical loading drug}] \times 100$$

The practical loading bioactive materials were measured as mentioned.

The release rate of encapsulated substance is usually determined by incubating few mg of the freeze-dried hydrogel samples in 10 mL PBS at specific pH at 37 °C in shaking water bath. At time intervals, 1 mL of the released medium was taken and 1 mL of the fresh medium is replaced. The absorbance readings of the filtered supernatant are recorded at specific nm using UV-Vis spectrophotometer, and finally, the released amount was calculated from standard calibration curve.

### 3.7 *Biological Impact*

In general, any substance or formula that comes into contact with human body should be clean and liberate no chemical agent that may be toxic or have adverse effects. In vitro cytotoxicity test is a useful technique for detecting such agents by using the yellow tetrazolium dye (MTT) assay to measure the cell viability (Nada et al. 2011).

The reduction of tetrazolium salts is now recognized as a safe and accurate method. The yellow tetrazolium salt is reduced in metabolically active cells to form insoluble purple formazan crystals, which are solubilized by the addition of a detergent. The color can then be quantified by spectrophotometric means. For each cell type, a linear relationship between cell number and absorbance is established to enable an accurate and straightforward quantification of changes in cell proliferation. Among the applications for MTT method are drug sensitivity, cytotoxicity, response to growth factors, and cell activation.

## 4 Hydrogel Applications

Alginate has been known for many applications such as food applications and textile printing (Ibrahim et al. 2006, 2011, 2013d) and recently used in the pharmaceutical applications. However, in the last few decades, alginate hydrogels have been explored in tissue engineering (Rowley et al. 1999) applications. Alginate hydrogel has been reported as stem cell (Zhao et al. 2010) scaffolds to guarantee cell proliferation (Ashton et al. 2007). Also, alginate cross-linked networks have gained great attention such as drug delivery matrices in which bioactive materials, protein (George and Abraham 2007), cells (Novikova et al. 2006; Tan and Takeuchi 2007), and drugs can be encapsulated and their release profiles are controlled (George and Abraham 2006).

Chitosan hydrogel has numerous applications in varied fields starting from textile industries, cosmetics, and medical purposes. Utilization of chitosan in tissue engineering, drug delivery, and medicine-related application makes chitosan as an important, exciting, and promising polysaccharide nowadays. Several studies have been done in using chitosan hydrogels in encapsulating bioactive molecules such as cells (includes stem cells), proteins, enzymes, and sensitive drugs. Chitosan and chitosan derivatives have covered a broad spectrum of pharmaceutical applications, providing wide degree of flexibility for reshaping and fitting the targeting sides. Also, chitosan-based hydrogel has been used as color and heavy metal removal substrate from water wastes (Ishihara et al. 2006; Hong et al. 2007; Chatterjee et al. 2009a; Ribeiro et al. 2009; Bhattarai et al. 2010).

Cellulose hydrogel is superior candidate over other polymers when biocompatibility and biodegradability are required for the final applications. Due to cellulose low cost and large availability, cellulose is regarded as appealing precursor



for hydrogel (Sannino et al. 2009). Final application of the produced cellulose-based hydrogel depends on the mechanical properties. Azide–alkyne functional cellulose hydrogel showed inert response to the active biomaterials. However, low mechanical properties of such cellulose-based hydrogel showed limited factor of wide applications (Koschella et al. 2011). Hydroxypropyl methylcellulose has been developed as suitable matrix for injectable hydrogel in the *in vitro* three-dimensional culture for rabbit articular chondrocytes (Vinatier et al. 2009). Also, cellulose-based graft by acylated monomers is provided in the market as superabsorbent hydrogels for personal care products (Sannino et al. 2009). Cellulose-based superabsorbent hydrogel can absorb up to 1000 mL of water per one gram of dry material. Such characteristic is main reason behind using cellulose-based hydrogel as water reservoirs in agriculture by which water consumption will be controlled and water resources will be optimized. Moreover, nutrients and/or plant pharmaceuticals have been encapsulated into such cellulose-based hydrogel to support plant by water and such loaded materials as needed (Sannino et al. 2009).

Cellulose-based hydrogel is also used to absorb the excess water from human body that is known in the market as body's water retainer. It requires pH-sensitive hydrogel that goes through the acid medium without swelling and it swells at pH 6–7 existed in the intestine region.

On contrary, hydrogel that swells in acidic medium has been employed as meal replacement to absorb liquids and swell inside the stomach resulting as sense of fullness. The latter characteristic of cellulose-based hydrogel is known in the market as stomach bulking agents.

Carboxymethylcellulose hydrogel and anionic hydrogel have been used extensively in oral drug delivery that relays mainly on polyelectrolyte hydrogels. Cellulose-based hydrogels have been reported as biodegradable and biocompatible matrices for scaffolds, regenerative medicine and for wound dressing.

Hyaluronic acid-based hydrogels, chemically crosslinked with divinyl sulfone, have been employed in preparing biocompatible hydrogels as scaffolds in order to deliver therapeutic molecules (Bhattacharyya et al. 2008). However, thermosensitive, hyaluronic acid-based hydrogels, crosslinked by using poly(*N*-isopropylacrylamide), have been used as an injectable matrices for adipose tissue engineering (Tan et al. 2009). In different manner, hyaluronic acid has been attached to contact lens, made of poly(2-hydroxyethyl methacrylate), as wetting agent in order to reduce the deposition of protein and lipid from tear fluids (Van Beek et al. 2008). Hydrogel prepared by the reaction between hyaluronic acid and phosphatidyl ethanolamine has been suggested to treat knee joint (Kitazono and Kaneko 2012). Due to the distinguished biological potentials of hyaluronic acid, many applications of the hyaluronic hydrogels have been reported especially in cell encapsulation (Ki et al. 2006) and scaffolds for bone regeneration (Patterson et al. 2010).

Starch is regarded as renewable, biocompatible, and abundant polysaccharide that has shown wide attraction for medical applications. For instance, starch-based hydrogel, crosslinked by glycidyl methacrylate, has been reported as potential carrier for drug delivery matrices (Reis et al. 2008).

## 5 Conclusion and Future Prospective

An overview of the polymer gel principles, definition, and types was covered in the first section of this review. Hydrogel formation based on hydrophilic polymers was covered in order to represent the difference between the physical and chemical crosslinking. Forces controlling each type of the crosslinking were described as well. Famous candidates of polysaccharides, namely alginate, chitosan, cellulose, hyaluronic acid, and starch, were highlighted with several examples on their physical and chemical crosslinking. Applications for each hydrogel have been represented with their potentials and limitations.

In conclusion, new trends have been emerged to design new shapes of hydrogel by using the bio-3D-printer in order to form suitable scaffolds for tissue engineering. Introducing amino acids to the carbohydrate polymers will enhance the biocompatibility of the final products in terms of cell attachments, cell proliferation, and cell migration. Different chemical cross-linkers with different spacing link will control the pore size of the hydrogel to cope with the encapsulation efficiency targeting specific applications. New series of interactive hydrogel can be generated to be sensitive to the surrounding environment such as pH, temperature, light/darkness, heavy metals, and bacterial infection. In polymeric carbohydrates whose chemical structures possess mainly hydroxyl functional groups, chemical modifications require high temperatures, agitation, and long reaction times to carry out any chemical reactions. However, such requirements are not favorable for pharmaceutical carriers designed for hosting and delivery bioactive materials such as drugs, cells, proteins, and enzymes. Click chemistry is a new expression for chemical reactions taking place in mild conditions with high-efficient and simple purification methods. Click chemistry that lies mainly in azide and alkyne precursors shows potentials to serve as a promising route in performing pharmaceutical materials taking in consideration ecoconcerns related to their synthesis and utilization in addition to economic issues.

## References

- Ahmed EM (2015) Hydrogel: preparation, characterization, and applications: a review. *J Adv Res* 6:105–121
- Alves NM, Mano JF (2008) Chitosan derivatives obtained by chemical modifications for biomedical and environmental applications. *Int J Biol Macromol* 43:401–414
- Ashton RS, Banerjee A, Punyani S, Schaffer DV, Kane RS (2007) Scaffolds based on degradable alginate hydrogels and poly(lactide-co-glycolide) microspheres for stem cell culture. *Biomaterials* 28:5518–5525
- Augst AD, Kong HJ, Mooney DJ (2006) Alginate hydrogels as biomaterials. *Macromol Biosci* 6:623–633
- Azlan K, Wan Saime WN, Lai Ken L (2009) Chitosan and chemically modified chitosan beads for acid dyes sorption. *J Environ Sci* 21:296–302

- Bacaita ES, Ciobanu BC, Popa M, Agop M, Desbrieres J (2014) Phases in the temporal multiscale evolution of the drug release mechanism in IPN-type chitosan based hydrogels. *Phys Chem Chem Phys* 16:25896–25905
- Bhattacharyya S, Guillot S, Dabboue H, Tranchant J-F, Salvétat J (2008) Carbon nanotubes as structural nanofibers for hyaluronic acid hydrogel scaffolds. *Biomacromolecules* 9:505–509
- Bhattarai N, Gunn J, Zhang M (2010) Chitosan-based hydrogels for controlled, localized drug delivery. *Adv Drug Deliv Rev* 62:83–99
- Burdick JA, Prestwich GD (2011) Hyaluronic acid hydrogels for biomedical applications. *Adv Mater* 23:41–56
- Chan AW, Whitney RA, Neufeld RJ (2009) Semisynthesis of a controlled stimuli-responsive alginate hydrogel. *Biomacromolecules* 10:609–616
- Chang C, Zhang L (2011) Cellulose-based hydrogels: Present status and application prospects. *Carbohydr Polym* 84:40–53
- Chang P-C, Liu B-Y, Liu C-M, Chou H-H, Ho M-H, Liu H-C, Wang D-M, Hou L-T (2007) Bone tissue engineering with novel rhBMP2-PLLA composite scaffolds. *J Biomed Mater Res A* 81:771–780
- Chang C, Duan B, Cai J, Zhang L (2010) Superabsorbent hydrogels based on cellulose for smart swelling and controllable delivery. *Eur Polym J* 46:92–100
- Chang C, He M, Zhou J, Zhang L (2011) Swelling behaviors of pH- and salt-responsive cellulose-based hydrogels. *Macromolecules* 44:1642–1648
- Chatterjee S, Lee DS, Lee MW, Woo SH (2009a) Congo red adsorption from aqueous solutions by using chitosan hydrogel beads impregnated with nonionic or anionic surfactant. *Bioresour Technol* 100:3862–3868
- Chatterjee S, Lee DS, Lee MW, Woo SH (2009b) Enhanced adsorption of congo red from aqueous solutions by chitosan hydrogel beads impregnated with cetyl trimethyl ammonium bromide. *Bioresour Technol* 100:2803–2809
- Chatterjee S, Chatterjee T, Woo SH (2010a) A new type of chitosan hydrogel sorbent generated by anionic surfactant gelation. *Bioresour Technol* 101:3853–3858
- Chatterjee S, Lee MW, Woo SH (2010b) Adsorption of congo red by chitosan hydrogel beads impregnated with carbon nanotubes. *Bioresour Technol* 101:1800–1806
- Cheng Y-H, Yang S-H, Su W-Y, Chen Y-C, Yang K-C, Cheng WT-K, Wu S, Lin F (2010) Thermosensitive Chitosan–Gelatin–Glycerol phosphate hydrogels as a cell carrier for nucleus pulposus regeneration: an in vitro study. *Tissue Eng Part A* 16:695–703
- Cheng Y, Nada AA, Valmikinathan CM, Lee P, Liang D, Yu X, Kumbar SG (2014) In situ gelling polysaccharide-based hydrogel for cell and drug delivery in tissue engineering. *J Appl Polym Sci*. <https://doi.org/10.1002/app.39934>
- Collins MN, Birkinshaw C (2013) Hyaluronic acid based scaffolds for tissue engineering—a review. *Carbohydr Polym* 92:1262–1279
- Csaba N, Köping-Höggård M, Alonso MJ (2009) Ionically crosslinked chitosan/tripolyphosphate nanoparticles for oligonucleotide and plasmid DNA delivery. *Int J Pharm* 382:205–214
- Dahou W, Ghemati D, Oudia A, Aliouche D (2010) Preparation and biological characterization of cellulose graft copolymers. *Biochem Eng J* 48:187–194
- El-Hag Ali A, Abd El-Rehim H, Kamal H, Hegazy DE-S (2008) Synthesis of carboxymethyl cellulose based drug carrier hydrogel using ionizing radiation for possible use as site specific delivery system. *J Macromol Sci Part A* 45:628–634
- Farag S, Al-Afaleq EI (2002) Preparation and characterization of saponified delignified cellulose polyacrylonitrile-graft copolymer. *Carbohydr Polym* 48:1–5
- George M, Abraham TE (2006) Polyionic hydrocolloids for the intestinal delivery of protein drugs: alginate and chitosan—a review. *J Control Release* 114:1–14
- George M, Abraham TE (2007) pH sensitive alginate-guar gum hydrogel for the controlled delivery of protein drugs. *Int J Pharm* 335:123–129
- Guo C, Zhou L, Lv J (2013) Effects of expandable graphite and modified ammonium polyphosphate on the flame-retardant and mechanical properties of wood flour-polypropylene composites. *Polym Polym Compos* 21:449–456

- Hong Y, Song H, Gong Y, Mao Z, Gao C, Shen J (2007) Covalently crosslinked chitosan hydrogel: properties of in vitro degradation and chondrocyte encapsulation. *Acta Biomater* 3:23–31
- Hong W, Liu Z, Suo Z (2009) Inhomogeneous swelling of a gel in equilibrium with a solvent and mechanical load. *Int J Solids Struct* 46:3282–3289
- Hurtado PI, Berthier L, Kob W (2007) Heterogeneous diffusion in a reversible gel. *Phys Rev Lett* 98:98–101
- Ibrahim NA, Abo-Shosha MH, El-Zairy EA, El-Zairy EM (2006) New thickening agents for reactive printing of cellulosic fabrics. *J Appl Poly Sci* 101(6):4430–4439
- Ibrahim NA, Eid BM, El-Zairy ER (2011) Antibacterial functionalization of reactive-cellulosic prints via inclusion of bioactive Neem oil/ $\beta$ CD complex. *Carbohydr Polym* 86:1313–1319
- Ibrahim NA, Eid BM, El-Aziz EA, Elmaaty TMA, Ramadan SM (2017) Loading of chitosan – Nano metal oxide hybrids onto cotton/polyester fabrics to impart permanent and effective multifunctions. *Int J Biol Macromol* 105: 769–776
- Ibrahim NA, Abou Elmaaty TM, Eid BM, Abd El-Aziz E (2013a) Combined antimicrobial finishing and pigment printing of cotton/polyester blends. *Carbohydr Polym* 95:379–388
- Ibrahim NA, Eid BM, Elmaaty TMA, El-Aziz EA (2013b) A smart approach to add antibacterial functionality to cellulosic pigment prints. *Carbohydr Polym* 94:612–618
- Ibrahim NA, Eid BM, Youssef MA, Ibrahim HM, Ameen HA, Salah AM (2013c) Multifunctional finishing of cellulosic/polyester blended fabrics. *Carbohydr Polym* 97:783–793
- Ibrahim NA, El-Zairy EMR, Abdalla WA, Khalil HM (2013d) Combined UV-protecting and reactive printing of cellulosic/wool blends. *Carbohydr Polym* 92:1386–1394
- Ibrahim NA, Khalil HM, El-Zairy EMR, Abdalla WA (2013e) Smart options for simultaneous functionalization and pigment coloration of cellulosic/wool blends. *Carbohydr Polym* 96:200–210
- Ishihara M, Obara K, Nakamura S et al (2006) Chitosan hydrogel as a drug delivery carrier to control angiogenesis. *J Artif Organs* 9:8–16
- Ito K (2007) Novel cross-linking concept of polymer network: synthesis, structure, and properties of slide-ring gels with freely movable junctions. *Polym J* 39:489–499
- Jameela SR, Lakshmi S, James NR, Jayakrishnan A (2002) Preparation and evaluation of photocrosslinkable chitosan as a drug delivery matrix. *J Appl Polym Sci* 86:1873–1877
- Jen AC, Wake MC, Mikos AG (1996) Review: hydrogels for cell immobilization. *Biotechnol Bioeng* 50:357–364
- Jeon O, Bouhadir KH, Mansour JM, Alsberg E (2009) Photocrosslinked alginate hydrogels with tunable biodegradation rates and mechanical properties. *Biomaterials* 30:2724–2734
- Jin R, Moreira Teixeira LS, Dijkstra PJ, Karperien M, van Blitterswijk CA, Zhong ZY, Feijen J (2009) Injectable chitosan-based hydrogels for cartilage tissue engineering. *Biomaterials* 30:2544–2551
- Kabiri K, Omidian H, Zohuriaan-Mehr MJ, Doroudiani S (2011) Superabsorbent hydrogel composites and nanocomposites: a review. *Polym Compos* 32:277–289
- Ki HB, Jun JY, Tae GP (2006) Fabrication of hyaluronic acid hydrogel beads for cell encapsulation. *Biotechnol Prog* 22:297–302
- Kim M-S, Choi Y-J, Noh I, Tae G (2007) Synthesis and characterization of in situ chitosan-based hydrogel via grafting of carboxyethyl acrylate. *J Biomed Mater Res, Part A* 83A:674–682
- Kitazono E, Kaneko H (2012) Hyaluronic acid compound, hydrogel thereof and joint treating material. 2
- Koschella A, Hartlieb M, Heinze T (2011) A “click-chemistry” approach to cellulose-based hydrogels. *Carbohydr Polym* 86:154–161
- Kriegel R (2004) Divinyl sulfone crosslinking agents and methods of use in subterranean applications
- Kulkarni RV, Sa B (2008) Evaluation of pH-sensitivity and drug release characteristics of (polyacrylamide-grafted-xanthan)-carboxymethyl cellulose-based pH-sensitive interpenetrating network hydrogel beads. *Drug Dev Ind Pharm* 34:1406–1414

- Laftah WA, Hashim S, Ibrahim AN (2011) Polymer hydrogels: a review. *Polym Plast Technol Eng* 50:1475–1486
- Lawrie G, Keen I, Drew B, Chandler-Temple A, Rintoul L, Fredericks P, Grøndahl L (2007) Interactions between alginate and chitosan biopolymers characterized using FTIR and XPS. *Biomacromolecules* 8:2533–2541
- Lee KY, Mooney DJ (2012) Alginate: properties and biomedical applications. *Prog Polym Sci* 37:106–126
- Lee KY, Bouhadir KH, Mooney DJ (2004) Controlled degradation of hydrogels using multi-functional cross-linking molecules. *Biomaterials* 25:2461–2466
- Lee F, Chung JE, Kurisawa M (2008a) An injectable enzymatically crosslinked hyaluronic acid-tyramine hydrogel system with independent tuning of mechanical strength and gelation rate. *Soft Matter* 4:880–887
- Lee HS, Singh P, Thomason WH, Fogler HS (2008b) Waxy oil gel breaking mechanisms: adhesive versus cohesive failure. *Energy Fuels* 22:480–487
- Li X, Xu S, Wang J, Chen X, Feng S (2009) Structure and characterization of amphoteric semi-IPN hydrogel based on cationic starch. *Carbohydr Polym* 75:688–693
- Lim S-H, Hudson SM (2004) Synthesis and antimicrobial activity of a water-soluble chitosan derivative with a fiber-reactive group. *Carbohydr Res* 339:313–319
- Marci G, Mele G, Palmisano L, Pulito P, Sannino A (2006) Environmentally sustainable production of cellulose-based superabsorbent hydrogels. *Green Chem* 8:439–444
- Marsano E, Bianchi E, Sciuotto L (2003) Microporous thermally sensitive hydrogels based on hydroxypropyl cellulose crosslinked with poly-ethyleneglicol diglycidyl ether. *Polymer (Guildf)* 44:6835–6841
- Mathur AM, Moorjani SK, Scranton AB (1996) Methods for synthesis of hydrogel networks: a review. *J Macromol Sci Part C Polym Rev* 36:405–430
- Mirzaei BE, Ramazani SAA, Shafiee M, Danaei M (2013) Studies on glutaraldehyde crosslinked chitosan hydrogel properties for drug delivery systems. *Int J Polym Mater* 62:605–611
- Müller FA, Müller L, Hofmann I, Greil P, Wenzel MM, Staudenmaier R (2006) Cellulose-based scaffold materials for cartilage tissue engineering. *Biomaterials* 27:3955–3963
- Muzzarelli RAA (2009) Genipin-crosslinked chitosan hydrogels as biomedical and pharmaceutical aids. *Carbohydr Polym* 77:1–9
- Nada AA, Hauser P, Hudson SM (2011) The grafting of per-(2,3,6-O-allyl)- $\beta$  cyclodextrin onto derivatized cotton cellulose via thermal and atmospheric plasma techniques. *Plasma Chem Plasma Process* 31:605–621
- Nada AA, James R, Shelke NB, Harmon MD, Awad HM, Nagarale RK, Kumbar SG (2014) A smart methodology to fabricate electrospun chitosan nanofiber matrices for regenerative engineering applications. *Polym Adv Technol* 25:507–515
- Nimmo CM, Owen SC, Shoichet MS (2011) Diels–Alder click cross-linked hyaluronic acid hydrogels for tissue engineering. *Biomacromolecules* 12:824–830
- Novikova LN, Mosahebi A, Wiberg M, Terenghi G, Kellerth JO, Novikov LN (2006) Alginate hydrogel and matrigel as potential cell carriers for neurotransplantation. *J Biomed Mater Res - Part A* 77:242–252
- Pal K, Singh VK, Anis A, Thakur G, Bhattacharya MK (2013) Hydrogel-based controlled release formulations: designing considerations, characterization techniques and applications. *Polym Plast Technol Eng* 52:1391–1422
- Park S, Okada T, Takeuchi D, Osakada K (2010) Cyclopolymerization and copolymerization of functionalized 1,6-heptadienes catalyzed by Pd complexes: Mechanism and application to physical-gel formation. *Chem A Eur J* 16:8662–8678
- Patterson J, Siew R, Herring SW, Lin ASP, Guldborg R, Stayton PS (2010) Hyaluronic acid hydrogels with controlled degradation properties for oriented bone regeneration. *Biomaterials* 31:6772–6781
- Pawar SN, Edgar KJ (2012) Alginate derivatization: a review of chemistry, properties and applications. *Biomaterials* 33:3279–3305

- Prabaharan M (2008) Review paper: chitosan derivatives as promising materials for controlled drug delivery. *J Biomater Appl* 23:5–36
- Qi H, Liebert T, Meister F, Heinze T (2009) Homogenous carboxymethylation of cellulose in the NaOH/urea aqueous solution. *React Funct Polym* 69:779–784
- Qin X, Lu A, Cai J, Zhang L (2013) Stability of inclusion complex formed by cellulose in NaOH/urea aqueous solution at low temperature. *Carbohydr Polym* 92:1315–1320
- Reis AV, Guilherme MR, Moia TA, Mattoso LHC, Muniz EC, Tambourgi EB (2008) Synthesis and characterization of a starch-modified hydrogel as potential carrier for drug delivery system. *J Polym Sci Part A: Polym Chem* 46:2567–2574
- Ribeiro MP, Espiga A, Silva D et al (2009) Development of a new chitosan hydrogel for wound dressing. *Wound Repair Regen* 17:817–824
- Rickett TA, Amoozgar Z, Tucek CA, Park J, Yeo Y, Shi R (2011) Rapidly photo-cross-linkable chitosan hydrogel for peripheral neurosurgeries. *Biomacromolecules* 12:57–65
- Rowley JA, Madlambayan G, Mooney DJ (1999) Alginate hydrogels as synthetic extracellular matrix materials. *Biomaterials* 20:45–53
- Ruel-Gariépy E, Leroux JC (2004) In situ-forming hydrogels—review of temperature-sensitive systems. *Eur J Pharm Biopharm* 58:409–426
- Sannino A, Madaghiele M, Lionetto MG, Schettino T, Maffezzoli A (2006) A cellulose-based hydrogel as a potential bulking agent for hypocaloric diets: an in vitro biocompatibility study on rat intestine. *J Appl Polym Sci* 102:1524–1530
- Sannino A, Demitri C, Madaghiele M (2009) Biodegradable cellulose-based hydrogels: design and applications. *Materials (Basel)* 2:353–373
- Singh A, Sharma PK, Garg VK, Garg G (2010) Hydrogels: a review. *Int J Pharm Sci Rev Res* 4:97–105
- Soleimani Dorcheh A, Abbasi MH (2008) Silica aerogel; synthesis, properties and characterization. *J Mater Process Technol* 199:10–26
- Song Y, Sun Y, Zhang X, Zhou J, Zhang L (2008a) Homogeneous quaternization of cellulose in NaOH/urea aqueous solutions as gene carriers. *Biomacromolecules* 9:2259–2264
- Song Y, Zhou J, Zhang L, Wu X (2008b) Homogenous modification of cellulose with acrylamide in NaOH/urea aqueous solutions. *Carbohydr Polym* 73:18–25
- Sudheesh Kumar PT, Lakshmanan VK, Anilkumar TV, Ramya C, Reshmi P, Unnikrishnan AG, Nair SV, Jayakumar R (2012) Flexible and microporous chitosan hydrogel/nano ZnO composite bandages for wound dressing: in vitro and in vivo evaluation. *ACS Appl Mater Interfaces* 4:2618–2629
- Tan WH, Takeuchi S (2007) Monodisperse alginate hydrogel microbeads for cell encapsulation. *Adv Mater* 19:2696–2701
- Tan H, Ramirez CM, Miljkovic N, Li H, Rubin JP, Marra KG (2009) Thermosensitive injectable hyaluronic acid hydrogel for adipose tissue engineering. *Biomaterials* 30:6844–6853
- Teng D, Wu Z, Zhang X, Wang Y, Zheng C, Wang Z, Li C (2010) Synthesis and characterization of in situ cross-linked hydrogel based on self-assembly of thiol-modified chitosan with PEG diacrylate using Michael type addition. *Polymer (Guildf)* 51:639–646
- Thakur VK, Thakur MK (2014a) Recent advances in graft copolymerization and applications of chitosan: a review. *ACS Sustain Chem Eng* 2:2637–2652
- Thakur VK, Thakur MK (2014b) Recent trends in hydrogels based on psyllium polysaccharide: a review. *J Clean Prod* 82:1–15
- Thakur VK, Thakur MK (2015) Recent advances in green hydrogels from lignin: a review. *Int J Biol Macromol* 72:834–847
- Thakur VK, Thakur MK, Gupta RK (2014) Graft copolymers of natural fibers for green composites. *Carbohydr Polym* 104:87–93
- Van Beek M, Jones L, Sheardown H (2008) Hyaluronic acid containing hydrogels for the reduction of protein adsorption. *Biomaterials* 29:780–789
- Van Vlierberghe S, Dubrue P, Schacht E (2011) Biopolymer-based hydrogels as scaffolds for tissue engineering applications: a review. *Biomacromolecules* 12:1387–1408

- Vinatier C, Gauthier O, Fatimi A et al (2009) An injectable cellulose-based hydrogel for the transfer of autologous nasal chondrocytes in articular cartilage defects. *Biotechnol Bioeng* 102:1259–1267
- Wakhet S, Singh VK, Sahoo S et al (2015) Characterization of gelatin-agar based phase separated hydrogel, emulgel and bigel: a comparative study. *J Mater Sci Mater Med* 26:118
- West ER, Xu M, Woodruff TK, Shea LD (2007) Physical properties of alginate hydrogels and their effects on in vitro follicle development. *Biomaterials* 28:4439–4448
- Xu L, Huang Y-A, Zhu Q-J, Ye C (2015) Chitosan in molecularly-imprinted polymers: current and future prospects. *Int J Mol Sci* 16:18328–18347
- Yang JS, Xie YJ, He W (2011) Research progress on chemical modification of alginate: a review. *Carbohydr Polym* 84:33–39
- Zhao L, Weir MD, Xu HHK (2010) An injectable calcium phosphate-alginate hydrogel-umbilical cord mesenchymal stem cell paste for bone tissue engineering. *Biomaterials* 31:6502–6510
- Zhou J, Zhang L, Cai J, Shu H (2002) Cellulose microporous membranes prepared from NaOH/urea aqueous solution. *J Memb Sci* 210:77–90
- Zhou J, Zhang L, Deng Q, Wu X (2004) Synthesis and characterization of cellulose derivatives prepared in NaOH/urea aqueous solutions. *J Polym Sci Part A: Polym Chem* 42:5911–5920
- Zhou Q, Zhang L, Li M, Wu X, Cheng G (2005) Homogeneous hydroxyethylation of cellulose in NaOH/urea aqueous solution. *Polym Bull* 53:243–248
- Zhou J, Chang C, Zhang R, Zhang L (2007) Hydrogels prepared from unsubstituted cellulose in NaOH/urea aqueous solution. *Macromol Biosci* 7:804–809

# Chapter 5

## Silica-Based Polymeric Gels as Platforms for Delivery of Phosphonate Pharmaceuticals



Konstantinos E. Papathanasiou, Maria Vassaki, Argyro Spinthaki, Argyri Moschona and Konstantinos D. Demadis

### 1 Matrices in Controlled Delivery Gel Systems: The Case of Silica

Polymeric matrices are a prominent option for the construction of drug delivery carriers, due to their easy chemical or physical modification and wide variety of potential applications (Mashkevich 2007). There are many different drug carrier matrix types depending on specific factors and the desired outcome, such as the drug type and the route of delivery. These are considered as “open systems”; therefore, polymer gel carriers play a dominant role in the pharmaceutical field because they are able to transport molecules that could act as drugs, through cross-linked networks. Hence, spontaneous, controlled release can be accomplished.

Gel formation can possess various degrees of difficulty depending on the choice of polymer, but research in the field is quite extensive. Some examples of gel types are hydrogels, stimuli-responsive, (bio)degradable (Binauld and Stenzel 2013), just to mention a few. For example, hydrogels are typically formed from a network of polymer chains, constructing a colloidal gel that can contain, up to 99% water (Soppimath et al. 2001).

Silica gels have drawn substantial interest of the scientific community over the past few years due to their low toxicity, stability, low manufacturing cost, and multiple usages. They appear in a variety of applications, such as promising polar adsorbents of, e.g., amino acids (Zhao 1992), and as drug carriers. Pure silica gels can be used as the stationary phase in chromatography (thin layer chromatography, reversed-phase chromatography, etc.), and functionalized silicon dioxide gels are often used in organic synthesis and purification of various reagents and products (Kennedy 1997).

---

K. E. Papathanasiou · M. Vassaki · A. Spinthaki · A. Moschona · K. D. Demadis (✉)  
Crystal Engineering, Growth and Design Laboratory, Department of Chemistry,  
University of Crete, Voutes Campus, 71003 Heraklion, Crete, Greece  
e-mail: demadis@uoc.gr



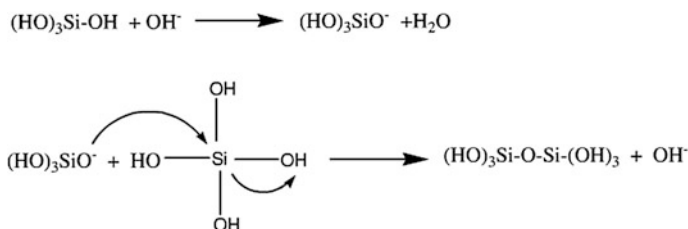


**Fig. 1**  $\text{S}_{\text{N}2}$ -like mechanism of silicic acid polycondensation

Silicic acid  $[\text{Si}(\text{OH})_4]$  polymerization has been the subject of intense research (Ehrlich et al. 2010). It can result in gel formation under adjustable pH values and appropriate supersaturated solutions. It is worthwhile to take a closer look at some significant details of silicon chemistry. In diluted aqueous solutions, soluble silica is found as ortho/monosilicic acid  $\text{Si}(\text{OH})_4$ . This is a monomer that exists in two forms in an about-neutral pH environment, the protonated species (major,  $\text{Si}(\text{OH})_4$ ), and the singly deprotonated species (minor,  $\text{Si}(\text{OH})_3\text{O}^-$ ). As pH increases, the concentration of the deprotonated form ( $\text{Si}(\text{OH})_3\text{O}^-$ ) increases. Increasing the silicate concentration and adjusting the pH value to  $\sim 7$  leads to condensation of two monomers, with simultaneous loss of one water molecule. The procedure follows a  $\text{S}_{\text{N}2}$ -type mechanism, in which a deprotonated silicic acid molecule attacks a fully protonated one (see Fig. 1) (Demadis 2008).

The aforementioned step is the most crucial one as far as the kinetics of the polycondensation is concerned and is the rate-determining step in the complex silica polycondensation process (Perry and Keeling-Tucker 1998). The next steps involve the formation of trimers, tetramers, and then higher oligomeric species until 1–2 nm amorphous silica nanoparticles are formed (Mann et al. 1983).

It is worth mentioning that the pKa of the polysilicic acids at these stages of the polymerization is about 6.5, and thus, above pH 7–8, negatively charged silicates become predominant (Coradin et al. 2004). In such conditions, silicic acid on the surface of colloidal species exists in equilibrium with dissolved silicic acid molecules, and, hence, due to the Ostwald ripening process, further particle growth occurs, leading to stable sols. In contrast, at pH regions below 7, particles can be only slightly charged, so no electrostatic repulsion prevents them from aggregation, leading to gel formation (Ning 2010).

A variety of methods have been published from different research groups regarding the fabrication of silica gels, which slightly differ from one another (Wang and Zhang 2007; Gommès et al. 2004). The easiest and most widely used method for gel preparation is a process that involves preparation of an aqueous solution of hydrated sodium silicate ( $\text{Na}_2\text{SiO}_3 \cdot x\text{H}_2\text{O}$ ), which is then acidified to form a gelatinous precipitate. After mild washing, the product can be dehydrated and the percentage of dehydration depends on the exact end use that it is intended for.

After gel formation, the remaining hydroxyl groups on the gel surface (silanols,  $-\text{Si-O-H}$ ) can either be immediately used as binding sites for other candidate molecules, or become guests of an array of chemical or physical modifications, due to their modifiable oxygen atoms. Thus, silica gels are ideal candidates for a huge array of applications.

Extensive research has been reported on controlled release systems involving silica-based drug carriers. The importance of the controlled release principle in a drug delivery system lies in the need to deliver the desired drug in the right (i) time, (ii) area/location, and (iii) concentration. More specifically, a drug delivery system of controlled release properties should be able to maintain the optimum drug concentration in the blood, with minimum fluctuation, to achieve predictable and reproducible release rates for an extended time period and, last but not least, to eliminate side effects. Thus, the synthesis of gels for a specific drug should be tailored considering the desired release kinetics, the loading level and, as expected, the physical properties of drugs (Martin del Valle et al. 2009).

## 2 Controlled Release Systems

In the past of few decades, several studies have been carried out on controlled delivery systems (Ramakrishna et al. 2001; Mestiri et al. 1995; Hughes et al. 2004; Szymura-Oleksiak et al. 2001). Controlled release systems are designed to support and enhance the treatment under study. The goal of these systems is to control the drug release through the passage of time, assist the drug to overtake natural potential barriers, hinder and prevent possible elimination/excretion of the drug from the body, guide the drug to the desired site of action and minimize the potential exposure of the drug to undesirable degradation effects (Siegel and Rathbone 2012).

The desired system should be able to maintain the optimum concentration of the drug in the blood, release the drug in a controlled and planned fashion, and have the ability to enhance the duration of action of the drug, particularly when it is short-lived. Also, a delivery system must be designed so as not to cause side effects to the patient, to avoid frequent doses, which lead to drug wastage. The target of a delivery system should be to provide an optimized treatment.

There are two common methods of controlled release, the temporal control, and the distribution control. In temporal control, the drug is protected by a device which has the ability for long-range transport at specific times during the treatment. This method is applicable to drugs which tend to be metabolized rapidly and eliminate from the body (see Fig. 2).

Temporal control may be accomplished by three mechanisms: delayed dissolution, diffusion controlled and drug solution flow control. In delayed dissolution, polymeric devices protect drug release by delaying the dissolution of the drug molecules, thus inhibiting diffusion or controlling the flow. In diffusion controlled release, an insoluble polymeric matrix delays and controls the diffusion of the drug

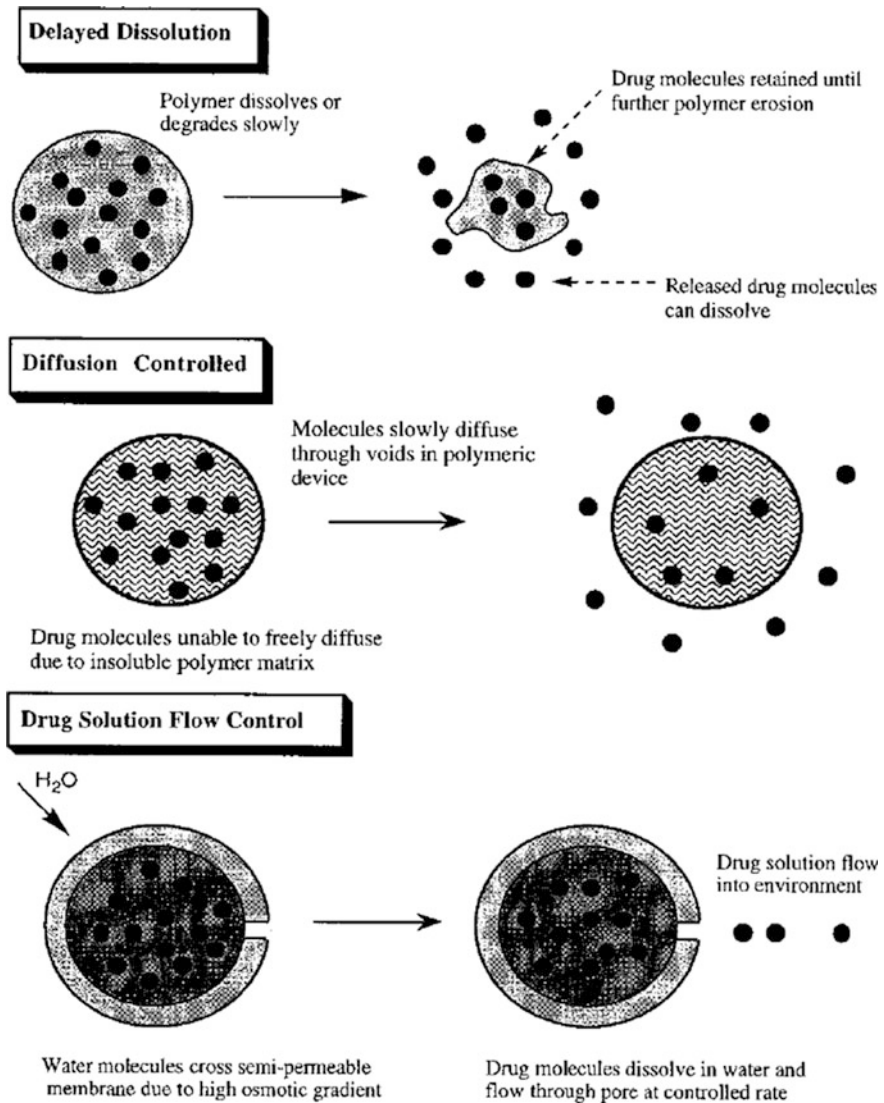


**Fig. 2** Examples of mechanisms of temporal controlled release. Reproduced with permission from Uhrich et al. (1999)

molecules. The drug should in this case travel through a tortuous path to come out of the matrix. Drug solution flow control is used in osmotic potential across the semipermeable barrier of the transfer devices in order to create pressure chambers which contain aqueous solutions of the drug. This pressure is equalized by the transfer of the solvent of the drug out of the matrix (Uhrich et al. 1999). In the case of distribution control, the delivery system is implanted directly to the area where

the drug needs to act (Walter et al. 1995). The implants which are suitable for this controlled released system are those which have no harmful side effects for the patient and the drug is unable to leave from the implant (Uhrich et al. 1999). Implantable drug delivery systems (IDDS) are classified into three major categories: biodegradable or non-biodegradable implants, implantable pump systems, and, the newest, atypical class of implants (Martin del Valle et al. 2009).

In biodegradable or non-biodegradable implants, the drug release depends on the solubility and diffusion of the drug in the delivery device. In implantable pump systems, controlled drug release is achieved by the microtechnology of electronic systems and the flow is controlled through the constant pressure difference. The atypical class of controlled release systems achieves targeted delivery of drug, minimization of wasting drug and side effects. In this case, the efficacy of the drug and the treatment (Martin del Valle et al. 2009).

### 3 Bisphosphonates (BPs) in Controlled Release Systems

In the last ten years, the scientific literature has seen about 10,000 scientific works on the topic of BPs. These compounds were first shown to inhibit calcification and hydroxyapatite dissolution in vitro and bone resorption in vivo (Francis et al. 1969). The pharmacological effect of BPs is related to their ability to bind to the bone mineral (hydroxyapatite). Equally important is their biochemical effect on the cells, predominantly osteoclasts (for a comprehensive review on bisphosphonate pharmacology see Russell et al. 2008). Representative members of the BP family are shown in Fig. 3.

Etidronate and clodronate (first generation of “-dronates”) do not contain nitrogen atoms in their structure. These compounds act as analogs of pyrophosphates and metabolized to a cytotoxic analog of ATP, adenosine-5'-( $\beta,\gamma$ -dichloromethylene)-triphosphate. That analog inhibits the mitochondrial adenine nucleotide translocase (ANT) and eventually triggers apoptosis (Frith et al. 1997; Lehenkari et al. 2002).

When a BP contains a nitrogen atom in its alkyl side chain, for example, aledronic acid or pamidronic acid (see Fig. 3), it becomes 10–100 times more potent than the non-nitrogen analogs (first-generation BPs). Studies with amino-bisphosphonates have shown that they are taken up by mature osteoclasts and inhibit an enzyme of the mevalonate pathway called farnesyl pyrophosphatase synthase (Dunford et al. 2001; Fisher et al. 1999; Luckman et al. 1998; Van Beek et al. 1999; Fleisch et al. 2002). Inhibition of inactive osteoclasts is a result of the domino impact from the involvement of BPs in biochemical pathways (Rodan and Reszka 2002).

Still nowadays, the final and fatal stage of cancer, metastasis, is an uncharted and incurable activity. Scientists reported that in some types of human cancers, such as breast cancer, thyroid cancer, renal carcinoma, prostate cancer, and multiple myelomas, more than 50% will get metastasized probably at a bone site in the advanced stages (Mundy 1997). As emphasized before, BPs are compounds/drugs

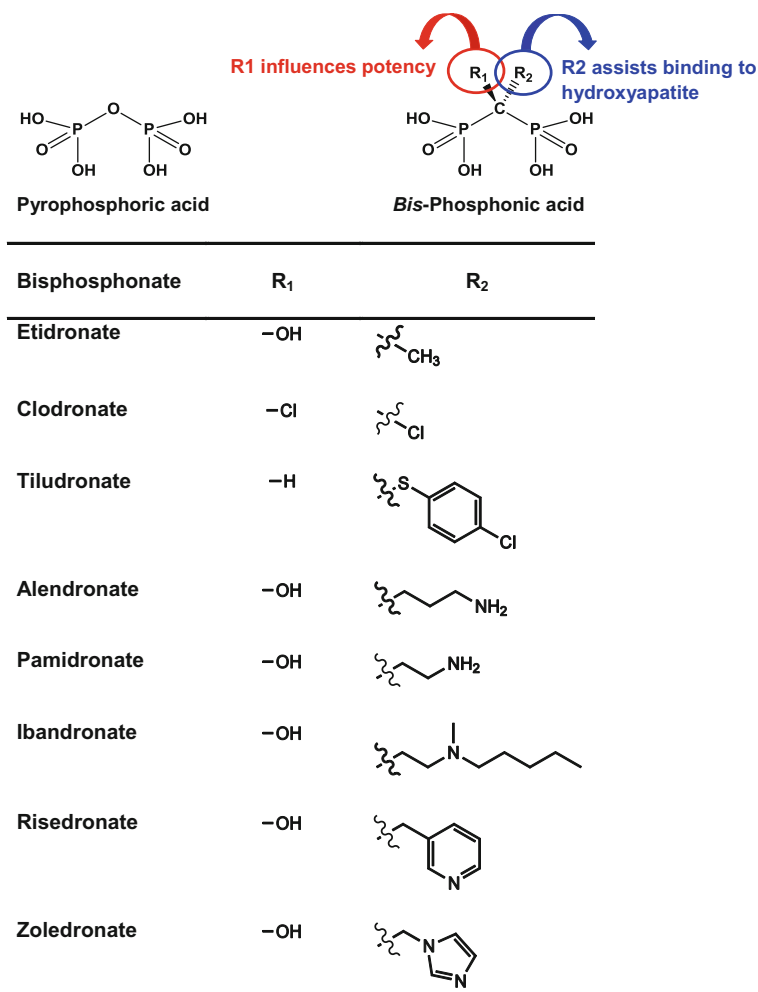


**Fig. 3** Schematic structures of bisphosphonates

that are able to reduce bone erosion and restore bone density in osteoporosis and other bone-related diseases. There are many clinical trials which proved that bone homeostasis is restored by the use of BPs (Shane 2010). The use of BPs induces the apoptosis of osteoclasts and, as a result, the actions of osteoclasts that are responsible for the bone erosion are inhibited (Weinstein et al. 2009). There is fast distribution and high accumulation in the bone (100 times) in comparison to  $C_{max}$  even after 6 months post use (Chen et al. 2002). This is due to the BPs strong affinity toward bone mineral (hydroxyapatite). An additional reason for the widespread use of BPs as bone imaging agents (besides high selectivity and affinity) is their synergy with radiopharmaceuticals. Some studied synergy examples are:

estradiol (Thompson et al. 1989), prostaglandin E2 (Gil et al. 1999), Src (protein tyrosine kinase pp60c-Src) homology 2 inhibitors (Shakespeare et al. 2003), diclofenac (Hirabayashi et al. 2001), fluroquinolone, *cis*-platin, melphalan, methotrexate (Hosain et al. 1996), radiopharmaceuticals like technetium ( $^{99m}\text{Tc}$ ) hydroxyethylidene disphosphonate,  $^{99m}\text{Tc}$  methylene disphosphonate,  $^{99m}\text{Tc}$  hydroxymethylene disphosphonate (Francis and Fogelman 1987), and samarium ( $^{153}\text{Sm}$ ) leixidronam (QuadrametR) (Lamb and Faulds 1997).

The phosphonate moiety ( $-\text{PO}_3\text{H}_2$ ) exhibits excellent binding properties to hydroxyapatite and metallic surfaces. BPs have been evaluated as formulating agents, especially for the steric stabilization of nanoparticles (Giger et al. 2013). Gittens et al. proposed peptides and proteins for conjugation with BPs to induce bone selectivity (Gittens et al. 2005). Hengst et al. (2007) have suggested the use of CHOL-TOE-BP as a targeting moiety for liposomal drug delivery to the bone. Also, BP conjugates were used as delivery anchors for treatment of osteoporosis (Gil et al. 1999). The use of alendronate- $\beta$ -cyclodextrin as a bone anabolic agent was demonstrated by Liu et al. (2008).

Studies on the applications of BPs in cardiac valve problems are discussed below in more detail. Tissue-derived valvular prostheses which consist of either human allograft or xenograft are commonly utilized in valve replacement surgery. Xenograft valve prostheses are most commonly built up from bovine pericardium or porcine aortic valves that cross-link glutaraldehyde. These replacement valves present problems due to calcification, with cuspal mineral deposition, leading to valvular regurgitation or stenosis. This is the most important reason for the clinical failure of these devices. Furthermore, aortic wall calcification has been observed, leading to gradual rigidity in long-term implants. Fresh aortic explants appeared less calcified than the glutaraldehyde-cross-linked aortic wall grafts. In order to prevent the above model systems from mineral deposition, calcification inhibitors were used as pretreatments or local controlled release polymer co-implants (Levy et al. 1985, 1990, 1995).

A great deal of studies on controlled release of BPs were performed, since the administration of BP compounds can limit the formation and growth of hydroxyapatite crystals. When these drugs are administered in efficient systemic dosages, severe adverse effects on skeletal mineral, and overall calcium metabolism result, so the dosage level is a significant factor. Local therapy was achieved with controlled release matrices that enclose the anticalcification factor, 1-hydroxyethylene diphosphonate (HEDP, or etidronate) dissipated in a copolymer of ethylene-vinyl acetate (EVA). These matrices were hemispherical (diameter 1 cm) and this geometric structure presented practically stable release rates in a plethora of test formulations. In cusps removed from animals with hemisphere implants containing ethylene-vinyl acetate HEDP, exhibited minimal calcification.

Local controlled release of HEDP (etidronate) from ethylene-vinyl acetate copolymer matrices directly into bioprosthetic cuspal implants inhibited calcification of the subcutaneous implants for up to 84 days without detectable problematic effects associated with the BP therapy. This long-term (84 days) controlled release system delivered etidronate at a nearly total body dosage of 6  $\mu\text{g}/\text{kg}$  and this very

low dosage requirement for local therapy was undoubtedly the reason for effective anticalcification therapy, which importantly was not associated with any adverse effects. In contrast, the control implants showed progressive extensive calcification (Levy et al. 1985, 1990, 1995).

In some studies, silicone matrices including  $\text{Na}_2\text{HEDP}$  or  $\text{Ca}_2\text{HEDP}$  (which is  $\sim 1000$  times less soluble) have demonstrated their efficacy as inhibitors for mineralization of bioprosthetic cusps. The drug load solubility affects the drug delivery rate. Thus, after 150 days approximately 80% of HEDP was released from matrices containing exclusively  $\text{Na}_2\text{HEDP}$  in comparison with lower levels of release from matrices loaded with (the less soluble)  $\text{Ca}_2\text{HEDP}$  (Golomb et al. 1987).

It must be noted that the required duration of drug delivery can be accommodated to range from several months to 10 or more years by varying the matrix geometry, polymer composition, and solubility of the HEDP salt used.

The BPs are capable of bone-specific delivery as it has been already reported. However, some of the BP derivatives exhibit some disadvantages from a toxicological point of view: After the BPs or their derivatives are taken up by the bone tissue, they can remain attached onto the bone mineral for a long time, thus causing side effects.

A prodrug-based delivery system was designed in order to overcome such problems, known as novel osteotropic delivery system (ODDS). This system operated not only as a bone-specific, but also as a controlled delivery system. The affinity for hydroxyapatite is the most definitive feature in order to attain the osteotropic drug delivery. The three main groups of the chemical compounds which can attach to the surface of hydroxyapatite are usually oxygen-based, such as carboxylate, phosphonate, and hydroxyl moieties. A drug is bound to a bisphosphonic promoiety via bioreversible bonds. The BP prodrug is principally taken up by the bone due to the chemical adsorption of bisphosphonic promoiety to hydroxyapatite. After systemic administration, a bisphosphonic prodrug is rapidly delivered to the bone and subjected to enzymatic and/or chemical hydrolysis to afford the parent drug, depending on its cleavage rate.

Because many previous studies showed that diphosphonic prodrug of carboxyfluorescein (CF-BP) is strongly adsorbed onto hydroxyapatite in vitro and strongly taken up into osseous tissues after intravenous injection, the CF-BP was synthesized as a standard compound. Moreover, CF was used because this compound and its prodrug (CF-BP) could be detected not only by a fluorescence detector but also by fluorescence microscopy. As soon as CF-BP was incorporated into the bone, it dissolved very slowly generating CF in the systemic compartment. It must be noted that the by-products, which are not taken up by the bone, are rapidly excreted from the body via the urinary system.

The P-C-P group in bisphosphonates is resistant to chemical and enzymatic degradation (Cremers et al. 2005). Hence, the elimination of CF-BP from the osseous tissue is the result of the hydrolysis of the ester bond, which was proposed on the basis of the presence of regenerated CF. Once the CF-BP is injected, the bone concentration of regenerated CF gradually increased during the following 7 days. In contrast, CF presents a really small skeletal distribution (0.9% of dose)

when it is injected intravenously. As a consequence, CF itself has no affinity for the bone. This phenomenon could be explained by the mechanism of the diffusion-limited release of regenerated CF through the bone mineral matrix. So, a skeletal diffusion-controlled system like the one described has the capacity to retain the plasma drug concentration for a long term and it could be helpful for effective therapies (Fujisaki et al. 1995, 1996a, b).

There are a variety of research efforts on biological and biologically inspired silica formation (Patwardhan 2011; Morse 1999; Lopez et al. 2005; Hildebrand 2008). These research studies put forth useful observations and conclusions. Based on such studies, it is now certain that an abundance of biomolecules (typically rich in amines) play a crucial role in biosilica deposition. It is now possible to develop new bioinspired green routes to nanostructured and porous silica by utilizing a wide variety of “additives” (analogs of biomolecules) (Patwardhan et al. 2005). The use of “Green Nanosilica” has a variety of advantages. Some of these are related to the safety of the process, routinely performed on the benchtop at room temperature, in water and takes about 5 min. The composition of “Green Nanosilica” can be controlled in order to modify the system properties, such as the pore and particle size (Belton et al. 2008). This can be achieved by making the “right” choice of an additive and synthesis conditions, as is shown by some SEM images (see Fig. 4) from a study of Steven et al. (2014). It is clear that the utilization of this approach offers a one step, “green” synthesis in contrast to the time-, energy-, and material-intensive methods for traditional materials (Patwardhan et al. 2005; Belton et al. 2005, 2008).

A very intuitive application of siliceous ordered mesoporous materials combined with bisphosphonates was studied by Balas et al. (2006). Aledronate in two different types of hexagonal ordered mesoporous materials, MCM-41 ( $D_p = 3.8$  nm) and SBA-15 ( $D_p = 9.0$  nm). Thomas et al. (2003) reviewed the adsorption from

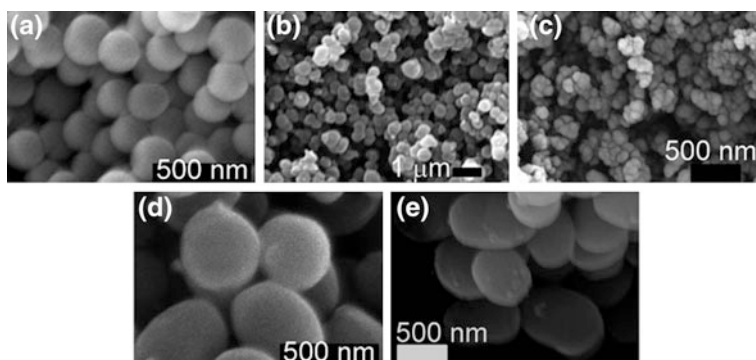


**Fig. 4** Scanning electron micrographs of silica particles used: **a** Stöber silica, **b** PEHA-GN, **c** PAH-GN, **d** APMSN, and **e** SAMSIN. Reproduced with permission from Steven et al. (2014)



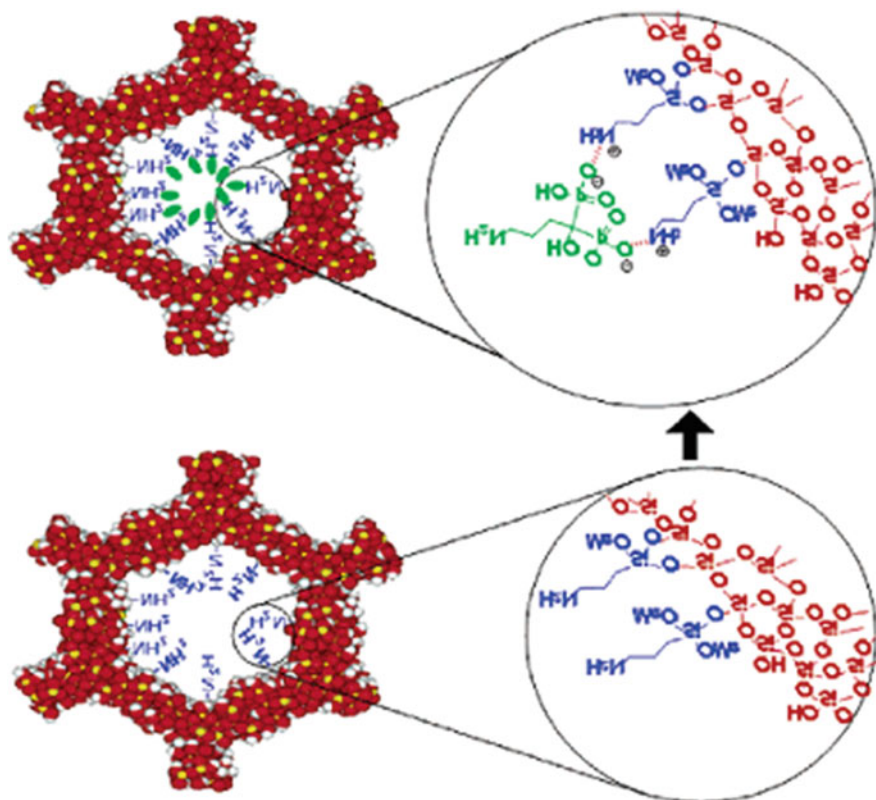


**Fig. 5** Alendronate adsorption on hexagonally ordered mesoporous silica, functionalized with propylamine groups. Reproduced with permission from Balas et al. (2006)

these systems/matrices (Fig. 5). In both cases, the surface of the pore internal walls had undergone modification with amine groups (Chong and Zhao 2003).

The amine functionalization was confirmed with the use of FT-IR,  $N_2$  adsorption, and elemental analysis techniques. X-ray diffraction patterns ensured that the ordered mesoporous framework of the materials was unaffected by the modification conditions. The grafting of propylamine to the pore walls in the modification process results to a decrease in the total pore volume and diameter, ca. 60% for MCM-41 and ca. 40% for SBA-15. After 24 h of immersion in an aqueous alendronate solution, the amine-modified materials showed a drug loading almost three times larger than that of the unmodified materials (Fig. 6). This difference is a consequence of the interaction between the phosphonate groups in alendronate and the silanol groups (in the case of unmodified materials) and from the amine groups covering the surface of the mesopore walls of the modified materials (Walcarius et al. 2003).

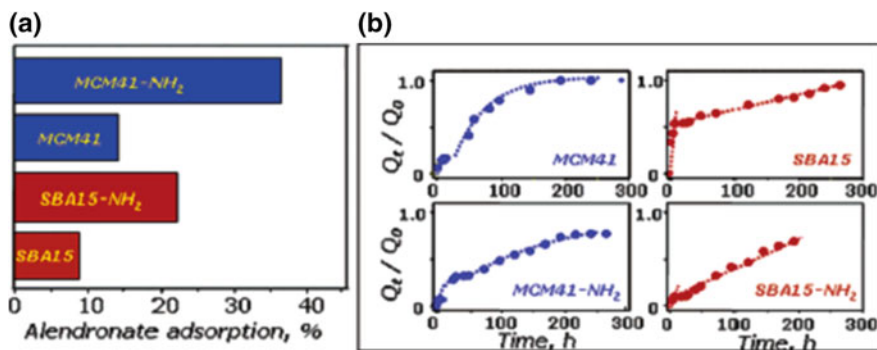


**Fig. 6** **a** Maximum load of alendronate in ordered mesoporous materials, **b** release profiles of alendronate from the pure siliceous and amino-modified ordered mesoporous materials. Reproduced with permission from Balas et al. (2006)

The interaction between silanol and phosphonate of the adsorbed drug is weaker than that of the amine to phosphonate under pH 4.8 loading conditions. This enhances the adsorption of alendronate molecules when the mesoporous materials are amine-modified, 22% in SBA-15-NH<sub>2</sub> and 37% in MCM-41-NH<sub>2</sub>.

## 4 Conclusions

Phosphonates are extensively used in osteoporosis-related treatments. In this chapter, we discussed the release/delivery of phosphonates as “active” pharmaceutical ingredients, with particular emphasis on silica matrices. Several delivery systems have been reported so far to mitigate the most significant problem of phosphonates, i.e., their poor bioavailability. Controlled delivery of phosphonate-based drugs is an opportune field. Thus, new tools and methods in bone targeting are investigated to effectively deliver these drugs under pathological conditions of bone diseases.

**Acknowledgements** K. E. Papathanasiou thanks the Onassis Foundation for a doctoral scholarship. K. D. Demadis thanks the EU for funding the Research Program SILICAMPS-153, under the ERA.NET-RUS Pilot Joint Call for Collaborative S&T projects.

## Bibliography

Balas F, Manzano M, Horcajada P, Vallet-Regí M (2006) Confinement and controlled release of bisphosphonates on ordered mesoporous silica-based materials. *J Am Chem Soc* 128: 8116–8117

- Belton DJ, Patwardhan SV, Perry CC (2005) Spermine, spermidine and their analogues generate tailored silicas. *J Mater Chem* 15:4629–4638
- Belton DJ, Patwardhan SV, Annenkov VV, Danilovtseva EN, Perry CC (2008) From biosilicification to tailored materials: optimizing hydrophobic domains and resistance to protonation of polyamines. *Proc Natl Acad Sci USA* 105:5963–5968
- Binauld S, Stenzel MH (2013) Acid-degradable polymers for drug delivery: a decade of innovation. *Chem Commun* 49:2082–2102
- Chen T, Berenson J, Vescio R, Swift R, Gilchick A, Goodin S, LoRusso P, Ma P, Ravera C, Deckert F, Schran H, Seaman J, Skerjanec A (2002) Pharmacokinetics and pharmacodynamics of zoledronic acid in cancer patients with bone metastases. *J Clin Pharmacol* 42:1228–1236
- Chong ASM, Zhao XS (2003) Functionalization of SBA-15 with APTES and characterization of functionalized materials. *J Phys Chem B* 107:12650–12657
- Coradin T, Eglin D, Livage J (2004) The silicomolybdic acid spectrophotometric method and its application to silicate/biopolymer interaction studies. *Spectroscopy* 18:567–576
- Cremers SC, Pillai G, Papapoulos SE (2005) Pharmacokinetics/pharmacodynamics of bisphosphonates: use for optimisation of intermittent therapy for osteoporosis. *Clin Pharmacokinet* 44:551–570
- Demadis KD (2008) Silica scale inhibition relevant to desalination technologies: progress and recent developments. In: Delgado DJ, Moreno P (eds) *Desalination research progress*. Nova Science Publishers, Inc., New York, pp 249–259
- Dunford JE, Thompspon K, Coxon FP, Luckman SP, Hahn FM, Poulter CD, Ebetino FH, Rogers MJ (2001) Structure-activity relationships for inhibition of farnesyl disphosphate syntase in vitro and inhibition of bone resorption in vivo by nitrogen-containing bisphosphonates. *J Pharm Exp Ther* 296:235–242
- Ehrlich H, Demadis KD, Koutsoukos PG, Pokrovsky O (2010) Modern views on desilicification: biosilica and abiotic silica dissolution in natural and artificial environments. *Chem Rev* 110:4656–4689
- Fisher JE, Rogers MJ, Halasy JM, Luckman SP, Hughes DE, Masarachia PJ, Wesolowski G, Russell RG, Rodan GA, Reszka AA (1999) Alendronate mechanism of action: geranylgeraniol, an intermediate in the mevalonate pathway, prevents inhibition of osteoclast formation, bone resorption and kinase activation in vitro. *Proc Natl Acad Sci USA* 96:133–138
- Fleisch H, Reszka A, Rodan G, Rogers G (2002) Bisphosphonates: mechanisms of action. In: Bilezikian JP, Raisz LG, Rodan GA (eds) *Principles of bone biology*. Academic Press, San Diego, pp 1361–1385
- Francis MD, Fogelman I (1987) 99 mTc diphosphonate uptake mechanism on bone. In: Fogelman I (ed) *Bone scanning in clinical practice*. Springer, New York, pp 7–17
- Francis MD, Graham R, Russell RGG, Fleisch H (1969) Diphosphonates inhibit formation of calcium phosphate crystals in vitro and pathological calcification in vivo. *Science* 165:1264–1266
- Frith JC, Mönkkönen J, Blackburn GM, Russell RGG, Rogers MJ (1997) Clodronate and liposome-encapsulated clodronate are metabolized to a toxic ATP analog, adenosine 5'-( $\beta$ ,  $\gamma$ -dichloromethylene) triphosphate, by mammalian cells in vitro. *J Bone Miner Res* 12:1358–1367
- Fujisaki J, Tokunaga Y, Takahashi T, Hirose T, Shimojo F, Kagayama A, Hata T (1995) Osteotropic drug delivery system (ODDS) based on bisphosphonic prodrug. I: synthesis and in vivo characterization of osteotropic carboxyfluorescein. *J Drug Target* 3:273–282
- Fujisaki J, Tokunaga Y, Sawamoto T, Takahashi T, Kimura S, Shimojo F, Hata T (1996a) Osteotropic drug delivery system (ODDS) based on bisphosphonic prodrug. III: pharmacokinetics and targeting characteristics of osteotropic carboxyfluorescein. *J Drug Target* 4:117–123
- Fujisaki J, Tokunaga Y, Takahashi T, Murata S, Shimojo F, Hata T (1996b) Physicochemical characterization of bisphosphonic carboxyfluorescein for osteotropic drug delivery. *J Pharm Pharmacol* 48:798–800
- Giger EV, Castagner B, Leroux J-C (2013) Biomedical applications of bisphosphonates. *J Control Release* 167:175–188

- Gil L, Han Y, Opas EE, Rodan GA, Ruel R, Seedor JG, Tyler PC, Young RN (1999) Prostaglandin E<sub>2</sub>-bisphosphonate conjugates: potential agents for treatment of osteoporosis. *Bioorg Med Chem* 7:901–919
- Gittens SA, Bansal G, Zernicke RF, Uludag H (2005) Designing proteins for bone targeting. *Adv Drug Deliv Rev* 57:1011–1036
- Golomb G, Dixon M, Smith MS, Schoen FJ, Levy RJ (1987) Controlled-release drug delivery of diphosphonates to inhibit bioprosthetic heart valve calcification: release rate modulation with silicone matrices via drug solubility and membrane coating. *J Pharm Sci* 76:271–276
- Gommes C, Blacher S, Goderis B, Pirard R, Heinrichs B, Alie C, Pirard JP (2004) In situ SAXS analysis of silica gel formation with an additive. *J Phys Chem B* 108:8983–8991
- Hengst V, Oussoren C, Kissel T, Storm G (2007) Bone targeting potential of bisphosphonate-targeted liposomes. Preparation, characterization and hydroxyapatite binding in vitro. *Int J Pharm* 331:224–227
- Hildebrand M (2008) Diatoms, biomineralization processes, and genomics. *Chem Rev* 108:4855–4874
- Hirabayashi H, Takahashi T, Fujisaki J, Masunaga T, Sato S, Hiroi J, Tokunaga Y, Kimura S, Hata T (2001) Bone specific delivery and sustained release of diclofenac, a non-steroidal anti-inflammatory drug, via bisphosphonic prodrug based on osteotropic drug delivery system (ODDS). *J Control Release* 70:183–191
- Hosain F, Spencer RP, Couthon HM, Sturtz GL (1996) Targeted delivery of antineoplastic agent to bone: biodistribution studies of technetium-99m-labeled gembisphosphonate conjugate of methotrexate. *J Nucl Med* 37:105–107
- Hughes LG, Vick TA, Wang JH (2004) Coated Implants. European Patent 1250164
- Kennedy JH (1997) HPLC purification of pergolide using silica gel. *Org Process Res Dev* 1:68–71
- Lamb HM, Faulds D (1997) Samarium <sup>153</sup>Sm leixidronam. *Drugs Aging* 11:413–418
- Lehenkari PP, Kellinsalmi M, Näpänkangas JP, Ylitalo KV, Mönkkönen J, Rogers MJ, Azhaye A, Väänänen HK, Hassinen IE (2002) Further insight into mechanism of action of clodronate: inhibition of mitochondrial ADP/ATP translocase by a nonhydrolyzable, adenine-containing metabolite. *Mol Pharmacol* 61:1255–1262
- Levy RJ, Wolfrum J, Schoen FJ, Hawley MA, Lund SA, Langer R (1985) Inhibition of calcification of bioprosthetic heart valves by local controlled-release diphosphonate. *Science* 228:190–192
- Levy RJ, Johnson TP, Sintov A, Golomb G (1990) Controlled release implants for cardiovascular disease. *J Control Release* 11:245–254
- Levy RJ, Qu X, Underwood T, Trachy J, Schoen FJ (1995) Calcification of valved aortic allografts in rats: effects of age, crosslinking, and inhibitors. *J Biomed Mater Res* 29:217–226
- Liu X, Wiswall AT, Rutledge JE, Akhter MP, Cullen DM, Reinhardt RA, Wang D (2008) Osteotropic  $\beta$ -cyclodextrin for local bone regeneration. *Biomaterials* 29:1686–1692
- Lopez PJ, Gautier C, Livage J, Coradin T (2005) Mimicking biogenic silica nanostructures formation. *Curr Nanosci* 1:73–83
- Luckman SP, Hughes DE, Coxon FP, Graham R, Russell RG, Rogers MJ (1998) Nitrogen-containing bisphosphonates inhibit the mevalonate pathway and prevent post-translational prenylation of GTP-binding proteins, including Ras. *J Bone Miner Res* 13:581–589
- Mann S, Perry CC, Williams RJP, Fyfe CA, Gobbi GC, Kennedy GJ (1983) The characterisation of the nature of silica in biological systems. *J Chem Soc Chem Commun* 4:168–170
- Martin del Valle EM, Galan MA, Carbonell RG (2009) Drug delivery technologies: the way forward in the new decade. *Ind Eng Chem Res* 48:2475–2486
- Mashkevich BO (ed) (2007) Drug delivery research advances. Nova Science Publishers Inc., New York
- Mestiri M, Benoit JP, Hernigou P, Devissaguet JP, Puisieux F (1995) Cisplatin-loaded poly(methyl methacrylate) implants: a sustained drug delivery system. *J Control Release* 33:107–113
- Morse DE (1999) Silicon biotechnology: harnessing biological silica production to construct new materials. *Trends Biotechnol* 17:230–232

- Mundy GR (1997) Mechanisms of bone metastasis. *Cancer* 80:1546–1556
- Ning RY (2010) Reactive silica in natural waters—a review. *Des Wat Treat* 21:79–86
- Patwardhan SV (2011) Biomimetic and bioinspired silica: recent developments and applications. *Chem Commun* 47:7567–7582
- Patwardhan SV, Clarson SJ, Perry CC (2005) On the role(s) of additives in bioinspired silicification. *Chem Commun* 1113–1121
- Perry CC, Keeling-Tucker T (1998) Aspects of the bioinorganic chemistry of silicon in conjunction with the biometals calcium, iron and aluminium. *J Inorg Biochem* 69:181–191
- Ramakrishna S, Mayer J, Wintermantel E, Leong KW (2001) Biomedical applications of polymer-composite materials: a review. *Compos Sci Technol* 61:1189–1224
- Rodan GA, Reszka AA (2002) Bisphosphonate mechanism of action. *Curr Mol Med* 2:571–577
- Russell RGG, Watts N, Ebetino F, Rogers M (2008) Mechanisms of action of bisphosphonates: similarities and differences and their potential influence on clinical efficacy. *Osteoporos Int* 19:733–759
- Shakespeare WC, Metcalf CA III, Wang Y, Sundaramoorthi R, Keenan T, Weigle M, Bohacek RS, Dalgarno DC, Sawyer TK (2003) Novel bone-targeted Src tyrosine kinase inhibitor drug discovery. *Curr Opin Drug Discov Devel* 6:729–741
- Shane E (2010) Evolving data about subtrochanteric fractures and bisphosphonates. *N Engl J Med* 362:1825–1827
- Siegel RA, Rathbone MJ (2012) Overview of controlled release mechanisms. In: Siepmann J, Siegel RA, Rathbone MJ (eds) *Fundamentals and applications of controlled release drug delivery*. Springer, New York, pp 19–43
- Soppimath KS, Aminabhavi TM, Kulkarni AR, Rudzinski WE (2001) Biodegradable polymeric nanoparticles as drug delivery devices. *J Control Release* 70:1–20
- Steven CR, Busby GA, Mather C, Tariq B, Lucia Briuglia M, Lamprou DA, Urquhart AJ, Grant MH, Patwardhan SV (2014) Bioinspired silica as drug delivery systems and their biocompatibility. *J Mater Chem B* 2:5028–5042
- Szymura-Oleksiak J, Slosarczyk A, Cios A, Mycek B, Paszkiewicz Z, Szklarczyk S, Stankiewicz D (2001) The kinetics of pentoxifyllinerelease in vivo from drug-loaded hydroxyapatite implants. *Ceram Int* 27:767–772
- Thomas JM, Johnson BFG, Raja R, Samkar G, Midgley PA (2003) High-performance nanocatalysts for single-step hydrogenations. *Acc Chem Res* 36:20–30
- Thompson WJ, Thompson DD, Anderson PS, Rodan GA (1989) Polymalonic acids as bone affinity agents. *European Patent* 0341961
- Uhrich KE, Cannizzaro SM, Langer RS, Shakesheff KM (1999) Polymeric systems for controlled drug release. *Chem Rev* 99:3181–3198
- Van Beek E, Pieterman E, Cohen L, Lowik C, Papapoulos S (1999) Nitrogen-containing bisphosphonates inhibit isopentenyl pyrophosphate isomerase/farnesyl pyrophosphate synthase activity with relative potencies corresponding to their antiresorptive potencies in vitro and in vivo. *Biochem Biophys Res Commun* 255:491–494
- Walcarius A, Etienne M, Lebeau B (2003) Rate of access to the binding sites in organically modified silicates. 2. Ordered mesoporous silicas grafted with amine or thiol groups. *Chem Mater* 15:2161–2173
- Walter KA, Tamargo R, Olivi A, Burger PC, Brem H (1995) Intratumoral chemotherapy. *Neurosurgery* 37:1129–1145
- Wang GH, Zhang LM (2007) Manipulating formation and drug-release behavior of new sol-gel silica matrix by hydroxypropyl guar gum. *J Phys Chem B* 111:10665–10670
- Weinstein RS, Robertson PK, Manolagas SC (2009) Giant osteoclast formation and long-term oral bisphosphonate therapy. *N Engl J Med* 360:53–62
- Zhao Z-G (1992) Adsorption of phenylalanine from aqueous solution onto active carbon and silica gel. *Chin J Chem* 10:325–330

# Chapter 6

## Polymeric Hydrogel: A Flexible Carrier System for Drug Delivery



Surbhi Dubey, Rajeev Sharma, Nishi Mody and S. P. Vyas

### 1 Introduction

Progress in modern drug delivery and in the area of polymer science has shifted the interest on polymer-based drug delivery systems to obtain spatiotemporal release of the therapeutics. The advent of effective and precise biological therapeutics has accelerated the polymer-based smart delivery systems for both pulsatile dose delivery and implantable reservoir systems. A great number of polymers of both natural and synthetic origin constitutes a vital area of biopharmaceutics in which linear or branched polymer chains have been exploited as polymeric drug carriers.

A through study of underlying mechanisms of transitional behaviour of polymers under applied stimulus can help design the polymers with well-ordered molecular and structural to give a well-defined reaction to the external conditions. Such stimuli responsive polymers are used for formulating sensitive carriers which deliver drug(s) in response to the varying biological conditions/stimulus present in body. Polymers carrying therapeutics can themselves be bioactive which in addition to drug provide their own therapeutic benefit as well. These polymers are biodegradable and prevent carrier accumulation in the biological system. Pharmaceutical agents can also be conjugated to the polymer through biologically labile bonds to dissociate in particular bioenvironment in response to change like pH, temperature, enzyme or ionic strength etc. The polymer-drug conjugation provides advantages including prolonged circulation half-life and sustained the drug release. Active targeting can be achieved by conjugating the polymeric backbone with the ligand specific to the overexpressed cell surface receptor of the affected tissue. The targeted nanocarriers which are taken up by the receptor mediated endocytosis are taken by the endosome follow an endolysosomal pathway

---

S. Dubey (✉) · R. Sharma · N. Mody · S. P. Vyas  
Drug Delivery Research Laboratory, Department of Pharmaceutical Sciences,  
Dr. H.S. Gour University Sagar, Sagar 470003, M.P., India  
e-mail: surbhi.dubey3@gmail.com

where majority of drug molecules are degraded, curtailing the intracellular therapeutic concentration. Hence, new polymeric materials are being explored and undergo endosomal escape preventing entry into the lysosomes and promoting cytoplasmic drug delivery. Therefore, drug delivery research based on polymeric material has produced precognitive systems which allow cytoplasmic delivery of novel therapeutics. The polymeric novel drug delivery carrier systems comprise of microspheres, nanoparticles, nanospheres, nanocapsules, polymeric micelle, polymer-drug conjugates, dendrimers, transdermal patches, and polymeric gels (hydrogel). Hydrogels offer a wide platform for the delivery of various types of therapeutics (small molecules, chemotherapeutics, proteins, antigens, conjugated) owing to their amenability be designed as bioadhesive as well as environment-sensitive systems using various stimuli-sensitive polymers as illustrated in Table 1.

Pharmaceutical gels are mainly represented by hydrogel. The hydrogel is a three-dimensional crosslinked network of hydrophilic polymers. These polymers are insoluble in water but are capable of absorbing large volume of water. Hydrogels can be structured as slabs, microparticles (microgel), nanoparticles (nanogel), coatings, and films from polymers of both natural and synthetic origins. Various kinds of material (polymers) used for the fabrication of hydrogels are classified in Table 2, and the properties of ideal material required for the formulation of hydrogel are given in Table 3.

### ***1.1 Advantages of Hydrogels***

- Hydrogels are highly flexible and elastic structures which can be tuned and tailored as per need by modifying crosslinking densities.
- Therapeutic molecules can be easily incorporated by anchoring them covalently to the polymer or entrapping into polymer matrix.
- Hydrogels offer three-dimensional milieus for molecular-level biological interactions.
- They possess lower tendency to adsorb biological proteins and adhere to cells because of their inert and hydrophilic surfaces. A hydrogel is a soft and rubbery substance that avoids irritation to the adjoining tissue.
- Hydrogel undergoes sol–gel transition; the property in particular renders these systems safe for in vivo use. Hydrogels can be manipulated to respond to externally applied factors (stimuli-sensitive), such as temperature, ionic strength, solvent polarity, electric/magnetic field, light, or small biomolecules.
- Hydrogels offer pharmacokinetic benefits for drug delivery as a depot formulation is created upon administration from which the drug is released slowly in the neighbouring tissue, thereby generating high local concentration of drug over prolonged period of time.

**Table 1** Hydrogel used in drug delivery

S.No	Polymer	Drug/ bioactive	Delivery site	Stimuli	Advantages/Application	Ref
1.	Poly(N-isopropylacrylamide) (PNIPAAm)	4-Cetamidophen	-	Temperature	Hydrogel microparticles into a crosslinked gelatin matrix	Klouda and Mikos (2008)
2.	IPNs of poly (acrylic acid) and polyacrylamide (PAAm) or P(AAm-co-BMA)	Ketoprofen	-	Temperature	Positive temperature dependence of swelling	Owens et al. (2007)
3.	Poly (ethylene oxide) (PEO) and poly(propylene oxide) (PPO) Pluronic® (or Poloxamers®) and Tetronics®.	Ketoprofen, Spirinolactone	-	Temperature	The release of a hydrophilic model drug (ketoprofen) and a hydrophobic model drug (spirinolactone) were first-order and S-shaped, respectively.	Qiu and park 2012
4.	Copolymers of methyl methacrylate and N,N'-dimethylaminoethyl methacrylate (DMAEM)	Caffeine	-	pH	It was not released at neutral pH, but released at zero-order at pH 3-5	Siegelet al. 1988
5.	Semi-IPN of crosslinked chitosan and PEO	Antibiotics, such as amoxicillin and metronidazole	-	pH	More swelling under acidic conditions	Patel and Amiji (1996)
6.	Hydrogels made of polyanions (e.g. PAA) crosslinked with azaromatic crosslinkers	Model drug	-	pH	Swelling of such hydrogels in the stomach is minimal and thus, the drug release is also minimal	Peppas and Peppas 1990; Khare and Peppas 1990
7.	NIPAAm, acrylic acid and 2-hydroxyethyl methacrylate	Streptokinase and heparin	-	Terpolymer hydrogels, pulsatile delivery	Function of stepwise pH and temperature changes	Vakkalanka et al. 1996; Brazel and Peppas 1996

(continued)



Table 1 (continued)

S.No	Polymer	Drug/ bioactive	Delivery site	Stimuli	Advantages/Application	Ref
8.	Nonionic poly (N-isopropylacrylamide) hydrogel	-	-	Specific ion-sensitive hydrogels	A sharp volume phase transition at a critical concentration of sodium chloride in aqueous solution	Starodoubtsev et al. (1995)
9.	N-isopropylacrylamide (NIPAAm) monomer and a dextran macromer containing multiple hydrolytically degradable oligolactate-(2-hydroxyethyl methacrylate) units (Dex-lactateHEMA)	insulin	-	thermoreponsive	Insulin release from the hydrogel occurs for duration of one week and the release kinetics can be modified by changing the polymer ratio of NIPAAm and Dex-lactateHEMA and altering the physical size of the hydrogels.	Misra et al. (2009)
10.	Poly(ethylene glycol) hydrogels	Doxycycline	Eye and skin	-	superior wound healing efficacy for mustard injuries in the eye and skin	Anumolu et al. (2010)
11.	polyacrylic acid polymers	metronidazole (MTZ)	skin		Bioadhesive	Calixto et al. (2015)
12.	PLGA-PEG-PLGA hydrogel	dexamethasone acetate	ocular	thermosensitive	thermosensitive in situ gel-forming material for ocular drug delivery, may improve the bioavailability, efficacy of some eye drugs.	Gaoa et al. (2010)
13.	dextrin grafted with poly (2-hydroxyethyl methacrylate) [Dxt-g-p(HEMA)]	omidazole	colon	pH	Controlled delivery of amidazole in the colonic region in a controlled way. first order kinetics by non-Fickian diffusion mechanism amidazole release from hydrogel follows	Das et al. (2013)
14.	Schiff's base cross-linked hydrogels (PFA/PPLL hydrogels)	metformin and 5-fluorouracil	colon carcinoma model	pH	pH dependant and controlled release of anticancer drug in colon	Wua et al. 2013

(continued)

Table 1 (continued)

S.No	Polymer	Drug/ bioactive	Delivery site	Stimuli	Advantages/Application	Ref
15.	poly-N-vinyl-2-pyrrolidone (PVP)	Acyclovir	nasal delivery		mucoadhesive polymeric hydrogels less damages to the nasal mucosal compared to formulation containing glycerol.	Aisarra et al. (2009)
16.	Pluronic F127 and carbopol 934P (C934P)	naproxen	oral		improve oral residence time and absorption of naproxen	Shin B-K et al. (2013)
17.	Supramolecular Hydrogel (methoxy poly(ethylene glycol) block polymer and $\alpha$ -cyclodextrin ( $\alpha$ -CD))	diclofenac	ocular		Extended the retention time on the corneal surface in rabbits, compared with a plain micellar formulation	Zhang et al. (2016)
18.	polysaccharide cross-linked hydrogel	Avastin	Ocular		Avastin was sustained release from hydrogel with well structure stability	Xu et al. (2013)
19.	dextrin grafted with poly (2-hydroxyethyl methacrylate) [Dxt-g-p(HEMA)]	Omidazole	colon	pH sensitive	delivers amidazole successfully in the colonic region in a controlled way omidazole release from hydrogel follows first order kinetics and a non-Fickian diffusion mechanism	
20.	crosslinked carboxymethyl sago pulp/pectin hydrogel beads	diclofenac sodium	colon	pH sensitive	Less than 9% of s released at pH 1.2 and the hydrogel beads sustain the drug release at pH 7.4 over 30 h.	Tan et al. (2016)
21.	P(CE-MAA-MEG)	5 - Aminosalicilic acid	colon	pH sensitive	Drug release in colon	Bai et al. (2016)
22.	chitosan-based hydrogel	Latanoprost		thermoresponsive	elevated intraocular pressure was significantly decreased within 7 days and remained at a normal level for the following 21 days in rabbit eyes	Cheng et al. (2016a)

(continued)

Table 1 (continued)

S.No	Polymer	Drug/ bioactive	Delivery site	Stimuli	Advantages/Application	Ref
23.	gellan or sodium alginate alone and combined with sodium carboxymethyl- $\beta$ -cellulose (NaCMC)	Gatifloxacin	ocular	Ion-activated mucoadhesive gel	mucoadhesive hydrogel longer corneal residence duration	Kesavan et al. (2015)
24.	micellar supramolecular hydrogel ( $\alpha$ -cyclodextrin ( $\alpha$ -CD) and onomethoxy poly(ethylene glycol)- $\beta$ -poly( $\epsilon$ -caplactone) (MPEG5000-PCL5000) micelles)	PTX	cancer	-	injectable drug delivery system. enhance the biological activity of encapsulated PTX compared to free PTX	Fu et al. 2016
25.	Supramolecular Hydrogel	10-Hydroxy Camptothecin	cancer		sustained long term and release of HCPT with high accumulated rate.	Ruixin et al. (2015)
26.	supramolecular hydrogels based on poly(ether-urethane) nanoparticles and $\alpha$ -CD	Hydrophobic (indomethacin) and hydrophilic drugs (rhodamine)	-	pH and oxidation dual-responsive	hydrogels demonstrate dual drug release behavior and the release rates could be appreciably accelerated by adding up of an oxidizing agent ( $H_2O_2$ ) or increasing the environmental pH.	Cheng et al. (2016b)
27.	bis-imidazolium based supramolecular hydrogel	anionic drugs like indomethacin and ibuprofen	topical		hydrogels are soft, stable in comparison to previous reported gels. Enhanced skin retention of drug Capable for the delivery of poor water soluble drugs used in the treatment of acute inflammation or other skin diseases.	Limón et al. (2015)
28.	Supramolecular hydrogel based on $\alpha$ -cyclodextrin ( $\alpha$ -CD) and a PEGylated doxorubicin prodrug	Doxorubicin	cancer	pH	hydrogels could be degraded in the acidic environment of tumor cells and achieved the controlled delivery of DOX	Fei et al. (2015)

**Table 2** Classification of polymers used for hydrogel fabrication

Natural polymer	<ul style="list-style-type: none"> <li>• Cellulose Derivatives: methyl cellulose (MC), carboxymethyl cellulose (CMC), and various grades of hydroxypropyl methylcellulose (HPMC)</li> <li>• Hydrocolloids/Polyssacharides: alginate, xanthan, guar gum, konjac, gellan, chitosan, carrageenan, scleroglucan, hyaluronic acid, pectin, gelati, agaraose, inulin</li> </ul>
Synthetic polymer	<ul style="list-style-type: none"> <li>• Poly (2-hydroxyethyl methacrylate) (polyHEMA)</li> <li>• Poly (Ethylene Glycol)</li> <li>• Poly (Vinyl Alcohol)</li> <li>• Polyacrylamide</li> <li>• Polyvinylpyrrolidone</li> <li>• Polyurethane</li> </ul>
Superdisintegrants	<ul style="list-style-type: none"> <li>• Crosslinked carboxymethyl cellulose [(Ac-Di-Sol® (FMC Biopolymer); Primellose® (DMV-Fonterra)]</li> <li>• Crosslinked polyvinylpyrrolidone [Crosopovidone Kollidone CL®, CL-M® (BASF); Polyplasdone XL®, XL10® (ISP)]</li> <li>• Crosslinked starch glycolate [Primojel® (DMV-Fonterra)]</li> </ul>
Stimuli sensitive	<ul style="list-style-type: none"> <li>• Temperature: poly(<i>N</i>-isopropylacrylamide) ( PNIPAAm), poly(<i>N,N'</i>-diethylacrylamide) (PDEAAm ) poly (ethylene oxide)-<i>b</i>-poly(propylene oxide)-<i>b</i>-poly (ethylene oxide) (Plurionics , Tetronics , poloxamer), xyloglucan, Poloxamers</li> <li>• pH: Polyelectrolytes, poly(2-hydroxyethyl methacryate) (PHEMA), polymethyl methacrylate (PMMA), polyacrylamide (PAAm), polyacrylic acid (PAA), poly dimethylaminoethylmethacrylate (PDEAEMA) and polyethylene glycol, Cellulose acetate phthalate (CAP)</li> <li>• Ion-sensitive hydrogels: Gelrite (anionic extra cellular polysaccharide), alginate</li> <li>• Glucose: Concanavalin A (Con A), ph sensitive polymers</li> <li>• Antigen: Semi-IPN with grafted antibodies or antigens.</li> </ul>

- Hydrogels can be prepared with properties in between two different materials, e.g. mix a swellable polymer with a temperature- or pH-responsive polymer to obtain the networks with a defined amount of swellability in response to changes in temperature or pH.
- Hydrogel can also be assembled to form various novel drug nanocarriers in tissue specific dimensions like microspheres, nanoparticles, nanogels, microgels, nanosponges.
- Hydrogels are highly biocompatible due to presence of high water content and the physiochemical similarity to the native extracellular matrix, both compositionally (particularly in the case of carbohydrate-based hydrogels) and mechanically.
- Hydrogel are highly flexible and deformable which enable them to acquire the shape of the surface to which they adhere thus rendering them suitable for drug delivery as mucoadhesive or bioadhesive dosage forms.

**Table 3** Desired properties of ideal hydrogel material

– Possess high absorption ability with maximum possible equilibrium swelling capability in saline
– Preferred particle size and porosity for desired rate of absorption as per the application requirement.
– High absorbency under load (AUL)
– The lowest residual monomer and soluble content
– Should be cheap
– Should be stable and durable during swelling in the application area and during storage.
– Biocompatible and biodegradable
– Degrade without the formation of toxic molecules or residue
– Maintain pH-neutrality after swelling in water
– Colorless, odorless and non-toxic
– Should be photo stable
– Re-wetting capability

## 1.2 Demerits of Hydrogel

- Hydrogels possess low tensile strength which may lead to their drainage from site of application and limits their use in drug-bearing applications.
- Lack of homogeneity and low drug loading capacity for hydrophobic drugs.
- Rapid release of drug because of high water content and large pore size of hydrogel.
- Lack of ease of application, as many of the hydrogels do not possess sufficient deformability in order to be injectable and hence require surgical procedure for their application.

## 2 Classification of Hydrogel

### 2.1 Classification Based on Polymeric Composition

#### 2.1.1 Homopolymeric Hydrogels

Polymer network of these hydrogels comprises of single monomer species that constitutes the basic structural units (Iizawa et al. 2007). Depending upon the properties of monomer and polymerization technique used, homopolymers may form a crosslinked skeletal.

### **2.1.2 Copolymeric Hydrogel**

These hydrogels are made of two types of monomeric units one of which is essentially hydrophilic in nature. The monomeric units may be organized in a block, random, or alternating configuration alongside the chain of the polymer network (Kubinova et al. 2010).

### **2.1.3 Multipolymer Interpenetrating Polymeric Hydrogel (IPN)**

The polymeric network of these hydrogels is constituted of two independent crosslinked polymers (natural or synthetic). IPN is prepared by intimate blending of two polymers, in which one of the polymers is produced or crosslinked in the immediate presence of the other from which hydrogel matrix is prepared. The resulting hydrogel matrix is generally highly dense, stiff and strong mechanically. Further, they have manageable physical properties, and more proficient drug loading capacity as compared to conventional hydrogels (Mohamadnia et al. 2007).

### **2.1.4 Semi-inter Penetrating Network (Semi-IPN)**

Semi-IPN consists of a combination of a crosslinked polymer and a linear polymer. Semi-IPN is formed when the linear polymer penetrates the crosslinked network of another polymer without formation of any chemical bond.

## ***2.2 Classification Based on Polymeric Composition***

Based upon the physical configuration and chemical composition, hydrogels can be classified as.

### **2.2.1 Amorphous Hydrogels**

Hydrogel (non-crystalline) in which chains are randomly arranged.

### **2.2.2 Semicrystalline Hydrogels**

These consist of a complex fusion of amorphous and crystalline phases along with the dense regions of ordered macromolecular arrangement.

### 2.2.3 Crystalline Hydrogels

The crystalline hydrogels have, chains which are arranged in proper sequence.

## 2.3 Classification Based on Type of Crosslinking

Based upon the nature of crosslinking connections in the polymeric network, hydrogels are classified into two following categories.

### 2.3.1 Physically Crosslinked Hydrogels/Reversible Hydrogels

Polymeric network is formed involving temporary interchain junctions arising from polymeric chains entanglements or physical interaction between polymer chains such as ionic interactions, hydrogen bonds, or hydrophobic interactions. Approaches employed for preparing physically crosslinked hydrogels include environmental triggers (pH, temperature, ionic strength) and a variety of physicochemical interactions (hydrophobic interactions, charge condensation, hydrogen bonding, stereo-complexation, or supramolecular chemistry) (Hoare and Kohane 2008).

### 2.3.2 Chemically Crosslinked Hydrogels/Permanent Hydrogel

These hydrogels are designed through formation of permanent junctions in the polymer network. Chemical crosslinking can be achieved by following methods: using crosslinkers (aldehydes, addition reactions, condensation reaction), grafting, or using radiation.

## 2.4 Classification According to Network Electrical Charge

Depending on the nature of charge present on the crosslinking chains, hydrogels are classified into four types (Mocanu et al. 2012, Deo et al. 2010 and Percec et al. 2002):

- 2.4.1 Anionic hydrogels (e.g. carboxymethylpullulan hydrogels, alginate);
- 2.4.2 Cationic hydrogels (e.g. *N*-isopropylacrylamide (NIPAM) and (3-acrylamidopropyl) trimethylammonium chloride (AAPTAC));
- 2.4.3 Neutral hydrogels (miscible composites from water-insoluble polymers like poly(2,4,4-trimethylhexamethylene terephthalamide);
- 2.4.4 Ampholytic hydrogels (e.g. acrylamide-based ampholytic hydrogels).

## ***2.5 Classification on the Basis of Stimuli***

These hydrogels are responsive to physical or chemical stimuli and releases drug as a result of the abrupt change in the physical nature of the network in response to the physical or chemical stimuli. Based on this property, hydrogels are classified as follows.

### **2.5.1 Physically Responsive Hydrogels**

The polymeric network of these hydrogels consists if such polymers which undergo structural change alteration in molecular interactions by physical stimuli like temperature, electric or magnetic field.

### **2.5.2 Chemically Responsive Hydrogel**

Drug release from these hydrogels occurs in response to the chemical stimulus like pH, change in ionic strength or presence of certain ions and chemical reagents as a result of molecular changes due to change in interaction between polymer chains and solvent.

## **3 Methods for Preparation of Hydrogel**

### ***3.1 Mechanism of Network Formation***

The formation of hydrogel involves the creation of elastic network of polymeric chains through crosslinking. Therefore, any method which can be incorporated to generate a crosslinked polymeric network can be used to create a hydrogel (Ahmed 2015). This process of formation of crosslinked network is known as gelation and can be defined as the linking of macromolecular chains together which initially leads to progressively larger branched yet soluble polymers depending on the structure and conformation of the starting material.

Such hydrogels exhibit sol–gel transition which is most commonly employed for the formation of injectable depot preparations and ophthalmic gels. Sol is defined as the blend of polydispersed branched and soluble polymers. As the linking process proceeds, the size of the branching polymers goes on increasing with decreasing solubility resulting in the formation of gel. The linking can occur through physical (physical gelation) or chemical (chemical gelation) means. This transition of polymer from definite branched polymeric to vast network structure is referred to as as sol–gel transition or gelation. The critical point at which gel appears is known as gel point.



## 3.2 Physically Crosslinked Hydrogel

Physically crosslinked hydrogel can be formed through following methods.

### 3.2.1 Heating/Cooling a Polymer Solution

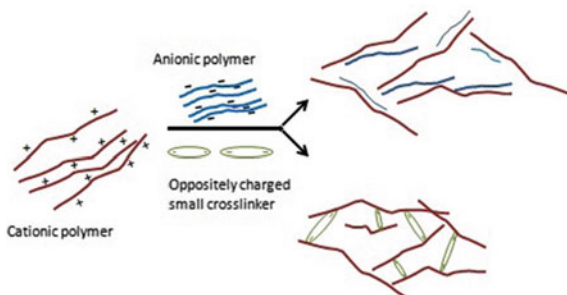
In this approach, the physically crosslinked gel is shaped upon cooling the hot solution of polymers. Upon cooling, the gel is formed as a result of helix formation, formation of junction, and association of helices (Funami et al. 2007). Example of polymer includes: carrageenan and gelatin. Above the melting transition temperature, the carrageenan is present in randomly coiled arrangement, and upon cooling, it transforms into rigid helical rods. In addition, stable aggregates are formed in the presence of positive ions ( $K^+$ ,  $Na^+$ , etc.) due to screening of repulsive forces between sulphonic groups and increased attractive forces between negative ( $SO_3^-$ ) and positive moieties of salt ( $Na^+$ ,  $K^+$ , etc.). Another simple approach which is used to obtain hydrogel is known as block copolymerization. It involves warming of polymeric solutions, for example hydrogel formed of polyethylene oxide–polypropylene oxide, polyethylene glycol–polylactic acid hydrogel.

### 3.2.2 Ionic Interaction-/Charge Interaction-Based Hydrogel

In this approach, charge interaction between a polymer and a counter ion or between two polymers of opposite charge leads to in situ formation of polymeric network to form hydrogel (Fig. 1). For example, under physiological conditions, elastin-like polypeptides are crosslinked through electrostatic interaction between the cationic lysine groups and anionic organophosphorus groups (Lim et al. 2007).

Polysaccharide, alginate is one of the most popular examples where crosslinks are formed through ionic linkage. Gel formation occurs incorporation of calcium ions which crosslink the mannuronic and glucuronic acid residues (Gacesa 1988). The crosslinking can be carried out at room temperature and at physiological pH, that is why alginate is widely used to encapsulate living cells and proteins in its matrix (Goosen et al. 1985).

**Fig. 1** Hydrogel formation through charge interaction



Another approach for the formation of ionic hydrogel does not necessitate the existence of ions on the polymer chain for the creation of ionic crosslinks. It is based on the ability of the metal ion to accumulate in the polymeric cage because of its small ionic radius, for example the formation of dextran, hydrogel in the presence of potassium ions. Dextran is deficient in ionic binding sites for cations; however, the ionic radius of the potassium ion easily and perfectly occupies the cage formed by six oxygen atoms of glucose entities of three polymer chains, in this manner making a microstructure (Watanabe et al. 1993). However, this dextran/potassium gel is less suitable for drug delivery purposes because it is unstable in water.

In addition, hydrogels can likewise be produced as a result of the formation of complex of polyanions with polycations, for example complex formation between chitosan and polyanions, such as dextran sulphate or polyphosphoric acid that generates ionically crosslinked chitosan hydrogels-based nanoparticles. (Janes et al. 2001). These chitosan hydrogel nanoparticles were loaded with doxorubicin, and reportedly shown a minimum burst release and exhibited good in vitro cytotoxicity due to the released drug.

pH-based ionic interactions can also lead to the formation of hydrogel. pH change promotes the ionization of the functional groups present on the polymer chain to form gel following interaction with the counter ion. Biodegradation of these hydrogels occurs easily by the ionic functionalities present in the extracellular fluid which bind competitively to the gel resulting in the breakdown of the polymeric network. For example, (i) peptides consisting of alternating positively and negatively charged groups can self-assemble through ionic interaction to form hydrogel in situ (Chen 2005) (ii) doxorubicin hydrochloride containing ionically crosslinked hydrogel formed from blend of quaternized chitosan and glycerophosphate which is optically clear and release drug as a function of pH (Wu et al. 2006).

Moreover, charge interactions can be used to crosslink gels to create three-dimensional particulate carriers like microparticle or nanoparticle with promising drug delivery properties. For example, dextran microspheres coated with anionic and cationic polymers reveal impulsive gelation upon mingling owing to ionic complex formation between the oppositely charged microparticles network (Van Tomme et al. 2005).

### 3.2.3 Crosslinking by Crystallization

#### Crystallization in Homopolymer Systems

Crystallization process involves subjecting the aqueous solution of water-soluble polymer to a series of freeze-thaw cycle resulting in crystallization of the polymer and formation of gel. For example, polyvinyl alcohol, a water-soluble polymer, forms a gel gradually when its aqueous solution is stored at room temperature but with weaker elasticity and strength. Surprisingly, when the solution of PVA was subjected to freeze-thaw process, a gel was formed having greater strength,

elasticity, and remained stable for 6 months at 37 °C (Yokoyama et al. 1986; Hassan and Peppas 2000). Mechanism for the formation of stronger gel is attributed to the formation of polymer crystals in the hydrogel network leading to more ordered arrangements of the polymeric chains and stronger anchorages. The properties of hydrogel are dependent on the molecular weight and concentration of PVA, temperature, time duration of freezing, and number of freeze-thaw cycle. This gel is ideal for encapsulation of proteins like BSA as the conformation of protein is retained during the release where the latter follows Fickian diffusion pattern.

The polymer crystals are also formed through hydrogen bonds formation does take place in the concentrated polymeric solution, and the gel gets converted into particulate form on stirring. For example, concentrated solution of dextran spontaneously formed hydrogel when stored at room temperature, and upon stirring, the solution of microspheres was obtained.

### Crosslinking by Stereocomplex Formation

Polymers consisting of chiral, optically active, monomeric units can form crystallites. Similarly, on mixing the polymer/s with regions of opposite chirality, these regions can associate to form racemic crystalline domains, which are known as stereocomplexes. Thus, stereocomplex hydrogels can be produced by combining enantiomerically enriched polymers of opposite chirality. Instead, they can be formed simply from one polymeric species having regions of opposed chirality. One of the most relevant stereocomplexes is formed by semicrystalline PLLA and PDLA, the homopolymers of L-lactic acid and D-lactic acid, respectively. The strong interaction between polylactide blocks with L- and D-stereochemistry can be utilized for in situ forming hydrogels with high storage moduli (up to 14 kPa) as illustrated schematically in Fig. 2. Star diblock copolymers or multi-arm PEG-PLA dendrimers interact through stereospecific crosslinking to form hydrogel with transition temperatures extending from 10 to 70 °C. The transition temperature is governed by the polymer concentration and length of the PLA block (Hiemstra et al. 2006). These hydrogels have enormous potential to be used in drug delivery. Stereocomplex formation also occurs in mixtures of triblock copolymers, for example PLLA-PEG-PLLA and PDLA-PEG-PDLA, which can be easily transformed into particulate carriers to carry number of drug- and protein-based therapeutics. For example, Lim et al. studied and compared the release of BSA from microspheres formed by these triblock copolymers with the microspheres formulated with single enantiomeric triblock copolymer and with PLLA microspheres (Lim and Park 2000). Natural polymers can also be crosslinked through stereocomplex formation by grafting of enantiomers on their backbone, for example grafting of D- and L-lactic acid oligomers on the dextran backbone (Hennink et al. 2004; Bos et al. 2004). Hydrogel is formed by spontaneous gelation in water without the need of any harsh condition or organic solvent or chemical crosslinkers or the hydrophobic domains thus they are suitable for the delivery of proteins. They have excellent biocompatibility and biodegradability.

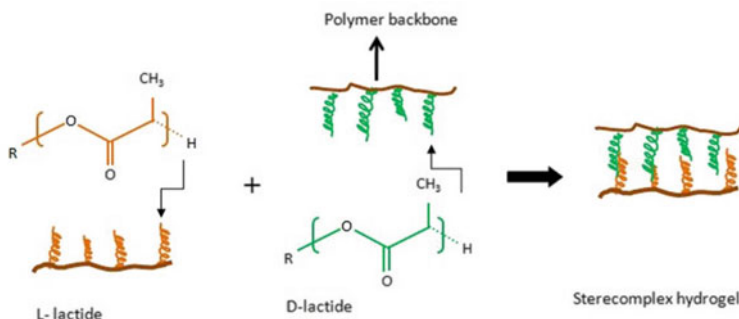


**Fig. 2** Hydrogel formation through stereocomplex formation

Hydrogels based on stereocomplex crosslinking, however suffer from demerit of limited range of polymers available which are capable of forming strong hydrogel. A small change in the composition or stoichiometry during synthesis can disrupt or weaken the stereochemical interaction. The stereocomplex hydrogels are degraded in biological conditions due to the existence of hydrolysable oligomeric lactide side chains and are used for drug delivery applications. They are also degraded in body by means of the degradable structure anchored on the polymer base or by tailoring polymeric backbone with degrading groups. For example, hydrogel can be made degradable by involving grafts and linking biosusceptible groups between the polymer chains.

However, many of the stereocomplex hydrogels do not contribute as a good candidate for controlled release formulation because the rate of hydrolysis is faster than that required to provide adequate gel strength and to assure drug retention over several weeks or months. Physiologically stable stereocomplex hydrogels capable of releasing drug for several weeks or months are still to be designed, devised and developed.

### 3.2.4 H-Bonding-Based Hydrogels

Hydrogen bonding-based physically crosslinked gel structure is formed by interaction between polymeric chains consisting of active oxygen and a chain consisting of hydrogen bonding atoms like H, N, or F. These hydrogels are formulated as injectable hydrogels based on sol-gel viscoelastic transition. Such individual polymers remain in solution form which upon blending undergo viscoelastic changes (rheological synergism) due to hydrogen bonding and form the gel. Upon subjecting to shear during injection, hydrogen bonds are cleaved, thereby allowing ease of administration; for example, polyacrylic acid (PAA) and polymethacrylic acid (PMA) make complexes with polyethylene glycol (PEG) as a result of hydrogen bonding interaction between oxygen of PEG and hydrogen from carboxylic group of PAA and PMA (England et al. 1994). The polymeric gel from

these polymers can also be prepared by dissolving in ethanol. This gel upon injecting into body diffuses ethanol and converts into gel which degrades gradually as the complex dissociates. Other examples of physically interconnected gel-like structures which are injectable too include combinations of natural polymers such as gelatin-agar (Liu et al. 2005), starch-carboxymethyl cellulose (Bajpai and Shrivastava 2005), and hyaluronic acid-methylcellulose (Gupta et al. 2006).

These hydrogels are formed only upon the protonation of carboxylic acid groups and exhibit pH-dependent swelling behaviour. However, on in vivo administration these hydrogen-bonded networks get diluted and disperse owing to inflow of water, hence constraining their usage to comparatively short-acting drug release systems unless additional crosslinking agent is also used.

Carboxylic group containing polymers can form hydrogel on lowering of pH. For example, sodium CMC forms a hydrogen-bonded hydrogel when dispersed in 0.1 M HCl solution (Takigami et al. 2007). The  $\text{Na}^+$  ion in CMC is replaced by the hydrogen ion present in the acid solution which results in the hydrogen bond formation followed by a decrease in the solubility of CMC and formation of hydrogel. Based on the similar mechanism, polyacrylic acid and polyethylene oxide (PEO-PAAc) also form a hydrogen-bonded hydrogel as the pH of the aqueous solution decreases (Hoffman 2002). Polymeric blend of xanthan and alginate forms an insoluble hydrogel network due to formation of strong intermolecular bonds.

### 3.2.5 Supramolecular Complex-Based Hydrogel

Supramolecular hydrogels represent a solid three-dimensional structure shaped involving non-covalent bonds like hydrogen bond, hydrophobic interaction, and cation- $\pi$  and  $\pi$ - $\pi$  interactions. While chemical crosslinkers are responsible for stabilizing the hydrogel network of the chemical gels, the non-covalent interactions in supramolecular three-dimensional structure provide strength and stability through the formation of macromolecular polymer and three dimensional gel network.

Supramolecular hydrogels are produced from hydrophilic molecules. Stimuli-responsive supramolecular hydrogel can be made by incorporating some reversible bonds. Furthermore, such reversible supramolecular hydrogels also show self-healing properties and have enormous potential to contribute in drug delivery application.

The most widely used supramolecular complexes include the inclusion complexes formed by the interaction of cyclodextrin and poly(alkylene oxide) polymers like PEO and PPO (Hoare and Kohane 2008). These are capable of forming reversible hydrogels which are easily injectable and therefore utilized to prepare controlled release injectable formulations. Combination of complexation with hydrophobic interaction has resulted in a stronger, denser, and/or more stable hydrogel network. For example, a self assembled supramolecular structure comprising of cyclodextrin and a biodegradable poly(ethylene oxide)-poly[(R)-3-hydroxybutyrate]-poly(ethylene oxide) (PEO-PHB-PEO) triblock copolymer

was reported by many researchers. The collaborative outcome of complexation of PEO segments with  $\alpha$ -cyclodextrin and the hydrophobic interaction between PHB blocks give rise to the development of the supramolecular hydrogel with a robust macromolecular network (Saboktakin and Tabatabaei 2015). Table 4 summarizes various types of supramolecular hydrogel and their compositions.

### 3.3 Covalently/Chemically Crosslinked Hydrogels

Chemical crosslinking involves the use of a crosslinking agent to link two polymer chains or grafting of monomers on the backbone of the polymers. The functional groups present on the natural or synthetic polymers can react with the crosslinkers (such as glutaraldehyde, adipic acid dihydrazide) resulting in the crosslinking of chains and formation of hydrogel.

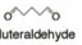
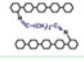
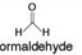
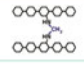
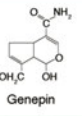
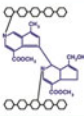
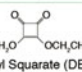
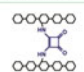
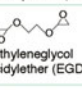
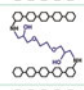
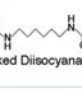
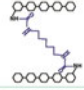
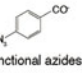
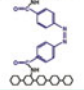
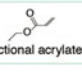
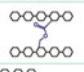
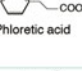
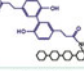
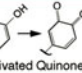
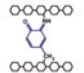
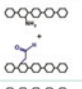
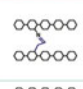
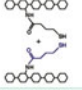
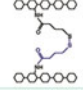
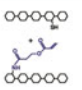
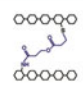
There are a number of approaches stated in the literature to form permanent chemical hydrogels. These methods are as illustrated in Fig. 3 and exemplified using chitosan. The major chemical methods employed are use of crosslinkers, grafting and radiation in solid and/or aqueous state. Other chemical crosslinking methods such as IPN (polymerize a monomer contained by additional solid polymer to form interpenetrating network structure) and hydrophobic interactions (including a polar hydrophilic group by hydrolysis or oxidation followed by covalent crosslinking) are also employed to achieve chemically crosslinked permanent hydrogels.

#### 3.3.1 Crosslinking by Radical Polymerization

Low molecular weight monomers (vinyl and acrylic acid) can be crosslinked in the presence of crosslinking agents. It proceeds through three processes, viz. initiation, propagation, and termination. Initiation of the reaction generates a free radical active site, which attaches monomers in a chain-like manner. Wichterle and Lim (1960) first described hydrogel based on poly(2-hydroxyethyl methacrylate) (pHEMA) polymer, and it is one of the commonly studied hydrogel system. This hydrogel is synthesized by polymerization of hydroxyethyl methacrylate (HEMA) in the presence of crosslinking agent like ethylene glycol dimethacrylate. This approach is used to synthesize pH- or a temperature-sensitive hydrogel by integrating methacrylic acid or *N*-isopropylacrylamide, respectively, in the vicinity of suitable crosslinking agents. For example, PVA has been crosslinked chemically with monomer (methacrylic acid) in aqueous medium using ethylene glycol dimethacrylate (EGDMA) as crosslinking agent and benzoyl peroxide as a reaction initiator to produce pH-sensitive hydrogel which is a promising delivery system for colonic delivery of 5-fluorouracil in colorectal cancer (Minhas et al. 2013). Various water soluble polymers of synthetic, semi-synthetic, and natural origin have been used for the design of hydrogels using this route. These water-soluble polymers

**Table 4** Types and properties of supramolecular hydrogels for drug delivery

S.No	Hydrogel Type	Polymer/ Mechanism of formation	Properties	Ref
1.	Supramolecular hydrogels as intrarenal drug delivery systems (UPy-modified prepolymers and UPy-functionalized peptides)	introduction of UPy-moieties on poly (ethylene glycol) (PEG) prepolymers enzyme-triggered drug release mechanism via the degradation of encapsulated hydrogels.	The drug release of occurs at physiological temperature. the drug release rate can be controlled by by changing the enzyme concentration and/or temperature.	Dolman et al. (2010)
2.	Injectable systems based on supramolecular hydrogels	in situgel-forming system composed of hyaluronic acid-tyramine (HA-Tyr) conjugates using a peroxidase-catalyzed oxidation (horseradish peroxidase) reaction.	Do not need surgical removal after treatment. No toxic molecules is formed on degradation in the body, Excellent biocompatibility and 2. biodegradability formation of hydrogels without any inflammation andredundant reactions, Prolonged and sustained drug release can be achieved bycontrolling the hydrogel degradation, can be programmed throughthe design of the cross-link density	Vemula et al. (2006)
3.	Supramolecular hydrogels based on nonsteroidalanti-inflammatory drugs and small peptides.	The covalent linkage of Phe–Phe and NSAIDs results in conjugates that self-assemble in water to form molecular nanofibers as the matrices of hydrogels	better selectivity toward their targets. peptides consisting of d-amino acids facilitate to protect the activities of NSAIDs. Offers a new molecular hydrogels for topical use.	
4.	Novel supramolecular hydrogels based on Cyclodextrin and copolymers	Hydrogel self-assembled between a-cyclodextrin and a biodegradablepoly (ethylene oxide)–poly[(R)-3-hydroxybutyrate]–poly(ethyleneoxide) (PEO–PHB–PEO) triblock copolymer The cooperation effect of complexation of PEO segments with a-cyclodextrin and the hydrophobic interaction between PHBblocks resulted in the formation of the supramolecular hydrogel with a strong macromolecular network	relatively long term sustained controlled release of drugs can be attained thixotropic and reversible	Takashima et al. (2012)

	Agent	Target Functional Groups	Reaction Conditions	Cross-linkage	Comments
Small Molecule	 Glutaraldehyde	Primary amines & aldehydes	Reaction favors basic & neutral pH		Reaction completes within 1 h; Difficult to remove trace glutaraldehyde
	 Formaldehyde	Primary amines & aldehydes	Basic & neutral pH		Reaction completes within 1 h; Difficult to remove trace formaldehyde
	 Genepin	Primary amines & aldehydes	Independent of pH		Nontoxic linker; Can undergo self polymerization
	 Diethyl Squarate (DES)	Primary amines	pH 4.5-5.5; Solution precipitates at higher pH; Reaction favors elevated temperatures		Reacts under mild conditions & is nontoxic; Long reaction time precludes use for in situ gelation
	 Ethylene glycol diglycidylether (EGDE)	Primary amines and oxiranes	Basic pH; Reaction favors elevated temperatures		Difficult to remove EDGE traces; Long reaction times & basic pH can yield hydrogel beads
	 Blocked Diisocyanate	Primary amines	Basic pH; Reaction requires elevated temperatures		Long reaction times & basic pH requirements preclude in situ gelation; Can produce hydrogel beads
Photo-Sensitive	 Functional azides	Primary amines	Independent of pH		Multi step crosslinker; Suitable for injectable hydrogel hydrogel preparation
	 Functional acrylates	Other acrylic acids	Independent of pH		Multi step crosslinker; Suitable for injectable hydrogel hydrogel preparation
Enzymatic	 Phloretic acid	Primary amines	Physiological pH		Fast gelation; Suitable for in situ gelation
	 Activated Quinone	Primary amines	pH 5.8-6 at 35°C		Gelation occurs under 2 hr; Suitable for in situ gelation
	Reaction	Reaction Conditions	Reactive Polymer Groups	Cross-linkage	Comments
Polymer-Polymer	Schiff Base Formation	Neutral pH			Good candidate for in situ gel formation; Hydrogel formation in around 10 min
	Disulfide Bonding	Neutral pH			Good candidate for in situ gel formation; Hydrogels have enhanced mucoadhesive properties
	Michael Addition	Weak base; Catalysts required			Good candidate for in situ gel formation; Hydrogels have enhanced mucoadhesive properties

**Fig. 3** Various crosslinking groups and structures in covalently crosslinked chitosan hydrogels

after being derivitized with polymerizable groups can be crosslinked into hydrogels by free radical polymerization, for example dextran, albumin, (hydroxyethyl) starch, poly-aspartamide, poly(vinyl alcohol), and hyaluronic acid. Among these polymers, dextran is most widely exploited for hydrogel preparation and explored for the delivery of drugs, proteins, and imaging agents (Mehvar 2000). In addition,



dextran-based hydrogels are under research as a colon delivery system due to the existence of dextranase in the colon. Polymerizable dextran is prepared by reacting aqueous solution of dextran with glyce dylacrylate to produce acryl dextran. Acryl dextran forms a hydrogel following free radical polymerization in the presence of  $N,N,N',N'$ -tetramethylene-diamine and ammonium peroxydisulphate as an initiator. Polyacryldextran hydrogel-based microspheres are capable of immobilizing enzyme efficiently with full retention of their activity.

### 3.3.2 Crosslinking by Complementary Groups Chemical Reaction

Hydrophilic groups, namely  $\text{NH}_2$ ,  $\text{COOH}$  and  $\text{OH}$  present on the hydrophilic polymers may be used for the hydrogel development. Covalent linkages among polymer chains occurs through the reactions, for example an amine-carboxylic acid or an isocyanate- $\text{OH}/\text{NH}_2$  reaction or Schiff base formation, which may be used to recognize covalent linkages between polymer chains.

### 3.3.3 Crosslinking with Aldehydes

$-\text{OH}$  groups carrying hydrophilic polymers, e.g. polyvinyl alcohol. may be cross-linked through glutaraldehyde (Zu et al. 2012). Conditions are applied (like low pH, methanol added as a quencher, high temperature) to establish crosslinking are well defined and required to be maintained carefully. However, polymer bearing amine functional group can be crosslinked even under mild conditions through the formation of intermediate Schiff base. This approach is used to form protein -based hydrogels like, gelatin and albumin and the amine containing polysaccharides.

### 3.3.4 By Addition Reactions

Water soluble polymer can be crosslinked to form hydrogels using bis or higher functional crosslinking agents such as divinylsulfone and 1,6-hexanedibromide through an addition reaction. The properties of hydrogel network can be simply customized to attain the desired characters by changing the concentration of crosslinking agent and the dissolved polymer. In this approach, the crosslinking reactions are performed in organic solvent since water may react with the crosslinking molecules if used. This increases the cost of synthesis and also the toxicity issues thereby, reducing the safety margin for in vivo use. In addition, the crosslinking agents are highly toxic which require the complete removal of unreacted reagent. The drug is loaded after the hydrogel preparation and reagent extraction which results in first-order drug release profile along with the narrow duration of the release and therefore renders such hydrogels unsuitable specifically for sustained and controlled release formulation.

### 3.3.5 By Condensation Reactions

Condensation reactions among hydroxyl (–OH) groups or amine (–NH<sub>2</sub>) with carboxyl group (–COOH) result in the formation of polyesters and polyamides, respectively. These reactions are used for the synthesis of hydrogel from water-soluble polymers. One of the most efficient and widely used crosslinking agents to crosslink water-soluble polymers with amide bonds is *N,N*-(3-imethylaminopropyl)-*N*-ethyl carbodiimide (EDC). This reaction involves the addition of *N*-hydroxysuccinimide (NHS) to suppress the side reactions and increase the density and yield of hydrogel (Kuijpers et al. 2000).

These hydrogels have potentials to deliver active pharmaceutical agent as well as protein-based therapeutics over a prolonged period of time. For example, hydrogel loaded with lysozyme could release the enzyme for 2 days both in vitro and in vivo. The loading capacity of these hydrogels can be increased by incorporating negatively charged agent; for example, addition of negatively charged polysaccharide chondroitin sulphate augmented the loading capability of protein in hydrogel besides retarding the release of the protein from hydrogel due to electrostatic interactions between the cationic protein and anionic polysaccharide.

Another method known as Passerini and Ugi condensation reaction is also used to prepare polysaccharides-based hydrogels (de Nooy et al. 2000). Passerini condensation employs a reaction between carboxylic acid and an aldehyde or ketone with an isocyanide to yield an  $\alpha$ -(acryloxy). These hydrogels are degradable at ambient temperature and at pH 9.5 because of the existence of ester bond in the crosslinks. Ugi condensation is extension of Passerini approach, in which amine is added to the above reaction mixture to finally yield  $\alpha$ -(acylamino) amide. These are more stable than Passerini hydrogel under similar conditions due to amide bond in crosslinks. The advantage of these methods is that the reaction can be supported out at room temperature and in water at slightly acidic pH.

## 3.4 Crosslinking by High Energy Irradiation

Unsaturated substances can be polymerized by employing high energy radiations like gamma and electron beams (Amin 2012). Hydrophilic polymers which are derivatized with vinyl group can be transformed into hydrogels by means of high energy radiation. Alternatively, radiation-induced polymerization can also be used to synthesize hydrogel from a fusion of a monofunctional acrylate (e.g. acryloyl-L-proline methyl ester) and an appropriate crosslinker (Caliceti et al. 2001).

High energy radiation can also induce formation of hydrogel from water-soluble polymer through free radical formation which do not require the presence of vinyl groups. Free radicals are formed from the polymeric chain (e.g. haemolytic fission of C–H bond) when the aqueous polymeric solution is irradiated. Additionally,

hydroxyl radicals are also generated by radiolysis of water molecules which can attack polymer chains resulting in the formation of macroradicals (Peppas and Mikos 1986). The macroradicals react with the polymeric chain functionality through covalent bond formation resulting in crosslinked structure. Radiation is usually accomplished in an inert (nitrogen, argon) atmosphere to avoid the generated macroradicals to react with oxygen. Well-acknowledged examples of polymers which can be crosslinked with high energy irradiation are poly(vinyl alcohol), poly(ethylene glycol), and poly(acrylic acid).

The characteristics of the gels, particularly swelling and permeability properties, are reliant on the amount of the polymer used and dose of radiation employed: In general, the crosslinking density rises with the increase in polymer concentration and amount of radiation dose. The major benefit of preparing hydrogel by means of radiation-induced crosslinking is that this synthesis can be used in presence of water under mild conditions (room temperature and physiological pH). In addition, the use of toxic crosslinking agents is not required. Nevertheless, the loading of biologically active compound is to be done after the formation of hydrogel to avoid radiation-induced damage to the pharmaceutically active substance and/or possible interaction between the radical and the therapeutic moiety. The gel formed from PEG and PVA are non-biodegradable due to presence of C–C bonds in the crosslinks.

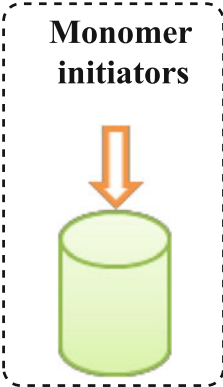
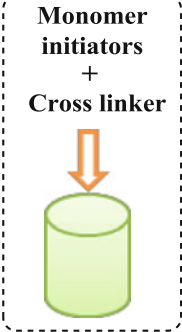
## 4 Polymerization Techniques in Hydrogel Synthesis

Hydrogels can be prepared from monomers or polymers of synthetic or natural polymers by using techniques which are capable of crosslinking these units through polymerization. The various synthesis polymerization techniques reported for the synthesis biomedical hydrogels are described in Table 5 (Ahmed 2015; Sahu et al. 2012).

## 5 Characterization of Hydrogel


Mostly, hydrogels are characterized for their various parameters such as morphological characterization, crystalline/thermal behaviour, morphological integrity, rheological, swelling, mechanical and biochemical properties, and in vitro release behaviour. The important features of hydrogels are summarized in Table 6 (Sahu et al. 2012; Chauhan et al. 2012; Rowley et al. 1999; Khare and Peppas 1995).

**Table 5** Various polymerization techniques employed in hydrogel formation

Name of technique	Description	Advantages	Disadvantages
Bulk polymerization 	<p>It is the simplest technique which involves only monomer and monomer-soluble initiators. The choice of a suitable initiator depends upon the type of monomers and solvents being used. In this method hydrogels can be prepared by using one or more types of monomers and owing to the high concentration of monomer, the high degree of polymerization and high rate polymerization occurs. However, the viscosity of the system is low initially to allow ready polymerization reaction and viscosity increases markedly with the conversions. In this polymerization process monomers make a homogeneous hydrogel system produces a very rigid, transparent, glassy polymer matrix. This glassy polymer matrix when put in contact with aqueous medium, swells to become soft and flexible gel. Ex. vinyl monomers based hydrogels (Suda 2007).</p>	<ul style="list-style-type: none"> <li>❖ Simple method</li> <li>❖ Minimum chance to contamination</li> </ul>	<ul style="list-style-type: none"> <li>❖ Irregular polymerization</li> <li>❖ An increase temp will increase the polymerization rate</li> <li>❖ Near the end of polymerization, the viscosity is very high and difficult to control the rate</li> </ul>
Cross-linking/Solution polymerization 	<p>In cross-linking method, the ionic or neutral monomers are mixed with or without cross-linking agents. It requires the correct selection of the solvents. Both the initiator and monomer be soluble in each other and that the solvent are suitable for boiling points, regarding the solvent-removal steps. The polymerization is initiated thermally by UV-irradiation or by a redox initiator system. The solvent is employed to lower the viscosity of</p>	<ul style="list-style-type: none"> <li>❖ Solvent reduces viscosity, making processing easier</li> <li>❖ Thermal control is easier than in the bulk</li> </ul>	<ul style="list-style-type: none"> <li>❖ Reduce monomer concentration which results in decreasing the rate of the reaction and the degree of polymerization</li> <li>❖ Difficult to remove solvent from final form, causing degradation of bulk properties</li> <li>❖ Not suitable for dry polymers</li> </ul>

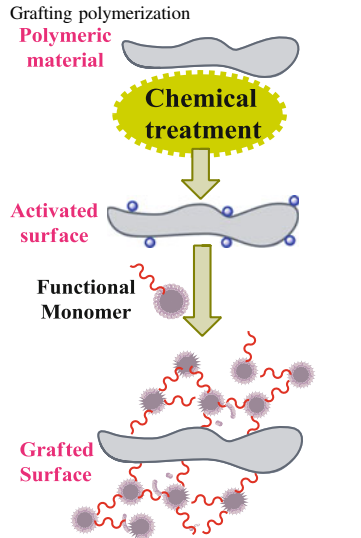
(continued)

**Table 5** (continued)

Name of technique	Description	Advantages	Disadvantages
	<p>the reaction thus help in the heat transfer and reduce auto acceleration is the major advantage of this method over bulk polymerization. In this technique, the prepared need to be washed hydrogels formulation with distilled/deionized water to remove the cross-linking agents, monomers, oligomers, initiators, and other impurities. Various cross-linking techniques such as ionic interactions, protein interaction, hydrogen bonds, crystallization, and crosslinking by hydrophobic interactions have been investigated for the synthesis of physically cross link gels (Ganji and Farahan 2009; Stringer and Peppas 1996).</p>		
<p>Suspension polymerization or inverse-suspension polymerization</p> <div style="border: 1px dashed black; padding: 10px; margin: 10px 0;"> <p style="text-align: center;"><b>Monomer</b> + <b>Inorganic stabilizer</b> + <b>Oil soluble initiator</b> + <b>Water</b></p>  </div>	<p>Suspension polymerization is an advantageous method since the products are obtained as powder or microspheres (beads), and thus, grinding is not required. Since water-in-oil (W/O) process is chosen instead of the more common oil-in-water (O/W), the polymerization is referred to as "inverse suspension". In this polymerization consists of an aqueous system with monomer as a dispersed phase and results in polymer as a dispersed solid phase. In this technique, the monomers and initiator are dispersed in the hydrocarbon phase as a homogenous mixture. The dispersion is</p>	<ul style="list-style-type: none"> <li>❖ Polymerization to high conversion</li> <li>❖ Low viscosity due to the suspension</li> <li>❖ Easy heat removal due to the high heat capacity of water</li> <li>❖ Excellent heat transfer because of the presence of the solvent</li> <li>❖ Solvent cost and recovery operation are cheap</li> </ul>	<ul style="list-style-type: none"> <li>❖ Contamination by the presence of suspension and other</li> <li>❖ Must separate and purify polymer, or accept contaminated product</li> <li>❖ Reactor cost may higher than the solution cost</li> </ul>

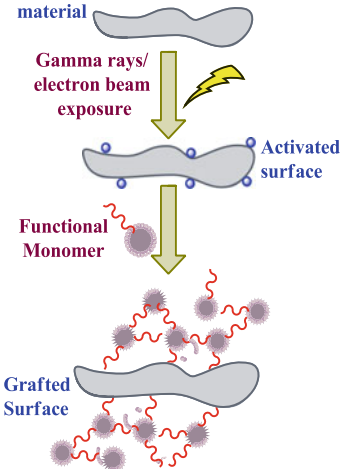
(continued)

**Table 5** (continued)

Name of technique	Description	Advantages	Disadvantages
	thermodynamically unstable and requires both continuous agitation and addition of a low hydrophilic–lipophilic-balance (HLB) suspending agent. Near the end of polymerization, the particles are hardened, are the bead or pearl shaped polymers recovered by filtration, and followed by washing step (Watanabe et al. 1993; Hunkeler 1992).		
<p>Grafting polymerization</p>  <p>The diagram illustrates the three stages of grafting polymerization. 1. <b>Polymeric material</b>: A grey, wavy polymer backbone. 2. <b>Chemical treatment</b>: A yellow starburst indicates the activation step, resulting in an <b>Activated surface</b> with blue dots representing active sites. 3. <b>Functional Monomer</b>: Red wavy chains with grey spheres (monomers) are shown attaching to the active sites, resulting in a <b>Grafted Surface</b> with multiple red wavy chains extending from the backbone.</p>	This involves the polymerization of a monomer on the backbone of a preformed polymer. In this process polymer chains are activated by the action of chemical reagents, or high energy radiation treatment. This technique involves the generation of free radicals onto a stronger support surface and then polymerizing monomers directly onto it as a result a chain of monomers are covalently bonded to the support (Tong and Zhang 2005; Said et al. 2004).	❖ To improve the mechanical properties	
Polymerization by irradiation	In this technique ionizing high energy radiations/ electron beams like gamma rays has been used to initiate the free radical polymerization of polymer on the backbone. Also, radiolysis of water molecules results in the generation of hydroxyl	❖ Initiator-free hydrogels and relatively pure	

(continued)

**Table 5** (continued)

Name of technique	Description	Advantages	Disadvantages
	<p>radicals, which also attack the polymer chains, resulting in the formation of macro-radicals. Recombination of the macro-radicals on different chains results in the formation of covalent bonds, so finally, cross-linked structure is formed. Some examples of polymers cross-linked by the radiation method are poly(acrylic acid), poly(ethylene glycol), poly(vinyl alcohol) etc (Enas et al. 2008; Das et al. 2006)</p>		

## 6 Smart Hydrogels

Stimuli-responsive hydrogels are of great potential with a number of applications. Some environmental variations like increased temperature and low pH are found in the body in diseased conditions, and due to this reason, either temperature-responsive and/or pH-responsive hydrogels can be used for site-specific controlled drug delivery. Hydrogels can also respond to specific molecules like antigen and glucose thus find applications in triggered drug delivery and as biosensors (Leda 2015). Apart from temperature and pH, hydrogels may also respond to light, pressure, and electrical variation, thereby giving rise to light-sensitive, pressure-responsive, and electro-sensitive hydrogels, respectively. The disadvantage associated with these stimuli-responsive hydrogels is that they respond very slowly, and to overcome this drawback, nowadays thinner and smaller hydrogels are formulated. Different stimuli-responsive hydrogels with their drug delivery applications are discussed as follows.

### 6.1 Temperature-Sensitive Hydrogel

Temperature-sensitive hydrogels are most likely and the most frequently studied group of stimuli-responsive hydrogel networks in drug delivery research (Qiu and Park 2012). A number of polymers show temperature-responsive phase transition

**Table 6** Characterization parameters of hydrogel

S. No.	Parameter	Description
1.	Morphological characterization	In general, morphological evaluations of hydrogels performed by using equipment like stereomicroscope. However, Scanning electron microscope (FE-SEM) and atomic force microscopic (AFM) methods are extensively used as a visualizing aid and to ensure the texture, real microstructure, composition, surface topography and other properties such as electrical conductivity of hydrogels. These are the powerful techniques widely used to capture the characteristic 'network' structure in hydrogels (Szepes et al. 2008).
2	Crystalline / Thermal behavior	This analysis is quite a popular study for the morphological characterization of hydrogels. This analysis helps to understand whether the polymers in hydrogel retain their crystalline structure or they get deformed during the fabrication processing or pressurization process. The retention of crystalline structure or their deformation during pressurization has played a vital role. The estimation of amorphous or crystalline characteristics or determines the pattern of the arrangement of layers in hydrogel is studied by diffraction analysis techniques. X-ray diffraction (XRD), Differential scanning calorimetry (DSC) and Thermo Gravimetric Analysis (TGA) techniques are commonly used for the evaluation of thermal or crystalline behavior which is related with stability of the hydrogels (Yu and Xiao 2008)
3.	Impurities/ Morphological integrity	By using spectroscopic techniques, it is an easy way to identify the presence of functional groups in a molecule which is present in hydrogels. Fourier Transform Infrared Spectroscopy (FTIR) is a useful technique for identifying chemical structure or chemical characterization of a substance and to confirm the identity of a pure compound or to detect the presence of certain impurities. Any change in the morphological integrity of hydrogels structure changes their IR absorption spectra due to stretching and O-H vibration. The stretching or bending vibrations are basically responsible for the changes in IR absorption spectra. This technique is widely used to investigate the structural arrangement in hydrogel by comparison with the starting materials (Mansur et al. 2004).
4.	Rheology	The rheological properties of hydrogels are important parameter and basically dependent on the types of structure such as cross-links, entanglement and association present in the system. Hydrogel formulations are evaluated for viscosity under constant temperature (usually 4°C) by using cone plate type viscometer and also determined by the simple equation of determining the angle of repose through which height and length is determined [Shultz et al., 2008]
6.	Swelling behavior	Swelling or rate of swelling is the most important characteristic and favorable property of the hydrogel system. It is ability to swell or water holding capacity, when put in contact with a compatible medium. It is determined by several physicochemical factors particularly the sample/particle size, porosity extent and the type of the porous structure. The time

(continued)



**Table 6** (continued)

S. No.	Parameter	Description
		and degree of swelling are significant because these effect on the release kinetic of loaded bioactive(s) from swelling controlled systems. The hydrophobic / hydrophilic balance of the hydrogels, the degree of cross-linking, and especially, the degree of ionization and its interaction with counterions are the important parameters which control the equilibrium swelling, dimensional change and the release patterns of drugs from these carriers [18]. Hence, in the past decades various mathematical models have gained considerable attention for predictability of swelling behavior. In case of polymeric hydrogels, the polar hydrophilic groups are first to be hydrated upon contact with aqueous medium or medium of specific pH to know the swellability of this polymeric network. These polymers show increase in dimensions related to swelling. The hydrogels swell in water to form the polymeric network. The formation of this polymeric network is responsible for the morphological characterization of drug. Polymers are characterized by light scattering and size exclusion chromatography, viscosity methods, osmometry etc. (Ganji and Farahan 2009; Yin et al. 2002, 2008)
7.	Mechanical properties	Mechanical properties of the hydrogels is important because the hydrogels could be used in various biomedical applications such as wound dressing material, ligament and tendon repair, tissue engineering as in cartilage replacement and matrix for drug delivery, which need hydrogels with different properties. FDA provides strict guidelines for the same depending upon the type of application. As for example, a drug delivery device should maintain its integrity during the lifetime of the application (Mi et al., 2001; Toshikazu et al. 1992)
8.	Biocompatible properties	Biocompatibility is also most important characteristic property required by the hydrogel. Biocompatibility means compatibility with the body immune system and its degradation products should be nontoxic. Ideally they should be metabolized into harmless products or can be excreted by the renal filtration process. Generally, hydrogels possess a good biocompatibility since their hydrophilic surface has a low interfacial free energy when in contact with body fluids, which results in a low tendency for proteins and cells to adhere to these surfaces. Moreover, the soft and rubbery nature of hydrogels minimizes irritation to surrounding tissue (De Groot et al. 2001; Anderson & Langone, 1999; Smetana 1993).
3.	<i>In-vitro</i> release profile	Since hydrogels are the swollen polymeric networks, interior of which is occupied by drug molecules, therefore, release studies are carried out to understand the mechanism of release over a period of application. The <i>in-vitro</i> diffraction study is quite popular for studying the release profile of hydrogel. One that basis the bioequivalence study is carried out to estimate the release of dosage forms. The parameters are matched with the standard plot so that the equivalence between the drug solutions is carried out (Szepes et al. 2008; Yu and Xiao 2008).

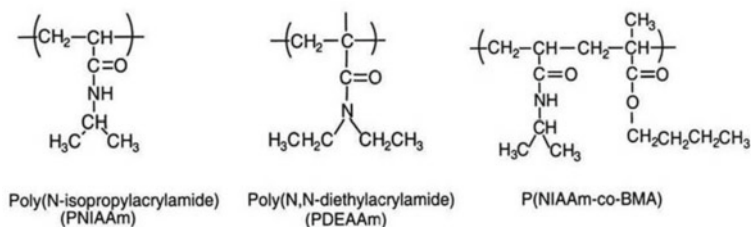


Fig. 4 Structures of some temperature-sensitive polymers

behaviour. The assemblies of some of those polymers are shown in Fig. 4. The presence of hydrophobic moieties like alkyl group is the most common characteristic of temperature-sensitive polymers. The **lower critical solution temperature (LCST)** represents that critical temperature below which the all the components of a mixture are miscible at every compositions. LCST is an important factor while selecting polymers for temperature-dependent hydrogels. Generally, polymers with LCST ranging from 28 to 32 °C are considered as good candidate to formulate temperature-sensitive drug delivery systems. Water-soluble polymers shows a proportional relation between solubility and temperature; i.e. as the temperature of the solvent is increased, the solubility of hydrophilic polymers also increases. Conversely, polymers possessing LCST follow inverse relation between temperature and aqueous solubility. Hydrogels comprising of such polymers undergo shrinkage as the temperature rises above LCST. The polymers chains of LCST polymers are linked by temperately hydrophobic groups or contain a mixture of hydrophilic and hydrophobic segments. If the chains are linked with severely hydrophobic groups, then the polymer will lose water solubility. As the temperature is lowered, the aqueous solubility of polymer increases because hydrogen bonding between hydrophilic segments and water molecules dominates the hydrophobic interaction. But, as the temperature increases the hydrophobic interactions among hydrophobic segments become stronger, the overall net effect leads to shrinkage of polymer to form hydrogel through strong hydrophobic interactions between segments of the chain. In general, increase in the hydrophobic constituents of the polymer chain leads to lowering of LCST (Schild 1992).

Different types of block copolymers made of poly (ethylene oxide) (PEO) and poly(propylene oxide) (PPO) also display an opposite temperature-sensitive property. The LCST of these polymers lies close to the physiological temperature, and hence, they are widely employed for the formulation of sol–gel-conversion-based controlled drug delivery systems.

Other temperature-sensitive polymers include poly (*N*-isopropylacrylamide) (PNIPAM) which is perhaps the most broadly used temperature-responsive polymer. Another example of such polymer which is widely employed as gel-sol system in vivo includes poly(*N,N*-diethylacrylamide) (PDEAM) because of its lower critical solution temperature (LCST) in the range of 25–32 °C, which is close to the body

temperature. The LCST of the polymers can be modified by adding other monomers; for example, copolymers of NIPAAm can be prepared using additional monomers, e.g. butylmethacrylate (BMA), to adjust the LCST (Cai and Suo 2011).

### 6.1.1 Properties of Temperature-Sensitive Hydrogels

Temperature-sensitive hydrogels can experience sol–gel phase transitions, alternative to the typical swelling–shrinking transitions if the polymer chains in hydrogels are non-covalently crosslinked. These thermally reversible gels with inverse temperature dependence are sol at elevated temperatures. Polymers that express this kind of behaviour are block copolymers of PEO and PPO.

Alternatively, the temperature-responsive hydrogels can also be prepared by using such crosslinking agents that possess temperature sensitivity.

Water soluble artificial polymer and a distinct protein-folding motif, the coiled coil were used to form a hybrid hydrogel system (Wang et al. 1999). The hydrogel experienced temperature-induced folding owing to the cooperative conformational shift. Incorporating temperature sensitivity through temperature-sensitive crosslinking agents provides an innovative platform in assembling temperature-sensitive hydrogels-based drug delivery systems.

### 6.1.2 Negatively Thermosensitive Drug Release Systems

Negatively thermo-responsive hydrogels are those polymers whose volume will decrease tends to increase in the temperature. Negatively responsive hydrogels can liberate encapsulated substances while shrinking with an increase of the temperature.

The examples of such hydrogels include crosslinked P(NIPAAm-co-BMA) hydrogels (Okuyama et al. 1993) and interpenetrating polymer networks (IPNs) of P(NIPAAm) and poly(tetra methylene ether glycol) (PTMEG). The mechanical strength of the NIPAAm gel can be increased by integrating hydrophobic comonomer BMA (Zhang et al. 2009). These hydrogel matrices are used to generate on–off drug release profile with varying temperature conditions; for example, the topically used indomethacin loaded hydrogel showed drug release (on) at low temperature while off at higher temperature. A dense and relatively impermeable layer of gel (designated as skin type barrier) was formed due to sudden temperature change resulting from faster collapse of the surface as compared to the interior part of the gel. This external shrinking was regulated by the length of the methacrylate alkyl side-chain, i.e. the hydrophobicity of the comonomer (Yoshida et al. 1991). The results, moreover, proposed that the drug in the polymeric matrices diffused from the inside to the surface during the off state even when no drug release was observed.

Temperature-sensitive hydrogels can also be positioned within a firm capsule bearing holes or apertures. The on–off release is accomplished by the flexible bulk variation of temperature-sensitive hydrogels (Dinarvand and Emanuele 1995; Gutowska et al. 1997). Such a device is named as a squeezing hydrogel as the drug release is affected by the dimensions and bulk volume of the hydrogel.

Temperature sensitive hydrogels can be strengthened by inserting in them a classified rigid matrix or by grafting them to the surface of rigid membranes. A composite membrane was prepared by dispersing PNIPAAm hydrogel microparticles into a crosslinked gelatin matrix (Chun and Kim 1996). The release of a model drug, 4-acetamidophen, was studied and was found to be dependent on the temperature which determined the swelling status of the PNIPAAm hydrogel microparticles in the microchannels of the membrane. A similar approach was used to develop a reservoir-type microcapsule drug delivery system by encapsulating the drug core with ethylcellulose containing nano-sized PNIPAAm hydrogel particles (Ichikawa and Fukumori 2000). For making stable thermally controlled on–off devices, PNIPAAm hydrogel can be grafted onto the entire surface of a rigid porous polymer membrane.

### 6.1.3 Positive Thermosensitive Drug Release Systems

Hydrogels formed by IPNs display positive thermosensitive effect which means that they swell at high temperature and shrink on lowering the temperature, for example IPNs of poly (acrylic acid) and polyacrylamide (PAAm) or P(AAm–co-BMA). The swelling behaviour of these hydrogels was reversible depending on the temperature which also resulted in concurrent reversible release of the drug like ketoprofen from that formulated monolithic system.

### 6.1.4 Thermo-Reversible Gels

Plurionics<sup>®</sup> and Tetronics<sup>®</sup> are the most popular form of thermo-reversible gels. Thermo-reversible hydrogels are not ideal for parenteral application since they are non-biodegradable. However, they can be converted to biodegradable form by replacing the PPO segment of PEO–PPO–PEO block copolymers by a biodegradable poly (L-lactic acid) segment (Jeong et al. 1999; Jeong et al. 2000).

The molecular architecture does not remain restricted to the A–B–A-type block copolymer, but can be extended into three-dimensional, hyper-branched structures, such as a star-shaped assembly. Gels with varying LCST values can be achieved by using appropriate combinations of molecular weight and polymer architecture. The hydrogel is formed by introducing the polymer loaded with drug (hydrophilic or hydrophobic) in aqueous solution, and the resulting hydrogel exhibits generally a first-order and S-shaped drug release, respectively.

## 6.2 *pH-Sensitive Hydrogels*

pH-sensitive polymers usually comprised of polyelectrolytes that either release or accept protons in response to change in the surrounding pH. They contain a large number of ionizable groups that undergo pH-dependent ionization. Poly (*N,N'*-diethylaminoethyl methacrylate) (PDEAEM) gets ionized at low pH, while poly (acrylic acid) (PAA) gets ionized at high pH. While the cationic polyelectrolytes, such as PDEAEM, display rapid dissolution and higher swelling when crosslinked at low pH owing to ionization of the polyanions, such as PAA, and undergo dissolution at high pH.

### 6.2.1 Properties of pH-Sensitive Hydrogels

Hydrogels prepared from crosslinked poly-electrolytes demonstrate vast differences in swelling properties in response to the changing pH of the environment. The pendant acidic or basic groups arranged on the polyelectrolytes undergo ionization parallel to acidic or basic groups of monoacids or monobases. However, the electrostatic forces applied by the neighbouring ionized groups render the ionization of polyelectrolytes difficult.

Polyelectrolyte polymers can show a swelling behaviour far better than the nonelectrolytic polymers because of the existence of ionizable groups arranged along polymer length. The reason behind the swelling of the polyelectrolyte based hydrogels is the presence of electrostatic repulsion between the charges that lie on the polymer chain. The extent of swelling depends on the magnitude of electrostatic repulsion under any condition like pH, ionic strength, and type of counterions present. The pH responsiveness and swelling can be further modified by adding neutral comonomers of different types. These monomers provide varying hydrophobic character to the polymer chain which results in different pH-responsive behaviour. Examples of such monomers include maleic anhydride, 2-hydroxyethyl methacrylate, and methyl methacrylate.

### 6.2.2 Applications of pH-Sensitive Hydrogels

#### Controlled Drug Delivery

pH-sensitive hydrogels are often used for developing controlled release formulations for oral administration because of varying pH conditions present in the gastrointestinal tract. The varying GIT pH range starting from neutral pH of mouth to acidic pH of the stomach to the alkaline pH of the intestine is exploited to elicit pH-dependent behaviour of polyelectrolyte hydrogels. The polycationic-based

hydrogels show minimal swelling at neutral pH, and hence, it is used for the delivery of offensive drugs in the neutral pH of mouth. Semi-IPNs made from polycationic hydrogels are employed for the delivery of drug in the stomach.

For example, semi-IPN of crosslinked chitosan and PEO presented more swelling when exposed to the acidic conditions which is ideal for localized delivery of antibiotics, such as amoxicillin and metronidazole, in the stomach for the management of *Helicobacter pylori* infection.

Furthermore, hydrogels which are functional at neutral pH are formulated using PAA or PMA. These hydrogels are used for delivering drug at neutral pH (Khare and Peppas 1993). Hydrogels can also be used for preparing enzyme sensitive drug delivery systems by incorporating crosslinkers through such bonds which can be cleaved by biological enzymes. These hydrogels are capable of providing localized or targeted drug delivery owing to the cleavage of bond in the environment (or tissue) where the enzyme responsible for bond cleavage is present. For example, for colon-specific drug delivery, drug loaded hydrogel is prepared by crosslinking polyanion like PAA by using azoaromatic crosslinkers. The drug is released in colon after the cleavage of azoaromatic bond by the azoreductase present in the microbial flora of the intestine (Fig. 5). These hydrogels show slower rate of swelling, and hence, drug release is also slow and minimal.

Depending upon the need of the therapy and site of drug release, the polymer composition and the type of crosslinker can be changed; for example, terpolymer-based hydrogels comprising of NIPAAm, acrylic acid, and 2-hydroxyethyl methacrylate were synthesized for the pulsatile delivery of streptokinase and

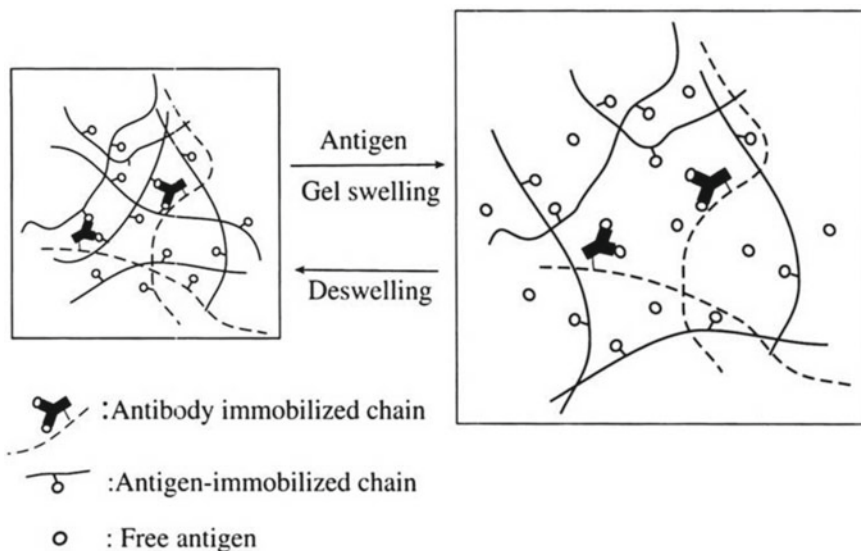


**Fig. 5** Swelling of an antigen–antibody-based semi-IPN hydrogel with the amount of free antigen

heparin based on the progressive pH and temperature variations (Vakkalanka et al. 1996; Brazel and Peppas 1996).

### **6.3 Specific Ion-Sensitive Hydrogels**

Salt concentration can affect the swelling behaviour of a few hydrogels. A nonionic poly (*N*-isopropylacrylamide) hydrogel showed a strident volume phase transition at a acute concentration of sodium chloride in aqueous solution. Below the LCST, the amount of water present in the hydrogel is dependent on the concentration of sodium chloride. The gel collapses suddenly at a critical concentration of sodium chloride which too is found to be dependent on the temperature. Rise in temperatures results into a equivalent drop in the critical concentration of sodium chloride.

A number of salts are tested, but none of them show such behaviour outside the salting-out region. However, sodium ions form the common part of all the salt taken under investigation, and hence, it is concluded that chloride ions perform a significant role in this phase transition. Although the mechanism of ion sensitivity is unknown, the LCST of the system was found to decrease on increasing the concentration of the chloride ions.

This exclusive phase transition behaviour could be applied for creating chloride ion-sensitive biosensors. The additional salts investigated for phase transition behaviour did not induce network collapse in the studied concentration range, and alternative theory known as ion pair and multiplet (ionomer effect) theory was suggested to clarify these interesting experimental outcomes.

### **6.4 Specific Antigen-Responsive Hydrogels**

For certain biomedical applications, it is essentially required being beneficial to cultivate a material or device, which generates response to particular proteins present in the biological system. One such device based on sol–gel phase-reversible hydrogels was prepared using antigen–antibody interactions which rely on the similar concept as used for glucose-sensitive phase-reversible hydrogels. A semi-interpenetrating network hydrogel was prepared by fixing an antigen and a corresponding antibody to dissimilar polymer grids. The spontaneous crosslinking interaction between antigen and antibody gives rise to a three-dimensional hydrogel network.

Hydrogel swelling is activated in the presence of free antigens that strive with the polymer-bound antigen, resulting in a reduction in the crosslinking density (Fig. 6).

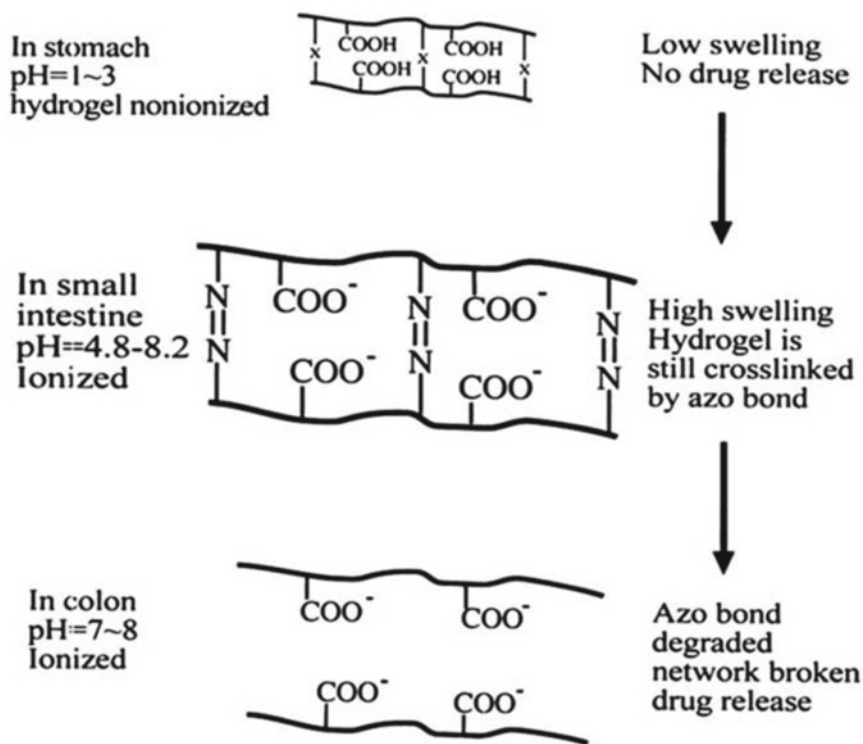


**Fig. 6** Representation of oral colon-specific drug delivery based on biodegradable and pH-sensitive hydrogels. The azoaromatic groups in the crosslinks are indicated by  $-N=N-$

## 7 Conclusion and Future Prospectives

Hydrogel-based drug delivery has emerged as a prospective drug delivery system owing to its distinctive characteristics, and a number of hydrogel-based patents are filed which are in different phase of clinical trials (Table 7). They are relatively biodegradable, elastic, flexible, soft, have minimum tendency to tissue adhesion, and possess high water content which makes them compatible to the living tissue, abolishing irritation to the tissue to which they are administered. However, the high water content of hydrogel results in poor mechanical strength which confers a major disadvantage for their use in drug delivery. Poor mechanical strength presents complexity in fabrication and administration and causes burst release with incomplete release of the active agent. To overcome the issue, hydrogel with improved mechanical strength is prepared through interpenetrating polymer network (IPN), but their synthesis requires the use of chemical crosslinkers which lead to toxicity following their degradation in body.



**Table 7** Few patents available on hydrogel

S.No.	Patent no	Patent name	Comment	Inventor/s
1.	EP 0 524 718 A1	hydrogels suitable for transdermal iontophoretic delivery of drugs	polyurethane hydrogel matrices, can be employed as passive transdermal reservoirs.	Hahn Soonkap
2.	US Patent 8,409,606 B2	a system that provided the release of specific drugs through punctal plugs.	soft biodegradable covalently crosslinked hydrogels, high-swelling capability, remain in situ (in the punctum or lacrimal canal) with greater comfort for the patient.	Amarpreet S. Sawhney, Peter Jarrett, Michael Bassett, Charles Blizzard
4.	US Patent 5,514,380	Biodegradable hydrogel copolymer as drug delivery matrix	Synthesized from a hydrophilic soft block and a hydrophobic, biodegradable hard block.	Soo S. Song, Ho H. Kim, Yil W. Yi
5.	US Patent 8,383,153 B2	Poly(amidoamine) oligomer hydrogel for drug delivery and drug carrier using the same	temperature- and pH-sensitive hydrogel, avoid the initial burst drug release and was instead capable of providing a sustained release.	Doo Sung Lee, Bong Sup KIM, Minh Khanh Nguyen
6.	US Patent 7,066,904 B2.	Triggered release hydrogel drug delivery system	triggering release of a drug from a hydrogel polymer to tissue at a desired location of the body using a catheter, catheter allows the inclusion and the immobilisation of a significant quantity of drug into the hydrogel, which is released by a triggering agent or under different condition in the desired location.	Arthur Rosenthal, James J. Barry, Ronald Sahatjian
7.	US Patent application WO1998043615 A1	Method for oral delivery of proteinsA hydrogel matrix	made of poly (methacrylic acid-g-ethylene glycol) cross-linked with tetraethylene glycol dimethacrylate for oral delivery of different active ingredients, e.g. non-steroidal anti-inflammatory drugs (NSAIDs) pH-sensitive swelling behavior	Nicholas A. Peppas, Anthony M. Lowman, Tsuneji Nagai, Mariko Moris

(continued)

**Table 7** (continued)

S.No.	Patent no	Patent name	Comment	Inventor/s
8.	US 20070122362 A1	Hydrogel sheets and shapes for oral care	Can be modified to afford a denture fixative or can be laden with a whitening agent or other loading materials for treatment of alveolitis or malodor, inter alia.	Martin Giniger, Matthew Spaid
9.	US 20150017105 A1	Anhydrous hydrogel composition and delivery system	mucoadhesive (oral compositions) or as topical agents, can be used deliver an active agent such as active pharmaceutical agents (API's), coagulants, fragrances, flavors, and other actives and excipients.	John Borja
10.	US 20020019369 A1	Injectable drug delivery systems with cyclodextrin-polymer based hydrogels	the composition may be injected subcutaneously, intramuscularly, intradermally, or intracranially.	Jun Li, Hanry Yu, Kam Leong
11.	US 20150366975 A1	Thermosensitive injectable hydrogel for drug delivery	Thermosensitive injectable hydrogel based on HA and a copolymer of polyethylene oxide (PEO) and polypropylene oxide (PPO), having a gel formation temperature from 30.degree. C. to 37.degree. C.	Hua-Jing Ho, Hsiu-O Sheu, Ming-Thau Shen, Shing Chuan Ho, Yuan Soon, Liu Jun-Jen
12.	WO 2001087276 A1	Hydrogel composition for transdermal drug delivery containing acrylate polymers like acrylic acid polymer, methacrylic acid polymer, alkyl acrylate polymer, alkyl methacrylate polymer or copolymers	enable both hydrophilic and lipophilic permeation enhancers to be applicable in the hydrogel composition in order to effectively control skin penetration of drugs.	Ho Chin Kim, Hye Jeong Yoon

(continued)

**Table 7** (continued)

S.No.	Patent no	Patent name	Comment	Inventor/s
13.	US 8409606 B2	Drug delivery through hydrogel plugs	a punctal plug comprising a Dehydrated covalently crosslinked synthetic hydrophilic polymer dehydrated hydrogel having dimensions to pass through a puncta lacrimali which absorb physiological water to swell to at least 1 mm in cross-sectional width to conformably fit a canaliculus, therapeutic agent dispersed through the hydrogel for sustained release through the proximal face to the tear film of the eye in an effective amount over a period of at least about seven days	Amarpreet S. Sawhney, Peter Jarrett, Michael Bassett, Charles Blizzard

Therefore, there is a need to form hydrogels with such gelators capable of providing ease of administration and have precise gelation temperature to provide smooth injectability evading gelation in the syringe. Furthermore, strategies are needed to be developed to form covalently crosslinked hydrogel without toxic crosslinkers or with biodegradable crosslinkers which are still to be explored.

There is also a need to develop hydrogels which vary in drug release kinetics. Such hydrogels will expand the area of application based on the release profile desired or required for both drug delivery and tissue application. Hydrogels can also be modulated to follow diverse degradation profile so as to meet the kinetic issues. The stimuli-responsive hydrogel system offers an approach where the rate of drug release can be modulated on off overtime so that hydrogel can be used in conditions where varying doses of drug are required over the time (e.g. delivery of insulin). There is also a need for improvement in hydrogel for the delivery of hydrophobic drugs as well as susceptible molecules like proteins, antibodies, or nucleic acids. The method of synthesis applied for in situ crosslinking the hydrogels (thermal, physically gelling polymers, or the functional group chemistry) may affect the biological properties of entrapped drug molecules. Therefore, an effective method for pre-encapsulation or complexation of these bioactive before the in situ gel formation is needed to be developed to solve this issue.

Although a number of interesting physical and chemical methods are presently known, there is certainly a need for other methods. It is expected that principles from the expanding research area of supramolecular chemistry will be applied to design novel type of hydrogels with tailored properties which can preferably be prepared in an aqueous environment. Also, protein engineering might contribute to the development of hydrogel systems with a very precise control over their microstructure and thus their properties. Finally, it can be foreseen that systems in which gel formation is induced by a specific trigger (temperature, pH, or a specific compound) will be developed precisely for application in pharmaceutical and biomedical purposes.

## References

- Ahmed EM (2015) Hydrogel: preparation, characterization, and applications: a review. *J Adv Res* 6:105–121
- Alsarra IA, Hamed AY, Mahrous GM, El Maghraby GM, Al-Robayan AA, Alanazi FK (2009) Mucoadhesive polymeric hydrogels for nasal delivery of acyclovir. *Drug Dev Ind Pharm* 35 (3):352–362
- Amin MCIM (2012) Synthesis and characterization of thermo and pH-responsive bacterial cellulose/acrylic acid hydrogels for drug delivery. *Carbohydr Polym* 88:465–473
- Anderson JM, Langone JJ (1999) Issues and perspectives on the biocompatibility and immunotoxicity evaluation of implanted controlled release systems. *J Control Rel* 57:107–113
- Anumolu SNS, DeSantis AS, Menjoge AR, Hahn RA, Beloni JA, Gordon MK, Sinko PJ (2010) Doxycycline loaded poly(ethylene glycol) hydrogels for healing vesicant-induced ocular wounds. *Biomaterials* 31(5):964–974
- Bai XY, Yan Y, Wang L, Zhao LG, Wang K (2016) Novel pH-sensitive hydrogels for 5-aminosalicylic acid colon targeting delivery: in vivo study with ulcerative colitis targeting therapy in mice. *Drug Deliv* 23(6):1926–1932
- Bajpai AK, Shrivastava J (2005) In vitro enzymatic degradation kinetics of polymeric blends of crosslinked starch and carboxymethyl cellulose. *Polym Int* 54(11):1524–1536
- Bos GW, Jacobs JLL, Koten JW, Van Tomme S, Veldhuis T, van Nostrum CF (2004) In situ crosslinked biodegradable hydrogels loaded with IL-2 are effective tools for local IL-2 therapy. *Eur J Pharm Sci* 21(4):561–567
- Brazel CS, Peppas NA (1996) Pulsatile local delivery of thrombolytic and antithrombotic agents using poly(N-isopropylacrylamide-co-methacrylic acid) hydrogels. *J Control Rel* 39:57–64
- Bromberg LE, Ron ES (1998) Temperature-responsive gels and thermogelling polymer matrices for protein and peptide delivery. *Adv Drug Deliv Rev* 31:197–221
- Cai S, Suo Z (2011) Mechanics and chemical thermodynamics of phase transition in temperature-sensitive hydrogels. *J Mech Phys Solid* 59:2259–2278
- Caliceti P, Salmaso S, Lante A, Yoshida M, Katakai R, Martellini F, Mei LHI, Carenza M (2001) Controlled release of biomolecules from temperature-sensitive hydrogels prepared by radiation polymerization. *J Control Release* 75:173–181
- Calixto G, Yoshii AC, Rocha e Silva H, Stringhetti Ferreira Cury B, Chorilli M (2015) Polyacrylic acid polymers hydrogels intended to topical drug delivery: preparation and characterization. *Pharm Dev Technol* 20(4):490–496
- Chan Y-P, Meyrueix R, Rivail C, Chatellier J (2011) Medusa: an innovative formulation. Approach to improve pharmacokinetic & safety profiles of biotherapeutics, [www.ondrugdelivery.com](http://www.ondrugdelivery.com), pp 4–6

- Chauhan S, Harikumar SL, Kanupriya (2012) Hydrogels: a smart drug delivery system. *IJRPC* 2(3):603–614
- Chen P (2005) Physicochemical and engineering aspects. *Colloids Surf A* 257–258:1–554
- Cheng X, Jinc Y, Suna T, Qia R, Lic H (2016a) An injectable, dual pH and oxidation-responsive supramolecular hydrogel for controlled dual drug delivery. *Colloid Surf B* 141:44–52
- Cheng Y-H, Tung-Hu Tsa, Jhan Y-Y, Chiu AW-H, Tsai K-L, Chien C-S, Chiou S-H, Liu CJL (2016b) Thermosensitive chitosan-based hydrogel as a topical ocular drug delivery system of latanoprost for glaucoma treatment. *Carbohydr Polym* 144:390–399
- Chun SW, Kim JD (1996) A novel hydrogel-dispersed composite membrane of poly (N-isopropylacrylamide) in a gelatin matrix and its thermally actuated permeation of 4-acetamidophen. *J Control Release* 38:39–47
- Das A, Wadhwa S, Srivastava AK (2006) Cross-linked guar gum hydrogels discs for colon-specific delivery of ibuprofen, formulation and in-vitro evaluation. *Drug Del* 13:139–142
- Das D, Das R, Ghosh P, Dhara S, Panda AB, Pal S (2013) Dextrin cross linked with poly(HEMA): a novel hydrogel for colon specific delivery of ornidazole. *RSC Adv* 3:25340–25350
- De Groot CJ, Van Luyn MJA, Van Dijk-Woltheris WNE, Cadee JA, Plantinga JA, Otter WD, Hennink WE (2001) In vitro biocompatibility of biodegradable dextran-based hydrogels tested with human fibroblasts. *Biomaterials* 22:1197–1203
- de Nooy AEJ, Capitani D, Masci G, Crescenzi V (2000) Ionic polysaccharide hydrogels via the Passerini and Ugi multicomponent condensations: synthesis, behavior and solid-state NMR characterization. *Biomacromolecules* 1:259–267
- Deo N, Ruetsch S, Ramaprasad K, Kamath Y (2010) Stable environmentally sensitive cationic hydrogels for controlled delivery applications. *J Cosmet Sci* 61:421
- Dinarvand RD, Emanuele A (1995) Use of thermoresponsive hydrogels for on-off release of molecules. *J Control Release* 36:221–227
- Dolman MEM, Harmsen S, Storm G, Hennink WE, Kok RJ (2010) Drug targeting to the kidney: advances in the active targeting of therapeutics to proximal tubular cells. *Adv Drug Deliv Rev* 62:1344–1357
- Eagland D, Crowther NJ, Butler CJ (1994) Complexation between polyoxyethylene and polymethacrylic acid—the importance of the molar mass of polyoxyethylene. *Eur Polym J* 30:767–773
- Enas M, Awad AM, Ahmed MA (2008) Development of a multicomponent fertilizing hydrogel with relevant techno-economic indicators. *Am-Euras J Agric Environ Sci* 3(5):764–770
- Fei L, Jinlin H, Mingzu Z, Kam CT, Peihong N (2015) Injectable supramolecular hydrogels fabricated from PEGylated doxorubicin prodrug and  $\alpha$ -cyclodextrin for pH-triggered drug delivery. *RSC Adv* 5:54658–54666
- Fu C, Lin X, Wang J, Zheng X, Li X, Lin Z, Lin G (2016) Injectable micellar supramolecular hydrogel for delivery of hydrophobic anticancer drugs. *J Mater Sci Mater Med* 27(4):735682–735689
- Funami T, Hiroe M, Noda S, Asai I, Ikeda S, Nishimari K (2007) Influence of molecular structure imaged with atomic force microscopy on the rheological behavior of carrageenan aqueous systems in the presence or absence of cations. *Food Hydrocolloids* 21:617–629
- Gacesa P (1988) Alginates. *Carbohydr Polym* 8:161–182
- Ganji F, Farahan EV (2009) Hydrogels in controlled drug delivery systems Iranian. *Polym J* 18(1): 63–88
- Gaoa Y, Sunb Y, Renc F, Shen Gao (2010) PLGA–PEG–PLGA hydrogel for ocular drug delivery of dexamethasone acetate. *Drug Dev Ind Pharm* 30(10):1131–1138
- Goosen MFA, O'Shea GM, Gharapetian HM, Chou S, Sun AM (1985) Optimization of microencapsulation parameters: semipermeable microcapsules as a bioartificial pancreas. *Biotechnol Bioeng* 27:146–150
- Gupta D, Tator CH, Shoichet MS (2006) Fast-gelling injectable blend of hyaluronan and methylcellulose for intrathecal, localized delivery to the injured spinal cord. *Biomaterials* 27(11):2370–2379

- Gutowska A, Bark JS, Kwon IC, Bae YH, Kim SW (1997) Squeezing hydrogels for controlled oral drug delivery. *J Control Release* 48:141–148
- Hassan CM, Peppas NA (2000) Structure and morphology of freeze/thawed PVA hydrogels. *Macromolecules* 33:2472–2479
- Hennink WE, De Jong SJ, Bos GW, Veldhuis TFJ, van Nostrum CF (2004) Biodegradable dextran hydrogels crosslinked by stereocomplex formation for the controlled release of pharmaceutical proteins. *Int J Pharm* 277(1–2):99–104
- Hiemstra C, Zhong ZY, Li LB, Dijkstra PJ, Jan FJ (2006) In-situ formation of biodegradable hydrogels by stereocomplexation of PEG-(PLLA) and PEG-(PDLA) star block copolymers. *Biomacromolecules* 7(10):2790–2795
- Hoare TR, Kohane DS (2008) Hydrogels in drug delivery: progress and challenges. *Polymer* 49:1993–2007
- Hoffman AS (2002) Hydrogels for biomedical applications. *Adv Drug Deliv Rev* 43:3–12
- Hunkeler D (1992) Synthesis and characterization of high molecular weight water-soluble polymers. *Polym Int* 27:23–33
- Ichikawa H, Fukumori Y (2000) Novel positively thermosensitive controlled-release microcapsule with membrane of nano-sized poly(N-isopropylacrylamide) gel dispersed in ethylcellulose matrix. *J Control Release* 63:107–119
- Iizawa T, Taketa H, Maruta M, Ishido T, Gotoh T, Sakohara S (2007) Synthesis of porous poly (N-isopropylacrylamide) gel beads by sedimentation polymerization and their morphology. *J Appl Polym Sci* 104:842–850
- Janes KA, Fresneau MP, Marazuela A, Fabra A, Alonso MJ (2001) Chitosan nanoparticles as delivery systems for doxorubicin. *J Control Release* 73:255–267
- Jeong B, Choi YK, Bae YH, Zentner G, Kim SW (1999) New biodegradable polymers for injectable drug delivery systems. *J Control Release* 62:109–114
- Jeong B, Bae YH, Kim SW (2000) Drug release from biodegradable injectable thermosensitive hydrogel of PEG–PLGA–PEG triblock copolymers. *J Control Release* 63:155–163
- Jhan MS, Andrade JD (1973) Water and hydrogels. *J Biomed Mater Res* 7(6):509–522
- Katono H, Maruyama A, Sanui K, Okano T, Sakurai Y (1991) Thermo-responsive swelling and drug release switching of interpenetrating polymer networks composed of poly(acrylamide-co-butyl methacrylate) and poly(acrylic acid). *J Control Release* 16:215–227
- Kesavan K, Kant S, Pandit JK (2015) Therapeutic effectiveness in the treatment of experimental bacterial keratitis with ion-activated mucoadhesive hydrogel. *Ocul Immunol Inflamm* 19:1–4
- Khare AR, Peppas NA (1993) Release behavior of bioactive agents from pH-sensitive hydrogels. *J Biomater Sci Polym* 4:275–289
- Khare AR, Peppas NA (1995) Swelling/deswelling of anionic copolymers gels. *Biomaterials* 16:559–567
- Klouda L, Mikos AG (2008) Thermoresponsive hydrogels in biomedical applications—a review. *Eur J Pharm Biopharm* 68(1):34–45
- Kubinova S, Horak D, Kozubenko N, Vanecek V, Proks V, Price J (2010) The use of superporous Ac-CGGASIKVAVS-OH-modified PHEMA scaffolds to promote cell adhesion and the differentiation of human fetal neural precursors. *Biomaterials* 31:5966–5975
- Kuijpers AJ, van Wachum PB, van Luyn MJA, Engbers GHM, Krijgsveld J, Zaat SAJ, Dankert J, Feijen J (2000) In vivo and in vitro release of lysozyme from crosslinked gelatin hydrogels: a model system for the delivery of antibacterial proteins from prosthetic heart valves. *J Control Release* 67:323–336
- Leda K (2015) Thermoresponsive hydrogels in biomedical applications: a seven-year update. *Eur J Pharmac Biopharma* 97(B):338–349
- Lim DW, Park TG (2000) Stereocomplex formation between enantiomeric PLA–PEG–PLA triblock copolymers: characterization and use as protein delivery microparticulate carriers. *J Appl Polym Sci* 75:1615–1623
- Lim DW, Nettles DL, Setton LA, Chilkoti A (2007) Rapid cross-linking of elastin-like polypeptides with (hydroxymethyl)phosphines in aqueous solution. *Biomacromol* 8(5):1463–1470

- Limón D, Amirthalingam E, Rodrigues M, Halbaut L, Andrade B, Garduño-Ramírez ML, Amabilino DB, Pérez-García L, Calpena AC (2015) Novel nanostructured supramolecular hydrogels for the topical delivery of anionic drugs. *Eur J Pharm Biopharm* 96:421–436
- Liu JH, Lin SQ, Li L, Liu E (2005) Release of theophylline from polymer blend hydrogels. *Int J Pharm* 298(1):117–125
- Mansur HS, Orefice RL, Mansur AAP (2004) Characterization of poly(vinyl alcohol)/poly(ethylene glycol) hydrogels and PVA-derived hybrids by small-angle X-ray scattering and FTIR spectroscopy. *Polymer* 45:7193–7202
- Mehvar R (2000) Dextran for the targeted and sustained delivery of therapeutic and imaging agents. *J Controlled Release* 69:1–25
- Minhas M, Ahmad M, Ali L, Sohail M (2013) Synthesis of chemically cross-linked polyvinyl alcohol-co-poly (methacrylic acid) hydrogels by copolymerization; a potential graft-polymeric carrier for oral delivery of 5-fluorouracil. *DARU J Pharm Sci* 21:44
- Misra GP, Singh RS, Aleman TS, Jacobson SG, Gardner TW, Lowe TL (2009) Subconjunctivally implantable hydrogels with degradable and thermoresponsive properties for sustained release of insulin to the retina. *Biomaterials* 30(33):6541–6547
- Mocanu G, Mihaï D, Dulong V, Picton L, Le Cerf D (2012) New anionic crosslinked multi-responsive pullulan hydrogels. *Carbohydr Polym* 87:1440–1446
- Mohamadnia Z, Zohuriaan-Mehr MJ, Kabiri K, Jamshidi A, Mobedi H (2007) pH-sensitive IPN hydrogel beads of carrageenan-alginate for controlled drug delivery. *J Bioact Compat Polym* 22:342–356
- Okuyama Y, Yoshida R, Sakai K, Okano T, Sakurai Y (1993) Swelling controlled zero order and sigmoidal drug release from thermo-responsive poly(N-isopropylacrylamide-co-butyl methacrylate) hydrogel. *J Biomater Sci Polym* 4:545–556
- Owens DE, Jian Y, Fang JE, Slaughter BV, Chen Y-H, Peppas NA (2007) Thermally responsive swelling properties of polyacrylamide/poly(acrylic acid) interpenetrating polymer network nanoparticles. *Macromolecules* 40(20):7306–7310
- Patel VR, Amiji MM (1996) Preparation and characterization of freeze-dried chitosan–poly(ethylene oxide) hydrogels for site-specific antibiotic delivery in the stomach. *Pharm Res* 13:588–593
- Peppas NA, Mikos AG (1986) Preparation methods and structure of hydrogels. In: Peppas NA (ed) *Hydrogels in medicine and pharmacy*, vol I. CRC Press, Boca Raton
- Percec V, Bera TK, Butera RJ (2002) A new strategy for the preparation of supramolecular neutral hydrogels. *Biomacromolecules* 23:272–279
- Qiu Y, Park K (2012) Poly(ethylene oxide) (PEO) and poly(propylene oxide) (PPO) Pluronics® (or Poloxamers®) and Tetronics® environment-sensitive hydrogels for drug delivery. *Adv Drug Deliv Rev* 64:49–60
- Rowley J, Madlambayan G, Faulkner J, Mooney DJ (1999) Alginate hydrogels as synthetic extracellular matrix materials. *Biomaterials* 20:45–53
- Ruixin L, Chang S, Wei W, Xiaoliang W, Hui L, Danke X, Wenying Z (2015) Encapsulation of 10-hydroxy camptothecin in supramolecular hydrogel as an injectable drug delivery system. *J Pharm Sci* 104(7):2266–2275
- Saboktakin RM, Tabatabaei RM (2015) Supramolecular hydrogels as drug delivery systems. *Int J Biol Macromol* 75:426–436
- Sahu NK, Gils PS, Ray D, Sahoo PK (2012) Hydrogels: *Rev Adv Polym Sci Tech: Int J* 2(4): 43–50
- Said HM, Alla SGA, El-Naggar AWM (2004) Synthesis and characterization of novel gels based on carboxymethyl cellulose/acrylic acid prepared by electron beam irradiation. *React Funct Polym* 61:397–404
- Schild HG (1992) Poly(N-isopropylacrylamide): experiment, theory and application. *Prog Polym Sci* 17:163–249
- Schuetz YB, Gurny R, Jordan O (2008) A novel thermoresponsive hydrogel of chitosan. *Eur J pharmBiopharm* 68:19–25

- Shin B-K, Baek EJ, Choi SG, Davaaa E, Nhoc Y-C, Limc Y-M, Parkc J-S, Huh KM, Park J-S (2013) Preparation and irradiation of Pluronic F127-based thermoreversible and mucoadhesive hydrogel for local delivery of naproxen. *Drug Dev Ind Pharm* 39(12):1874–1880
- Siegel RA, Falamarzian M, Firestone BA, Moxley BC (1998) pH-controlled release from hydrophobic/polyelectrolyte copolymer hydrogels. *J Control Release* 8:179–182
- Smetana K (1993) Cell biology of hydrogels. *Biomaterials* 14:1046–1050
- Starodoubtsev SG, Khokhlov AR, Sokolov EL, Chu B (1995) Evidence for polyelectrolyte/ionomer behavior in the collapse of polycationic gels. *Macromolecules* 28:3930–3936
- Stringer JL, Peppas NA (1996) Diffusion in radiationcrosslinked poly(ethyleneoxide) hydrogels. *J Control Release* 42:195–202
- Suda K (2007) Superabsorbent polymers and superabsorbent polymer composites. *Sci Asia* 33(Suppl):139–143
- Szepes A, Makai Z, Blumer C, Mader K, Kasa P, Revesz PS (2008) Characterization and drug delivery behaviour of starch based hydrogels prepared via isostatic ultrahigh pressure. *Carbohyd Polym* 72:571–575
- Takashima Y, Yuting Y, Otsubo M, Yamaguchi M, Harada A, Beilstein (2012) *J Org Chem* 8:1594–1600
- Takigami M, Amada H, Nagasawa N, Yagi T, Kasahara T, Takigami S, Tamada M (2007) Preparation and properties of CMC gel. *Trans Mater Res Soc Jpn* 32(32):713–716
- Tan HL, Tan LS, Wong YY, Muniyandy S, Hashim K, Pushpamalar J (2016) Dual crosslinked carboxymethyl pulp/pectin hydrogel beads as potential carrier for colon-targeted drug delivery. *J Appl Polym Sci* 133(19)
- Telitel S, Dumur F, Faury T, Graff B, Tehfe M-A, Gigmès D, Fouassier J-P, Lalevée J (2013) New core-pyrene  $\pi$  structure organophotocatalysts usable as highly efficient photoinitiators. *Beilstein J Org Chem* 9:877–890
- Tong Q, Zhang G (2005) Rapid synthesis of a superabsorbent from a saponified starch and acrylonitrile/AMPS graft copolymers. *Carbohyd Polym* 62:74–79
- Toshikazu T, Hisahiko K, Kenji U, Toshiro M (1992) Structure and mechanical properties of poly(vinyl alcohol) gels swollen by various solvents. *Polymer* 33(11):2334–2339
- Vakkalanka SK, Brazel CS, Peppas NA (1996) Temperature- and pH-sensitive terpolymers for modulated delivery of streptokinase. *J Biomater Sci Polym* 8:119–129
- Van Tomme SR, van Steenberghe MJ, De Smedt SC, van Nostrum CF, Hennink WE (2005) *Biomaterials* 26(14):2129–2135
- Vemula PK, Li J, George J, Am J (2006) *Chem Soc* 128:8932–8938
- Wang C, Stewart RJ, Kopecek J (1999) Hybrid hydrogels assembled from synthetic polymers and coiled-coil protein domains. *Nature* 397:417–420
- Watanabe N, Hosoya Y, Tamura A, Kosuge H (1993) Characteristics of water-absorbent polymer emulsions. *Polym Int* 30:525–531
- Watanabe T, Ohtsuka A, Murase N, Barth P, Gersonde K (1996) NMR studies on water and polymer diffusion in dextran gels. Influence of potassium ions on microstructure formation and gelation mechanism. *Magn Reson Med* 35:697–705
- Wichterle O, Lim D (1960) Hydrophilic gels for biological use. *Nature* 185:117–118
- Wu J, Su ZG, Ma GH (2006) A thermo- and pH-sensitive hydrogel composed of quaternized chitosan/glycerophosphate. *Int J Pharm* 315(1–2):1–11
- Wu X, He C, Wu Y, Chen X (2016) Synergistic therapeutic effects of Schiff's base cross-linked injectable hydrogels for local co-delivery of metformin and 5-fluorouracil in a mouse colon carcinoma model. *Biomaterials* 75:148–162
- Xu X, Weng Y, Xu L, Chen H (2013) Sustained release of avastin<sup>®</sup> from polysaccharides cross-linked hydrogels for ocular drug delivery. *Macromolecules* 60:272–276
- Yin Y, Yang Y, Xu H (2002) Swelling behavior of hydrogels for colon-site drug delivery. *J Appl Polym Sci* 83:2835–2842
- Yin Y, Ji X, Dang H, Ying Y, Zhing H (2008) Study of the swelling dynamics with overshooting effect of hydrogels based on sodium alginate-g-acylic acid. *Carbohyd Polym* 71:682–689



- Yokoyama F, Masada I, Shimamura K, Ikawa T, Monobe K (1986) Morphology and structure of highly elastic poly-(vinyl alcohol) hydrogel prepared by repeated freezing-and-melting. *Colloid Polym Sci* 264
- Yoshida M, Asano M, Kumakura M, Katakai R, Mashimo T, Yuasa H, Yamanaka H (1991) Thermo-responsive hydrogels based on acryloyl-L-proline methyl ester and their use as long-acting testosterone delivery systems. *Drug Des Deliv* 7:159–174
- Yu H, Xiao C (2008) Synthesis and properties of novel hydrogels from oxidized Konjac glucomannan cross linked gelation for in-vitro drug delivery. *Carbohydr Polym* 72:479–489
- Zhang JT, Bhat R, Jandt KD (2009) Temperature-sensitive PVA/PNIPAAm semi-IPN hydrogels with enhanced responsive properties. *Acta Biomater* 5(1):488–497
- Zhang Z, He Z, Liang R, Ma Y, Huang W, Jiang R, Shi S, Chen H, Li X (2016) Fabrication of a micellar supramolecular hydrogel for ocular drug delivery. *Biomacromolecules* 17(3):798–807
- Zheng X, Li X, Lin Z, Lin G (2016) Injectable micellar supramolecular hydrogel for delivery of hydrophobic anticancer drugs. *J Mater Sci Mater Med* 27(4):73
- Zu Y, Zhang Y, Zhao X, Shan C, Zu S, Wang K, Li Y, Ge Y (2012) Preparation and characterization of chitosan-polyvinyl alcohol blend hydrogels for the controlled release of nano-insulin. *Int J Biol Macromol* 50(1):82–87

# Chapter 7

## Gel-Based Approaches in Genomic and Proteomic Sciences



Rafael A. Baraúna, Diego A. Graças, Joriane T. C. Alves,  
Ana Lídia Q. Cavalcante and Artur Silva

### 1 Introduction

Genomics is defined as the study of the structure and function of the genome. The word genomics was created by the geneticist Thomas H. Roderick in 1986 to name a new scientific journal that aimed to publish works on DNA sequencing, mapping, and other DNA analysis technologies (Kuska 1998). Conceptually, genomics was the first omics technology to emerge in scientific publications. Due to the rapid technological development, in the subsequent decades, several omics technologies were created, such as transcriptomics, proteomics, and metabolomics.

The first non-viral genome to be completely sequenced was that of the bacterium *Haemophilus influenzae* Rd (Fleischmann et al. 1995). Its genome is comprised of one chromosome that is 1.8 mpb in size. The small size of the genome favored their sequencing using the Sanger technology available at that time. In 2004, with the emergence of the 454 sequencing platform from Roche, the DNA sequencing workflow that previously required months of hard work could now be completed in a few days. Since then, several other specific analyses have been developed and

---

R. A. Baraúna (✉) · D. A. Graças · J. T. C. Alves · A. L. Q. Cavalcante · A. Silva  
Institute of Biological Sciences, Center of Genomics and Systems Biology,  
Laboratory of Genomics and Bioinformatics, Federal University of Pará, Belém, Brazil  
e-mail: rabarauna@ufpa.br

D. A. Graças  
e-mail: diego.a87@gmail.com

J. T. C. Alves  
e-mail: joriannealves@gmail.com

A. L. Q. Cavalcante  
e-mail: analidiabio2011@gmail.com

A. Silva  
e-mail: asilva@ufpa.br

have gained notoriety in the field of genomics, such as the description of functional genes and pseudogenes, the determination of GC content, and the identification of transposons, plasmids, and repetitive regions, among other analyses.

Thus, the field of genomics has become divided into: structural genomics, which aims to clarify the structural characteristics of the genome by determining synteny rates and genome rearrangements among other analyses; functional genomics, which aims to provide a functional description of open reading frames (ORFs) and coding sequences (CDSs) detected in the genome; and comparative genomics, which aims to compare the structural and functional characteristics described above between genomes from different taxonomic levels.

According to the central dogma of molecular biology postulated by Francis Crick in 1970 (Crick 1970), proteins are the final products of gene expression. They have important functional activities in living organisms and are highly abundant in cells. The term proteome was first used by Wilkins et al. (1995) to describe the set of proteins expressed by a genome. As with the field of genomics, the field of proteomics has grown, being applied to studies of post-translational modifications, protein–protein or protein–DNA interactions, and the characterization of alternative splice products, among other analyses. In contrast to the genome, the proteome of an organism is extremely variable. It responds to environmental modifications or to endogenous gene regulation.

Over decades of basic and applied research, gel-based molecular approaches have been used in the fields of genomics and proteomics. Two such techniques are constantly being updated to produce more accurate and reproducible results and, thus, are still being used in current studies. Pulsed-field gel electrophoresis (PFGE) and two-dimensional gel electrophoresis (2DE) are fractionation molecular techniques with broad applications. PFGE has been used to determine the size of prokaryotic genomes, for the detection of plasmids, and in epidemiological studies of pathogenic microorganisms (Folster et al. 2012; Bengtsson et al. 2012), while 2DE has been used to analyze the differential expression of genes and to characterize post-translational modifications (Morimoto et al. 2013).

Basically, in these gel-based techniques, molecules are fractionated according to their physicochemical characteristics such as molecular weight (MW) or isoelectric point (pI). In the following sections, we will describe and discuss the functionality and applications of 2DE and PFGE, two old techniques with modern applications that are commonly used in the fields of genomics and proteomics.

## 2 Gel-Based Molecular Approaches

### 2.1 Two-Dimensional Gel Electrophoresis (2DE)

Two-dimensional gel electrophoresis was one of the first techniques to analyze a high number of proteins in one single experiment. In 1975, Patrick H. O'Farrell published the proteome of the model microorganism *Escherichia coli* in a

two-dimensional polyacrylamide gel. For many researchers, this work marked the birth of proteomics (O'Farrell 1975). In subsequent years, a number of technical improvements have allowed the use and dissemination of 2DE in the field of cell physiology. The creation of polyacrylamide gel strips with an immobilized pH gradient for use in the first dimension and the use of the fluorescent markers Cy2, Cy3, and Cy5 are examples of advances that have improved the technique.

Proteins are highly complex molecules with at least three important physico-chemical properties: the isoelectric point (pI), the quaternary structure, and the molecular weight (MW). In each step of 2DE, these three characteristics are taken into account to perform the fractionation experiment. An overview of 2DE with the respective events that occur in each step of the technique is shown in Fig. 1.

In general, 2DE is performed in three steps: an initial chemical treatment and an isoelectric focusing (IEF) followed by separation with denaturing polyacrylamide gel electrophoresis (SDS-PAGE). The chemical treatment preserves the primary structure of the extracted proteins and generally involves the use of urea, CHAPS (3-[(3-cholamidopropyl)dimethylammonio]-1-propanesulfonate), and DTT ((2*S*,3*S*)-1,4-bis(sulfanyl)butane-2,3-diol). Urea is a neutral chaotropic agent used to denature and solubilize proteins. CHAPS is a zwitterionic detergent that ensures complete

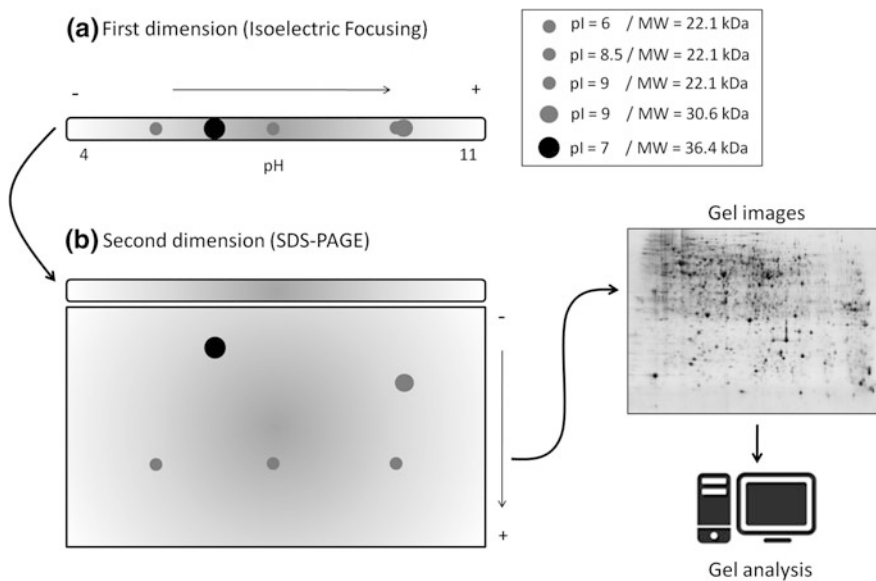


**Fig. 1** Schematic representation of the steps of two-dimensional gel electrophoresis. Proteins are represented by circles of different sizes according to their MW. The hypothetical values of pI and MW for each protein are described inside the box. **a** In the first dimension, proteins are separated according to their pI. The represented gel strip has a pH ranging from 4 up to 11. **b** In the second dimension, proteins are separated according to their molecular mass. High molecular weight proteins are retained at the top of the gel. Subsequently, the gels are scanned and analyzed with bioinformatics software

sample solubilization and prevents protein aggregation through hydrophobic interactions. DTT is a reducing agent that breaks any disulfide bonds present in the molecule, thereby maintaining all proteins in their fully reduced state. At the end of the first step, all proteins are solubilized in their primary structure, so the differential quaternary structures are no longer a problem for the fractionation process.

In the second step, the solubilized proteins are applied to a gel strip with an immobilized pH gradient. These strips can have broad or narrow pH ranges. When an electric field is applied to the strip, the proteins tend to migrate to the pH value corresponding to their pI. The isoelectric point is defined as the pH value where the net charge of the protein is zero. This phenomenon occurs because the proteins are zwitterionic molecules that change their net charge depending on the environmental value of pH. At the end of the first dimension, the proteins are fractionated according to their pI values (Fig. 1).

After IEF, a step of gel equilibration must be performed. The strips containing the proteins are treated again with the reducing agent DTT and with the alkylating agent iodoacetamide. A third component of the equilibration buffer plays an important role in the process. Sodium dodecyl sulfate (SDS) is an anionic surfactant that binds to the proteins forming negatively charged complexes. This negative charge allows the proteins to migrate toward the anode in the second dimension. If the strips were not equilibrated with SDS, it would be difficult for the proteins to migrate under an electric field through the second dimension because their charge in the strip is zero after isoelectric focusing. Finally, the fractionated proteins trapped in the gel of the first dimension must pass in the same position for the gel of the second dimension, in which they will be separated according to their molecular weights. To perform this task, the first dimension strip is placed in contact with the polyacrylamide gel of the second dimension and sealed with 1% agarose. Once the procedure is complete, the proteins of an organism or group of organisms are chemically treated and separated according to their pI (first dimension) and MW (second dimension) to generate a map of proteins that corresponds to the proteome of the biological sample (Fig. 1). Each spot visualized in the gel after staining is considered to be a protein or a variation of a protein.

In both the first and second dimensions, polyacrylamide gels are used to separate the molecules. This gel is formed by the chemical copolymerization of acrylamide monomers with bisacrylamide (*N,N'*-methylenebisacrylamide) in the presence of ammonium persulfate (APS) and tetramethylethylenediamine (TEMED). TEMED catalyzes the formation of APS free radicals, which, in turn, initiates and accelerates the polymerization reaction between the acrylamide and bisacrylamide to form the gel matrix.

The polymerized gel can physically withstand the separation of molecules. Different gel pore sizes can be achieved, depending on the concentration of the monomers of acrylamide and bisacrylamide. The pore dimensions are estimated from 0.5 up to 500 nm. The higher the monomer concentration, the smaller the pore size. Commonly, acrylamide gels may be prepared in concentrations ranging from 3 to 30%. The polyacrylamide matrix is commonly used because it is chemically inert

and is easily stained with silver nitrate or Coomassie Blue, in addition to generating high resolution due to the small pore sizes.

## ***2.2 Two-Dimensional Differential Gel Electrophoresis (2D-DIGE)***

In the method described above, each two-dimensional gel is loaded with one sample, which means that, to compare two different physicochemical states of an organism in triplicate, it is necessary to run six gels. The problem is that the greater the number of analyzed gels, the greater the bias created due to manipulation in the process of the benchtop analysis. To minimize this bias and increase the resolution of the analysis, two-dimensional differential gel electrophoresis (2D-DIGE) was developed (Marouga et al. 2005). In this method, samples are labeled with three different fluorophores that emit light in different wavelengths. The fluorophores are called Cy2, Cy3, and Cy5.

Using the 2D-DIGE technique, two samples can be loaded in one single gel. Each sample is marked with a different dye. The third dye is usually used as an internal standard to compare the volume of the spots in a protein expression analysis. The steps of the analysis are similar to those described in the previous section. The proteome of each condition is distinguished using a scanner that captures the signals emitted by the fluorophores. Cy2, Cy3, and Cy5 have excitation wavelengths of 488, 532, and 633 nm, respectively (Marouga et al. 2005). It is important to note that all three dyes have the same molecular mass and charge, which allows for the same protein labeled with different dyes to have the same pattern of migration within the gel. The chemical composition of the gel is the same as that used in conventional 2DE.

## ***2.3 Pulsed-Field Gel Electrophoresis (PFGE)***

Pulsed-field gel electrophoresis (PFGE) is a separation technique for large-sized DNA molecules (often greater than 40 kilobases). It was first reported by Schwartz and Cantor (1984) and involves a gel containing DNA molecules and the application of an electric field, the direction of which is periodically modified with pulse times ranging from 0.1 to 1,000 s or more (Heintz and Gong 2001) so that the DNA molecules move from negative and which now allows for the separation of up to 5 megabase (Mb) molecules. The differences between common electrophoresis and PFGE are that the number of electrodes is greater in the latter and the directions in which these electrodes move nucleic acids are different. Figure 2 illustrates the basic operation of the two forms.

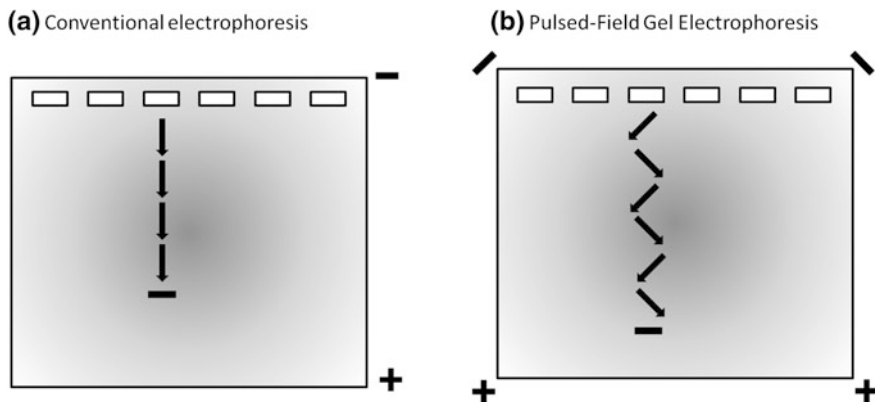


**Fig. 2** Comparing the pattern of DNA migration in **a** conventional electrophoresis and **b** pulsed-field gel electrophoresis. The arrows indicate the movement of the DNA molecule in the gel according to the type of applied electric field

In common electrophoresis, only two electrodes operate continuously; i.e., both are connected permanently making the nucleic acid (e.g., DNA) migrate from the negative pole to the positive pole. In PFGE, there are four electrodes that are turned on and off periodically in diagonal pairs, causing the nucleic acid to migrate down and to the left, then down and to the right, thus covering a much larger distance than if it were in a rectilinear form.

According to the well-established protocols, the larger the DNA fragment to be separated, the greater the time that each electric field should be activated. This is due to the fact that the DNA molecules must be fully stretched before going through the pores; so the larger the DNA molecule, the greater the time required for it to be in the correct conformation and migrate after a change of direction of the electrodes.

There are several types of PFGE that differ from each other by the apparatus used for running the gels. There are basically four commonly used types that are defined below.

- I. The vertical pulsed-field system: This type of electrophoresis employs two pairs of linear electrodes, but there is an angle of  $110^\circ$  between the electrodes that are alternated.
- II. Field inversion (FIGE): This type of electrophoresis uses only one pair of electrodes with an angle of  $180^\circ$  between them; however, in contrast to ordinary electrophoresis, the field is alternated periodically so that the nucleic acid moves in both directions.
- III. Rotating gels: This is a system where, instead of changing electrodes, the gel is rotated to change the angle in which the nucleic acid moves. Only one pair of electrodes is used.
- IV. Contour-clamped homogeneous electric field: A device with multiple electrodes hexagonal with an angle of  $120^\circ$ . The main feature of this type of PFGE is that it generates a homogeneous electric field.

There are several factors that affect the resolution of the fragments during electrophoresis such as pulse time, field strength, buffer composition, type and concentration of agarose, and an obtuse angle between the fields. In general, only the pulse time is changed, and the larger the fragments are, the slower it moves. If voltage is also increased, the large fragments can be separated more easily, but some voltage limits of increase should be considered.

The angle of the applied electric field is a minor factor that affects migration, but there are studies showing that the 90° angle provides the best results (Bancroft and Wolk 1988). PFGE is run at temperatures of 4–15 °C, and the higher the temperature, the faster migration occurs.

### 3 Applications in Microbial Genomics and Proteomics

The three above-mentioned techniques are constantly used in the field of genomics and proteomics to analyze the molecular behavior of free-living microbes. These applications have been called “environmental omics,” and according to Ge et al. (2013), it can be divided into three main fields of application: (i) chemical toxicity and environmental monitoring; (ii) adverse human health outcomes and environmental impacts; and (iii) ecological functions and environmental adaptation of organisms.

Both 2DE and 2D-DIGE were used to evaluate the differential expression of proteins in free-living bacterial species in response to several environmental variations such as metal concentration (Poirier et al. 2013), temperature (Dall’Agnol et al. 2014), pH (Mangold et al. 2013), and other parameters. Using 2DE, García-Descalzo et al. (2014) identified several isoforms of heat shock proteins in the bacteria *Shewanella frigidimarina* in response to heat. Similarly, Dall’Agnol et al. (2014) identified several isoforms of cold shock proteins in a bacterium isolated from Antarctica *Exiguobacterium antarcticum* B7 in response to cold. The post-translational modifications leading to the production of protein isoforms are easily visualized in two-dimensional gels by the gel-shift patterns in both the vertical or horizontal directions. Changes in the horizontal position of a spot occur in protein isoforms with altered pI values. This change is caused by mechanisms such as phosphorylation. On the other hand, the vertical shift of a spot is associated with changes in the molecular mass of the protein isoforms. This second change is caused by mechanisms such as proteolysis.

Proteomic methods have also been applied to evaluate the molecular response of bacteria to heavy metals. These groups of microorganisms have important applications for the industry of bioleaching and biomining. One of the main acidophilic and chemolithoautotrophic species used in bioleaching is *Acidithiobacillus ferrooxidans*. Modifications on the proteome of *A. ferrooxidans* were described when the bacteria were grown with high concentrations of uranium (Dekker et al. 2016), ferrous iron (Ouyang et al. 2013), copper (Almácegui et al. 2014), and pyrite (Vera et al. 2013).



Independently of the experimental question, proteins involved in general stress responses such as detoxification of reactive oxygen species are very commonly detected in proteomics assays. In fact, the most represented proteins in bacterial proteomes belong to essential metabolic pathways for the cell. These ‘housekeeping’ proteins are expressed in large amounts regardless of the physicochemical condition. A list of these differentially expressed proteins, repeatedly identified in several proteomic studies, was published by Petrak et al. (2008). Despite this bias created by the differential concentration of cellular proteins, several metabolic adaptations were determined using gel-based proteomics techniques. Using 2D-PAGE, Almácegui et al. (2014) demonstrated that a group of putative periplasmic disulfide isomerases were upregulated in the presence of copper in *A. ferrooxidans*, suggesting that these proteins are responsible for restoring copper-damaged disulfide bonds in the exposed cell wall.

The PFGE technique is an approach that is used to analyze and compare the natural diversity of the genomes (Aires et al. 2010) by the separation of DNA fragments in gels, which are distinguished by size and then visualized after staining by ethidium bromide (Soll 2000). It is frequently used for prokaryotic organisms, where it is considered a “gold standard” technique mainly for genomic studies of the epidemiology of pathogenic bacteria such as *Salmonella typhi* (Nair et al. 1994), *Yersinia enterocolitica* (Najdenski et al. 1994), *Staphylococcus aureus* (Tenover et al. 1995), and *E. coli* (Davis et al. 2003), and it allows for grouping and differentiation between the species studied.

However, this technique can also be used for eukaryotic genomes, although it is first necessary to use specific restriction enzymes that will cleave the DNA in up to 2 kilobases fragments, which can then be separated by PFGE (Aires et al. 2010). The advantage of this technique is the use of the entire genome for analysis, allowing for the identification of polymorphisms and variation in virulence factors that can be used in the construction of genomic libraries and will aid in the development of vaccines (Pooideh et al. 2015).

In a study with *S. aureus*, PFGE distinguished the bacterial isolates by the patterns of polymorphisms that could not be differentiated by the antibiogram or plasmid analysis (Ichiyama et al. 1991). Furthermore, PFGE provides species information that is not yet characterized such as ploidy and chromosomal size. In metagenomic studies, PFGE is one of the tools used that can identify the variety of species present in the samples (Sommer et al. 2010).

Therefore, PFGE is an advantageous tool for analyzing, grouping, and differentiating many pathogenic bacteria based on the DNA size of the analyzed organisms, the restriction enzymes used, the electrical resistance field (FS), the pulse time, and the buffer composition. Thus, to analyze the karyotype of prokaryotic genomes, PFGE stands out as the best tool (Bart-Delabesse et al. 1993; Caetano-Allóles 1993). Due to the methodology of this technique, PFGE is widely used in epidemiological studies, allowing for the identification of the clonal similarities between strains at the molecular level, which provides useful information on the spread of disease. The results of these analyses can be correlated with disease infection sites to aid in the development of preventive measures to control the spread of pathogens (Pooideh et al. 2015).

## 4 Conclusions and Future Perspective

The technological development in genetics, molecular biology, and cellular biology has led to the emergence of high throughput “omic” technologies. As a result, a large amount of data have been generated and stored in public databases for the past twenty years. According to Genomes Online Database (GOLD), a total of 12,122 complete genome projects have been conducted in 2016, an extraordinary difference when compared to the thirty-five incomplete projects registered in 1997. While *in silico* analyses have evolved in the last twenty years, benchtop approaches have also evolved and are continuously being applied in genomics and proteomics. The World-2DPAGE Constellation project was implemented on the ExPASy server to promote and provide information of the proteomes from several organisms through different databases such as SWISS-2DPAGE (Hoogland et al. 2008). These numbers and initiatives demonstrate the large scientific and technological production of the “omics” fields in the last two decades.

Currently, one of the main goals of the “omic” sciences is correlating a large amount of data generated with biological processes to answer important questions in microbiology. Several species such as the model bacterium *E. coli*, the psychrotrophic bacterium *E. antarcticum* B7, and the free-living bacterium *P. putida* have been studied on all three omic scales: genomic, transcriptomic, and proteomic (Taniguchi et al. 2010; Carneiro et al. 2012; Ray et al. 2013; Dall’Agnol et al. 2014; Gulez et al. 2014; Ying et al. 2016). Connecting the results obtained in these omic profiles is of great importance for the elucidation of unknown metabolic pathways, for characterizing the structures of operons, for the correction of pseudogenes, and for the detection of protein isoforms, as well as for several other applications.

Systems biology and synthetic biology are branches of the molecular biology field that seek to understand the biological systems from a holistic perspective. Therefore, they are guided by genomic and proteomic results. In this context, the benchtop techniques discussed in this chapter, such as 2DE, 2D-DIGE, and PGFE, become increasingly important for the *in vitro* determination of the hypothetical biological mechanisms studied in bioinformatics and, therefore, can be considered ancient techniques with current applications.

## References

- Aires J, Anglade P, Baraige F, Zagorec M, Champomier-Vergès M, Butel M (2010) Proteomic comparison of the cytosolic proteins of three *Bifidobacterium longum* human isolates and *B. longum* NCC2705. *BMC Microbiol* 10:29
- Almácegui RJ, Navarro CA, Paradela A, Albar JP, von Bernath D, Jerez CA (2014) New copper resistance determinants in the extremophile *Acidithiobacillus ferrooxidans*: a quantitative proteomic analysis. *J Proteome Res* 13(2):946–960
- Bancroft I, Wolk CP (1988) Pulsed homogeneous orthogonal field gel electrophoresis (PHOGE). *Nucl Acids Res* 16(15):7405–7418

- Bart-Delabesse E, Boiron P, Carlotti A, Dupont B (1993) *Candida albicans* genotyping in studies with patients with AIDS developing resistance to fluconazole. *J Clin Microbiol* 31(11):2933–2937
- Bengtsson S, Naseer U, Sundsfjord A, Kahlmeter G, Sundqvist M (2012) Sequence types and plasmid carriage of uropathogenic *Escherichia coli* devoid of phenotypically detectable resistance. *J Antimicrob Chemother* 67(1):69–73
- Caetano-Allóles G (1993) Amplifying DNA with arbitrary oligonucleotide primers. *Genome Res* 3:85–94
- Carneiro AR, Ramos RTJ, Dall’Agnol H, Pinto AC, Soares SC, Santos AR, Guimarães LC, Almeida SS, Baraúna RA, Graças DA et al (2012) Genome sequence of *Exiguobacterium antarcticum* B7, isolated from a biofilm in Ginger Lake, King George Island, Antarctica. *J Bacteriol* 194(23):6689–6690
- Crick F (1970) Central dogma of molecular biology. *Nature* 227:561–563
- Dall’Agnol HPMB, Baraúna RA, de Sá PHCG, Ramos RTJ, Nóbrega F, Nunes CIP, Graças DA, Carneiro AR, Santos DM, Pimenta AMC et al. (2014) Omics profiles used to evaluate the gene expression of *Exiguobacterium antarcticum* B7 during cold adaptation. *BMC Genomics* 15:986
- Davis MA, Hancock DD, Besser TE, Call DR (2003) Evaluation of pulsed-field gel electrophoresis as a tool for determining the degree of genetic relatedness between strains of *Escherichia coli* O157:H7. *J Clin Microbiol* 41(5):1843–1849
- Dekker L, Arsène-Ploetze F, Santini JM (2016) Comparative proteomics of *Acidithiobacillus ferrooxidans* grown in the presence and absence of uranium. *Res Microbiol* 167(3):234–239
- Fleischmann RD, Adams MD, White O, Clayton RA, Kirkness EF, Kerlavage AR, Bult CJ, Tomb JF, Dougherty BA, Merrick JM et al (1995) Whole-genome random sequencing and assembly of *Haemophilus influenzae* Rd. *Science* 269(5223):496–512
- Folster JP, Pecic G, Rickert R, Taylor J, Zhao S, Fedorka-Cray PJ, Whichard J, Mcdermott P (2012) Characterization of multi-resistant *Salmonella enterica* serovar Heidelberg from a ground Turkey-associated outbreak in the United States in 2011. *Antimicrob Agents Chemother* 56(6):3465–3466
- García-Descalzo L, García-Lopez E, Alcázar A, Baquero F, Cid D (2014) Proteomic analysis of the adaptation to warming in the Antarctic bacteria *Shewanella frigidimarina*. *Biochemica et Biophysica Acta (BBA)—Proteins Proteomics* 1844(12):2229–2240
- Ge Y, Wang DZ, Chiu JF, Cristobal S, Sheehan D, Silvestre F, Peng X, Li H et al (2013) Environmental OMICS: current status and future directions. *J Integr OMICS* 3(2):75–87
- Gulez G, Altıntaş A, Fazli M, Dechesne A, Workman CT, Tolker-Nielsen T, Smets BF (2014) Colony morphology and transcriptome profiling of *Pseudomonas putida* KT2440 and its mutants deficient in alginate of all EPS synthesis under controlled matrix potentials. *MicrobiologyOpen* 3(4):457–469
- Heintz N, Gong S (2001) Working with bacterial artificial chromosomes and other high-capacity vectors. In: Green MR, Sambrook J (eds) *Molecular cloning: a laboratory manual*. Cold Spring Harbor Laboratory Press, New York, p 301
- Hoogland C, Mostaguir K, Appel RD, Lisacek F (2008) The World-2DPAGE Constellation to promote and publish gel-based proteomics data through the ExpASY server. *J Proteomics* 71(2):245–248
- Ichiyama S, Ohta M, Shimokata K, Kato N, Takeuchi J (1991) Genomic DNA fingerprinting by pulsed-field gel electrophoresis as an epidemiological marker for study of nosocomial infections caused by methicillin-resistant *Staphylococcus aureus*. *J Clin Microbiol* 29(12):2690–2695
- Kuska B (1998) Beer, Bethesda, and biology: how “genomics” came into being. *J Natl Cancer Inst* 90(2):93
- Mangold S, Jonna V, Dopson M (2013) Response of *Acidithiobacillus caldus* toward suboptimal pH conditions. *Extremophiles* 17(4):689–696
- Marouga R, David S, Hawkins E (2005) The development of the DIGE system: 2D fluorescence difference gel analysis technology. *Anal Bioanal Chem* 382:669–678

- Morimoto H, Kuwano M, Kasahara Y (2013) Gene expression profiling of *Pseudomonas putida* F1 after exposure to aromatic hydrocarbon in soil by using proteome analysis. *Arch Microbiol* 195(12):805–813
- Nair S, Poh CL, Lim YS, Tay L, Goh KT (1994) Genome fingerprinting of *Salmonella typhi* by pulsed-field gel electrophoresis for subtyping common phage types. *Epidemiol Infect* 113(3): 391–402
- Najdenski H, Itean I, Carniel E (1994) Efficient subtyping of pathogenic *Yersinia enterocolitica* strains by pulsed-field gel electrophoresis. *J Clin Microbiol* 32:2913–2920
- O'Farrell (1975) High resolution two-dimensional electrophoresis of protein. *J Biol Chem* 250(10):4007–4021
- Ouyang J, Liu Q, Li B, Ao J, Chen X (2013) Proteomic analysis of differential protein expression in *Acidithiobacillus ferrooxidans* grown on ferrous iron or elemental sulfur. *Ind J Microbiol* 53(1):56–62
- Petrak J, Ivanek R, Toman O, Cmejla R, Cmejlova J, Vyoral D, Zivny J, Vulpe CD (2008) Déjà vu in proteomics. A hit parade of repeatedly identified differentially expressed proteins. *Proteomics* 8(9):1744–1749
- Poirier I, Hammann P, Kuhn L, Bertrand M (2013) Strategies developed by the marine bacterium *Pseudomonas fluorescens* BA3SM1 to resist metals: a proteome analysis. *Aquat Toxicol* 128:215–232
- Pooideh M, Jabbarzadeh I, Ranjbar R, Saifi M (2015) Molecular epidemiology of *Mycobacterium tuberculosis* isolates in 100 patients with tuberculosis using pulsed field gel electrophoresis. *Jundishapur J Microbiol* 8(7):e18274
- Ray P, Girard V, Gault M, Job C, Bonneau M, Mandrand-Berthelot MA, Singh SS, Job D, Rodrigue A (2013) *Pseudomonas putida* KT2440 response to nickel or cobalt induced stress by quantitative proteomics. *Metallomics* 5:68–79
- Schwartz DC, Cantor CR (1984) Separation of yeast chromosome-sized DNAs by pulsed field gradient gel electrophoresis. *Cell* 37(1):67–75
- Soll DR (2000) The ins and outs of DNA fingerprinting the infectious fungi. *Clin Microbiol Rev* 13:322–370
- Sommer MO, Church GM, Dantas G (2010) A functional metagenomic approach for expanding the synthetic biology toolbox for biomass conversion. *Mol Syst Biol* 6:360
- Taniguchi Y, Choi PJ, Li GW, Chen H, Babu M, Hearn J, Emili A, Xie XS (2010) Quantifying *E. coli* proteome and transcriptome with single-molecule sensitivity in single cells. *Science* 329(5991):533–538
- Tenover FC, Arbeit RD, Goering RV, Mickelsen PA, Murray BE, Persing DH, Swaminathan B (1995) Interpreting chromosomal DNA restriction patterns produced by pulsed-field gel electrophoresis: criteria for bacterial strain typing. *J Clin Microbiol* 33(9):2233–2239
- Vera M, Krok B, Bellenberg S, Sand W, Poetsch A (2013) Shotgun proteomics study of early biofilm formation process of *Acidithiobacillus ferrooxidans* ATCC 23270 on pyrite. *Proteomics* 13(7):1133–1144
- Wilkins MR, Sanchez JC, Gooley AA, Appel RD, Humphery-Smith I, Hochstrasser DF, Williams KL (1995) Progress with proteome projects: why all proteins expressed by a genome should be identified and how to do it. *Biotechnol Genet Eng Rev* 13:19–50
- Ying BW, Yama K, Kitahara K, Yomo T (2016) The *Escherichia coli* transcriptome linked to growth fitness. *Genom Data* 7:1–3

# Chapter 8

## Polymer Gels in Vaginal Drug Delivery Systems



María-Dolores Veiga, Roberto Ruiz-Caro, Araceli Martín-Illana,  
Fernando Notario-Pérez and Raúl Cazorla-Luna

### 1 Anatomy and Physiology of the Vagina

The vagina is a thin-walled fibromuscular tube located between the rectum, urethra and bladder in women, and extending from outside the body to the cervix, which is the central organ of reproduction in women (Alexander et al. 2004; Forsberg 1996; Huszar 1986; Sjoberg 1992). Although the anterior and posterior walls of the vagina are in contact with each other in a relaxed state, it is an easily distensible organ and may be considered as a potential area, albeit not a real open area (Baloglu et al. 2009; Huszar 1986; Woolfson et al. 2000). It performs multiple functions, such as providing an outlet for menstrual fluids, facilitating the entry of seminal fluid, and during childbirth is the organ that provides structure at the base of the birth canal (Baloglu et al. 2009).

The interindividual variability of the dimensions of the vagina is extremely high and is especially modified depending on age and sexual arousal. The average length of the vagina in women of reproductive age varies between 6 and 8 cm for the front wall and up to 14 cm for the back wall, including the length of the cervix (Pendergrass et al. 1996). The average vaginal surface area, important for drug administration through this route, is 87.46 cm<sup>2</sup> (which may vary within a range of 65–107 cm<sup>2</sup>) (Pendergrass et al. 2003). However, the prevalence of vaginal folds greatly hinders its calculation, and the above data are therefore only an estimate of the true area (Ferguson and Rohan 2011).

Not only is the size of the vagina highly variable, but the shape also changes significantly from one woman to another, although a common pattern has been found in the form acquired by the vagina in women of the same race (Pendergrass et al. 1996, 2000, 2003). The different potential forms of the vagina are also

---

M.-D. Veiga (✉) · R. Ruiz-Caro · A. Martín-Illana · F. Notario-Pérez · R. Cazorla-Luna  
Department of Pharmaceutical Technology, Faculty of Pharmacy,  
Complutense University of Madrid, Madrid, Spain  
e-mail: mdveiga@ucm.es

important from the point of view of pharmaceutical development, as this factor may affect the acceptability of certain forms of vaginal dosage and require the development of multiple dosage forms for vaginal administration, with formulations always designed to cover the largest possible vaginal area. In some applications such as vaginal microbicides for the prevention of sexually transmitted diseases, there is speculation as to the possible influence of the amount of vaginal surface covered by the formulation, and it remains to be seen whether the microbicide must completely cover the vagina to achieve complete protection (Ferguson and Rohan 2011).

Both the vagina and the ectocervix (the portion of the cervix exposed to the vaginal environment) are lined by keratinized and non-keratinized stratified squamous epithelium composed of several layers, which is continually renewed during the reproductive years. There are three clearly differentiated areas in this epithelium: a basal layer composed of germinal cells, a middle zone also called stratum spinosum—the most abundant—and finally the surface area where the most mature cells are found and whose function is to protect the cells below and the subepithelial vasculature from trauma and infection (Huszar 1986). During ripening, the cells migrate from the basal layer to the surface layer, while their morphology also changes to become flatter with smaller nuclei and an increase in cell volume (Rohan and Sassi 2009). As already mentioned, the vaginal mucosa also has multiple roughened folds which increase the absorption surface. Squamous cells are characterized by having gaps in their connecting links that form a series of canals between adjacent cells which allow the movement of molecules and electrolytes, and the absorption of certain drugs (Huszar 1986).

The thickness of the squamous epithelium varies (from 0.2 to 0.5 mm) and is substantially affected by age. The thickness of the vaginal epithelium is modified during the menstrual cycle in response to changes in oestrogen levels, while the decrease in oestrogen levels after menopause leads to a reduction in epithelial thickness. These variations must also be taken into consideration from the pharmacological point of view, since the study of this epithelium is essential for drug administration with both local and systemic action. Drug permeability through the vaginal surface has important consequences, as it can influence the distribution and pharmacokinetics of some vaginally administered drugs, and will therefore have a significant impact on their efficacy and toxicity profiles (Woolfson et al. 2000; Vermani and Garg 2000; Rohan and Sassi 2009). The vagina is coated in a mucous layer consisting mainly of water, but also of a matrix of mucins—glycoproteins with high molecular weight—and plasma proteins, enzymes, amino acids, cholesterol, lipids, together with a range of inorganic ions (Burruano et al. 2002; Katz 1986; Zavos and Cohen 1980). The sources of mucous secretions include goblet cells in the epithelium of the endocervix and Bartholin glands; the squamous epithelium of the vagina and ectocervix is not involved in the production of mucus. The physical characteristics, composition and volume of mucosal secretions depend on the menstrual cycle, as their production is oestrogen dependent. Hence, the secretions are more abundant at the time of ovulation, leading to an increase in the total volume of vaginal fluid, a higher pH and mucin content, and a decrease in

viscosity. The structure of this mucosa is similar to a complex net of tangled microfibrils. The mucus layer is less viscous during ovulation, while at non-ovulatory stages it becomes dense and compact. This mucus layer may facilitate or impede the effectiveness of a drug, and the fluctuations occurring in the mucosal net and its pore size may affect the pharmacodynamics of certain active ingredients (Ferguson and Rohan 2011).

Mucus has the ability to maintain a minimum layer over the epithelial surface. The depth of this layer is determined by the balance between the secretion rate and the abruption or degradation rate. Drugs administered vaginally, whose therapeutic target is within the mucosa, must be able to penetrate this layer before they are eliminated or degraded (Cone 2009).

Another significant factor is the vaginal fluid, since this can be both a useful tool and a barrier to drug delivery. This is a liquid that accumulates inside the vagina, covers the vaginal epithelium, and is produced from the mucous membranes of the endometrium and transudate serum. This transudate comes from blood vessels that surround the vagina, goes through the vaginal wall, and mixes with secretions from the sebaceous, sweat and Skene glands. It can also contribute to the endometrial and oviductal fluids in the vagina (Rencher 2001; Rohan and Sassi 2009; Valore et al. 2002); vaginal fluid is thus enormously complex. Although its main component is cell mucus and elements associated with the innate microflora of the vaginal epithelium, it also contains various components such as amino acids, proteins, carbohydrates, enzymes, enzyme inhibitors, ion and lipids, and possibly macrophages, lymphocytes, plasma cells, Langerhans cells, eosinophils and mastocytes (Huszar 1986). The physical presence of a fluid layer on the epithelium and the enzyme activity in vaginal fluid has been identified as a significant barrier to drug delivery and absorption. As this fluid is the medium in which the drug is dissolved, it plays a crucial role in ensuring the active substance reaches its target. However, its components may have the ability to interfere with the drug activity, either destabilizing it or by non-specific binding between the drug and some of these components (Rohan and Sassi 2009). Dynamic changes in the volume and composition of vaginal fluid must be considered, as this can modify the release profile of drugs administered by this route. This fluid is the volume where the active ingredient is dissolved for absorption, and these variations may even affect the distribution of drugs in the body (Ferguson and Rohan 2011). Finally, the vaginal fluid also affects the residence time and bioadhesion of the formulation (Rohan and Sassi 2009).

Another factor in vaginal fluid influencing drug delivery is its pH. The normal pH value in an adult woman of childbearing age is between 4 and 4.5. This acid pH is due to commensal *Lactobacillus* sp., which produces lactic acid from the glycogen from the sloughed epithelial cells of the mucosa. High pH may increase the risk or be indicative of an infection. This should be considered when administering drugs vaginally, as the active ingredient must be stable in this pH, and the formulation must be able to release the drug in a medium with this acidity. The pH of vaginal fluid in adult women rises during menstruation and after vaginal intercourse, since both the menstrual fluid and the ejaculate are alkaline in nature.

These alterations in the pH must also be evaluated, as they can modify the release profile of pH-sensitive drugs from vaginal administration formulations (Woolfson et al. 2000).

Vaginal microflora is variable, with the possible presence of both cocci and bacilli species of Gram-positive and Gram-negative bacteria (Larsen and Monif 2001; Lamont et al. 2011), and a general presence of small amounts of anaerobic microorganisms. It can be affected by many factors such as age, menarche, the time of the menstrual cycle, pregnancy, menopause, infections and douching practices. The normal vaginal flora plays an important role in determining the environment in which the drug must be released. Any system of vaginal drug delivery must take into account the presence of these bacteria and their contribution to creating barriers to drug delivery. Caution should be exercised since commensal bacteria are responsible for maintaining a healthy vaginal environment, and the formulations should not be toxic to the vaginal microbiota (Rohan and Sassi 2009). Some vaginal bacterial infections caused by several pathogenic microorganisms have the ability to alter the enzyme composition of the vagina and the vaginal fluid. Enzyme activity in the vagina and the vaginal fluid—although it has not yet been fully characterized—may affect the stability of some drugs and their passage through the vaginal epithelium (Woolfson et al. 2000); the most abundant enzymes are aminopeptidase, which contribute to the degradation of proteins and peptides, although lysozyme and other enzymes have also been found (Rohan and Sassi 2009).

## 2 Vaginal Drug Administration

Despite the multitude of challenges for drug delivery posed by the anatomy and physiology of the vagina, vaginal drug delivery is often used for both local drug administration and to achieve a systemic action (Ferguson and Rohan 2011).

The vaginal route for drug administration has been recognized since ancient Egypt, when this was the route used for various substances for contraception (Ferguson and Rohan 2011). The vagina has traditionally been the application site for local action drugs, but it also has great potential for systemic administration due to its large surface area and high blood supply (Rohan and Sassi 2009). Products that are usually administered vaginally are antimicrobials for the treatment of vaginal infections, spermicides, contraceptive agents, and drugs for hormone replacement, induction of labour and the interruption of pregnancy (Garg et al. 2002; Vermani and Garg 2000). The most common vaginal administration dosage forms include solids such as suppositories and tablets, and semisolid forms such as creams and gels. Intravaginal rings (IVR), films and foams are also used (Garg et al. 2003). The choice of vaginal administration depends on multiple variables ranging from drug properties to clinical requirements for acceptability by the user (Woolfson et al. 2000).

Vaginal drug delivery offers several advantages (Alexander et al. 2004; Baloglu et al. 2009; Vermani and Garg 2000; Woolfson et al. 2000). The vagina provides a



convenient and easy access route due to the easy self-administration of the formulations. It represents a noninvasive route of administration, since it avoids the discomfort, tissue damage and possible infections associated with parenteral administration. Drugs that are administered vaginally avoid the effect of hepatic first pass, and the high vascularity of the vagina allows adequate blood supply for drugs needing systemic administration (Ozyazici et al. 2006; Rohan and Sassi 2009). Absorption by this route can occur both through passive diffusion and active transport. Vaginal administration also avoids the incidence of many side effects such as those affecting the gastrointestinal tract and liver, which may be associated with the oral and parenteral administration of drugs (Ozyazici et al. 2006). The vagina provides high permeability for drugs with certain physicochemical characteristics, as absorption is defined by the molecular weight and the ionization and dissolution properties of the active ingredient (Ferguson and Rohan 2011).

The vaginal route has other clear advantages when seeking to achieve a local effect of the drug, such as when treating infections of the female reproductive system or preventing sexually transmitted diseases. In these cases, the most obvious advantage of vaginal administration is that the drug concentration is much greater in the area in which it is required to exercise its effect that could be achieved by other routes. This route has a limited systemic drug exposure compared to the oral or parenteral route, thus avoids the incidence of adverse reactions to the active substance, or limits their severity (Ferguson and Rohan 2011).

### 3 Pharmaceutical Forms for Vaginal Administration

A proper formulation of drugs is essential for the development of a safe, stable, effective and acceptable pharmaceutical product. There are therefore many considerations when developing a product for effective vaginal administration (Rohan and Sassi 2009). The choice of dosage form depends directly on the physical and chemical characteristics of the drug, its mechanism of action, the target of the formulation and patient comfort (Buckheit et al. 2010; Rohan and Sassi 2009).

Several pharmaceutical forms have been used for vaginal drug delivery. Although there is a predominance of more traditional formulations such as creams (Khanna et al. 2007, 2008), gels (Burns et al. 2015; Hladik et al. 2015; Laeyendecker et al. 2015; Marrazzo et al. 2015; Yang et al. 2014) and tablets (Clark et al. 2014; Sánchez-Sánchez et al. 2015), other more novel dosage forms include films (Akil et al. 2015) and intravaginal rings (Johnson et al. 2010; Smith et al. 2015; Srinivasan et al. 2014).

Gels are possibly the most widely studied dosage form for the vaginal route (Rohan and Sassi 2009). These are semisolid systems consisting of a liquid and a solid component that acts as a gelling agent by trapping the liquid within its three-dimensional structure, producing the characteristic consistency of these solid-liquid mixtures.

Based on the polarity of the liquid component, we can distinguish between hydrogels and organogels. Hydrogels contain a polar solvent (such as water), while in organogels the liquid component is apolar (such as vegetable oils). Hydrogels are used in the food industry, tissue engineering and the pharmaceutical industry for the administration of active principle on skin and/or mucous membranes, as they are widely accepted by patients for being refreshing, hydrating, easy to extend; they can be removed by washing with water and are not greasy to touch. However, drug release from these gels and the consequent absorption through the lipophilic skin barrier is hampered by their hydrophilicity. Meanwhile, patients' poorer acceptance of organogels, in research since the 1990s, is offset by their ability to cross the skin barrier (Rehman et al. 2014; Sagiri et al. 2015, Singh et al. 2014a).

The mixture of hydrogel and organogel in defined ratios results in the formation of a bigel. The properties of both gels can be exploited by combining both gel types, and lipophilic and hydrophilic drugs can be included in the same dosage form for topical or transdermal administration. Research into the field of bigels is still in its early stages. For example, Rehman et al. (2014) prepared bigels with different compositions and concluded that these systems represent suitable carriers for topical and transdermal drug delivery with a higher permeability than hydrogel-based systems (Rehman et al. 2014).

Gels have the advantage of being easily and conveniently applied because they can be administered by the women themselves, so treatment adherence is significantly improved and is the reason for their great acceptability with patients (Coggins et al. 1998; Hardy et al. 1998; Rosen et al. 2008; Tien et al. 2005). They are optimal formulations for ensuring the prompt action of the drug, since by extending the gel in a thin layer over the vaginal mucosa the drug is rapidly released and absorbed. Gels have a further advantage over other formulations when they are not used for treatment but to prevent infections, as they are able to cover a larger area of the vaginal mucosa. They thus offer greater protection against external pathogens, as apart from the effects of the drug itself they form a physical barrier that protects the vagina. Their ease of production means the manufacturing costs are low, especially when compared to more complex dosage forms such as vaginal rings; this is a very important consideration, especially for middle- and low-income countries (Ferguson and Rohan 2011; Forbes et al. 2011, 2014). Finally, it is also worth noting that several studies on women's preferences have highlighted a clear trend towards hydrogels, as water-based products are more popular than those with an oily base (Auslander et al. 2007; Braunstein and van de Wijgert 2005; Cohen et al. 2007; Darroch and Frost 1999; Holt et al. 2006; Rader et al. 2001).

However, as with all formulations, gels also have their drawbacks. After vaginal gel utilization within trials, reports of leakage or messiness are extremely common (Jespers et al. 2007; Lacey et al. 2010; Nel et al. 2009, 2010; Schwartz et al. 2008). The fact that it is a semisolid formulation makes it very difficult to ensure the uniformity of the dose, so drugs administered using gels as vehicles must have a sufficiently broad therapeutic margin to ensure their effectiveness despite possible small variations depending on the person applying it or even between different applications. Another limitation is that gels have little ability to control drug release,

so if continuous treatment were required, repeat administrations of the formulation would be necessary (Forbes et al. 2011).

Another consideration is the possibility of developing vaginal administration tablets containing hydrophilic polymers as excipients (Sánchez-Sánchez et al. 2015). These tablets would be administered vaginally, and a gel would form in situ as the polymers capture water from the vaginal environment. The active ingredient in these matrices is uniformly distributed within a polymer, and drug release depends on the type, ratio, particle size and solubility of the polymer; the solubility and particle size of the drug; and the geometry of the matrix. These matrices become hydrated and swollen in contact with water, forming a gel through which the drug diffuses. The active ingredient is released from these systems through two simultaneous mechanisms. First, the outermost (and least consistent) gel layers erode and the active ingredient dissolves in the medium. The drug then diffuses through the gel, which acts as a barrier. The release rate will depend on the consistency of the polymer gel and the aqueous solubility of the drug, so when the gel is very weak or drug solubility very low, diffusion has little influence and release depends on the speed of erosion of the matrix (Sánchez et al. 2010). However, when the drug solubility is moderate or high, three stages can be distinguished in the release process: an initial phase in which the drug is dissolved on the matrix surface and the polymer begins to gel; a stationary phase in which the entry of water in the matrix causes the gel to expand and drug release is controlled by diffusion through the gel layer; and finally a depletion phase that begins after the gelling of the polymer matrix, where the drug concentration is lower than its solubility coefficient (Rabasco 1997). This mechanism of release can be visually observed in Fig. 1.

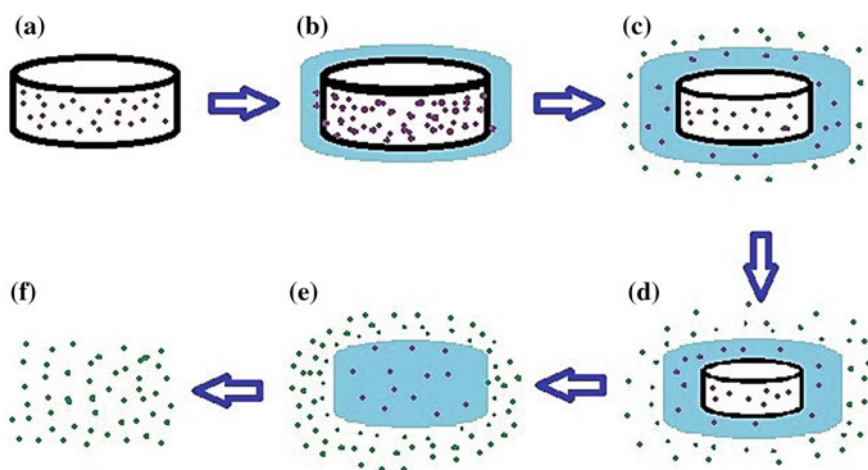


**Fig. 1** Swelling behaviour in hydrophilic tablets

Tablets that are capable of gelling in the vaginal environment offer several advantages over traditional gels. They are still easy to manufacture, which makes them inexpensive, and—like gels—they can be applied by the user. As they are solid formulations, they are more convenient to implement, as their greater stability ensures accuracy in the dose administered. However, the overriding advantage of these formulations is their capacity to control drug release according to therapeutic needs. Depending on the desired outcome, different polymers could be used to achieve rapid gelling and release of the active ingredient for an immediate effect. The opposite scenario is also possible, where release could be delayed through the processes of water uptake, swelling, dissolution of the active ingredient and its dissemination through the gel by developing sustained release formulations, as can be achieved by intravaginal rings, but with a much lower manufacturing cost (Sánchez-Sánchez et al. 2015).

## 4 Desirable Features in Gels

A number of essential features are required when developing formulations of vaginal gels. The first of these is mucoadhesion. The relatively new term “bioadhesion” describes the ability of certain synthetic and biological macromolecules to adhere to the body’s tissues. This definition is probably sufficient to identify the phenomenon of simple adherence. Thanks to the viscous nature of the surface layer, any material can adhere to a biological tissue, and particularly to mucous membranes, without the intervention of specific tissue and polymer bindings. There can be no real bioadhesion without some interrelation between specific chemical groups of polymers and biological tissues, or the interpenetration of chains (Rodríguez et al. 2000). Administration forms that bind to mucous are called “mucoadhesive” and are designed to remain fixed at the site of the release and/or absorption of the drug by prolonging their residence time, despite opposing natural circumstances. Mucoadhesive capacity is essential for vaginal gels, since this is the only way to achieve the permanence of the formulation in the vaginal environment after administration. To optimize the mucoadhesion of gels, we need to know the nature of the interactions occurring in the mucosa–gel interface and the mucoadhesive specificity of polymer gel to mucin, which prevents it from adhering to other surfaces (Rodríguez et al. 2000). The bioadhesion process first requires the physical or mechanical interactions that occur as a result of direct contact between the bioadhesive polymer and the mucosa, causing interpenetration of the polymer molecules in the gel mucus or resulting in semipermanent non-specific joints. This adhesion is time-dependent and requires the diffusion of the polymer molecules and the formation of complex structures between the chains. Second, covalent or ionic chemical bonds are established between gel and mucosa, resulting in highly stable links (Lyra et al. 2007). In order for mucoadhesion to occur, the attractive interaction must be higher than the non-specific repulsion. Attractive interactions are caused by van der Waals force, electrostatic attraction, hydrogen bonds and

hydrophobic interaction. Repulsive interactions occur by electrostatic and steric repulsion (Rodríguez et al. 2000).

Certain polymers adhere non-specifically to various surfaces through hydration. The presence of hydroxyl, carboxyl, or amino groups promotes adhesion of the polymer (Lyra et al. 2007). All mucoadhesive systems owe their properties to the inclusion of one or more polymers which, under appropriate conditions, are able to interact with the mucosal surface, thus maintaining the dosage form fixed. The conditions under which each polymer reveals its bioadhesive capacity will depend on its chemical and structural characteristics, and also on physiological factors. A substantial number of polymers have been studied for their mucoadhesive capacity, mainly natural or semisynthetic polymers such as gum tragacanth, guar gum, karaya gum, sodium alginate, gelatine, chitosan, cellulose derivatives (such as methyl cellulose, sodium carboxymethylcellulose, hydroxyethylcellulose or hydroxypropylcellulose), polyethylene glycols, polyvinyl alcohol, carbopol, polymers and copolymers of acrylic and methacrylic acid, polyalkylcyanoacrylates or polycarophil (Rodríguez et al. 2000; Valenta 2005). However, other polymers have been specifically synthesized to achieve high mucoadhesion, and there are combinations of different polymers whose qualitative and quantitative composition have been the subject of patents (Rodríguez et al. 2000).

The success of vaginal gels depends on the selection of formulations that are compatible with the vaginal mucosa. Another essential factor is thus the biocompatibility of polymers; that is, they must not trigger an immune response in the body. The polymers used to develop these gels and their byproducts should not be mutagenic, carcinogenic, antigenic or toxic and must of course be compatible with the host tissue, in this case is the vaginal mucosa.

Cytotoxicity assays are the first stage in biocompatibility testing. Their function is reliably and reproducibly to detect any negative effects on cell functions at an early stage. *In vitro*, studies are usually the first step in testing biocompatibility. Cell cultures are ideal systems for the study and observation of a specific cell type for specific conditions, since these systems are not as complex as an *in vivo* system, with its large number of interacting variables (Martínez Palau 2008). Cytotoxicity assessment forms the basis of *in vitro* test methods in national and international standards. *In vitro* assays assess the morphology, cytotoxicity and secretory functions of different cell types. The assays may be direct—through contact between the cells and the material—or indirect, by adding a material extract to the cell culture. If *in vitro* toxicity is defined as a negative parameter, or the deterioration of an agent in normal biochemical cell functions, these negative effects may manifest in different ways and lead to a variety of possibilities for assessing cytotoxicity (Martínez Palau 2008). The assessment is done after an appropriate exposure time—typically 24 to 72 h—using qualitative morphological observation, quantitative measurements of cell death, cell growth inhibition, cell proliferation, protein accumulation and release of one or more enzymes, or other measurable parameters (Hanson et al. 1996).

*In vitro* assays are only one phase in the evaluation of biocompatibility, since it is too risky to extrapolate *in vitro* methods to the situation *in vivo* (Hanson et al. 1996).

The polymers categorized as biocompatible *in vitro* must therefore be further evaluated by *in vivo* methods. The development of vaginal dosage forms requires a series of safety studies, first in animal models and then in women. It must be demonstrated that vaginal administration has no significant cytotoxicity in women and no toxicity to the vaginal mucosa.

Another aspect to consider when developing vaginal gels is the biodegradability of the polymers. Biodegradable polymers erode in contact with body fluids; they have a volume of water in their structure and subsequently undergo hydrolysis, which disintegrates the polymer chains. Polymer fragments are ultimately metabolized by the body.

There are two types of bioerosion: heterogeneous or surface erosion, and homogeneous or mass erosion. Surface erosion occurs when the rate at which water penetrates the material is lower than the rate of conversion of the polymer into soluble fragments. This surface attack has the effect of reducing the thickness of the material. The polymer must be hydrophobic to prevent water penetration; polyorthoesters and polyanhydrides are examples of materials that undergo this type of erosion. In mass erosion, the amount of water entering the solid is greater than needed by the polymer to be transformed into a soluble material; excess water causes erosion that affects the entire mass of the solid. This kind of erosion occurs in two phases. In the first phase, water penetrates the material by attacking the chemical bonds of the amorphous phase and converting long polymer chains into shorter water-soluble fragments. Because this phenomenon occurs initially in the amorphous phase, there is a reduction in molecular weight without any loss of physical properties, since the matrix material is still supported by the crystalline regions. The second phase consists of the enzymatic attack and metabolization of the fragments, resulting in a rapid loss of polymer mass.

Hydrolysis is the most significant degradation mechanism in most biodegradable polymers. The degradation rate of biodegradable polymers depends on their hydrophilicity and on the accessibility of their hydrolytically unstable bindings to body fluids. The hygroscopicity of the polymer, its morphology, crystallinity and molecular weight are key parameters in the kinetics of polymer degradation. Several factors can influence the degradation rate, although the main one is polymer hygroscopicity; it is also affected by other factors such as the type of chemical bond, the pH and the copolymer composition (Martínez Palau 2008).

Biodegradable polymers may be classified basically into four main categories: natural polymers (such as cellulose, starch and proteins), modified natural polymers (such as cellulose acetate or polyalkenoate), composite materials combining biodegradable particles (for example, starch, regenerated cellulose, or natural gums) with synthetic polymers (for example, mixtures of starch and polystyrene, or starch and polycaprolactone), and synthetic polymers (such as polyesters, polyesteramides and polyurethanes). In terms of chemical composition, the most widely used biodegradable polymers can be divided into three categories: sugar derivatives, polyesters and polyvinyl alcohol type (Contó Rigante 2008).

The fundamental advantages of biodegradable polymers when developing vaginal gels are that the gel does not need to be removed after it has served its

purpose, and may also offer a way to control the release of the active ingredient depending on the degradation rate of the polymer.

## 5 Characterization Methods of Vaginal Gels

During research, pharmaceutical gels are characterized through numerous assays. Some of the most interesting tests for evaluating pharmaceutical gels are described below.

### 5.1 Swelling of the Formulations

A crucial factor when developing polymer gels is their swelling in aqueous medium, as this is a good indicator for predicting the mucoadhesive and cohesive capabilities of the polymer being tested. The stability of the polymer and the drug release from the formulation are both directly related to this swelling.

Hintzen et al. (2013) proposed to determine this swelling using a mechanism based on gravimetry. Solid formulations are attached to a needle after being accurately weighed. Each of the formulations to be tested is then immersed in a buffer solution similar to vaginal pH at a constant temperature of 37 °C. At set times, the formulations are extracted, and excess water is removed using a paper filter. The formulations are weighed and returned to the solution. The process is repeated at predetermined times until a constant swelling percentage is achieved or until the matrix is completely eroded or dissolved.

The following equation is used to determine swelling in each formulation:

$$\text{Swelling (\%)} = \frac{(W_t - W_0)}{W_t} \times 100$$

where

- $W_t$  is the weight at each set measuring time
- $W_0$  is the initial weight.

The following equation (Ceschel et al. 2001) can also be used to determine the percentage of erosion or dissolution of the matrix (DS) for formulations that do not completely disappear during the test:

$$\text{DS} = \frac{(W_0 - W_f)}{W_0} \times 100$$

where

- $W_0$  is the initial weight and
- $W_f$  is the weight once the formulation is completely dry after the end of the test.

## 5.2 Mucoadhesion

Mucoadhesion can be determined by an ex vivo process after fixing the formulations to a sample of vaginal mucosa of animal origin. These tests can be done with a choice of two types of method.

### 5.2.1 The Glass Plate Method

The formulations are placed on a fragment of animal mucosa (previously affixed to a glass plate with acrylic adhesive). A 50 g weight is placed on top for 5 min to promote adhesion. The resulting batches are then placed in an apparatus consisting of a basket immersed in a phosphate buffer (pH 7.2). The time the gels remain adhered to the mucosa until their complete detachment, dissolution, or the erosion of the dosage form is observed and recorded (Fig. 2) (Sagiri et al. 2015).

### 5.2.2 The Beaker Method

Correctly, cut tissues are affixed to the surface of a beaker using a methyl cyanoacrylate polymer. After wetting with 50  $\mu$ L of simulated vaginal fluid,

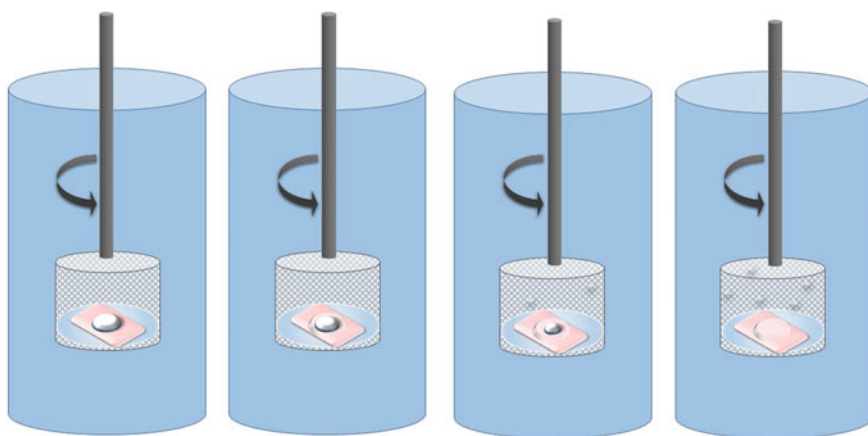


**Fig. 2** Mucoadhesion time determination by the glass plate method



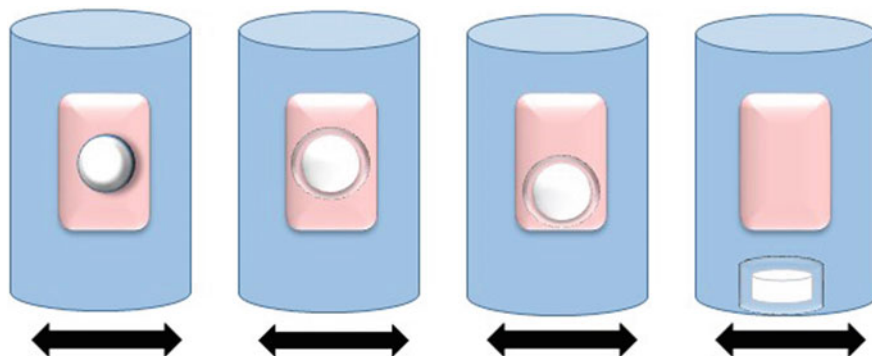


**Fig. 3** Mucoadhesion time determination by the beaker method

the samples are affixed to the surface of the mucosa by applying a constant force for 20 s. The beaker is filled with a volume of 800 mL of simulated vaginal fluid and kept at 37 °C. Once the test has started, the mucoadhesion is monitored until the complete dissolution, erosion, or detachment of the dosage form is observed (Fig. 3) (Perioli et al. 2008).

### 5.2.3 The Rotating Cylinder Method

The sample of vaginal mucosa is affixed with an acrylic adhesive to a stainless steel prism. Each formulation is placed on top of this sample, and a constant weight is applied for a period of time. The prism is then placed in a USP 1 dissolution apparatus containing 500 mL of simulated vaginal fluid at 37 °C, and the submerged prism is rotated at a constant stirring rate of 30 rpm. The time when the detachment of the mucosa, erosion and/or complete dissolution of the dosage forms is observed to occur is evaluated visually in duplicate (Fig. 4) (Kast et al. 2002).

### 5.2.4 The Stainless Steel Slab Method

In this method, it was determined how long the formulation remains attached to the vaginal mucosa through a new ex vivo mucoadhesion test. A sample of freshly excised vaginal mucosa was fixed to a stainless steel plate. The formulation was adhered to the mucosa. The plate was placed inside a beaker containing simulated vaginal fluid, so that the mucosa with the compact adhered was submerged into the medium (Fig. 5). Beakers were placed in a shaking water bath (37 °C, 15 rpm). Bioadhesion time was evaluated by daily observation of the samples (Notario-Pérez et al. 2017).

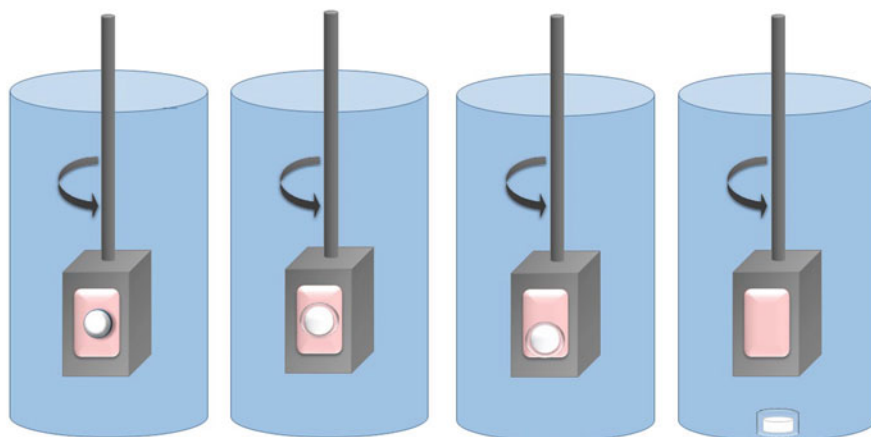


**Fig. 4** Mucoadhesion time determination by the rotating cylinder method

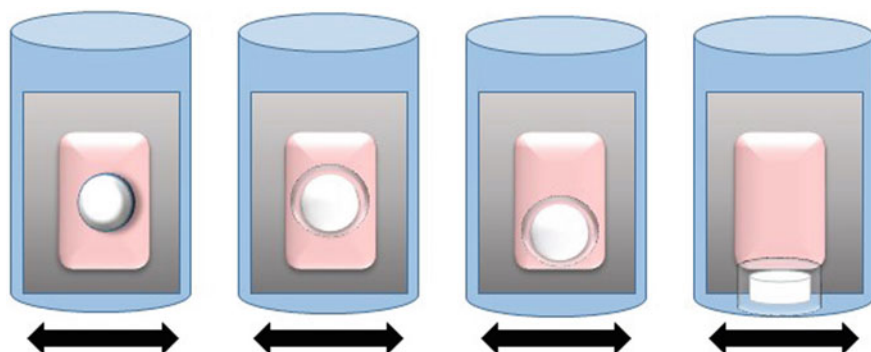


**Fig. 5** Mucoadhesion time determination by the stainless steel slab method

### 5.3 *In Vitro* Drug Permeation and Release

It is vital to determine the drug release profiles of any polymer formulations developed. Systems have therefore been designed to accurately characterize the drug release kinetics using an *in vitro* procedure. The problem lies in simulating the exact conditions found in the vagina to achieve greater verisimilitude in the results.

The technique commonly used to evaluate these properties is Franz diffusion cell, which was developed in 1975. This has become the most widely applied method for assessing cutaneous permeation and drug release from dosage forms, especially those with controlled drug release. It comprises two chambers with a

human, animal, or synthetic membrane between them. The donor chamber contains a solution or dispersion of the drug, and the receptor one is used for sampling. The amount of drug that diffuses from one chamber to another through the membrane is evaluated using analytical techniques such as UV or HPLC spectroscopy (Baena et al. 2011).

#### ***5.4 In Vitro Biocompatibility***

These studies are usually performed on cell lines known as HaCaT cells, which are human epidermal keratinocytes. The formulation (1 g) is provided in a dialysis bag and immersed in 50 mL of phosphate saline buffer (pH = 7.2). After 24 h incubation, the resulting leachate is sterilized by passing through a filter and 20  $\mu$ L is added per well in a 96-well plate. Each well is previously incubated for 12 h with 1 or  $2 \times 10^4$  HaCaT cells, 95% humidity, 5% CO<sub>2</sub>, 37 °C, in Dulbecco's modified Eagle's medium (DMEM), and 10% foetal bovine serum (FBS) for correct adhesion. After 1 and 5 days of incubation, biocompatibility is determined by the MTT method (3-(4,5-dimethylthiazol-2-yl)-2,5-diphenyltetrazolium bromide); the medium (DMEM-10% FBS cell) is replaced, and 100 $\mu$ L of MTT is added to each well. After 3 h of incubation at 37 °C, the medium is discarded, and 200  $\mu$ L of dimethylsulphoxide (DMSO) is added to dissolve the insoluble formazan crystals formed, resulting in a purple-coloured solution. The intensity of the colour is directly related to the number of viable cells (Sagiri et al. 2015; Singh et al. 2014a, b).

#### ***5.5 Mechanical Characterization (Viscosity)***

Rheological properties—viscosity and flow—are commonly assessed using a cone-plate viscometer at room temperature. Mechanical properties (stress relaxation, gel strength, spreadability and backward extrusion) of the bigels are usually studied using a static mechanical tester (Singh et al. 2014a).

### **6 Polymers Used for Gel Development**

There are different polymers that can be used for the development of pharmaceutical gels. According to their origin, they can be classified as natural, semisynthetic, or synthetic polymers (Table 1).

**Table 1** Classification of polymers according to their origin

<i>Natural polymers</i>			
Obtained from plants	Obtained from seaweed	Obtained from bacteria	Obtained from animals
Tragacanth Guar gum Karaya gum/sterculia gum Locust bean gum Arabic gum/acacia gum Starch Pectin	Alginate Carrageenan Agarose Ulvan Fucoidan	Xanthan gum	Gelatine Chitosan Hyaluronic acid
<i>Semisynthetic polymers</i>			
Cellulose derivatives			
<i>Synthetic polymers</i>			
Acrylic acid derivatives Polyethylene glycols Polyvinyl alcohols Polyvinylpyrrolidone			

## 6.1 Natural Polymers

The most noteworthy of this group of polymers are hydrocolloids; these are macromolecules with high water affinity which dissolve at different rates, modifying their rheology and enhancing their viscosity; they are even able to form a gel which gives the liquid the appearance of a solid. Fibres with high water catchment capability (such as agar, alginates, gum arabic, pectin and others) are generally long linear or ramified chains consisting of different carbohydrates. Depending on the characteristics of their chains (length, branches and electric charges), hydrocolloids may be soluble in cold thinners (as occurs with alginate, guar gum, gum arabic, or xanthan gum) or require prior heat treatment to aid dissolution (agar, pectin, carrageenan, locust bean gum and others). Most hydrocolloids are obtained from plant products and consist of fragments of fibres purified to varying degrees by means of physicochemical processes which can be chemically modified to enhance their properties. Others are obtained through biotechnology, by cultivating microorganisms that secrete mucilage or gums (Lupo Pasin 2015).

### 6.1.1 Polymers Obtained from Plants

Some of the main polysaccharides from plants are gums, which are obtained either from vegetal exudates or from their seeds. The most commonly used gums in the pharmaceutical industry are:

- Tragacanth

This is a polysaccharide obtained from the dry sap of several species of *Astragalus*. This gum oozes spontaneously when wounds are made in its stems. It varies in colour from white to pale yellow and is odourless and flavourless.

In contact with water, tragacanth swells quickly, independently of the process temperature, and holds approximately ten times its weight. It generates a very viscous gelatine-like and highly mucoadhesive structure. Tragacanth is usually added to water at 1–10%. The highest viscosity is obtained at pH 8, and its maximum stability is observed at pH 5.

Tragacanth's solubility in water is conditioned by the presence of carboxyl groups, but it is not soluble in alcohol or in other organic solvents.

Tragacanth-based solutions are highly resistant to acid environments, so this gum would be appropriate for using a medium such as vaginal fluid (Sharma et al. 2015; Acartürk 2009).

- Guar gum

Guar gum is a biodegradable and biocompatible heteropolysaccharide obtained from the seed of *Cyamopsis tetragonoloba* (Fig. 6). It is a highly water-soluble beige powder with no need for heat treatment and can hold up to fifteen times its weight in water, resulting in a flavourless viscous gel. Guar gum is not soluble in ethanol. The viscosity of the gel depends on the length of the galactomannan chains. It undergoes hydrolysis in an acid medium such as vaginal fluid, which reduces the viscosity of the gel. Guar gum-based gels are highly spreadable and, as their viscosity is reduced in acid media, this leads to higher gel extensibility (Tasdighi et al. 2012). Guar gum is used in vaginal gels to provide a rigid gel and a prolonged release component. They show integrity beyond 7 h and do not dissolve

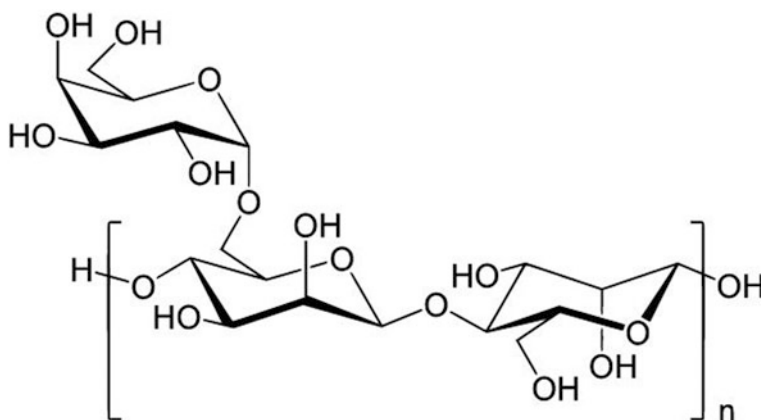


Fig. 6 Guar gum chemical structure

completely even after this time. These gums achieved prolonged integrity and release when used as a rigid gel structure forming agent, as they have a very slow erosion/dissolution rate (Ahmad et al. 2008).

This compound is commonly used as a demulcent or gastric mucosa protector, and its inclusion in vaginal formulations would thus protect the vaginal mucosa. It is highly compatible with most plant hydrocolloids (such as tragacanth, karaya gum, gum arabic, agar, alginates, or carrageenans) and also with almost all starches and cellulose derivatives. Although the mucoadhesive properties of guar gum have been poorly studied, one study shows that its mucoadhesive strength is similar to HPMC (Tasdighi et al. 2012). It is used in the pharmaceutical industry as a binder or a disintegrant in tablets, but there are several references to its use in vaginal dosage forms. Guar gum has been found in bioadhesive vaginal gels and also combined with HPMC to develop a bioadhesive vaginal tablet formulation (Baloğlu et al. 2006; Ahmad et al. 2008).

- Karaya gum/*Sterculia* gum:

Karaya gum is a recently discovered gum previously used as a tragacanth substitute, when it was considered an adulterant. Today, karaya gum is thought to have several advantages over other gums, and its usefulness in pharmaceutical formulations is highlighted by European Pharmacopoeia. It is obtained by making wounds in *Sterculia urens* trees and is commonly found in the form of a colourless and translucent granulate or powder. It is almost insoluble in ethanol and poorly soluble in water, but quickly swells in contact with water to reach sixty to one hundred times its volume, producing a highly viscous gel (Chivate et al. 2008). Karaya gum is often used in the formulation of mucoadhesive paste and could potentially be used to develop mucoadhesive vaginal gels that remain attached to vaginal mucosa for a substantial period of time. Several studies also suggest this polymer as a possible agent for the development of controlled drug release formulations. Gels based on this polymer would offer a more convenient dosage for patients—for use in the treatment or prevention of infections—as it would require fewer applications per day (Chivate et al. 2008).

- Locust bean gum

This polymer is obtained from the endosperm of the seeds of *Ceratonia siliqua*. Locust bean gum is a practically odourless white or pale yellow powder (Fig. 7) (Meunier et al. 2014).

It is insoluble in organic media, and a colloidal dispersion is obtained in cold water. However, as the temperature rises, locust bean takes water until dissolution is finally obtained. This solution gels with the addition of small amounts of sodium borate with a high pH (over 7.5). Gels obtained this way are stable, plastic and transparent (Demirci et al. 2014).

Locust bean gum is generally added to the medium when formulating these gels, as concentrations higher than 2–3% lead to a viscous paste that is unable to gel.

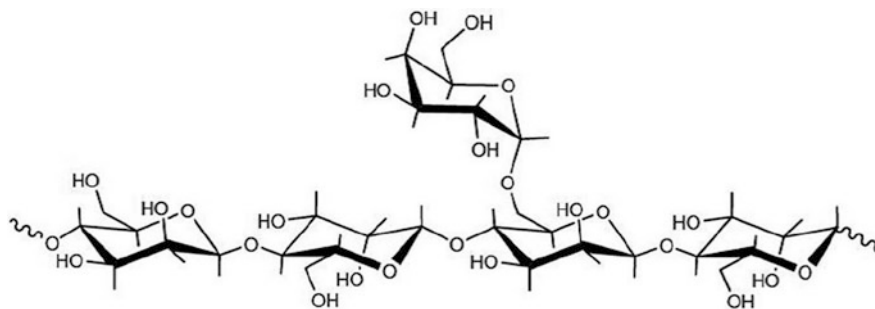


**Fig. 7** Locust bean gum chemical structure

The conventional use of locust bean gum as an excipient in drug products generally depends on the thickening, gel forming and stabilizing properties (Prajapati et al. 2013).

- Gum arabic/Acacia gum

This is the result of the gummy exudate obtained from stems and branches of *Acacia senegal* and other African species in the same genus (Fig. 8). It varies in colour from white to pale yellow or slightly pink. It is semitransparent and odourless, and has a mild mucilaginous flavour (Kuklinski 2000).

It is freely soluble in water and insoluble in ethanol and organic solvents. Gels based on this gum are often not very viscous, so it is always necessary to combine gum arabic with other polymers in order to increase its viscosity and obtain highly mucoadhesive gels (Kaddam et al. 2015; Davaatseren and Hong 2014). This gum is also incompatible with highly oxidizable materials. However, the importance of this polymer in this field is due to its prebiotic properties; when fermented by

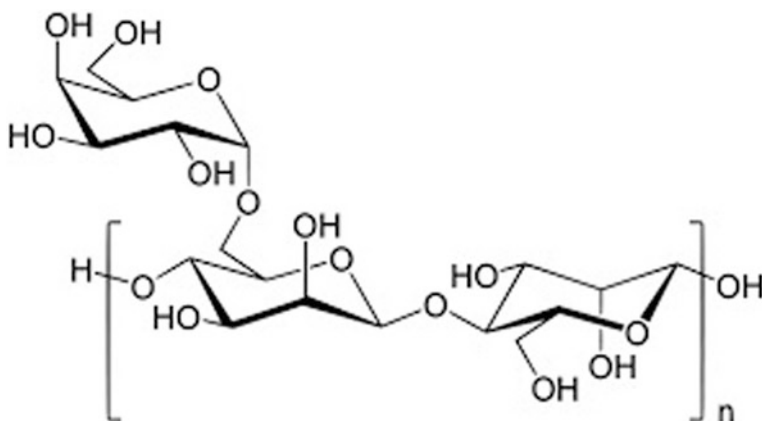


**Fig. 8** Arabic gum chemical structure

*Lactobacillus* bacteria—which colonize the vaginal tract—short-chain fatty acids are released into the medium, which have been shown to have anticarcinogenic, antioxidant and anti-inflammatory properties (Mohamed et al. 2015). The gum also contains cyanogenic glycosides and several enzymes such as oxidases, peroxidases and pectinases, which give it antimicrobial properties. Gum arabic is therefore a potential excipient for the development of mucoadhesive microbicide gels (Pradeep et al. 2012). The availability of other cheaper products has led to a decrease in its use today.

In addition to these gums, gels can also be obtained from several structural and reserve polymers. Some of these polymers are:

- Starch

This is a macromolecule comprising two polysaccharides: amylose (Fig. 9) and amylopectin (Fig. 10). It is the main glucidic reserve in the plant world. Starch granules are insoluble in water but capture water as the temperature rises, triggering a gelling phenomenon. Total gelling of the medium is observed at a wide range of temperatures, and the weight of the granules is another determining factor. When starch dissolves in water, amylose and amylopectin lose their crystallinity and capture water to form a gel. However, when the temperature decreases, the molecules reorganize their structure to form linear chains arranged in parallel lines attached by hydrogen bonds. When this phenomenon occurs, water escapes from the polymer and the phases become separated. Nevertheless, starch granules have been developed that are highly soluble in cold water (Pacheco de Delahaye and Techeira 2009). Starch is also mildly bioadhesive, a property that has been assessed for the development of mucoadhesive vaginal gels (Valenta 2005). Today, starch is more frequently used in the food industry than in the pharmaceutical industry. Pharmaceutical gels containing this modified starch are usually added to other polymers such as chitosan to improve the characteristics of the gel (Kamoun 2016).

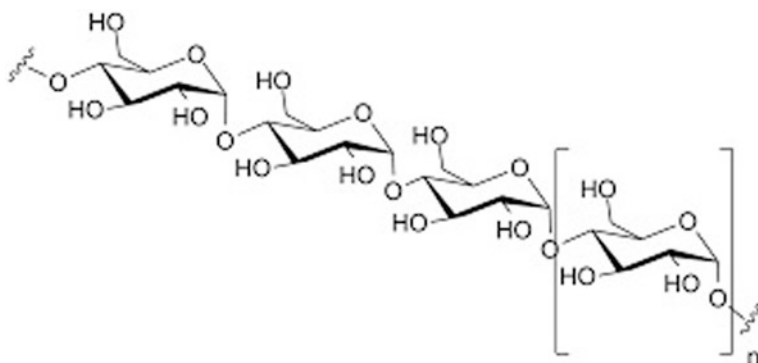


**Fig. 9** Amylose chemical structure



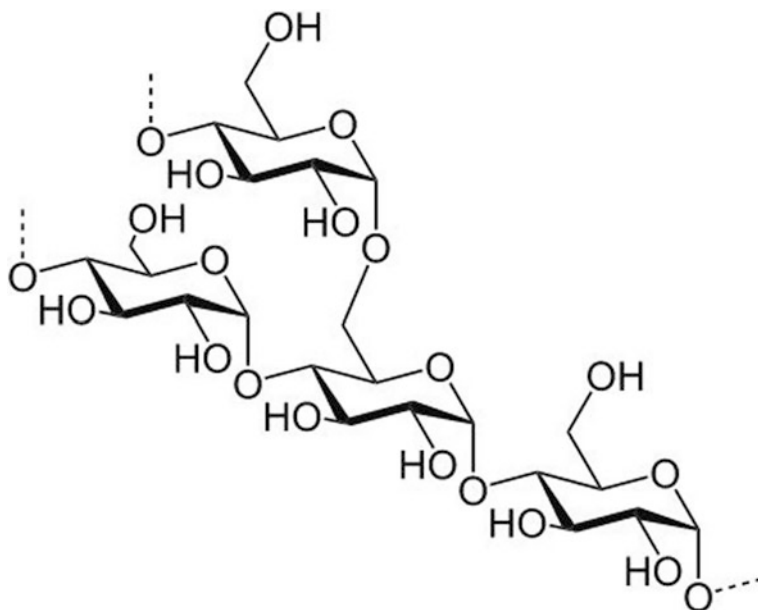


**Fig. 10** Amylopectin chemical structure

- Pectin

The term pectin comprises a group of heteropolysaccharide-based polymers, formed by partially methoxylated polygalacturonic acids (Fig. 11). It is the main component of the middle lamella in plants and is obtained by acid extraction of the inner portion of the pericarp of citric fruits or apples (USP Pharmacopoeia 2016). It consists of linear chains of 1-4 galacturonic acid inserted in 1-2 rhamnoses which may or may not be attached to arabinoses or galactoses.

It is a pale yellow powder, moderately soluble in water, which forms a viscous colloidal and opalescent solution with good flow properties. It is practically insoluble in ethanol and other organic solvents. However, it dissolves more easily in water if it is previously wetted with ethanol or glycerol (USP Pharmacopoeia 2016).

The interleaved rhamnoses generate pectic elbows, whose number conditions the potential to capture water. Pectin-based systems generate swellable, mucoadhesive systems and biocompatible gels. These compounds may therefore be possible potential excipients for the development of vaginal mucoadhesive systems (Mamani et al. 2015).

In recent years, pectin has aroused considerable interest as it can be used for very different applications depending on its physical–chemical parameters and biodegradability.

Pectins are divided into two main groups depending on their degree of esterification: highly methoxylated pectins, poorly methoxylated pectins and other pectic substances such as unmethylated pectins or amidated pectins (Vandamme et al. 2002).

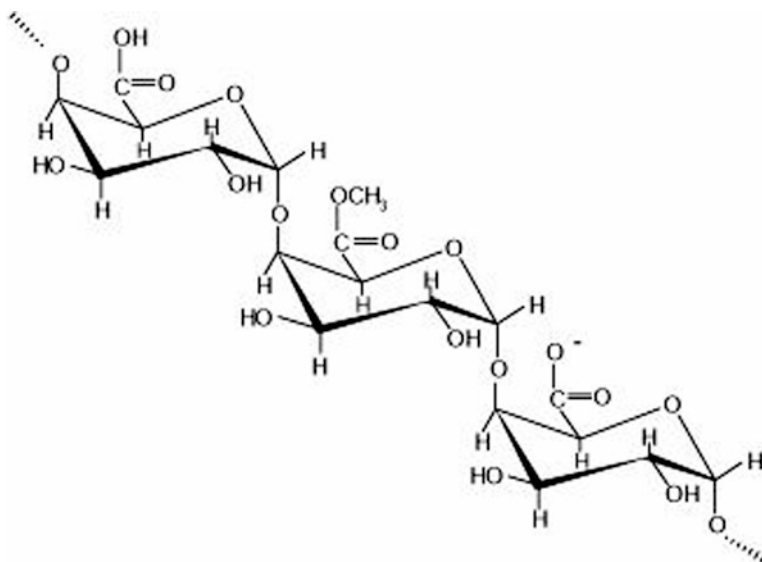


**Fig. 11** Pectin chemical structure

Highly methoxylated pectins have methoxylation values of between 60 and 75%, whereas this value decreases to 20–40% in poorly methoxylated pectins. This difference in the degree of methoxylation directly influences the gelling ability of each pectin; thus, highly methoxylated pectins require a pH range of close to 3 to form gels, are generally soluble in hot water, and must contain a dispersing agent such as dextrose to prevent clumping during gelling. On the other hand, poorly methoxylated pectins produce gels regardless of the pH of the medium, but require the presence of a controlled amount of calcium ions or other divalent cations, and are thus more interesting than highly methoxylated pectins for use in pharmaceutical technology (Sriamornsak 2003; Mamani et al. 2015).

Pectin has been described by the FDA as a safe additive with no daily consumption limit and is widely used as an excipient in matrix tablets, gels, coated tablets and others.

These advantages have led to the use of pectin in the formulation of vaginal gels, as it is completely and quickly biodegradable and leaves little residue after application (Caswell and Kane 2002). It also has bioadhesive properties (Acartürk 2009; Baloğlu et al. 2006; Valenta 2005).

The goal today is to improve mucoadhesive properties and the control of drug release from the polymer. An S-protected thiolated pectin has been synthesized, which shows an increase in the time required for the formulations to disaggregate and has improved rheological properties. This produces a long-lasting formulation in the area of application (Hintzen et al. 2013).

### 6.1.2 Polymers Obtained from Seaweed

The huge biodiversity of seaweed makes this a source of natural polymers with multiple applications, most of them still to be discovered. This group includes some well-known polymers commonly used in the pharmaceutical industry and others with enormous potential that should be studied in more depth.

- Alginate

Alginates are structural components of the cell wall of brown seaweed and are the most abundant polysaccharides in marine algae (Fig. 12). This polymer constitutes up to 40% of the dry weight of seaweed, and its main function is to confer stiffness, elasticity, flexibility and ability to catch water (Avendaño-Romero et al. 2013).

Alginates are mainly extracted from three species of brown algae: *Laminaria hyperborea*, *Ascophyllum nodosum* and *Macrocystis pyrifera*. In their natural state, alginates are presented as a mixture of calcium, magnesium and sodium salts, present in seawater (Lupo Pasin 2015).

Alginates contain varying amounts of  $\beta$ -D-mannuronic acid and  $\alpha$ -L-guluronic acid, which determines the physical properties of the polymer. A hard brittle gel is obtained if their structure contains predominantly  $\alpha$ -L-guluronic acid, while  $\beta$ -D-mannuronic acid endows the gel with softness and elasticity (Madan et al. 2009).

Alginate can be described as a pale white or yellowish-brown odourless powder. It is poorly soluble in water, where it forms a viscous colloidal solution, and practically insoluble in ethanol.

The viscosity of alginate-based solutions depends on the length of the molecules; the longer the chain, the higher the viscosity. When dissolved in water, the molecules become hydrated and its viscosity increases. Viscosity may also vary depending on the polymer concentration, pH, or the presence of metal ions. In acid media, alginates form a high-viscosity gel, as the carboxylic groups of the uronic acids accept protons, which leads to the formation of bonds between molecules of  $\alpha$ -L-guluronic acid (Avendaño-Romero et al. 2013). However, when the pH of the medium is below 4, an inhomogeneous white gel is formed by the precipitation of

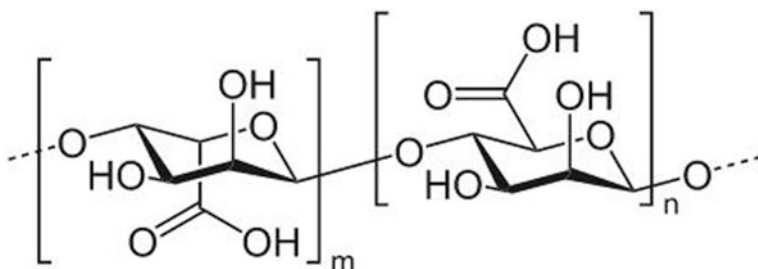


Fig. 12 Alginate chemical structure

alginic acid, producing an increased viscoelastic response due to the presence of a material with the characteristics of an alginate gel. It is therefore not recommended to work below this pH (Lupo Pasin 2015). Although the vaginal environment has an acid pH, under normal conditions it does not fall below pH 4, so alginate gels may be used to develop formulations for vaginal administration. However, in infections which cause acidification of the vaginal environment—such as infections by *Candida albicans*—the use of alginate-based gels may lead to reduced efficacy due to the precipitation of alginic acid and the subsequent modification of the gel's characteristics.

However, although some studies found certain bioadhesive properties (Smart et al. 1984; Szekalska et al. 2015), this polymer has a limited number of sites of interaction with the mucosa (Fuongfuchat et al. 1996). It is an anionic-type polysaccharide, and since the vaginal mucosa has negative charges, mucoadhesion is not prolonged over time. This is why alginate is combined with other polymers with adhesive properties such as chitosan or cellulose derivatives when developing vaginal mucoadhesive formulations (El-Kamel et al. 2002). There are numerous formulations of vaginal gels containing alginate, frequently combined with other polymers, in many different applications (Tasdighi et al. 2012; Zhou et al. 2013).

- Carrageenan

This is a natural sulphated polymer derived from the *Rhodophyceae* family of red algae. It is located in the cell wall and the intercellular matrix of seaweed tissue. It is currently widely used as a food additive, as it is safe for human consumption.

Carrageenans consist of galactose and/or anhydrogalactose joined by alternating  $\alpha$  (1–3) and  $\beta$  (1–4) bonds, resulting in polymers with varying molecular weights, and which have no gelling properties below 100 kDa. Depending on the sulphation positions and the number of sulphate ester groups, there are three main types of carrageenan:  $\iota$ -carrageenan (Fig. 13),  $\kappa$ -carrageenan (Fig. 14), and  $\lambda$ -carrageenan (Fig. 15). Higher levels of sulphation imply lower gel strength and low solubilization temperature. Gelling is easier on  $\kappa$ -carrageenan, which contains between 32% and 39% sulphation, followed by  $\iota$ -carrageenan, with 28–35%, and most difficult on  $\lambda$ -carrageenan, with a sulphation rate of between 25 and 30%.

All carrageenan types are soluble in hot water at temperatures above the gel melting temperature—usually between 40 and 70 °C—but only  $\lambda$ -carrageenan, and  $\kappa$ -carrageenan and  $\iota$ -carrageenan salts dissolve in cold water.

Hot  $\kappa$ -carrageenan and  $\iota$ -carrageenan solutions form thermoreversible gels as they cool. As a hot carrageenan solution cools, its viscosity gradually increases until it reaches gelling temperature, when viscosity suddenly increases dramatically.

Carrageenans have great stability since they retain their properties at high temperatures and at a wide range of pH. Decreases in pH cause the carrageenan to hydrolyse, resulting in decreased viscosity and gel strength. However, no hydrolysis occurs once the gel is formed—even at low pH (3.5–4)—and the gel remains

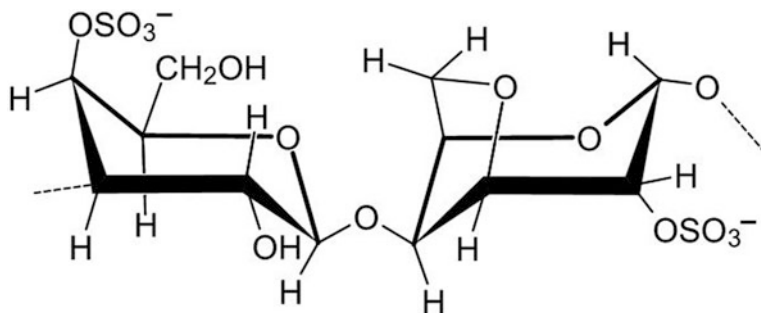


**Fig. 13**  $\alpha$ -Carrageenan chemical structure

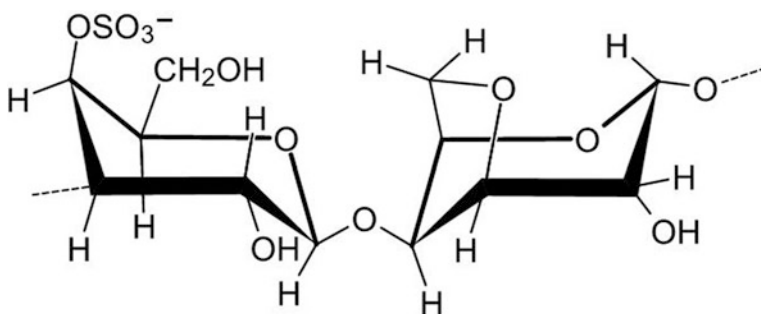


**Fig. 14**  $\kappa$ -Carrageenan chemical structure

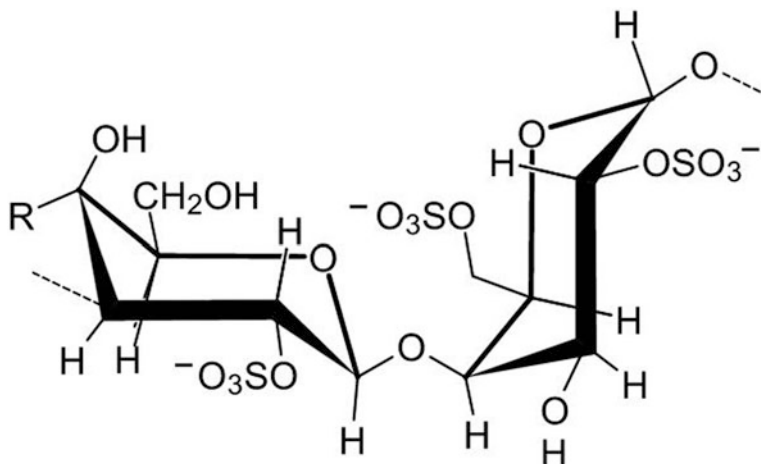


**Fig. 15**  $\lambda$ -Carrageenan chemical structure

stable and can maintain its effectiveness for hours within the vagina. As it is not absorbed, it produces no systemic effects (Valenta 2005).

Their uses include the development of gels with Poloxamer<sup>®</sup>. Results show that the higher the polymer concentration, the greater the control over the release of the drug, and the lower the erosion of the system (Liu et al. 2009). Carrageenan also has a synergy with locust bean gum, as the association improves water retention and gel texture, and forces the brittle gel to become resilient. Another association studied is with starches; the viscosity of the resulting gel is markedly improved compared to carrageenan-based gels.

These compounds have slightly microbicide properties, as they are capable of binding to the surface of some viruses and preventing their adherence to the vaginal mucosa (Sánchez-Sánchez et al. 2015). Thanks to this feature, studies are currently underway into the development of vaginal gels for the prevention of sexually transmitted diseases. For example, Carraguard<sup>®</sup> is an investigational gel whose active ingredient is carrageenan. Studies have shown that it is safe for use in women and that the associated side effects are mild and infrequent. However, phase II trials have failed to demonstrate its effectiveness in preventing HIV transmission (Skoler-Karhoff et al. 2008). Also, under-assessment is a carrageenan-based gel for use as a vehicle for the inclusion of antiretrovirals, such as the combination of MIV-150 and zinc acetate, which are able to inhibit the simian–human immunodeficiency virus from binding to cells (Barnable et al. 2015). Another possibility is to include Griffithsin to prevent the transmission of herpes simplex type 2 or human papillomavirus (Levendosky et al. 2015).

- Agarose

Agar-agar is a structural carbohydrate present in *Agarophyte* seaweed in the genera *Gelidium* and *Gracilaria*. It is a complex mixture of polysaccharide, composed mainly of agarose and agaropectin (Fig. 16). Agarose—which is the gelling fraction—typically represents at least two-thirds of the natural agar.

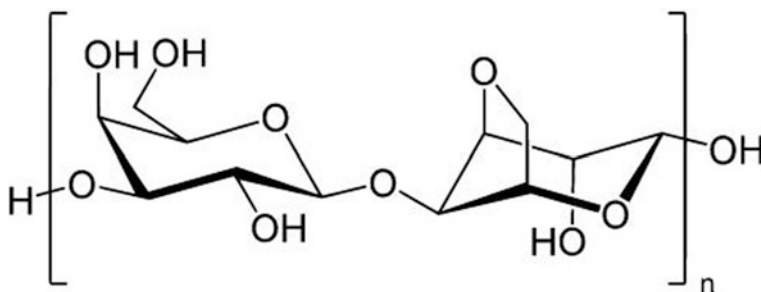


**Fig. 16** Agarose chemical structure

It is insoluble in cold water, but dissolves quickly at temperatures above 65 °C, although there are modified agaroses for which the gelling temperature varies between 17 and 40 °C.

The solution can be cooled to obtain thermoreversible gels even with very low concentrations of agar (0.5–1%). The pH significantly affects the gel strength, whose force decreases in acid media.

Drug delivery systems have been developed based on agarose gels thanks to these properties (Marras-Márquez et al. 2014).

- Ulvan

Ulvan refers to a group of complex sulphated polysaccharides derived from the cell walls of the green algae species *Ulva* and *Enteromorpha* (Robic et al. 2009).

This little-studied polysaccharide has interesting physical–chemical and biological characteristics. It is mainly composed of rhamnose, glucuronic acid, iduronic acid and xylose. It has high charge density, which determines its water solubility. It is a hydrophobic substance which when dissolved in saline solution has low intrinsic viscosities, but is capable of forming gels with borate and divalent cations through mechanisms that remain unclear (Robic et al. 2009). Ulvan-based gels have been found to be thermoreversible, and ion concentration and variations in pH may affect the conformation of the polymer and thus the gelling (Cunha and Grenha 2016).

Its physicochemical, rheological and biological properties suggest it has great potential for future biomedical applications, including drug delivery systems (Cunha and Grenha 2016).

- Fucoidan

Fucoidan is a viscous substance obtained from brown algae (*Phaeophyta*). This is a group of sulphated polysaccharides, which—like ulvan—does not refer to a specific structure, but is the general term given to a family of polysaccharides with a high fucose content.

It is important to determine the solubility and rheological properties of fucoidan to understand its nature and establish different applications. Fucoidan is highly soluble in water, which is directly related to the level of branching and the sulphate group content.

However, despite its hygroscopic behaviour, it is unable to form high-viscosity solutions, so its gelling power is minimal. Its viscoelastic behaviour is maintained over a wide range of pH (5.8–9.5) (Cunha and Grenha 2016).

Unlike other seaweed-based polymers such as carrageenan or ulvan, there is little evidence of the gelling properties of fucoidan. In fact, gelling is observed up to concentrations above 25% (Venugopal 2011), although gels can be formed by combining it with polymers of the opposite charge, due to the electrostatic interactions between the negatively charged sulphate groups from fucoidan and other positively charged polymers such as chitosan (Sezer et al. 2008).

### 6.1.3 Polymers Obtained from Bacteria

- Xanthan gum:

Xanthan is an extracellular polysaccharide produced by fermentation of glucose by the bacterium *Xanthomonas campestris* (Fig. 17). It is a white or cream-coloured odourless powder.

It dissolves in water independently of temperature. Solutions with low concentrations of xanthan gum have a relatively high viscosity, so it is commonly used in concentrations of 1% or less. These solutions are stable over a wide range of pH, temperature and salinity (García-Ochoa et al. 2000).

Its unique characteristics of stability point to this polymer as having significant potential for developing gels which would be able to maintain their viscosity over a wide range of pH and temperature (Sherafudeen and Vasantha 2015; Kocatürk et al. 2015; Shinde and Kanojiya 2014).

It has been studied in the development of medical gels due to its high compatibility with other polymers. When combined with hydroxypropyl methylcellulose (HPMC), it can be used to develop a non-irritating gel capable of remaining attached to the mucosa for extended periods of time (Sherafudeen and Vasantha 2015). The compatibility of xanthan has also been assessed with other gums such as guar gum, and formulations have been developed that are capable of delaying drug release and producing the sustained release of the active ingredient. Xanthan gum has been found to allow better control over drug release compared to guar gum or HPMC (Mughal et al. 2011).

Xanthan gum is one of the polymers that has been observed to provide the best mucoadhesive properties for the development of vaginal gels, thanks to the presence of charged functional groups capable of binding to charges present in the

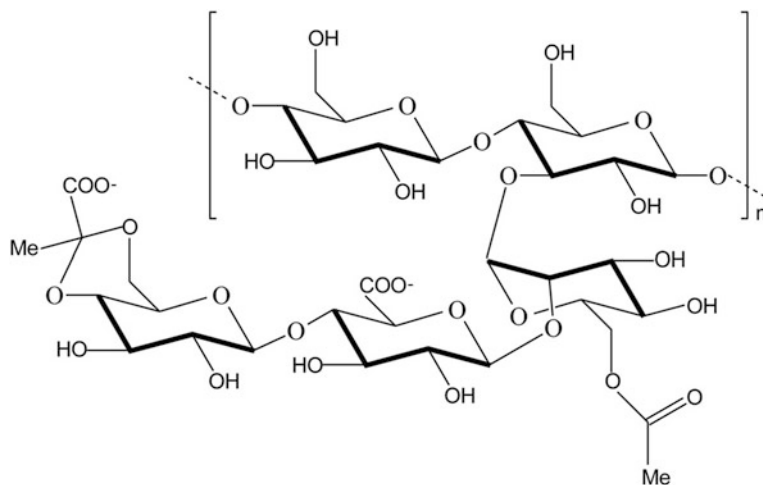


**Fig. 17** Xanthan gum chemical structure



mucosa. It also forms stronger hydrogen bridges than neutral polymers such as guar gum or HPMC hydrogen. Drug release profiles can also be controlled by using anionic polymers such as sodium alginate or xanthan (Tasdighi et al. 2012).

#### 6.1.4 Polymers Obtained from Animals

Gels can also be developed from animal polymers, although they are less common than plant polymers.

- Gelatine

Gelatine is a pure natural protein obtained from animal raw materials through the selective hydrolysis of collagen. The vast majority of gelatines are produced as a white, odourless and tasteless powder.

Gelatine is a thermoreversible hydrocolloid capable of forming a gel when cooling a warm solution. The gel can be melted again at any time.

There are countless types of gelatine that are identified with different parameters. One of the most important of these is the “bloom value” which specifies gelatine gelling ability.

The versatility of gelatine is demonstrated by the large number of applications it has in the pharmaceutical industry. It is especially valued for its ability to form films, its thermoreversible gelling, and its adhesive properties. This polymer is not only used to formulate gels, but it is also the main component of capsules and is present in some tablet formulations.

Gelatine provides the formulation with elasticity, transparency and gloss and melts at body temperature, enabling rapid release of the active ingredients.

The oldest known vaginal drug delivery systems were based on gelatine and so can be considered to be the first mucoadhesive release systems. Although there are numerous gelling polymers today that offer an alternative to gelatine, some gels still include this polymer (Zhuang et al. 2016; Pawar and Pande 2015).

- Chitosan

Chitosan is a natural polycationic copolymer of glucosamine and N-acetylglucosamine obtained by partial deacetylation of chitin, a structural element in the exoskeleton of crustaceans (Fig. 18) (Ruiz-Caro et al. 2012).

Chitin is the most abundant organic substance in nature after cellulose, but is highly insoluble in water—which limits its applications—and has low reactivity. Chitosan is N-deacetylated chitin, a modification that offers better reactivity and solubility properties. It is obtained by replacing the acetamide groups in chitin with amino groups by treating chitin with a strong alkali (Mármol et al. 2011).

The presence of hydroxyl and amino groups permits adhesion to the mucosa by hydrogen bonds. They also give the polymer an acid pKa, so they are protonated in the vaginal environment and improve adhesion as the mucosa has a negatively charged surface.

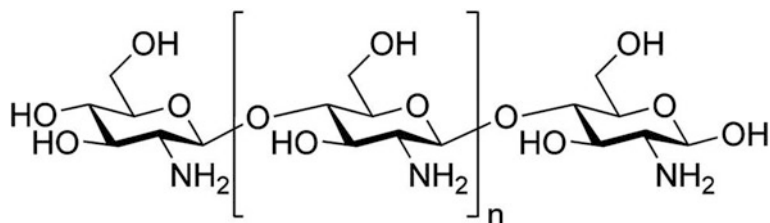


**Fig. 18** Chitosan chemical structure

Chitosan is biocompatible and biodegradable and has been used to develop numerous systems for vaginal administration such as tablets, emulsions and gels. Formulations containing this excipient have sustained release (Illum 1998; Dodane and Vilivalam 1998), mucoadhesive properties (Sánchez-Sánchez et al. 2015) and antimicrobial activity (Kim et al. 2003; Luessen et al. 1996).

The introduction of thiol groups can improve the mucoadhesive properties of the formulation while maintaining biocompatibility (Berknop-Snürch et al. 2004), which can lead to drug release over a longer period of time in the application area (Duchene and Ponchel 1992). This can be useful in systems with long-lasting controlled drug release, as formulations can be obtained that are more convenient for the patient.

Formulations based on chitosan salts—such as chitosan citrate—have also been studied and yield gels capable of modulating the release of acyclovir and promoting its absorption in the vaginal mucosa. They have microbicide properties due to the presence of citrate, which is responsible for complexing the calcium and zinc ions, and this is directly related to the infection process (Bonferoni et al. 2008).

- Hyaluronic acid

Hyaluronic acid is a polymer in the glycosaminoglycan group, composed of disaccharide units of N-acetylglucosamine and glucuronic acid linked by a glycosidic bond (Fig. 19). It is found naturally in the body carrying out a structural function, signifying it is absolutely biocompatible. It is also capable of modulating drug release.

It is a sticky crystalline substance both in the human body and when produced synthetically. Hyaluronic acid is a hydrophilic molecule with the ability to increase its size a thousand times thanks to its water uptake. It has anti-inflammatory, regenerating and healing properties. The use of vaginal gels based on this polymer for the treatment of infections not only prevents irritation even after continuous applications, but would have a beneficial effect on the vaginal mucosa.

There are numerous references to its use in gels and creams for vaginal application, usually based on the specific therapeutic properties offered by the polymer (Hedén et al. 2016). Other active ingredients can be included in this gel, such as oestrogen for the treatment of vaginal atrophy in postmenopausal women (Jokar et al. 2016).

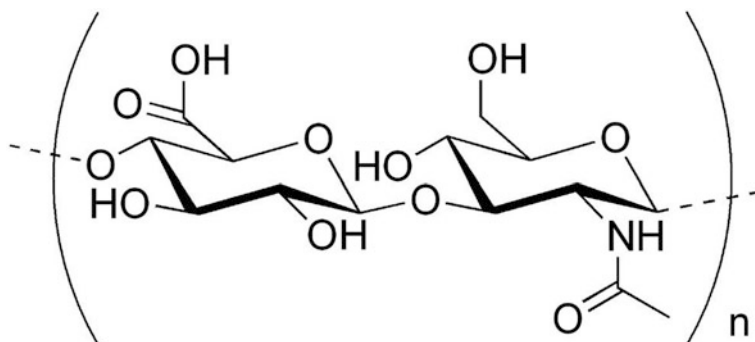


**Fig. 19** Hyaluronic acid chemical structure

Hyaluronic acid microspheres have been formulated as vaginal drug delivery systems thanks to their ability to modulate drug release. Studies are currently underway into the development of microspheres comprising hyaluronic esters in order to slow the release of active ingredients by the same route (Richardson and Trevor 1999).

## 6.2 Semisynthetic Polymers

### 6.2.1 Cellulose Derivatives

Cellulose is the most abundant organic biomolecule in the world, as it is the main structural component in plants. Cellulose derivatives are semisynthetic polymers obtained by chemically modifying cellulose to obtain more inert substances with different solubility or higher mechanical strengths. They are usually less sensitive to the action of microorganisms, besides having excellent qualities of stability and application (Shokri and Adibkia 2013; Granström 2009). They are widely used in the pharmaceutical industry, and the most important are cellulose ethers such as ethyl cellulose (Fig. 20), methyl cellulose (Fig. 21), carboxymethyl cellulose (Fig. 22), hydroxypropyl cellulose (Fig. 23), hydroxymethyl cellulose and hydroxymethylpropyl cellulose (Fig. 24) (Shokri and Adibkia 2013).

Cellulose ethers are high molecular weight compounds produced by substituting hydrogen atoms in the hydroxyl groups in the anhydroglucose units of cellulose with alkyl or substituted alkyl groups. The properties conferred by each derivative depend on their molecular weight, chemical structure, the distribution of substituent groups and the degree of substitution. These characteristics affect their solubility, solution viscosity and stability to biodegradation, heat, hydrolysis and oxidation (Shokri and Adibkia 2013).

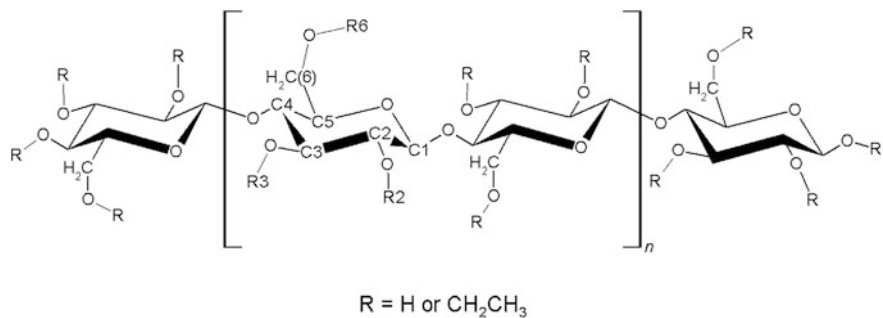


**Fig. 20** Ethyl cellulose chemical structure

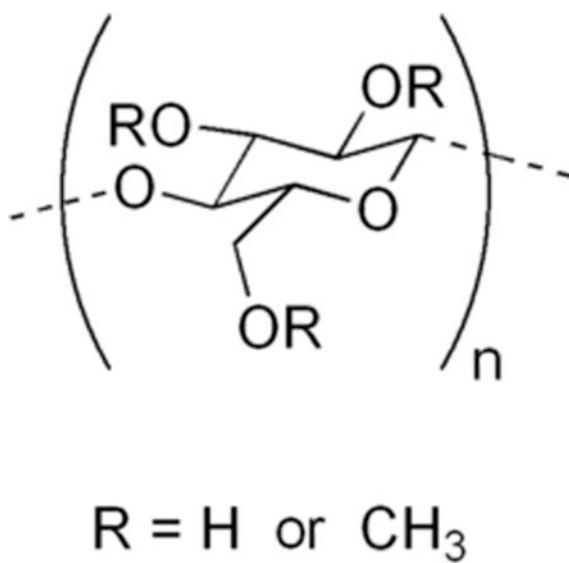


**Fig. 21** Methyl cellulose chemical structure

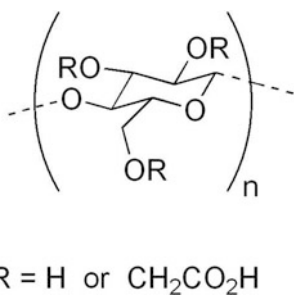


**Fig. 22** Carboxymethyl cellulose chemical structure

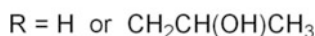
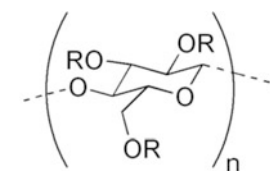


**Fig. 23** Hydroxypropyl cellulose chemical structure

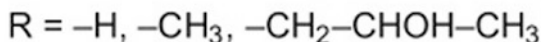
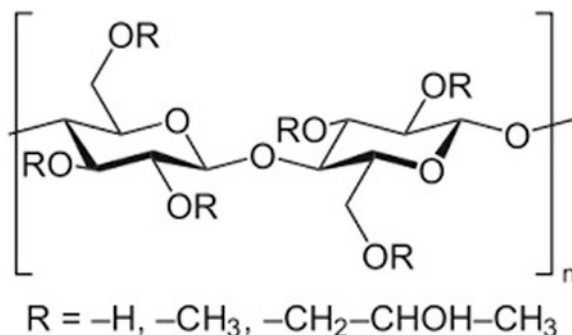


**Fig. 24** Hydroxypropylmethyl cellulose chemical structure

These nonionic compounds are soluble in water and simple alcohols, and in some organic solvents.

In terms of their application in vaginal formulations, a variety of studies have shown that formulations with these polymers can remain for several days in the mucosa without any significant toxic effects or physiological changes, which could prolong drug residence at the site of action (Ceschel et al. 2001).

Cellulose ethers are generally hydrophilic and form a hydrogel when exposed to water. Although some are water insoluble, as is the case of ethylcellulose, most are soluble in aqueous medium (methyl cellulose, hydroxypropyl cellulose or hydroxypropyl methyl cellulose) (Shokri and Adibkia 2013).

Numerous vaginal gels are formulated with cellulose derivatives, such as hydroxyethyl cellulose (Richardson et al. 2013; Li et al. 2012), hydroxypropyl methyl cellulose (Wu et al. 2015; Tasdighi et al. 2012; Chatterjee et al. 2011) and sodium carboxymethyl cellulose (Tasdighi et al. 2012). So, frequent is the use of these polymers in the development of vaginal gels that a hydroxyethyl cellulose gel known as “universal placebo” is often used to assess the effectiveness of vaginal gels in clinical trials (Ravel et al. 2012; Anton et al. 2012). Solid formulations obtained by compression, and consisting solely of HPMC, have shown mucoadhesion times of over 70 h and a sustained drug release of over 40 h. These results

point to this polymer as an interesting excipient for the development of mucoadhesive tablets capable of gelling in the vaginal environment, thereby allowing a sustained release of the drug (Perioli et al. 2011; Notario-Pérez et al. 2018).

## 6.3 Synthetic Polymers

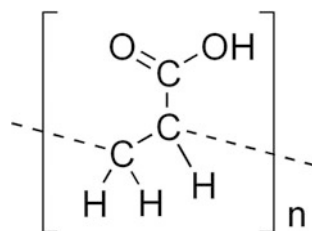
### 6.3.1 Acrylic Acid Derivatives

This group includes synthetic derivatives of polyacrylic acids from the polymerization of acrylic acid esters and salts (Fig. 25).

Polyacrylic acid is a synthetic polymer with a high molecular weight. It is an anionic polymer which loses protons and acquires negative charge in aqueous solution, giving it the ability to absorb and retain water and swell to many times its original volume, so it acts as a hydrogel. Due to its solubility and viscosity, it is used primarily as an adhesive agent. The bioadhesive properties of polyacrylic acids are widely known, and they have great potential for the development of vaginal mucoadhesive formulations. They can interact with mucous membranes by means of hydrogen bonds through the ionized carbonyl groups (Shah and Donovan 2007).

These polymers have excellent rheological (high viscosity) and swelling characteristics, favouring a sustained release of the active ingredient. They also have good adhesive properties (well known even at the industrial level), which has led to research into their use in ocular, oral and vaginal formulations, with promising results (Dittgen et al. 1997). Hydrogels containing these polymers are often found as mucoadhesive drug delivery systems (Nishikawa et al. 2008). The properties of acrylic acid derivatives make them good candidates for vaginal gels, such as BufferGel<sup>®</sup>, an aqueous gel based on Carbopol<sup>®</sup> that has proved to be spermicidal and to have some activity against HIV and herpes simplex type 2 (Rohan and Sassi 2009). Different formulations combine these derivatives with other polymers in the development of vaginal mucoadhesive gels (Cevher et al. 2008).

**Fig. 25** Polyacrylic acid chemical structure



### 6.3.2 Polyethylene Glycols

This polyether is widely used in pharmaceutical industry and is also known as macrogol, polyethylene oxide, or polyoxyethylene (Fig. 26). It is generally associated with a number referring to the molecular mass of the polymer. It is soluble in water; the higher the molecular weight of the polymer, the greater its solubility.

Its multiple potential uses vary depending on the molecular weight and the specific hydration and diffusion coefficient of the gels generated; these factors modify the release profile of the drug from the dosage form.

There are some examples of vaginal gels including this polymer, although the gels were never formulated solely with polyethylene glycol, but combined with other polymers (Rajan et al. 2014; Pedersen et al. 2014).

### 6.3.3 Polyvinyl Alcohol

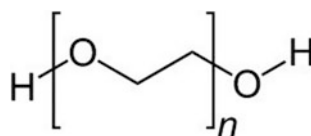
Polyvinyl alcohol has excellent adhesive and film-forming properties, besides being odourless and non-toxic (Fig. 27). It forms a reversible colloid in hot water and is insoluble in cold water. At 20 °C, it swells and forms a gel when it is used in concentrations of between 38 and 75%.

Hydrogels with potential biomedical applications can therefore be developed based on polyvinyl alcohol (Arredondo et al. 2011; Hwang et al. 2010).

### 6.3.4 Polyvinyl pyrrolidone

Polyvinyl pyrrolidone, also known as povidone, is another completely harmless polymer (Fig. 28). Its properties are similar to polyvinyl alcohol, which is noted for its excellent bioadhesion. It is soluble in water and other polar solvents, and has high hygroscopicity, with the ability to absorb up to 40% of its weight in water. Gels are therefore formulated with this polymer for administration on mucosa (Vokurka et al. 2011).

**Fig. 26** Polyethylene glycol chemical structure



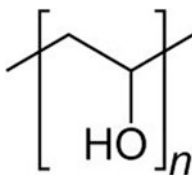


**Fig. 27** Polyvinyl alcohol chemical structure

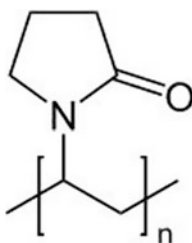


**Fig. 28** Polyvinyl pyrrolidone chemical structure

## 7 Applications of Vaginal Gels

Because of all the advantages of vaginal gels, as stated above, they are possibly the most commonly used dosage form for vaginal administration. Vaginal gels can therefore be found with very different active ingredients and a wide variety of applications. The main uses of vaginal gels are described below.

### 7.1 *Lubricants and Contraceptives*

Vaginal dryness is a common condition in women of all ages, but particularly prevalent around menopause (Edwards and Panay 2016). Vaginal lubricants are commonly used by women either prior to sex for comfort and to avoid pain or independent of relations for the treatment of vaginal dryness (Edwards and Panay 2016; Carati et al. 2016). Hydrogels are the optimal dosage form for this purpose, as they are a quick and easy method of relieving short-term symptoms and produce a moisturizing and refreshing effect which alleviates dryness. The use of a water-soluble vaginal lubricant during sexual intercourse is more advisable than products such as Vaseline or mineral oils that can damage latex condoms or diaphragms (Edwards and Panay 2016).

The use of contraceptive gels is also common prior to intercourse; these tend to have a dual effect as a lubricant and contraceptive. They typically contain



spermicidal substances which immobilize or inactivate sperm to prevent conception (Gupta et al. 2016; Jain et al. 2014).

## **7.2 *Hormone Replacement Therapy (HRT)***

Another use of vaginal gels is for hormone replacement therapy in postmenopausal women. The most widespread are gels containing oestrogen or progesterone that help the overall symptomatology, but also relieve urogenital atrophy, prevent osteoporosis, and pose a lower cardiovascular risk than oral administration (Delgado et al. 2016).

There are numerous studies on vaginal gels for the treatment of vaginal atrophy (Al-Saqi et al. 2016). Tuğcu-Demiröz et al. developed long-acting mucoadhesive gels containing oxybutynin as a drug and compared them to oxybutynin immediate release tablets. The polymers they included in the formulations were chitosan, hydroxypropylmethyl cellulose and poloxamer 407. Gels with hydroxypropylmethyl cellulose showed the highest viscosity and adhesiveness, cohesiveness and mucoadhesion and had adequate permeation across the vaginal mucosa and the highest relative bioavailability (compared to tablets). These vaginal gels represent an alternative in the treatment of overactive bladder and vaginal dryness in postmenopausal women (Tuğcu-Demiröz et al. 2013).

The moisturizing effect of these gels makes them the most appropriate form for administering the treatment, as the gel lubricates and moisturizes the vaginal mucosa and the hormones in the formulation prevent dryness (Caruso et al. 2016).

## **7.3 *Labour Induction***

Although the use of intravenous oxytocin is still the main method of inducing labour, the vaginal administration of formulations to induce labour once pregnancy has reached term is increasingly being recommended. Again, vaginal gels are the dosage form of choice, as the most common treatment is a vaginal gel with prostaglandin E2 (Beckmann et al. 2016; Kehl et al. 2016; Beckmann et al. 2015). The administration of this gel produces the onset of contractions and also ensures the cervix is in a more favourable environment for giving birth (Beckmann et al. 2015).

## **7.4 *Treatment of Vaginal Infections***

Local drug delivery is usually the first treatment option in the case of vaginal infections, as higher concentrations of the active ingredient can be delivered at the site where it must exert its action, and there are fewer side effects as systemic drug

exposure is reduced. Vaginal gels are an easy form of application able to release the drug quickly, thereby taking effect more quickly than other dosage forms.

For example, mucoadhesive and thermosensitive gels for vaginal controlled release of Cidofovir have been developed and characterized. The polymers used were chitosan, Carbopol® 974P, HPMC and poloxamer 407. As in the other work, gels with HPMC showed the highest viscosity, adhesiveness, cohesiveness and mucoadhesion values. The *in vitro* antitherpetic effect of these gels containing the drug was demonstrated using Vero cells. These formulations may therefore be a promising alternative for the treatment of genital herpes and human papilloma virus infections in women (Tuğcu-Demiröz et al. 2015). It is also worth mentioning a mucoadhesive *in situ* gel containing clotrimazole for treating vaginal candidiasis that was formulated and evaluated by Rençber et al. (2016). They used poloxamer 407 and 188 as gelling agents, and HPMC K100M as an excipient for improving mechanical, mucoadhesive and vaginal residence time. They concluded that gels with 20% poloxamer 407, 10% poloxamer 188 and 0.5% HPMC could be alternative clotrimazole formulations in vaginal candidiasis therapy based on their properties and their vaginal mucosa residence time (even 24 h after application).

Gels are therefore commonly used to treat infections of this kind, such as bacterial vaginosis (Masoudi et al. 2016; Melis et al. 2016; Schwebke et al. 2015; Xiao et al. 2015), vaginitis (Karamisheva and Nachev 2015), candidiasis (Berretta et al. 2013; Rençber et al. 2016) and genital herpes (Tuğcu-Demiröz et al. 2015).

In addition to traditional gels, there are also examples of bigels developed to treat vaginal infections. Sagiri et al. (2015) developed bigels composed of a gelatine-based hydrogel and a stearic acid-based gel with sesame or pea oil as an organic solvent. The resulting bigels were mucoadhesive and biocompatible and allowed the release of ciprofloxacin through a diffusion mechanism, resulting in good antimicrobial efficacy against *E. coli*. Singh et al. prepared bigels with sesame oil and sorbitan monostearate as components in the organogel and a Carbopol® 934-based hydrogel. These gels contained metronidazole for the treatment of bacterial vaginosis and showed biocompatibility, diffusion-mediated drug release and good antimicrobial effectiveness against *E. coli* (Singh et al. 2014a). In another study, Singh et al. developed and characterized bigels consisting of a guar gum-based hydrogel, an organogel with sesame oil as a solvent and sorbitan monostearate as organogelling for controlled drug release. These bigels were biocompatible, and ciprofloxacin showed release kinetics based on zero-order diffusion, which is highly suited to control release formulations. They had good antimicrobial efficiency against *Bacillus subtilis* and showed promise as topical drug delivery alternatives (Singh et al. 2014b).

## 7.5 Microbicides

Although not many vaginal microbicide formulations are currently commercially available, they are becoming considerably interesting. There are numerous studies

on the development of microbicides against various infectious agents, since this has been the main focus of the research on microbicides in the last two decades. Pre-exposure topical prophylactic microbicides are products that can be applied vaginally to protect the user from sexually transmitted diseases.

The effectiveness of any microbicide product depends on the effectiveness of the product and the willingness and ability of the user to use the product as directed (acceptability and adherence). The formulation of a microbicide is evidently therefore of great importance. Gels have historically been the most common dosage form for microbicide products for vaginal administration. These gels typically require a daily dose or a single dose before and/or after sexual intercourse. The advantages of vaginal gels include the patient's familiarity with their use for this purpose, the lubricating effect which favours sexual pleasure, and the fact that they are easy and inexpensive to manufacture (Ferguson and Rohan 2011).

In addition to providing a suitable administration route for the active ingredient, vaginal gels can provide additional benefits to the user. Lubrication—as mentioned previously—is one such advantage, as it may reduce the likelihood of genital abrasions induced by penetration and thus the risk of acquiring sexually transmitted diseases. Once applied, vaginal gels can provide a physical barrier to prevent epithelial penetration of the infectious agent (Ferguson and Rohan 2011).

We found vaginal microbicides under research for the prevention of many infectious agents including HIV, due to the severity of the infection and the lack of a treatment to eliminate the virus once acquired (Doggett et al. 2015; Jarrett et al. 2016; Tintori et al. 2016).

Vaginal administration of these drugs may be advantageous given that the female lower genital tract is the site of acquisition of sexually transmitted male-to-female diseases (Ferguson and Rohan 2011).

## 8 Smart Gels: Hydrogels Responsive to Stimulation

Although one of the traditional limitations of gels is the lack of control over drug release, significant progress has been made in this area in the last decade. Not only have controlled release systems been successfully developed that are capable of providing sustained release of the active ingredient, but it is now also possible to develop gels that are sensitive to certain stimuli, in the presence of which they are able to release the drug (Masteiková et al. 2003).

### 8.1 Gels Sensitive to Temperature

These gels swell or deflate depending on temperature variations in the environment. They may be “sensitive to negative temperature” and release drugs at temperatures below the “low critical solution temperature”, but not above. Pulsatile releases are

achieved with copolymer structures of N-isopropyl acrylamide. These types of hydrogels are very interesting for modified protein release and may also be sensitive to positive temperature, when they swell at temperatures above the high critical solution temperature, while no drug is released below this threshold. They include polyacrylic acid, polyacrylamide and poly (acrylamide-co-butyl methacrylate) gels. Solutions of some polymers—such as poloxamer—are easy to administer as a liquid that gels at body temperature. Polymer formulations have been developed for vaginal drug delivery which gel in situ based on their thermoplastic behaviour. They are currently being used to study prolonged release of oestrogen, peptides, proteins, progestins and nonoxynol-9. Chang et al. (2002) have proposed a mucoadhesive thermosensitive gel with greater and more prolonged release of clotrimazole than conventional formulations.

## ***8.2 Gels Sensitive to pH***

The polymers constituting these gels have acid and/or basic groups and undergo proton exchange with the environment depending on its pH. Hydrogels with polymers containing weakly acidic groups will have increased swelling in basic media. Conversely, if the polymer groups are weakly basic, this property of the gel will decrease in high pH environments. Carbopol<sup>®</sup> is a notable example of the first group (Soppimath et al. 2002).

## ***8.3 Gels Sensitive to Electrical Signals***

Gelling polymers usually have ionizable functional groups that are responsible for the shrinking or swelling of these gels in the presence of an electric field. The polymers studied for inclusion in controlled release hydrogels by this method include chitosan and chondroitin 4-sulphate (Jensen et al. 2002; Ramanathan and Block 2001).

## ***8.4 Gels Sensitive to Light***

Formation in situ by photo-polymerization with injection or application has been studied in tissue engineering, wound healing and controlled drug release (Anseth et al. 2002; Obara et al. 2003). For example, Matsuda (2002) developed an adhesive system based on the formation of a gelatine gel in damaged tissue with the consequent sustained release of a drug.

### **8.5 Gels Sensitive to Ions**

These are polymer structures that gel in the presence of certain ions. For example, iota-carrageenan and alginic acid form gels in the presence of calcium ions, while gellan gum does so in the presence of magnesium, sodium and potassium ions (Bhardwaj et al. 2009; Guo et al. 1998).

### **8.6 Gels Sensitive to Glucose**

The polymers in the gel swell and release the insulin contained within their structure and increase blood glucose (Podual et al. 2000). This is caused by a change in pH, so they could be said to be a subtype of pH-sensitive hydrogels.

## **9 Conclusions and Future Perspectives**

All these considerations point to vaginal administration as a potential route for both local and systemic administration of drugs, although it is worth noting the continual fluctuations in the parameters that affect drug release and absorption.

Gels are the most common dosage form, as they allow easy and convenient administration by the patient, and are widely accepted by users. They are also easy to produce, and their manufacturing costs are therefore not very high.

Current research is aimed at developing vaginal gels based on polymers with good mucoadhesive and gelling capabilities, with the ultimate goal of achieving an inexpensive and of course biocompatible product. It is particularly worth highlighting polymers derived from seaweed, as although they are still uncommon, they may have enormous potential for application in pharmaceutical development.

The gels currently on the market are incapable of retaining the drug for long periods of time, so future research could be directed towards designing gels that allow controlled and sustained release of the active ingredient. For example, new controlled release products currently in research are directed towards the uterine mucus, where they are deposited and could serve as a reservoir for such systems, releasing the drug in a controlled manner (Rohan and Sassi 2009).

Most of the present and undoubtedly the future research into clinical applications will focus on developing vaginal microbicides, which are needed to provide women with readily available methods for preventing sexually transmitted diseases that they can control themselves. Several factors are involved in developing these microbicides, because although their safety and efficacy are of paramount importance, other significant aspects that contribute significantly to decision making in the design of delivery systems for vaginal microbicides include acceptance by the patient and treatment adherence (Rohan and Sassi 2009).

## References

- Acartürk F (2009) Mucoadhesive vaginal drug delivery systems. *Recent Pat Drug Deliv Formul* 3:193–205
- Ahmad FJ, Alam MA, Khan ZI, Khar RK, Ali M (2008) Development and in vitro evaluation of an acid buffering bioadhesive vaginal gel for mixed vaginal infections. *Acta Pharm* 58: 407–419
- Akil A, Agashe H, Dezzutti CS, Moncla BJ, Hillier SL, Devlin B, Shi Y, Uranker K, Rohan LC (2015) Formulation and characterization of polymeric films containing combinations of antiretrovirals (ARVs) for HIV prevention. *Pharm Res* 32:458–468
- Alexander NJ, Baker E, Kaptein M, Karck U, Miller L, Zampaglione E (2004) Why consider vaginal drug administration. *Fertil Steril* 82:1–12
- Al-Saqi SH, Jonasson AF, Naessén T, Uvnäs-Moberg K (2016) Oxytocin improves cytological and histological profiles of vaginal atrophy in postmenopausal women. *Post Reprod Health* 22:25–33
- Anseth KS, Metters AT, Bryant SJ, Martens PJ, Elisseff JH, Bowman CN (2002) In situ forming degradable networks and their application in tissue engineering and drug delivery. *J Control Release* 78:199–209
- Anton PA, Cranston RD, Kashuba A, Hendrix CW, Bumpus NN, Richardson-Harman N, Elliott J, Janocko L, Khanukhova E, Dennis R, Cumberland WG, Ju C, Carballo-Diéguez A, Mauck C, McGowan I (2012) RMP-02/MTN-006: A phase 1 rectal safety, acceptability, pharmacokinetic, and pharmacodynamic study of tenofovir 1% gel compared with oral tenofovir disoproxil fumarate. *AIDS Res Hum Retroviruses* 28:1412–1421
- Arredondo A, Patiño JF, Londoño ME, Echeverri CE (2011) Matriz a partir de un hidrogel de alcohol polivinílico (PVA) combinada con sulfadiazina de plata con potencial aplicación en el manejo y control de la sepsis en heridas dérmicas. *Revista Iberoamericana de Polímeros* 12:178–187
- Auslander BA, Perfect MM, Breitkopf DM, Succop PA, Rosenthal SL (2007) Microbicides: information, beliefs, and preferences for insertion. *J Womens Health* 16:1458–1467
- Avendaño-Romero GC, López-Malo A, Palou E (2013) Propiedades del alginato y aplicaciones en alimentos. *Temas Selectos de Ingeniería de Alimentos* 7:87–97
- Baena Y, Dallos LJ, Manzo RH, Ponce D'León LF (2011) Estandarización de celdas de Franz para la realización de ensayos de liberación de fármacos a partir de complejos con polielectrolitos. *RevDOI Colomb Cienc Quím Farm* 40(2):174–188
- Baloglu E, Ozyazici M, Yaprak Hizarcioğlu S, Senyigit T, Ozyurt D, Pekçetin C (2006) Bioadhesive controlled release systems of ornidazole for vaginal delivery. *Pharm Dev Technol* 11:477–484
- Baloglu E, Senyigit ZA, Karavana SY, Bernkop-Schnurch A (2009) Strategies to prolong the intravaginal residence time of drug delivery systems. *J Pharm Pharm Sci* 12:312–336
- Barnable P, Calenda G, Bonnaire T, Menon R, Levendosky K, Gettie A, Blanchard J, Cooney ML, Fernández-Romero JA, Zydowsky TM, Teleshova N (2015) MIV-150/zinc acetate gel inhibits cell-associated simian-human immunodeficiency virus reverse transcriptase infection in a macaque vaginal explant model. *Antimicrob Agents Chemother* 59:3829–3837
- Beckmann M, Kumar S, Flenady V, Harker E (2015) Prostaglandin vaginal gel induction of labor comparing amniotomy with repeat prostaglandin gel. *Am J Obstet Gynecol* 213:1–9
- Beckmann M, Merollini K, Kumar S, Flenady V (2016) Induction of labor using prostaglandin vaginal gel: cost analysis comparing early amniotomy with repeat prostaglandin gel. *Eur J Obstet Gynecol Reprod Biol* 199:96–101
- Berknop-Snürch A, Hornof M, Guggi D (2004) Thiolated chitosans. *Eur J Pharm Biopharm* 57:9–17
- Berretta AA, de Castro PA, Cavalheiro AH, Fortes VS, Bom VP, Nascimento AP, Marquete-Oliveira F, Pedrazzi V, Ramalho LN, Goldman GH (2013) Evaluation of mucoadhesive gels with propolis (EPP-AF) in preclinical treatment of candidiasis vulvovaginal infection. *Evid Based Complement Alternat Med* 2013:641480

- Bhardwaj TR, Kanwar M, Lal R, Gupta A (2009) Natural gums and modified natural gums as sustained-release carriers. *Drug Devel Ind Pharm* 26:1025–1038
- Bonferoni MC, Sandri G, Rossi S, Ferrari F, Gibin S, Caramella C (2008) Chitosan citrate as multifunctional polymer for vaginal delivery. Evaluation of penetration enhancement and peptidase inhibition properties. *Eur J Pharm Sci* 33:166–176
- Braunstein S, van de Wijgert J (2005) Preferences and practices related to vaginal lubrication: implications for microbicide acceptability and clinical testing. *J Womens Health* 14:424–433
- Buckheit RW, Watson KM, Morrow KM, Ham AS (2010) Development of topical microbicides to prevent the sexual transmission of HIV. *Antiviral Res* 85:142–158
- Burns RN, Hendrix CW, Chaturvedula A (2015) Population pharmacokinetics of tenofovir and tenofovir-diphosphate in healthy women. *J Clin Pharmacol* 55:629–638
- Burruano BT, Schnaare RL, Malamud D (2002) Synthetic cervical mucus formulation. *Contraception* 66:137–140
- Carati D, Zizza A, Guido M, De Donno A, Stefanizzi R, Serra R, Romano I, Ouedraogo C, Megha M, Tinelli A (2016) Safety, efficacy, and tolerability of differential treatment to prevent and treat vaginal dryness and vulvovaginitis in diabetic women. *Clin Exp Obstet Gynecol* 43:198–202
- Caruso S, Cianci S, Amore FF, Ventura B, Bambili E, Spadola S, Cianci A (2016) Quality of life and sexual function of naturally postmenopausal women on an ultralow-concentration estriol vaginal gel. *Menopause* 23:47–54
- Caswell M, Kane M (2002) Comparison of the moisturization efficacy of two vaginal moisturizers: Pectin versus polycarbophil technologies. *J Cosmet Sci* 53:81–87
- Ceschel GC, Maffei P, Lombardi BS, Ronchi C, Rossi S (2001) Development of a mucoadhesive dosage form for vaginal administration. *Drug Dev Ind Pharm* 27:541–554
- Cevher E, Sensov D, Taha MA, Araman A (2008) Effect of thiolated polymers to textural and mucoadhesive properties of vaginal gel formulations prepared with polycarbophil and chitosan. *AAPS PharmSciTech* 9:953–965
- Chang JY, Oh YK, Kong HS, Kim EU, Jang DD, Nam KT, Kim CK (2002) Prolonged antifungal effects of clotrimazole-containing mucoadhesive thermosensitive gels on vaginitis. *J Control Release* 82:39–50
- Chatterjee A, Bhowmik BB, Thakur YS (2011) Formulation, in vitro and in vivo pharmacokinetics of anti-HIV vaginal bioadhesive gel. *J Young Pharm* 3:83–89
- Chivate AA, Poddar SS, Abdul S, Savant G (2008) Evaluation of *Sterculia foetida* gum as controlled release excipient. *AAPS PharmSciTech* 9:197–204
- Clark MR, Peet MM, Davis S, Doncel GF, Friend DR (2014) Evaluation of rapidly disintegrating vaginal tablets of Tenofovir, Emtricitabine and their combination for HIV-1 prevention. *Pharmaceutics* 6:616–631
- Coggins C, Elias CJ, Atisook R, Bassett MT, Ettiègne-Traoré V, Ghys PD, Jenkins-Woelk L, Thongkrajai E, VanDevanter NL (1998) Women's preferences regarding the formulation of over-the-counter vaginal spermicides. *AIDS* 12:1389–1391
- Cohen JA, Steele MS, Urena FI, Beksinska ME (2007) Microbicide applicators: understanding design preferences among women in the dominican republic and South Africa. *Sex Transm Dis* 34:15–19
- Cone RA (2009) Barrier properties of mucus. *Adv Drug Deliv Rev* 61:75–85
- Contó Rigante K (2008) Modificación química de almidones mediante el uso de sales cuaternarias de amonio. PhD thesis, Simón Bolívar University, Venezuela
- Cunha L, Grenha A (2016) Sulfated seaweed polysaccharides as multifunctional materials in drug delivery applications. *Mar Drugs* 14:42
- Darroch JE, Frost JJ (1999) Women's interest in vaginal microbicides. *Fam Plann Perspect* 31:16–23
- Davaatseren M, Hong GP (2014) Effect of NaCl, gum arabic and microbial transglutaminase on the gel and emulsion characteristics of porcine myofibrillar proteins. *Korean J Food Sci Anim Resour* 34:808–814

- Delgado JL, Estevez J, Radicioni M, Loprete L, Moscoso Del Prado J, Nieto Magro C (2016) Pharmacokinetics and preliminary efficacy of two vaginal gel formulations of ultra-low-dose estriol in postmenopausal women. *Climacteric* 19:172–180
- Demirci ZO, Yilmaz I, Demirci AŞ (2014) Effects of xanthan, guar, carrageenan and locust bean gum addition on physical, chemical and sensory properties of meatballs. *J Food Sci Technol* 51:936–942
- Dittgen M, Durrani MJ, Lehmann K (1997) Acrylic polymers: a review of pharmaceutical applications. *STP Pharma* 7:403–437
- Dodane V, Vilivalam VD (1998) Pharmaceuticals applications of chitosan. *J Pharm Sci Technol* 1:246–253
- Doggett EG, Lanham M, Wilcher R, Gafos M, Karim QA, Heise L (2015) Optimizing HIV prevention for women: a review of evidence from microbicide studies and considerations for gender-sensitive microbicide introduction. *J Int AIDS Soc* 18:20536
- Duchene D, Ponchel G (1992) Principle and investigation of bioadhesion mechanism of solid dosage forms. *Biomaterials* 13:709–714
- Edwards D, Panay N (2016) Treating vulvovaginal atrophy/genitourinary syndrome of menopause: how important is vaginal lubricant and moisturizer composition? *Climacteric* 19:151–161
- El-Kamel A, Sokar M, Naggar V, Al Gamal S (2002) Chitosan and sodium alginate-based bioadhesive vaginal tablets. *AAPS PharmSci* 4:E44
- Ferguson LM, Rohan LC (2011) The importance of the vaginal delivery route for antiretrovirals in HIV prevention. *TherDeliv* 2:1535–1550
- Forbes CJ, Lowry D, Geer L, Veazey RS, Shattock RJ, Klasse PJ, Mitchnick M, Goldman L, Doyle LA, Muldoon BC, Woolfson AC, Moore JP, Malcolm RK (2011) Non-aqueous silicone elastomer gels as a vaginal microbicide delivery system for the HIV-1 entry inhibitor maraviroc. *J Control Release* 156:161–169
- Forbes CJ, McCoy CF, Murphy DJ, Woolfson AD, Moore JP, Evans A, Shattock RJ, Malcolm RK (2014) Modified silicone elastomer vaginal gels for sustained release of antiretroviral HIV microbicides. *J Pharm Sci* 103:1422–1432
- Forsberg JG (1996) A morphologist's approach to the vagina. *Acta Obstet Gynecol Scand Suppl* 163:3–10
- Fuongfuchat A, Jamieson AM, Blackwell J, Gerken TA (1996) Rheological studies of the interaction of mucins with alginate and polyacrylate. *Carbohydr Res* 284:85–99
- García-Ochoa F, Santos VE, Casas JA, Gómez E (2000) Xanthan gum: production, recovery, and properties. *Biotechnol Adv* 18:549–579
- Garg S, Vermani K, Kohli G, Kandarapu R, Tambwekar KR, Garg A, Waller DP, Zaneveld LJ (2002) Survey of vaginal formulations available on the Indian market: physicochemical characterization of selected products. *Int J Pharmaceut Med* 16:141–152
- Garg S, Tambwekar KR, Vermani K, Kandarapu R, Garg A, Waller DP, Zaneveld LJ (2003) Development pharmaceuticals of microbicide formulations. Part II: formulation, evaluation, and challenges. *AIDS Patient Care STDS* 17:377–399
- Granström M (2009) Cellulose derivatives: synthesis, properties and applications. Academic dissertation, University of Helsinki, Finland
- Guo JH, Skinner GW, Harcum WW, Barnum PE (1998) Pharmaceutical applications of naturally occurring water-soluble polymers. *Pharm Sci & Technol Today* 1:254–261
- Gupta S, Kaur IP, Prabha V (2016) Evaluation of antifertility effect of gel formulation containing sperm immobilizing factor: in vitro and in vivo studies. *Eur J Pharm Sci* 81:67–74
- Hanson S, Lalor P, Niemi S, Northup S, Ratner B, Spector M, Vale BM, Willson J (1996) In Biomaterials science, Academic Press, 215
- Hardy E, Jiménez AL, de Padua KS, Zaneveld LJD (1998) Women's preferences for vaginal antimicrobial contraceptives III: Choice of a formulation, applicator, and packaging. *Contraception* 58:245–249
- Hedén P, Sarfati I, Clough K, Olenius M, Sellman G, Trevidic P (2016) Safety and efficacy of stabilized hyaluronic acid gel for breast enhancement. *Plast Reconstr Surg Glob Open* 3:e575



- Hintzen F, Hauptstein S, Perera G, Bernkop-Schnürch A (2013) Synthesis and in vitro characterization of entirely S-protected thiolated pectin for drug delivery. *Eur J Pharm Biopharm* 85:1266–1273
- Hladik F, Burgener A, Ballweber L, Gottardo R, Vojtech L, Fourati S, Dai JY, Cameron MJ, Strobl J, Hughes SM, Hoesley C, Andrew P, Johnson S, Piper J, Friend DR, Ball TB, Cranston RD, Mayer KH, McElrath MJ, McGowan I (2015) Mucosal effects of tenofovir 1% gel. *Elife* 4
- Holt BY, Morwitz VG, Ngo L, Harrison PF, Whaley KJ, Pettifor A, Nguyen AH (2006) Microbicide preference among young women in California. *J Womens Health* 15:281–294
- Huszar G (1986) The physiology and biochemistry of the uterus in pregnancy and labor. CRC Press Inc, Boca Raton, pp 239–260
- Hwang MR, Kim JO, Lee JH, Kim YI, Kim JH, Chang SW, Jin SG, Kim JA, Lyoo WS, Han SS, Ku SK, Yong CS, Choi HG (2010) Gentamicin-loaded wound dressing with polyvinyl alcohol/dextran hydrogel: gel characterization and in vivo healing evaluation. *AAPS PharmSciTech* 11:1092–1103
- Illum L (1998) Chitosan and its use as pharmaceutical excipient. *Pharm Res* 15
- Jain A, Kumar L, Kushwaha B, Sharma M, Pandey A, Verma V, Sharma V, Singh V, Rawat T, Sharma VL, Maikhuri JP, Gupta G (2014) Combining a synthetic spermicide with a natural trichomonacide for safe, prophylactic contraception. *Hum Reprod* 29:242–252
- Jarrett AM, Gao Y, Hussaini MY, Cogan NG, Katz DF (2016) Sensitivity analysis of a pharmacokinetic model of vaginal anti-HIV microbicide drug delivery. *J Pharm Sci* 105:1772–1778
- Jensen M, Hansen PB, Murdan S, Frokjaer S, Florence AT (2002) Loading into electro-stimulated release of peptides and proteins from chondroitin 4-sulphate hydrogels. *Eur J Pharm Sci* 15:139–148
- Jespers VA, Van Roey JM, Beets GI, Buve AM (2007) Dose-ranging Phase I study of TMC120, a promising vaginal microbicide, in HIV-negative and HIV-positive female volunteers. *J Acquir Immune Defic Syndr* 44:154–158
- Johnson TJ, Gupta KM, Fabian J, Albright TH, Kiser PF (2010) Segmented polyurethane intravaginal rings for the sustained combined delivery of antiretroviral agents dapivirine and tenofovir. *Eur J Pharm Sci* 39:203–212
- Jokar A, Davari T, Asadi N, Ahmadi F, Foruhari S (2016) Comparison of the hyaluronic acid vaginal cream and conjugated estrogen used in treatment of vaginal atrophy of menopause women: a randomized controlled clinical trial. *Int J Community Based Nurs Midwifery* 4:69–78
- Kaddam L, FdleAlmula I, Eisawi OA, Abdelrazig HA, Elnimeiri M, Lang F, Saeed AM (2015) Gum Arabic as fetal hemoglobin inducing agent in sickle cell anemia; in vivo study. *BMC Hematol* 15:19
- Kamoun EA (2016) N-succinyl chitosan-dialdehyde starch hybrid hydrogels for biomedical applications. *J Adv Res* 7:69–77
- Karamisheva V, Nachev A (2015) Saforelle—a new approach to treat vaginitis. *Akush Ginekolog* 54 (Suppl 2):22–24
- Kast CE, Valenta C, Leopold M, Bernkop-Schnürch A (2002) Design and in vitro evaluation of a novel bioadhesive vaginal drug delivery system for clotrimazole. *J Control Rel* 81:347–354
- Katz DF (1986) Human cervical mucus: research update. *Am J Obstet Gynecol* 165:1984–1986
- Kehl S, Weiss C, Wamsler M, Beyer J, Dammer U, Heimrich J, Faschingbauer F, Sütterlin M, Beckmann MW, Schleussner E (2016) Double-balloon catheter and sequential vaginal prostaglandin E2 versus vaginal prostaglandin E2 alone for induction of labor after previous cesarean section. *Arch Gynecol Obstet* 293:757–765
- Khanna N, Dalby R, Tan M, Arnold S, Stern J, Frazer N (2007) Phase I/II clinical safety studies of terameprocol vaginal ointment. *Gynecol Oncol* 107:554–562
- Khanna N, Dalby R, Connor A, Church A, Stern J, Frazer N (2008) Phase I clinical trial of repeat dose terameprocol vaginal ointment in healthy female volunteers. *Sex Transm Dis* 35:577–582

- Kim KW, Thomas RL, Lee C, Park HJ (2003) Antimicrobial activity of native chitosan, degraded chitosan and O-carboxymethylated chitosan. *J Food Prot* 66:1495–1498
- Kocatürk T, Gençgönül A, Balica F, Özbağcivan M, Çakmak H (2015) Combined eye gel containing sodium hyaluronate and xanthan gum for the treatment of the corneal epithelial defect after pterygium surgery. *Clin Ophthalmol* 9:1463–1466
- Kuklinski C (2000) Farmacognosia, estudio de las drogas y sustancias medicamentosas de origen natural. Ed Omega
- Lacey CJ, Woodhall S, Qi Z, Sawant S, Cowen M, McCormack S, Jiang S (2010) Unacceptable side-effects associated with a hyperosmolar vaginal microbicide in a phase I trial. *Int J STD AIDS* 21:714–717
- Laeyendecker O, Redd AD, Nason M, Longosz AF, Karim QA, Naranbhai V, Garrett N, Eshleman SH, Abdool Karim SS, Quinn TC (2015) Antibody maturation in women who acquire HIV infection while using antiretroviral preexposure prophylaxis. *J Infect Dis* 212:754–759
- Lamont RF, Sobel JD, Akins RA, Hassan SS, Chaiworapongsa T, Kusanovic JP, Romero R (2011) The vaginal microbiome: new information about genital tract flora using molecular based techniques. *BJOG* 118:533–549
- Larsen B, Monif GR (2001) Understanding the bacterial flora of the female genital tract. *Clin Infect Dis* 32:69–77
- Levendosky K, Mizenina O, Martinelli E, Jean-Pierre N, Kizima L, Rodriguez A, Kleinbeck K, Bonnaire T, Robbiani M, Zydowsky TM, O’Keefe BR, Fernández-Romero JA (2015) Griffithsin and carrageenan combination to target herpes simplex virus 2 and human Papillomavirus. *Antimicrob Agents Chemother* 59:7290–7298
- Li L, Ben Y, Yuan S, Jiang S, Xu J, Zhang X (2012) Efficacy, stability, and biosafety of sifuvirtide gel as a microbicide candidate against HIV-1. *PLoS ONE* 7:e37381
- Liu Y, Zhu Y, Wei G, Lu W (2009) Effect of carrageenan on poloxamer-based in situ gel for vaginal use: improved in vitro and in vivo sustained-release properties. *Eur J Pharm Sci* 37:306–312
- Luessen HL, de Leeuw BJ, Langemeyer MW, de Boer AB, Verhoef JC, Junginger HE (1996) Mucoadhesive polymers in peroral peptide drug delivery: VI. Carbomer and chitosan improve the intestinal absorption of the peptide drug Buserelin in vivo. *Arch Pharm Res* 13:1668–1672
- Lupo Pasin B (2015) Estudio de gelificación de alginatos para encapsulación: caracterización, preparación y aplicaciones en alimentos funcionales. PhD thesis, University of Barcelona, Spain
- Lyra MAM, Soares-Sobrinho JL, Brasileiro MT, de la Roca MF, Barraza JA, Viana OS, Rolim-Neto PJ (2007) Hydrophilic matrix and mucoadhesive systems for drug controlled release. *Lat Am J Pharm* 26:784–793
- Madan M, Bajaj A, Lewis S, Udupa N, Baig JA (2009) In Situ forming polymeric drug release systems. *Indian J Pharm Sci* 71:242–251
- Mamani PL, Ruiz-Caro R, Veiga MD (2015) Pectin/anhydrous dibasic calcium phosphate matrix tablets for in vitro controlled release of water-soluble drug. *Int J Pharm* 494(1):235–243
- Masoudi M, Miraj S, Rafeian-Kopaei M (2016) Comparison of the effects of *Myrtus Communis* L, *Berberis Vulgaris* and metronidazole vaginal gel alone for the treatment of bacterial vaginosis. *J Clin Diagn Res* 10:QC04–QC07
- Mármol Z, Páez G, Rincón M, Araujo K, Aiello C, Chandler C, Gutiérrez E (2011) Chitin and chitosan friendly polymer. A review of their applications. *Revista Tecnocientífica URU* 1:53–58
- Marras-Márquez T, Peña J, Veiga-Ochoa MD (2014) Agarose drug delivery systems upgraded by surfactants inclusion: Critical role of the pore architecture. *Carbohydr Polym* 103:359–368
- Marrazzo JM, Ramjee G, Richardson BA, Gomez K, Mgodhi N, Nair G, Palanee T, Nakabiito C, van der Straten A, Noguchi L, Hendrix CW, Dai JY, Ganesh S, Mkhize B, Taljaard M, Parikh UM, Piper J, Mäse B, Grossman C, Rooney J, Schwartz JL, Watts H, Marzinke MA, Hillier SL, McGowan IM, Chirenje ZM (2015) Tenofovir-based preexposure prophylaxis for HIV infection among African women. *N Engl J Med* 372:509–518

- Martínez Palau M (2008) Síntesis, estructura y aplicaciones de poliésteres secuenciales derivados de ácido glicólico y w-hidroxiácidos. PhD thesis, Polytechnic University of Catalonia, Spain
- Masteiková R, Chalupová Z, Sklbalová Z (2003) Stimuli-sensitive hydrogels in controlled and sustained drug delivery. *Medicina (Kaunas)* 39(Suppl 2):19–24
- Matsuda T (2002) Device-directed therapeutic drug delivery systems. *J Control Release* 78:125–131
- Melis GB, Marotto MF, Orrù MM, Pilloni M, Zedda P, D'Alterio M, Paoletti AM (2016) Bacterial vaginosis: efficacy of a local treatment with a gel containing a fraction derived from propionibacterium acnés. *Minerva Ginecol* 68:1–8
- Meunier L, Garthoff JA, Schaafsma A, Krul L, Schrijver J, van Goudoever JB, Speijers G, Vandenplas Y (2014) Locust bean gum safety in neonates and young infants: an integrated review of the toxicological database and clinical evidence. *Regul Toxicol Pharmacol* 70:155–169
- Mohamed RE, Gadour MO, Adam I (2015) The lowering effect of Gum Arabic on hyperlipidemia in Sudanese patients. *Front Physiol* 6:160
- Mughal MA, Iqbal Z, Neau SH (2011) Guar gum, xanthan gum, and HPMC can define release mechanisms and sustain release of propranolol hydrochloride. *AAPS PharmSciTech* 12:77–87
- Nel AM, Coplan P, van de Wijert JH, Kapiga SH, von Mollendorf C, Geubbels E, Vyankandondera J, Rees HV, Masenga G, KIWELU I, Moyes J, Smythe SC (2009) Safety, tolerability, and systemic absorption of dapivirine vaginal microbicide gel in healthy, HIV-negative women. *AIDS* 23:1531–1538
- Nel AM, Smythe SC, Habibi S, Kaptur PE, Romano JW (2010) Pharmacokinetics of 2 dapivirine vaginal microbicide gels and their safety vs. Hydroxyethyl cellulose-based universal placebo gel. *J Acquir Immune Defic Syndr* 55:161–169
- Nishikawa M, Onuki Y, Isowa K, Takayama K (2008) Formulation optimization of an indomethacin-containing photocrosslinked polyacrylic acid hydrogel as an anti-inflammatory patch. *AAPS PharmSciTech* 9:1038–1045
- Notario-Pérez F, Martín-Illana A, Cazorla-Luna R, Ruiz-Caro R, Peña J, Veiga MD (2018) Improvement of Tenofovir vaginal release from hydrophilic matrices through drug granulation with hydrophobic polymers. *Eur J Pharm Sci* 117:204–215
- Notario-Pérez F, Martín-Illana A, Cazorla-Luna R, Ruiz-Caro R, Bedoya LM, Tamayo A, Rubio J, Veiga MD (2017) Influence of Chitosan Swelling Behaviour on Controlled Release of Tenofovir from Mucoadhesive Vaginal Systems for Prevention of Sexual Transmission of HIV. *Mar Drugs* 15(2):50
- Obara K, Ishihara M, Ishizuka T, Fujita M, Ozeki Y, Maehara T, Saito Y, Yura H, Matsui T, Hattori H, Kikuchi M, Kurita A (2003) Photocrosslinkable chitosan hydrogel containing fibroblast growth factor-2 stimulates wound healing in healing-impaired db/db mice. *Biomaterials* 24:3437–3444
- Ozyazici M, Gökçe E, Hizarcioglu SY, Taner MS, Köseoglu K, Ertan G (2006) Dissolution and vaginal absorption characteristics of metronidazole and ornidazole. *Pharmazie* 61:855–861
- Pacheco de Delahaye E, Techeira N (2009) Chemical and functional properties of native and modified yam (*dioscorea alata*) starch. *Interciencia* 34:280–285
- Pawar S, Pande V (2015) Oleic acid coated gelatin nanoparticles impregnated gel for sustained delivery of zaltoprofen: formulation and textural characterization. *Adv Pharm Bull* 5:537–548
- Pedersen C, Slepkin A, Andersson SB, Fagerberg JH, Bergström CA, Peterson EM (2014) Formulation of the microbicide INP0341 for in vivo protection against a vaginal challenge by *Chlamydia trachomatis*. *PLoS ONE* 9:e110918
- Pendergrass PB, Reeves CA, Belovicz MW, Molter DJ, White JH (1996) The shape and dimensions of the human vagina as seen in three-dimensional vinyl polysiloxane casts. *Gynecol Obstet Invest* 42:178–182
- Pendergrass PB, Reeves CA, Belovicz MW, Molter DJ, White JH (2000) Comparison of vaginal shapes in Afro-American, caucasian and hispanic women as seen with vinyl polysiloxane casting. *Gynecol Obstet Invest* 50:54–59
- Pendergrass PB, Belovicz MW, Reeves CA (2003) Surface area of the human vagina as measured from vinyl polysiloxane casts. *Gynecol Obstet Invest* 55:110–113

- Perioli L, Ambrogi V, Pagano C, Massetti E, Rossi C (2008) Chitosan and a modified chitosan as agents to improve performances of mucoadhesive vaginal gels. *Colloids Surf B Biointerfaces* 66:141–145
- Perioli L, Amrogi V, Pagano C, Massetti E, Rossi C (2011) New solid mucoadhesive systems for benzydamine vaginal administration. *Colloids Surf B Biointerfaces* 84:413–420
- Podual K, Doyle FJ III, Peppas NA (2000) Dynamic behavior of glucose oxidase-containing microparticles of poly(ethylene)-grafted cationic hydrogels in an environment of changing pH. *Biomaterials* 21:1439–1450
- Pradeep AR, Agarwal E, Bajaj P, Naik SB, Shanbhag N, Uma SR (2012) Clinical and microbiologic effects of commercially available gel and powder containing *Acacia arabica* on gingivitis. *Aust Dent J* 57:312–318
- Prajapati VD, Jani GK, Moradiya NG, Randeria NP, Nagar BJ (2013) Locust bean gum: A versatile biopolymer. *Carbohydr Polym* 94(2):814–821
- Rabasco A (1997) Nuevas formas de administración de medicamentos. In *Tecnología Farmacéutica, Vol. II: Formas Farmacéuticas* 8:379–445
- Rader M, Marks G, Mansergh G, Crepaz N, Miller LC, Appleby PR, Murphy S (2001) Preferences about the characteristics of future HIV prevention products among men who have sex with men. *AIDS Educ Prev* 13:149–159
- Rajan SS, Turovskiy Y, Singh Y, Chikindas ML, Sinko PJ (2014) Poly(ethylene glycol) (PEG)-lactic acid nanocarrier-based degradable hydrogels for restoring the vaginal microenvironment. *J Control Release* 194:301–309
- Ramanathan S, Block LH (2001) The use of chitosan gels as matrices for electrically-modulated drug delivery. *J Control Release* 70:109–123
- Ravel J, Gajer P, Fu L, Mauck CK, Koenig SS, Sakamoto J, Motsinger-Reif AA, Doncel GF, Zeichner SL (2012) Twice-daily application of HIV microbicides alter the vaginal microbiota. *MBio* 3(6):e00370-12.
- Rehman K, Mohd Amin MC, Zulfakar MH (2014) Development and physical characterization of polymer-fish oil bigel (hydrogel/oleogel) system as a transdermal drug delivery vehicle. *J Oleo Sci* 63(10):961–970
- Rencher WB (2001) Vaginal microbicide formulations workshop. Arlington, VA: Lippincott-Raven
- Rençber S, Karavana SY, Şenyiğit ZA, Eraç B, Limoncu MH, Baloğlu E (2016) Mucoadhesive in situ gel formulation for vaginal delivery of clotrimazole: formulation, preparation, and in vitro/in vivo evaluation. *Pharm Dev Technol* 7:1–11
- Richardson BA, Kelly C, Ramjee G, Fleming T, Makanani B, Roberts S, Musara P, Mkandawire N, Moench T, Coletti A, Soto-Torres L, Karim SA (2013) Appropriateness of hydroxyethylcellulose gel as a placebo control in vaginal microbicide trials: a comparison of the two control arms of HPTN 035. *J Acquir Immune Defic Syndr* 63:120–125
- Richardson JL, Trevor TI (1999) Vaginal delivery of calcitonin by hyaluronic acid formulations. *Drugs Pharm Sci* 98:563–599
- Robic A, Gaillard C, Sassi JF, Lerat Y, Lahaye M (2009) Ultrastructure of ulvan: a polysaccharide from green seaweeds. *Biopolymers* 91:652–664
- Rodríguez IC, Cerezo A, Salem II (2000) Bioadhesive delivery systems. *Ars Pharmaceutica* 41:115–128
- Rohan LC, Sassi AB (2009) Vaginal drug delivery systems for HIV prevention. *AAPS J* 11:78–87
- Rosen RK, Morrow KM, Carballo-Diéguez A, Mantell JE, Hoffman S, Gai F, Maslankowski L, El-Sadr WM, Mayer KH (2008) Acceptability of tenofovir gel as a vaginal microbicide among women in a phase I trial: a mixed-methods study. *J Womens Health* 17:383–392
- Ruiz-Caro R, Gago-Guillan M, Otero-Espinar FJ, Veiga MD (2012) Mucoadhesive Tablets for Controlled Release of Acyclovir. *Chem Pharm Bull* 60(10):1249–1257
- Sagiri SS, Singh VK, Kulanthaivel S, Banerjee I, Basak P, Battachrya MK, Pal K (2015) Stearate organogel-gelatin hydrogel based bigels: physicochemical, thermal, mechanical characterizations and in vitro drug delivery applications. *J Mech Behav Biomed Mater* 43:1–17

- Sánchez R, Damas R, Domínguez P, Cerezo P, Salcedo I, Aguzzi C, Viseras C (2010) Uso de la HidroxiPropilMetilCelulosa (HPMC) en liberación modificada de fármacos. *Farmaespaña industrial*
- Sánchez-Sánchez MP, Martín-Illana A, Ruiz-Caro R, Bermejo P, Abad MJ, Carro R, Bedoya LM, Tamayo A, Rubio J, Fernández-Ferreiro A, Otero-Espinar Veiga MD (2015) Chitosan and Kappa-Carrageenan vaginal acyclovir formulations for prevention of genital herpes. *In vitro and ex vivo evaluation*. *Mar Drugs* 13:5976–5992
- Schwartz JL, Kovalevsky G, Lai JJ, Ballagh SA, McCormick T, Douville K, Mauck CK, Callahan MM (2008) A randomized six-day safety study of an antiretroviral microbicide candidate UC781, a non-nucleoside reverse transcriptase inhibitor. *Sex Transm Dis* 35:414–419
- Schwebke JR, Marrazzo J, Beelen AP, Sobel JD (2015) A phase 3, multicenter, randomized, double-blind, vehicle-controlled study evaluating the safety and efficacy of metronidazole vaginal gel 1.3% in the treatment of bacterial vaginosis. *Sex Transm Dis* 42:376–381
- Sezer AD, Cevher E, Hatipoğlu F, Oğurtan Z, Baş AL, Akbuğa J (2008) Preparation of fucoidan-chitosan hydrogel and its application as burn healing accelerator on rabbits. *Biol Pharm Bull* 31:2326–2333
- Shah AJ, Donovan MD (2007) Formulating gels for decreased mucociliary transport using rheologic properties: polyacrylic acids. *AAPS PharmSciTech* 8:E48–E53
- Sharma H, Sharma BD, Talukder S, Ramasamy G (2015) Utilization of gum tragacanth as bind enhancing agent in extended restructured mutton chops. *J Food Sci Technol* 52:1626–1633
- Sherafudeen SP, Vasantha PV (2015) Development and evaluation of in situ nasal gel formulations of loratadine. *Res Pharm Sci* 10:466–476
- Shinde UA, Kanojiya SS (2014) Serratiopeptidase niosomal gel with potential in topical delivery. *J Pharm* 2014:382959
- Shokri J, Adibkia K (2013) Application of cellulose and cellulose derivatives in pharmaceutical industries. In *cellulose—medical, pharmaceutical and electronic applications*
- Singh VK, Anis A, Banerjee I, Pramanik K, Bhattacharya MK, Pal K (2014a) Preparation and characterization of novel carbopol based bigels for topical delivery of metronidazole for the treatment of bacterial vaginosis. *Mater Sci Eng C Mater Biol Appl* 44:151–158
- Singh VK, Banerjee I, Agarwal T, Pramanik K, Bhattacharya MK, Pal K (2014b) Guar gum and sesame oil based novel bigels for controlled drug delivery. *Colloids Surf B Biointerfaces* 123:582–592
- Sjoberg I (1992) The vagina. Morphological, functional and ecological aspects. *Acta Obstet Gynecol Scand* 71:84–85
- Skoler-Karpoft S, Ramjee G, Ahmed K, Altini L, Plagianos MG, Friedland B, Govender S, De Kock A, Cassim N, Palanee T, Dozier G, Maguire R, Lahteenmaki P (2008) Efficacy of Carraguard for prevention of HIV infection in women in South Africa: a randomised, double-blind, placebo-controlled trial. *Lancet* 372:1977–1987
- Smart JD, Kellaway IW, Worthington HE (1984) An in-vitro investigation of mucosa-adhesive materials for use in controlled drug delivery. *J Pharm Pharmacol* 36:295–299
- Smith JM, Srinivasan P, Teller RS, Lo Y, Dinh CT, Kiser PF, Herold BC (2015) Tenofovir disoproxil fumarate intravaginal ring protects high-dose depot medroxyprogesterone acetate-treated macaques from multiple SHIV exposures. *J Acquir Immune Defic Syndr* 68:1–5
- Soppimath KS, Aminabhavi TM, Dave AM, Kumbar SG, Rudzinski WE (2002) Stimulus-responsive “smart” hydrogels as novel drug delivery systems. *Drug Dev Ind Pharm* 28:957–974
- Sriamornsak P (2003) Chemistry of pectin and its pharmaceutical uses: a review. *Silpakorn Univ Int J* 3:206–228
- Srinivasan P, Dinh C, Zhang J, Pau CP, McNicholl JM, Lo Y, Herold BC, Teller R, Kiser P, Smith JM (2014) Pharmacokinetic evaluation of tenofovir disoproxil fumarate released from an intravaginal ring in pigtailed macaques after 6 months of continuous use. *J Med Primatol* 43:364–369
- Szekalska M, Winnicka K, Czajkowska-Kośnik A, Sosnowska K, Amelian A (2015) Evaluation of alginate microspheres with metronidazole obtained by the spray drying technique. *Acta Pol Pharm* 72:569–578

- Tasdighi E, Jafari Azar Z, Mortazavi SA (2012) Development and in-vitro evaluation of a contraceptive vaginal-adhesive propranolol hydrochloride gel. *Iran J Pharm Res* 11:13–26
- Tien D, Schnaare RL, Kang F, Cohl G, McCormick TJ, Moench TR, Doncel G, Watson K, Buckheit RW, Lewis MG, Schwartz J, Douville K, Romano JW (2005) In vitro and in vivo characterization of a potential universal placebo designed for use in vaginal microbicide clinical trials. *AIDS Res Hum Retroviruses* 21:845–853
- Tintori C, Brai A, Dasso Lang MC, Deodato D, Greco AM, Bizzarri BM, Cascone L, Casian A, Zamperini C, Dreassi E, Crespan E, Maga G, Vanham G, Ceresola E, Canducci F, Ariën KK, Botta M (2016) Development and in vitro evaluation of a microbicide gel formulation for a novel non-nucleoside reverse transcriptase inhibitor belonging to the N-Dihydroalkoxybenzoxypyrimidines (N-DABOs) family. *J Med Chem* 59:2747–2759
- Tuğcu-Demiröz F, Acartürk F, Erdoğan D (2013) Development of long-acting bioadhesive vaginal gels of oxybutynin: formulation, in vitro and in vivo evaluations. *Int J Pharm* 457(1):25–39
- Tuğcu-Demiröz F, Acartürk F, Özkul A (2015) Preparation and characterization of bioadhesive controlled-release gels of cidofovir for vaginal delivery. *J Biomater Sci Polym Ed* 26:1237–1255
- USP Pharmacopoeia. 39th edn (2016)
- Valenta C (2005) The use of mucoadhesive polymers in vaginal delivery. *Adv Drug Deliv Rev* 57:1692–1712
- Valore EV, Park CH, Igteti SL, Ganz T (2002) Antimicrobial components of vaginal fluid. *Am J Obstet Gynecol* 187:561–568
- Vandamme TF, Lenourry A, Charrueau C, Chaumeil JC (2002) The use of polysaccharides to target drugs to the colon. *Carbohydr Polym* 48:219–231
- Venugopal V (2011) Polysaccharide from seaweed and microalgae. In *Marine Polysaccharides: Food Applications*. Taylor and Francis Group, Boca Raton, pp 111–122
- Vermani K, Garg S (2000) The scope and potential of vaginal drug delivery. *Pharm Sci Technol Today* 3:359–364
- Vokurka S, Skardova J, Hruskova R, Kabatova-Maxova K, Svoboda T, Bystricka E, Steinerova K, Koza V (2011) The effect of polyvinylpyrrolidone-sodium hyaluronate gel (Gelclair) on oral microbial colonization and pain control compared with other rinsing solutions in patients with oral mucositis after allogeneic stem cells transplantation. *Med Sci Monit* 17:CR572–CR576
- Woolfson AD, Malcolm RK, Gallagher R (2000) Drug delivery by the intravaginal route. *Crit Rev Ther Drug Carrier Syst* 17:509–555
- Wu N, Zhang X, Li F, Zhang T, Gan Y, Li J (2015) Spray-dried powders enhance vaginal siRNA delivery by potentially modulating the mucus molecular sieve structure. *Int J Nanomedicine* 10:5383–5396
- Xiao BB, Zhang D, Chen R, Shi HR, Xin XR, Wang HL, Pang YC, Zhu SN, Yao C, Liao QP (2015) Sucrose gel for treatment of bacterial vaginosis: a randomized, double-blind, multi-center, parallel-group, phase III clinical trial. *Beijing Da Xue Xue Bao* 47:925–932
- Yang KH, Hendrix C, Bumpus N, Elliott J, Tanner K, Mauck C, Cranston R, McGowan I, Richardson-Harman N, Anton PA, Kashuba AD (2014) A multi-compartment single and multiple dose pharmacokinetic comparison of rectally applied tenofovir 1% gel and oral tenofovir disoproxil fumarate. *PLoS ONE* 9:e106196
- Zavos PM, Cohen MR (1980) The pH of cervical mucus and the postcoital test. *Fertil Steril* 34:234–238
- Zhou Q, Zhong L, Wei X, Dou W, Chou G, Wang Z (2013) Baicalein and hydroxypropyl- $\gamma$ -cyclodextrin complex in poloxamer thermal sensitive hydrogel for vaginal administration. *Int J Pharm* 454:125–134
- Zhuang H, Bu S, Hua L, Darabi MA, Cao X, Xing M (2016) Gelatin-methacrylamide gel loaded with microspheres to deliver GDNF in bilayer collagen conduit promoting sciatic nerve growth. *Int J Nanomedicine* 11:1383–1394

# Chapter 9

## Gel Formation by Non-covalent Cross-Linking from Amylose Through Enzymatic Polymerization



Tomonari Tanaka and Jun-ichi Kadokawa

### 1 Introduction

Polysaccharides are one of the sustainable products distributed widely in nature and acting significant role as structural materials and providers of energy (Schuerch 1986). Because their annual huge production, natural polysaccharides are identified as very important biomass resources (Brown and Brown 2014; Pappu et al. 2015, 2016). Accordingly, the production of environmentally benign functional materials can be expected by the efficient approaches using natural polysaccharide resources (Mohanty et al. 2002; Rouilly and Rigal 2002; Trache et al. 2017; Corobea et al. 2016; Voicu et al. 2016; Miculescu et al. 2016). For example, cellulose, the most abundant organic resource on the earth, composed of  $\beta(1 \rightarrow 4)$ -linked glucose repeating units, has been used in a number of traditional applications including its use in furniture, clothing, and medical products (Klemm et al. 2005; Lejeune and Deprez 2009).

Some polysaccharides are known to spontaneously form hydrocolloid gels with aqueous solutions, which widely behave close to a liquid or to a solid (Piculell 1998; Nishinari et al. 2000; Nishinari and Takahashi 2003). Because of such a wide variety of the properties, hydrocolloid polysaccharides are used as stabilizers, viscous agents, and structure providers in food industries (Stephen et al. 2006). Therefore, the artificial formation of gels from abundant polysaccharides by appropriate procedures is one of the efficient approaches to obtain environmentally

---

T. Tanaka

Department of Biobased Materials Science, Graduate School of Science and Technology,  
Kyoto Institute of Technology, Matsugasaki, Sakyo-Ku, Kyoto 606-8585, Japan

J. Kadokawa (✉)

Department of Chemistry, Biotechnology, and Chemical Engineering,  
Graduate School of Science and Engineering, Kagoshima University,  
1-21-40 Korimoto, Kagoshima 860-0065, Japan  
e-mail: kadokawa@eng.kagoshima-u.ac.jp

benign materials, which have a potential in practical applications in biomedical and tissue engineering fields.

Amylose is one component of starch and a linear polysaccharide composed of  $\alpha(1 \rightarrow 4)$ -linked glucose repeating units (Schuerch 1986). A pure amylose is difficult to be prepared by the complete separation from amylopectin, the other component of starch (Lenz 1993). The enzymatic polymerization method is only the way to obtain a pure amylose sample with desired molecular weight. Two enzymes have been known to catalyze the enzymatic polymerization to produce amylose, that is, phosphorylase and amylosucrase (Ziegast and Pfannemüller 1987; Fujii et al. 2003; Yanase et al. 2006; Ohdan et al. 2006; Seibel et al. 2006a, b).

Because amylose acts as an energy resource in nature, it is hard to obtain structural materials solely from amylose; this is completely different from the case of cellulose. A single amylose chain shows water solubility, but spontaneously forms an antiparallel double helix with the other amylose chain owing to its helical conformation to produce a water-insoluble material (Eisenhaber and Schulz 1992; Hinrichs et al. 1987). Besides such double helix formation, amylose is known to act as a host molecule to construct inclusion complexes in the presence of appropriate guest molecules (Sarko and Zugenmaier 1980; Putseys et al. 2010). Because of hydrophobicity of the cavity in the amylose helix, hydrophobic interaction is the driving force for inclusion by amylose, and accordingly, hydrophobicity is required for guest molecules, which are efficiently incorporated in the cavity of the amylose helix.

The gelling system from amylose with suitable polymeric components has been reported, which is constructed by the formation of amylose double helix or inclusion complex as non-covalent cross-linking points through the phosphorylase-catalyzed enzymatic polymerization (Fig. 1) (Izawa and Kadokawa 2009; Kadokawa and Kobayashi 2010; Kadokawa 2011b, 2014; Kadokawa and Kaneko 2013; Shoda et al. 2016). This chapter overviews the gel formation cross-linked from amylose through the phosphorylase-catalyzed enzymatic polymerization.

## 2 Phosphorylase-Catalyzed Enzymatic Polymerization

Phosphorylase is an enzyme that catalyzes phosphorolysis of  $\alpha(1 \rightarrow 4)$ -glucans at the nonreducing end in the presence of inorganic phosphate (Pi) to produce  $\alpha$ -D-glucose 1-phosphate (Glc-1-P) (Fig. 2) (Kitaoka and Hayashi 2002; Nakai et al. 2013). Phosphorylase can catalyze the glucosylation reaction using Glc-1-P as a glycosyl donor and produce  $\alpha(1 \rightarrow 4)$ -glucosidic linkage under the selected conditions because the reaction shows reversibility (Fig. 2). As glycosyl acceptors,  $\alpha(1 \rightarrow 4)$ -glucans with the larger degrees of polymerization (DPs) than the smallest one, which is recognized by the enzyme are used. The smallest glycosyl acceptor recognized by phosphorylase isolated from potato (potato phosphorylase), the most well-known phosphorylase, is maltotetraose (Glc<sub>4</sub>). It has been found that the substrate specificities of phosphorylases were relatively weak depending on their



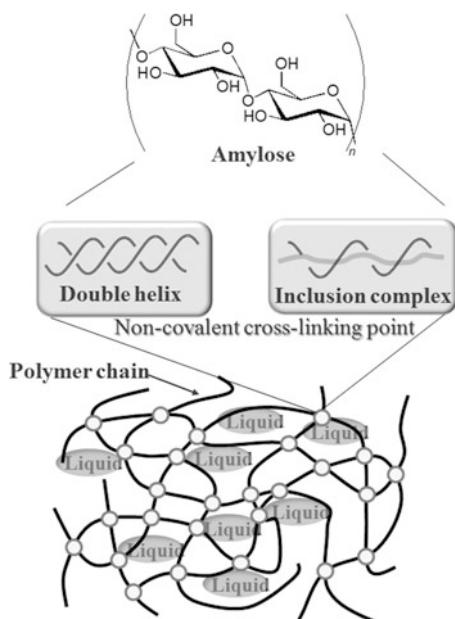


**Fig. 1** Schematic image of amylose supramolecular gel constructed by non-covalent cross-linking points through formation of double helix or inclusion complex

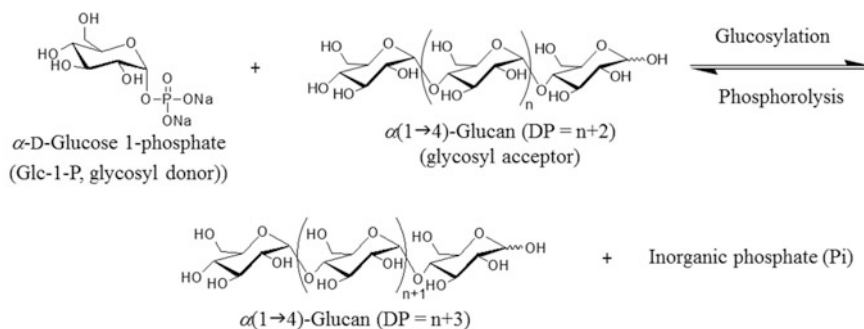


**Fig. 2** Phosphorylase-catalyzed reversible phosphorolysis and glucosylation

sources. Accordingly, phosphorylases catalyze glycosylations using some analog glycosyl donors of Glc-1-P which have phosphate structures of the different monosaccharide residues at the anomeric (C-1) position (Kadokawa 2011a, b, 2013b, 2015b; Shoda et al. 2016). For example, potato phosphorylase was found to catalyze glucosamylation of Glc<sub>4</sub> with  $\alpha$ -D-glucosamine 1-phosphate (GlcN-1-P) to obtain a pentasaccharide having a GlcN unit at the nonreducing end (Fig. 3a) (Nawaji et al. 2008). In addition to the glucosamylation, it has been reported that

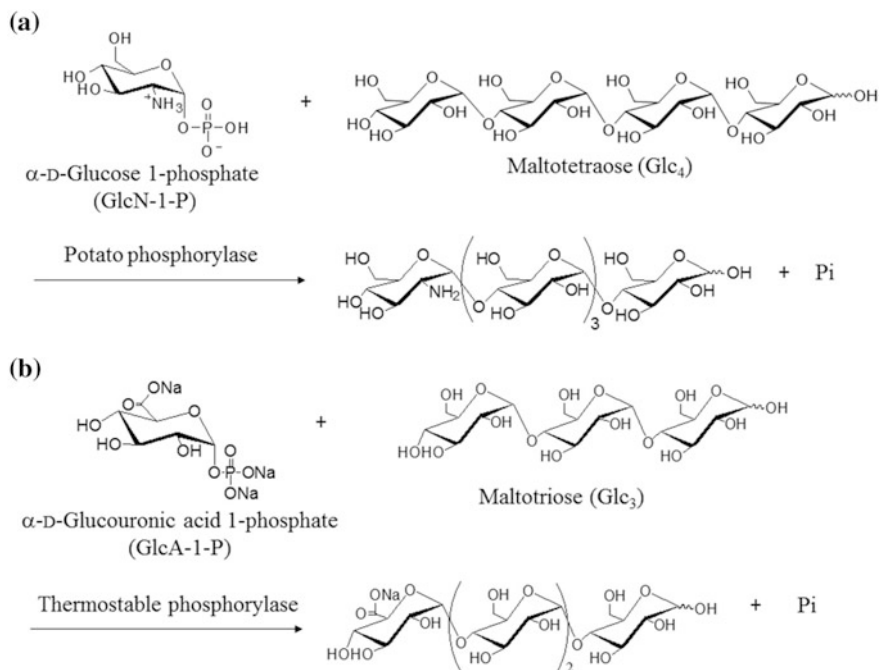


**Fig. 3** Phosphorylase-catalyzed **a** glucosamylation of maltotetraose (Glc<sub>4</sub>) with  $\alpha$ -D-glucosamine 1-phosphate (GlcN-1-P) and **b** glucuronylation of maltotriose (Glc<sub>3</sub>) with  $\alpha$ -D-glucuronic acid 1-phosphate (GlcA-1-P)

phosphorylase isolated from thermophilic bacteria (thermostable phosphorylase) also catalyzes glucuronylation of maltotriose (Glc<sub>3</sub>), which is the smallest glycosyl acceptor for this enzyme, using  $\alpha$ -D-glucuronic acid 1-phosphate (GlcA-1-P) as a glycosyl donor to obtain a tetrasaccharide having a GlcA unit at the nonreducing end (Fig. 3b) (Umegatani et al. 2012). Potato phosphorylase, on the other hand, does not recognize GlcA-1-P, indicating the more tolerance of thermostable phosphorylase for the recognition of glycosyl donors.

In the presence of the larger equivalents of Glc-1-P for the glycosyl acceptor, phosphorylase induces enzymatic polymerization of Glc-1-P as a monomer and succeeds glycosylations to produce a polysaccharide, that is, amylose (Fig. 4) (Ziegast and Pfannemüller 1987; Fujii et al. 2003; Yanase et al. 2006; Ohdan et al. 2006). To take place the polymerization, maltooligosaccharides larger than the smallest one recognized by phosphorylase have to be present in the reaction system and the elongation of amylose chain is exactly initiated at the nonreducing end of maltooligosaccharide. Accordingly, maltooligosaccharide is often called a primer of the enzymatic polymerization. The phosphorylase-catalyzed enzymatic polymerization can control the molecular weights of the produced amyloses by Glc-1-P monomer/primer feed ratios, and their distributions are relatively narrow because the enzymatic reaction belongs to the manner of chain-growth polymerization and

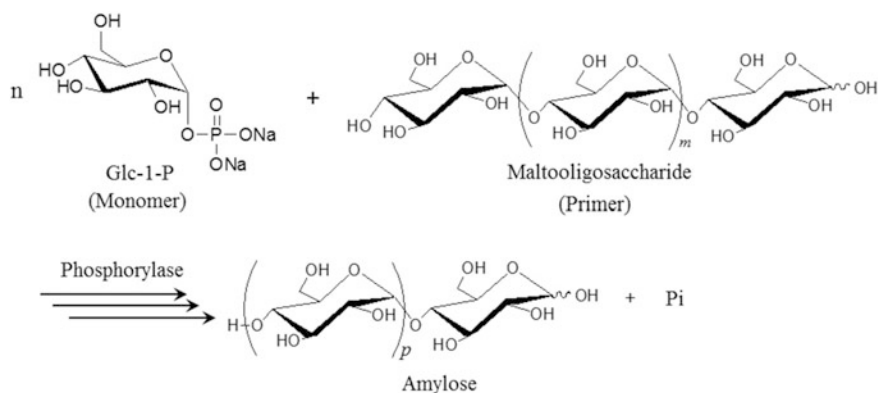


**Fig. 4** Phosphorylase-catalyzed enzymatic polymerization to produce amylose

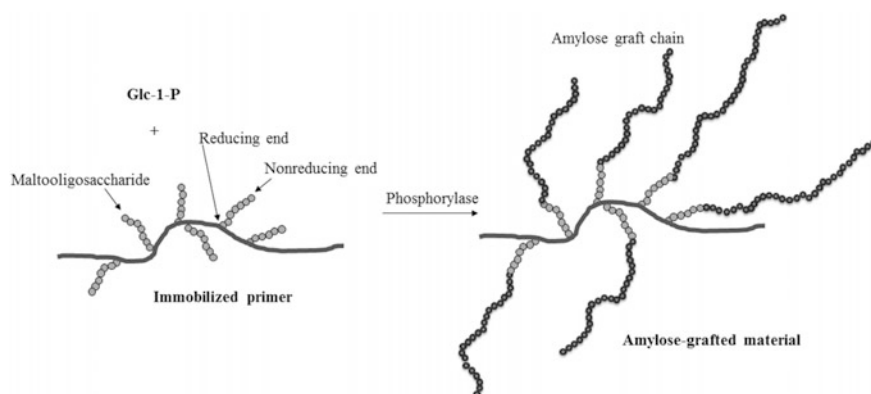


**Fig. 5** Synthesis of amylose-grafted material by phosphorylase-catalyzed enzymatic polymerization using immobilized primer

is progressed analogously to living polymerization without the occurrence of termination and chain-transfer reaction (Kitamura 1996).

Because the reducing end of maltooligosaccharide does not participate into the phosphorylase-catalyzed enzymatic polymerization, the enzymatic reaction can be conducted using immobilized primers, where the reducing end is covalently linked to other substances such as polymeric chains, giving rise to amylose-grafted materials (Fig. 5) (Kitamura et al. 1982; Izawa and Kadokawa 2009; Kadokawa 2014). Furthermore, when plural maltooligosaccharides are attached onto the substance, the primer shows multifunction to produce plural amyloses by the enzymatic polymerization initiated from each nonreducing end.

### 3 Hydrogelation by Double Helix Formation of Enzymatically Produced Amyloses

Glycogen is a water-soluble natural polysaccharide with high molecular weight and has been used as a multifunctional primer for the phosphorylase-catalyzed enzymatic polymerization to produce a glycogen hydrogel (Kadoakwa 2012, 2013). Glycogen has a highly branched structure composed of  $\alpha(1 \rightarrow 4)$ -glucosidic chains which are branched by  $\alpha(1 \rightarrow 6)$ -glucosidic linkages (Calder 1991; Manners 1991). Glycogen exhibits multifunction for the phosphorylase-catalyzed enzymatic polymerization because it has a number of  $\alpha(1 \rightarrow 4)$ -glucan nonreducing ends. When the potato phosphorylase-catalyzed enzymatic polymerization of Glc-1-P from glycogen was carried out and then stand further at room temperature for 24 h, the reaction mixture turned into a hydrogel (Fig. 6) (Izawa et al. 2009). The product formed hydrogel in which amylose chains elongated among glycogen molecules and constructed the cross-linked double helix. The stress–strain curves of the hydrogels under compressive mode suggested that they became harder and then turned to exhibit brittle nature with increasing the amounts of glycogen molecules. Increasing the number of elongated amylose chains, that is, increasing amount of glycogen, caused the increasing of the hydrogel strength as more double helix cross-linking points. However, further increases in the number of cross-linking points probably induced the brittle nature.

Lyophilization of the hydrogels facilely provided cryogels with porous morphology as shown in the SEM image in Fig. 7. The stress–strain curves of the products under compressive mode showed that the mechanical properties were strengthened when the amounts of glycogen used for the preparation of the hydrogels increased. This is owing to the formation of smaller networks because of being the higher cross-linking densities from the larger amounts of glycogen. The powder X-ray diffraction (XRD) pattern of the cryogel showed diffraction peaks assignable to the crystalline structure of double helix conformation of amylose. This result indicated that the elongated double helical amylose chains were entangled and constructed the network in the cryogel.

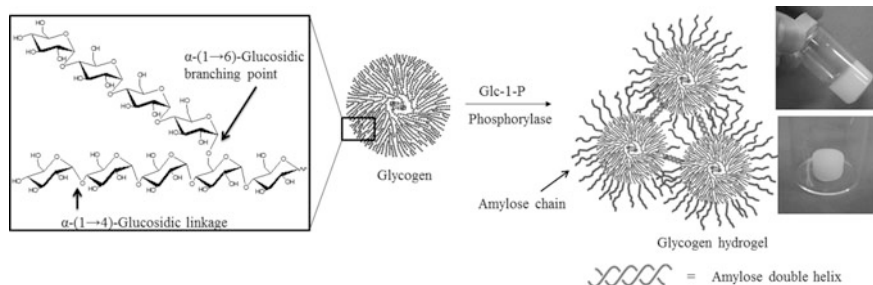


**Fig. 6** Preparation of glycogen hydrogel by phosphorylase-catalyzed enzymatic polymerization using glycogen as multifunctional primer

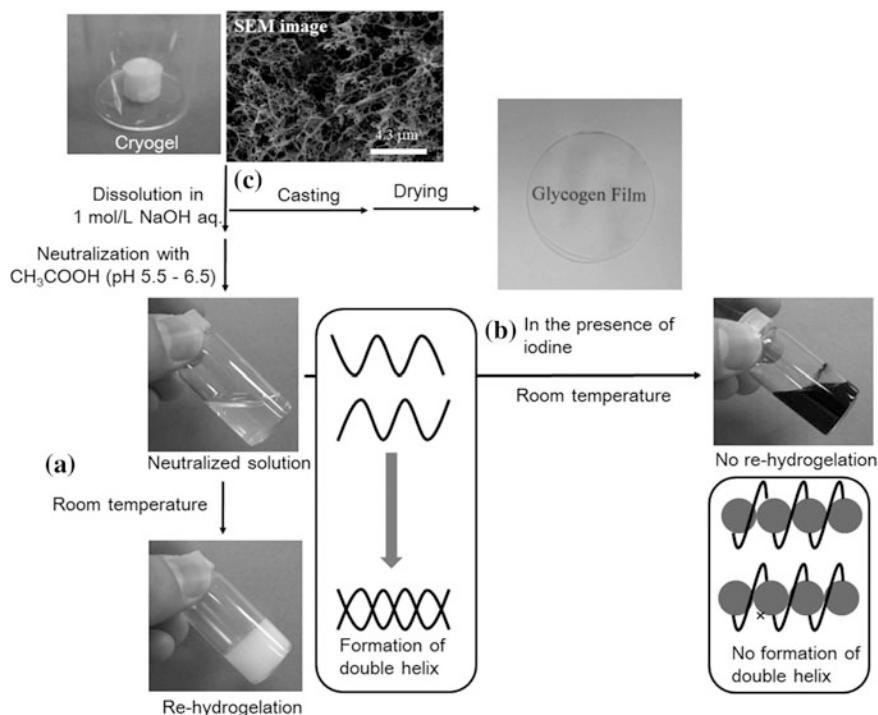


**Fig. 7** Photograph and SEM image of cryogel and **a** re-hydrogelation, **b** suppression of re-hydrogelation, and **c** formation of film

The cryogel was solubilized in aqueous NaOH because the amylose double helical conformation was known to be dissociated under strong alkaline (basic) conditions. When the alkaline solution was neutralized by acetic acid to pH 5.5–6.5, re-hydrogelation occurred owing to the re-formation of double helix cross-linking points by amyloses (Fig. 7a). When the standard iodine–iodide solution was added to the neutralized solution immediately after it was prepared and the resulting mixture was left standing, on the other hand, such re-hydrogelation did not take place (Fig. 7b). In this experiment, the elongated amylose chains included iodines, forming the well-known amylose/iodine inclusion complexes, and avoided the formation of the double helix as cross-linking point. Furthermore, a transparent film was obtained by casting the alkaline solution of the cryogel on a glass plate and drying (Fig. 7c).

pH-responsive amphoteric glycogen hydrogels were also fabricated by means of the similar approach through the phosphorylase-catalyzed enzymatic polymerization (Takata et al. 2015). Amphoteric glycogens having both GlcA and GlcN units at the nonreducing ends were first prepared by thermostable phosphorylase-catalyzed successive glucuronylation using GlcA-1-P and glucosamylation using GlcN-1-P (Fig. 8). The feed ratio of GlcA-1-P/GlcN-1-P can control the

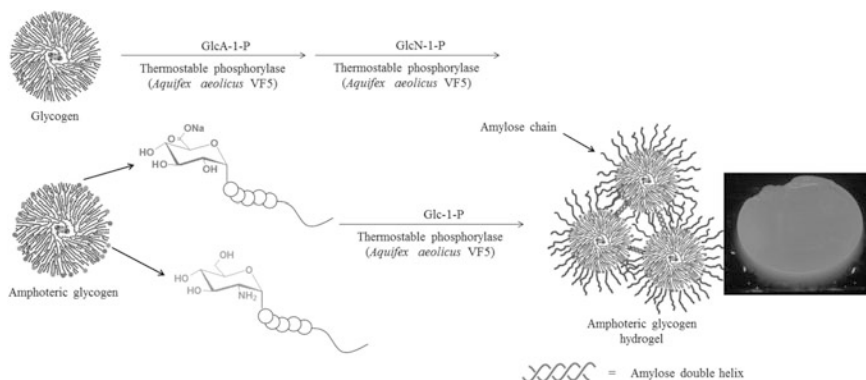


**Fig. 8** Preparation of amphoteric glycogen hydrogel by phosphorylase-catalyzed successive glucuronylation, glucosaminylation, and polymerization

functionalities of the products and change the  $\zeta$  potential values from positive to negative depending on the pH change from acidic to basic. The inherent isoelectric point (pI) values were calculated as the pH values at the zero charge of the  $\zeta$  potentials, which were reasonably changed in accordance with the GlcA/GlcN ratios in the amphoteric products.

Then, the amphoteric glycogens were converted into hydrogels by the formation of double helix cross-linking points of the elongated amylose chains by the thermostable phosphorylase-catalyzed enzymatic polymerization of Glc-1-P from the nonfunctionalized, nonreducing ends (Fig. 8). Then, pH-responsive behavior of the resulting amphoteric hydrogels was investigated. Under strong basic conditions by addition of aqueous NaOH, the gels totally turned into solutions by disruption of cross-linking points because of the dissociation of amylose double helices under such conditions (Fig. 9). By changing pH to weak basic by addition of aqueous acetic acid, the amylose chains reconstructed cross-linking points of double helices, resulting in re-hydrogelation (Fig. 9). Furthermore, the following pH-dependent shrinking/swelling behavior of the hydrogels was observed (Fig. 9). At pH = pI, the hydrogels are shrunk owing to neutral charges on the surfaces and the absence of intermolecular repulsive forces. At both weak acidic and basic pHs shifted from pI, the surfaces of glycogens were charged, leading to swelling of the hydrogels owing to cationic/cationic or anionic/anionic electrostatic repulsion.

Synthetic multifunctional polysaccharide primers having plural maltooligosaccharide chains have also been used for the phosphorylase-catalyzed enzymatic polymerization, giving rise to hydrogels. Reductive amination of free maltooligosaccharides with amino groups on basic polysaccharides using reductants is applicable to synthesize such maltooligosaccharide-grafted polysaccharide primers (Fig. 10a). Another method to synthesize maltooligosaccharide-grafted polysaccharide primers is condensation using condensing agents between amine-functionalized maltooligosaccharides and acidic polysaccharides having carboxylate groups

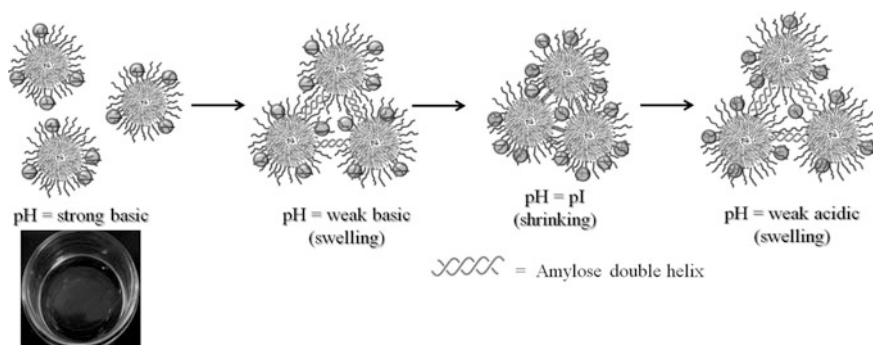


**Fig. 9** Plausible mechanism for pH-responsive behavior of amphoteric glycogen hydrogel

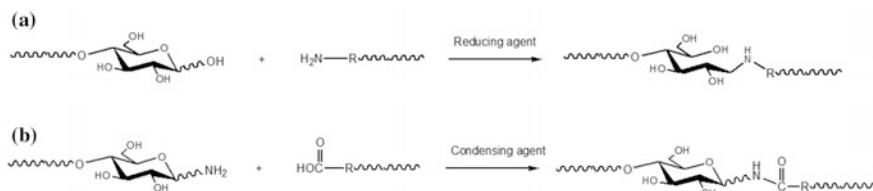


**Fig. 10** Immobilization reactions of maltooligosaccharide primer at reducing end by **a** reductive amination and **b** condensation

(Fig. 10b) (Kaneko and Kadokawa 2009a; Kadokawa 2011b, 2012, 2013, 2014, 2015a). By means of the former reaction, followed by the phosphorylase-catalyzed enzymatic polymerization (chemoenzymatic approach), amylose-grafted chitosan and cellulose hydrogels have been prepared (Kaneko et al. 2007; Matsuda et al. 2007; Omagari et al. 2009).

Chitosan is an aminopolysaccharide, composed of  $\beta(1 \rightarrow 4)$ -linked GlcN repeating units, which is obtained by *N*-deacetylation of a natural polysaccharide, chitin (Pillai et al. 2009). Maltoheptaose (Glc<sub>7</sub>) was introduced onto the chitosan chain by the reductive amination of Glc<sub>7</sub> with amino groups at C-2 position in chitosan using NaBH<sub>3</sub>CN in a mixed solvent of aqueous acetic acid/methanol, giving rise to a maltooligosaccharide-grafted chitosan (Fig. 11). Then, the phosphorylase-catalyzed enzymatic polymerization of Glc-1-P from the maltooligosaccharide primers on the product was performed to obtain an amylose-grafted chitosan. The hydrogel of the product was produced by drying the reaction mixture slowly in the vessel at 40–50 °C (Fig. 11). The hydrogelation was caused by the formation of double helix cross-linking points between the amylose graft chains on the chitosan chains.

For the production of the amylose-grafted cellulose hydrogel by the chemoenzymatic method, amino groups were first introduced to cellulose by the following successive reactions; partial tosylation of the OH groups at C-6 position,

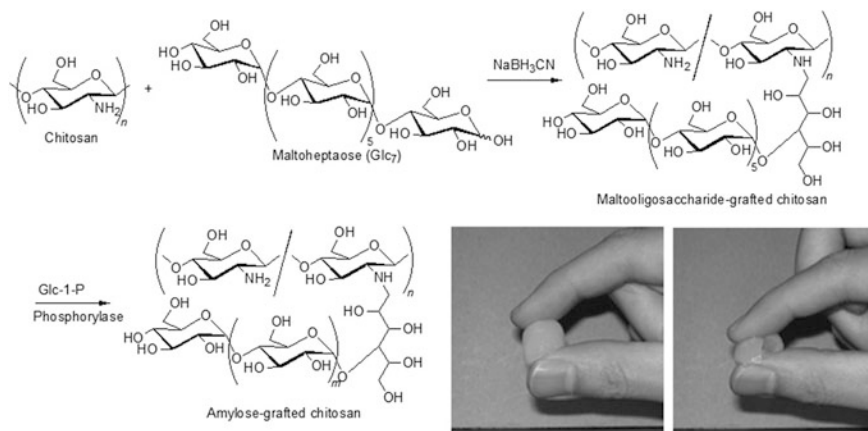


**Fig. 11** Chemoenzymatic preparation of amylose-grafted chitosan hydrogel

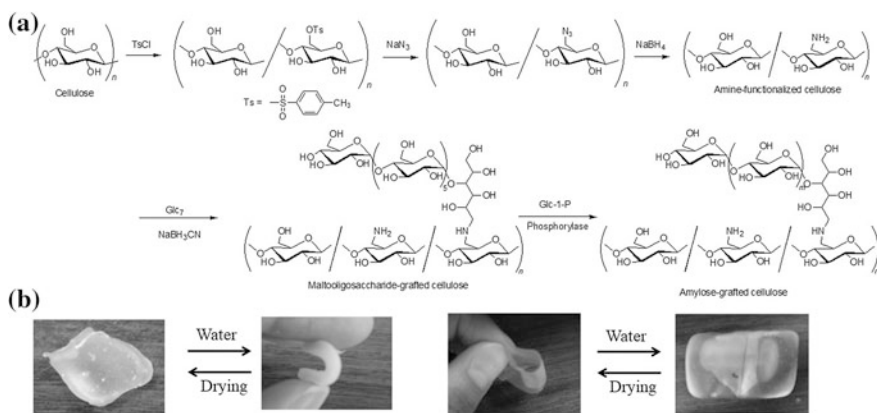


**Fig. 12 a** Chemoenzymatic preparation of amylose-grafted cellulose and **b** wetting-drying process of its hydrogel

displacement of the tosylates by azido groups; and reduction to amino groups (Fig. 12a). The maltooligosaccharide-grafted cellulose, which was prepared by reductive amination using the amine-functionalized cellulose and free Glc<sub>7</sub>, was synthesized by the reductive amination method. Subsequently, an amylose-grafted cellulose was obtained by the phosphorylase-catalyzed enzymatic polymerization of Glc-1-P from the maltooligosaccharide primers on the cellulose backbone (Fig. 12a). When the reaction mixture was left standing on a Petri dish at room temperature for several days, it totally turned into the gelling form. The resulting hydrogel was tougher than that formed from the amylose-grafted chitosan after washing with water several times to remove some contaminants such as the



unreacted Glc-1-P. The hydrogel was converted further into the solid material by drying under the ambient atmosphere. The addition of water to the solid returned to the hydrogel again. The cycle between the hydrogel and solid was able to be repeated by the wetting and drying process (Fig. 12b). Furthermore, the above property of the amylose-grafted cellulose allowed the formation of a film. The thinly spread enzymatic polymerization mixture was left standing at room temperature, resulting in a wet and swollen film, which was converted into the soft film by drying under the ambient atmosphere. The cycle between the swollen and dried films was also repeated by wetting and drying (Fig. 12b).

For the latter condensation reaction with acidic polysaccharides having carboxylate groups in the chemoenzymatic approach, Glc<sub>7</sub> must have an amino group at the reducing end because it needs to react with the carboxylate groups by condensation to obtain the maltooligosaccharide-grafted polysaccharides (Fig. 13). First, Glc<sub>7</sub> lactone was prepared by I<sub>2</sub>/KOH oxidation at the reducing end and subsequent cation exchange and intramolecular dehydrative condensation (Kobayashi et al. 1996). Then, the product was reacted with 2-azidoethylamine, followed by reduction by NaBH<sub>4</sub> to give an amine-functionalized maltooligosaccharide. Xanthan gum and carboxymethyl cellulose sodium salt (NaCMC) have been employed for condensation with the product and the subsequent phosphorylase-catalyzed enzymatic polymerization (Arimura et al. 2011; Kadokawa 2012; Hatanaka et al. 2014).

Xanthan gum, which is a water-soluble polysaccharide produced by *Xanthomonas campestris*, has a β(1 → 4)-glucosidic backbone as well as cellulose and trisaccharide side-chains (mannose-β(1 → 4)-glucuronic acid-β(1 → 2)-mannose-α(1 → 3)-) attached to alternating glucose units in the main-chain (Melton et al. 1976). The C-6 position of α-mannoside unit is acetylated, and the C-4 and -6 positions of β-mannoside unit are partially pyruvated. For the chemoenzymatic approach, the maltooligosaccharide primers were first introduced on the xanthan gum chain by condensation of an amine-functionalized maltooligosaccharide with carboxylate groups using water-soluble carbodiimide (WSC)/*N*-hydroxysuccinimide (NHS) as the condensing agent to produce a maltooligosaccharide-grafted xanthan

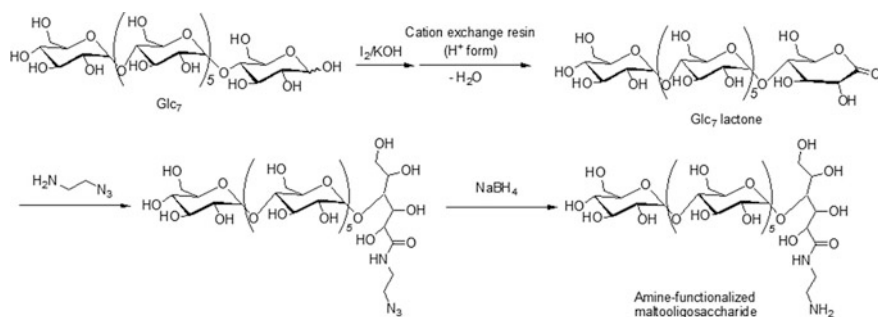


**Fig. 13** Synthesis of amine-functionalized maltooligosaccharide

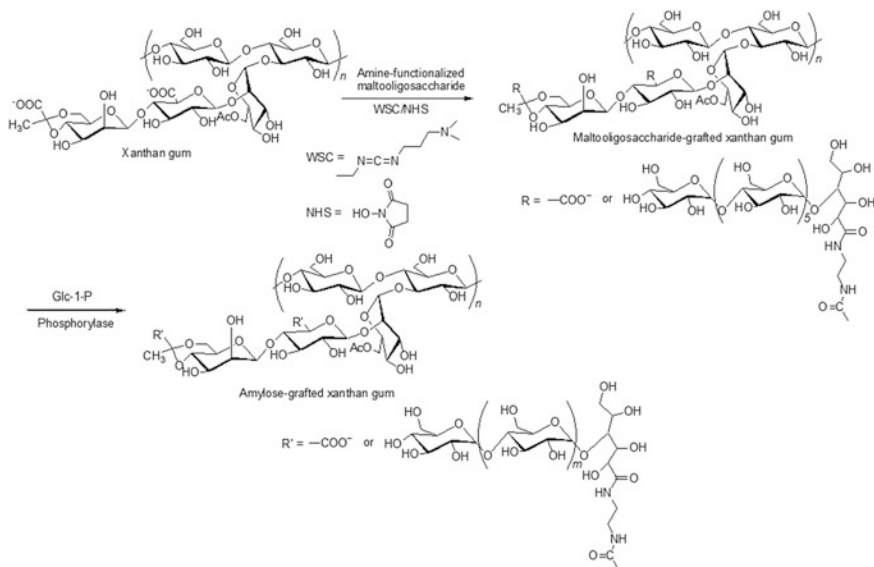


**Fig. 14** Chemoenzymatic synthesis of amylose-grafted xanthan gum

gum (Fig. 14). Then, an amylose-grafted xanthan gum was obtained by means of the phosphorylase-catalyzed enzymatic polymerization of Glc-1-P from the maltooligosaccharide primers on the xanthan gum main-chain (Fig. 14). The product formed an ion gel with an ionic liquid, 1-butyl-3-methylimidazolium chloride (BMIMCl), when the mixture was stirred until it became homogeneous (Fig. 15a). The hydrogel with high water content was obtained by soaking the ion gel in water (Fig. 15b). The hydrogel converted to an ionically cross-linked hydrogel with trivalent metal cations by soaking in aqueous  $\text{FeCl}_3$  (Fig. 15c). When the mechanical properties of the ionically cross-linked hydrogels with  $\text{Fe}^{3+}$  were evaluated by compressive testing, the fracture strain values increased with increasing functionalities or DPs of the amylose graft chains. It was suggested that the  $\text{Fe}^{3+}$ -treated hydrogels were fabricated by not only ionically cross-linking with  $\text{Fe}^{3+}$  and double helix conformation of the xanthan gum chains, but also double helix conformation of the amylose graft chains. The formation of looser network structures in the hydrogels was conceived by the presence of the double helix structure between the amylose graft chains, which probably contributed to resulting in the enhancement of elasticity.

An amylose-grafted NaCMC was also synthesized by the same way to the amylose-grafted xanthan gum (Fig. 16). NaCMC is water-soluble cellulose derivative with a carboxymethyl group at 6-position of the glucose unit (Stephen et al. 2006). The maltooligosaccharide-grafted NaCMC was synthesized by the condensation reaction between an amine-functionalized maltooligosaccharide and a carboxylate group of NaCMC in the presence of WSC/NHS under the same

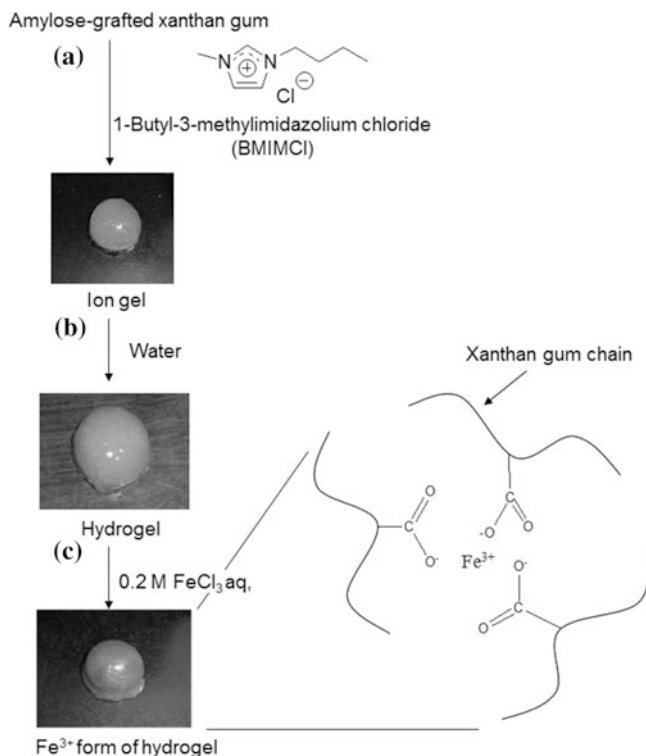


**Fig. 15** **a** Formation of ion gel of amylose-grafted xanthan gum with 1-butyl-3-methylimidazolium chloride (BMIMCl), **b** conversion into hydrogel, and **c** cross-linking with trivalent Fe<sup>3+</sup> ion

conditions as those using xanthan gum to obtain the maltooligosaccharide-grafted NaCMC. When the phosphorylase-catalyzed enzymatic polymerization of Glc-1-P using the maltooligosaccharide-grafted NaCMC with the functionality of 35.4% was carried out in the feed ratio of Glc-1-P/maltooligosaccharide = 500 in sodium acetate buffer, the hydrogel was formed in the resulting reaction mixture. After lyophilization of the hydrogel, the average DP value of the amylose graft chains was calculated on the basis of the elemental analysis data and the functionality of the maltooligosaccharide chain to be 214.

A film was fabricated by drying a thinly spread alkaline solution of the product in aqueous NaOH; the film still contained NaOH. The morphology of nanofibers with highly entangled fashion was shown in the SEM image of the film (Fig. 17). After the immersion of the film in water to remove NaOH from the film, merged nanofibers each other at interfacial area with remaining the fiber arrangements were observed by the SEM observation (Fig. 17).

On the basis of the above results, the self-assembling generative (bottom-up) process has been proposed, leading to the formation of the nanofiber film as shown

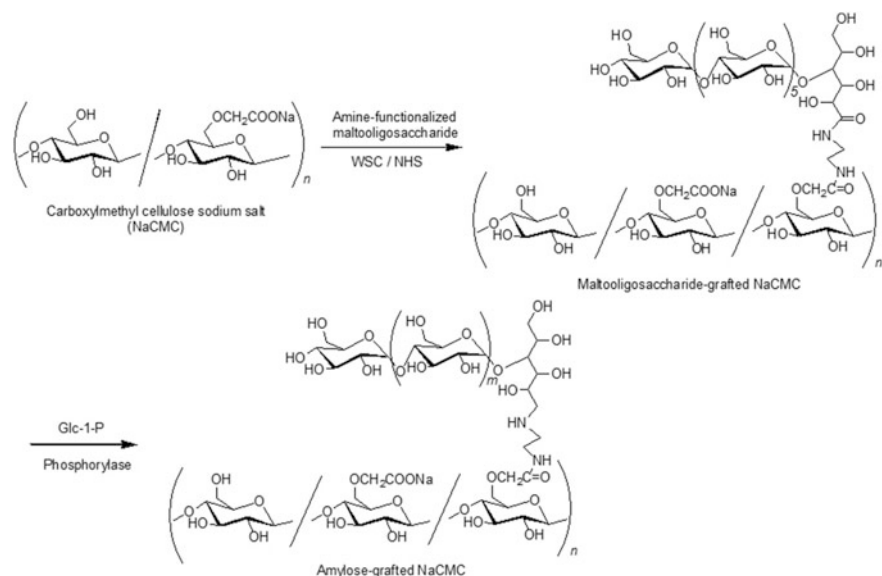


**Fig. 16** Chemoenzymatic synthesis of amylose-grafted carboxymethyl cellulose sodium salt (NaCMC)

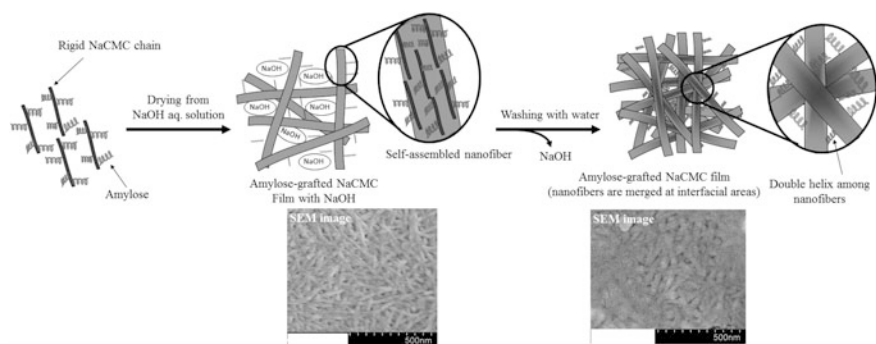


**Fig. 17** Plausible mechanism for formation of nanofiber films from amylose-grafted NaCMC and their SEM images

in Fig. 17. The introduction of the amylose graft chains on NaCMC avoided forming the random-coil conformation, providing the rigid nature of the NaCMC chain. During drying the aqueous alkaline solution, some of these rigid materials regularly organized to induce nanofibrillation with the slight double helix formation from the amylose graft chains on NaCMCs, but they did not form large aggregates because of the prevention of the double helix formation from the most of the amylose chains under the strong basic conditions. By washing out NaOH from the

film, the further formation of double helices on the nanofibers was induced, resulting in merging on the surface of the fibers.

#### 4 Fabrication of Supramolecular Gels by Inclusion Complexation of Enzymatically Produced Amyloses in Vine-Twining Polymerization

Inclusion complexes of amylose with polymeric guest compounds have attracted increasingly attention as elemental components to hierarchically fabricate supramolecular functional materials rather than those with monomeric guest molecules. However, the study regarding the direct complexation of amylose and polymeric molecules was limited (Shogren et al. 1991; Shogren 1993; Star et al. 2002; Ikeda et al. 2006; Kida et al. 2007; Kaneko et al. 2011a; Rachmawati et al. 2013a; Kumar et al. 2013; Rachmawati et al. 2013b, 2014). It is difficult for the amylose to include the long chains of polymeric guests into the cavity because the driving force for complexation between guest molecules and amylose is only weak hydrophobic interaction. The authors have considered to develop the new methodology for the direct preparation of inclusion complexes composed of amylose and polymeric guests in the enzymatic polymerization field. Such a method was achieved to obtain the inclusion complex catalyzed by the phosphorylase in the dispersion of hydrophobic polymers with aqueous buffer solvents. The elongating process from the shorter  $\alpha(1 \rightarrow 4)$ -glucan (maltooligosaccharide) to the longer  $\alpha(1 \rightarrow 4)$ -glucan (amylose) induced inclusion complexation with hydrophobic guest polymers (Kaneko and Kadokawa 2005, 2006, 2009b; Kadokawa 2011b, 2012, 2013a, 2014, 2015c). The representation of the elongation process in the phosphorylase-catalyzed enzymatic polymerization system is similar as the way that vine of plant grows twining around a rod (Fig. 18). Accordingly, we have proposed that this enzymatic manner for the construction of amylose-polymer inclusion complexes is named ‘vine-twining polymerization.’

The authors reported that the first example of the vine-twining polymerization to produce an amylose-inclusion complex by using poly(tetrahydrofuran) (PTHF) as a hydrophobic guest polymer (Fig. 19) (Kadokawa et al. 2001b, 2002). When the vine-twining polymerization using Glc-1-P monomer and Glc<sub>7</sub> primer catalyzed by

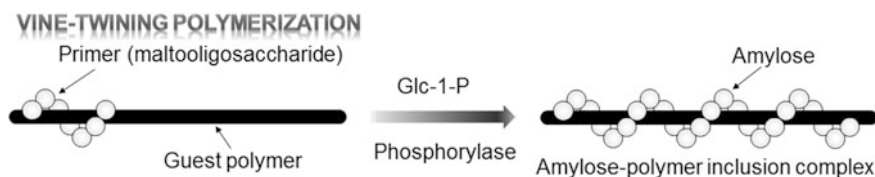


**Fig. 18** Image of vine-twining polymerization to produce amylose-polymer inclusion complex through phosphorylase-catalyzed enzymatic polymerization

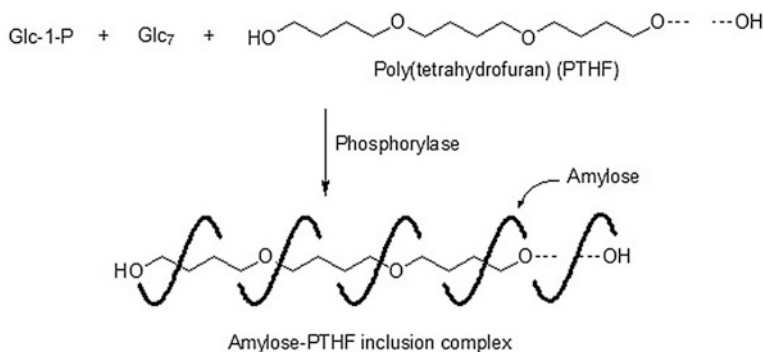


**Fig. 19** Vine-twining polymerization using poly(tetrahydrofuran) (PTHF) as a guest polymer

phosphorylase was conducted in the presence of PTHF dispersed with sodium citrate buffer as a polymerization solvent, the inclusion complex composed of amylose and PTHF was gradually precipitated with the progress of the polymerization. No inclusion complex was produced by the simple mixing of amylose and PTHF in a buffer solvent, strongly suggesting a possibility for complexation during the above enzymatic polymerization progress. On the other hand, the produced amylose did not form the inclusion complex when poly(ethylene glycol) with two methylene lengths was used as a hydrophilic guest polymer. This result suggested that hydrophobicity of guest polymers strongly affected whether complexation by amylose was progressed in the vine-twining polymerization system.

On the basis of significance in hydrophobicity of guest polymers on the formation of inclusion complexes, the use of three polyesters, poly( $\epsilon$ -caprolactone) (PCL), poly( $\delta$ -valerolactone) (PVL), and poly(glycolic acid-*co*- $\epsilon$ -caprolactone), as hydrophobic guest polymers in the vine-twining polymerization successfully provided the amylose-inclusion complexes (Fig. 20) (Kadokawa et al. 2001a, 2003; Nomura et al. 2011). When three kinds of poly(lactide)s (PLAs) were used as optically active guest polymers, i.e. poly(L-lactide) (PLLA), poly(D-lactide), and poly(DL-lactide), it was found that the amylose produced by the vine-twining polymerization perfectly recognized the chirality in PLAs on complexation and consequently it only formed an inclusion complex with PLLA (Kaneko et al. 2011b). The selectivity of inclusion complexation by amylose toward PLLA is probably owing to their same helical direction, that is, left-handed helix, resulting in the conformational suitability for complexation.

Taking the vine-twining polymerization manner around a guest polymer into consideration, the authors investigated to hierarchically fabricate supramolecular polymers composed of amylose-PLLA inclusion complex by using primer-guest conjugate substrates. This approach is based on the following strategic manner, in which a propagating amylose chain started from Glc<sub>7</sub> moiety in the conjugate substrate in the phosphorylase-catalyzed enzymatic polymerization potentially includes a PLLA segment in another substrate, and consequently, such inclusion

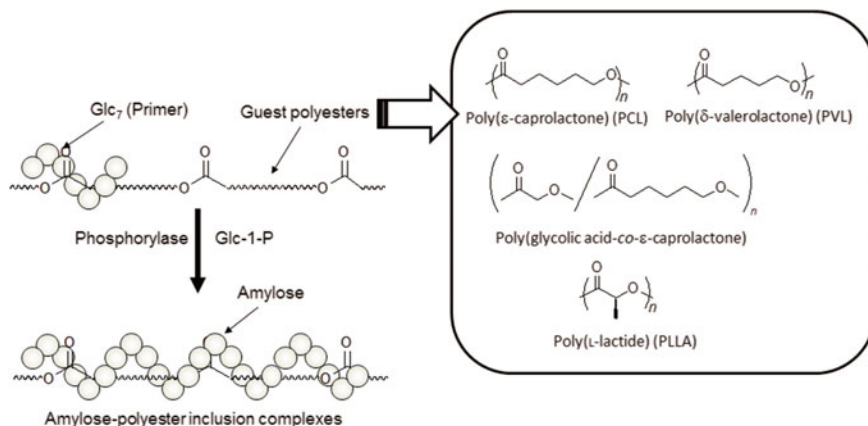


**Fig. 20** Vine-twining polymerization using various polyesters as guest polymers

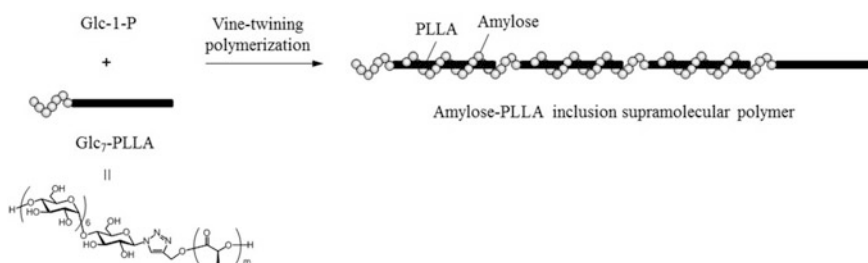


**Fig. 21** Synthesis of amylose-PLLA inclusion supramolecular polymer by vine-twining polymerization using  $\text{Glc}_7$ -PLLA as a primer-guest polymer conjugate

complexation among the substrates successively takes place, resulting in amylose-inclusion supramolecular polymeric materials. To carry out the strategy,  $\text{Glc}_7$ -functionalized PLLA ( $\text{Glc}_7$ -PLLA) was synthesized by copper(I)-catalyzed azide-alkyne cycloaddition reaction (CuAAC) using maltoheptaosyl azide and alkyne-terminated PLLA (Tanaka et al. 2013a), and used as a primer-guest conjugate substrate in the vine-twining polymerization (Fig. 21) (Tanaka et al. 2013b). The morphology and solubility of the product using  $\text{Glc}_7$ -PLLA were completely different from those of the previously reported amylose-PLLA inclusion complex which was synthesized by means of vine-twining polymerization using  $\text{Glc}_7$  and PLLA as a primer and a guest polymer, respectively. The similar XRD pattern of the product was observed with that of the amylose-PLLA inclusion complex. The  $^1\text{H}$  NMR spectrum of the product showed signals not only due to amylose but also due to PLLA. The solubility of the resulting product with DMSO was poor although the amylose-PLLA inclusion complex using  $\text{Glc}_7$  and PLLA was properly dissolved with DMSO. Compared with that of DMSO-soluble fraction of the

product using Glc<sub>7</sub>-PLLA, the GPC peak of the alkaline hydrolysate of the product shifted to lower molecular weight region. These results supported that vine-twining polymerization using Glc<sub>7</sub>-PLLA as a primer-guest conjugate substrate produced a polymeric continuum of inclusion complex in which PLLA was included by an amylose chain enzymatically elongated from the other Glc<sub>7</sub>-PLLA substrate; that is, a linear inclusion supramolecular polymer composed of amylose and PLLA. Another linear supramolecular polymer composed of amylose and PTHF was also synthesized using Glc<sub>7</sub>-functionalized PTHF as a primer-guest conjugate substrate in vine-twining polymerization (Tanaka et al. 2015b). Although these linear inclusion supramolecular polymers were film-formable, they did not exhibit gel formation.

On the other hand, a hyperbranched inclusion supramolecular polymer composed amylose and PLLA by means of vine-twining polymerization was gel-formable. When a Glc<sub>7</sub>-functionalized branched PLLA (Glc<sub>7</sub>-PLLA<sub>2</sub>), which was synthesized by CuAAC using maltoheptaosyl azide and alkyne-terminated branched PLLA, was used as a primer-guest conjugate substrate in vine-twining polymerization, a hyperbranched inclusion supramolecular polymer composed of amylose and PLLA was obtained (Fig. 22) (Tanaka et al. 2015a). The XRD, <sup>1</sup>H NMR, and GPC measurements of the product using Glc<sub>7</sub>-PLLA<sub>2</sub> and its alkaline hydrolysate supported that the hyperbranched structure including PLLA by elongated amylose was formed due to biantennary structure of the primer-guest conjugate substrate. The solution of the product using Glc<sub>7</sub>-PLLA<sub>2</sub> with an ionic liquid, BMIMCl, formed an ion gel (Fig. 23). Such ion gel was not formed by the same procedure from the linear amylose-PLLA inclusion supramolecular polymer using Glc<sub>7</sub>-PLLA, indicating that the hyperbranched structure constructed by amylose and PLLA strongly contributed to exhibiting ability of the gel formation.

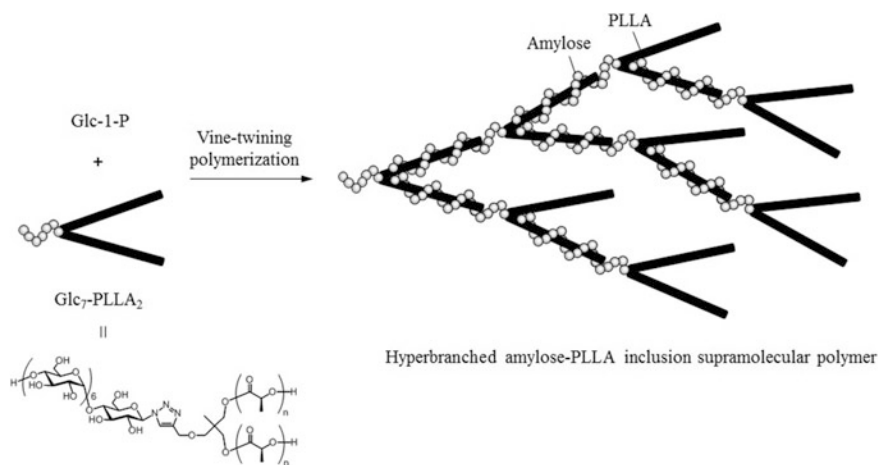


**Fig. 22** Synthesis of hyperbranched amylose-PLLA inclusion supramolecular polymer by vine-twining polymerization using Glc<sub>7</sub>-PLLA<sub>2</sub> as a primer-guest polymer conjugate



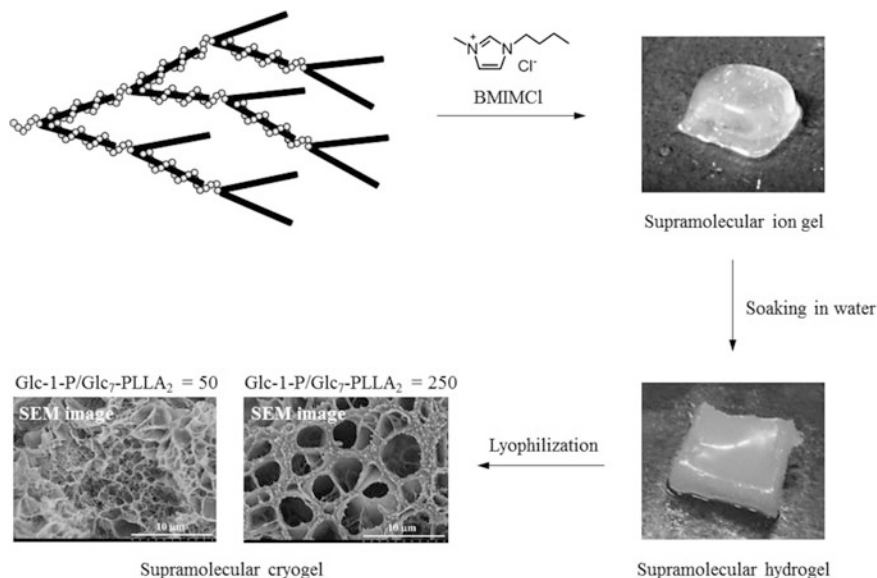


**Fig. 23** Preparation of ion gel of hyperbranched amylose-PLLA inclusion supramolecular polymer with BMIMCl and its conversion into hydrogel and subsequently into cryogel

The frequency dependence of storage and loss modulus ( $G'$  and  $G''$ , respectively) of the ion gel showed signature of typical viscoelastic material with predominance of storage modulus on the whole frequency range. No gelation from the solution of linear inclusion supramolecular polymer with BMIMCl was supported by the dynamic viscoelastic result because the  $G''$  values were mostly larger than the  $G'$  values. The hydrogel was obtained from the ion gel by exchanging of dispersion media from BMIMCl to water by soaking. The successful conversion into the hydrogel was confirmed by the dynamic viscoelastic data of the resulting material from ion gel, in which the  $G'$  values were always larger than the  $G''$  values. The significant difference in the dynamic viscoelastic results of the ion and hydrogels from both the Glc-1-P/Glc<sub>7</sub>-PLLA<sub>2</sub> feed ratios = 50 and 250 was not appeared. After the lyophilization, the hydrogel converted to the cryogel. The SEM image of the cryogel showed porous morphology. The average pore sizes of the cryogel made bigger from 2.0 to 3.7  $\mu\text{m}$  as increasing Glc-1-P/Glc<sub>7</sub>-PLLA<sub>2</sub> feed ratio from 50 to 250. Accordingly, the SEM results suggest that the hyperbranched fashion in cryogels affects the porous morphologies.

The other way to fabricate supramolecular gels by means of the vine-twining polymerization was achieved using graft copolymers having hydrophobic graft polyesters, such as PCL and PVL. Complexation of amylose with the graft chains between the intermolecular graft copolymers by the vine-twining polymerization afforded cross-linking points, giving rise to supramolecular gels (Fig. 24) (Kadokawa 2015c). To design the suitable graft copolymer structure, it has to

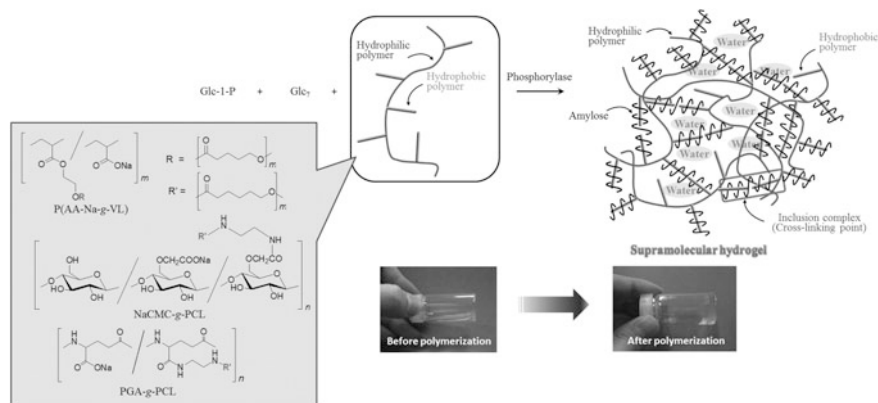


**Fig. 24** Fabrication of supramolecular hydrogels through formation of inclusion complex cross-linking points by vine-twining polymerization using graft copolymers composed of hydrophilic main chains and hydrophobic graft chains

exhibit water-solubility as a component of hydrogel, whereas hydrophobicity is necessary to be acted as guest polymers for complexation by amylose.

Taking these antagonistic properties for the graft copolymer structure into account, the authors designed  $\delta$ -valerolactone-grafted poly(acrylic acid sodium salt) (PAA-Na-g-PVL) that had poly(acrylic acid sodium salt) (PAA-Na) segment as a strong hydrophilic polymer to contribute to enhancing water-solubility of the graft copolymer and poly(valerolactone) (PVL) segment to induce complexation by amylose in the vine-twining polymerization.

When the phosphorylase-catalyzed vine-twining polymerization was carried out using Glc-1-P and the Glc<sub>7</sub> primer in the presence of PAA-Na-g-PVL in sodium acetate buffer, a hydrogel was produced in the reaction mixture (Fig. 24) (Kaneko et al. 2010). Complexation by amylose toward the PVL graft chains was confirmed by the XRD measurement of the powdered sample prepared by lyophilization of the produced hydrogel. The typical diffraction peaks which corresponded to the structure of an amylosic inclusion complex were shown on the XRD analysis. The XRD pattern was completely different from that of a sole amylose. This result indicated that PVL graft chains acted as cross-linking points with amylose in the vine-twining polymerization system to induce inclusion complexes in the intermolecular (PAA-Na-g-PVL)s for the hierarchically formation of the supramolecular hydrogel.

The enzymatic disruption and reproduction of the resulting hydrogel was demonstrated by using two amylose-related enzymes, amylase, and phosphorylase, because amylose was hydrolyzed by amylase and produced by phosphorylase. The pure hydrogel sample was first prepared by adding aqueous sodium acetate buffer to the aforementioned powdered sample. The mixture of the hydrogel and  $\beta$ -amylase was totally converted to a solution after the enzymatic reaction. This disruption behavior indicated that the cross-linking points in the hydrogel composed of

amylose were cleavage by the hydrolysis catalyzed by  $\beta$ -amylase. The subsequent phosphorylase-catalyzed enzymatic polymerization, that is the addition of the phosphorylase and G-1-P, in the resulting solution was reproduced the hydrogel. Maltooligosaccharides, which were produced by the hydrolysis of the amylose components catalyzed by  $\beta$ -amylase and present in the solution after the above hydrolysis, acted as a primer for the enzymatic polymerization. The enzymatically produced amylose included the PVL graft chains in the intermolecular (PAA-Na-g-PVL)s forming cross-linking points. The enzymatic disruption-reproduction cycle was repeatable, indicating the enzymatically recyclable behavior of the present supramolecular hydrogel.

This methodology can be applied to another graft copolymer fabricating a supramolecular film through hydrogelation by the vine-twinning polymerization. To provide the film form from the amylosic supramolecule, NaCMC was employed as the main-chain of the graft copolymer because of its water solubility and film formability. A supramolecular hydrogel was obtained by the means of phosphorylase-catalyzed vine-twinning polymerization in sodium acetate buffer using NaCMC-g-PCL as a guest polymer-grafted copolymer (Kadokawa et al. 2013). The XRD profile of a powdered sample, which was obtained by lyophilization of the hydrogel, showed the typical diffraction pattern assignable to an amylosic inclusion complex, supporting the progress of gelation owing to complexation by amylose with the PCL graft chains in the intermolecular (NaCMC-g-PC)s for cross-linking. A supramolecular film was then obtained by addition of water to the powdered material, and subsequent drying (Fig. 25). This methodology provided the several films from the hydrogels which had the different amounts and molecular weights of the amylose molecules because they were controllably changed by the conditions in the phosphorylase-catalyzed enzymatic polymerization. The enhancement of the mechanical properties of the resulting films, which were composed of the moderate amounts and molecular weights of amylose, compared with a CMC film was observed by tensile testing. This result suggested that the supramolecular cross-linking structure in the films contributed to enhancing the mechanical properties.

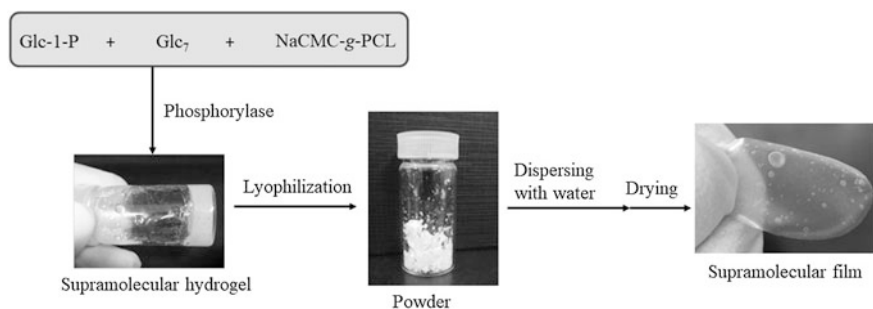


**Fig. 25** Fabrication of supramolecular film through hydrogelation by vine-twinning polymerization using NaCMC-g-PCL

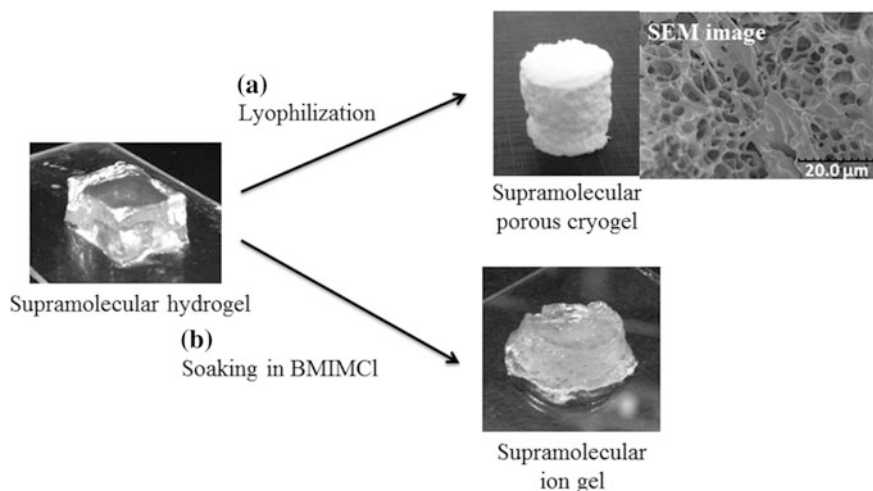


**Fig. 26** Conversion of supramolecular hydrogel, obtained from PGA-*g*-PCL, into **a** cryogel and **b** ion gel with BMIMCl

A self-standing supramolecular hydrogel with superior mechanical property was fabricated by the vine-twining polymerization using poly( $\gamma$ -glutamic acid-*graft*- $\epsilon$ -caprolactone) (PGA-*g*-PCL) (Kadokawa et al. 2015). The improvement of the mechanical property compared to the other hydrogels obtained using PAA-*g*-PVL and NaCMC-*g*-PCL was probably because of the high water retention and moisturizing properties of PGA. The presence of inclusion complexes in the resulting hydrogel was confirmed by the XRD measurement of the lyophilized sample (cryogel). The SEM image of the cryogel showed porous morphology (Fig. 26a). Furthermore, the cryogels from the hydrogels, fabricated by the larger amounts of Glc<sub>7</sub>, had the smaller pore sizes, because of the formation of the smaller networks from the larger amounts of Glc<sub>7</sub>. Soaking the hydrogel in BMIMCl induced exchange of dispersion media to produce an ion gel (Fig. 26b). The mechanical properties of the cryogels and ion gels were strongly affected by the enzymatic polymerization conditions for the hydrogelation.

Because the hydrogel was composed of supramolecular networks by the cross-linked inclusion complexation of amylose with the PCL graft chains, macroscopic interfacial healing through the phosphorylase-catalyzed enzymatic polymerization was demonstrated (Fig. 27). A sodium acetate buffer solution containing phosphorylase and Glc-1-P was applied to the surfaces of the two pieces, which were prepared by cutting of hydrogel.

After the surfaces were placed in contact and then left to stand at 40 °C for 6 h during the enzymatic polymerization, the two pieces had cohered at the interface. On the other hand, when the same procedure was conducted using a sole sodium

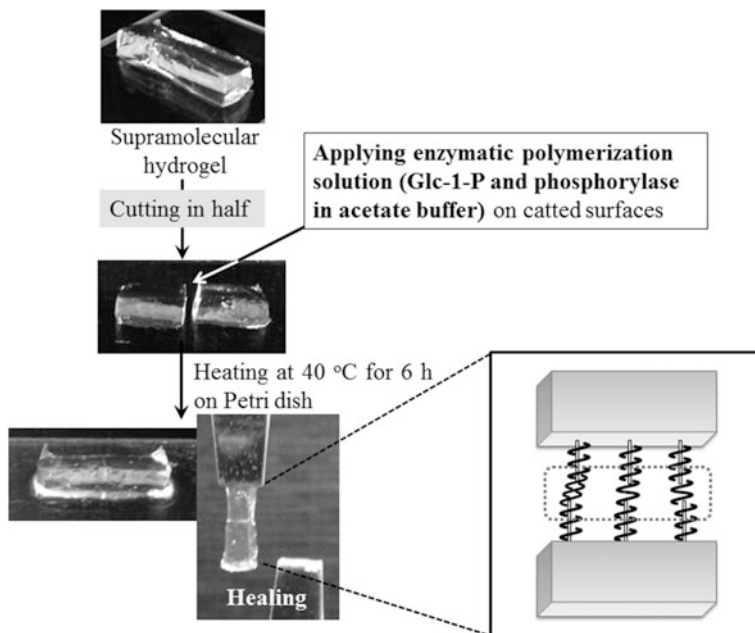


**Fig. 27** Macroscopic interfacial healing of supramolecular hydrogel, obtained from PGA-g-PCL, through phosphorylase-catalyzed enzymatic polymerization

acetate buffer, the surfaces were not cohered. The healing of the hydrogels on a macroscopic level was induced by complexation of the enzymatically produced amylose molecules with the PCL graft chains at the interface.

## 5 Conclusion

This chapter overviewed the fabrication of supramolecular gels composed of non-covalent cross-linking points of amylose through the phosphorylase-catalyzed enzymatic polymerization. Two kinds of non-covalent assemblies, double helix and inclusion complex, for cross-linking have been employed on the basis of specific properties of amylose owing to its helical conformation. Because amylose does not solely form gelling state, the other appropriate polymeric components have been employed for the gel formation with amylose. When the phosphorylase-catalyzed enzymatic polymerization was conducted using both the natural and synthetic multifunctional primer substances, the elongated amylose chains efficiently formed double helices among the substances to produce the supramolecular hydrogels. The other approach to the supramolecular hydrogel formation from amylose was achieved by inclusion complexation in the vine-twining polymerization process

using the designed graft copolymers. The resulting hydrogels exhibited unique and specific properties such as formability of cryo- and ion gels and macroscopic healing ability. The approaches described in this chapter will lead to fabricate further high-performance supramolecular gels from amylose. Furthermore, the amylose supramolecular gels have a potential to be used as biobased functional materials in biomedical, tissue engineering, and environmentally benign applications in the future.

## References

- Arimura T, Omagari Y, Yamamoto K, Kadokawa J (2011) Chemoenzymatic synthesis and hydrogelation of amylose-grafted xanthan gums. *Int J Biol Macromol* 49:498–503
- Brown RC, Brown TR (2014) *Biorenewable resources: engineering new products from agriculture*, 2nd edn. Wiley Blackwell, Chichester
- Calder PC (1991) Glycogen structure and biogenesis. *Int J Biochem* 23:1335–1352
- Corobea MC, Muhulet O, Miculescu F, Antoniac IV, Vuluga Z, Florea D et al (2016) Novel nanocomposite membranes from cellulose acetate and clay-silica nanowires. *Polym Adv Technol* 27(12):1586–1595
- Eisenhaber F, Schulz W (1992) Monte-carlo simulation of the hydration shell of double-helical amylose—a left-handed antiparallel double helix fits best into liquid water-structure. *Biopolymers* 32:1643–1664
- Fujii K, Takata H, Yanase M, Terada Y, Ohdan K, Takaha T, Okada S, Kuriki T (2003) Bioengineering and application of novel glucose polymers. *Biocatal Biotransform* 21:167–172
- Hatanaka D, Takemoto Y, Yamamoto K, J-i Kadokawa (2014) Hierarchically self-assembled nanofiber films from amylose-grafted carboxymethyl cellulose. *Fibers* 2:34–44
- Hinrichs W, Buttner G, Steifa M, Betzel C, Zabel V, Pfannemuller B, Saenger W (1987) An amylose antiparallel double helix at atomic resolution. *Science* 238:205–208
- Ikeda M, Furusho Y, Okoshi K, Tanahara S, Maeda K, Nishino S, Mori T, Yashima E (2006) A luminescent poly(phenylenevinylene)-amylose composite with supramolecular liquid crystallinity. *Angew Chem Int Ed* 45:6491–6495
- Izawa H, Kadokawa J (2009) Preparation of functional amylosic materials by phosphorylase-catalyzed polymerization. In: Kadoakwa J (ed) *Interfacial researches in fundamental and material sciences of oligo- and polysaccharides*. Transworld Research Network, Trivandrum, pp 69–86
- Izawa H, Nawaji M, Kaneko Y, Kadokawa J (2009) Preparation of glycogen-based polysaccharide materials by phosphorylase-catalyzed chain elongation of glycogen. *Macromol Biosci* 9:1098–1104
- Kadoakwa J (2012) Synthesis of amylose-grafted polysaccharide materials by phosphorylase-catalyzed enzymatic polymerization. In: Smith PB, Gross RA (eds) *Biobased monomers, polymers, and materials*, vol 1043. ACS Symposium Series 1105. American Chemical Society, Washington, DC, pp 237–255
- Kadoakwa J (2013) Synthesis of new polysaccharide materials by phosphorylase-catalyzed enzymatic  $\alpha$ -glycosylations using polymeric glycosyl acceptors. In: Cheng HN, Gross RA, Smith PB (eds) *Green polymer chemistry: biocatalysis and materials II*, vol 1144. ACS Symposium Series 1144. American Chemical Society, Washington, DC, pp 141–161
- Kadokawa J (2011a) Facile synthesis of unnatural oligosaccharides by phosphorylase-catalyzed enzymatic glycosylations using new glycosyl donors. In: Gordon NS (ed) *Oligosaccharides: sources, properties and applications*. Nova Science Publishers Inc, Hauppauge, pp 269–281

- Kadokawa J (2011b) Precision polysaccharide synthesis catalyzed by enzymes. *Chem Rev* 111:4308–4345
- Kadokawa J (2012) Preparation and applications of amylose supramolecules by means of phosphorylase-catalyzed enzymatic polymerization. *Polymers* 4:116–133
- Kadokawa J (2013a) Architecture of amylose supramolecules in form of inclusion complexes by phosphorylase-catalyzed enzymatic polymerization. *Biomolecules* 3:369–385
- Kadokawa J (2013b) Synthesis of non-natural oligosaccharides by  $\alpha$ -glucan phosphorylase-catalyzed enzymatic glycosylations using analogue substrates of  $\alpha$ -D-glucose 1-phosphate. *Trends Glycosci Glycotechnol* 25:57–69
- Kadokawa J (2014) Chemoenzymatic synthesis of functional amylosic materials. *Pure Appl Chem* 86:701–709
- Kadokawa J (2015a) Chemoenzymatic synthesis of amylose-grafted cellulose derivatives. In: Mondal MIH (ed) *Cellulose and cellulose derivatives*. Nova Science Publishers Inc, Hauppauge, pp 299–311
- Kadokawa J (2015b) Enzymatic synthesis of non-natural oligo- and polysaccharides by phosphorylase-catalyzed glycosylations using analogue substrates. In: Cheng HN, Gross RA, Smith PB (eds) *Green polymer chemistry: biobased materials and biocatalysis*, vol 1192. ACS Symposium Series 1192. American Chemical Society, Washington, DC, pp 87–99
- Kadokawa J (2015c) Hierarchically fabrication of amylosic supramolecular nanocomposites by means of inclusion complexation in phosphorylase-catalyzed enzymatic polymerization field. In: Thakur KV, Thakur KM (eds) *Eco-friendly polymer nanocomposites: processing and properties*. Springer, New Delhi, pp 513–525
- Kadokawa J, Kaneko Y (2013) Engineering of polysaccharide materials—by phosphorylase-catalyzed enzymatic chain-elongation. Pan Stanford Publishing Pte Ltd., Singapore
- Kadokawa J, Kobayashi S (2010) Polymer synthesis by enzymatic catalysis. *Curr Opin Chem Biol* 14:145–153
- Kadokawa J, Kaneko Y, Nakaya A, Tagaya H (2001a) Formation of an amylose-polyester inclusion complex by means of phosphorylase-catalyzed enzymatic polymerization of  $\alpha$ -D-glucose 1-phosphate monomer in the presence of poly( $\epsilon$ -caprolactone). *Macromolecules* 34:6536–6538
- Kadokawa J, Kaneko Y, Tagaya H, Chiba K (2001b) Synthesis of an amylose-polymer inclusion complex by enzymatic polymerization of glucose 1-phosphate catalyzed by phosphorylase enzyme in the presence of polythf: a new method for synthesis of polymer-polymer inclusion complexes. *Chem Commun*, 449–450
- Kadokawa J, Kaneko Y, Nagase S, Takahashi T, Tagaya H (2002) Vine-twinning polymerization: Amylose twines around polyethers to form amylose—polyether inclusion complexes. *Chem Eur J* 8:3321–3326
- Kadokawa J, Nakaya A, Kaneko Y, Tagaya H (2003) Preparation of inclusion complexes between amylose and ester-containing polymers by means of vine-twinning polymerization. *Macromol Chem Phys* 204:1451–1457
- Kadokawa J, Nomura S, Hatanaka D, Yamamoto K (2013) Preparation of polysaccharide supramolecular films by vine-twinning polymerization approach. *Carbohydr Polym* 98:611–617
- Kadokawa J, Tanaka K, Hatanaka D, Yamamoto K (2015) Preparation of multiformable supramolecular gels through helical complexation by amylose in vine-twinning polymerization. *Polym Chem* 6:6402–6408
- Kaneko Y, Kadokawa J (2005) Vine-twinning polymerization: a new preparation method for well-defined supramolecules composed of amylose and synthetic polymers. *Chem Rec* 5:36–46
- Kaneko Y, Kadokawa J (2006) Synthesis of nanostructured bio-related materials by hybridization of synthetic polymers with polysaccharides or saccharide residues. *J Biomater Sci Polym Ed* 17:1269–1284
- Kaneko Y, Kadokawa J (2009a) Chemoenzymatic synthesis of amylose-grafted polymers. In: Ito R, Matsuo Y (eds) *Handbook of carbohydrate polymers: development, properties and applications*. Nova Science Publishers Inc, Hauppauge, pp 671–691

- Kaneko Y, Kadokawa J (2009b) Preparation of polymers with well-defined nanostructure in the polymerization field. In: Lee JN (ed) *Modern trends in macromolecular chemistry*. Nova Science Publishers Inc, Hauppauge, pp 199–217
- Kaneko Y, Matsuda S, Kadokawa J (2007) Chemoenzymatic syntheses of amylose-grafted chitin and chitosan. *Biomacromol* 8:3959–3964
- Kaneko Y, Fujisaki K, Kyutoku T, Furukawa H, Kadokawa J (2010) Preparation of enzymatically recyclable hydrogels through the formation of inclusion complexes of amylose in a vine-twining polymerization. *Chem Asian J* 5:1627–1633
- Kaneko Y, Kyutoku T, Shimomura N, Kadokawa J (2011a) Formation of amylose-poly (tetrahydrofuran) inclusion complexes in ionic liquid media. *Chem Lett* 40:31–33
- Kaneko Y, Ueno K, Yui T, Nakahara K, Kadokawa J (2011b) Amylose's recognition of chirality in polylactides on formation of inclusion complexes in vine-twining polymerization. *Macromol Biosci* 11:1407–1415
- Kida T, Minabe T, Okabe S, Akashi M (2007) Partially-methylated amyloses as effective hosts for inclusion complex formation with polymeric guests. *Chem Commun*, 1559–1561
- Kitamura S (1996) Starch polymers, natural and synthetic. In: Salamone C (ed) *The polymeric materials encyclopedia, synthesis, properties and applications*, vol 10. CRC Press, New York, pp 7915–7922
- Kitamura S, Yunokawa H, Mitsui S, Kuge T (1982) Study on polysaccharide by the fluorescence method 2. Micro-brownian motion and conformational change of amylose in aqueous-solution. *Polym J* 14:93–99
- Kitaoka M, Hayashi K (2002) Carbohydrate-processing phosphorolytic enzymes. *Trends Glycosci Glycotechnol* 14:35–50
- Klemm D, Heublein B, Fink HP, Bohn A (2005) Cellulose: fascinating biopolymer and sustainable raw material. *Angew Chem Int Ed* 44:3358–3393
- Kobayashi K, Kamiya S, Enomoto N (1996) Amylose-carrying styrene macromonomer and its homo- and copolymers: synthesis via enzyme-catalyzed polymerization and complex formation with iodine. *Macromolecules* 29:8670–8676
- Kumar K, Woortman AJJ, Loos K (2013) Synthesis of amylose-polystyrene inclusion complexes by a facile preparation route. *Biomacromol* 14:1955–1960
- Lejeune A, Deprez T (2009) *Cellulose: structure and properties, derivatives and industrial uses*. Nova Science Publishers, Hauppauge
- Lenz RW (1993) Biodegradable polymers. *Adv Polym Sci* 107:1–40
- Manners DJ (1991) Recent developments in our understanding of glycogen structure. *Carbohydr Polym* 16:37–82
- Matsuda S, Kaneko Y, Kadokawa J (2007) Chemoenzymatic synthesis of amylose-grafted chitosan. *Macromol Rapid Commun* 28:863–867
- Melton LD, Mindt L, Rees DA (1976) Covalent structure of the extracellular polysaccharide from *Xanthomonas campestris*: evidence from partial hydrolysis studies. *Carbohydr Res* 46:245–257
- Miculescu M, Thakur VK, Miculescu F, Voicu SI (2016) Graphene-based polymer nanocomposite membranes: a review. *Polym Adv Technol* 27(7):844–859
- Mohanty AK, Misra M, Drzal LT (2002) Sustainable bio-composites from renewable resources: opportunities and challenges in the green materials world. *J Polym Environ* 10:19–26
- Nakai H, Kitaoka M, Svensson B, Ohtsubo K (2013) Recent development of phosphorylases possessing large potential for oligosaccharide synthesis. *Curr Opin Chem Biol* 17:301–309
- Nawaji M, Izawa H, Kaneko Y, Kadokawa J (2008) Enzymatic  $\alpha$ -glucosaminylation of maltooligosaccharides catalyzed by phosphorylase. *Carbohydr Res* 343:2692–2696
- Nishinari K, Takahashi R (2003) Interaction in polysaccharide solutions and gels. *Curr Opin Colloid Interface Sci* 8:396–400
- Nishinari K, Zhang H, Ikeda S (2000) Hydrocolloid gels of polysaccharides and proteins. *Curr Opin Colloid Interface Sci* 5:195–201
- Nomura S, Kyutoku T, Shimomura N, Kaneko Y, Kadokawa J (2011) Preparation of inclusion complexes composed of amylose and biodegradable poly(glycolic acid-co- $\epsilon$ -caprolactone) by



- vine-twinning polymerization and their lipase-catalyzed hydrolysis behavior. *Polym J* 43: 971–977
- Ohdan K, Fujii K, Yanase M, Takaha T, Kuriki T (2006) Enzymatic synthesis of amylose. *Biocatal Biotransform* 24:77–81
- Omagari Y, Matsuda S, Kaneko Y, Kadokawa J (2009) Chemoenzymatic synthesis of amylose-grafted cellulose. *Macromol Biosci* 9:450–455
- Pappu A, Patil V, Jain S, Mahindrakar A, Haque R, Thakur VK (2015) Advances in industrial prospective of cellulosic macromolecules enriched banana biofibre resources: a review. *Int J Biol Macromol* 79:449–458
- Pappu A, Saxena M, Thakur VK, Sharma A, Haque R (2016) Facile extraction, processing and characterization of biorenewable sisal fibers for multifunctional applications. *J Macromol Sci Part A* 53(7):424–432
- Piculell L (1998) Gelling polysaccharides. *Curr Opin Colloid Interface Sci* 3:643–650
- Pillai CKS, Paul W, Sharma CP (2009) Chitin and chitosan polymers: chemistry, solubility and fiber formation. *Prog Polym Sci* 34:641–678
- Putseys JA, Lamberts L, Delcour JA (2010) Amylose-inclusion complexes: formation, identity and physico-chemical properties. *J Cereal Sci* 51:238–247
- Rachmawati R, Woortman AJJ, Loos K (2013a) Facile preparation method for inclusion complexes between amylose and polytetrahydrofurans. *Biomacromol* 14:575–583
- Rachmawati R, Woortman AJJ, Loos K (2013b) Tunable properties of inclusion complexes between amylose and polytetrahydrofuran. *Macromol Biosci* 13:767–776
- Rachmawati R, Woortman AJJ, Loos K (2014) Solvent-responsive behavior of inclusion complexes between amylose and polytetrahydrofuran. *Macromol Biosci* 14:56–68
- Rouilly A, Rigal L (2002) Agro-materials: a bibliographic review. *J Macromol Sci Polym Rev C*42:441–479
- Sarko A, Zugenmaier P (1980) Crystal structures of amylose and its derivatives. In: French AD, Gardner KH (eds) *Fiber diffraction methods*, vol 141. ACS Symposium Series 141. American Chemical Society, Washington, DC, pp 459–482
- Schuerch C (1986) Polysaccharides. In: Mark HF, Bilkales N, Overberger CG (eds) *Encyclopedia of polymer science and engineering*, vol 13. 2nd edn. Wiley, New York, pp 87–162
- Seibel J, Beine R, Moraru R, Behringer C, Buchholz K (2006a) A new pathway for the synthesis of oligosaccharides by the use of non-leloir glycosyltransferases. *Biocatal Biotransform* 24:157–165
- Seibel J, Jordening HJ, Buchholz K (2006b) Glycosylation with activated sugars using glycosyltransferases and transglycosidases. *Biocatal Biotransform* 24:311–342
- Shoda S, Uyama H, Kadokawa J, Kimura S, Kobayashi S (2016) Enzymes as green catalysts for precision macromolecular synthesis. *Chem Rev* 116:2307–2413
- Shogren RL (1993) Complexes of starch with telechelic poly( $\epsilon$ -caprolactone) phosphate. *Carbohydr Polym* 22:93–98
- Shogren RL, Greene RV, Wu YV (1991) Complexes of starch polysaccharides and poly(ethylene-co-acrylic acid)—structure and stability in solution. *J Appl Polym Sci* 42:1701–1709
- Star A, Steuerman DW, Heath JR, Stoddart JF (2002) Starched carbon nanotubes. *Angew Chem Int Ed* 41:2508–2512
- Stephen AM, Phillips GO, Williams PA (2006) *Food polysaccharides and their applications*. Food science and technology, 2nd edn. CRC/Taylor & Francis, Boca Raton
- Takata Y, Yamamoto K, Kadokawa J (2015) Preparation of pH-responsive amphoteric glycogen hydrogels by  $\alpha$ -glucan phosphorylase-catalyzed successive enzymatic reactions. *Macromol Chem Phys* 216:1415–1420
- Tanaka T, Fukuhara H, Shoda S, Kimura Y (2013a) Facile synthesis of oligosaccharide-poly (L-lactide) conjugates forming nanoparticles with saccharide core and shell. *Chem Lett* 42:197–199
- Tanaka T, Sasayama S, Nomura S, Yamamoto K, Kimura Y, Kadokawa J (2013b) An amylose-poly (L-lactide) inclusion supramolecular polymer: enzymatic synthesis by means of vine-twinning polymerization using a primer-guest conjugate. *Macromol Chem Phys* 214:2829–2834

- Tanaka T, Gotanda R, Tsutsui A, Sasayama S, Yamamoto K, Kimura Y, Kadokawa J (2015a) Synthesis and gel formation of hyperbranched supramolecular polymer by vine-twinning polymerization using branched primer-guest conjugate. *Polymer* 73:9–16
- Tanaka T, Tsutsui A, Gotanda R, Sasayama S, Yamamoto K, Kadokawa J (2015b) Synthesis of amylose-polyether inclusion supramolecular polymers by vine-twinning polymerization using maltoheptaose-functionalized poly(tetrahydrofuran) as a primer-guest conjugate. *J Appl Glycosci* 62:135–141
- Trache D, Hazwan Hussin M, Mohamad Haafiz MK, Kumar Thakur V (2017) Recent progress in cellulose nanocrystals: sources and production. *Nanoscale* 9(5):1763–1786
- Umegatani Y, Izawa H, Nawaji M, Yamamoto K, Kubo A, Yanase M, Takaha T, Kadokawa J (2012) Enzymatic  $\alpha$ -glucuronylation of maltooligosaccharides using  $\alpha$ -glucuronic acid 1-phosphate as glycosyl donor catalyzed by a thermostable phosphorylase from *Aquifex aeolicus* VF5. *Carbohydr Res* 350:81–85
- Voicu SI, Condruz RM, Mitran V, Cimpean A, Miculescu F, Andronesu C, Thakur VK et al (2016) Sericin covalent immobilization onto cellulose acetate membrane for biomedical applications. *ACS Sustain Chem Eng* 4(3):1765–1774
- Yanase M, Takaha T, Kuriki T (2006)  $\alpha$ -Glucan phosphorylase and its use in carbohydrate engineering. *J Sci Food Agric* 86:1631–1635
- Ziegast G, Pfannemüller B (1987) Linear and star-shaped hybrid polymers. 4. phosphorolytic syntheses with Di-functional, Oligo-Functional and Multifunctional Primers. *Carbohydr Res* 160:185–204

# Chapter 10

## New Aspects to Physicochemical Properties of Polymer Gels in Particularly the Coordination Biopolymeric Metal–Alginate Iontropic Hydrogels



Refat M. Hassan (El-Moushy), Khalid S. Khairou and Aida M. Awad

### 1 Preface

Polymer gels are consisting of crosslinked elastic polymer network inflated with a solvent such as water. The network of the polymer envelopes and holds the liquid inside the interstitial spaces to prevent it from flowing out as well as gives the gel its solidity (Yashihito and Gong 1998). These polymeric materials can be classified into a variety of ways. One of these ways was based on their origin, into natural and synthetic (and sometimes including a third category of semi-natural or synthetic modifications of natural polymers). A further and more useful classification was based on the physical properties of such gels in particularly with respect to its elastic modulus and the degree of elongation which ranges from strong, weak to pseudo-gels. These physical properties can be controlled from hard rubbery plastics to soft hydrogel by manipulating the microstructure of the polymer backbone and its surrounding liquid (Grillet et al. 2012). The gelation process occurs when the polymeric chains are effectively interacted with each other physically by hydrogen bonds and entanglement of the polymer chains, or chemically by formation of ionic and/or covalent bonds yielding a crosslinkage network which spanning the whole volume of the gel. This means that the gels are formed by the use of physical or

---

This Chapter Dedicated for My Family

---

R. M. Hassan (El-Moushy) (✉)

Department of Chemistry, Faculty of Science, Assiut University, Assiut 71516, Egypt  
e-mail: rmhassan2002@yahoo.com

K. S. Khairou

Department of Chemistry, Faculty of Applied Sciences, Umm Al-Qura University,  
Makkah Al-Mukarramah 13401, Kingdom of Saudi Arabia

A. M. Awad

Department of Chemistry, Faculty of Science, Sohag University, Sohag 82524, Egypt

© Springer Nature Singapore Pte Ltd. 2018

V. K. Thakur and M. K. Thakur (eds.), *Polymer Gels*, Gels Horizons: From Science to Smart Materials, [https://doi.org/10.1007/978-981-10-6083-0\\_10](https://doi.org/10.1007/978-981-10-6083-0_10)

chemical crosslinkers (Gennes 1979; Ross-Murphy 1995; Dentini et al. 2006). In case of chemical bonding, the formed gels are irreversible since they cannot dissolve again in the surrounding solvents (Kara et al. 2003). Here, the strength of chelation of the existed chemical bonding as well as the geometrical structure can be considered as the controlling factors of the corresponding physicochemical properties of the formed gels (Haug et al. 1967; Hassan 1993a, b).

Polymer gels in particularly that related to biodegradable materials such as alginate and its derivatives have attracted much attention owing to its wide applications ranging from medicine, pharmacy, food and drug delivery (Ross-Murphy 1995; Draget 2009; Draget et al. 2005, 2006; Andrews and Jones 2006; Tunic 2010) to adhesives (Creton and Papon 2003) and consumer products (Solomon and Spicer 2010). Recently, keen attempts have been exerted for development of new types of hydrogels so-called smart biopolymeric gels for application in the context biomedical devices (Chaterji et al. 2007) which ranging from tissue engineering with human cells for hard tissue (Putnam and Mooney 1996; Shi 2004; Despong et al. 2005; Dittrich et al. 2006), nerve regeneration (Prang et al. 2006) to biomedical sensing, medical adhesives, gastrointestinal tract, kidney, dental, maxillofacial surgery, medical textiles and immobilization and biocatalysts (Zhang et al. 1996; Park and Park 1996; Dumitriu 2002; Anand et al. 2006; Saha et al. 2008, 2011; Sarai et al. 2009; Roy et al. 2010a, b). This new type of gels can be obviated by engineering the interconnected pores of the polymer structure in order to form capillary networks in the matrix by either downscaling the polymer size or significant decrease in the diffusion paths (Putnam and Mooney 1996; Pratt et al. 2004).

This chapter concerns with hydrogel polymer—in particularly that created from polysaccharides by crosslinking the functional groups of alginate macromolecule as anionic polyelectrolyte with metal cations forming the corresponding coordination biopolymer metal–alginate ionotropic hydrogel complexes in either jelly or granule forms (MAG complexes). Here, a sort of bridge is formed between the carboxylate and hydroxyl functional groups of alginate macromolecular chains and the interdiffused metal ions by partially ionic and partially coordinate bonds, respectively. It also aims of shedding more light on the physicochemical properties of the metal–alginate ionotropic hydrogels in terms of the stability of these complexes based on the strength of chelation related to the geometrical configuration. Moreover, it includes pertinent discussion on the morphology and behavior of these ionotropic hydrogel complexes in aqueous, organic, and buffer solutions.

## 2 Materials and General Aspects

### 2.1 Alginate Polysaccharide

Alginate is a linear copolysaccharide isolated from seaweeds brown algae (Chanda et al. 1952; Fisher and Dorfel 1955; Whistler and Kirby 1952; Haug and Larsen 1962) or using certain bacteria (Sutherland 1991; Draget et al. 2006). It consists of a

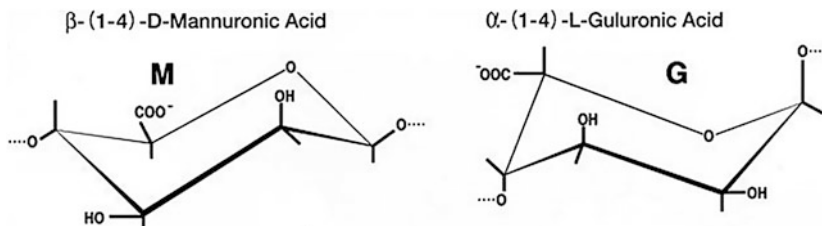


**Fig. 1** Structure configuration of alginate polysaccharide

binary heteropolymer containing 1,4-linked  $\beta$ -D-mannuronic (M) and  $\alpha$ -L-guluronic (G-) acid units which are configurational isomers to each other with a varying proportions depending on the source from which the alginate reagent is isolated (Schweiger 1962; Drummond et al. 1962; Hirst et al. 1964; Haug 1964; Braccini et al. 1999; Dentini et al. 2006). The monomers are arranged in blockwise fashion along the macromolecular chains in a linear block copolymer structure (Haug et al. 1966, b; Rees and Samuel 1967; Rees 1972; Smidsrod 1974; Morris et al. 1978). The blocks (G) and (M) residues are arranged in homopolymeric sequences of both types and in regions which the dipolysaccharides are approximately representing the repeating structure units. The secondary alcoholic groups on C-2 and C-3 are being in cis-position. If the conformational is considered, an axial-equatorial position is existed, whereas the carboxylate group on the monomer is being in equatorial position (Aspinal 1982). A simple configuration of the alginate structure is shown in Fig. 1.

Literature survey on the structure, some properties, and applications of alginate polysaccharide has been reviewed elsewhere (Muzzarelli 1973; Davidson 1980; Park and Park 1996; Draet 2009).

## 2.2 Preparation of Alginate Sols

Sodium alginate (Cica Reagent Chem. Co.) was used without further purifications. Stock solutions of alginate sols (2, 3 and 4%) were prepared by stepwise addition of the reagent powder to deionized water (w/w) while rapidly and vigorously stirring the solution to prevent the formation of coagulate lumps, which swell with difficulty. The prepared alginate sols were left at room temperature (25 °C) for about 24 h in order to become air bubbles-free. Then, it kept in a refrigerator to avoid any bacterial attack. The validity of the prepared alginate sol for using is about two weeks. After removing the alginate sol from the refrigerator, it should be kept at room temperature for about 1–2 h to be easy for handling before using in experiments.

## 2.3 *Physicochemical Properties of Na-Alginate Sol*

### 2.3.1 Viscosity

The measured viscosities for 4% alginate sol in doubly distilled water (w/w) using Ubbelohde viscometer were found to be 2.78 and 9.87 dl g<sup>-1</sup> at 20 °C for the inherent and reduced viscosities, respectively (Hassan et al. 1993).

### 2.3.2 Ionization Constant and Degree of Substitution

The ionization constant of alginic acid has been determined potentiometrically at a constant ionic strength of 1.0 mol dm<sup>-3</sup>. The value of pK was found to be 2.93, whereas alginic acid takes up 5.4 mequiv Na<sup>+</sup>/g at pH 3.3 (Hassan and Abd-Alla 1991). The degree of substitution was found to be 4.34 mmol g<sup>-1</sup> (0.95 mol mol<sup>-1</sup>) at 25 °C (Khairou et al. 2003). Most alginic acid reagents are expected to be deprotonated at the carboxylate functionalities due to their relative pK<sub>a</sub> values (Thomas et al. 2006). It was found that polysaccharides involving alginate sol have high tendency for deprotonation in alkaline solutions (Hassan 1993b; Hassan et al. 2014b), whereas it has high affinity for protonation in acidic media (Abdel-Hamid et al. 2003; Hassan et al. 2012a; Fawzy 2016).

### 2.3.3 Oxidation of Alcoholic Functional Groups

Polysaccharides involving alginate substrate are considered to be good reductants of many inorganic substrates like chromium (VI), and hence, it can be used for purification of water from contaminated toxic and carcinogen Cr (VI) ion (Lin and Wang 2012). This property can be achieved by the high efficiency of alginate polysaccharide to reduce chromium from its soluble form Cr (VI) to Cr (III) form which has a high tendency to form insoluble complexes (Bellu et al. 2008; Bertoni et al. 2014). This capability is attributed to presence of electron-donor oxidizable alcoholic groups within the monomers of the alginate macromolecular chains. The oxidation kinetics of secondary alcoholic groups on C-2 and C-3 positions has been investigated using various oxidizing agents such as permanganate ion in alkaline solutions (Hassan 1993b), hexacyanoferrate (III) in alkaline solutions (Hassan et al. 2014b), chromic acid (Bertoni et al. 2014), and cerium (IV) in acidic media (Fawzy 2016). The oxidation of alginate polysaccharide was found to afford the formation of mono- and/or diketoalginate coordination biopolymeric derivative precursors as oxidation products depending on the stoichiometric molar ratio of the oxidant (Hassan 1993c). This means that the secondary alcoholic groups of alginate polysaccharide are oxidized to its corresponding keto forms without occurrence of any cleavage between the C-2 and C-3 bonding during investigation under those experimental conditions used. On contrary, it was reported that oxidation of

alginate substrate by chromium (VI) in acidic solutions at 60 °C affords the formation of  $\text{CO}_2/\text{HCO}_2\text{H}$  with C–C bonding cleavage (Betroni et al. 2014). The kinetics and mechanisms of oxidation of alginate and some other polysaccharides by various oxidants have been reviewed in more detail (Hassan 2013, 2016), respectively.

The activation parameters and second-order rate constants for oxidation of alginate polysaccharide by various oxidants in aqueous solutions are summarized in Table 1. Although the solvents used as media were different, it seems that the magnitude of oxidation rates decreased in the order  $\text{MnO}_4^- > \text{CrO}_4^{2-} > \text{Ce}^{4+} > [\text{Fe}(\text{CN})_6]^{3-}$ , respectively. Again, the high negative entropies of activation observed in these redox systems indicated that the formed intermediates prior to the rate-determining steps are more compactness than the reactants in these redox systems. The experimental kinetics indicated that these redox reactions are preferred to proceed by one-electron transfer process in case of cerium (IV) and ferricyanide oxidants; and by one- and/or two-electron changes in case of permanganate (VII) and chromium (VI) oxidants, respectively, through inner-sphere mechanisms for electron transfer rather than the outer-sphere type in all cases.

On the other hand, the oxidation of carbohydrates and polysaccharides by periodate ion (Dyhurst 1970; Sharon 1975; Gomez et al. 2007) or by hypochlorite (Whistler and Schweiger 1958) is considered as classical techniques used for determination of the structure of polysaccharides. The oxidation of polysaccharides involving alginate substrate by periodate ion as an oxidant indicated the bond cleavage between C-2 and C-3 positions and formation of aldehyde groups of the oxidized sugar residues spontaneously form of six-membered hemiacetal rings with closet hydroxyl groups on the neighboring unit (Parnter and Larsen 1970; Kristiansen et al. 2010). Again, the alginate polysaccharide showed a high tendency for degradation in the presence of other reducing compounds such as ascorbic acid (Smidsrod et al. 1963) or hydrogen peroxide in the presence of iron salts (Smidsrod et al. 1965). The degradation of alginate is caused by the hydroxyl radicals formed during the oxidation processes along with ring rupture and a decrease in viscosity. Since polymer systems have been used for several applications in drug-controlled delivery, the oxidized product precursors of alginate may also present more reactive groups and fast degradation for such purpose (Gomez et al. 2007).

### 2.3.4 Acetylation and Hydrolysis of Na-Alginate

The acetylation (or esterification) and the hydrolysis of the hydroxyl groups of polysaccharides are generally considered as one of the most important chemical procedures for changing the properties of polysaccharides as well as a specific tool in order to support the assumptions on the nature of conformational chelation between the functional groups of alginate and the chelated metal cations in particularly with calcium (II) ion. It has been noticed that activation of polysaccharides

**Table 1** Activation parameters and second-order rate constants for oxidation of alginate polysaccharides by various oxidants in aqueous solutions (Medium) = 0.1 and  $I = 1.0 \text{ mol dm}^{-3}$  at 25 °C

Oxidant	Medium (mol dm <sup>-3</sup> )	$E_a^\ddagger$ (kJ mol <sup>-1</sup> )	$\Delta S^\ddagger$ (J mol <sup>-1</sup> K <sup>-1</sup> )	$\Delta H^\ddagger$ (kJ mol <sup>-1</sup> )	$\Delta G^\ddagger$ (kJ mol <sup>-1</sup> )	$10^2 k$ (dm <sup>3</sup> mol <sup>-1</sup> s <sup>-1</sup> )	References
MnO <sub>4</sub> <sup>-</sup>	NaOH	53.54	-58.46	50.29	67.71	85.01	Hassan (1993b)
[Fe (CN) <sub>6</sub> ] <sup>3-</sup>	NaOH	60.24	-110.6	57.46	90.94	1.02	Hassan et al. (2014b)
CrO <sub>4</sub> <sup>2-</sup>	HClO <sub>4</sub>	-	-	-	-	35.39 <sup>a</sup>	Bertoni et al. (2014)
Ce <sup>4+</sup>	HClO <sub>4</sub>	47.73	-98.94	44.15	73.63	9.65	Fawzy (2016)
	H <sub>2</sub> SO <sub>4</sub>	26.08	-167.11	23.36	73.16	6.76	Fawzy (2016)

<sup>a</sup>Measured at 60 °C



before achieving any acetylation will be more convenient for performing this process. The activation can be achieved by subjecting the alginic acid for swelling process in strong acid as a catalyst for about 15 min before acetylation (Hirst et al. 1964; Hirst and Rees 1965). Schweiger (1962) reported that alginic acid can be either partially or completely acetylated with acetic anhydride and catalytic amounts of perchloric acid as a catalyst to give soluble diacetyl alginate. Again, the partial acid hydrolysis of alginic acid in 1 mol dm<sup>-3</sup> oxalic acid at 100 °C was found to be one of the essential techniques for supporting the structure of alginic acid (Haug et al. 1966, b).

### 2.3.5 Chromatographic Separation

Alginic acid as anionic polyelectrolyte was successfully used as a stationary phase for TLC in separation of metal cations (Cozzi et al. 1968, 1969, b, c; Hassan et al. 1992b), amino acids (Cozzi et al. 1969, b, c), primary aromatic amines (Cozzi et al. 1969, b, c; Lepri et al. 1970), and purine and pyrimidines (Lepri et al. 1972). It concluded from chromatographic separation technique that the ion exchange process is not only the controlled mechanism but the influence of the two hydroxyl groups on the retention capacity of alginic acid is also important. The experimental results indicate that alginic acid is considered as a good stationary phase in TLC and more suitable for analytical purposes.

## 2.4 *Preparation of Coordination Biopolymer Crosslinked Metal—Alginate Ionotropic Hydrogel Complexes (MAG)*

Solutions of cationic or anionic polyelectrolytes can be transformed to gels through the diffusion of anionic or cationic polyvalent metal ions, respectively. Coordination polymeric metal–alginate hydrogels with elastic modulus, clarity, and fine network structures can be prepared in different shapes such as spheres (pellets), membranes (disks), fibers, and columns depending on the apparatus and method of preparation used (Mongar and Wassermann 1952; Segeren et al. 1974; Awad et al. 1980a, b; Hassan et al. 2013a, b, 2014c).

This type of gels has anisotropic properties and called ionotropic gels where the sol-gel transformation is accompanied by orientation of the solvent molecules and macromolecular chains toward the chelated metal ion (Thiele and Longmaack 1957; Schweiger 1964). The degree of orientation depends on whether the direction of metal ion diffusion into the alginate sol whether is upward or downward (Thiele and Hallich 1955a, b).

#### 2.4.1 Preparation of Hydrogels of Membrane and Column Shapes

In case of membranes or column shape hydrogels, petri dishes or one-side closed columns (with cellophane paper) were internally smeared with a very thin layer of the alginate sol used and dried in an electric oven at about  $\sim 90$  °C for about 10–15 min, left to cool at the ambient temperature. These petri dishes or columns are filled to about two-thirds of its height with alginate sol of known concentration and immersed in vessels containing metal ion electrolytes of known concentrations and left for a certain period of time depending on the thickness wanted of the formed membrane or column hydrogels. For example, for 2% alginate sol, the gel grew for a height of 1 cm in about 10 h for membranes and  $\sim 24$  h for column gels.

As soon as the alginate sol comes in contact with the metal ion electrolyte, a thin primary membrane film is formed on the surface of alginate sol which prevents it from the deterioration into the electrolyte solution. Then, an ion exchange process starts to occur between the leaved  $\text{Na}^+$  counter ions of alginate macromolecule and the metal ions from the electrolyte forming the corresponding coordination biopolymer metal–alginate ionotropic hydrogel complexes (Hassan et al. 1991, 1992a, b, c). The formed membranes or columns were carefully removed from the petri dishes or glass columns and washed frequently with deionized water until the resultant washing became free from the non-chelated metal ions. This can be confirmed by measuring the conductivity of the washing water. The washed membranes or column or column hydrogels were then kept in doubly distilled conductivity water for use.

#### 2.4.2 Preparation of Hydrogels of Spherical Shape (Pellets)

Ionotropic gels of spherical shapes (pellets) can be prepared by dropping sodium alginate sols into electrolyte solutions of polyvalent metal cations or silver (I) ions using a dropper or syringe (Hassan 1991a, b, 1993a, c). In this case, a similar thin primary membrane film is formed around the alginate sol droplet which gives it the symmetrical spherical shape. At the beginning, the droplet will float at just below the surface of the metal ion electrolyte solution for a while. Then an ion exchange process will occur between the  $\text{Na}^+$  counter ions of alginate polyelectrolyte and the exchanging metal ions. After the completion of exchange, the droplet starts to sink down into the electrolyte solution with a certain velocity. In a similar manner to that followed in case of membrane and column gels, the formed pellets were removed from the container vessel of electrolyte and washed frequently with deionized water until the resultant washing became free from the non-chelated metal ions. The washed pellets were then kept in doubly distilled conductivity water for use.

### 2.4.3 Preparation of Gel Complexes of Granule Nature

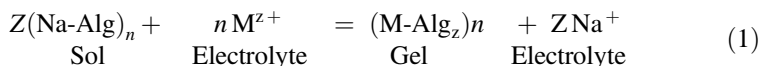
It is more convenient to use metal–alginate complexes of granule solid nature rather than other phases such as jellies for the FTIR spectra, thermal decomposition, electrical properties, ion exchange, and chemical equilibria studies, since the macromolecules of the granule solids have rigid networks. The granule solids can be prepared by stepwise addition of alginate powder to a metal ion electrolyte solution with rapidly and vigorously stirring the solution to avoid the formation of lumps, which form lumps. After the completion of the exchange between the  $\text{Na}^+$  counter ions of alginate polysaccharide and the interdiffused metal ions from the electrolyte ( $\sim 5$  h), the granule solid gel complexes were filtered off and washed several times with deionized water until the washing water becomes free of non-chelated metal ion as previously described. Then, the granules are dried in an electric oven at about 100–105 °C until constant weight (24 h) and kept in a desiccator over anhydrous  $\text{CaCl}_2$  or  $\text{P}_2\text{O}_5$  for use.

## 3 Physicochemical Properties of Coordination Biopolymer Ionotropic Hydrogel Complexes

### 3.1 Stoichiometry of Sol-Gel Transformation (Gelation)

The stoichiometry of gelation is of great significant which offers a route for determining the average number of chains in each polyguluronate junction zones (Morris et al. 1978). The ion exchange phenomenon is inherently a stoichiometric process (Hellferich 1962). This means that the ion exchange requires that the fluxes of the two exchanging counter ions be equal in magnitude, even though the counter ion motilities may be quite different in order to maintain the electroneutrality. Therefore, any  $\text{Na}^+$  counter ions produced from the dissociation of sodium alginate as anionic polyelectrolyte leaves the matrix of alginate macromolecular chains must be replaced by an equivalent amount of other polyvalent metal ions. This exchange process leads to the formation of the corresponding coordination biopolymer metal–alginate ionotropic hydrogel complexes.

The chelated metal ions in these formed hydrogel complexes can be completely replaced by frequent addition of hydrogen ions (using dilute mineral acids such as HCl or  $\text{HClO}_4$  as eluent). Then, the concentration of the metal ion produced in the washing solution can be determined complexometrically. The experimental analysis of the results indicated that one mole of each mono-, divalent-(or uranyl-), trivalent-, and tetravalent metal ions chelates one, two, three, and four moles of sodium alginate monomer units, respectively. This result conform to the following stoichiometric equation:



where the symbol Na-Alg denotes sodium alginate sol, M-Alg<sub>z</sub> is the metal–alginate hydrogel, and M denotes the metal ion and Z stands to its valency, respectively. This means that no dimerization occurred under our experimental conditions as was expected in some other cases (Morris et al. 1978).

These results were confirmed by the gravimetric analyses of these studied metal–alginate complexes. The gravimetric technique was based on previous determination of the decomposition temperature for each studied hydrogel complex (TGA and DTA curves of non-isothermal decomposition techniques). This was performed by heating a known weight of the metal–alginate ionotropic hydrogel complex at about 105 °C until it reached a constant weight in order to evaluate the water contents into the gels. Then, the dried gels were heated over the determined decomposition temperature for about 24 h until reached a constant weight of the formed metal oxide as final product of decomposition. The stoichiometric ratio can be evaluated from both weights of the dehydrated metal–alginate complex and the final metal oxide. The experimental results obtained from both complexometric and gravimetric techniques were found to be in good agreement with each other within experimental errors confirming the stoichiometric results obtained.

### ***3.2 Affinity and Selectivity of Na-Alginate for Chelation with Polyvalent Metal Cations***

Polysaccharides are versatile macromolecules that may be either neutral such as methyl cellulose and pectin or ionic such as alginate, pectate, and carboxymethyl cellulose. This in addition to the presence of another type of polysaccharides so-called sulfated polysaccharides which contain more sulfate moieties which present in the macromolecular chains such as carrageenans and chondroitin macromolecules. The ionic character of alginate polysaccharide was due to the presence of anionic carboxylate group moieties in the polymeric backbone monomers. Therefore, this kind of polysaccharides exhibits specific physicochemical properties owing to its polyelectrolyte character and the features resulting from their stereoregularity (Braccini et al. 1999).

One of these characters is the high affinity of alginate for chelation with polyvalent metal cations in particularly divalent metal ions to form coordination biopolymer ionotropic hydrogel complexes (Thiele and Anderson 1955; Thiele and Longmaack 1957a, b; Takahashi and Emura 1960; Haug 1961; Takahashi and Emura 1960; Hellferich 1962; Schweiger 1964; Smidsrod and Haug 1965, 1968, 1972; Panteleev et al. 1972; Yonese et al. 1988; Mimura et al. 2001; Wu et al. 2009). When an electrolyte solution of a polyvalent metal ion is added to a half-neutralized sample of alginic acid, the pH decreases and this may be

considered as an indication for the affinity between the chelated metal ions and the alginate macromolecule. It was found that the ion exchange behavior between the alginate sol and the metal ions varies from one alginate to another depending on the source of alginate reagent. The ability of alginate to form ionotropic hydrogels of porous structure through ion exchange processes with polyvalent metal ions will extend the application of alginate for using as metal absorbent for separation and recovery of many metal ions through hybrid microcapsulation enclosed with suitable extractants. For example, microcapsulated alginates were used for selective uptake of Sr-90 (Sapozhnikov et al. 1996); americium (Mimura et al. 2001) and silver (Outokesh et al. 2006); toxic As (V) ions (Tiwari et al. 2008); radioactive uranium and rare earth elements (Sakamoto et al. 2008) as well as other metal ions (Wu et al. 2008); and plutonium (Wu et al. 2009). This property in particular with calcium ions may be the key to extend its applications to the biological functions (Braccini and Perez 2001) as well as for predictive environmental modeling, numerous industrial and more other technological applications (Thomas et al. 2006).

The amount of polyvalent metal ion which is necessary to bring about gel formation or precipitation of alginate was found to be dependent on the chemical composition of alginate polysaccharide (Haug 1961). The precipitation for divalent metal ions with alginate was found to increase in the order: Ba < Pb < Cu < Sr < Cd < Ca < Zn < Ni < Co < M, Fe, Mg-alginates (Haug and Smidsrod 1965). It has been found that the selectivity coefficient in those Na<sup>+</sup>-M<sup>2+</sup> series was mainly attributed to the guluronic residues more than the mannanuronic ones of alginate macromolecule. Again, the alginate as cation exchanger was found to increase in the order: alginic acid < calcium alginate ≤ sodium alginate (Takahasi and Emura 1960).

The divalent metal ions were arranged in an ionotropic series by measuring the capillary diameters of the formed gels which increased in the following order: Pb < Cu < Cd < Ba < Sr < Ca < Zn, Co, Ni-alginates (Thiele and Hallich 1957). Again, the stability of different metal-alginate complexes was studied by determining the viscosity of solutions obtained by adding EDTA to the insoluble alginate derivatives which was found to increase in the following order: Mg < Mn < Co < Zn < Ca < Ni < Sr < Cu < Cd < Ba-alginates (Schweiger 1964). Since magnesium alginate is a water-soluble complex, it is difficult to form stable Mg-coordination biopolymeric hydrogels as was observed with other divalent metal ions.

The affinity of alginate polyelectrolyte for chelation with alkaline metal cations was found to increase in the order Mg ≪ Ca ≪ Sr ≪ Ba-alginates, a unique property of alginate compared to other polyanions (Smidsrod 1974; Draget 2009). This selectivity increases markedly with increasing the content of α-L-guluronate residue in the chains, whereas the polymannuronate blocks and alternating blocks were almost with a lower or without selectivity. Hence, the mode of binding cannot be explained by only non-specific electrostatic interaction, but also by the structural features of the G and M blocks. The GG blocks are characterized by a selective binding in particular to Ca (II) ions, and hence, the mechanical strength of

calcium alginate can mainly be attributed to the junctions formed by GG blocks (Smidsrod 1974).

Selective ion exchange behavior of alginate for a specified metal ion in a mixture of different metal ions such as Sr–Mg and Co–Ca ions indicated that the manuronic acid residues had a selectivity coefficient value close to unity, while those due to the guluronic acid residues varied from the value 1.5 for (Sr–Mg) to 0.17 for (Co–Ca) mixtures (Haug and Smidsrod 1967; Smidsrod and Haug 1968, 1972). Therefore, the selectivity was almost attributed to the guluronic acid residues. On the other hand, in Ca–Sr and Cu–Ca mixtures, both types of uronic acid residues were found to exhibit selectivity for  $\text{Ca}^{2+}$  and  $\text{Cu}^{2+}$  ions, respectively. Again, the selectivity in mixtures containing more than two metal ions of the same or different valencies of the metal ions in the mixture has been investigated by (Takahashi and Emura 1960; Takahashi et al. 1963). For example, in mixtures of ( $\text{Cu}^{2+}$ – $\text{Ni}^{2+}$ – $\text{Co}^{2+}$ ), ( $\text{Fe}^{3+}$ – $\text{Ni}^{2+}$ – $\text{Cu}^{2+}$ – $\text{Co}^{2+}$ ), ( $\text{Sn}^{4+}$ – $\text{Fe}^{3+}$ ), ( $\text{Pb}^{2+}$ – $\text{Cd}^{2+}$ – $\text{Zn}^{2+}$ ), and ( $\text{Cr}^{3+}$ – $\text{Cd}^{2+}$ – $\text{Zn}^{2+}$ ), it has been found that the most retained selective metal ions were  $\text{Cu}^{2+}$ ,  $\text{Fe}^{3+}$ ,  $\text{Sn}^{4+}$ ,  $\text{Pb}^{2+}$ , and  $\text{Cr}^{3+}$ , respectively. Moreover, the exchange selectivity for mixtures of copper with other divalent metal ions indicated that the  $\text{Cu}^{2+}$  ion was the most strongly retained metal ion among other divalent metal ions. The selectivity coefficient for separation of a mixture of  $\text{Cu}^{2+}$  and  $\text{Co}^{2+}$  ions on columns of alginate sol or ca(II)-alginate was found to be 1.9 at 25 °C (Hassan et al. 1992b).

In view of the above aspects, alginate has a high selectivity for metal ions but it differs from one metal ion to another depending on the strength of chelation between the metal ion and the hydroxyl and carboxylate functional groups of alginate macromolecular chains, nature of metal ion such as its ionic radius and polarizability, pH and viscosity of the media, temperature, and the structure and source of alginate reagent (Hassan et al. 1992a, c; Hassan et al. 2012b).

### 3.3 FTIR Spectra

Although the infrared spectrum does not add new light on the gelation itself, it is very important to offer some knowledge on the interaction between the interdiffused metal ions and the carboxylated and hydroxyl groups as functional groups of alginate macromolecule. As shown in Fig. 2, alginate has bands at 1600 and 1400  $\text{cm}^{-1}$  corresponding to the stretching vibrations of  $\nu_{\text{as}}$  OCO and  $\nu_{\text{s}}$  OCO groups, respectively, and strong band at 1735  $\text{cm}^{-1}$  assigned to the free carboxylate group, whereas the band at 3500  $\text{cm}^{-1}$  belongs to the stretching vibrations of the hydrogen bond of the hydroxyl OH groups (Pearson et al. 1960; Higgins et al. 1961; Bellamy 1966; Muzzarelli 1973).

The vibrational assignment of FTIR bands for studied MAG complexes is summarized in Table 2. It is noticed that the bands at 1600 and 1400  $\text{cm}^{-1}$  in alginate are shifted to more or less wave numbers indicating the participation of OCO groups in the coordination. On the other hand, the enhancement of the band of alginate at wavelength of 1735 nm may confirm such participation, whereas the

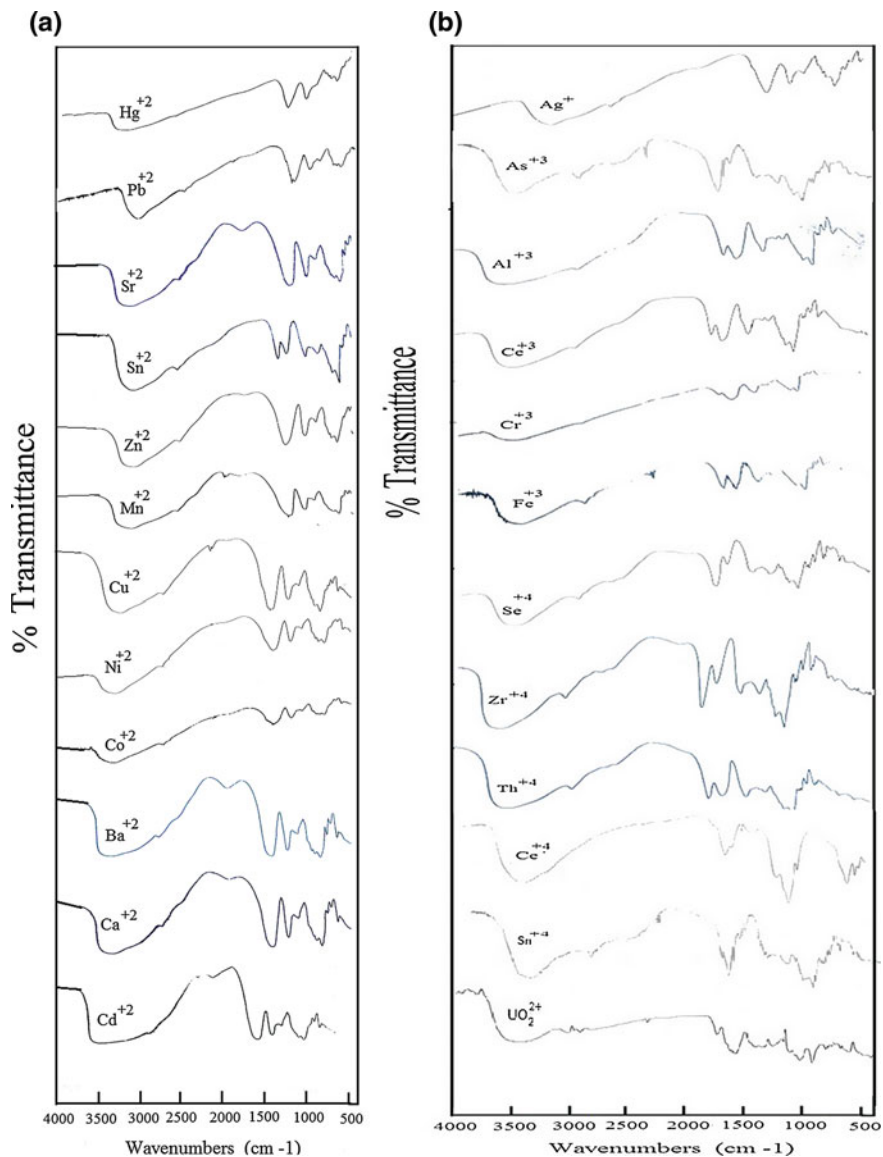


**Fig. 2** **a** FTIR of some coordination biopolymeric of divalent metal–alginate gel complexes. **b** FTIR of some coordination biopolymers of mono-, tri-, and tetravalent metal–alginate gel complexes

displacement of the band of 3500 to lower wave numbers may indicate the sharing of the OH groups in chelation. These results indicated that trivalent and tetravalent metal ions also have high affinity to chelate with the functional groups of alginate polysaccharide on contrary to that reported elsewhere (Schweiger 1964).

**Table 2** FTIR spectra of some coordination biopolymeric metal–alginate gel complexes of granule nature

Complex	$\nu_s\text{OCO}$	$\nu_{as}\text{OCO}$	$\nu_{\text{OH}}$	$\nu_{\text{M-O}}$	Formula
Na (I)-alginate	1400	1600	3500	850	$\text{C}_6\text{H}_7\text{O}_6\text{Na}$
Ag (I)-alginate	1405	1597	3444	830	$\text{C}_6\text{H}_7\text{O}_6\text{Ag}$
$\text{UO}^{2+}$ -alginate	1410	1591	3457	817	$\text{C}_{12}\text{H}_{14}\text{O}_{11}\text{UO}_2$
Co (II)-alginate	1415	1579	3219	816	$\text{C}_{12}\text{H}_{14}\text{O}_{11}\text{Co}.3\text{H}_2\text{O}$
Ni (II)-alginate	1417	1595	3450	814	$\text{C}_{12}\text{H}_{14}\text{O}_{11}\text{Ni}.3\text{H}_2\text{O}$
Cu (II)-alginate	1406	1636	3325	817	$\text{C}_{12}\text{H}_{14}\text{O}_{11}\text{Cu}.3\text{H}_2\text{O}$
Zn (II)-alginate	1411	1602	3280	816	$\text{C}_{12}\text{H}_{14}\text{O}_{11}\text{Zn}.3\text{H}_2\text{O}$
Sn (II)-alginate	1403	1634	3421	813	$\text{C}_{12}\text{H}_{14}\text{O}_{11}\text{Sn}.2\text{H}_2\text{O}$
Pb (II)-alginate	1407	1631	3448	815	$\text{C}_{12}\text{H}_{14}\text{O}_{11}\text{Pb}.2\text{H}_2\text{O}$
Cd (II)-alginate	1418	1601	3489	820	$\text{C}_{12}\text{H}_{14}\text{O}_{11}\text{Cd}.2\text{H}_2\text{O}$
Hg (II)-alginate	1405	1620	3461	816	$\text{C}_{12}\text{H}_{14}\text{O}_{11}\text{Hg}.2\text{H}_2\text{O}$
Ca (II)-alginate	1421	1595	3288	816	$\text{C}_{12}\text{H}_{14}\text{O}_{11}\text{Ca}.3\text{H}_2\text{O}$
Sr (II)-alginate	1417	1595	3440	813	$\text{C}_{12}\text{H}_{14}\text{O}_{11}\text{Sr}.3\text{H}_2\text{O}$
Ba (II)-alginate	1413	1593	3280	814	$\text{C}_{12}\text{H}_{14}\text{O}_{11}\text{Ba}.3\text{H}_2\text{O}$
Ce (IV)-alginate	1424	1603	3445	809	$\text{C}_{18}\text{H}_{21}\text{O}_{17}\text{Ce}.4\text{H}_2\text{O}$
As (III)-alginate	1408	1634	3467	818	$\text{C}_{18}\text{H}_{21}\text{O}_{17}\text{As}.4\text{H}_2\text{O}$
Al (III)-alginate	1425	1648	3490	830	$\text{C}_{18}\text{H}_{21}\text{O}_{17}\text{Al}.4\text{H}_2\text{O}$
Cr (III)-alginate	1420	1637	3463	810	$\text{C}_{18}\text{H}_{21}\text{O}_{17}\text{Cr}.4\text{H}_2\text{O}$
Fe (III)-alginate	1422	1630	3448	820	$\text{C}_{18}\text{H}_{21}\text{O}_{17}\text{Fe}.4\text{H}_2\text{O}$
La (III)-alginate	1419	1698	3426	815	$\text{C}_{18}\text{H}_{21}\text{O}_{17}\text{La}.4\text{H}_2\text{O}$
Ce (III)-alginate	1421	1618	3441	815	$\text{C}_{18}\text{H}_{21}\text{O}_{17}\text{Ce}.4\text{H}_2\text{O}$
Se (IV)-alginate	1408	1629	3387	806	$\text{C}_{24}\text{H}_{28}\text{O}_{22}\text{Se}.3\text{H}_2\text{O}$
Zr (IV)-alginate	1408	1629	3447	813	$\text{C}_{24}\text{H}_{28}\text{O}_{22}\text{Zr}.4\text{H}_2\text{O}$
Th (IV)-alginate	1419	1635	3462	806	$\text{C}_{24}\text{H}_{28}\text{O}_{22}\text{Th}.4\text{H}_2\text{O}$
Sn (IV)-alginate	1414	1634	3457	810	$\text{C}_{24}\text{H}_{28}\text{O}_{22}\text{Sn}.4\text{H}_2\text{O}$

### 3.4 X-Ray Diffraction

The X-ray diffraction patterns provide evidence for formation of ordered domains in which the alginate polymers are latterly associated. It also provides some knowledge on the crystal structure and hydrogen bonding (Nishima et al. 2002). It has been reported that most of water-swollen hydrogels are generally amorphous in nature and have no particular ordered structure at the molecular level, except for some biological gels where some high-ordered aggregates were observed in the junction zones as existed in the cited hydrogels (Osada et al. 1955). Experimental observations of X-ray diffraction patterns for the cited metal–alginate ionotropic hydrogels indicated that these gels are amorphous in nature as shown in Fig. 3 (Hassan 1993a, c).



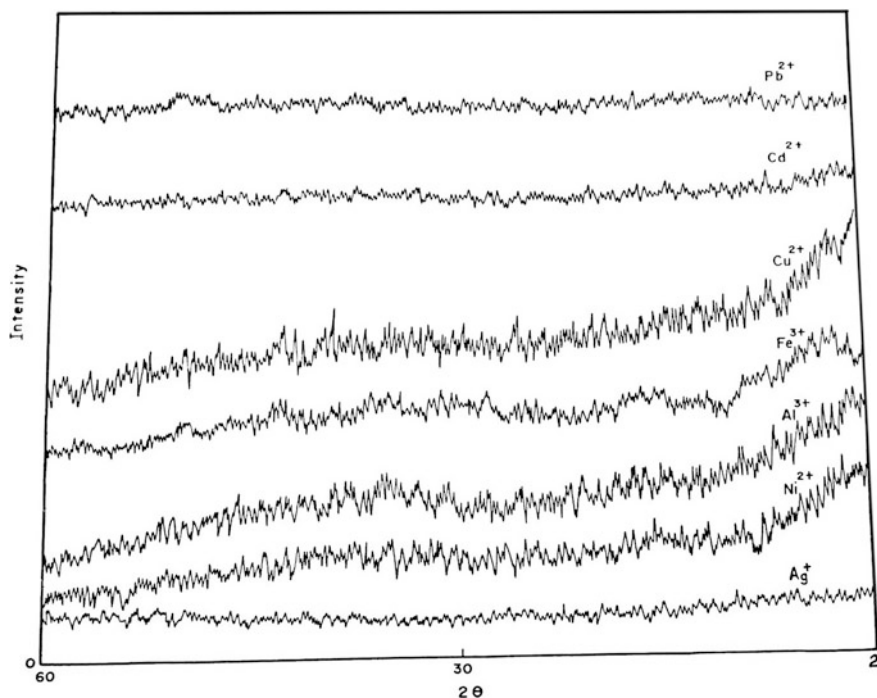


Fig. 3 X-ray diffraction of some coordination biopolymeric metal-alginate gel complexes

### 3.5 Morphology

However, the morphology of ionotropic gels has received much attention owing to its wide applications in industrial technology. The solvation in their structure does not always permit them to be maintained unchanged during investigation. Generally, the diffusion of certain counter ions in particularly the divalent metal ions into anionic polyelectrolytes such as alginate results in formation of ionotropic gels of ordered structures with parallel aligned and channel-like pores (Thiele and Anderson 1953; Higdon 1958). These gels were characterized by anisotropic property, birefringence, capillary structure, swelling, reversibility of the ion exchange processes as well as distinct morphological structures depending on the direction of diffusion of metal cations toward the alginate sol (upward or downward) in order to replace the leaving Na<sup>+</sup> counter ions resulting from the dissociation of alginate polyelectrolyte sol. This anisotropic property of gels was attributed to the orientation of the solvent molecules and the macromolecular chains toward the chelated metal ions (Thiele and Awad 1966; Awad and El-Cheikh 1980; Hassan et al. 1991). The anisotropic property of such formed gels by direct diffusion is of great interest from the standpoint of physical and colloidal chemistry in terms of biological and medical significance (Thiele 1967; Thiele and Awad 1969).

When the metal ions are allowed to diffuse upward such as in case of columns (where one side of the column was previously closed with a cellophane paper) filled with alginate sol and immersed in electrolyte solution, non-capillary structural gels were formed. This method of gel preparation is called “ascending technique.” On the other hand, when the metal ions are diffused downward as in case of sphere and membrane hydrogels, the direction of diffusion becomes trapping-capillaries that are parallel and symmetrically identical. The latter method is termed “descending technique.” In either ascending or descending techniques, the diffusion process takes place stepwise and the continuity of such diffusion leads to the formation of such corresponding MAG complexes of multilayers as mentioned before (Thiele and Hallich 1957; Obolonkova et al. 1974; Tolstoguzof 1975; Awad and El-Cheikh 1980; Hassan et al. 1989a, b, 1991). A Brownian dynamic model was suggested for the orientation of chains in these ionotropic hydrogels (Woelki and Kohler 2003). It was found that some of these properties such as birefringence, coherent network structure and, hence, a membrane of capillary-structure can be maintained even after splitting off the functional groups (Purz 1972).

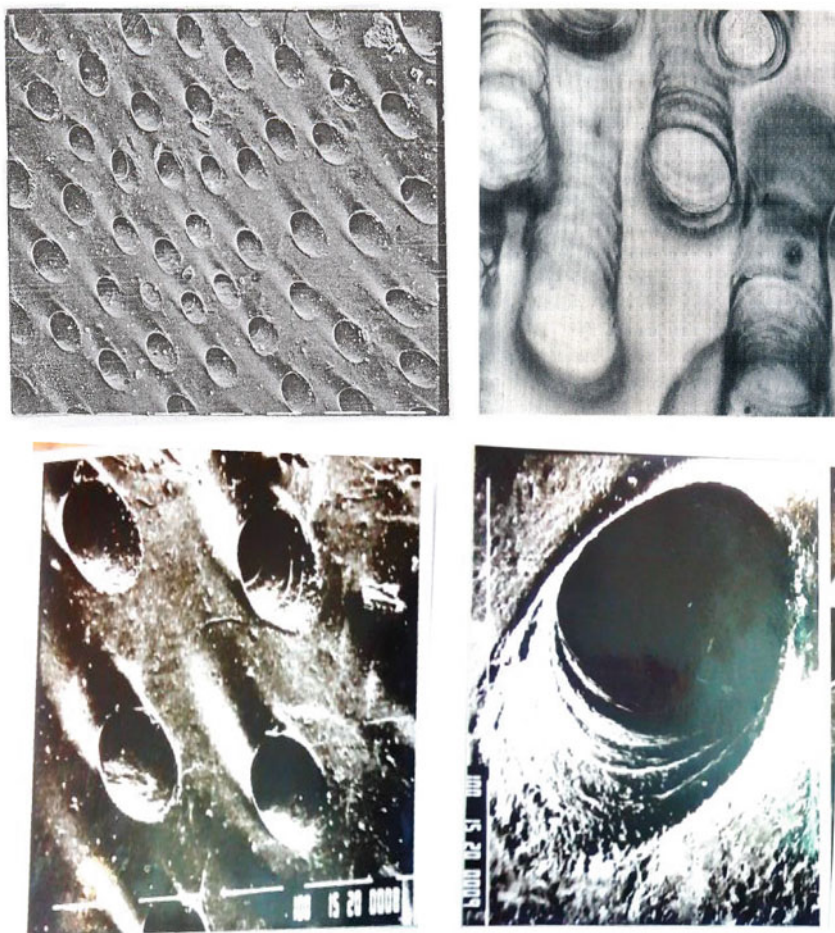
These ionotropic hydrogels were firstly created by gelation of alginate sol polysaccharide with some specific divalent metal cations in particularly Ca (II) ion. Therefore, in order to apply such ionotropic hydrogels of porous structures in medical purposes, the chelated metal ions need to be replaced by acidic exchange or ion substitution processes. Ionotropic hydrogels of membrane shapes were successfully applied as filters (Thiele and Hallich 1959) as well as for analytical purposes of separation the metal ions (Moll 1963; Hassan et al. 1991; Sapozhnikov et al. 1996; Mimura et al. 2001; Outokesh et al. 2006; Tiwari et al. 2008; Sakamoto et al. 2008; Wu et al. 2008, 2009).

Morphological structures in these MAG complexes were investigated by optical, polarization, and electron microscopy techniques (Hassan et al. 1991, 2012b; Hassan 1991a, b, 1993a, c; Khairou et al. 2002a, b; Zaafarany 2013). The corresponding photographs are shown in Fig. 4a–f. The optical images showed uniform capillaries perpendicular to the ion front as shown in Fig. 4a. This structural regularity of the investigated hydrogels was showing birefringence and uniform capillary structure as was reported by (Thiele et al. 1962). These capillaries appear to be of spiral or cone shapes on polarizing microscope as shown in Fig. 4b. When a traverse section is made in the capillary zone of the formed hydrogel, porous structure shapes are obtained as shown in Fig. 4c. The formed pores seem to be identical and with the same diameters and sizes. The diameter of these pores was dependent on several factors such as the nature of the interdiffused metal ions (ionic radii and polarizability), the pH and viscosity of the electrolyte, concentration of both alginate sol and metal ion electrolyte, and the orientation of the solvent molecules and macromolecular chains of alginate toward the chelated metal ion. The diameter size in these pores could be controlled successfully by changing the pHs of the alginate sol through adding some electrolytes (Hassan et al. 1991). The width of such capillaries plays an important role in the magnitude of the rate of ion exchange processes in these ionotropic hydrogel complexes (Hassan 1991a, b). Electron microscopy scanning (SEM and TEM) of the hydrogel structures is shown



**Fig. 4** **a** A longitudinal section in Cu (II)-alginate ionotropic hydrogel polymembrane showing the capillary structure (Hassan et al. 1991). **b** Electron microscopy photographs inside the pores of metal–alginate ionotropic hydrogel showing spiral and cone structures (Hassan 1993a; Khairou et al. 2002a, b). **c** Transverse sections in the capillaries showing the pores for some metal–alginate ionotropic hydrogels (Hassan et al. 1991, 2012b; Khairou et al. 2002a, b). **d** Electron microscopy scanning in the interspaces between the layers in Cu (II)-alginate ionotropic hydrogels (Hassan et al. 1991, 2012b). **e** Electron microscopy scanning in metal–alginate ionotropic hydrogels of granule nature. **f** Electronmicroscopic and optical photographs of the thin layers separated from cu-alginate polymembrane (Hassan et al. 1991, 1993a)

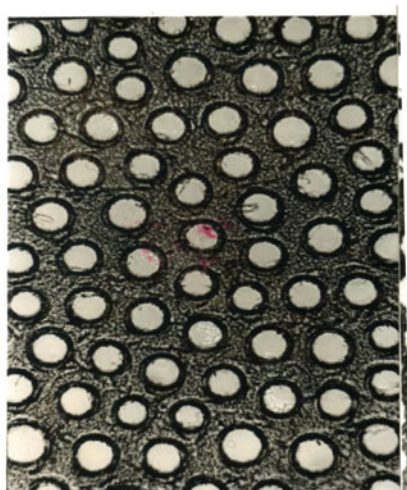
(b)

**Fig. 4** (continued)

in 4d, e respectively. Recently, atomic force microscopy (AFM) is used to investigate the microstructure in gel layers of MAG complexes (Kerchov and Elimelech 2007).

The results of investigations for such ordered gels may reflect the polymembrane formation and the respective geometrical structures in these MAG complexes. The gelation process is generally a colloidal chemical process where the diffusion takes place stepwise in the formed capillary polymembrane structure. Again, the dehydration of solvent molecules from polymembrane gels gives the observed transparent film of homogeneity. These multilayer membranes were successfully separated into very thin layers (Hassan et al. 1991) as shown in Fig. 4f. The thin layers are

(c)



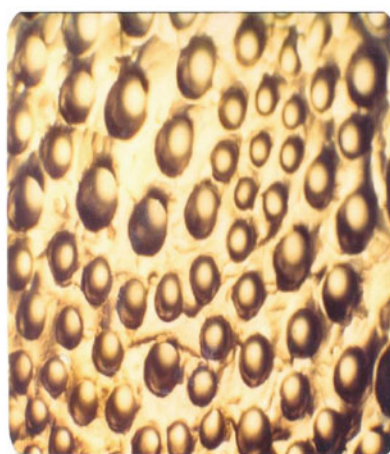
Zn(II)



Cd(II)



Co(II)



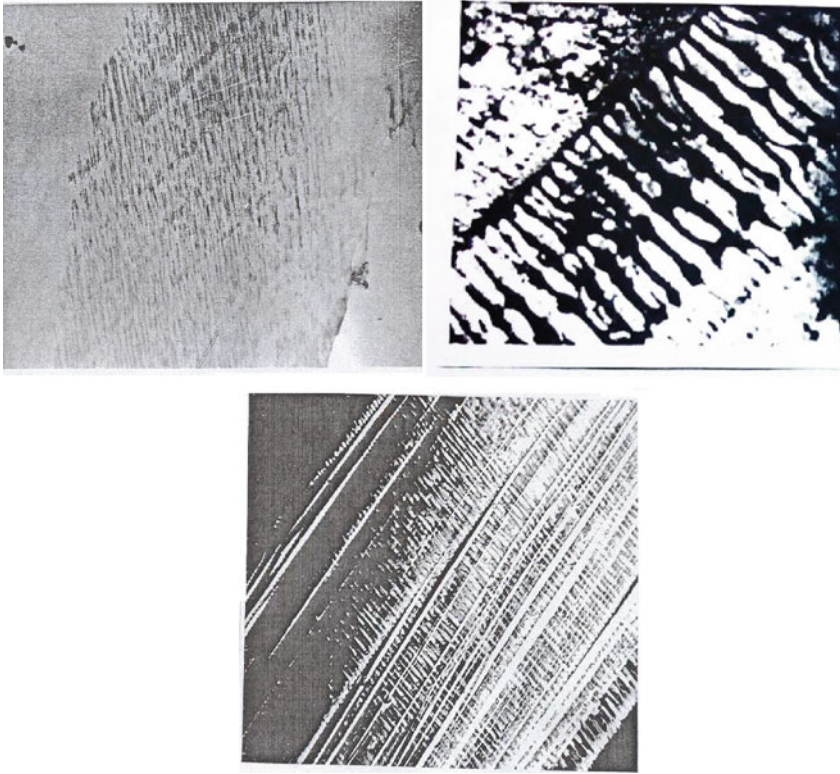
Ni(II)

Fig. 4 (continued)

promising in technological applications such as in electro-photoconductography as cellular reinforcement screens for X-rays and photographing the electron beams of oscillography (Zaafarany 2010).

Moreover, in order to increase the elasticity and softness of such multilayer membranes, 1,6-hexamethylene diisocyanate was used as a crosslinker of the free

(d)



**Fig. 4** (continued)

hydroxyl groups of the macromolecular chains for alginate macromolecule or copper-alginate polymembranes (Hassan 1991a, b). The crosslinked polymembranes were found to possess high affinities and selectivities for separation of metal ions from mixtures. For example, in a mixture of mono-, di-, and trivalent metal ions, the selectivity of separation was found to increase in the order  $M^{1+} < M^{2+} < M^{3+}$ . Moreover, for a mixture of  $Cu^{2+}$ ,  $Ni^{2+}$ , and  $Co^{2+}$ , the separation factor was found to decrease in the order  $Cu^{2+} > Ni^{2+} > Co^{2+}$  ions. Again, these crosslinked polymembranes were successfully used for ultrafiltration of fine bacteria and viruses (Hassan et al. 1991).

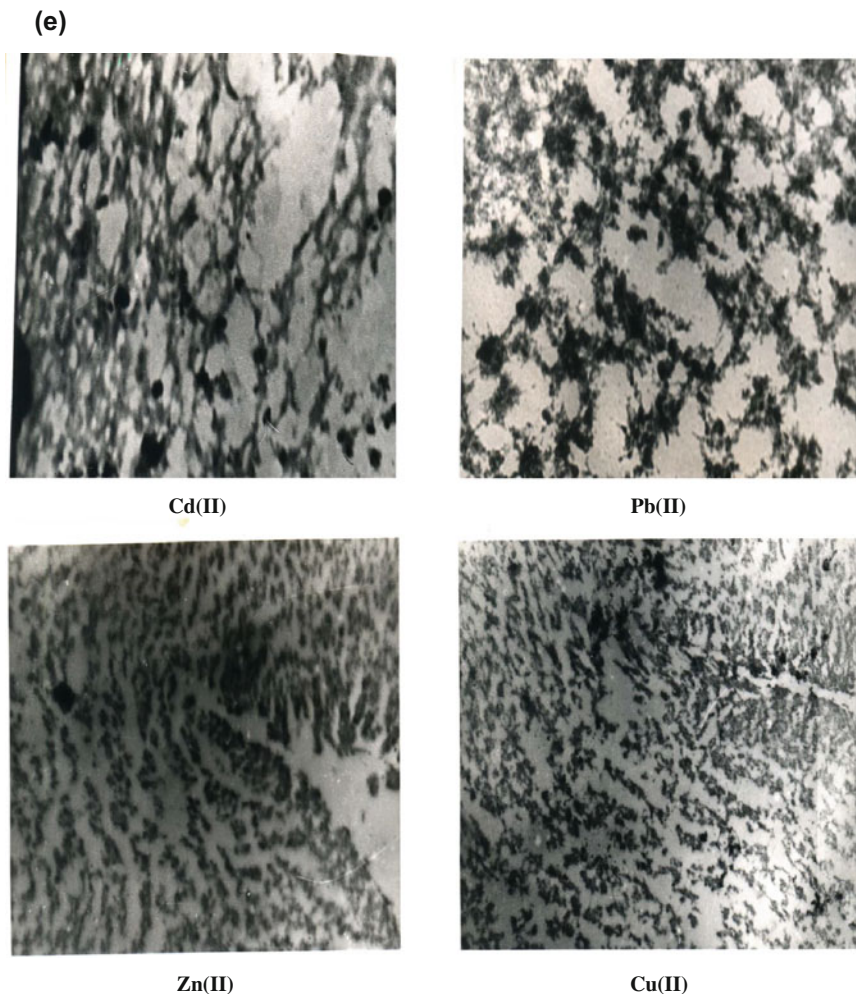


Fig. 4 (continued)

### 3.6 *Kinetics and Mechanisms of Sol-Gel Transformation in Ionotropic Hydrogels*

#### 3.6.1 In Case of Hydrogels of Membrane and Column Shapes

##### Kinetics of Sol-Gel Transformation

The kinetics of sol-gel transformation between polyvalent metal cations and sodium alginate sols for formation of ionotropic hydrogels in either membrane or column shapes were studied, complexometrically. Some transition divalent metal ions such

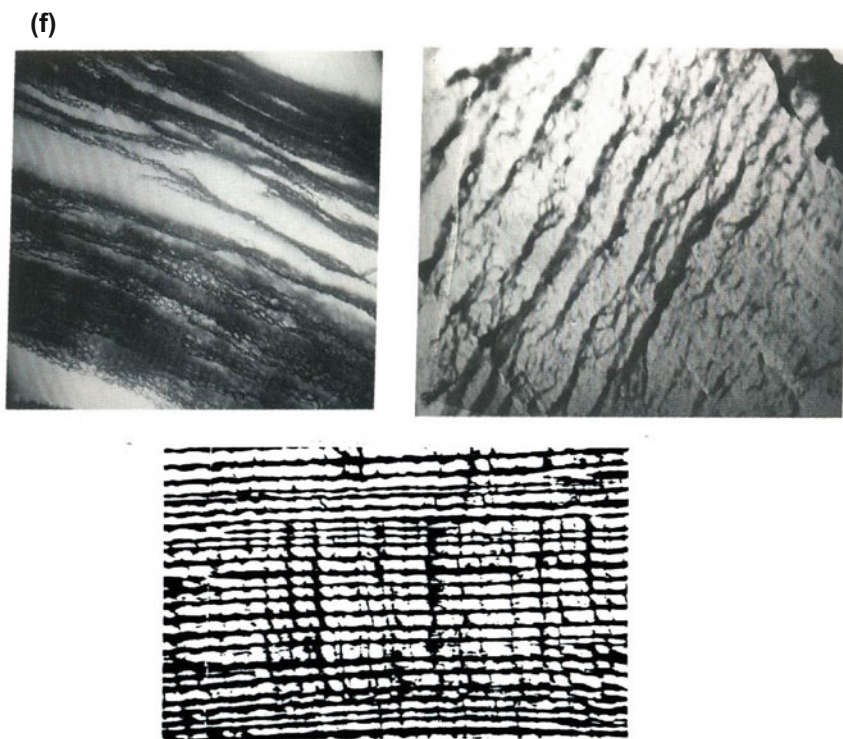


Fig. 4 (continued)

as Ni (II) (Hassan et al. 1988b), Cu (II) (Hassan et al. 1988a), Co (II) (Awad et al. 1980b; Hassan et al. 1989a); alkaline earth metals such as Ca (II), Sr (II), and Ba (II) (Hassan et al. 2013, b); heavy metal ions such as Zn (II), Sn (II), Cd (II), Hg (II), and Pb (II) (Khairou et al. 2002a, b) as well as trivalent and tetravalent metal ions such as Al (III), La (III), and Th (IV) (Zaafarny 2013) were investigated complexometrically. Pseudo-first-order conditions were employed in which the alginate sol concentration was present in a large excess over that of the metal ion concentrations. Plots of  $(\ln [C])$  vs. time) were found to be of sigmoidal S-shaped nature with two distinct stages for the gelation rates. The first part was significantly fast at early stages, followed by a slow decrease in the gelation rates at longer time periods. This indicates that the cited gelation reactions obey a behavior of the following rate-law expression (Frost and Pearson 1965).

$$C_t - C_\infty = B_0 e^{-k_f t} + P_0 e^{-k_s t} \quad (2)$$

where  $k_f$  and  $k_s$  are the observed pseudo-first-order rate constants for the fast and slow gelation steps, respectively,  $B_0$  and  $P_0$  represent the initial concentration of the



sol in the two gelation processes, and  $C_t$  and  $C_\infty$  are the concentration of the metal at times  $t$  and infinity.

The relatively fast initial stages were explained by fast formation of primary membranes on the surface of alginate sols. The second slow stage seems to be an ion exchange between the exchanging  $\text{Na}^+$  and metal counter ions and is controlled by the compactness of the network of the already formed primary gel membrane. Hence, two possible rate-determining steps may be considered. They are the exchange of the counter ion across the interface between the sol and the metal ion electrolyte (Dickel and Meyer 1953) or the true exchange reaction at the fixed ionic groups (Tetenboum and Gregor 1956). Since, the rate-controlling by ion exchange across the interface is unlikely (Richman and Tomas 1956), it is worthwhile to consider the exchange of the interdiffused ions in either fast or slow stages as the rate-controlling steps. Again, the magnitude of the activation energies obtained may support the suggested mechanism of the rate-controlling step for ion exchange process (Awad and El-Cheikh 1980).

Moreover, the second-order rate constants of gelation or gel growth ( $R_g/[\text{alginate sol}]$ ) for the fast stage of gelation as well as the activation parameters obtained which calculated from the temperature dependence of the gelation rates by the least squares method using Arrhenius and Eyring equations (Glasstone et al. 1941) are summarized in Table 3. The observed large negative entropies of activation can be interpreted by the necessity of the interdiffused metal ions to penetrate one pair or more of adjacent large carboxylate groups of alginate macromolecule in order to

**Table 3** Activation parameters and rates of gelation growth for sol-gel transformation between alginate polysaccharide and some metal ions using membrane and column-shaped hydrogels

Metal alginate	$E_a^\ddagger$ (kJ mol <sup>-1</sup> )	$\Delta S^\ddagger$ (J mol <sup>-1</sup> K <sup>-1</sup> )	$\Delta H^\ddagger$ (kJ mol <sup>-1</sup> )	$\Delta G^\ddagger$ (kJ mol <sup>-1</sup> )	$10^4 R_g^*$ (dm <sup>3</sup> mol <sup>-1</sup> s <sup>-1</sup> )
Ca <sup>2+</sup>	11.49	-288.25	8.86	94.75	2.12
Ba <sup>2+</sup>	14.67	-260.85	12.59	90.52	5.36
Sr <sup>2+</sup>	16.97	-265.62	14.29	93.44	3.90
Zn <sup>2+</sup>	27.50	-240.09	24.79	96.34	1.57
Cd <sup>2+</sup>	62.99	-116.56	60.34	95.68	6.36
Pb <sup>2+</sup>	24.46	-238.29	21.80	92.81	6.60
Sn <sup>2+</sup>	16.25	-257.76	13.56	90.37	13.56
Hg <sup>2+</sup>	12.62	-285.99	8.72	93.47	2.81
Cu <sup>2+</sup>	15.73	-176.64	37.80	90.44	6.53
Ni <sup>2+</sup>	29.83	-224.49	25.29	92.19	9.31
Co <sup>2+</sup>	38.69	-260.89	14.77	92.50	12.92
Al <sup>3+</sup>	26.51	-242.06	23.81	95.94	1.90
La <sup>3+</sup>	12.65	-282.64	9.98	94.21	2.59
Th <sup>4+</sup>	15.46	-272.47	12.69	93.89	3.10

Measured at 45 °C

bring them together in bridges for forming the corresponding coordination biopolymer metal–alginate ionotropic hydrogel complexes.

In spite of the variety of metal ions used in those gelation processes, it seems that the magnitude of the free energy of activation is remained unaltered significantly as shown in Table 3. Again, a plot of  $\Delta H^\ddagger$  against  $\Delta S^\ddagger$  of the isokinetic relationship (Leffler and Grunwald 1963) was found to be linear. The magnitude of the slope of the isokinetic relationship is significant and may be considered as a deserved comment of the reactivity of these gelation processes. The approximate similarity of the free-energy values along with the linearity of the isokinetic relationship may indicate that the mechanisms of gelation processes in these sol-gel transformation systems are similar. Moreover, the magnitude of the activation energies may reflect the stability in these metal–alginate hydrogel complexes. The activation-energy values indicate that the stability increases in the order  $M^{3+} < M^{2+} \leq M^{4+}$ -alginate complexes. This means that trivalent metal–alginate hydrogels are less stable complexes and can be explained from the thermodynamic point of view by the energy strains in the geometrical configuration.

Generally, the magnitude of the rate constants of gelation (rate of gel growth) depends on many factors such as the ionic radii and polarizability of the interdiffused metal ions, the concentrations of both metal ion and alginate sol, pH and viscosity of the electrolyte. It noticed that the rate constants of gelation for a group of metal cations, to be decreased in the order: Sn > Pb > Cd > Hg > Zn–alginate hydrogel complexes (Table 3). This order was found to be in good consistent with the reported ionic radii and polarizability of these metal ions (Cotton and Wilkinson 1972).

### Mechanism of Sol-Gel Transformation

As the alginate sol gets in contact with the metal ion electrolyte, a thin layer of primary membrane is formed on the surface of the alginate sol in order to prevent the deterioration of the alginate sol from the petri dish or column into the surrounding metal ion electrolytes. This membrane will separate the sol from the surrounding electrolyte, whereas the macromolecular chains of alginate polyelectrolyte start to distribute themselves statistically below the already formed primary membrane. As the steady-state conditions are established, the  $Na^+$  counter ions produced from the dissociation of the alginate macromolecule began to migrate from the alginate sol outward into the electrolyte solution through that formed primary membrane. Simultaneously, an equivalent amount of metal ions must go inward and occupy the places left by  $Na^+$  counter ions with the alginate macromolecule in order to maintain the electroneutrality. The net process is an exchange process between the counter ions in both the sol and electrolyte phases (Hassan 1989; Hassan et al. 1989a, b, 1991). The continuity of such exchange process resulting from the transfer of both counter ions leads to gradual growing of multilayer membrane involving crosslinked metal ions with the functional groups of alginate macromolecule. The thickness and properties of such multilayer membrane

depend on the concentrations of both metal ion and alginate sol, pH and viscosity of the electrolyte, nature of the metal ion and temperature. The time of growth increases with increasing the sol concentration and vice versa with respect to the concentration of metal ion electrolyte.

### 3.6.2 In Case of Hydrogels of Sphere Shapes

#### Kinetics and Mechanism of Sol-Gel Transformation

When an alginate sol droplet is allowed to get in contact with a metal ion electrolyte placed in a container such as beaker or cylinder, a primary membrane is rapidly formed around the droplet which separates the alginate sol inside the droplet from deterioration into the electrolyte solution as well as to keep the droplet in a symmetrical spherical shape. At the beginning, the droplet floats just below the surface of the metal ion electrolyte inside the container since the density of the alginate sol is smaller than that of the metal ion electrolyte. In a similar manner to that mentioned previously in case of membranes and column hydrogels, an ion exchange process between the  $\text{Na}^+$  counter ions of alginate sol and the interdiffused metal ions of the electrolyte will take place. When the density of the metal–alginate droplet exceeds that of the electrolyte, the formed metal–alginate pellet starts to sink down into the container with a certain velocity which may be called the velocity of acceleration ( $V$ ) which differs from one metal ion to another. The spent time between the floating and the sinking of the droplet may be called the relaxation time ( $\Delta\tau$ ). In fact, the relaxation time is usually terminated in a very brief periods of time, but for sol-gel transformation the structural peculiarities and the hindrance of the relative movements of the particles to various interchain linkages may cause some shifts to take place very slowly (Awad et al. 1980a, b; Yonese et al. 1988). In complex structures of polymer gels as in the cited work, the response of the gel to the external variables varies widely depending on the timescale. So, the polymer chain has a certain relaxation time, i.e., it relaxes to avoid any deformation (Larson 1988). The largest relaxation time of free polymer may reflect the rheological behavior of these MAG complexes.

#### Influence of Diffusion Controls on Sol-Gel Transformation

The relaxation time is affected by the rate of the formation of the primary membrane. It has been found that the rate of formation of the primary membrane and the gel growth are high in metal ion electrolytes of lower concentrations rather than in higher electrolyte concentration, and this may be attributed to the fast mobility of the metal ions in the former case. On contrary, the rates were found to be larger in higher concentrations of alginate sols rather than that in sols of lower concentration owing to the presence of many exchange sites within the alginate macromolecular chains in the former case in comparison with that of the latter sols. Hence, the

relaxation time decreases with increasing the concentration of the alginate sol and temperature, whereas it increases with increasing the metal ion concentration. The relaxation times ( $\Delta\tau$ ) and velocity of acceleration ( $V$ ) as one of the diffusion controls which affect the sol-gel transformation of spherical shape hydrogels have been examined for some divalent (Awad et al. 1979, 1980a, b; Hassan et al. 1992a, b, c, d, 1995a, b; Khairou et al. 2003) and trivalent metal cations (Hassan et al. 1995a, b). The kinetics were performed by dropping a droplet of sodium alginate sol of known concentration in calibrated cylinder containing metal ion electrolyte of known concentration which were previously thermostated into a constant temperature water- or air-bath within  $\pm 0.1$  °C. The time interval ( $\Delta\tau$ ) between the moment at which the droplet gets in contact with the surface of electrolyte and the moment at which the droplet starts to sink into the electrolyte was recorded. Here, the increase in the droplet density with time  $d\rho/dt$  may be taken as a measure of the rate of gel growth, and hence, the value of  $(\rho_1 - \rho_2)/\Delta\tau$  is considered to be a measure of the gelation rate, thus

$$\text{Rate} = \frac{\rho_1 - \rho_2}{\Delta\tau} = kA \quad (3)$$

where  $\rho_1$  denotes the density of the electrolyte,  $\rho_2$  is the density of the sol,  $k$  is the rate constant of gelation, and  $A$  is the proportional constant. Since the increase in the density of the sol droplet is mainly due to metal ion diffusion inside the sol droplet rather than the diffusion of  $\text{Na}^+$  counter ions out to the electrolyte solution, Eq. (3) can be simplified to give:

$$\text{Rate} = R_g = \frac{d\rho_1}{\Delta\tau} = kA \quad (4)$$

By plotting  $\rho_1$  versus  $\Delta\tau$  for different electrolyte concentrations, straight lines were obtained from whose slopes the rate of gel growth ( $R_g$ ) can be evaluated. These values were calculated by using the method of least squares and are summarized in Table 4. Consequently, the values of  $(\rho_1 - \rho_2)/(\Delta\tau)$  can be considered as a measure of the exchange rate ( $k$ ), i.e., the rate of sol-gel transformation.

It has been found that the calculated rates of sol-gel transformation (gelation) using either pseudo-first-order kinetics or change in the droplet density techniques were in good agreement with each other within the experimental errors. Again, the time ( $t$ ) for constant distance ( $Y$ ) covered by the droplet while sinking into the electrolyte under the influence of the gravitational forces was recorded.

All experiments were repeated with alginate sol and different metal ion electrolytes of different concentrations at various temperatures for at least five experimental runs. For each alginate sol and metal ion electrolyte, some precautions were taken into consideration in order to maintain a nearly constant sol droplet. These precautions were: (1) using the same syringe as a dropper; (2) constancy of the distance from the tip of the syringe to the surface of the electrolyte solution; (3) the force exerted upon the piston of the syringe was maintained constant.

**Table 4** Values of gelation rate growth, relaxation time, and velocity of acceleration for sol-gel transformation between alginate polysaccharide and some metal ions using sphere-shaped hydrogels at 23 °C

Metal ions	$10^4 \text{ d}\rho_1/\text{d}\Delta\tau$ ( $\text{g}/\text{cm}^3 \text{ s}$ )	$\Delta\tau$ (min)	$V$ ( $\text{cm s}^{-1}$ )
$\text{Ca}^{2+}$	1.4	34.6	0.21
$\text{Sr}^{2+}$	2.0	33.4	0.27
$\text{Ba}^{2+}$	2.5	32.2	0.29
$\text{Mn}^{2+}$	5.8	27.1	0.23
$\text{Co}^{2+}$	7.8	30.0	0.14
$\text{Ni}^{2+}$	8.7	31.5	0.21
$\text{Cu}^{2+}$	9.5	33.1	0.24
$\text{Zn}^{2+}$	9.2	30.1	0.26
$\text{Al}^{3+}$	1.5	46.1	–
$\text{Fe}^{3+}$	1.1	58.0	–
$\text{La}^{3+}$	1.9	23.6	0.32
$\text{Ce}^{3+}$	1.7	23.0	0.42
$\text{Cd}^{2+}$	2.0	33.6	0.28
$\text{Sn}^{2+}$	1.5	38.4	0.26
$\text{Pd}^{2+}$	3.5	14.3	0.32
$\text{Hg}^{2+}$	1.6	28.4	0.23

An approach of mathematical treatment was suggested to calculate the velocity of acceleration ( $V$ ) from the kinetic data as well as to explain the behavior of sinking for the metal–alginate droplet into the calibrated cylinder which containing the electrolyte solution. Let us assume that there are three forces acting on the spherically shape metal–alginate droplet. The first one is the weight of the sol droplet toward the gravitational of acceleration in the downward direction ( $F_1$ )

$$F_1 = \frac{4}{3} \pi r^3 \rho_2 g \downarrow \quad (5)$$

where  $r$  is the radius of the sol droplet which depends on the radius of metal ion ( $r^*$ ) and  $g$  is the gravitational force. The second force is the Archimedean force which tends to raise the sol droplet upward ( $F_2$ ), thus

$$F_2 = \frac{4}{3} \pi r^3 \rho_1 g \uparrow \quad (6)$$

The third one is the dragging force ( $F_3$ ) which increases with increasing the velocity of the falling droplet:

$$F_3 = B m V \uparrow \quad (7)$$

where  $m$  is the mass of the droplet and  $B$  is the proportional constant which depends on the viscosity of the medium and the radius of the falling droplet, and

$$B = \frac{6\pi r \zeta}{m} \quad (8)$$

where  $\zeta$  denotes the viscosity of the electrolyte solution and  $V$  is the velocity of the falling droplet.

At the beginning, the velocity of the droplet is equal to zero, and hence, the dragging force ( $F_3$ ) can be omitted, then,

$$\frac{4}{3}\pi r^3 \rho_2 g < \frac{4}{3}\pi r^3 \rho_1 g \quad (9)$$

When the density of the droplet exceeds that of the surrounding metal ion electrolyte solution ( $>\Delta\tau$ ), it starts to sink into the electrolyte solution with an appreciable velocity. The behavior of sinking is controlled by the conditions

$$\frac{4}{3}\pi r^3 \rho_2 g > \frac{4}{3}\pi r^3 \rho_1 g + 6\pi r \zeta V \quad (10)$$

Equation (10) requires that the velocity of the droplet ( $V$ ) should be less than the factor  $2g r^2 (\rho_2 - \rho_1)/9\zeta$  as was experimentally observed. It seems that both relaxation time and velocity of acceleration are depending on the physical properties of the metal–alginate droplet such as mass, volume, elasticity as well as the nature of the metal ion such as its radius and polarizability, pH of the media, concentration of both alginate sol and metal ion electrolyte and temperature.

In order to account the effect of the diffusion controls on the acceleration of velocity, the following equation of motion is suggested

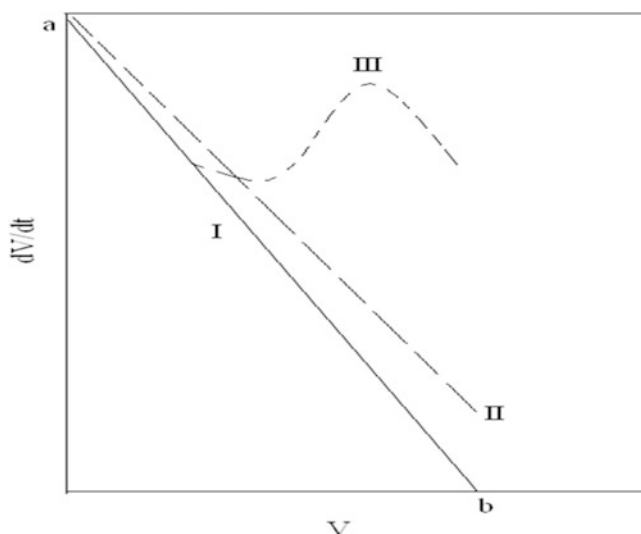
$$m \frac{dV}{dt} + (V - U) \frac{dm}{dt} = B - AmV \quad (11)$$

where  $U$  is the velocity of the reduced mass just after leaving the droplet of the electrolyte surface and  $B$  is constant equal to  $[g(\rho_2 - \rho_1)]/\rho_2$ .

Assuming that the reduced mass becomes immediately at rest after droplet leaving ( $U = 0$ ), hence Eq. (11) reduces to Eq. (12), thus

$$\frac{dV}{dt} = B - \left( A + \frac{dm/dt}{m} \right) V \quad (12)$$

The analysis of Eq. (12) can be clarified by using the following theoretical diagram:



Theoretical sketch for the diffusion controls

This diagram can be completely understood if we considered the following assumptions.

**Case I:**

Assuming that both the mass and density of the droplet are constants during the gelation process ( $dm/dt = 0$ ), Eq. (12) leads to Eq. (13),

$$\frac{dV}{dt} = B - AV \quad (13)$$

where

$$V = A/B(1 - e^{-Bt}) \quad (14)$$

Equation (12) requires that the plots of  $dV/dt$  against  $V$  should be linear with a negative slope equals to  $(-A)$  and intercept on  $dV/dt$  axis equals to  $(B)$ . This straight line may be represented by  $(a - b)$  line on the theoretical diagram.

**Case II:**

Assuming that the mass of the droplet remains constant while its density is subjected to change as a result of crosslinking of the interdiffused metal ions as well as the orientation of the macromolecular chains and solvent molecules toward the chelated metal ion. Then Eq. (12) leads to Eq. (13), but with variables  $A$  and  $B$ .

The term  $B$  increases by increasing  $\rho_2'$  due to the decrease in  $r$ , while the term  $A$  is consequently decreases. The values of  $dV/dt$  are increased when compared with that obtained in Case I. On the other hand, if the droplet radius decreases with a continuous increase in its density, a behavior similar to that illustrated by the line (II) is obtained. Moreover, if the decrease in the radius of the droplet occurs in a rhythmic manner, i.e., in a pulsed way, then we will obtain the line (III), which coincides with the line (I) for the same interval time.

### Case III:

If the mass of the droplet decreases while its radius remains constant owing to the outward flux of water (dehydration), then the  $B$  term increases while the  $A$  term is decreased. Therefore, the term  $B - AV$  yields a decrease in  $dV/dt$  in Eq. (13). At the same time, the term  $dm/dt$  will increase in magnitude and possesses a negative sign. The resultant of  $dV/dt$  will depend on whether or not the rate of  $(A - BV)$  decrease is greater than the rate of  $dm/dt$  increase. If  $dV/dt < 6\pi\eta r$ , then  $\frac{dm/dt}{m}$  may even assume to be a negative value.

The acceleration of velocity can be determined from  $Y-t$  plots. Then the term  $dV/dt$  can be evaluated using the well-known graphical methods Awad et al. (1979, 1980a). The results are summarized in Table 4. In view of the above interpretations and the observed pulsed behavior of  $dV/dt - V$  plots (Fig. 5), the gel growth in these MAG complexes is a rhythmic process in nature.

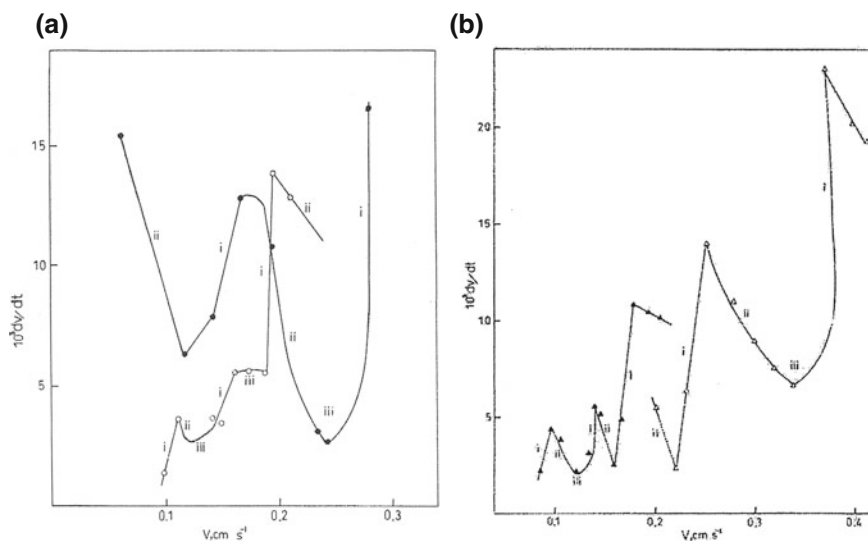


**Fig. 5** Rhythmic curves of  $(dV/dt)$  versus  $V$  plots for some coordination biopolymeric metal-alginate gel complexes. **a**  $\text{Sn}^{2+}$  (o),  $\text{Cd}^{2+}$  (.); **b**  $\text{Sn}^{2+}$  (▲),  $\text{Hg}^{2+}$  (Δ)



### 3.7 Other Fundamental Properties of Coordination Biopolymeric Metal Alginate Iontropic Hydrogels

#### 3.7.1 Water Contents

The water content in these metal–alginate hydrogels was determined by drying the hydrogel complexes in the form of sphere shapes (pellets) in an electric oven at 105 °C until it reached a constant weight. The water content was calculated as follows

$$\text{Water content (\%)} = [100 - (W'/W_0) \times 100] \quad (15)$$

where  $W_0$  and  $W'$  denote the weights of the gel sphere before and after dryness, respectively. The water contents were calculated and are summarized in Table 5. It has been shown that water content in these studied ionotropic hydrogel exceeds 90% of the hydrogel weight. The pore size distribution has a large tendency to vary with simultaneous contraction of the gel during drying. This may be interpreted by the huge capillary stresses and resistance of fluid-flow in the narrow and small pores of the hydrogel network (Hassan et al. 2012b, 2014a).

#### 3.7.2 Rheological Properties

Rheological characterization of polymer gels has attracted the attention of many investigators owing to its wide applications in biomedical industry (Segeren et al. 1974; Kavanagh and Ross-Murphy 1998; Andrews and Jones 2006; Anand et al. 2006; Saha et al. 2011). The properties of the polymer gels can be controlled by

**Table 5** Degree of swelling and shrinking and water contents for some coordination biopolymeric metal–alginate ionotropic hydrogel spheres

Metal ion	Degree of swelling <sup>a</sup> (%)	Water content <sup>b</sup> (%)		Metal ion	Degree of shrinking <sup>a</sup> (%)	Water content <sup>b</sup> (%)	
		2%	4%			2%	4%
Ca <sup>II</sup>	19.1	97.78	95.12	Cu <sup>II</sup>	2.4	97.46	94.56
Mn <sup>II</sup>	96.4	97.83	94.33	Cd <sup>II</sup>	16.7	97.48	91.33
Co <sup>II</sup>	106.5	97.85	93.75	Sn <sup>II</sup>	9.6	97.71	94.31
Ni <sup>II</sup>	70.9	97.54	95.25	Ba <sup>II</sup>	3.2	96.56	93.04
Sr <sup>II</sup>	12.2	96.94	92.47	Pb <sup>II</sup>	6.0	96.33	93.76
Se <sup>IV</sup>	21.8	98.74	95.89	Al <sup>III</sup>	11.9	97.98	92.15
				Cr <sup>III</sup>	12.2	98.43	93.62
				Fe <sup>III</sup>	8.8	98.23	93.40

<sup>a</sup>[Alg] = 2%, Room temp. = 22 °C, immersing time = for about one month

<sup>b</sup>Drying temperature = 105 °C for about 72 h

treatment of the microstructure of the polymer backbone and its surrounding liquid. The polymer can be made stiffer by increasing the spacing of the crosslinks either by increasing the molecular weight of the polymer chain connecting the crosslinks or diluting the gel with a solvent such as water (Grillet et al. 2012).

### Shape, Elasticity, Transparency, Mass, Volume, and Radius

The physical properties of spherical metal–alginate hydrogels such as shape, elasticity, transparency, mass, volume, and radius were determined by the well-known methods and are summarized in Table 6. The trivalent metal–alginate hydrogels were found to be a little soft, brittle, and of non-transparency nature (Hassan et al. 2014a, 2012b). This fact may be owing to the presence of some geometrical energy strain and will be discussed later.

### Swelling and Shrinking

#### Swelling and Shrinking in Aqueous Solutions

The swelling properties of polymer gels are of great importance for application in industrial technology such as in immobilization systems and water-based drilling fluids which depend on rheological performance and ecological considerations (Ricka and Tanaka 1984; Navarette et al. 2001; Sharma et al. 2006; Torres et al. 2011).

Nowadays, ethanol is considered as competitive alternative to the current fossil fuels in the whole world. Therefore, an increase interest for production of ethanol on a large scale has been realized in industry. It was found that addition of calcium alginate spheres as biocatalyst will increase the performance of ethanol production (Torres et al. 2011). Again, the calcium alginate pellets were used as biocatalyst for removal of phenol and chlorophenols from water (Torres et al. 1998).

It is well known that hydrogels exhibit some changes on swelling and shrinking under the influence of environmental variables such as the solvent composition, pH, UV, visible light, ionic strength of the solvent media, surfactants, and temperature. The complexed matrix of alginate with polyvalent metal ions can adopt divergent swelling behaviors as the conditions of the surrounding solution change. Generally, the polymer hydrogel consists of an elastic crosslinked network (using physical or chemical crosslinks). These crosslinks prevent the long polymers from dissolving in the external solvent, and hence, the polymer gel can swell or shrink reversibly by either adsorption or desorption of a significant fraction of the immersing fluid where the small molecules migrate in and out into the gel network (Osada et al. 1955; Hong et al. 2008). In other words, the polymer hydrogel swells when imbibing an amount of solvent from the surrounding media, whereas it shrinks when release an amount of its internal solvent to the surrounding. This ability is considered as one of the most remarkable properties of biomaterials which makes the polymer hydrogels of promising intelligent in the diverse biotechnologies including medical devices and drug delivery.... (Hassan et al. 2012b, 2014a).

**Table 6** Physical properties of some coordination biopolymeric metal–alginate ionotropic hydrogel spheres.  $[Alg] = 2\%$  at 25 °C

Metal–alginate	Shape	Elasticity	Transparency	$10^2 m_e$ (g) <sup>a</sup>	$10^2 m_i$ (g) <sup>a</sup>	$10^2 v_e$ (cm <sup>3</sup> ) <sup>b</sup>	$10^2 v_i$ (cm <sup>3</sup> ) <sup>b</sup>	$n$	$K$
Mn (II)	Spherical	Elastic	Transp.	5.72	4.10	5.41	3.45	0.581	0.076
Co (II)	Spherical	Elastic	Transp.	8.01	3.72	8.05	3.87	1.254	0.004
Ni (II)	Spherical	Elastic	Transp.	5.50	3.07	5.13	3.55	1.004	0.012
Ca (II)	Spherical	Elastic	Transp.	3.67	3.26	3.65	2.97	0.23	0.362
Sr (II)	Spherical	Elastic	Transp.	3.20	2.87	2.97	2.70	0.210	0.391
Se (IV)	Spherical	Elastic	Transp.	6.09	5.50	5.92	5.27	–	–
Cu (II)	Spherical	Elastic	Transp.	3.33	3.44	3.29	3.55	0.085	0.68
Sn (II)	Spherical	Brittle	Not	5.79	5.90	5.41	5.68	0.096	0.733
Ba (II)	Spherical	Elastic	Transp.	2.45	2.65	3.38	3.46	0.160	0.480
Pb (II)	Spherical	Elastic	Transp.	2.92	3.07	2.70	2.87	0.104	0.627
Al (III)	Flat	Brittle	Semi	4.99	5.46	4.73	5.34	–	–
Cr (III)	Flat	Brittle	Not	4.82	5.44	4.54	4.80	–	–
Fe (III)	Flat	Brittle	Not	5.41	4.99	4.80	5.47	–	–

<sup>a</sup> $m_i$  and  $m_e$  are the masses of the droplet before and after equilibrium<sup>b</sup> $v_i$  and  $v_e$  are the volumes of the droplet before and after equilibrium

The swelling or shrinking property comprised with measurements of either water absorbed or released by swelling or shrinking, respectively (Hassan et al. 2014a, 2012b). The procedure of measurement takes place by immersing the hydrogel spheres into containers contained fixed volumes of deionized conductivity water which were previously thermostated at the desired temperatures within  $\pm 0.1$  °C. After intervals of time, the swollen or shrunk spheres were removed from the water in the container and blotted quickly by means of filter paper strips to remove the excess water adhered on the surfaces, and then the weights and volumes of these examined gels were determined. The degree of water uptake (swelling) was calculated from the relationship

$$\text{Swelling (\%)} = ((W - W_0) / W_0) \times 100 \quad (16)$$

where the symbols  $W_0$  and  $W$  represent the initial weight of pellets before and after immersing, respectively.

The observed swelling may be attributed to the tendency of the ionogenic groups of the monomeric units (carboxylate and hydroxyl moieties) to surround themselves by some solvent molecules which causes a stretching of the alginate matrix. As an equilibrium condition is attained, the elastic forces of the matrix will balance with the absorption tendency, and hence, the matrix expansion is stopped.

On the other hand, in a similar manner the degree of the released water (shrinking) can be determined from the following equation

$$\text{Shrinking (\%)} = ((W_0 - W) / W_0) \times 100 \quad (17)$$

The results are summarized in Table 5. All cited data were an average of five experimental runs.

The swelling process is known as a kinetic process depending on the interaction between the polymer network and the solvent. Many theories have been formulated to describe or predict the swelling kinetics by coupling the mass transport and mechanical deformation of the gels on the basis of interaction between the polymer network and the solvent. Linear and nonlinear concepts were suggested to explain the swelling kinetics (Tanaka and Filmore 1999; Durning and Moorman 1993; Dolbow et al. 2004, 2005; Tsi et al. 2004; Hong et al. 2008; Bouklas and Huang 2012). The two theories are consistent within the linear regime under the conditions of small perturbation from anisotropically swollen state of the gel. However, another technique can be also applied to characterize the rheological properties such as the adhesion and mechanical response of the swollen hydrogels.

Concerning the cited MAG complexes, the gel network consists of very strong and very large polymer chain which spans the whole volume of the entire gel. So, if the crosslink is broken, the network cannot be reformed again. This means that the gel strength is proportional to the density of the crosslinks (Grillet et al. 2012). Therefore, we are avoided to apply those linear and nonlinear concepts for

explaining the swelling kinetics. Alternatively, the kinetics of swelling and shrinking were examined by a simple kinetic equation of (Rigter and Peppes 1987):

$$m_t/m_e = k t^n \quad (18)$$

The linearized form of this equation can be rewritten as follows:

$$\ln(m_t/m_e) = \ln k + n \ln t \quad (19)$$

where  $m_t$  and  $m_e$  are the weights of the hydrogels at time  $t$  and at equilibrium, respectively, whereas  $k$  and  $n$  are constants. The values of the constants  $k$  and  $n$  are dependent on the degrees of swelling and shrinking in terms of expansion or constriction of the matrix network, respectively. Plots of the left-hand side of  $\ln(m_t/m_e)$  against  $\ln t$  gave good straight lines from whose slopes and intercept of the values of  $n$  and  $k$  can be evaluated. These values were calculated by the least squares method and are summarized in Table 6. It is noticed that the value of ( $n$ ) is function of either swelling or shrinking magnitudes. The ( $n$ ) value was found to increase with increasing either the degrees of swelling or shrinking which are related to the expansion or constriction of the matrix network, respectively. Hence, the values of ( $n$ ) may be considered as an indirect evidence for the ability of those hydrogels to swell or shrink in aqueous solutions. On the other hand, the constant ( $k$ ) depends on the nature of metal ion such as its ionic radius and the polarizability as well as on the orientation of the solvent molecules and macromolecular chains toward chelated metal ion.

It is well known that polymer hydrogels tend to equilibrate with the external solvent through swelling or shrinking. Therefore, the gels are swollen by uptaking or imbibing some water or other solvent molecules from the swelling media. The rate of swelling is gradually increased with time as shown in Fig. 6a, b. When an equilibrium condition is attained, no change in the swelling rate of the gel is observed. The equilibrium is established if the chemical potential of the solvent in the swelling media is equal to that of the swollen gel. It has been found that  $Mn^{II}$ ,  $Ni^{II}$ ,  $Ca^{II}$ ,  $Sr^{II}$ , and  $Se^{IV}$ —metal alginates—having a great tendency for swelling in water. The degree of swelling was found to increase in the order  $Sr < Ca < Se < Ni < Mn < Co$ -alginates, whereas the crosslinks did not affected by the chemical potential of the solvent inside the gel. This may be explained by the mixing property of the free energy of alginate as anionic polyelectrolyte and that of the solvent, the extension of the macromolecule network, and the mixing property of both the solvent and mobile ions. Again, the experimental observations indicated that the volume swelling is closely related to the weight swelling during the swelling process as shown in Fig. 6b.

Some other hydrogels tend to shrink by removal of the liquid from the gel network to the external media. In this case, the weight of the gel is gradually decreased by time as shown in Fig. 6c. This behavior may be interpreted by alternation of the swelling heat caused by the large number of segments of adjacent chains which are situated in juxtapositions. These juxtapositions were prevented from taking up positions of relatively high statistical probability for some

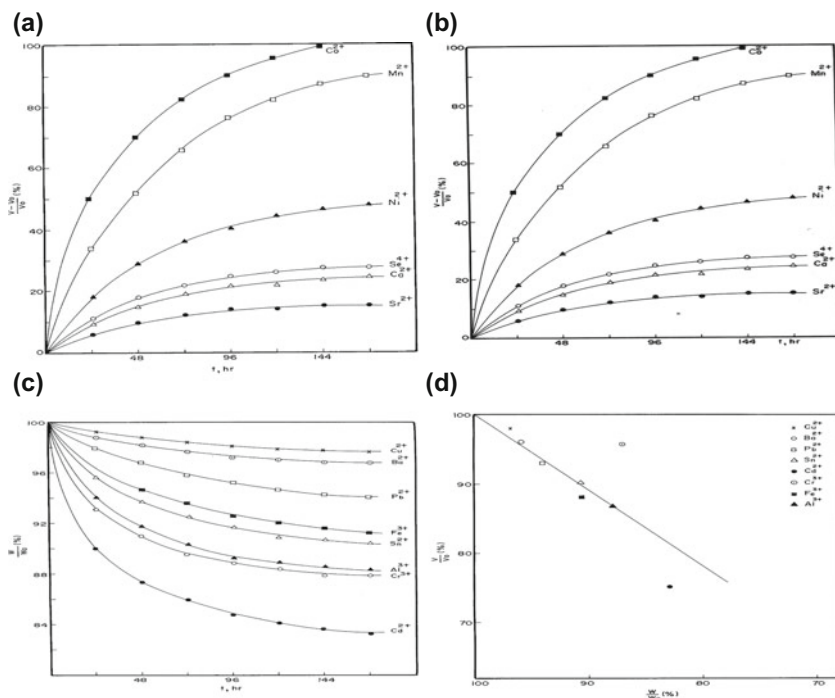


**Fig. 6** **a** Change in weight-swelling plots with aging time at 22 °C for some coordination biopolymeric metal–alginate ionotropic hydrogel complexes. **b** Change of volume-swelling plots with aging time at 22 °C for some coordination biopolymeric metal–alginate ionotropic hydrogel complexes. **c** Plots of the degree of shrinking as a function of time at 22 °C for some coordination biopolymeric metal–alginate ionotropic hydrogel complexes. **D.** Plots of volume-shrinking-weight-loss for some coordination biopolymeric metal–alginate ionotropic hydrogel complexes

stereochemical reasons. The degree of shrinking was also found to decrease in the order:  $\text{Cd} > \text{Cr} > \text{Al} > \text{Sn} > \text{Fe} > \text{Pb} \approx \text{Ba} > \text{Cu}$ -alginates. A plot of volume shrinking vs. weight loss was fairly linear as shown in Fig. 6d. This linearity may indicate that the volume reduction is closely related to the weight loss, i.e., to the density of the gel by about  $0.95 \text{ g/cm}^3$  in a very close value of the density of water as a swelling media (Hassan et al. 2014a, b, c) (Fig. 7).

It is of importance that the gels must possess acceptable properties for their handling in practical use. Therefore, the stress–strain (Smirsdod 1973) and percent elongation (Smidsrod 1973; Gemeiner et al. 1989) for metal–alginate gels have been examined in more detail elsewhere. It concluded that these ionotropic hydrogels may change some of their physicochemical properties by either shrinking or swelling. The experimental observations indicated that the swelling is accompanied by a remarkable alternation in the macroscopical shape and optical properties in these gels. The increase in volume and pore size by swelling of the gel can be explained by the increase in the wideness of the network capillaries. Again, the increase in the gel transparency on swelling may be attributed to the birefringence loss in the gel (Mongar and Wassermann 1952). As the gel shrinks, its stiffness increases because

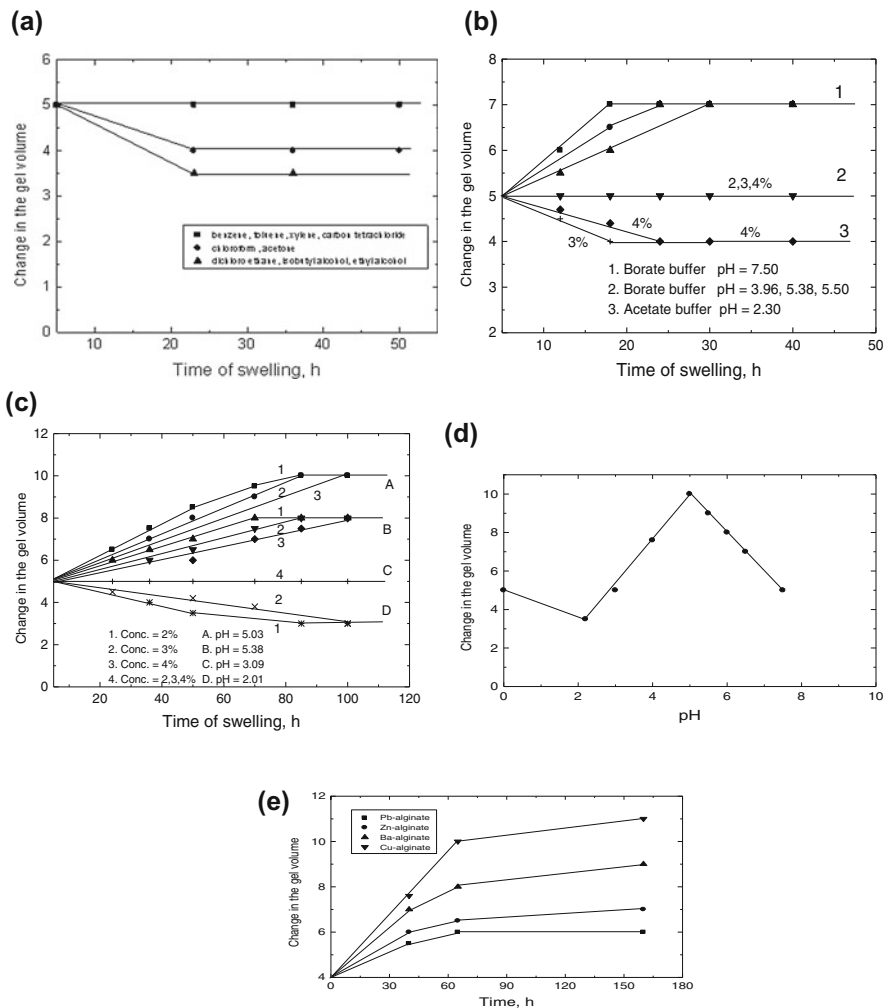


**Fig. 7** **a** Plots of swelling versus time in different solvents for some coordination biopolymeric metal-alginate ionotropic hydrogel complexes. **b** Plots of swelling versus time for some coordination biopolymeric metal-alginate ionotropic hydrogel complexes in buffer solutions. **c** Plots of swelling versus time at various values of alginate concentration and pHs for some coordination biopolymeric metal-alginate ionotropic hydrogel complexes. **d** Effect of pH on the change of hydrogel volume for some coordination biopolymeric metal-alginate ionotropic hydrogel complexes. **e** Plots of swelling versus time for some coordination biopolymeric metal-alginate ionotropic hydrogel complexes

the network becomes more tightly packed. Hence, a decrease in the volume, pore size, and the birefringence of the gel should follow the shrinking process. The shrinking behavior with respect to the volume and size decreasing can be interpreted

by the expulsion of the liquid from the hydrogel pores to the external media which cause a reduction in the gel/liquid interfacial area. Again, the decrease in the birefringence can be attributed to the removal of water molecules from the gel which was sharing for the increase of the orientation property toward the chelated metal ions.

The factors which affect the behavior of metal–alginate gels in aqueous solutions such as temperature, concentration of alginate sol, width of capillaries, and the radii of the metal ions have been examined elsewhere (Katchalsky and Michael 1955). These factors were explained by some variation that occurs in the chemical potential between the swelling media and the water content of the gel, and the free energy of the gel-stretching in the gel network (the free energy of the gel is apart from the standard free energy of the components which results from mixing of the gel with water and the electrostatic free energy). This variation leads to a contraction in the network of the gel.

The degree of swelling or shrinking was found to be largely affected by the sol concentration. As the alginate sol increases, the swelling or shrinking rate is increased. This fact can be interpreted by the increase in the bridging bonds which causes swelling or contraction of the gel network, respectively. The magnitude of swelling or shrinking was found to agree with the order of capillary width in these metal alginate ionotropic hydrogels reported by (Thiele and Hallich 1957). As the width of capillaries increases, the swelling process is also increased, whereas that of the shrinking is decreased.

The slope of the curves obtained from swelling (or shrinking) time plots may be considered as a determining factor for the mechanical stability of these metal–alginate ionotropic gels. The experimental observations indicated that the magnitude of mechanical stability is decreased in the following order  $\text{Cu} > \text{Ba} > \text{Sr} > \text{Cu} > \text{Pb} > \text{Mn} > \text{Co}$ -alginate gels in good consistent with the reported stability of these ionotropic gel series (Schweiger 1964; Thiele and Anderson 1955). The high mechanical stability of copper-alginate gel may be attributed to its high degree of orientation (Thiele and Anderson 1955; Awad and El-Cheikh 1980) and its distorted octahedral structure (Hassan et al. 1992a, 2012b). The speculated geometrical structure for chelation in these metal–alginate gel complexes was suggested and discussed in more detail (Hassan 1993a).

Segeren et al. (1974) investigated the swelling of calcium (II) alginate in the presence of sugar in order to obtain information on the number of statistical chain elements in sodium alginate chain. It has been found that the number of statistical chain elements is an average of strand between crosslinks, but was very smaller to be examined according to the rubberlike elasticity theory.

## Swelling and Shrinking in Organic Solvents

### Behavior of Cu (II)-Alginate Membranes in Various Organic Solvents

Copper-alginate membranes were cut into cubes of the same dimensions, and their outer surfaces were blotted quickly by means of filter paper strips and then immersed into Erlenmeyer flasks containing 50 ml of either the tested organic solvent (or buffer solution).



The change in volume was followed periodically until it reached a constant value (Hassan et al. 2012). The results are summarized in Table 7a–e. The suffered changes in the volume for copper-alginate membrane cubes (4%) immersed in organic solvents for about 120 h are shown in Table 7a. However, the non-polar solvents showed no change in the physical properties of examined gel membranes, and a remarkable shrinking of the gels was observed in case of polar solvents. It seems that the dielectric constants or polarity of the organic solvents used have no influence on such properties. This result was found to be in good agreement with that observed for calcium (II)-alginate spheres immersed in organic solvents (Torres et al. 2011). The observed shrinking in polar solvents can be explained by desorption phenomenon where some water molecules should be released from the gel matrix to the external solution in order to preserve the gel in an equilibrium state with that external surrounding solvent. In case of non-polar solvents, no change in volume or other properties was observed. This behavior may be attributed to the imbibition phenomena in which the water content in the gel matrix is just replaced by the solvent molecules with no expansion of the gel matrix. This means that no change in the already existed steady-state conditions by substitution of such non-polar solvent molecules

### Swelling and Shrinking in Buffer Solutions

As shown in Table 7b–e, the swelling and shrinking properties of copper-alginate polymembranes in the buffer solutions are mainly dependent on the pH of the buffer solution used. For example, these tested hydrogels tend to swell in moderate pHs (5.03–5.08), but tend to shrink in universal buffers of lower pHs (2.03) as shown in Table 7b, c respectively. In the former case, the swollen effect may be attributed to the tendency of the gels to equilibrate with the external buffer solution, and hence, this property can be attained by the gel sorption of some buffer molecules. The swelling process will cease gradually with time until it stops completely as the equilibrium is reached between the hydrogel matrix and the external buffer solution. The ability of the hydrogels for swelling was pronounced in gels of lower alginate concentrations rather than that in gels of higher concentration. At lower pHs, the equilibrium between the gel and the external buffer solution is attained by desorption process for some water molecules from the internal gel to outside onto the external buffer solution. The change in volume as a function of pH is shown in Table 7d respectively. This behavior indicates that the pH of the buffer solution is the determining factor in the volume change property. As the pH of the buffer solution decreases, the capillary width of the gel zones becomes more narrow, and hence, a decrease in the gel volume is observed, i.e., a shrinking process occurs (Khairou et al. 2002a, b). On the other hand, an increase of the pH of the buffer will in turn increases the capillary width of the gel zone, i.e., the volume of the gel increases (swelling). On contrary, the hydrogels were found to deteriorate at higher pHs more than  $\geq 10$ .

**Table 7** A. The effect of some organic solvents on the volume of copper-alginate ionotropic hydrogels of polymembrane shapes (4%). B. Behavior of copper-alginate hydrogels of polymembrane shapes in universal buffer solution. C. Behavior of copper-alginate hydrogel of polymembrane shapes in borate and acetate buffer solutions. D. The maximum change of volume for copper-alginate ionotropic hydrogels of polymembrane shapes in universal buffer solution. E. Behavior of different metal–alginate ionotropic hydrogel spheres in universal buffer solutions (pH = 5.33)

(a)						
Solvent	Volume of solvent (ml)	pH of solvent	Volume of gel (ml)	Changing in the gel volume (cm <sup>3</sup> ) with time/h		
				24 h	48 h	120 h
Isobutyl alcohol	50	3.12	5	3.5	3.5	3.5
Toluene	50	3.48	5	5.0	5.0	5.0
Chloroform	50	3.52	5	4.0	4.0	4.0
Xylene	50	4.41	5	5.0	5.0	5.0
Ethyl alcohol	50	5.69	5	3.5	3.5	3.5
Dichloroethane	50	6.40	5	3.5	3.5	3.5
Acetone	50	6.60	5	4.0	4.0	4.0
Benzene	50	–	5	5.0	5.0	5.0
Carbon tetrachloride	50	–	5	5.0	5.0	5.0

(b) Changing in the gel volume in different buffers										
Buffer	Concn. of gel (%)	Volume of gel (cm <sup>3</sup> )	Volume of solution (ml)	pH of solution	Changing in the gel volume (cm <sup>3</sup> ) with time/h					
					12 h	18 h	24 h	30 h	100 h	100 h
Borate	2	5	50	7.5	6.0	7.0	7.0	7.0	7.0	7.0
	3	5	50	7.5	5.5	6.5	7.0	7.0	7.0	7.0
	4	5	50	7.5	5.0	6.0	6.5	7.0	7.0	7.0
	2,3,4	5	50	5.5	No changing occurs in the gel volume					
	2,3,4	5	50	8.3						
	2,3,4	5	50	9.2						
	2,3,4	5	50	5.38						

(continued)

**Table 7** (continued)

<b>(b) Changing in the gel volume in different buffers</b>																						
Buffer	Concn. of gel (%)	Volume of gel (cm <sup>3</sup> )					Volume of solution (ml)	pH of solution	Changing in the gel volume (cm <sup>3</sup> ) with time/h													
		5	5	5	5	5			12 h	18 h	24 h	30 h	100 h	100 h								
	2,3,4	5	50				3.94															
Acetate	3	5	50				2.3					4.0	4.0	4.0	4.0	4.0	4.0	4.0	4.0	4.0	4.0	-
	4	5	50				2.3					4.0	4.0	4.0	4.0	4.0	4.0	4.0	4.0	4.0	4.0	

<b>(c) Changing in the gel volume (cm<sup>3</sup>) with time/h.</b>												
150 h	100 h	85 h	80 h	75 h	70 h	50 h	36 h	24 h	pH of solution	Volume of solution (ml)	Volume of gel, cm <sup>3</sup>	Concn. of gel (%)
8.0	8.0	8.0	8.0	7.5	6.0	6.0	6.0	6.0	5.58	50	5	2
8.0	8.0	8.0	8.0	7.5	6.0	6.0	6.0	5.5	5.58	50	5	3
8.0	7.5	7.5	7.0	6.0	6.0	6.0	6.0	5.0	5.58	50	5	4
10.0	10.0	10.0	9.5	8.5	7.5	6.5	6.5	6.5	5.03	50	5	2
10.0	10.0	10.0	9.0	8.0	7.0	6.0	6.0	6.0	5.03	50	5	3
10.0	10.0	9.0	8.5	7.0	6.5	6.0	6.0	6.0	5.03	50	5	4
No changing occurs in the gel volume												
3.0	3.0	3.0	-	3.5	4.0	4.5	4.5	4.5	3.09	50	5	2, 3, 4
3.0	3.0	3.5	-	4.0	4.5	4.5	4.5	4.5	2.01	50	5	3
3.0	3.0	3.5	-	4.0	4.5	4.5	4.5	4.5	2.01	50	5	4

<b>(d) Changing in the gel volume as a function of pH</b>		
pH of solvent	Volume of gel (cm <sup>3</sup> )	Maximum change in the gel volume (cm <sup>3</sup> )
2.10	5	3.3
3.09	5	5.0
4.01	5	7.5
5.03	5	10.0
5.38	5	9.0

(continued)

**Table 7** (continued)

(d) Changing in the gel volume as a function of pH						
pH of solvent	Volume of gel (cm <sup>3</sup> )	Maximum change in the gel volume (cm <sup>3</sup> )				
5.58	5	8.0				
6.50	5	7.0				
7.50	5	5.0				
(e) Changing in the gel volume for various metal ions in the hydrogel complex						
Metal-alginate	Concn. of gel (%)	Volume of gel (cm <sup>3</sup> )	Volume of solution (ml)	Changing in the gel volume (cm <sup>3</sup> ) with time/h.		
				24 h	68 h	164 h
Ca-alginate	4	4	50	6.5	7.5	8.5
Cu-alginate	4	4	50	7.5	10.0	10.5
Zn-alginate	4	4	50	6.0	6.5	7.0
Ba-alginate	4	4	50	7.0	8.0	9.0
Ca-alginate	4	4	50	5.5	6.0	6.0

Some experimental runs were performed using metal–alginate hydrogels of sphere nature (2%) in universal buffers of pH = 5.33. The results are summarized in Table 7e and Fig. 7e respectively. It seems that the hydrogel spheres have high tendency for swelling at that cited pH used. It is reported that calcium(II)-alginate hydrogel spheres were suffered different damages depending on the nature of solvent used except of water as solvent (Torres et al. 2011). The pellets were lost a proportion of volume, i.e., it suffered shrinking and lost for about 16% in n-hexane; 19% in methanol; 19.5% in ethanol; 22% in diesel; 76.55% in acetone; 80% in isopropyl alcohol and total loss and destruction in THS and acetonitrile. They found difficulties to explain such observed behavior on the basis of dielectric constants or polarity of those solvents. This means that the nature of solvent will affect the mechanical properties and rheology of polymer gels (Mrozek et al. 2011).

On the other hand, superporous hydrogel classes (smart polymeric gels) were found to behave fast-swelling with pore size much larger than that of typical mesh sizes conventional hydrogels (where the mesh size is below 100 nm (Chen et al. 1999; Chen and Park 2000)). The differences in swelling or kinetics between the conventional and superporous types of hydrogels are attributed to the difference in morphology such as mesh size of the two classes of hydrogels. Moreover, both crosslinked hydrophobic and hydrophilic copolymer gels which swollen in organic solvents undergo spontaneous motion when immersed in water. The transitional and rotational mode of motion depends on the gel shape. Disk-shaped gel exhibits transitional motion, whereas triangular and square shaped exhibit rotational motion (Osada et al. 1955). This motion is produced by chemical free-energy of the polymer network to reach a state of equilibrium

### 3.8 Thermal Decomposition

#### 3.8.1 Analyses of TGA and DTA Thermal Decomposition Thermograms

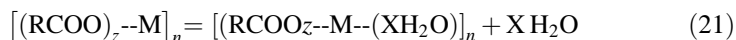
Thermal decomposition of polymer complexes is considered as an evaluation tool to determine the reactivity of polymers. The degradation mechanism includes the dehydration, formation of intermediate fragments, chain scission as well as depolymerization. All these changes together will lead to physical and optical property changes of the molecular weight of the polymer as well as some typical property changes which include reduced ductility and embrittlement, chalking, color changes, cracking and general reduction in most other describable properties.

Generally, the thermal decomposition and kinetic studies of polymers have proceeded in two directions. One of them is the use of the powdered materials, whereas the other one concerns with the single crystals. The essential features of solid-state decomposition are the destruction of the crystal lattice of the reactants, breaking and redistribution of chemical bonds, formation of crystal lattice of the decomposition product, and the diffusion of one component or the other through the

product layer for further propagation of the dissociation reaction (Mousa et al. 1990). Using granule solid samples in the cited technique has the advantages that the macromolecules have a rigid network for the reaction rather than other phases like jellies. Here, a chemical reaction results from molecular collisions (or atoms) which could be described by equations involving times and number of molecules (or atoms) and could be independent of the space coordinate. Thermal decomposition of solids depends to a large extent on the geometry of the crystal lattice, nature, and the direction of chemical bonds (Hassan et al. 1992d).

Dynamic thermogravimetry has been used to study the thermal decomposition of reactions. The analysis includes the change in weight as a function of time or temperature as the sample is heated. Application of thermoanalytical techniques to the cited coordination polymeric metal–alginate complexes presents an example to provide studies of bonding, kinetics, and mechanisms of decomposition. Here, a comparative explanation has been made on application of various thermogravimetric (TGA) and differential thermogravimetric (DTA) thermograms in order to afford the way by which these coordination complexes can be decomposed under the influence of non-isothermal conditions.

Thermal decomposition studies on such MAG complexes involving monovalent silver(I) (Said et al. 1994; Hassan et al. 2014c); divalent—(Said and Hassan 1993; Khairou 2002; El-gahami et al. 2003; Zaafarany et al. 2012); trivalent—(Zaafarany 2010; Tirkistani and Hassan 2012); tetravalent—(Said et al. 1994; Hassan et al. 2014a, b, c) and hexavalent metal–alginate complexes (Said et al. 1994) have been investigated. The experimental results of non-isothermal decomposition of the cited MAG complexes indicate that the degradation of these complexes exhibits three stages of weight loss (TGA curves) associated with a series of thermal decomposition (DTA curves). Typical examples are shown in Fig. 8a–d. The weight loss observed in first stage was corresponding to the dehydration of the coordinated water molecules except in silver– and uranyl–alginate complexes which was corresponding to the release of water of crystallization as illustrated by Eqs. (20) and (21), respectively,



where RCOO represents to alginate monomers which equals  $\text{C}_6\text{H}_7\text{O}_6$  in;  $\text{C}_{12}\text{H}_{14}\text{O}_{11}$ ,  $\text{C}_{18}\text{H}_{21}\text{O}_{17}$ , and  $\text{C}_{24}\text{H}_{28}\text{O}_{22}$  in case of monovalent-, divalent- (and uranyl)-, trivalent-, and tetravalent metal–alginate complexes, respectively, and M corresponds to the chelated metal, Z is the valance of metal, and X is the number of coordination water molecules (or waters of crystallization in case of Ag and U where have zero coordination water molecules) chelated metal ions which X equals zero. The weight loss associated with the second stage was found to be in good agreement with the calculated weight loss which associated with the formation of metal oxalates, carbonates or hydroxide in case of as intermediate fragments, respectively.

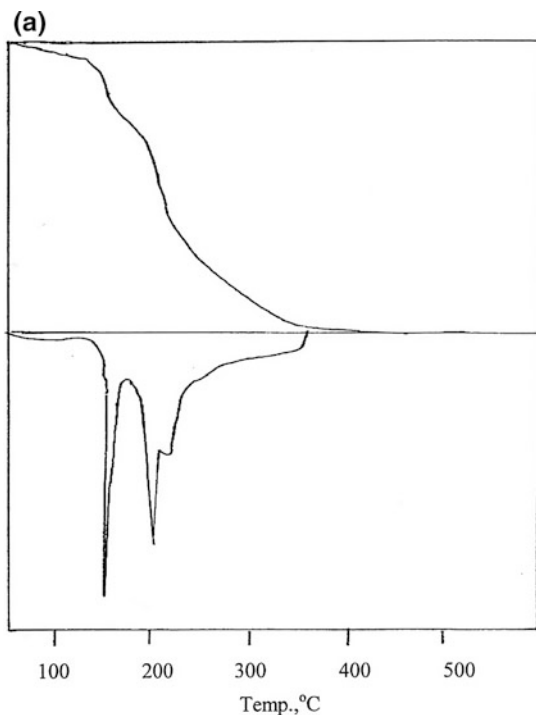
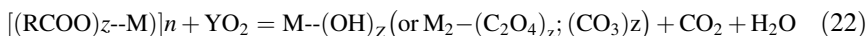
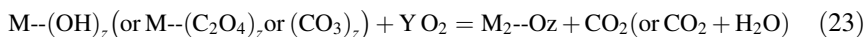


**Fig. 8** **a** TGA and DTA curves of Ag (I) as monovalent metal–alginate gel complex. **b** TGA and DTA curves of divalent metal–alginate gel complexes. **c** TGA and DTA curves of trivalent metal–alginate gel complexes. **d** TGA and DTA curves of tetravalent metal–alginate gel complexes

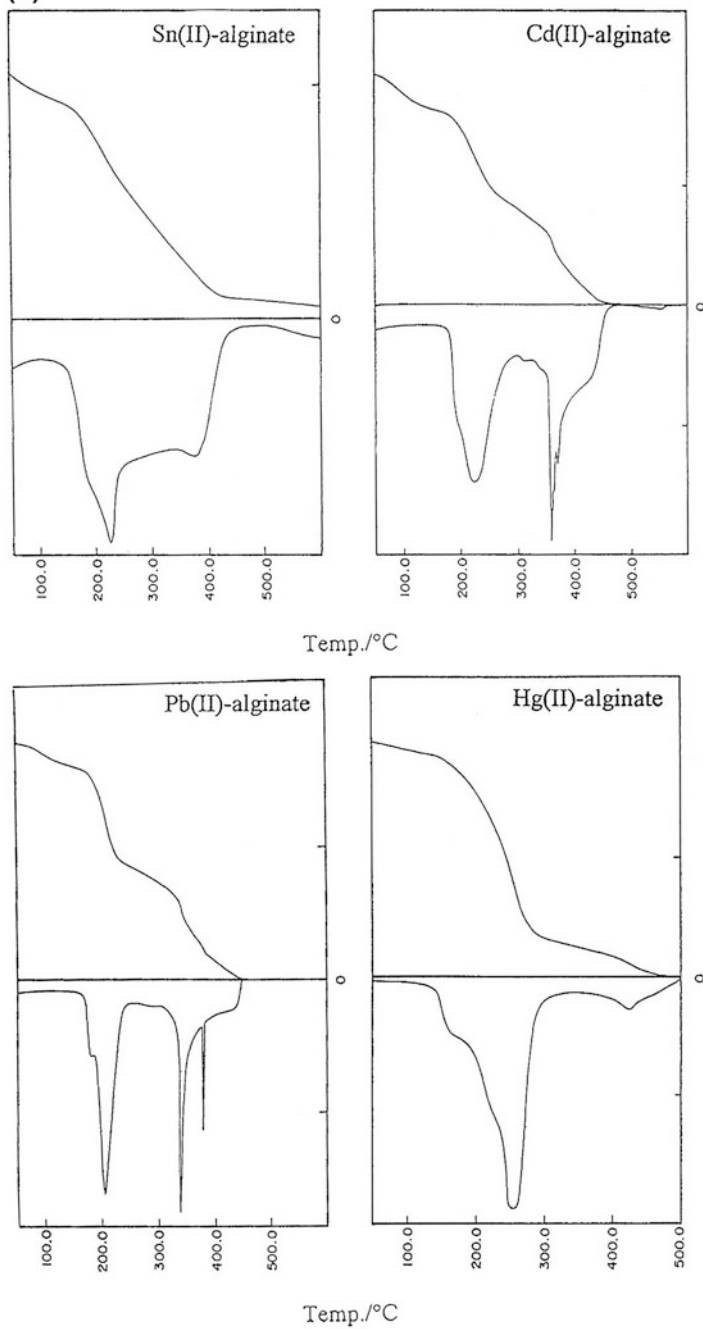


These intermediate fragments were decomposed in the third stage of weight loss to give rise to the corresponding metal oxides as final decomposition products



The total weight loss, the number of water molecules in the dehydration step, and maximal temperature of decomposition are summarized in Table 8. The thermal decomposition is usually endothermic as heat is required to break the chemical bonds of the sample undergoing decomposition. If the decomposition is sufficiently exothermic, then a positive feedback loop is created producing thermal runaway and possibly an explosion occurs.

As is shown in Table 8, the maximal temperature differs from one metal–alginate complex to another depending on the strength of bonding between the chelated metal ion and the carboxylate and hydroxyl functional groups of alginate in the

**(b)****Fig. 8** (continued)



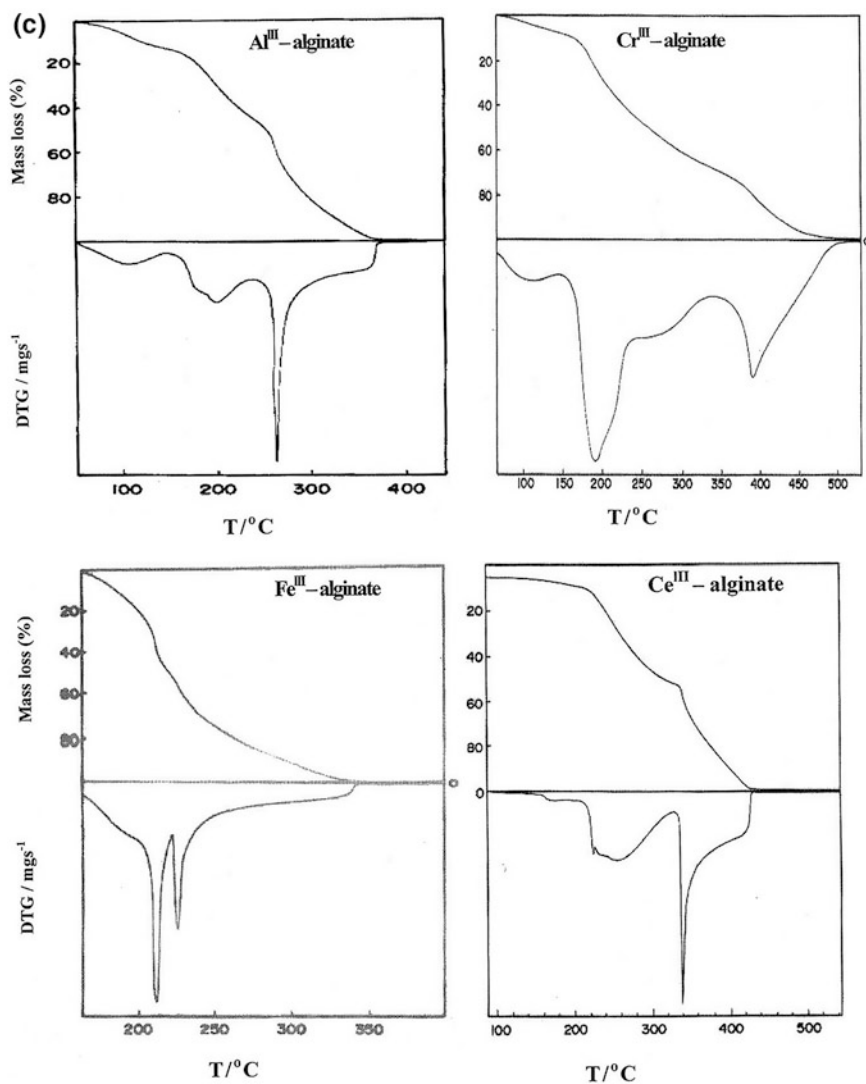


Fig. 8 (continued)

complex. The maximal temperature is the decomposition temperature of a substance at which the substance is chemically decomposed. When the bonding is strong, the complex decomposes at high temperature and vice versa at lower temperatures.

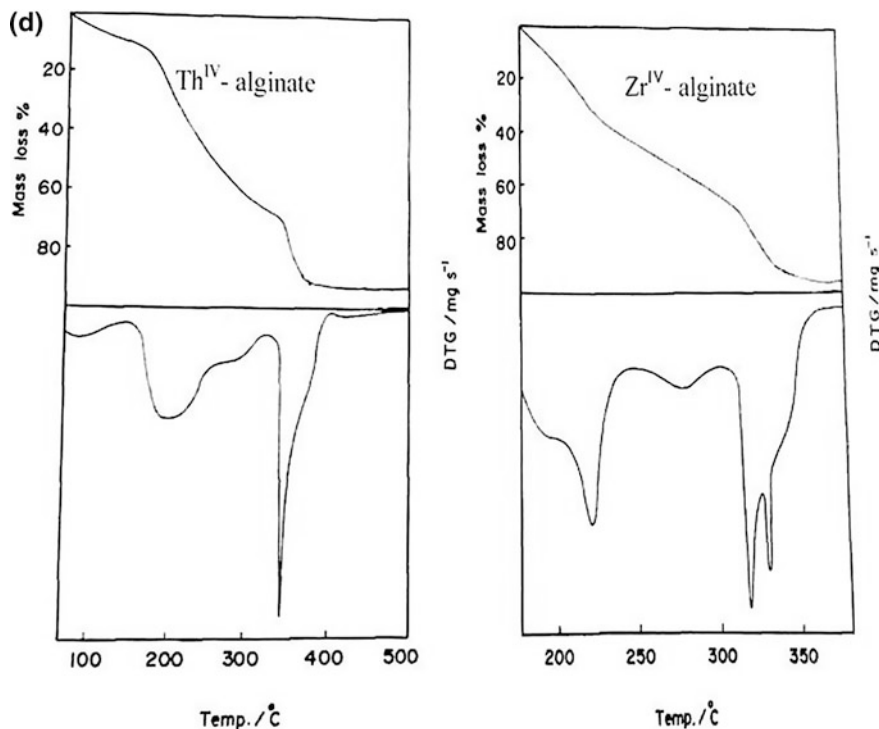


Fig. 8 (continued)

### 3.8.2 Kinetics of Thermal Decomposition

Generally, solid reactions are very complex from the kinetic point of view since suffering several physical and chemical stages of changes (Welch 1955). The literature survey includes extensive information from non-isothermal techniques rather than isothermal ones. The advantages of determining the kinetic parameters by non-isothermal methods were based on the fewer data required, the calculation over an entire temperature which ranges in a continuous manner, the easiness to predict the decomposition mechanism and avoiding the difficulties, and the questionable results being arisen when the sample undergoes reaction by raising the temperature in case of isothermal techniques. The amount of kinetic information on such complex systems as cited in the present chapter may be greatly extended by application of differential mass spectrometric analysis such as TGA, DSC, and DTA which measure the rates of weight changes and the heat liberation.

An important task of the kinetic analysis is to determine the numerical values of the mathematical parameters of the suggested kinetic model based on the experimental data. The use of dynamic mass spectrometry and computers proves to be the most effective techniques in study of non-isothermal decomposition (Sestak 1966;

**Table 8** Kinetic parameters, kinetic model, total weight loss, maximal temperature, nature of intermediate fragments for the first dehydration step of some coordination biopolymeric metal–alginate gel complexes of granule nature

Complex	Wt. loss (%)	Tc	Kinetic model	E (kJ mol <sup>-1</sup> )	$\Delta S^\ddagger$ (J mol <sup>-1</sup> K <sup>-1</sup> )	Z (mol S <sup>-1</sup> )	Intermediate fragments	Formula
Na (I)-Alg	64.3	180						C <sub>6</sub> H <sub>7</sub> O <sub>6</sub> Na
Ag (I)-Alg	66.5	210	R3	86.5	-77.5	$8.2 \times 10^8$	Oxalate	C <sub>6</sub> H <sub>7</sub> O <sub>6</sub> Ag
U (VI)-Alg	55.1	230	-	-	-	-	Oxalate	C <sub>12</sub> H <sub>14</sub> O <sub>11</sub> UO <sub>2</sub>
Mn (II)-Alg	91.8	205	F1	102.5	-39.9	$6.3 \times 10^{10}$	Oxalate	C <sub>12</sub> H <sub>14</sub> O <sub>11</sub> Mn.3H <sub>2</sub> O
Co (II)-Alg	87.5	206	F1	80.4	-86.5	$2.5 \times 10^8$	Oxalate	C <sub>12</sub> H <sub>14</sub> O <sub>11</sub> Co.3H <sub>2</sub> O
Ni (II)-Alg	85.8	214	A3	116.4	-45.9	$3.2 \times 10^{10}$	Oxalate	C <sub>12</sub> H <sub>14</sub> O <sub>11</sub> Ni.3H <sub>2</sub> O
Cu (II)-Alg	88.1	220	A3	199.7	-22.8	$6.3 \times 10^{11}$	Oxalate	C <sub>12</sub> H <sub>14</sub> O <sub>11</sub> Cu.3H <sub>2</sub> O
Zn (II)-Alg	86.2	208	A3	76.9	-110.0	$1.3 \times 10^7$	Oxalate	C <sub>12</sub> H <sub>14</sub> O <sub>11</sub> Zn.3H <sub>2</sub> O
Sn (II)-Alg	67.9	224	A3	96.2	-39.6	$6.0 \times 10^{10}$	Oxalate	C <sub>12</sub> H <sub>14</sub> O <sub>11</sub> Sn.2H <sub>2</sub> O
Pb (II)-Alg	64.5	204	F1	136.7	-1.4	$6.5 \times 10^{12}$	Oxalate	C <sub>12</sub> H <sub>14</sub> O <sub>11</sub> Pb.2H <sub>2</sub> O
Cd (II)-Alg	75.6	225	A3	170.2	-21.8	$5.6 \times 10^{11}$	Oxalate	C <sub>12</sub> H <sub>14</sub> O <sub>11</sub> Cd.2H <sub>2</sub> O
Hg (II)-Alg	79.5	252	F1	288.3	-25.2	$5.3 \times 10^{11}$	Carbonate	C <sub>12</sub> H <sub>14</sub> O <sub>11</sub> Hg.2H <sub>2</sub> O
Ca (II)-Alg	78.6	230	F1	135.4	-10.1	$2.3 \times 10^{12}$	Oxalate	C <sub>12</sub> H <sub>14</sub> O <sub>11</sub> Ca.3H <sub>2</sub> O
Sr (II)-Alg	70.4	226	R3	95.6	-52.7	$1.4 \times 10^9$	Oxalate	C <sub>12</sub> H <sub>14</sub> O <sub>11</sub> Sr.3H <sub>2</sub> O
Ba (II)-Alg	67.1	223	R3	120.2	-18.7	$8.1 \times 10^{11}$	Oxalate	C <sub>12</sub> H <sub>14</sub> O <sub>11</sub> Ba.3H <sub>2</sub> O
Al (III)-Alg	93.9	220	A3	88.0	-80.9	$6.0 \times 10^8$	Hydroxide	C <sub>18</sub> H <sub>21</sub> O <sub>17</sub> Al.4H <sub>2</sub> O
Cr (III)-Alg	97.2	207	F1	102	-59.8	$7.6 \times 10^9$	Carbonate	C <sub>18</sub> H <sub>21</sub> O <sub>17</sub> Cr.4H <sub>2</sub> O
Fe (III)-Alg	97.3	205	R3	214	+9.0	$3.1 \times 10^{12}$	Carbonate	C <sub>18</sub> H <sub>21</sub> O <sub>17</sub> Fe.4H <sub>2</sub> O
La (III)-Alg	74.7	260	A3	292	-	-	Carbonate	C <sub>18</sub> H <sub>21</sub> O <sub>17</sub> La.4H <sub>2</sub> O
Ce(III)-Alg	76.2	203	A3	198	-	-	Carbonate	C <sub>18</sub> H <sub>21</sub> O <sub>17</sub> Ce.4H <sub>2</sub> O
Se (IV)-Alg	90.1	217	A3	100.5	-70.4	$1.6 \times 10^9$	Oxalate	C <sub>24</sub> H <sub>28</sub> O <sub>22</sub> Se.3H <sub>2</sub> O
Zr (IV)-Alg	91.6	221	A3	88.9	-70.3	$2.2 \times 10^{12}$	Carbonate	C <sub>24</sub> H <sub>28</sub> O <sub>22</sub> Zr.4H <sub>2</sub> O
Th (IV)-Alg	82.6	204	A3	116.7	-58.8	$8.1 \times 10^8$	Carbonate	C <sub>24</sub> H <sub>28</sub> O <sub>22</sub> Th.4H <sub>2</sub> O

Sestak and Bergenn 1971). Again, evaluation of the kinetic data from the DTA curves can be obtained through the well-known equation (Freeman and Carrol 1958). Here, some aspects should be taken into consideration. The first criterion is the greater the linearity interval of the tested plots of  $g(\alpha)$ . The second criterion is the value of the standard deviation with the linearity interval should be considered. Again, the value of the pre-exponential factor ( $Z$ ) may be assistance to exclude the less probable models (Skvara and Satava 1970).

The close similarity and the identical similarity of DTA and TGA curves under certain conditions prompted us to use DTA equations for analyzing the TGA curves by correlating the reaction rates with height and the amount reacted or present with area of the curves. However, there are many methods for analysis; the methods of (Satava 1971) together with (Coats and Redfern 1964) were found to be the more accurate and reliable ones in the cited studies. The mechanisms of non-isothermal decompositions may be predicted from the trend and behavior of TGA curves. Sharp et al. (1966) suggested a reduced-time theoretical method in order to distinguish between different methods where the timescale in the kinetic equation is:

$$g(\alpha) = k t \quad (24)$$

where  $g(\alpha)$  is the integrated form of  $F(\alpha)$  which altered so that the data become curves of the form  $\alpha - (t/t_{1/2})$  plots

$$g(\alpha) = A(t/t_{1/2}) \quad (25)$$

Here, the term  $(t_{1/2})$  is the time for 50% decomposition and  $A$  is constant depending on the form of  $g(\alpha)$ . The  $(t_{1/2})$  values corresponding to  $\alpha = 0.5$  were determined from the experimental data  $(t/t_{1/2})$  plots. The data were analyzed by linear regression analysis for various kinetic model functions.

The activation energies ( $E^\ddagger$ ) were calculated from the following relationship

$$\text{Log} \frac{g(\alpha)}{T^2} = \log \frac{ZR}{\Phi E} - \log \frac{2ZRR^2Tp}{\Phi E^2} - \frac{E^\ddagger}{2.303 T} \quad (26)$$

where  $Z$  denotes the frequency factor,  $\Phi$  is the heating rate,  $T$  is the absolute temperature,  $T_c$  is the maximal temperature of decomposition rate ( $T_{\max}$ ), and  $R$  is the gas constant. Plots of  $g(\alpha)/T^2$  against  $1/T$  gave good straight lines from whose slopes of the values of ( $E^\ddagger$ ) were evaluated. The entropies of activation ( $\Delta S^\ddagger$ ) were calculated from the following relationship

$$Z = (k_B T p / h) \exp^{(-\Delta S^\ddagger / R)} \quad (27)$$

where  $k_B$  is Boltzmann's constant and  $h$  is Planck's constant. The results were numerically computed by employing the integral methods for evaluation the kinetic parameters. The models and the kinetic parameters of the initial dehydration stages are summarized in Table 8. The negative values of entropies of activation at the

initial dehydration steps indicate that the reactants are more ordered than that of the activated complexes formed during the dehydration processes and vice versa for complexes of positive values of activation entropies. It is clear that the phase-boundary (*R3*) and the random nucleation (*A3*) models are prevailing as the best fitting for the kinetic models compared with other models for the first dehydration stages. The *A3* function indicated that the nucleation of the thermal decomposition of the compound is a random process followed by a rapid surface growth. As the nuclei grow larger, they may eventually impinge upon one another, so that a decrease of growth occurs on touching. On the other hand, the *R3* function showed that the decomposition is controlled by movement of the interface at constant velocity, and hence, the phase decomposition is the phase-boundary decomposition control.

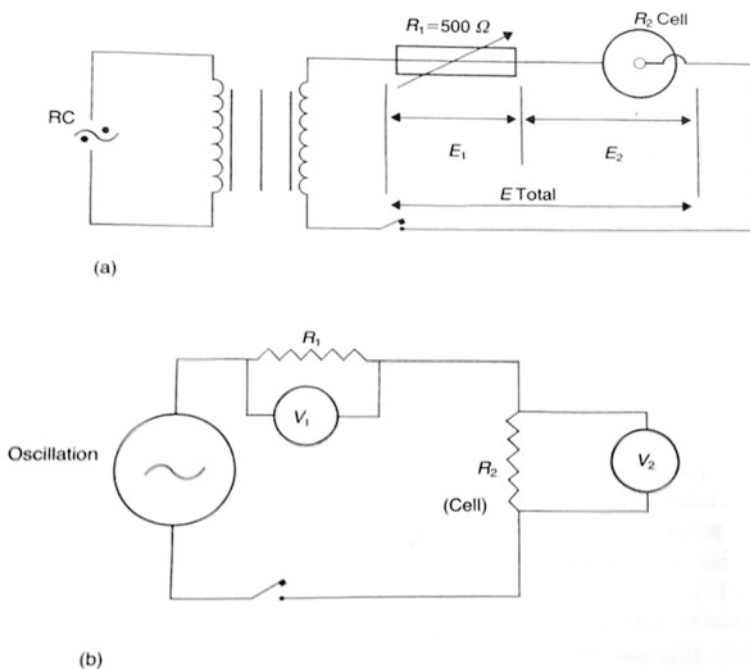
### 3.9 Electrical Properties

Polymeric materials are unique because the structural forms can be synthesized and the way of which the changes can be locally made in the structure by a general way. Conducting polymers offered the promise for achieving a new generation of polymers which have the semiconductors' properties (Kondawar et al. 2011). Again, appreciable knowledge on the structure of such materials can be accomplished through electrical conductivity measurement. Polymers in particularly that exhibit semiconductor behavior has been the subject for many investigations in recent years owing to its wide application in electrical devices such as electron photography and solar cells, memory phenomenon, and film devices (El-Dessouky et al. 1986).

#### 3.9.1 Electrical Conductance of Iontropic Hydrogels Complexes of Jelly Nature

The specific mechanical properties of the cited MAG complexes of jelly characters make the measurements of their electrical conductances by the usual methods difficult. Therefore, a new technique was developed to overcome such a difficulty (El-Cheikh et al. 1974; Awad and El-Cheikh 1980; Hassan et al. 1989b; Hassan 1989). The metal–alginate ionotropic hydrogels applied in this technique were of column shapes and prepared by ascending technique. This technique was preferred than that the descending ones as no pores are formed as well as homogenous structures of gels are obtained. The instrument used for measurement is based on voltage drop across different components of the circuit such as valve voltmeter with higher internal resistance. Therefore, the total resistance of any component of the used circuit could change in the range  $\pm 0.01\%$ . It consists of an outer electrode made of a thin sheet of copper. The inner electrode consists of a thin copper tube.

The tip of the inner electrode was cut so as not to cause any destruction on dipping inside the gel of column shapes. The electrical device is shown below.



The AC source used was an RC generator with a wide range of frequency. By measuring the voltage drops across the fixed pure Ohmic resistance  $R_1$  ( $500 \Omega$ ) which is connected in series with the cell and across the cell itself, the resistance  $R_2$  of the cell can be calculated as follows:

$$\frac{E_1}{E_2} = \frac{R_1}{R_2} + \frac{500}{R_2} \quad (28)$$

Equation (28) is valid under the following conditions, thus

$$E_{\text{total}} = E_1 + E_2 \quad (29)$$

where  $E_{\text{total}}$  is the total voltage drop across the cell and the Ohmic resistance  $R_1$  and  $E_2$  is the voltage drop across the cell  $R_1$  and  $E_2$  is the voltage drop across the cell  $R_2$ , respectively. Thus, the specific resistance of the cell is given by the relationship:

$$\rho = \frac{2L}{2.303 \log a/b} R_2 \quad (30)$$

where  $\rho$  is the specific resistance,  $R_2$  is the measured resistance,  $L$  is the length of the outer electrode (1.5 cm),  $a$  is the radius of the inner electrode (0.25 mm), and  $b$  is the radius of the outer electrode (0.75 mm). The specific conductance of the metal alginate gel is given by

$$k = 1/\rho \quad (31)$$

#### Electrical Conductivity of Divalent and Trivalent Metal–Alginate Ionotropic Hydrogels

The specific conductances of some divalent (El-Cheikh et al. 1974; Hassan et al. 1989a, b), trivalent metal–alginates and alginic acid ionotropic gels (Hassan 1989) of concentrations (3 and 4%) were measured as function of wide frequencies (up to  $10^6$  Hz). Some typical plots of the specific conductance against the logarithms of frequencies gave curves with two definite inflection points, and four regions of frequencies are shown in Fig. 9a, b. This behavior seems to be common for all divalent- and trivalent metal–alginate ionotropic hydrogels, but not for alginic acid. At frequencies up to  $10^3$  Hz, the values of ( $k$ ) were gradually increased with increasing the applied frequency. At the frequencies  $10^3$  and  $10^5$  Hz, no appreciable changes in ( $k$ ) values were observed. At frequencies of  $10^5$ – $10^6$  Hz, a large increment of ( $k$ ) values with a slight increase of the applied frequency has been observed with respect to both divalent and trivalent MAG complexes. At very high frequencies  $>10^6$ , no change of the specific conductance with increasing the applied frequency, i.e., a steady state, is attained. Every metal–alginate complex is characterized by a particular limiting frequency ( $l_r$ ) at which the value of the specific conductance was remarkably increased depending on the strength of chelation between the chelated metal ion and the functional groups of alginate macromolecule. The results are summarized in Table 9.

The slight increase of the specific conductance ( $k$ ) observed before the first inflection point can be attributed to the elimination of the relaxation effects resulting from the cleavage of the weak coordinate bonds between the metal ions and the functional hydroxyl groups of alginate macromolecule. On the other hand, the large increase observed in the values of ( $k$ ) before the second inflection point can be explained by the elimination of the relaxation effects resulting from the cleavage of the strong ionic bonds between the carboxylate groups of alginate substrate and chelated metal ions. The stronger the bonds, the higher is the frequency at which the specific conductivity increased and vice versa for weak bonds. Therefore, ionic radius, polarizability, and mobility of the chelated metal ions as well as the orientation of the solvent molecules and the macromolecular chains toward the chelated metal ion play an important role in such magnitude. The metal ion of smaller ionic radius is the highest mobility and, hence, the larger the value of electrical

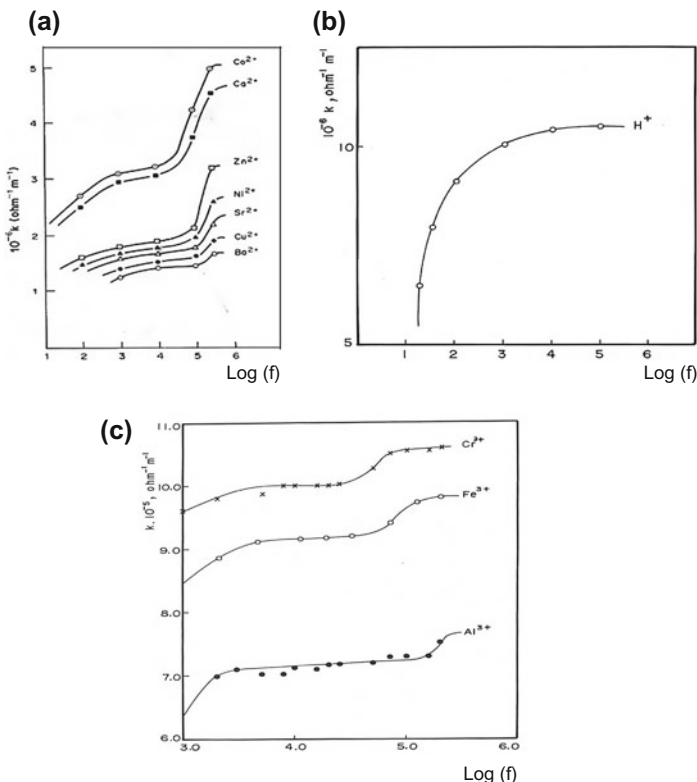


**Fig. 9** Plots of  $\log f$  versus  $k$  for divalent (a); trivalent (b) metal ions of coordination biopolymeric ionotropic hydrogel complexes and alginic acid hydrogel (c)

conductivity, while metal ions of highest polarizability showed the lowest electrical conductivity. The more oriented chelated metal ions possess smaller  $R_c$  values and higher stability. The orientations are decreased in the order  $\text{Ba} > \text{Cu} > \text{Sr} > \text{Ni} > \text{Zn} > \text{Ca} > \text{Co}$ -alginates in good agreement with the orientation order reported by (Thiele and Anderson 1955). This orientation was also found to be in good agreement with the results obtained of decreasing the specific resistance ( $R_c$ ) and increasing the limiting frequency in the same order. Consequently, we expect that the stability of these metal alginate hydrogel complexes is decreased in the same order as reported by (Schweiger 1964). In a similar manner with respect to the trivalent metal–alginate ionotropic hydrogels, the experimental results indicated that stability of these complexes was increased in the order  $\text{Al} < \text{Fe} \leq \text{Cr}$ -alginates in good consistent with decreasing the observed specific conductivities in the same order. This result was found to be agreed with the magnitude of the orientation



**Table 9** Specific conductance of acid, divalent and trivalent metal–alginate ionotropic hydrogels of column shapes at temperature of 30 °C

[Alg <sup>-</sup> ]	Frequency (kHz)	10 <sup>-5</sup> k (Ω <sup>-1</sup> m <sup>-1</sup> )							
		Cd <sup>2+</sup>	Ba <sup>2+</sup>	Cu <sup>2+</sup>	Sr <sup>2+</sup>	Ni <sup>2+</sup>	Zn <sup>2+</sup>	Ca <sup>2+</sup>	Co <sup>2+</sup>
3%	10 <sup>3</sup>	–	16.52	18.63	24.01	24.95	28.55	44.55	47.85
	10 <sup>4</sup>	–	17.21	19.80	25.57	26.60	30.05	47.45	50.05
	10 <sup>6</sup>	–	22.64	27.62	37.43	42.26	53.09	71.63	78.08
4%	10 <sup>3</sup>	12.6	24.15	23.30	32.12	33.43	36.01	60.14	64.66
	10 <sup>4</sup>	–	25.83	24.70	34.21	35.61	37.62	64.05	67.51
	10 <sup>6</sup>	19.9	32.08	33.95	49.91	56.52	65.83	95.03	102.09
		H <sup>+</sup>	Cr <sup>3+</sup>	Fe <sup>3+</sup>	Al <sup>3+</sup>				
3%	10 <sup>3</sup>	<b>120.0</b>	<b>16.5</b>	<b>14.4</b>	<b>9.8</b>				
	10 <sup>4</sup>	132.0	17.4	15.2	10.5				
	10 <sup>5</sup>	134.5	17.9	15.8	11.0				
4%	10 <sup>3</sup>	160.1	18.1	16.8	14.2				
	10 <sup>4</sup>	180.3	18.8	17.7	14.7				
	10 <sup>5</sup>	183.0	19.4	18.3	15.1				

which decreased in the same order. The main difference lies in the magnitude of  $R_c$  and  $l_f$  values.

#### Electrical Conductivity of Alginate Acid Hydrogel

On the other hand, only one inflection point with two regions of frequencies was observed for alginate acid hydrogels as shown in Fig. 9c. At frequencies less than 10<sup>4</sup> Hz, the specific conductance was rapidly increased with increasing the applied frequency. No appreciable change in  $k$  values is observed beyond 10<sup>3</sup> Hz of the applied frequency. The behavior of increment the values of  $k$  with frequency may be explained by elimination of the weak relaxation effect resulting from the cleavage of the very weak hydrogen bonds chelated the carboxylate functional groups of alginate macromolecular chain. The observed large values of ( $k$ ) for alginate acid may reflect its higher electrical properties in comparison with other divalent and trivalent metal–alginate ionotropic hydrogels. This behavior may be explained on the basis of strength of chelated bonds which decreased in the order ionic > covalent > hydrogen bonds, respectively. The frequency of the applied field usually reduces the oscillation time. As the oscillation time becomes smaller than that needed for bond cleavage, the relaxation effects will disappear, and hence, the value of  $k$  will not be affected. This may be noticed at frequencies greater than >10<sup>3</sup> in case of the alginate acid: >10<sup>4</sup>–10<sup>5</sup> Hz for trivalent metal complexes and more than >10<sup>6</sup> Hz for divalent metal alginate complexes, respectively, at which steady-state conditions are attained.

### 3.9.2 Electrical Conductance of Ionotropic Hydrogel Complexes of Granule Nature

Since the electrical properties of polymers depend not only on their chemical decomposition and structural features, but also on the degree of molecular order, it is of interesting to study their conductivities as a function of temperature. In such case, it is more convenient to use metal–alginate gel complexes in granule solid nature owing to the rigid network of their macromolecules. Thus in turn, the dispersion behavior associated with molecular configuration and its ordering will affect the trend of conductivity of these systems. Much attention has been paid to the measurements of electrical conduction of polymers sandwiched between two metal electrodes owing to their wide applications as sensors in electronic devices (Zaafarany et al. 2015).

The electrical conductivities ( $\sigma$ ) of some metal alginate complexes of granule solid shapes for monovalent (Hassan 1991b; Said et al. 1994), divalent (Hassan 1993a; Khairou and Hassan 2002) trivalent (Hassan et al. 1995a, b; Zaafarany et al. 2010; Zaafarany 2014), tetravalent (Said et al. 1994; Zaafarany et al. 2009a, b; Hassan et al. 2013a; Zaafarany et al. 2015), and hexavalent metal–alginate complexes (Hassan et al. 1993a; Said et al. 1994) have been measured using Keithley 610 °C electrometer over temperatures ranging from 290 to 500 °C by applying AC conductance measurements. This was performed using electrodes of circular shape forming M-S-M sandwich, where M symbol represents the two electrodes and S is the specimen. The metal alginates were sandwiched between two standard electrodes (graphite, copper or silver paste) mounted into a specially designed temperature-controlled electric furnace provided with a standard copper–constantan thermocouple. The samples were kept short circuited for 3–5 h to make it ready for measurements. The electrical resistances of the samples were measured, and from these values, the electrical conductivities ( $\sigma$ ) were calculated as follows:

$$\sigma = \frac{1}{R} \cdot \frac{L}{a} \quad (32)$$

where  $R$  is the resistance ( $\Omega$ ),  $a$  is the area of the sample surface ( $\text{cm}^2$ ), and  $L$  is the thickness of the specimen (cm).

Plots of the logarithms of the electrical conductivity ( $\sigma$ ) against  $1/T$  for the studied MAG complexes are shown in Fig. 10a–d. The behavior of conduction seems to be of complexity. In case of silver (I) as monovalent metal ion, some trivalent, tetravalent, and hexavalent metal–alginate complexes, the obtained curves of such plots showed parabola zones at the initial stages of raising the temperature. The electrical conductivity is gradually increased with increasing the temperature at the initial stages until reaches a maximum, then starts to decrease with raising the temperature. On the other hand, for divalent and some trivalent (La (III) and Ce (III)) metal–alginate complexes, the absence of such parabola zones has been revealed.

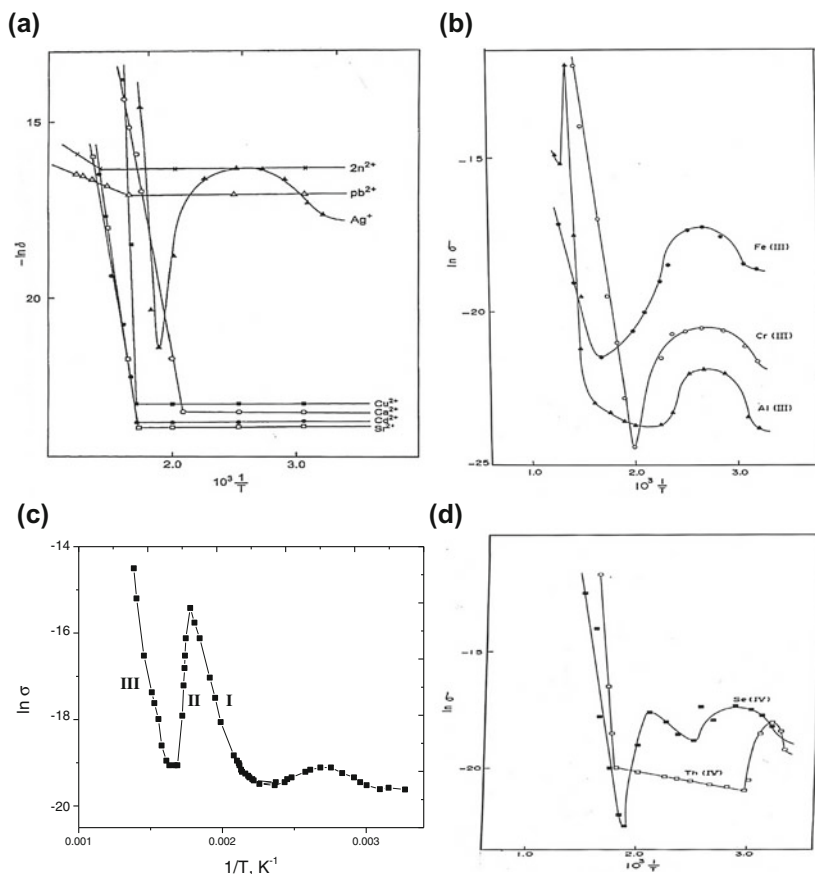


**Fig. 10** Typical plots of  $\ln \sigma$  against  $1/T$  for some coordination biopolymeric metal–alginate ionotropic hydrogel complexes

The number of parabola zones seems to be related to the number of available stable oxidation states resulting from the reduction of the chelated metal ions. For example, for metals which have only two oxidation states, such as Cr (III)–Cr (II) and Fe (III)–Fe (II), only one parabola is observed at the early stages on increasing the applied temperature, whereas two parabola zones were observed for metals which possess more than two oxidation states such as selenium, zirconium, and tin metal ions. Since uranium metal ion exhibits multi-equivalent oxidation states, more than two parabolas could be expected as was experimentally observed. On the other hand, it is surprising that the electrical conductance behavior of monovalent metal ions such as silver (I) which has zero oxidation state on reduction shows one parabola, whereas no parabola has been observed with respect to some trivalent metal ions such as La (III) and Ce (III) in their complexes. At high

temperatures ( $>250$  °C), a continuous increase in the electrical conductance with increasing the temperature was observed for all cited MAG complexes.

The TGA and DTA diagrams of thermal decomposition for these cited metal–alginate complexes indicated that the degradation of these complexes exhibits three stages of weight loss (TG curves) associated with a series of thermal decomposition (DTA curves). The first stage was corresponding to the dehydration of either the waters of crystallization (in case of silver- and uranyl complexes) or the coordinated water molecules for all other complexes. Therefore, if the parabola zones shown at the early stages of  $(\ln \sigma - 1/T)$  plots are attributed to the hydration processes, all complexes should behave the same behavior of existing these parabola zones. The absence of such parabola in complexes of all divalent metal ions as well as in some trivalent metal–alginate complexes such as La (III) and Ce (III) may lead us to suggest different conduction mechanisms for electrical conduction in the studied complexes.

Furthermore, the activation energies for increasing the electrical conductance with increasing the temperature at the first stage  $E_I$  as well as during the formation of the metal oxide at the elevated temperatures  $E_{II}$  were evaluated from the  $\ln \sigma - 1/T$  plots using the following relationship

$$\sigma = A \exp\left(-E^{\neq}/k_B T\right) \quad (33)$$

where  $k_B$  is Boltzmann's constant. The values of activation energies and electrical conductivities were calculated by the least squares method and are summarized in Table 10.

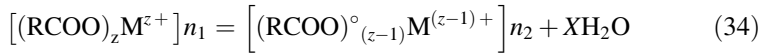
In view of the above aspects and the experimental results, two conduction mechanisms may be suggested. The first mechanism concerns with complexes which has no parabola zones, and their chelated metal ions has only one oxidation state such as divalent metal ions and both La (III) and Ce (III) trivalent metal ions. Here, there are three stages of conduction. The first stage is corresponding to the dehydration of the coordinated water molecules or waters of crystallization to give anhydrous complexes. The second stage represents the degradation of these formed anhydrous complexes to give the intermediate fragments (metal oxalate or metal carbonate), followed by decomposition of these fragments to give rise to metal oxides as final products at the third final stage. This mechanism is quite similar to the behavior of TGA curves observed in case of non-isothermal decomposition (Eqs. 20–23).

The second mechanism is quite different and concerns with complexes which are characterized by the presence of parabola zones at the early stages of conductivity measurements (such as complexes of silver, trivalent and tetravalent metal ions). It has been reported earlier that alginate macromolecule forms free radicals by heating (Kasahara 1954). However, the chelated metals ions have the capability for reduction by accepting electrons from reducing agents such as alginates. Hence, it is reasonable to postulate a conduction mechanism based on free radicals intervention. The increment in the values of  $(\sigma)$  with increasing temperature during the formation

**Table 10** Electrical conductivity and activation energy for some coordination biopolymeric metal–alginate gel complexes of granule nature at 20 °C

Complex	$E_I$ (eV) (initial stage)	$E_{II}$ (eV) (final stage)	$\sigma$ ( $\Omega^{-1} \text{ cm}^{-1}$ )	Coordinated water ( $\text{H}_2\text{O}$ )	References
Ag (I)- alginate	0.21	3.15	$1.80 \times 10^{-8}$	–	Hassan (1991b) Khairou et al. (2002a, b)
$\text{UO}^{+2}$ - alginate	0.37	1.69	$1.70 \times 10^{-12}$	–	Hassan et al. (1993a)
Co (II)- alginate	–	2.24	$2.24 \times 10^{-12}$	$3\text{H}_2\text{O}$	Khairou and Hassan (2002)
Ni (II)- alginate	–	1.92	$1.92 \times 10^{-12}$	$3\text{H}_2\text{O}$	Khairou and Hassan (2002)
Cu (II)- alginate	–	5.21	$1.83 \times 10^{-12}$	$3\text{H}_2\text{O}$	Khairou and Hassan (2002)
Zn (II)- alginate	–	0.22	$1.13 \times 10^{-7}$	$3\text{H}_2\text{O}$	Khairou and Hassan (2002)
Pb (II)- alginate	–	0.18	$1.84 \times 10^{-12}$	$2\text{H}_2\text{O}$	Khairou and Hassan (2002)
Cd (II)- alginate	–	1.75	$2.40 \times 10^{-12}$	$2\text{H}_2\text{O}$	Khairou and Hassan (2002)
Ca (II)- alginate	–	2.12	$1.34 \times 10^{-12}$	$3\text{H}_2\text{O}$	Khairou and Hassan (2002)
Sr (II)- alginate	–	1.54	$1.30 \times 10^{-13}$	$3\text{H}_2\text{O}$	Khairou and Hassan (2002)
As (III)- alginate	0.13	1.64	$2.80 \times 10^{-9}$	$4\text{H}_2\text{O}$	Zaafarany (2014)
Al (III)- alginate	0.48	4.11	$2.37 \times 10^{-10}$	$4\text{H}_2\text{O}$	Hassan et al. (1995b)
Cr (III)- alginate	0.16	2.74	$1.02 \times 10^{-10}$	$4\text{H}_2\text{O}$	Hassan et al. (1995b)
Fe (III)- alginate	0.22	1.41	$2.0 \times 10^{-9}$	$4\text{H}_2\text{O}$	Hassan et al. (1995b)
Ce (III)- alginate	–	1.19	$1.01 \times 10^{-9}$	$4\text{H}_2\text{O}$	Zaafarany (2010)
La (III)- alginate	–	1.47	$1.30 \times 10^{-9}$	$4\text{H}_2\text{O}$	Zaafarany (2010)
Se (IV)- alginate	0.25	1.17	$6.01 \times 10^{-9}$	$.3\text{H}_2\text{O}$	Zaafarany et al. (2009b)
Zr (IV)- alginate	0.36	0.85	$1.16 \times 10^{-9}$	$4\text{H}_2\text{O}$	Hassan et al. (2013a)
Th (IV)- alginate	0.86	1.20	$2.01 \times 10^{-9}$	$4\text{H}_2\text{O}$	Zaafarany et al. (2014c)
Ce (IV)- alginate	0.28	0.84	$1.04 \times 10^{-9}$	$4\text{H}_2\text{O}$	Zaafarany et al. (2015)
Sn (IV)- alginate	0.33	0.98	$1.11 \times 10^3$	$3\text{H}_2\text{O}$	Hassan et al. (2013a)

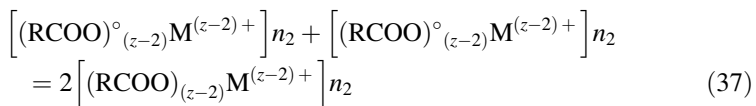
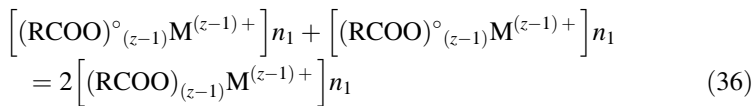
of the first parabola at the early stages can be explained by the transfer of one electron from carboxylate functional group of alginate macromolecule to the chelated metal ion forming free radical intermediate complex involving chelated metal ions of lower oxidation states along with a simultaneous dehydration of coordination water molecules as follows:



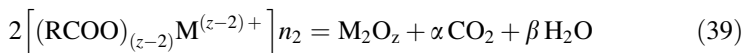
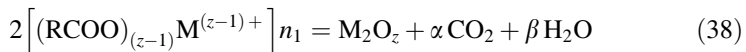
where  $\text{RCOO}^-$  and  $\text{RCOO}^\circ$  refer to the alginate macromolecule and the free radical alginate, M denotes the metal and Z stands to its valency, respectively. On the other hand, the observed second increase in the electrical conductivities with respect to the second parabolas or more can be interpreted in a similar manner by transfer of further electrons from alginate radical substrates to the reduced forms of chelated metal ions as follows:



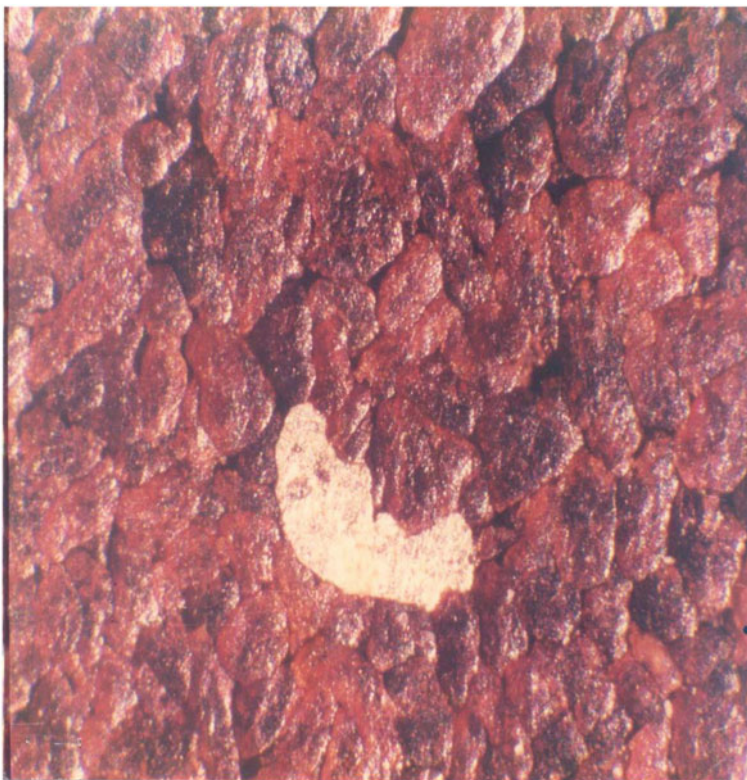
Again, the decrease of the electrical conductivity with increasing temperature through both the first and/or the second parabola zones can be attributed to the dimerization of the free radical substrates as defined by Eqs. (36) and (37), respectively,



The sharp increase in  $\sigma$  values observed at elevated temperatures can be interpreted by the degradation of the intermediate fragments to give rise to the corresponding metal oxides as final products as follows:



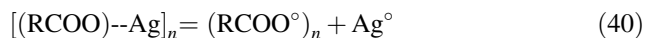
It is surprising that the degradation of the intermediate fragments in case of silver–alginate complex leads to the formation of silver metal ( $\text{Ag}^\circ$ ) which deposited on the surface of measured disk instead of formation of silver oxide as shown in Fig. 11 (Hassan 1991b). This means that the conduction mechanism of silver–alginate complex involves the formation of silver metal and alginate radical



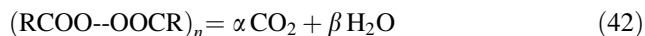
**Deposited Ag(0)**

**Fig. 11** Deposited silver–alginate on the surface of the investigated disk

at the first stage of increasing the electrical conductivity with increasing the temperature at early stage (first parabola). This was followed by the dimerization of the alginate radical to form dimer at the second stage of decreasing the electrical conductivity with raising the temperature as defined by Eqs. (40) and (41), respectively,



Then, a degradation process of the dimer occurs to give carbon dioxide and water in the third stage at the elevated temperatures as follows:



A question of basic interest may be arisen here is whether the chelated metal ions are reduced by successive one-electron transfer mechanism ( $\text{M}^{Z+} \rightarrow \text{M}^{(Z-1)+} \rightarrow \text{M}^{(Z-2+)}$ ) in a sequence or through two-electron changes in a single step ( $\text{M}^{Z+} \rightarrow \text{M}^{(Z-2+)}$ ) for complexes of two parabola zones. The presence of two transition zones may indicate the presence of both mechanisms, but from the thermodynamic points of view, the former one-electron transfer mechanism is the more probable ones. It noticed that uranyl and divalent metal–alginate complexes exhibit poor electrical conductivity in the range of insulators, whereas the complexes of silver (I), trivalent and tetravalent metal ions exhibit electrical conductivities similar to that of semiconductors.

Again, the values of the electrical conductivities obtained using different electrodes were found to be in good agreement with each other confirming the reproducibility on the techniques of measurements applied. This also means that the nature of electrodes has no influence on the behavior of electrical conductivity.

On the other hand, the influence of the applied frequency on the behavior of electrical conduction as a function of temperature for some metal–alginate complexes of granule solid nature has been examined elsewhere (Ahmed et al. 1997; Abd-Wahab et al. 1997). Plots of logarithms of ( $\sigma$ ) against  $1/T$  showed parabola zone followed by small shoulders at the early stages for all studied complexes with respect to all ranges of the applied frequencies (8–900 kHz). In the other hand, at elevated temperatures the electrical conductance was remarkably increased with increasing temperature for all complexes. This behavior seems to be gathered between the behavior of both electrical conduction of ionotropic hydrogel shapes under the influence of applied frequencies and that of granule solid shapes as a function of temperature. This means that the applied frequency is firstly created some vibration effects before elimination of the relaxation frequencies, followed by breaking the chelated bonds in order to form the corresponding metal oxides as final products at elevated temperatures.

Generally, the electrical conduction in polymeric compounds occurs via two conduction mechanisms so-called ionic and electronic conductions. This depends on the charge carriers existing within the network of the macromolecular chains (Sulaneck et al. 1990). The magnitude of the electrical conductivity is considered as indirect evidence of the conduction mechanism. When the value of the activation energy,  $E_a$ , is larger than unity, this means that the cationic mechanism is the more prominent one, whereas the values that are lower than unity correspond to the electronic mechanism. Hence, the observed lower values for ( $E_a$ ) observed for MAG complexes may reflect the prominent of electronic conduction mechanism.

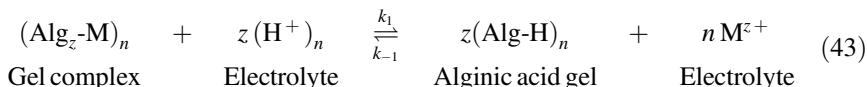


### 3.10 Ion Exchange and Chemical Equilibria

It has been found that the coordination biopolymeric metal–alginate complexes in either hydrogel spheres or granule nature possessed appreciable tendency for ion exchange processes by replacing the chelated metal counter ions with another equivalent amount of metal cations or hydrogen ions with maintaining the electroneutrality in its complexes. Hydrogen ions were selected for such purpose as an exchanging counter ion based on its simplicity for exchange and the stability of formed alginic acid (Hassan et al. 1991) as well as the distinct motilities between the two exchanging metal and hydrogen counter ions (Conway 1952; White et al. 1984).

The exchange of chelated metal counter ions in either hydrogel spheres or granule nature, such as monovalent (Hassan et al. 1995b, 1991b), divalent (Hassan 1991a; Hassan et al. 1992c, 1993a), trivalent (Zaafarany et al. 2010, Hassan et al. 1992c); tetravalent (Hassan et al. 1992c; Zaafarany et al. 2009a, b), and hexavalent metal ion (Hassan et al. 1993a) by hydrogen ions, has been investigated by titrimetric, complexometric, pH-metric, and electrical techniques.

On using hydrogel spheres in the exchange process between the chelated counter ions in coordination biopolymeric metal–alginate complexes and the  $H^+$  ions, the exchange process can be expressed by the following stoichiometric equation



where  $k_1$  and  $k_{ss}$  are the rate constants of exchange for the forward and reverse reactions,  $(\text{Alg}_z\text{-M})_n$  denotes the metal–alginate gel complex,  $(\text{Alg-H})_n$  is the alginic acid gel, M is the metal, and Z stands to its valency. The empirical rate-law expression of exchange is:

$$\begin{aligned}
 \text{Rate} &= -d[(\text{Alg}_z\text{-M})_n]/dt = -1/z d[\text{H}^+]/dt \\
 &= k_1 [(\text{Alg}_z\text{-M})_n][\text{H}^+] - k_{-1} [(\text{Alg-H})_n][\text{M}^{z+}]
 \end{aligned} \quad (44)$$

Under pseudo-first-order conditions where  $[(\text{Alg}_z\text{-M})_n] \gg [\text{H}^+]$ , the observed pseudo-first-order rate constant of exchange ( $k_{ex}$ ) for such reversible reaction can be hold by the following relationship (Glasstone et al. 1941; Frost and Person 1965; Capellos and Bileski 1972)

$$k_{ex} = k_1 [(\text{Alg}_z\text{-M})_n] + k_{-1} \quad (45)$$

The values of  $k_{ex}$  can be determined by various methods such as conductometric technique:

**Table 11** Activation parameters and rate of exchange and the related equilibrium constants for exchanging of chelated metal counter ions by hydrogen ions in some coordination biopolymeric metal–alginate ionotropic hydrogel spheres

Metal alginate	$10^{-2} K^a$	$\Delta S^\ddagger$ (J mol <sup>-1</sup> K <sup>-1</sup> )	$\Delta H^\ddagger$ (kJ mol <sup>-1</sup> )	$\Delta G^\ddagger$ (kJ mol <sup>-1</sup> )	$10^2 R_{ex}$ (s <sup>-1</sup> ) <sup>*</sup>	References
Ag (I)	0.08	–	–	–	3.23	Hassan et al. (1991b,1995b)
Ni (II)	1.59	–145.85	34.18	77.64	0.78	Hassan (1991a)
Cu (II)	0.72	–158.42	31.93	79.14	0.48	Hassan (1991a)
Co (II)	1.93	–138.90	35.99	77.38	0.85	Hassan (1991a)
Al (III)	0.74	–106.37	44.27	75.97	0.52	Hassan et al. (1992c)
Fe (III)	0.46	–97.59	47.87	76.95	0.33	Hassan et al. (1992c)
Se (IV)	0.85	–122.93	42.75	79.20	0.14	Hassan et al. (1992c)
Ce (IV)	0.86	–139.20	39.28	80.76	0.08	Hassan et al. (1992c)

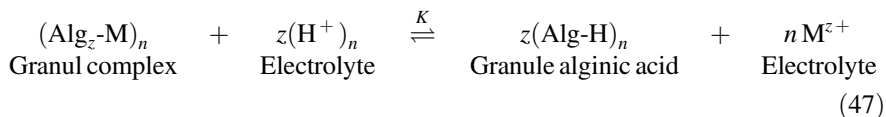
<sup>a</sup>Measured at 25 °C

$$\ln(\lambda_t - \lambda_e) = k_{ex}t + \alpha \quad (46)$$

where  $\lambda_t$  and  $\lambda_e$  are the conductivities at time  $t$  and equilibrium, respectively, and  $\alpha$  is constant. The parameter ( $\alpha$ ) allows the best fit to the data without the restrictions that the extrapolated value is used. The equilibrium constant values,  $K$ , were evaluated from the rate constant values of both the forward and reverse reactions ( $K = k_1/k_{-1}$ ). These values along with the activation parameters for exchange were calculated by the least squares method and are summarized in Table 11.

It is clear that the rate of exchange between the chelated metal ions in their corresponding metal–alginate complexes and H<sup>+</sup> counter ions decreased in the order monovalent > divalent > trivalent > tetravalent metal ions. This fact can be explained by the steric hindrance resulting from the crowdedness of the adjacent large carboxylate groups within the monomers of chelation in particularly in case of high chelated polyvalent metal cations. Thus in turn will obstacle the penetration of the small hydrogen ions in order to replace the leaving large chelated metal cations. This crowdedness increases with increasing the number of sharing carboxylate groups, and hence, it decreases the magnitude of exchange rate in the same order. The observed large negative values of activation entropies may reflect that the metal–alginate complexes are more compactness, ordered, and more stable than the alginic acid gel product. Despite the variety of the chelated metal ions used, the values of activation energies seem to be remained nearly the same indicating that the mechanisms of exchange are quite similar.

On the other hand, when using coordination biopolymeric metal–alginate complexes of granule spheres, the chemical equilibrium of ion exchange between the two exchanging counter ions can be expressed thermodynamically by the following stoichiometric equation:



where  $K$  is the thermodynamic equilibrium constant. Applying the mass action-law for heterogeneous systems and assuming that the activities of the solid phases are always unity (Glasstone and Lewis 1960) and the ratio of the activity coefficients in the solid phase is constant (Haug and Larsen 1962), the following relationship is obtained:

$$K_a = K_c \gamma \text{M}^{z+} / \gamma^z \text{H}^+ \quad (48)$$

where the symbol  $\gamma$  is the activity coefficient of the respective ions,  $K_a$  is the true thermodynamic equilibrium constant which may vary with the composition of the solid phase, and  $K_c$  is quotient equilibrium constant for concentration ( $K_c = [\text{M}^{z+}] / [\text{H}^+]^z$ ). The values of the thermodynamic equilibrium constants were calculated by the method of least squares along with other thermodynamic parameters (evaluated from the well-known equations:  $\Delta G^\circ = -RT \ln K$  and  $\Delta S^\circ = (\Delta H^\circ - \Delta G^\circ) / T$ ) and are summarized in Table 12. The negative values of  $\Delta H^\circ$  indicate that the ion exchange processes are of exothermic nature.

The calculated values of the equilibrium constants ( $K$ ), which deduced kinetically in case of hydrogel spheres, were found to be a little larger than that obtained thermodynamically in case of complexes of granules solid nature. This fact can be explained by the presence of capillaries in the network of the hydrogel spheres but not in case of granule solid complexes. These capillaries may enhance the exchange processes to proceed from the reactants to products and, hence, will lead to affect the true values of the thermodynamic equilibrium constants. Thus in turn may be considered as an indication that the complexes of granule solid nature are more stable than the complexes of hydrogel nature.

### 3.11 Geometrical Configuration of Metal–Alginate Ionotropic Hydrogel Complexes

In contrast to most polysaccharides, alginic acid consists mainly of (M) blocks and a minor percentage of (G) blocks. The acetylation of alginic acid (Schweiger 1962; Hirst et al. 1964; Hirst and Rees 1965) and oxidation of alginic acid by either periodate ion (Dyhurst 1970; Sharon 1975; Gomez et al. 2007) or hypochlorite oxidants (Whistler and Schweiger 1958) are considered as specific methods used

**Table 12** Thermodynamic parameters and the thermodynamic equilibrium constants for exchanging of chelated metal counter ions by hydrogen ions in some coordination biopolymeric metal–alginate complexes of granule nature

Metal alginate	$K_c^a$	$\Delta S^\circ$ (J mol <sup>-1</sup> K <sup>-1</sup> )	$\Delta H^\circ$ (kJ mol <sup>-1</sup> )	$\Delta G^\circ$ (kJ mol <sup>-1</sup> )	References
Ag (I)	4	–	–	–3.26	Hassan et al. (1991b, 1995b)
Ca (II)	34	–28.88	–17.32	–8.73	Hassan et al. (1992c)
Sr (II)	26	–26.24	–15.89	–8.06	Hassan et al. (1992c)
Ba (II)	17	–26.41	14.89	–7.01	Hassan et al. (1992c)
Zn (II)	46	–31.27	–18.81	–9.48	Hassan et al. (1992c)
Cd (II)	27	–27.52	–16.37	–6.68	Hassan et al. (1992c)
Pb (II)	30	–32.32	–18.05	–8.42	Hassan et al. (1992c)
La (III)	72	–15.20	–20.83	–16.28	Zaafarany (2010)
Ce (III)	33	–28.88	–22.63	–14.35	Zaafarany (2010)
Se (IV)	55	–49.66	–24.73	–9.93	Zaafarany et al. (2009b)
Th (IV)	26	+10.92	–4.76	–8.05	Zaafarany et al. (2009a)
UO <sub>2</sub> <sup>2+</sup> (VI)	16	–	–	–6.79	Hassan et al. (1993a)

<sup>a</sup>Measured at 25 °C

for supporting the conformational structure suggested for chelation between metal ions and the functional groups of alginate macromolecule. Schweiger (1962) suggests that chelation of divalent metal ions in particularly Ca (II) ion with alginate polysaccharide occurred through complex formation involving two carboxylate groups from neighboring monomer units (ionic bonds) and two vicinal hydroxyl groups of a unit of probably another chain (coordinate bonds), whereas trivalent and tetravalent metal ions were suggested to form precipitates with alginate and may not make any crosslink with alginate or make chelation but with other mechanism. The coordinate bonding is extended to two vicinal hydroxyl groups of another third unit, i.e., the chelation takes place through intermolecular association mechanism. However, there is no conclusive evidence for sharing the hydroxyl groups in chelation (Cozzi et al. 1968).

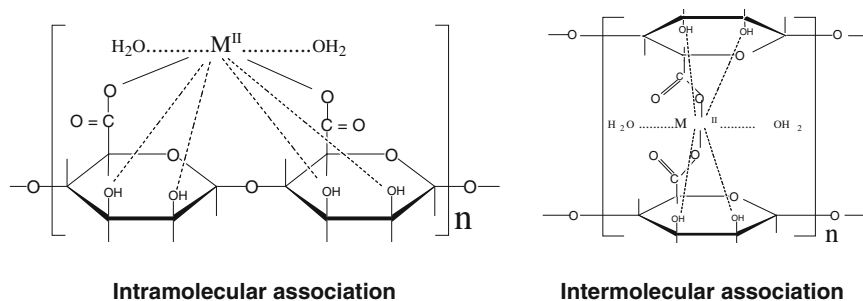
A model for chelation between alginate polysaccharide and divalent Ca (II) was suggested. It involves the formation of sort of bridges between the chelated Ca (II) and the functional groups of alginate macromolecule through partially ionic and partially coordinate bonds, respectively, in an egg-box-like structure (Hirst and Rees 1965; Rees and Samuel 1967; Rees 1972a, b; Grant et al. 1973; Rees and Walesh 1977). This model was used to describe the junction zones of alginate gels which suggests that helical chains are strongly associated by the specific sequestration and binding of calcium ions. Again, it reported that the high selectivity of similar ions such as in case of alkaline earth metals cannot be considered as an indication that the mode of binding is the only specific electrostatic interaction, but

also some chelation may be caused by structural features of G-blocks (Draget 2009). Hence, the formation of dimers by aggregations (Morris et al. 1978) may also contribute to the final structure of the formed gels (Braccini and Perez 2001; Thomas et al. 2006). This means that the ability of different urinate to bind calcium ions demonstrates high stereo-specificity of the interaction between  $\text{Ca}^{2+}$  and the  $\alpha$ -(1-4) linked polymers. This means that the  $\beta$ -(1-4)-linked polysaccharides may display a weak calcium interaction with no particularly favorable binding site.

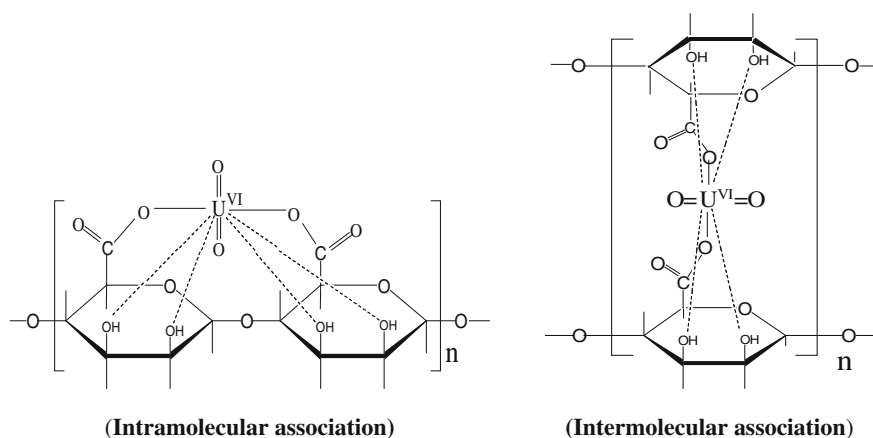
Moreover, investigations into the structure of Ca (II)-alginate junction zones by X-ray scattering revealed that the popular egg-box model may not be the only possible structure for the junction zones where a reversible aggregation of junction zones was found during the dehydration and rehydration processes (Li et al. 2007a, b). This means that MG-block or short G-block is also contributed to the junction zones. It is also suggested that sometimes the Ca (II) chelates with four carboxyl-oxygens from two possible carboxyl groups belonging to different polyglacturonate units and four oxygen atoms belonging to water molecules (in case of dimer formation) on contrary to the classical egg-box model (Plazinski 2011).

In view of the above aspects and our experimental results and interpretation, it may reasonable to suggest geometrical conformational and configurational structures on the nature of chelation between polyvalent metal ions and the functional groups of alginate polysaccharide. Two geometrical structures were suggested depending on the nature and valence of chelated metal ion (Hassan 1993a, b, c). The first one is corresponding to intramolecular association mechanism in which the functional groups involved in chelation belong to the same macromolecular chain of alginate. Here, the plane involving the chelated metal ion is parallel to the plane of alginate macromolecule, i.e., it corresponds to a planar geometry. The second type of chelation corresponds to intermolecular association mechanism in which the plane of the metal ions is perpendicular to the plane of alginate, i.e., the functional groups involved in chelation are related to different macromolecular chains. This geometry corresponds to non-planar type.

Divalent metal ions of octahedral coordination geometry in their complexes (Cotton and Wilkinson 1972) have the choice to chelate via either inter- or intramolecular association mechanisms. The priority of these two mechanisms depends on the stability of geometrical structure of the formed complex. It suggested that divalent metal ions are preferred to chelate by intramolecular association mechanism rather than the intermolecular ones. On the other hand, trivalent and tetravalent metal ions have no choice rather than to chelate by intermolecular association mechanism based on geometrical reasons in order to attain more stability for their complexes (Hassan 2013). Speculated mechanisms for chelation are illustrated in Schemes 1 and 2. The preferability of intermolecular association in case of trivalent and tetravalent complexes may be explained by the tendency of the chelated metal ions to decrease the stretching strain resulting from metal–oxygen bond elongation in case of chelation by intramolecular association (Scheme 3).



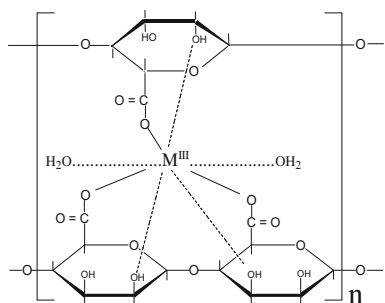
**Scheme 1** Chelation in divalent metal ion complexes



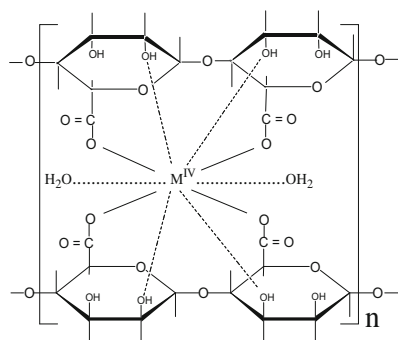
**Scheme 2** Chelation in uranyl ion complexes

Although, both silver (I), uranyl ion,  $\text{UO}_2^{2+}$ , and alginate have the choice to chelate by either inter- or intramolecular association mechanisms. Silver (I) prefers to chelate by non-planar geometry mechanism, while uranyl ion (VI) tends to chelate by intramolecular association mechanism as shown in Schemes 2, 4, and 5. The preferability for chelation by these two conduction mechanisms was explained on the basis of the observed conduction behavior and the magnitudes of the electrical conductivities obtained (Fig. 10a–d; Table 10). It has been found that divalent and uranyl metal–alginate complexes possess poor electrical conductivity, whereas the complexes of trivalent, tetravalent, and silver (I) metal ions possessed large values of the electrical conductivity in the range of semiconductors. Since the charge carriers tend to drift their velocity in case of intermolecular association mechanism which was supported by presence of channels around the planes which containing the chelated metal ions, the electrical conductivity will be expected to be higher in complexes of non-planar types rather than that in complexes of planar geometry. Therefore, the complexes of divalent and uranyl metal ions which are

**Chelation in trivalent metal ion complexes**

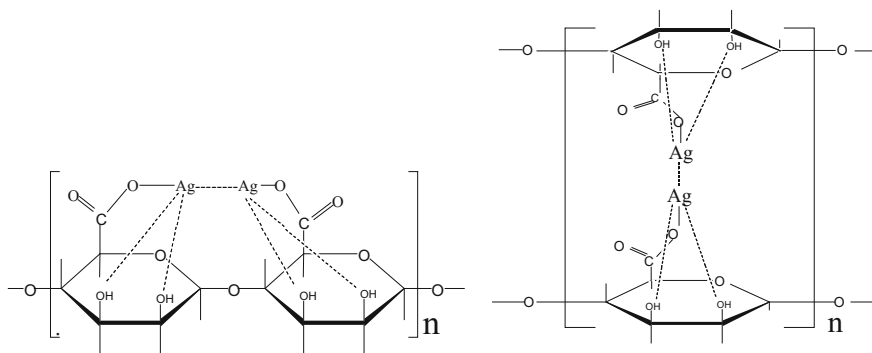


**Chelation in tetravalent metal ion complexes**



**Intermolecular association**

**Scheme 3** Chelation in tri- and tetravalent metal ions

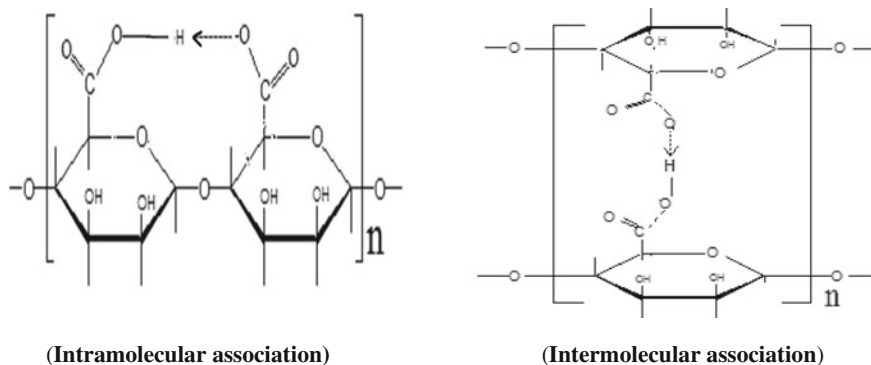


**(Intramolecular association)**

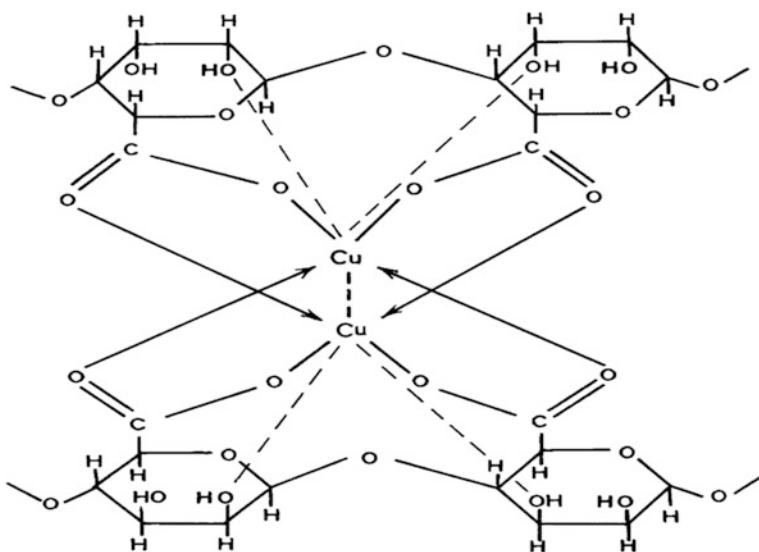
**(Intermolecular association)**

**Scheme 4** Chelation in silver (I) as monovalent metal ion complexes

characterized by poor conductivity may tend to exhibit the intramolecular association mechanism in their chelation, whereas silver (I), trivalent, and tetravalent metal–alginate complexes of the larger electrical conductivity may prefer to chelate the functional groups of alginate macromolecule by non-planar geometrical geometry. The high stability and selectivity of copper (II)–alginate complex may be attributed to its distorted structure as shown in Scheme 6.



**Scheme 5** Chelation in alginic acid complexes



**Scheme 6** Distorted chelation in copper-alginate hydrogel complexes

**Acknowledgements** The authors would like to present their grateful acknowledgement with thanks to Dr. Samia M. Ibrahim, Assistant Professor, Faculty of Science, Assiut University, New-Valley Branch, and Egypt and—Dr. Ishaq A. Zaafarany, Faculty of Applied Sciences, Umm Al-Qura University, Kingdom of Saudi Arabia, for their valuable help during the preparation of this chapter.



## References

- Abdel-Hamid MI, Khairou KS, Hassan RM (2003) Kinetics and mechanism of permanganate oxidation of pectin polysaccharide in acid perchlorate media. *Eur Polym J* 39:381–387
- Abd El-Wahab SM, Ahmed MA, Radwan FA, Hassan RM, El-Refae AM (1997) Relative permittivity and electrical conductivity of some divalent metal alginate complexes. *Mater Lett* 20:183–195
- Ahmed MA, El-Refae AM, Radwan FA, Abd El-Wahab SM, Hassan RM (1997) Temperature and frequency dependence of the electrical properties of metal alginate complexes. *Ind J Chem* 71:395–407
- Anand SC, Kennedy JF, Miraftab M, Rajendran S (2006) *Medial textiles and biomaterials for healthcare*. Woodhead Publishing Ltd, Cambridge
- Andrews GP, Jones DS (2006) Rheological characterization of bioadhesive binary polymeric systems designed as platforms for drug delivery implants. *Biomacromol* 7:899–906
- Aspinal CO (1982) *The polysaccharides*. Academic Press Inc, New York
- Awad A, El-Cheikh F (1980) Electric resistance and anisotropic properties of some metal alginate gels. *J Coll Sci* 80:107–110
- Awad A, El-Cheikh F, Hassan RM (1979) Kinetics of sol-gel transformation especially ionotropic gels. *Rev Roum Chim* 24:563–568
- Awad A, El-Cheikh F, Shaker A (1980a) The diffusion control in sol-gel transformation. *J Ind Chem Soc* 57:728–732
- Awad A, El-Cheikh F, Shaker A (1980b) Kinetic studies of cobalt alginate gels. *Coll Polym Sci* 258:1244–1249
- Bell SE, Conzalez JC, Garcia SI, Sognorella SR, Sala LF (2008) Kinetics and mechanism of oxidation of apple pectin by Cr(VI) in aqueous acid media. *J Phys Org Chem* 21:1–10
- Bellamy LJ (1966) *The infrared spectra of complex molecules*, 2nd edn. p 354
- Bertoni FA, Bellu SE, Conzalez JC, Sala LF (2014) Reduction of hypervalent chromium in acidic media by alginic acid. *Carbohydr Polym* 114:1–11
- Bouklas N, Huang R (2012) Swelling kinetics of polymer gels: comparison of linear and nonlinear theories. *Soft Matter* 8:8194–8200
- Braccini I, Grasso RP, Perez S (1999) Conformational and configurational features of acidic polysaccharides and their interactions with calcium ions: a molecular modeling investigation. *Carbohydr Res* 317:119–130
- Braccini I, Prez S (2001) Molecular basis of induced gelation in alginates and pectins. the egg box model revisited. *Biomacromolecules* 2:1089–1096
- Capellos C, Bielski BHJ (1972) *Kinetic systems*. Wiley, New York
- Chanda SK, Hirst EL, Percival EG, Rees DA (1952) Structure of alginic acid. *J Chem Soc*, 1833–1937
- Chateriji S, Kwon IIK, Park K (2007) Smart polymeric gels redefining the limits of biomedical devices. *Prog Polym Sci* 32:1083–1112
- Chen J, Park H, Park K (1999) Synthesis of superporous hydrogels: hydrogels with fast swelling and superabsorbent properties. *J Biomed Mater Res* 44:53–62
- Chen J, Park K (2000) Synthesis and characterization of superporous hydrogel composites. *J Controlled Release* 65:73–82
- Coats AW, Redfern JP (1964) Kinetic parameters from thermogravimetric data. *Nature* 20:68–69
- Conway BE (1952) *Electrochemical data*. Elsevier, London
- Cotton FA, Wilkinson G (1972) *Advanced inorganic chemistry*, 3rd edn. New York
- Cozzi D, Desideri PG, Lepri L, Ciantell G (1968) Alginic acid. A new thin layer material. Part I. *J Chrom* 35:396–404
- Cozzi D, Desideri PG, Lepri L (1969a) The mechanism of ion exchange with alginic acid. Part II. *J Chrom* 40:130–137
- Cozzi D, Desideri PG, Lepri L, Coas V (1969b) Ion-exchange thin layer chromatographic separation of amino acids on alginic acid. Part III. *J Chrom* 40:138–144

- Cozzi D, Desideri PG, Lepri L, Coas V (1969c) Thin-layer chromatographic and electrophoretic behavior of primary aromatic amines on weak ion exchangers. *J Chrom* 43:463–472
- Creton C, Papon E (2003) Advances in polymer science. *Polymer Therapeutics I*, pp 1–8
- Davidson RL (1980) *Handbook of water soluble gums and resins*. McGraw Hill Book Company, New York
- De Gennes PG (1979) *Scaling concepts in polymer physics*. Cornell University Press, Ithaca
- Dentini M, Rinaldi G, Barbelta A, Risica D, Skjak-Break G (2006) Acid gel formation in (pseudo) alginates with and without G-blocks produced by epimerizing mannuronan with C5 epimerases. *Carbohyd Polym* 63:519–526
- Despang F, Borner A, Dittrich R, Tomandl G, Pompe W, Gelinsky M (2005) Alginate/calcium phosphate scaffolds with oriented tube-like pores. *Materialwissenschaft und Werkstofftechnik* 36:761–767
- Dickel G, Meyer A (1953) Kinetics of ion exchange on resin exchanges. *Z Electrochem* 57:901–908
- Dittrich R, Despang F, Bernhardt A, Mannschatz A, Hanke Th, Tomandl G, Pompe W, Gelinsky M (2006) Mineralized Scaffolds for hard tissue engineering by ionotropic gelation of alginate, In: Vincenzini P (ed) *Advances in science and technology*, vol 49, pp 159–164, Trans Tech Publication Inc
- Delbow J, Fried E, Jia HD (2004) Chemically induced swelling of hydrogels. *J Mech Phys Solids* 52:51–84
- Delbow J, Fried E, Ji H (2005) A numerical strategy for investigating the kinetic response of stimulus-responsive hydrogels. *Comput Methods Appl Mech Eng* 194:4474–4485
- Dragnet KI, Smidsrod O, Skjaak –Barak G (2005) Alginates from algae. In: Steinbuechel A, Rhee SK (eds) *Polysaccharides and polyamides in the food industry, properties, production, and patents*. Wiley, Wein
- Dragnet KI, Moe ST, Skjak-Barak G, Smidsrod O (2006) Food polysaccharides and their applications. In: Slephan A, Philips CO, Williams PA (eds). *CRC Press*, Boca Raton, pp 289–234
- Dragnet KI (2009). In: Phillips GO, Williams PA (eds) *Handbook of hydrocolloids*, 2nd edn. Norwegian University of Science and Technology, Woodhead Publishing Limited, Chapter 29, pp 807–828
- Drummond DW, Hirst EL, Percival E (1962) The structure of alginic acid. Part IV. Partial hydrolysis of the reduced polysaccharides. *J Chem Soc* 1493–1499
- During CJ, Moorman KN (1993) Nonlinear swelling of polymer gel. *J Chem Phys* 98:4275–4293
- Dumitriu S (2002) *Polymeric biomaterials*, 2nd edn. Marcel Dekker Publisher, New York
- Dyhurst D (1970) Periodate oxidation of diols and other functional groups. Analytical and structural application. Pergamon Press, Oxford
- El-Dessouky MM, Hegazy EA, Dessouki AM, El-Sawy NM (1986) Electrical conductivity of anionic graft copolymers obtained by radiation grafting of 4-vinylpyridine onto poly (Vinyl chloride). *Radiat Phys Chem* 27:443–446
- EL-Cheikh F, Issa IM, Awad A (1974) About the electric conductance and relaxation effects in metal alginate gels. *Bull Fac Sci, Assiut, Egypt* 3:199–210
- El-Gahami MA, Khairou KS, Hassan RM (2003) Thermal decomposition of Sn(II), Pb(II), Cd(II) and Hg(II) cross-linked metal-alginate complexes. *Bull Polish Acad Sci* 51:105–113
- Fawzy A (2016) Oxidation of alginate and pectate biopolymers by cerium (IV) in perchloric and sulfuric acid solutions: a comparative kinetic and mechanistic study. *Carbohyd Polym* 138:356–364
- Fisher FG, Dorfel M (1955) The polyuronic acid in brown algae. *Zeitschrift Fur Physiologische Chemie* 302:186–194
- Freeman ES, Carroll B (1958) The Application of thermoanalytical techniques to reaction kinetics. The thermogravimetric evaluation of the kinetics of the decomposition of calcium oxalate monohydrate. *J Phys Chem* 62:394–397
- Frost AA, Pearson RG (1965) *Kinetics and mechanisms*, 2nd edn. Wiley, New York

- Gemeiner P, Kurillova L, Malovikova A, Toth D, Tomasovicova D (1989) Properties of spherical calcium pectate and alginate gels and their use in diffusion chromatography, solids separations and immobilization of enzymes and cells. *Folia Microbiol* 34:214–227
- Glasstone S, Laidler KJ, Eyring H (1941) The theory of rate processes, 2nd edn. Wiley, New York
- Glasstone S, Lewis D (1960) Elements of physical chemistry, 2nd edn. Van Nostrand
- Gomez CG, Rinaudo M, Villar MA (2007) Oxidation of sodium alginate and characterization of the oxidized derivatives. *Carbohydr Polym* 67:296–304
- Grant GT, Morris ER, Rees DA, Smith JC, Thom D (1973) Biological interactions between polysaccharides and divalent cations: the egg-box model. *Fed Eur Biochem Soc (FEBS)* 32:195–198
- Grillet AM, Wyatt NB, Gloe LM (2012). In: Vicente JD (ed) Rheoly, polymer gel rheology and adhesions, 1 st edn. Intech Publisher, Chapter 3, pp 59–80 ([www.intechopen.com](http://www.intechopen.com))
- Hassan RM, El-Shatoury SA, Mousa MA, Hassan A (1988a) Kinetics and mechanism of sol-gel transformation for polyelectrolytes of capillary copper alginate ionotropic membranes. *Eur Polym J* 24:1173–1175
- Hassan RM, Wahdan MH, Hassan A (1988b) Kinetics and mechanism of sol-gel transformation on polyelectrolytes of nickel alginate ionotropic membranes. *Eur Polym J* 24:281–283
- Hassan RM, Summan AM, Hassan MK, El-Shatoury SA (1989a) Kinetics and mechanism of sol-gel transformation on polyelectrolytes of some transition metal ions especially cobalt alginate ionotropic membranes. *Eur Polym J* 25:1209–12012
- Hassan RM (1989) Influence of frequency on electrical properties of acid and trivalent metal alginate ionotropic gels. A correlation between strength of chelation and stability of polyelectrolyte gels. *High Perform Polym* 1:275–284
- Hassan RM, Makhlof MTh, Summan AM, Awad A (1989b) Influence of frequency on specific conductance of polyelectrolyte gels with special correlation between strength of chelation and stability of divalent metal alginate ionotropic gels. *Eur Polym J* 25:993–996
- Hassan RM, Abd-All MA (1991) Ionotropic gels of alginate polyelectrolyte. I. Potentiometric determination of the ionization constant of alginic acid polyelectrolyte in relation to sol-gel transformation mechanism. *Acta Polym* 42:447–450
- Hassan RM (1991a) Alginate polyelectrolyte ionotropic gels. III. Kinetics of exchange of chelated divalent transition metal ions especially cobalt (II) and copper (II) by hydrogen ions in capillary ionotropic metal alginate polymembrane gels. *J Mater Sci* 26:5806–5810
- Hassan RM (1991b) Alginate polyelectrolyte ionotropic Ggels. VII. Physicochemical studies on silver (I) alginate complex with special correlation to the electrical properties and geometrical structure. *Coll Surf* 60:203–212
- Hassan RM, Awad A, Hassan A (1991) Separation of metal alginate ionotropic gels to polymembranes with special evidence on the position of chelation in copper alginate complex. *J Polym Sci* 29:1645
- Hassan RM, El-Shatoury SA, Makhlof MTh (1992a) Alginate polyelectrolyte ionotropic gels. IX. Diffusion control effects on the relaxation time of sol-gel transformation of divalent metal alginate ionotropic gel complexes. *Coll Polym Sci* 12:1237–1242
- Hassan RM, El-Shatoury SA, Makhlof MTh (1992b) Alginate polyelectrolyte ionotropic gels. XII. Chromatographic separation of metal ions in mixture solutions. *High Perform Polym* 4:49–54
- Hassan RM, El-Shatoury SA, Said AA (1992c) Alginate polyelectrolyte ionotropic gels. XVI. Kinetics and chemical equilibria studies for heterogeneous ion exchange of polyvalent metal ions in alginate gel complexes. *High Perform Polym* 4:173–179
- Hassan RM, Farid T, El-Bellihi (1992d) Kinetics of thermal decomposition of gamma—irradiated and unirradiated of mandelhydroxamic acid. *J Radioanal Nucl Chem Lett* 165:277–286
- Hassan RM (1993a) Alginate polyelectrolyte ionotropic gels. XIII. Geometrical aspects for chelation in metal alginate complexes related to their physicochemical properties. *Polym Inter* 31:81–86

- Hassan RM (1993b) Alginate polyelectrolyte ionotropic gels. XIV. Kinetics and mechanism of formation of intermediate complex during the oxidation of alginate polysaccharide by alkaline permanganate with a spectrophotometric evidence of manganite (VI) transient species 31:51–59; 31:1147–1151
- Hassan RM (1993c) Alginate polyelectrolyte ionotropic gels. II. Kinetics and mechanism of exchange of chelated nickel (II) by hydrogen ions in capillary ionotropic nickel alginate polymembrane gel complex. *J Mater Sci* 28:384–388
- Hassan RM, Ikeda Y, Tomiyasu H (1993a) Alginate polyelectrolyte ionotropic gels. XV. Physicochemical properties of uranyl alginate complex especially the chemical equilibrium and electrical conductivity related to the coordination geometry. *J Mater Sci* 28:5143–5147
- Hassan RM, Abd-Alla MA, El-Zohary MF (1993b) Alginate polyelectrolyte ionotropic gels. VI. Novel synthesis of diketoalginate as bipolymer precursor. *J Appl Polym Sci* 47:1649–1652
- Hassan RM, El-Shatoury SA, Azab HA (1995a) Alginate polyelectrolyte ionotropic gels. XVII. Influence of diffusion controls on relaxation time of gelation between alginate polyelectrolyte and polyvalent metal ions. *Asw Sc Tech Bull* 16:62–73
- Hassan RM, El-Shatoury SA, Osman MA, El-Korashy A (1995b) Alginate polyelectrolyte ionotropic gels. VIII. Electrical properties of di- and trivalent metal alginate complexes specially iron (III) and chromium (III) alginate resins. *Bull Fac Sci Assiut Univ Egypt* 24:141–153
- Hassan RM, Dahy A, Ibrahim SM, Zaafrany IA, Fawzy A (2012a) Oxidation of some macromolecules. Kinetics and mechanism of oxidation of methyl cellulose polysaccharide by permanganate ion in acid perchlorate solutions. *Indust Eng Chem Res* 51:5424–5432
- Hassan RM, Tirkistani FA, Zaafrany IA, Fawzy A, Khairy M, Iqbal S (2012b) Polymeric biomaterial hydrogels. I. Behavior of some ionotropic cross-linked metal-alginate hydrogels especially copper-alginate membranes in some organic solvents and buffer solutions. *Advan Biosci Biotechnol* 3:845–854
- Hassan RM (2013). Recent development in carbohydrate research. In: Pandalai SG (ed) *Transworld Research Network*, vol 3, pp 27–63 (A Review Article)
- Hassan RM, Zaafrany IA, Gobouri A (2013a) Temperature-dependence of electrical conductivity of some natural coordination polymeric biomaterials especially cross-linked tetravalent metal-alginate complexes with correlation between the coordination geometry and complex stability. *Advan Biosci Bioelectron* 2:16–24
- Hassan RM, Gobouri A, Zaafrany IA (2013b) Kinetics and mechanism of sol-gel transformation between sodium alginate anionic polyelectrolyte and some alkaline earth metal ions with formation of coordination biopolymer ionotropic polymembrane hydrogels of capillary structures. *Advan Biosci Bioelectron* 2:47–56
- Hassan RM, Zaafrany IA, Gobouri AA, Fawzy A, Takagi HD (2014a) Polymeric biomaterial hydrogels: II. Behavior of some coordination biopolymeric metal-alginate ionotropic hydrogels in aqueous solutions. *J Life Medicine* 1:41–47
- Hassan RM, Zaafrany IA, Gobouri AA (2014b) Base-catalyzed oxidation of some anionic polyelectrolytes: kinetic and mechanistic aspects to electron-transfer process into hexacyanoferrate (III) oxidation of alginate polysaccharide in alkaline media. *J Mol Cat A* 386:28–34
- Hassan RM, Zaafrany IA, Tirkistani FA, Ashgar BH, Takagi HD (2014c) Physicochemical studies on some coordination biopolymeric thorium (IV)-complexes: Kinetics and mechanism of non-isothermal decomposition of cross-linked thorium (IV)-alginate complex with correlation between coordination geometry and thermal stability. *Current Advan Chem Res* 1:7–14
- Hassan RM (2016). In: Taylor JC (ed) *Advances in chemistry research*, vol 30, Chapter 8, Nova Science Publishers, USA
- Haug A (1961) The affinity of some divalent metals on the properties of alginate. *Acta Chem Scand* 15:1794–1799
- Haug A, Larsen B (1962) Quantitative of the uronic acid composition of alginates. *Acta Chem Scand* 16:1908–1918

- Haug A (1964) Composition and properties of alginate. Thesis. Norwegian Institute of Technology, Trondheim, Norway, p 123
- Haug A, Smidsrod O (1965) The effect of divalent metals on the properties of alginate solutions II. Comparison of different metal ions. *Acta Chem Scand* 19:341–351
- Haug A, Larsen B, Smidsrod O (1966a) A study of the constitution of alginic acid by partial acid hydrolysis. *Acta Chem Scand* 20:183–190
- Haug A, Larsen B, Smidsrod O (1966b) A study of the constitution of alginic acid by partial acid hydrolysis. *Proc Int Seaweed Symp* 5:271–277
- Haug A, Smidsrod O (1967) Strontium-calcium selectivity of alginate. *Nature* 215:757–759
- Haug A, Myklestad S, Larsen B, Smidsrod O (1967) Correlation between chemical structure and physical properties of alginates. *Acta Chem Scand* 21:768–778
- Hellferich (1962) Ion exchange. Mc-Graw Hill, New York
- Higdon WT (1958) Studies of ionotropy: a special case of gelation. *J Phys Chem* 62:1277–1281
- Higgins HG, Cm Stewart, Harrington KJ (1961) Infrared spectra of cellulose and related polysaccharides. *J Polm Sci* 51:59–84
- Hirst EL, Percival E, Wold JK (1964) The structure of alginic acid Part IV. Partial hydrolysis of the reduced polysaccharide. *J Chem Soc* 1493–1499
- Hirst E, Rees DA (1965) The structure of alginic acid. Part V. Isolation and unambiguous characterization of some hydrolysis products of the methylated polysaccharides. *J Chem Soc* 1182–1187
- Hong W, Zhao X, Zhou J, Suo Z (2008) A theory of coupled diffusion and large deformation in polymeric gels. *J Mechan Phys Solid* 56:1779–1793
- Kara S, Tamber C, Bermek H, Pekean O (2003) Cation effects on sol-gel and gel-sol phase transitions of *k*-carrageenan—water system. *Inter J Biolog Macromol* 31:177–185
- Kasahara F (1954) Formation of free acid radicals and depolymerization mechanism in heating of sodium alginate. *Kimitsu Kagaku Kogyo* 62:551–594
- Katchalsky A, Michael I (1955) Polyelectrolyte gels in salt solutions. *J Polm Sci* 15:69–86
- Kavanagh GM, Ross-Murphy SB (1998) Rheological characterization of polymer gels. *Prog Polym Sci* 23:533–562
- Kerchova AJ, Elimelech M (2007) Formation of polysaccharide gel layers in the presence of Ca<sup>2+</sup> and K<sup>+</sup> ions. Measurements and mechanisms. *Biomacromol* 8:113–121
- Khairou KS, Hassan RM (2002) Temperature-dependence of electrical conductivity for cross-linked mono- and divalent metal alginate complexes. *High Perform Polym* 14:93–102
- Khairou KS, Al-Gethami WM, Hassan RM (2002a) Kinetics and mechanism of sol-gel transformation between sodium alginate polyelectrolyte and some heavy divalent metal ions with formation of capillary structure polymembrane ionotropic gels. *J Memb Sci* 209:445–456
- Khairou KS, Al-Gethami WM, Hassan RM (2002b) Kinetics and mechanism of sol-gel transformation on polyelectrolyte of divalent metal ions alginate complexes with formation of capillary ionotropic polymembrane. *Bull Polish Acad Sci* 49:299–305
- Khairou KS (2002) Kinetics and mechanism of the non-isothermal decomposition 1. Some divalent cross-linked metal-alginate ionotropic gels. *J Therm Anal Calor* 69:583–588
- Khairou KS, Al-Gethami WM, Hassan RM (2003) Diffusion controls relaxation time and acceleration of velocity of sol-gel transformation for cross-linked metal alginate ionotropic gel complexes. *Bull Polish Acad Sci* 51:207–220
- Kondawar S, Mahore R, Dahegaonkar A, Agrawal S (2011) Electrical conductivity of cadmium oxide nanoparticles embedded polyaniline nanocomposites. *Advanc Appl Sci Res* 2:401–406
- Kristiansen KA, Potthast A, Christensen E (2010) Periodate oxidation of polysaccharides for modification of chemical and physical properties. *Carbohydr Res* 345:1264–1271
- Larson RG (1988) Constitutive equations for polymer melts and solutions, Butterworths, Boston, ISBN 0909901199
- Li L, Fang Y, Vreeker R, Appelqvist I (2007a) Reexamining the egg-box model in calcium-alginate gels with X-ray diffraction. *Biomacromol* 8:464–468
- Leffler L, Grunwald E (1963) Rates and equilibria of organic reactions. Wiley, New York

- Lepri L, Desideri PG, Coas V, Cozzi D (1970) Separation of primary amine on alginic acid and carboxymethyl cellulose columns. *J Chrom* 49:239–248
- Lepri L, Desideri PG, Coas V (1972) Chromatographic and electrophoretic behavior of purines and pyrimidines on layers of weak and strong cation exchangers. *J Chrom* 64:271–284
- Li L, Fang Y, Vreeker R, Appelqvist I (2007b) Reexamining the egg-box model in calcium—alginate gels with X-ray diffraction. *Biomacromolecules* 8:464–468
- Lin YC, Wang SL (2012) Chromium (VI) reactions of polysaccharide biopolymers. *Chem Eng J* 181–182:479–485
- Makhlouf MTh, El-Shatoury SA, Hassan RM (1992) Alginate polyelectrolyte ionotropic gels. XIX. Spectrophotometric detection of short-lived intermediate in alkaline permanganate oxidation of alginate polysaccharide. *High Perform Polym* 4:89–91
- Mimura H, Ohta H, Hoshi H, Akiba K, Wakui Y, Onedera Y (2001) Uptake behavior of americium on alginic acid and alginate polymer gel. *J Radioanal Nucl Chem* 247:33–40
- Moll G (1963) Application of Al-alginate gels with channel-like pores as reversible filter for bacteria and viruses. *Zeitschrift Fur Hygiene* 149:297–314
- Mongar JL, Wassermann A (1952) Influence of ion exchange on optical properties. Shape and elasticity of fully-swollen alginate fibers. *J Chem Soc* 500–510
- Morris ER, Rees DA, Thom D, Boyd J (1978) Chiroptical and stoichiometric evidence of aspecific primary dimerization process in alginate gelation. *Carbohydr Res* 66:145–154
- Mousa MA, Summan AM, Al-Sousi GN (1990) Kinetics of isothermal decomposition of gamma-irradiated and unirradiated cobalt (II) malonate complex. *Thermochim Acta* 165:23–29
- Mrozek RA, Cole PJ, Qim KJ, Shull KR, Lenhart JL (2011) Influence of solvent size on the mechanical properties and rheology of polydimethylsiloxane-based polymeric gels. *Polymer* 52:3422–3430
- Muzzarelli RAA (1973) Natural chelating polymers, 1st edn. Pergamon Press, Oxford
- Navarette RC, Seheult JU, Coffey MD (2001) New biopolymer for drilling, drill-in, completions, spacer, and coil-tubing fluids. Part II SPE inter-symposium on oilfield chemistry, Houston, Texas, USA
- Nishima Y, Langan P, Chanzy H (2002) Crystal structure and hydrogen-bonding system in cellulose 1b from synchrotron, X-ray and neutron fiber diffraction. *J Am Chem Soc* 124:9074–9082
- Obolonkova ES, Belavtseva EM, Braudo EE, Tolstoguzov VB (1974) Formation of structures of anisotropic gels. II. Electron-microscope investigation of anisotropic calcium alginate gels. *Coll Polym Sci* 252:526–529
- Osada Y, Gong JP, Uchida M, Isogi N (1955). *J Appl Phys Jpn* 34: 1–511
- Outokesh M, Mimura H, Niboroi Y, Tanaka K (2006) Equilibrium and kinetics of silver uptake by multinuclear alginate microcapsules comprising an ion exchanger matrix and cyanex organophosphonic acid extractant. *Indus Eng Chem Res* 50:487–493
- Park H, Park K (1996) In: Ottenbrite RM, Huang SJ, Park K (eds) *Hydrogels and biodegradable polymers for bioapplications*, Chapter 1, ACS Symposium Series 627, Library of Congress Cataloging, Washington, USA
- Panteleeva AP, Dolmatova MYU, Dolmatov Yu (1972) Ion exchange interaction of some divalent cations with alginate. *Radiokhimiya* 14:741–743
- Parmer T, Larsen B (1970) Formation of hemiacetals between neighbouring hexauronic acid residues during the periodate oxidation of alginate. *J Polym Sci* 24:813–833
- Pearson FG, Marchesault CY, Liang CY (1960) Infrared spectra of crystalline polysaccharides V. Chitin. *J Polym Sci* 43:101–116
- Plazinski W (2011) Molecular basis of calcium binding by polyguluronate chains. Revising the egg-box model. *J Comput Chem* 32:2988–2995
- Prang P, Muller R, Eljaouhari A, Heckmann K, Kunz W, Weber T, Faber C, Vroemen M, Bogdahn U, Weidner N (2006) The promotion of oriented axonal regrowth in the injured spinal cord by alginate-based anisotropic capillary hydrogels. *Biomaterials* 27:3560–3569
- Pratt AB, Weber FE, Schmoekel HG, Muller R, Hubbel JA (2004) Synthetic extracellular matrices for in situ tissue engineering. *Biotec Bioeng* 86:27–36

- Purz HJ (1972) Morphological investigations of ordered gel formation in polyelectrolytes. *J Polym Sci* 78:405–409
- Putnam AJ, Mooney DJ (1996) Tissue engineering using synthetic extracellular matrices. *Nat Med* 2:824–826
- Rees DA, Samuel JWB (1967) The structure of alginic acid. Part VI. Minor features and structural variation. *J Chem Soc C* 2295–2297
- Rees DA (1972a) Polysaccharide gels. A molecular view. *Chem Indust* 16:630–636
- Rees DA (1972) Shapely Polysaccharide; The eighth colworth medal lecture. *Biochem J* 126:257–273
- Rees DA, Walesh EJ (1977) Secondary and tertiary structure of polysaccharides in solution gels. *Angew Chem Int Ed English* 16:214–224
- Ricka J, Tanaka T (1984) Swelling of ionic gels: quantitative performance of the Donnan theory. *Macromolecules* 17:2916–2921
- Richman D, Thomas H (1956) Self diffusion of sodium ion in cation exchange resin. *J Phys Chem* 60:237–239
- Rigter PI, Peppas NA (1987) Simple equation for description of solute release. II. Fickian and analogous release from swellable devices. *J Contr Rel* 5:37–42
- Ross-Murphy SB (1995) Structure property relationships in food biopolymer gels and-solutions. *J Rheology* 39:1451–1463
- Roy N, Saha N, Kitano T, Saha P (2010a) Development and characterization of novel medicated hydrogel wound dressing. *Soft Materials* 8:130–148
- Roy N, Saha N, Humpolicek P, Saha P (2010b) Permeability and biocompatibility of novel medicated hydrogel wound dressing. *Soft Materials* 8:338–357
- Saarai A, Saha N, Kitano T, Saha P (2009) Natural resource based medicated hydrogel for health care. In: *Proceedings frontiers in polymer science, international symposium celebrating the 50th anniversary of the Journal Polymer, Mainz, Germany*
- Saha N, Roy N, Saha P (2008) Allicin containing novel anti-microbial hydrogel. In: *Proceedings fifth international conference on polymer modification, degradation and stabilization, Liege, Belgium, September*
- Saha N, Sarrai A, Roy N, Kilano T, Shasaho P (2011) Polymeric biomaterials based hydrogels for biomedical application. *J Biomed Nanotech* 85:85–90
- Said AA, Hassan RM (1993) Thermal decomposition of some divalent metal alginate gel compounds. *J Polym Degrad Stabil* 39:393–397
- Said AA, Abd El-Wahab MM, Hassan RM (1994) Thermal and electrical studies on some metal alginate compounds. *Therm Chem Acta* 233:13–24
- Sakamoto N, Kano N, Imaizumi H (2008) Bisorption of uranium and rare earth elements using biomass of algae. *Biorg Chem Appl* 2008:1–8. <https://doi.org/10.1155/2008/706240>
- Sapozhnikov YuA, Kalmykov SN, Efimov IP, Remez VP (1996) The sorption of Sr-90 from waters by alginates. *Appl Radiat Isot* 47:887–888
- Satava V (1971) Mechanism and kinetics from non-isothermal TG traces. *Thermochem Acta* 2:423–428
- Schweiger RG (1962) Acetylation of alginic acid. I. Preparation and viscosities of align acetate. *J Org Chem* 27:1786–1789; II. Reaction of align acetates with calcium and other divalent ions. *J Org Chem* 27:1786–1791
- Schweiger RG (1964) Complexing of alginic acid with metal ions. *Kolloid Z Z Polym* 196:47–53
- Segeren AJM, Boskamp JV, Tempel MVD (1974) Rheological and swelling properties of alginate gels. *Fard Dissc Chem* 57:255–262
- Sestak JL, Bergenn G (1971) Study of the kinetics of the mechanism of solid-state reactions at increasing temperatures. *Thermochimi Acta* 3:42–47
- Sestak JK (1966) Errors of kinetic data obtained from thermogravimetric curves at increasing temperature. *Talanta* 13:567–572
- Sharp JP, Brindely GW, Achar BNN (1966) Numerical data for some commonly used solid state reaction equations. *Am Chem Soc* 49:379–382

- Sharma VP, Mahto V (2006) Studies of less-expensive environmentally safe polymers for development of water based drilling fluids. SPE Asia Pacific oil and gas conference and exhibition, Adelaide, Australia
- Sharon N (1975) Complex carbohydrates. Their chemistry, biosynthesis and functions. Addison-Wesley Publishing Company, Reading Mass
- Shi D (2004) Biomaterials and tissues engineering. Springer, Berlin
- Skvara F, Satava V (1970) Kinetic data from DTA measurements. *J Therm Anal* 2:325–335
- Smidsrod O, Haug A, Larsen B (1963) Degradation of alginic acid in the presence of reducing compounds. *Acta Chem Scand* 17:2628–2637
- Smidsrod O, Haug A, Larsen B (1965) Kinetic studies of the degradation of alginic acid by hydrogen peroxide in the presence of iron salts. *Acta Chem Scand* 19:143–152
- Smidsrod O, Haug A (1968) Dependence upon uronic acid composition of some ion exchange properties of alginates. *Acta Chem Scand* 22:1989–1997
- Smidsrod O, Haug A (1972) Dependence upon the sol-gel state of the ion exchange properties of alginates. *Acta Chem Scand* 26:2063–2074
- Smidsrod O (1973) Some physical properties of alginates in solution and in the gel state. Thesis. Norwegian Institute of Technology, Trondheim
- Smidsrod O (1974) Molecular basis for some physical properties of alginates in the gel state. *Farad Disc Chem Soc* 57:263–274
- Solmon MJ, Speicer PT (2010) Microstructural regimes of colloidal rod suspensions, Gels and glasses. *Soft Matter* 6:1391–1400
- Sulaneck WR, Clark DT, Samuelson EJ (1990) Science and application of conducting polymers. IOP Publishing Ltd, UK
- Sutherland IW (1991) In: Byron D (ed) Biomaterials: novel materials from biological sources. Stockton Press, New York, pp 39–311
- Takahashi E, Emura E (1960) Ion exchange of alginic acid. II. Selective ion exchange properties of alginate for metallic ions. *Kogyo Kawagaku Zasshi JPH* 63:1025–1030
- Takahashi E, Ishiwatari Y, Shirai H (1963) Selective ion exchange properties of alginate in mixed solutions of metal ions. *Kogyo Kawagaku Zasshi Jpn* 63(66):1458–1465
- Tanaka T, Filmore DJ (1999) Kinetics of swelling gels. *J Chem Phys* 76:1214–1218
- Tentenboom M, Greger HP (1956) Self diffusion of cations, non-exchange anions and solvent in a cation exchange resin system. *J Phys Chem* 21:150–162
- Thiele H, Anderson G (1955a) Ionotropic gels of polyuronic gels. Part III. Degree of order. *Koll Z* 76:140–145
- Thiele H, Anderson G (1955) Ionotropic gels. Part II. Orders. *Colloid and Polymer Science* 142:5–24; Part III. Order of Ionotropic Gels. *Coll Polym Sci* 142:5–24
- Thiele H, Anderson G (1953) Identical structure and pattern of deca classified collagen and ionotropic gel. *Naturwissenschaften* 40:366–366
- Thiele H, Longmaack (1957a) Structure formation by ion diffuse, simplex ionotropism. *Z Naturforsch* 12B:14–23
- Thiele H, Longmaack (1957b) Structure formation by ion diffuse, Simplex ionotropism. *Z Naturforsch* 12:14B–23B
- Thiele H, Hallich K (1957) Capillary structure in ionotropic gels. *Koll Z* 151:1–12
- Thiele H, Hallich K (1959) Application of capillary structure of ionotropic alginate gels as filters. *Coll Polym Sci* 163:115–122
- Thiele VH, Plohnke K, Brandt E, Moll G (1962) Order of polyelectrolyte for ion diffusion. *Kolloid Z Poly* 182:24–34
- Thiele H, Awad A (1966) Ions and their biological effects. Investigation on ionotropic gels. *Biotechnology* 3:63–75
- Thiele H (1967) Histalyse and Histogenese. Gewebe und ionotrope gele. Prinzip einer Strturbildung, Frankfurt
- Thiele H, Awad A (1969) Nucleation and oriented crystallization apatite in ionotropic gels. *J Biomed Mater Res* 3:431–432



- Thomas DP, Randal TC, Ralph M (2006) Molecular models of alginic acid interaction with calcium ions and calcite surface. *Geochim et Cosmochim Acta* 70:3508–3532
- Tirkistani FAA, Hassan RM (2012) Kinetics and mechanisms of non-isothermal decomposition of some cross-linked metal-alginate complexes especially trivalent-metal-alginate complexes. *Orient J Chem* 28:913–920
- Tiwari A, Dewangan T, Bajpai AK (2008) Removal of toxic As(V) ions onto alginate and carboxymethyl cellulose beads. *J Chin Chem Soc* 55:952–961
- Tolstoguzov VB (1975) Formation and structure of anisotropic gels. 1. Anisotropic gels of alaminated structure. *Coll Polym Sci* 253:109–116
- Torres LG, de Sanchez LV, Beltran NA, Jimenez BE (1998) Production and characterization of Ca-alginate biocatalyst for removal of phenol and chlorophenol from water. *Process Biochem* 33:625–634
- Torres LG, Velasquez A, Mrito-Arias MA (2011) Ca-alginate spheres behavior in presence of some solvents and water-solvent mixtures. *Advanc Biosci Biotech* 2:8–12
- Tsi H, Pence TJ, Kirkinis E (2004) Swelling induced finite strain flexure in a rectangular block of an isotropic elastic material. *J Elasticity* 75:69–89
- Tunic MH (2010) Small-strain dynamic rheology of food protein networks. *J Agric Food Chem* 59:1481–1486
- Yonese M, Baba K, Kishimoto H (1988) Stress relaxation of alginate gels crosslinked by various divalent metal ions. *Bull Chem Soc Jpn* 61:1857–1862
- Yashihito O, Gong JP (1998) Soft and wet materials polymer gels. *Adv Mater* 10:827–837
- Welch AJE (1955) In: Carner WE (ed) *Chemistry of the solid state*. Butterworth, London, p 318
- Whistler RL, Kirby KW (1952) Polysaccharides of marine algae. Compounds and behavior of polysaccharides. *Z Physiol Chem* 314:46–51
- Whistler RL, Schweiger R (1958) Oxidation of alginic acid with hypochlorite at different hydrogen ion concentrations. *J Am Chem Soc* 80:57015704
- White RE, Bockris JOM, Conway BE, Yeager E (1984) *Comprehensive treatise of electrochemistry*. Plenum Press, New York
- Woelki S, Kohler HH (2003) Orientation of chain molecules in ionotropic gels. A Brownian dynamic model. *Chem Phys* 293:323–340
- Wu Y, Mimura H, Niibori (2009) Selective uptake of plutonium (IV) on calcium alginate gel polymer. *TBP microcapsule J Radioanal Nucl Chem* 281:513–517
- Wu Y, Outokesh M, Mimura H, Niibori Y (2008) Selective uptake properties of metal ions by hybrid microcapsules enclosed with TBP. *Prog Nucl Energy* 50:487–493
- Zaafarany IA, Khairou KS, Hassan RM (2009a) Physicochemical studies on cross-linked thorium (IV)-alginate complex especially the electrical conductivity and chemical equilibrium related to the coordination geometry. *Arab Saudi J* 2:1–10
- Zaafarany IA, Khairou KS, Hassan RM, Ikeda Y (2009b) Physicochemical studies on some natural polymeric complexes of quadrivalent metal cations. Electrical conductivity and chemical equilibrium of cross-linked selenium (IV)-alginate complex with correlation between the complex stability and geometrical structure. *Saudi Chem Soc* 13:49–80
- Zaafarany IA (2010) Non-isothermal decomposition of Al, Cr and Fe cross-linked trivalent metal-alginate complexes. *JKAU Sci* 22:193–202. <https://doi.org/10.4197/sci.22-1.13>
- Zaafarany IA, Khairou KS, Hassan RM (2010) Physicochemical studies on some cross-linked trivalent metal-alginate complexes especially the electrical conductivity and chemical equilibrium related to the coordination geometry. *High Perform Polym* 22:69–81
- Zaafarany IA (2010b) Non-isothermal decomposition of Al, Cr and Fe cross-linked trivalent metal-alginate complexes. *Bulletin JKAU* 22:193–201
- Zaafarany IA, Khairou KS, Tirkistani FA, Iqbal S, Khairy M, Hassan RM (2012) Kinetics and mechanisms of non-isothermal decomposition of Ca(II)-, Sr(II)- and Ba(II)-cross-linked divalent metal-alginate complexes. *Inter J Chem* 4:7–14

- Zaafarany IA (2013) Kinetics and mechanism of sol-gel transformation between some trivalent- and tetravalent- metal ions and sodium alginate anionic polyelectrolyte with formation of coordination biopolymeric structure polymembrane hydrogels of capillary structures. Exner-correlation for some gelation processes. *J Advanc Chem* 3:133–142
- Zaafarany IA (2014) Temperature dependence of electrical conductivity for some natural coordination polymeric biomaterials especially cross-linked trivalent metal—alginate complexes with correlation between the coordination geometry and complex stability. *Advanc Chem Eng* 4:1–7
- Zaafarany IA, Altass H, Alfahemi J, Khairou KS, Hassan RM (2015) Electrical conductivity and chemical equilibria of coordination biopolymeric cerium (IV) alginate complex with correlation between the structure and complex stability. *Int J Chem* 7:57–67
- Zhang I, Shung KK, Edwards DA (1996) Hydrogels with enhanced mass transfer for transdermal drug delivery. *J Pharm Sci* 85:1312–1313

# Chapter 11

## Smart Polymer Gels



Waham Ashaier Laftah

### 1 Introduction

Polymer gels (PGs) are defined as viscoelastic cross-linked hydrophilic three-dimensional polymeric networks with dissociated ionic functional groups. PGs can absorb large amount of water or other biological fluids in short time and release them under certain conditions (Thakur and Thakur 2014a, b, 2015). Smart polymer gels (SPGs) are one class of polymer gels with a special characteristic which is the response to the environment change such as temperature, electric, light, sound field, magnetic fields, and pH. The response to the environment change gives this class of materials wide range of application in many fields such as medical and water treatment. SPGs are polymerized via normal polymerization methods such as solution, suspension, and emulsion polymerization. Cross-linking process of SPGs occurs via chemical (using cross-linking agent) or physical method (entanglements or crystallites).

### 2 Classification of Smart Polymer Gels

SPGs are classified depending on their response to surrounding environment as illustrated in Fig. 1.

---

W. A. Laftah (✉)

Department of Polymer Engineering, Faculty of Chemical Engineering,  
Universiti Teknologi Malaysia (UTM), 81310 Skudai, Johor, Malaysia  
e-mail: waham1980@yahoo.com.my

W. A. Laftah

College of Oil and Gas Engineering, Basrah University for Oil and Gas,  
61004 Basrah, Iraq

© Springer Nature Singapore Pte Ltd. 2018

V. K. Thakur and M. K. Thakur (eds.), *Polymer Gels*, Gels Horizons: From Science to Smart Materials, [https://doi.org/10.1007/978-981-10-6083-0\\_11](https://doi.org/10.1007/978-981-10-6083-0_11)

355

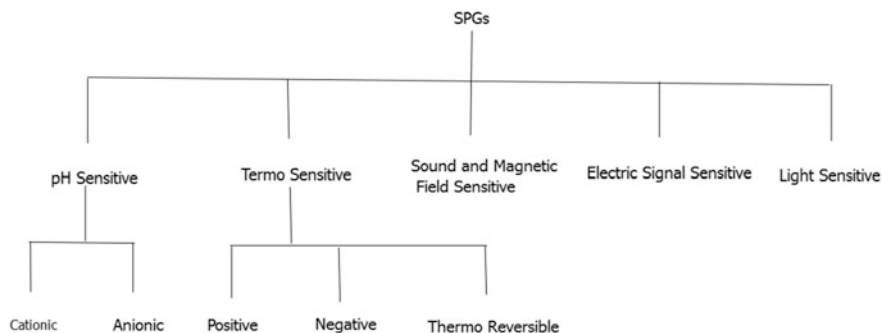


**Fig. 1** Classification of SPGs according to their response to the external medium

## 2.1 Thermosensitive Gels

This class of SPGs is defined by its ability to swell and shrink when the temperature of surrounding fluid is change (Hongyan He 2006). This kind of PGs can be divided into three classes: negative temperature sensitive, positive temperature sensitive, and thermoreversible.

### 2.1.1 Negative Temperature Sensitive

This class of SPGs has critical parameter called low critical solution temperature (LCST), which means that SPGs will shrink when the temperature increases above LCST and showing swelling behavior at temperature less LCST. LCST of this class of SPGs can be controlled using different ways such as changing the molar ratio of ionic copolymer or by changing the solvent composition. In general, LCST of polymer of more hydrophobic constituent shifts to low degree which means changing the percentage ratio of hydrophobic to hydrophilic contents of SPGs leads to change LCST (Schild 1992; Hongyan He 2006). Figure 2 shows the structures of some of these polymers.

From the structure of negative thermosensitive SPGs, it can be seen that the polymers have two parts; the first is hydrophilic part  $-\text{CONH}-$ , and the second is hydrophobic part  $-\text{R}-$  (Zhang et al. 2003). At temperatures lower than LCST water or fluid interact with the hydrophilic part by forming hydrogen bonds which leads to dissolution and swelling behavior. At temperature higher than LCST hydrophobic interaction among hydrophobic part will be stronger and hydrogen bonds will become weaker; therefore, network shrinking occurs due to inter-polymer chain association (Qiu and Park 2001), and the absorbed fluid will go out of the structure (de-swelling process).

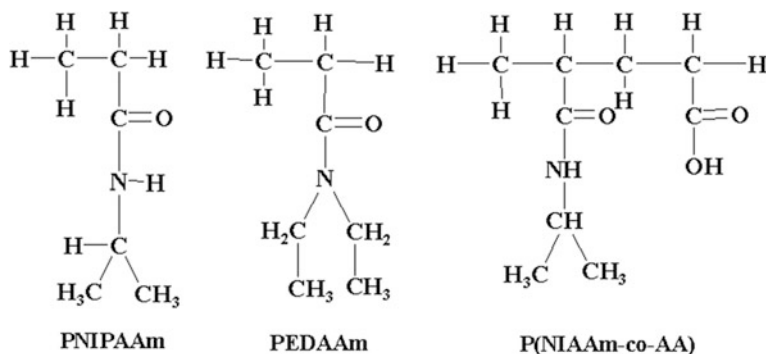


Fig. 2 Negatively pH-sensitive polymer gels

### 2.1.2 Positive Temperature Sensitive

Positive temperature SPGs are known with their upper critical solution temperature (UCST) (Peppas et al. 2000). When the temperature is below UCST network structure contract and release absorbed fluids (dehydration). Network relaxation occurs at temperature higher than UCST (swelling). This type of PGs is retrogressive with negatively temperature sensitive gels. This class of SPGs is shrinking at low temperature due to the formation of complex structure via hydrogen bonds. Network structure dissociates at high temperature due to breaking of hydrogen bonds and SPGs swelling to maximum possible extent rapidly above the UCST. There are a wide range of polymers and copolymers that are positive temperature such as poly(AAm-co-BMA), and poly(AA-co-AAm-co-BMA) (Hongyan He 2006).

### 2.1.3 Thermoreversible

This class SPGs has similar structure and contents of negative and positive temperature SPGs with deference in kind of bonds. Polymer chains in this class are not covalently cross-linked, and SPG undergoes sol-gel phase transitions instead of swelling-shrinking transition (Hongyan He 2006). Sol-gel phase transformation depends on glucose concentration in the surrounding medium. Sol-gel reversible SPGs require glucose response cross-linking. The most commonly used thermoreversible gels are pluronic and tetronic compounds as illustrated in Fig. 3 (Qiu and Park 2001).

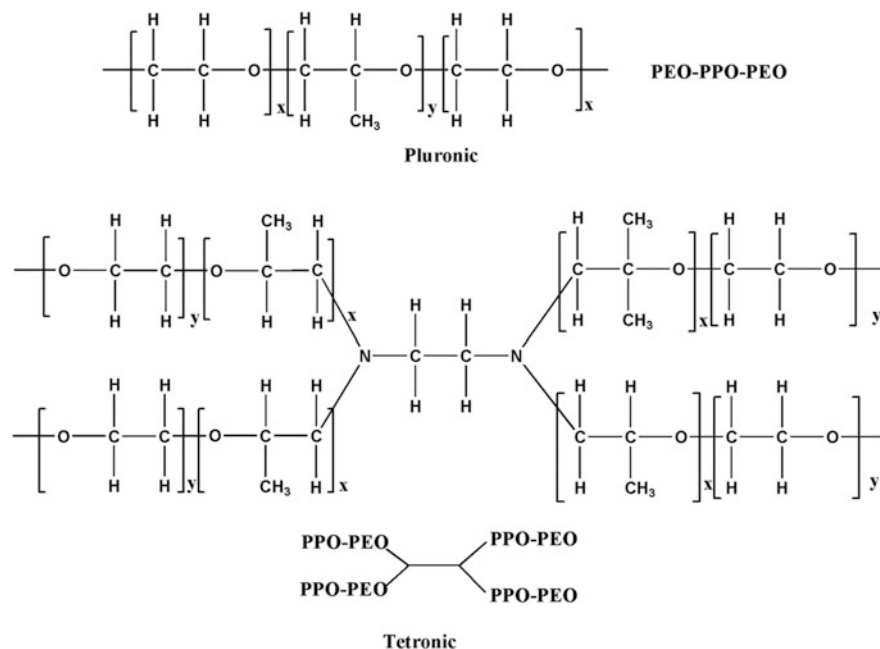


**Fig. 3** Polymer structures of pluronic and tetronic

## 2.2 pH-Sensitive Polymer Gels

pH-sensitive gels are materials that respond to pH values of surrounding medium. Swelling behavior occurs due to changes in hydrophobic–hydrophilic nature of chains or due to hydrogen bonds and the complexation of inter- and intramolecular or electrostatic repulsion. Depending on nature of polymer pendant group, pH-sensitive PGs are classified into anionic and cationic polymer gels (Hongyan He 2006).

### 2.2.1 Anionic Polymer Gels

This class of SPGs often has carboxylic or sulfonic acid groups (Qiu and Park 2001). The more important parameter of anionic gels is the relation between  $pK_a$  of the polymer and pH of surrounding environment, which means that, when  $pK_a$  is higher than pH of surrounding medium, the ionized structure will increase the electrostatic repulsion of the network and enhance the swelling properties (Hongyan He 2006). Examples of anionic pH-sensitive PGs are shown in Fig. 4.

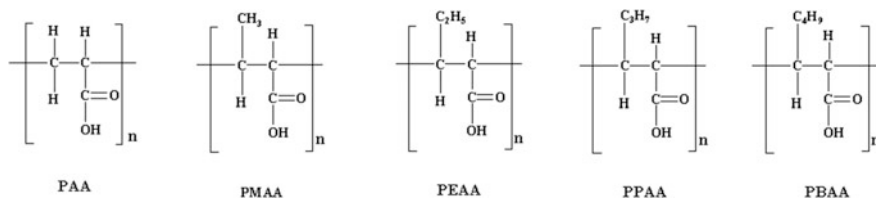


**Fig. 4** Anionic pH-sensitive polymer gels

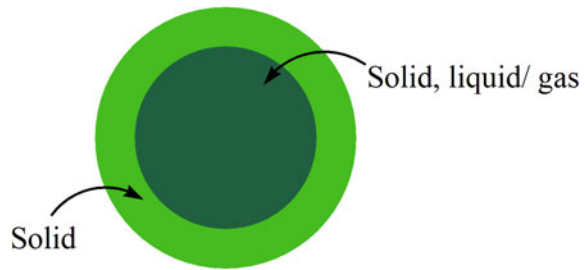
### 2.2.2 Cationic Polymer Gels

Cationic SPGs usually have pendant group such as amine (Qiu and Park 2001). The more important parameter in these materials is the relation between polymer pKb and pH of surrounding medium. When pH of environment is lower than polymer pKb amine group is changing from  $\text{NH}_2$  to  $\text{NH}_3^+$  which subsequently increase the hydrophilicity, electrostatic repulsion, and absorption capacity (Peppas et al. 2000). Polyacrylamide (PAAm) is the most used polymer as cationic polymer gels.

## 2.3 Electric Signal Sensitive

Raw matrix of this class is polyelectrolyte which is similar to pH-sensitive SPGs. Electric-sensitive SPG undergoes swelling and de-swelling as a response of applied electric signal. Electric-sensitive PGs have three kinds of transition phases: swelling, shrinking or de-swelling, and bending. These phases depend on a number of conditions such as the system that has been used to apply electric field (contact system or spread system) (Kim et al. 2003; Hongyan He 2006). In the last decades, new class of smart gels has been emerged called core-shell gels. Core-shell gels are structured composite particles consisting of at least two different components: one in principle forms the core and the other the shell of the particles (Ha et al. 2002). This class of materials has attracted much attention because of the combination of superior properties not possessed by the individual components. The systems might combine the characteristics and properties of both shell and core (Hendrickson et al. 2010). Core-shell gels might be pH and thermosensitive at same time. This characteristic granted this class of gels numbers of applications as impact modifiers, surface coatings, printing, catalysis, pollution control, sensing, and drug delivery in biomedical application (Jones and Lyon 2003; Li and Stöver 2000; Sasa and Yamaoka 1994; Khan et al. 2008). Core-shell gels are usually prepared in spherical form, implying a particle structure with the initially polymerized polymer located at the center of the particle, and the later-formed polymers becoming incorporated into the outer shell layer as illustrated in Fig. 5 (Dimonie et al. 1997). The core part may be a solid or a liquid or a gas; however, the shell materials usually a solid but its

**Fig. 5** Core-shell polymers (CSPs) consisting of central part may be a solid, liquid, or a gas and shell part usually a solid



nature depends on the type of applications (Jones and Lyon 2003). Core-shell polymer gels can be in nanosize and microsize according to preparation methods and targeted applications (Blackburn and Lyon 2008; Berndt et al. 2006).

### 3 Composites of Smart Polymer Gels

Composite of different materials can be possible solution to get special desired properties for particular applications or to gain the desired properties from each material in the compound. SPG composite has been carried out using different kind of polymers, fibers, and fillers of different sizes from micro- to nanosize. Many minerals have been used to act as filler for production of SPG composite such as kaolin, diatomite, potassium humate, glass, smectite, kaolinite, sodium silicate, bentonite, and montmorillonite (Kabiri et al. 2011). Natural fibers also have been used in some areas such as study by Rui Liang et al. used wheat straw (WS) to improve PGs properties and investigate the effect of WS on absorption capacity of PAA superabsorbent hydrogel in distilled water and 0.9% sodium chloride (NaCl). The result showed that the maximum absorbency attained at 20% of WS and absorbency started decreasing after further increase in WS % as shown in Fig. 6 (Liang et al. 2009). Composite of SPGs was prepared to improve mechanical properties, swelling behavior, and reduce cost. In fact, composites of polymer gels were successfully prepared and utilized in many filed when mechanical properties is needed. More information on polymer gel composites can be found in very good review by Kabiri et al. (2011).

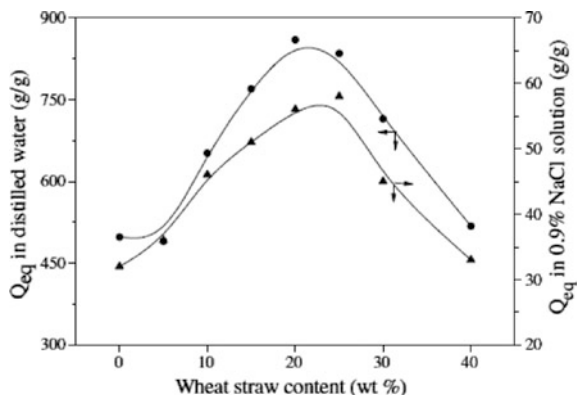
## 4 Properties of Smart Polymer Gels

### 4.1 Absorption Properties

Swelling behavior and absorption capacity (AC) are the most important properties that give SPGs wide applications. In general, swelling and absorption properties are



**Fig. 6** Influence of wheat straw content on the absorbency of WS/APP superabsorbent composites



attributed to the presence of hydrophilic groups such as  $-\text{OH}-$ ,  $\text{CONH}-$ ,  $-\text{CONH}_2-$ , and  $-\text{SO}_3\text{H}$  in the chemical structure of the network (Hamidi et al. 2008). The ratio of sample weight at swelling and de-swelling actions is called swelling ratio (SR) (Tang et al. 2008; Kim et al. 2003; Zuo Chun et al. 2007). There are many factors affecting SR and AC of SPG such as chemical compositions (Karadag et al. 2005; Guilherme et al. 2005), network structure (Patachia et al. 2007), cross-linking ratio, specific stimuli or the surrounding medium (Peppas et al. 2000; Hongyan He 2006), polymers molecular weight (Raj et al. 2009), and chemical structure of polymer repeating unit (Chun et al. 2009). The swelling process of SPGs can be explained as follows: The solvent tries to penetrate the polymer networks to produce 3D-molecular network at the same time expanding the molecular chains between the cross-linked points, thus decreasing the configuration enthalpy value. The molecular network has an elastic contractive force which tries to make the networks contract. When these opposite forces reach equilibrium, the expansion and contraction also reach a balance. In this process, the osmotic pressure is the driving force for expansion of swelling and network elastic force is the driving force of the contraction of gel. AC is estimated using volumetric, gravimetric, spectroscopic, and microwave method. The volumetric method measures the sample volume changes or absorbed fluid before and after absorption. The gravimetric method depends on measuring sample weight changes. Spectrometric method uses UV-spectrum of sample change, and the microwave method measures microwave absorption by energy changes. Absorbed water in network structure of PAA can exist in three states: bound, half-bound, and free water. Free water shows freezing point when the environment temperature is around  $0^\circ\text{C}$ . However, this freezing point cannot be seen with bound water. The half-bound water shows property between them. Bounded water is usually  $0.39\text{--}1.18\text{ g/g}$ . Absorption capacity of SPG mainly depends on osmotic pressure, network affinity, and network cross-linking density.

### 4.1.1 Cross-Linker and Cross-Linking Density

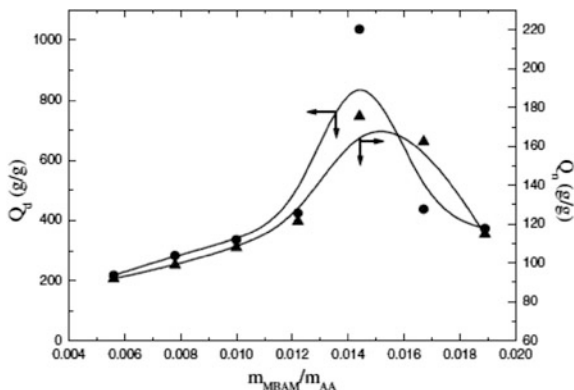
Cross-linker plays major role to adjust SPGs properties in terms of absorption and mechanical properties. Cross-linking density of SPGs is controlled by the fraction of cross-linking agent present in the polymerization and double bond conversion. Therefore, smaller amount of cross-linking agent leads to different cross-linking degree and change in AC of PGs. At low percentage of cross-linking agent, the three-dimensional PGs do not form effectively and the water molecules cannot be held resulting in SR and AC decrease. At high concentration of cross-linker a large number of growing polymer chains are involved to produce an additional network structure. High tied network does not allow water to enter the network and decrease AC (Turkington and Paradise 2005; Peppas et al. 2000). Effect of cross-linker content on SR of copolymer of carboxymethyl chitosan-g-polyacrylic acid is shown in Fig. 7 (Shah et al. 2010).

Some researchers reported that the number of functional groups of cross-linker has affected AC of polymer gels. Different AC of PGs of polyacrylamide (PAAm) and polyacrylamide sodium acrylate (PAAm/SA) was obtained using different type of cross-linker as shown in Fig. 8. AC via using 1,4-butanediol dimetacrylate (BDMA), ethylene glycol dimethacrylate (EGDMA), N,N'-methylenebisacrylamide (MPA), and trimethylolpropane triacrylate (TMPTA) were in the following order:

$$\text{MPA} > \text{BDMA} > \text{EGDMA} > \text{TMPTA}$$

Different AC is observed as a result of functional groups of each type of cross-linker. MPA, BDMA, and EGDMA are tetrafunctional cross-linkers and TMPTA is hexafunctional cross-linker. NH group of MPA increases SR and AC via causing new hydrophilic interaction. Using TMPTA cross-linker led to many cross-linking sites; therefore, the cross-linking density is higher than using other cross-linker at same concentration which leads to decreased AC (Ren and Sun 2010). The chemical structure of cross-linker can affect absorption properties. Cross-linking agent with hydrophilic property such as MPA enhances the AC as a result of presences of amide groups (Vital et al. 2008). In addition, water solubility,

**Fig. 7** Effect of MBAN/ mAA on the swelling ratio of superabsorbent polymer



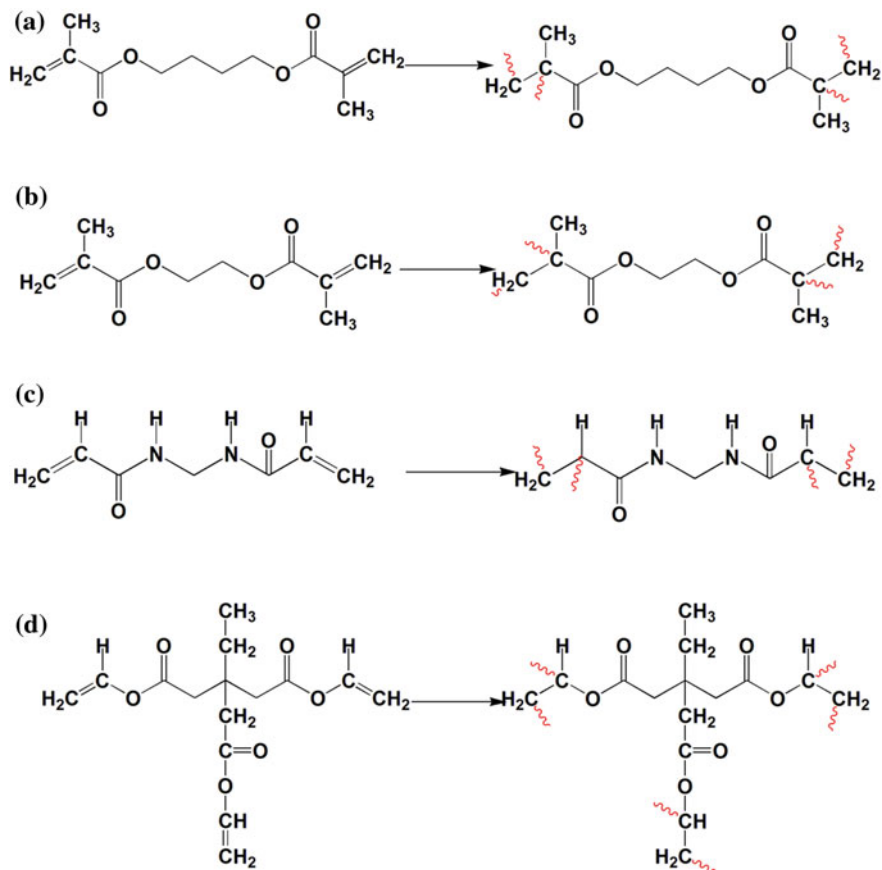


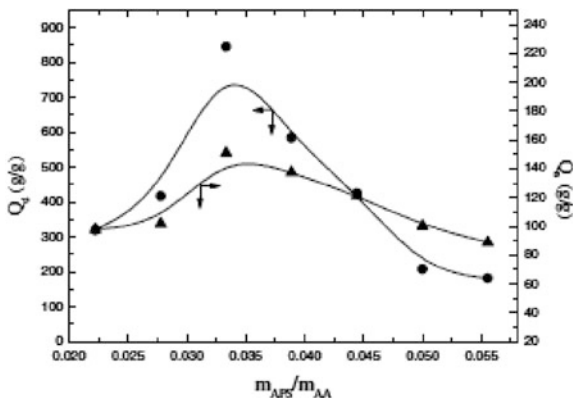
**Fig. 8** Linking sites of **a** 1,4-butanediol dimethacrylate (BDMA), **b** ethylene glycol dimethacrylate (EGDMA), **c** N,N-methylenebisacrylamide (MPA), **d** trimethylolpropane triacrylate (TMPTA)

short chains, and high activity of MPA give this kind of cross-linker wide use in free radical polymerization (Turkington and Paradise 2005).

#### 4.1.2 Initiator Content

Absorption capacity of SPGs is affected by the initiator content as a result of change in polymer molecular weight. At low molecular weight, the relative amount of polymer chain ends increases (polymer chain ends do not contribute to AC); therefore, AC will decrease at high content of initiator (D'Ulivo 2004). Moreover, when the content of initiator is low, the polymerization reaction takes place slowly and leads high molecular weight and network structure with big pore size.

**Fig. 9** Effect of mAPS/mAA on the swelling ratio of superabsorbent polymers



Network with large voids has less ability to hold water and less WAC. At high initiator content, the polymerization rate is high and the product has smaller space size and that prevents fluid molecules from entering the network (Lin et al. 2007). Figure 9 shows the effect of ammonium persulfate (Desrosiers et al. 2000) on water absorbency of copolymer of PAA-co-PAAm filled with inorganic clay (Li and Wang 2005). From above-mentioned, there is an optimum voids size to get maximum WAC and that can be controlled via initiator content.

#### 4.1.3 Degree of Neutralization (DON)

DON is normally used between 0 and 80% for most polymerization process (Talpur et al. 2009; Pourjavadi et al. 2004). Neutralization of acrylic acid (AA) using sodium hydroxide (NaOH), the negatively charged carboxyl groups attached to polymer chains, produces an electrostatic repulsion (ESR) which leads to network expansion which means high AC is associated with high ESR. After certain degree of neutralization, AC decreases with a corresponding increase in chain stiffness and counterion condensation on the polyion “(screening effect)” (Dall and Sharples 1991). At low DON, the ESR is low which ultimately decreasing the absorption capacity of the hydrogel networks. When DON start to increase the content of  $-\text{CO}_2-\text{Na}$  groups increases leading to enhancement in osmotic pressure between the inside and outside network and enhancing AC of SPGs. However, AC stop’s at certain value of DON and starts to decline. The main cause of decline in AC is the presence of  $\text{Na}^+$  ions which leads to shielding of carboxylate anions on PAA chains and inhibits anion–anion repulsion forces (El Bakouri et al. 2008). Table 1 shows DON effect on water absorbency of PAA hydrogel at various cross-linking agent concentrations (Yadvinder et al. 2005).

**Table 1** The effect of neutralization degree of acrylic acid at various cross-linking agent concentrations on water absorbency of the synthesized beads

Neutralization degree of acrylic acid %	Water absorption capacity g g <sup>-1</sup>		
	<i>N,N</i> -MBA		
	0.025 mol%	0.05 mol%	0.075 mol%
100	775 ± 99	568 ± 27	476 ± 15
76	581 ± 18	557 ± 51	471 ± 42
59	570 ± 68	523 ± 39	428 ± 28
46	507 ± 59	476 ± 17	447 ± 14

#### 4.1.4 Solvent Volume and Concentration

Network structure of SPGs is affected by solvent concentration as a result of enhanced primary cyclization rate of multi-vinyl monomer during the polymerization process. Increasing the reaction solvent volume leads to decrease in contents reaction of cross-linking agent, initiator, and monomer and finally decreases in polymerization rate and cross-linking density. Low solvent volume means reaction contents' viscosity is high and difficult movement for free radicals and monomer in the reaction (El Bakouri et al. 2008; Munshi et al. 1978). Solvent concentration affects network properties by affecting radical propagation dynamics. At low solvent concentration, the double bond concentration surrounding by free radical is relatively high. This leads to fast propagation step and less opportunity for free radicals to recycle by reacting with its own pendant double bond. Solvent type and quality have been reported to affect SPGs properties. Poor solvent use results in loose network structure, and firm networks are a result of using good solvent (Elliott and Bowman 2002). Previous study indicated that high solubility monomer and homopolymer in solvent lead to difficulty in grafting polymerization. In the same study, effect of solvent contents was determined by fixing other reaction contents. The result showed that the maximum percentage of grafting was obtained at 50-ml-total reaction mixture. As a conclusion of this section, solvent concentration can be used to control free radical polymerization in both microscopic and molecular levels.

#### 4.1.5 Fiber Type and Content

AC of SPGs is highly affected by chemical composition and concentration of used fibers. Hydrophilic groups on fiber surface contribute to enhance network absorption capacity. If the fibers act as additional cross-linking agent inside SPGs network, high concentration of fibers leads to rigid network structure and less. Previous work on sodium alginate (Na–Ag) grafted with carboxymethylcellulose (CMC) showed that SR of polymer gels increase gradually with increase in Na–Ag content, and the maximum AC is achieved at 0.5 weight ratio of Na–Ag/CMC.

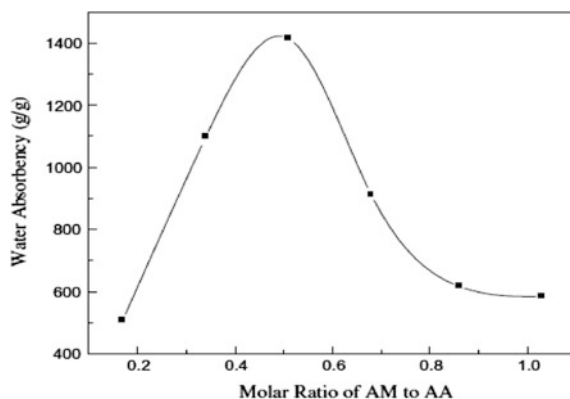
After this ratio, AC decreases as a result of increase in viscosity of reaction mixture which hindered reactants movement (Yang et al. 2003; Shah et al. 2010). Kappa-carrageenan (kC) used as a fiber showed that WAC of the network was increased with increase in kC content. Same result has been obtained using CMC grafted with polyacrylonitrile (PAN), and starch-poly(sodium acrylate-co-acrylamide) (Pourjavadi et al. 2007a; Bonakdar et al. 2010; Seoudi 2008). Another study indicated that absorption properties of SPG were enhanced by filling the structure with inorganic clay (attapulgit) (Li and Wang 2005).

#### 4.1.6 Chemical Structure and Monomer Molar Ratio

Blending of two monomers to produce desirable properties of SPGs has been studied intensively in the area of gels (Adem et al. 2009; Abd El-Rehim et al. 2006; Kadlubowski et al. 2007; Zhang et al. 2009; Mahdavinia et al. 2008). The effect of molar ratio of poly(acrylamide-acrylic acid) is shown in Fig. 10.

Increasing the polyacrylamide to more than 0.51 molar ratios leads to decrease AC, and counter result was observed at ratio less than this value. This study reported that the incorporation in suitable ratio of hydrophilic groups ( $-\text{CONH}$ ,  $\text{COONa}$ , and  $\text{COOH}$ ) inside the network reduces the repelling action and increases water absorbency (Li and Wang 2005). The chemical structure of polymer repeating unit affects SR and AC by changing the ratio of hydrophilic to hydrophobic groups (Chun et al. 2009). Network of high contents of hydrophilic groups swells to higher degree than those of high hydrophobic groups. Hydrophobic groups may collapse in the presence of water. The collapse chains minimize their exposure to water molecule as such lower absorption capacity and swelling rate.

**Fig. 10** Effect of molar ratio of AM to AA content on water absorbency of superabsorbent polymer



### 4.1.7 pH of Absorbed Fluid

Swelling behavior and absorption capacity of SPGs are affected by surrounding medium (Peppas et al. 2000; Hongyan He 2006). Affect of swollen pH on absorption and swelling capacity of polyelectrolytes has been considered in many studies (Varshosaz and Falamarzian 2001; Liu et al. 2006; Sahoo et al. 2007; Yoo et al. 2000; Kim and Park 2010; Karppi et al. 2007, 2008; Zhang et al. 2004; Wang et al. 2008; Singh et al. 2007; Sheikh et al. 2010; Yang et al. 2009, Abd El-Rehim et al. 2006). Effect of pH medium on swelling ratio of PAA hydrogel in Fig. 11 indicates that the high swelling ratio was at pH 4.9 solution. The cause of this value is associated with pKa of polyacrylic acid (PAA) and swollen medium. PAA has pKa of 4.9; therefore, when pH of swollen sample is less than pKa of PAA that leads to high strength of H<sup>+</sup> which affect carboxylic group ionization. At pH higher than pKa of PAA, more carboxylic ions are formed which enhances electrostatic repulsion and create more network free space and lead to increase in swelling ratio (Sheikh et al. 2010).

## 4.2 Releasing Behavior

Definition of SPG indicated that the network has the ability to release absorbed fluid as a response to environmental change (temperature, pH, ions, electric signal, sound, and magnetic field). Releasing behavior of SPGs draws great attention of many researches (Lee and Chen 2006; Kim and Peppas 2003; Tomic et al. 2007; Liu et al. 2006; Chen et al. 2009; Lee et al. 2008; Fundueanu et al. 2001; Siemoneit et al. 2006; Uchida et al. 2003; Issa et al. 1990; Huynh et al. 2009; Alemzadeh and Vossoughi 2002; Chun et al. 2005; Tada et al. 2005). Releasing character of SPGs via its sensitivity to environmental change grants this class of materials' advantages

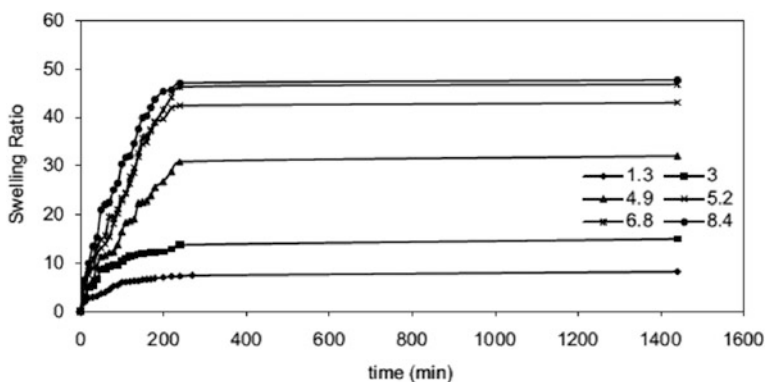
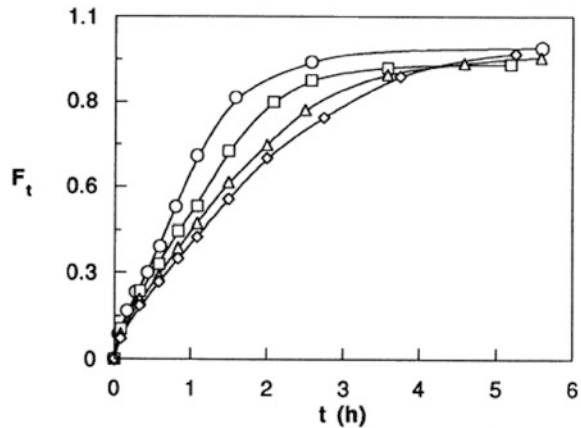


Fig. 11 Swelling ratio of PAA in media of different pH values as function of time

**Fig. 12** Fractional release profiles of theophylline at  $310 \pm 0.2$  K from glassy poly(acrylic acid-co-acrylamide) (50/50%)/MBAAm gels in water: (○) (0.67%) MBAAm, (□) (1.00%) MBAAm, (△) (1.25%) MBAAm, (◇) (1.50%) MBAAm



to be used in drug control release in medical and water treatment applications. Theophylline release from P(AA-co-AAm) hydrogel in distilled water indicated that low release rate related with samples of high degree of cross-linking as illustrated in Fig. 12 (Katime et al. 1999).

### 4.3 Mechanical Properties SPGs

Applications of SPGs are limited in some areas because of their poor mechanical properties (Tanaka et al. 2005). Mechanical properties of SPG are very important in applications such as drug delivery system and agriculture when the hydrogel has to withstand certain pressure in deep placement process (Omidian et al. 2005). There are some methods such as increasing the cross-linking density, copolymerizing of two kinds of polymer, and grafting with rigid substrates used to enhance mechanical properties of polymer gels in general (Cauich-Rodriguez et al. 1996; Katime et al. 2001). Mechanical properties of SPG can be controlled by changing system cross-linking degree. High cross-linking degree leads to more brittle and stronger network structure. Therefore, to achieve a relatively strong and elastic property network, suitable cross-linking degree has to be optimized. Also, mechanical properties are affected by the main monomers used to synthesize SPGs which means copolymerization of two types of repeating unit (hydrophilic-hydrophobic) (Katime et al. 2001; Patachia et al. 2007). The structural strength of polymer gels can be enhance by introducing a comonomer to the main networks which contribute to new hydrogen bonding and stable network structure (Solpan et al. 2003; Peppas et al. 2000). Mechanical properties are improved using nanomaterials, such as inorganic nanoclay and carbon nanotubes to produce nanocomposites network structure (Xiang et al. 2006; Pourjavadi et al. 2007a).



## 5 Application of Smart Polymer Gels

Unique properties of PGs such as absorption, swelling and de-swelling behavior, hydrophobicity, biocompatibility, and sensitivity to environmental change are the main reason for its wide applications. Homopolymer and copolymer of PGs have been used in various applications in our daily life such as agricultural, biomedical, water treatment, and other industrial applications (Katime et al. 1999, 2004; Liang et al. 2009; Solpan et al. 2008; Shukla et al. 2009; Zhao et al. 2004; M'Bareck et al. 2006; Devine et al. 2006; Nho et al. 2004; Hoffman 2002).

### 5.1 Biomedical Application

SPGs materials have wide application in biomedical and pharmaceutical because of their desirable properties such as minimal interfacial tension with surrounding biological fluids, gas permeation, diffusion of low molecular weight, less mechanical, and friction irritation to tissue (Cauch-Rodriguez et al. 1996). One of the difficulties biomedical experts are facing nowadays is how to deliver such a drug completely to particular place in the human body. Experts used a system called drug delivery system to manage release and deliver drug to specific positions (Wang et al. 2010; Blanco et al. 1996; Lukowski et al. 1992; Miao et al. 2010; Kakoulides et al. 1998; Kamath and Park 2010; Gong et al. 2009; Kaetsu 1996; Miyata et al. 2002; Geever et al. 2008; Nam et al. 2004; El-Hag et al. 2009; Bhattarai et al. 2010; Adnadjevic and Jovanovic 2009; Li et al. 2009; Cheddadi et al. 2011; Tu et al. 2010). SPGs of thermosensitive and pH sensitive are widely used in medical application as drug delivery system because of their sensitivity to pH and temperature of human body. Many monomer and polymer were used in this kind of application but the most used are PAA and PAAm and their copolymers. PAA grafted with *n*-alkyl methacrylate was prepared to study swelling and release kinetics of theophylline and aminophylline. This study indicated that the release of theophylline is fairly independent of alkyl chain length while the release of aminophylline is highly dependent on alkyl chain length (Katime et al. 2001). Copolymer of P(AA-co-AAm) hydrogel was used for theophylline release in distilled water (Katime et al. 1999). SPG based of PAA filled with cotton fiber was synthesized for gentamicin release. The outcome of this study showed the release of drug from the grafted network is a chain relaxation controlled manner (Bajpai and Das 2011). SPG of PAA grafted with gelatin (Ge) and cotton fiber was prepared for gentamicin sulfate release (Changez et al. 2003; Bajpai and Das 2011; Changez et al. 2004). The result of these studies regarded to use hydrogel based on PAA to deliver gentamicin sulfate in controlled manner. Loaded gentamicin sulfate showed fair antibacterial action against *Escherichia coli*. Grafted PAA with polyethylene oxide using radiation polymerization was prepared as insulin carrier. This study

indicated that insulin loaded on hydrogel has higher effect on lowering of blood glucose over injection insulin solution (Nho et al. 2004).

SPGs of pH-sensitive material are able to convert chemical energy to mechanical energy as such can serve as actuators or artificial muscles in medical applications. SPGs have also been used in many other biomedical application including diagnostic, therapeutic, and implantable devices such as catheters, biosensors (Pourjavadi et al. 2007b; Adhikari and Majumdar 2004), artificial skin (Devine et al. 2006), and tissue engineering (Kim et al. 2008; Landers et al. 2002).

## 5.2 Water Treatment Application

Water pollution is considered as one of the most important issues facing humanity these days. Usually, water is polluted by different undesirable ions and dyes. The sources of these contaminants are either industrial or agricultural. Most factories effluents are discarded into water (rivers, lakes, and seas). These ions and dyes change the biological system of rivers and lakes and affect life of several kinds of species. Wastewater has been treated using several methods such as biological treatment, chemical precipitation, supercritical water oxidation, steam-stripping, microwave radiation, ion exchange, and absorption methods. Absorption method gets high attention because of its low energy consumption and easy operation (Zheng and Wang 2009). Therefore, using the ability of such material to absorb and separate particular ions or dyes from solution can be helpful (Guilherme et al. 2007; Paulino et al. 2007). SPGs have been used in this field for past forty years. Some researchers studied AC of copolymer of PAA-PAAm-polysaccharide to methylene blue (MB) from water. The result showed good AC of this copolymer and excellent methylene blue removal (48 mg of dye per 1 g of SAP) (Paulino et al. 2006). In another study, SPGs of PAA grafted with chitosan was prepared for ammonium removal applications. This study indicated that PGs have high absorption capacity of 30 mg/g ammonium nitrogen in a wide pH range of 4–9 (Zheng et al. 2009). In another work, grafted PAA/chitosan/vermiculite gels were synthesized for adsorption of methylene blue from water. The results showed that grafted hydrogel has high adsorption for MB dye and suggested that it has the potential as adsorbent for cationic dye removal from wastewater (Liu et al.). Many other SPGs based on PAA copolymer were synthesized and absorption of cationic dyes such as methylene blue, safranin-O (SO), magenta (M), Janus Green B (JGB), and ions such as lead ( $Pb^{+2}$ ), cadmium ( $Cd^{+2}$ ), copper ( $Cu^{+2}$ ), ( $Ni^{+2}$ ), iron ( $Fe^{+3}$ ), ( $Mn^{+2}$ ) were studied (Solpan et al. 2008; Xiong et al. 2009; Zheng et al. 2010; Duran et al. 1999; Li et al. 2011; Kangwansupamonkon et al. 2010; Dai et al. 2011; Zheng et al. 2011; El-Hag et al. 2003; Wei et al. 2009; Shirsath et al. 2011).

## 6 Conclusion

SPGs are polymer gels that respond to the surrounding environmental change in their swollen and dry state. Conventional polymerization techniques were used to syntheses and prepare SPGs such as solution, suspension, emulsion, and radiation polymerization. Solution polymerization is the most widely used technique because of its advantage of pure product (free of surfactants and other contaminants). SPGs are classified depended on their sensitivity to thermo, pH, electric, magnetic, and sound-sensitive gels. Swelling, release, and mechanical properties are the most important criteria to select the correct SPGs for particular application. SPGs properties are affected by initiator content, cross-linker kind and content, chemical composition of polymer network, fiber content pH, and ion concentration of surrounding medium. SPGs properties granted these materials very wide applications in biomedical and water treatment.

## References

- Abd El-Rehim, HA, Hegazy ESA, Abd El-Mohdy HL (2006) Effect of various environmental conditions on the swelling property of PAAm/PAAcK superabsorbent hydrogel prepared by ionizing radiation. *J Appl Polym Sci* 101:3955–3962
- Adem E, Burillo G, Bucio E, Magaña C, Avalos-Borja M (2009) Characterization of interpenetrating networks of acrylic acid (AAc) and N-isopropylacrylamide (NIPAAm) synthesized by ionizing radiation. *Radiat Phys Chem* 78:549–552
- Adhikari B, Majumdar S (2004) Polymers in sensor applications. *Prog Polym Sci* 29:699–766
- Adnadjevic B, Jovanovic J (2009) A comparative kinetics study of isothermal DRUG release from poly(acrylic acid) and poly(acrylic-co-methacrylic acid) hydrogels. *Colloids Surf B* 69:31–42
- Alemzadeh I, Vossoughi M (2002) Controlled release of paraquat from poly vinyl alcohol hydrogel. *Chem Eng Process* 41:707–710
- Ali AE, Shawky HA, El Rehim HA, Hegazy EA (2003) Synthesis and characterization of PVP/AAc copolymer hydrogel and its applications in the removal of heavy metals from aqueous solution. *Eur Polym J* 39:2337–2344
- Bajpai SK, Das P (2011) Gentamicin-loaded poly(acrylic acid)-grafted cotton fibers, part 1: synthesis, characterization, and preliminary drug release study. *J Appl Polym Sci* 122:366–374
- Berndt I, Pedersen JS, Richtering W (2006) Temperature-sensitive core-shell microgel particles with dense shell. *Angew Chem* 118:1769–1773
- Bhattarai N, Gunn J, Zhang M (2010) Chitosan-based hydrogels for controlled, localized drug delivery. *Adv Drug Delivery Rev* 62:83–99
- Blackburn W, Lyon LA (2008) Size-controlled synthesis of monodisperse core/shell nanogels. *Colloid Polym Sci* 286:563–569
- Blanco MD, García O, Trigo RM, Teijón J, Katime I (1996) 5-Fluorouracil release from copolymeric hydrogels of itaconic acid monoester: I. Acrylamide-co-monomethyl itaconate. *Biomaterials* 17:1061–1067
- Bonakdar S, Emami SH, Shokrgozar MA, Farhadi A, Ahmadi SA, Amanzadeh A (2010) Preparation and characterization of polyvinyl alcohol hydrogels crosslinked by biodegradable polyurethane for tissue engineering of cartilage. *Mater Sci Eng C* 30:636–643

- Cauich-Rodríguez JV, Deb S, Smith R (1996) Effect of cross-linking agents on the dynamic mechanical properties of hydrogel blends of poly(acrylic acid)-poly(vinyl alcohol-vinyl acetate). *Biomaterials* 17:2259–2264
- Changez M, Burugapalli K, Koul V, Choudhary V (2003) The effect of composition of poly (acrylic acid)-gelatin hydrogel on gentamicin sulphate release: in vitro. *Biomaterials* 24:527–536
- Changez M, Koul V, Krishna B, Dinda AK, Choudhary V (2004) Studies on biodegradation and release of gentamicin sulphate from interpenetrating network hydrogels based on poly(acrylic acid) and gelatin: in vitro and in vivo. *Biomaterials* 25:139–146
- Cheddadi M, López-Cabarcos E, Slowing K, Barcia E, Fernández-Carballido A (2011). Cytotoxicity and biocompatibility evaluation of a poly(magnesium acrylate) hydrogel synthesized for drug delivery. *Int J Pharm* 413:126–133
- Chen J, Liu M, Liu H, Ma L (2009) Synthesis, swelling and drug release behavior of poly(N, N-diethylacrylamide-co-N-hydroxymethyl acrylamide) hydrogel. *Mater Sci Eng, C* 29:2116–2123
- Chun KW, Lee JB, Kim SH, Park TG (2005) Controlled release of plasmid DNA from photo-cross-linked pluronic hydrogels. *Biomaterials* 26:3319–3326
- Chun C, Lee SM, Kim SY, Yang HK, Song S-C (2009) Thermosensitive poly(organophosphazene)-paclitaxel conjugate gels for antitumor applications. *Biomaterials* 30:2349–2360
- Dai J, Yan H, Yang H, Cheng R. (2011) Simple method for preparation of chitosan/poly(acrylic acid) blending hydrogel beads and adsorption of copper(II) from aqueous solutions. *Chem Eng J* 165:240–249
- Dall W, Sharples DJ (1991) References. *Advances in marine biology*. Academic Press
- Desrosiers G, Savenkoff C, Olivier M, Stora G, Juniper K, Caron A, Gagne JP, Legendre L, Mulsow S, Grant J, Roy S, Grehan A, Scaps P, Silverberg N, Klein B, Tremblay JE, Therriault JC (2000) Trophic structure of macrobenthos in the Gulf of St. Lawrence and on the Scotian Shelf. *Deep-Sea Res Part II-Topical Stud Oceanogr* 47:663–697
- Devine DM, Devery SM, Lyons JG, Geever LM, Kennedy JE, Higginbotham CL (2006) Multifunctional polyvinylpyrrolidone-polyacrylic acid copolymer hydrogels for biomedical applications. *Int J Pharm* 326:50–59
- Dimonie VL, Daniels ES, Shaffer OL, El-Aasser MS (1997) Control of particle morphology. In: Lovell P, El-Aasser MS (eds) *Emulsion polymerization and emulsion polymers*. Wiley, West Sussex, England
- D'Ulivo A (2004) Chemical vapor generation by tetrahydroborate(III) and other borane complexes in aqueous media: a critical discussion of fundamental processes and mechanisms involved in reagent decomposition and hydride formation. *Spectrochim Acta, Part B* 59:793–825
- Duran S, Solpan D, Güven O (1999) Synthesis and characterization of acrylamide-acrylic acid hydrogels and adsorption of some textile dyes. *Nucl Instrum Methods Phys Res, Sect B* 151:196–199
- El Bakouri H, Aassiri A, Morillo J, Usero J, Khaddor M, Ouassini A (2008) Pesticides and lipids occurrence in Tangier agricultural soil (northern Morocco). *Appl Geochem* 23:3487–3497
- El-hag Ali A, Alarifi A (2009) Characterization and in vitro evaluation of starch based hydrogels as carriers for colon specific drug delivery systems. *Carbohydr Polym*
- Elliott JE, Bowman CN (2002) Effects of solvent quality during polymerization on network structure of cross-linked methacrylate copolymers. *J Phys Chem B* 106:2843–2847
- Fundueanu G, Mocanu G, Constantin M, Carpov A, Bulacovschi V, Esposito E, Nastruzzi C (2001) Acrylic microspheres for oral controlled release of the biguanide buformin. *Int J Pharm* 218:13–25
- Geever LM, Cooney CC, Lyons JG, Kennedy JE, Nugent MJD, Devery S, Higginbotham CL (2008) Characterisation and controlled drug release from novel drug-loaded hydrogels. *Eur J Pharm Biopharm* 69:1147–1159

- Gong C, Shi S, Wu L, Gou M, Yin Q, Guo Q, Dong P, Zhang F, Luo F, Zhao X, Wei Y, Qian Z (2009) Biodegradable in situ gel-forming controlled drug delivery system based on thermosensitive PCL-PEG-PCL hydrogel. Part 2: Sol-gel-sol transition and drug delivery behavior. *Acta Biomaterialia*, In Press, Corrected Proof
- Guilherme MR, Reis AV, Takahashi SH, Rubira AF, Feitosa JPA, Muniz EC (2005) Synthesis of a novel superabsorbent hydrogel by copolymerization of acrylamide and cashew gum modified with glycidyl methacrylate. *Carbohydr Polym* 61:464–471
- Guilherme MR, Reis AV, Paulino AT, Fajardo AR, Muniz EC, Tambourgi EB (2007) Superabsorbent hydrogel based on modified polysaccharide for removal of Pb<sup>2+</sup> and Cu<sup>2+</sup> from water with excellent performance. *J Appl Polym Sci* 105:2903–2909
- Ha J-W, Park IJ, Lee S-B, Kim D-K (2002) Preparation and characterization of core-shell particles containing perfluoroalkyl acrylate in the Shell. *Macromolecules* 35:6811–6818
- Hamidi M, Azadi A, Rafiei P (2008) Hydrogel nanoparticles in drug delivery. *Adv Drug Deliv Rev* 60:1638–1649
- Hendrickson GR, Smith MH, South AB, Lyon LA (2010) Design of multiresponsive hydrogel particles and assemblies. *Adv Func Mater* 20:1697–1712
- Hoffman AS (2002) Hydrogels for biomedical applications. *Adv Drug Deliv Rev* 54:3–12
- Hongyan He MS (2006) Multifunctional medical device based on PH-sensitive hydrogels for controlled drug delivery. PhD, Ohio State University
- Huynh DP, Im GJ, Chae SY, Lee KC, Lee DS (2009) Controlled release of insulin from pH/temperature-sensitive injectable pentablock copolymer hydrogel. *J Controlled Release* 137:20–24
- Issa R, Akelah A, Rehab A, Solaro R, Chiellini E (1990) Controlled release of herbicides bound to poly[oligo(oxyethylene) methacrylate] hydrogels. *J Controlled Release* 13:1–10
- Jones CD, Lyon LA (2003) Shell-restricted swelling and core compression in poly(N-isopropylacrylamide) core-shell microgels. *Macromolecules* 36:1988–1993
- Kabiri K, Omidian H, Zohuriaan-Mehr MJ, Doroudiani S (2011) Superabsorbent hydrogel composites and nanocomposites: a review. *Polym Compos* 32:277–289
- Kadlubowski S, Henke A, Ulanski P, Rosiak JM, Bromberg L, Hatton TA (2007) Hydrogels of polyvinylpyrrolidone (PVP) and poly(acrylic acid) (PAA) synthesized by photoinduced crosslinking of homopolymers. *Polymer* 48:4974–4981
- Kaetsu I (1996) Biomedical materials, devices and drug delivery systems by radiation techniques. *Radiat Phys Chem* 47:419–424
- Kakoulides EP, Smart JD, Tsibouklis J (1998) Azocross-linked poly(acrylic acid) for colonic delivery and adhesion specificity: synthesis and characterisation. *J Controlled Release* 52:291–300
- Kangwansupamonkon W, Jitbunpot W, Kiatkamjornwong S (2010) Photocatalytic efficiency of TiO<sub>2</sub>/poly[acrylamide-co-(acrylic acid)] composite for textile dye degradation. *Polym Degradation Stability* 95:1894–1902
- Karadag E, Üzüüm ÖB, Saraydin D, Güven O (2005) Dynamic swelling behavior of [gamma]-radiation induced polyelectrolyte poly(AAm-co-CA) hydrogels in urea solutions. *Int J Pharm* 301:102–111
- Karppi J, Akerman S, Akerman K, Sundell A, Nyssönen K, Penttilä I (2007) Isolation of drugs from biological fluids by using pH sensitive poly(acrylic acid) grafted poly(vinylidene fluoride) polymer membrane in vitro. *Eur J Pharm Biopharm* 67:562–568
- Karppi J, Akerman S, Akerman K, Sundell A, Nyssönen K, Penttilä I (2008) Erratum to “Isolation of drugs from biological fluids by using pH sensitive poly(acrylic acid) grafted poly(vinylidene fluoride) polymer membrane in vitro”. *Eur J Pharm Biopharm* 68:847–850 (*Eur J Pharm Biopharm* 67:562–568 (2007))
- Katime I, Novoa R, Diaz de Apodaca E, Mendizábal E, Puig J (1999) Theophylline release from poly(acrylic acid-co-acrylamide) hydrogels. *Polym Testing* 18:559–566

- Katime I, Novoa R, Zuluaga F (2001) Swelling kinetics and release studies of theophylline and aminophylline from acrylic acid/*n*-alkyl methacrylate hydrogels. *Eur Polym J* 37:1465–1471
- Katime I, Novoa R, De Apodaca ED, Rodrii Guez E (2004) Release of theophylline and aminophylline from acrylic acid/*n*-alkyl methacrylate hydrogels. *J Polym Sci, Part A: Polym Chem* 42:2756–2765
- Khan AK, Ray BC, Dolui SK (2008) Preparation of core-shell emulsion polymer and optimization of shell composition with respect to opacity of paint film. *Prog Org Coat* 62:65–70
- Kim K-S, Park S-J (2010) Effect of porous silica on sustained release behaviors of pH sensitive Pluronic F127/poly(acrylic acid) hydrogels containing tulobuterol. *Colloids Surf B* 80:240–246
- Kim B, Peppas NA (2003) In vitro release behavior and stability of insulin in complexation hydrogels as oral drug delivery carriers. *Int J Pharm* 266:29–37
- Kim SJ, Yoon SG, Lee YM, Kim SI (2003) Electrical sensitive behavior of poly(vinyl alcohol)/poly(diallyldimethylammonium chloride) IPN hydrogel. *Sens Actuators B: Chem* 88:286–291
- Kim J, Lee KW, Hefferan TE, Currier BL, Yaszemski MJ, Lu L (2008) Synthesis and evaluation of novel biodegradable hydrogels based on poly(ethylene glycol) and sebacic acid as tissue engineering scaffolds. *Biomacromol* 9:149–157
- Landers R, Hübner U, Schmelzeisen R, Mülhaupt R (2002) Rapid prototyping of scaffolds derived from thermoreversible hydrogels and tailored for applications in tissue engineering. *Biomaterials* 23:4437–4447
- Lee W-F, Chen Y-C (2006) Effects of intercalated hydrotalcite on drug release behavior for poly(acrylic acid-co-*N*-isopropyl acrylamide)/intercalated hydrotalcite hydrogels. *Eur Polym J* 42:1634–1642
- Lee C-F, Lin C-C, Chien C-A, Chiu W-Y (2008) Thermosensitive and control release behavior of poly(*N*-isopropylacrylamide-co-acrylic acid)/nano-Fe<sub>3</sub>O<sub>4</sub> magnetic composite latex particle that is synthesized by a novel method. *Eur Polymer J* 44:2768–2776
- Li W-H, Stöver HDH (2000) Monodisperse cross-linked core-shell polymer microspheres by precipitation polymerization. *Macromolecules* 33:4354–4360
- Li A, Wang A (2005) Synthesis and properties of clay-based superabsorbent composite. *Eur Polym J* 41:1630–1637
- Li D, Omalley BW, Paulson D (2009) Composition for controlled release delivery for treating otorhinolaryngology—and head and neck-associated pathologies e.g. allergy and laryngology comprises Chitosan-glycerophosphate hydrogel, and agent for treatment of the pathologies
- Li S, Zhang H, Feng J, Xu R, Liu X (2011) Facile preparation of poly(acrylic acid-acrylamide) hydrogels by frontal polymerization and their use in removal of cationic dyes from aqueous solution. Desalination, In Press, Corrected Proof
- Liang R, Yuan H, Xi G, Zhou Q (2009) Synthesis of wheat straw-g-poly(acrylic acid) superabsorbent composites and release of urea from it. *Carbohydr Polym* 77:181–187
- Lin J, Tang Q, Wu J (2007) The synthesis and electrical conductivity of a polyacrylamide/Cu conducting hydrogel. *React Funct Polym* 67:489–494
- Liu MZ, Liang R, Zhan F, Liu Z, Niu AZ (2006) Synthesis of a slow-release and superabsorbent nitrogen fertilizer and its properties. *Polym Adv Technol* 17:430–438
- Lukowski G, Müller RH, Müller BW, Dittgen M (1992) Acrylic acid copolymer nanoparticles for drug delivery: I. Characterization of the surface properties relevant for in vivo organ distribution. *Int J Pharm* 84:23–31
- Mahdavinia GR, Pourjavadi A, Zohuriaan-Mehr MJ (2008) Synthesis and properties of highly swelling PAAm/chitosan semi-IPN hydrogels. *Macromolecular Symposia* 274:171–176
- M'Bareck CO, Nguyen QT, Alexandre S, Zimmerlin I (2006) Fabrication of ion-exchange ultrafiltration membranes for water treatment: I. Semi-interpenetrating polymer networks of polysulfone and poly(acrylic acid). *J Membr Sci* 278:10–18
- Miao Q, Xu D, Wang Z, Xu L, Wang T, Wu Y, Lovejoy DB, Kalinowski DS, Richardson DR, Nie G, Zhao Y (2010) Amphiphilic hyper-branched co-polymer nanoparticles for the controlled delivery of anti-tumor agents. *Biomaterials* 31:7364–7375

- Miyata T, Uragami T, Nakamae K (2002) Biomolecule-sensitive hydrogels. *Adv Drug Deliv Rev* 54:79–98
- Munshi SK, Singh R, Vij VK, Jawanda JS (1978) Mineral composition of leaves in relation to degree of granulation in sweet orange. *Sci Hort* 9:357–367
- Nam K, Watanabe J, Ishihara K (2004) The characteristics of spontaneously forming physically cross-linked hydrogels composed of two water-soluble phospholipid polymers for oral drug delivery carrier I: hydrogel dissolution and insulin release under neutral pH condition. *Eur J Pharm Sci* 23:261–270
- Nho YC, Mook Lim Y, Moo Lee Y (2004) Preparation, properties and biological application of pH-sensitive poly(ethylene oxide) (PEO) hydrogels grafted with acrylic acid(AAc) using gamma-ray irradiation. *Radiat Phys Chem* 71:239–242
- Omidian H, Rocca JG, Park K (2005) Advances in superporous hydrogels. *J Controlled Release* 102:3–12
- Patachia S, Valente AJM, Baciuc C (2007) Effect of non-associated electrolyte solutions on the behaviour of poly(vinyl alcohol)-based hydrogels. *Eur Polym J* 43:460–467
- Paulino AT, Guilherme MR, Reis AV, Campese GM, Muniz EC, Nozaki J (2006) Removal of methylene blue dye from an aqueous media using superabsorbent hydrogel supported on modified polysaccharide. *J Colloid Interface Sci* 301:55–62
- Paulino AT, Guilherme MR, Reis AV, Tambourgi EB, Nozaki J, Muniz EC (2007) Capacity of adsorption of Pb<sup>2+</sup> and Ni<sup>2+</sup> from aqueous solutions by chitosan produced from silkworm chrysalides in different degrees of deacetylation. *J Hazard Mater* 147:139–147
- Peppas NA, Bures P, Leobandung W, Ichikawa H (2000) Hydrogels in pharmaceutical formulations. *Eur J Pharm Biopharm* 50:27–46
- Pourjavadi A, Harzandi AM, Hosseinzadeh H (2004) Modified carrageenan 3. Synthesis of a novel polysaccharide-based superabsorbent hydrogel via graft copolymerization of acrylic acid onto kappa-carrageenan in air. *Eur Polym J* 40:1363–1370
- Pourjavadi A, Hosseinzadeh H, Mahdavinia GR, Zohuriaan-Mehr MJ (2007a) Carrageenan-g-poly(sodium acrylate)/kaolin superabsorbent hydrogel composites: synthesis, characterisation and swelling behaviour. *Polym Polym Compos* 15:43–51
- Pourjavadi A, Hosseinzadeh H, Sadeghi M (2007b) Synthesis, characterization and swelling behavior of gelatin-g-poly(sodium acrylate)/kaolin superabsorbent hydrogel composites. *J Compos Mater* 41:2057–2069
- Qiu Y, Park K (2001) Environment-sensitive hydrogels for drug delivery. *Adv Drug Deliv Rev* 53:321–339
- Raj Singh TR, McCarron PA, Woolfson AD, Donnelly RF (2009) Investigation of swelling and network parameters of poly(ethylene glycol)-crosslinked poly(methyl vinyl ether-co-maleic acid) hydrogels. *Eur Polym J* 45:1239–1249
- Ren JL, Sun RC (2010) Hemicelluloses. Cereal straw as a resource for sustainable biomaterials and biofuels. Elsevier, Amsterdam
- Sahoo A, Ramasubramani KRT, Jassal M, Agrawal AK (2007) Effect of copolymer architecture on the response of pH sensitive fibers based on acrylonitrile and acrylic acid. *Eur Polym J* 43:1065–1076
- Sasa N, Yamaoka T (1994) Surface-activated photopolymer microgels. *Adv Mater* 6:417–421
- Schild HG (1992) Poly(N-isopropylacrylamide): experiment, theory and application. *Progress Polym Sci* 17:163–249
- Seoudi R (2008) Effect of polyvinyl alcohol molecular weight and UV-photoactivation on the size of gold nanoparticle. *Physica B* 403:4236–4240
- Shah CP, Singh KK, Kumar M, Bajaj PN (2010) Vinyl monomers-induced synthesis of polyvinyl alcohol-stabilized selenium nanoparticles. *Mater Res Bull* 45:56–62
- Sheikh N, Jalili L, Anvari F (2010) A study on the swelling behavior of poly(acrylic acid) hydrogels obtained by electron beam crosslinking. *Radiat Phys Chem* 79:735–739
- Shirsath SR, Hage AP, Zhou M, Sonawane SH, Ashokkumar M (2011) Ultrasound assisted preparation of nanoclay Bentonite-FeCo nanocomposite hybrid hydrogel: a potential responsive sorbent for removal of organic pollutant from water. Desalination

- Shukla NB, Daraboina N, Madras G (2009) Oxidative and photooxidative degradation of poly (acrylic acid). *Polym Degrad Stab* 94:1238–1244
- Siemoneit U, Schmitt C, Alvarez-Lorenzo C, Luzardo A, Otero-Espinar F, Concheiro A, Blanco-Méndez J (2006) Acrylic/cyclodextrin hydrogels with enhanced drug loading and sustained release capability. *Int J Pharm* 312:66–74
- Singh B, Chauhan GS, Kumar S, Chauhan N (2007) Synthesis, characterization and swelling responses of pH sensitive psyllium and polyacrylamide based hydrogels for the use in drug delivery (I). *Carbohydr Polym* 67:190–200
- Solpan D, Duran S, Saraydin D, Güven O (2003) Adsorption of methyl violet in aqueous solutions by poly(acrylamide-co-acrylic acid) hydrogels. *Radiat Phys Chem* 66:117–127
- Solpan D, Duran S, Torun M (2008) Removal of cationic dyes by poly(acrylamide-co-acrylic acid) hydrogels in aqueous solutions. *Radiat Phys Chem* 77:447–452
- Tada D, Tanabe T, Tachibana A, Yamauchi K (2005) Drug release from hydrogel containing albumin as crosslinker. *J Biosci Bioeng* 100:551–555
- Talpur FN, Bhanger MI, Memon NN (2009) Milk fatty acid composition of indigenous goat and ewe breeds from Sindh, Pakistan. *J Food Compos Anal* 22:59–64
- Tanaka Y, Gong JP, Osada Y (2005) Novel hydrogels with excellent mechanical performance. *Prog Polym Sci* 30:1–9
- Tang Q, Wu J, Sun H, Fan S, Hu D, Lin J (2008) Superabsorbent conducting hydrogel from poly (acrylamide-aniline) with thermo-sensitivity and release properties. *Carbohydr Polym* 73:473–481
- Thakur VK, Thakur MK (2014a) Recent trends in hydrogels based on psyllium polysaccharide: a review. *J Clean Prod* 82:1–15
- Thakur VK, Thakur MK (2014b) Recent advances in graft copolymerization and applications of Chitosan: a review. *ACS Sustain Chem Eng* 2(12):2637–2652
- Thakur VK, Thakur MK (2015) Recent advances in green hydrogels from lignin: a review. *Int J Biol Macromol* 72:834–847
- Tomic SL, Micic MM, Filipovic JM, Suljovrujic EH (2007) Swelling and drug release behavior of poly(2-hydroxyethyl methacrylate/itaconic acid) copolymeric hydrogels obtained by gamma irradiation. *Radiat Phys Chem* 76:801–810
- Tu H, Qu Y, Hu X, Yin Y, Zheng H, Xu P, Xiong F (2010) Study of the sigmoidal swelling kinetics of carboxymethylchitosan-g-poly(acrylic acid) hydrogels intended for colon-specific drug delivery. *Carbohydr Polym* 82:440–445
- Turkington AV, Paradise TR (2005) Sandstone weathering: a century of research and innovation. *Geomorphology* 67:229–253
- Uchida R, Sato T, Tanigawa H, Uno K (2003) Azulene incorporation and release by hydrogel containing methacrylamide propyltrimethylammonium chloride, and its application to soft contact lens. *J Controlled Release* 92:259–264
- Varshosaz J, Falamarzian M (2001) Drug diffusion mechanism through pH-sensitive hydrophobic/polyelectrolyte hydrogel membranes. *Eur J Pharm Biopharm* 51:235–240
- Vital SA, Fowler RW, Virgen A, Gossett DR, Banks SW, Rodriguez J (2008) Opposing roles for superoxide and nitric oxide in the NaCl stress-induced upregulation of antioxidant enzyme activity in cotton callus tissue. *Environ Exp Bot* 62:60–68
- Wang B, Xu X-D, Wang Z-C, Cheng S-X, Zhang X-Z, Zhuo R-X (2008) Synthesis and properties of pH and temperature sensitive P(NIPAAm-co-DMAEMA) hydrogels. *Colloids Surf B* 64:34–41
- Wang Q, Xie X, Zhang X, Zhang J, Wang A (2010). Preparation and swelling properties of pH-sensitive composite hydrogel beads based on chitosan-g-poly (acrylic acid)/vermiculite and sodium alginate for diclofenac controlled release. *Int J Biol Macromol* 46:356–362
- Wei Q, Li J, Qian B, Fang B, Zhao C (2009) Preparation, characterization and application of functional polyethersulfone membranes blended with poly (acrylic acid) gels. *J Membr Sci* 337:266–273
- Xiang Y, Peng Z, Chen D (2006) A new polymer/clay nano-composite hydrogel with improved response rate and tensile mechanical properties. *Eur Polym J* 42:2125–2132



- Xiong Z, Chen H, Xu LA, Zhang LF, Xiong CD, Huang X (2007) Preparation and properties of thermo-sensitive hydrogels of konjac glucomannan grafted *N*-isopropylacrylamide for controlled drug delivery. *Iran Polym J* 6:425–431
- Xiong C, Yao C, Wang L, Ke J (2009) Adsorption behavior of Cd(II) from aqueous solutions onto gel-type weak acid resin. *Hydrometallurgy* 98:318–324
- Yadvinder S, Bijay S, Timsina J, Donald LS (2005) Crop residue management for nutrient cycling and improving soil productivity in rice-based cropping systems in the tropics. *Advances in agronomy*. Academic Press
- Yang C-C, Lin S-J, Hsu S-T (2003) Synthesis and characterization of alkaline polyvinyl alcohol and poly(epichlorohydrin) blend polymer electrolytes and performance in electrochemical cells. *J Power Sources* 122:210–218
- Yang S, Li J, Shao D, Hu J, Wang X (2009) Adsorption of Ni(II) on oxidized multi-walled carbon nanotubes: effect of contact time, pH, foreign ions and PAA. *J Hazard Mater* 166:109–116
- Yoo MK, Sung YK, Lee YM, Cho CS (2000) Effect of polyelectrolyte on the lower critical solution temperature of poly(*N*-isopropyl acrylamide) in the poly(NIPAAm-co-acrylic acid) hydrogel. *Polymer* 41:5713–5719
- Zhang JT, Cheng SX, Huang SW, Zhuo RX (2003) Temperature-sensitive poly (*N*-isopropylacrylamide) hydrogels with macroporous structure and fast response rate. *Macromol Rapid Commun* 24:447–451
- Zhang X, Wu D, Chu CCC-C (2004) Synthesis and characterization of partially biodegradable, temperature and pH sensitive Dex-MA/PNIPAAm hydrogels. *Biomaterials* 25:4719–4730
- Zhang YT, Fan LH, Zhi TT, Zhang L, Huang H, Chen HL (2009) Synthesis and characterization of poly(acrylic acid-co-acrylamide)/hydrotalcite nanocomposite hydrogels for carbonic anhydrase immobilization. *J Polym Sci Part A Polym Chem* 47:3232–3240
- Zhao H, Li J, Jiang L (2004) Inhibition of HIV-1 TAR RNA-Tat peptide complexation using poly (acrylic acid). *Biochem Biophys Res Commun* 320:95–99
- Zheng Y, Wang A (2009) Evaluation of ammonium removal using a chitosan-g-poly (acrylic acid)/rectorite hydrogel composite. *J Hazard Mater*
- Zheng Y, Hua S, Wang A (2010) Adsorption behavior of Cu<sup>2+</sup> from aqueous solutions onto starch-g-poly(acrylic acid)/sodium humate hydrogels. *Desalination* 263:170–175
- Zheng Y, Huang D, Wang A (2011) Chitosan-g-poly(acrylic acid) hydrogel with crosslinked polymeric networks for Ni<sup>2+</sup> recovery. *Analytica Chimica Acta* 687:193–200

# Chapter 12

## Neuro-Evolutive Techniques Applied for Modeling Processes Involving Polymer Gels



Silvia Curteanu and Elena-Niculina Dragoi

### 1 Artificial Neural Networks—General Aspects

Artificial neural networks (ANNs) are efficient tools for complex, nonlinear process modeling, especially when the development of the phenomenological models is difficult or impossible to perform. Processes involving polymer gels are typical examples, because, in many situations, the chemical and physical laws that govern them are unknown or mathematical models do not provide accurate results. Empirical modeling, based on experimental data, becomes a suitable alternative, with good chances to design reliable models.

The main advantages of ANN-based techniques are: (i) They work with input–output data, detailed knowledge of the phenomenology of the processes not being required; (ii) compared with phenomenological models, ANNs are much simpler and the necessary calculations are faster—an important aspect for process control applications; (iii) once developed and trained, they can make multiple predictions in a facile manner; (iv) in the majority of cases, their results are accurate and reliable; (v) they can be combined with other techniques resulting efficient hybrid configuration tools.

On the other hand, in the context of chemical applications, particularly polymer gels, the neural network modeling results can provide useful information for experimental practice, such as: (i) substitute or better schedule the experiments that are materials, energy, and time consuming; (ii) emphasize the maximum performance of the systems and the conditions necessary to accomplish them; (iii) within the molecular design, the predictions clearly underline the structure–properties relationship. In addition, these achievements bring important economic benefits, the use of the modeling techniques representing an important stage in the optimal

---

S. Curteanu (✉) · E.-N. Dragoi

Department of Chemical Engineering, Faculty of Chemical Engineering and Environmental Protection, “Gheorghe Asachi” Technical University, Iasi, Romania  
e-mail: [silvia\\_curteanu@yahoo.com](mailto:silvia_curteanu@yahoo.com)

control engineering. Through the improvement in process performance and the possibility of hierarchical control, the consumption of energy can be reduced and final products of greater purity can be obtained with the same exploitation cost, while increasing the safety of the processes.

The flexibility of the neural network modeling (as result of the empirical character of using only input–output data) determines the general character of the methodology, which means an easy adaption and application to different processes and systems.

Undoubtedly, the methodology for modeling with neural networks should take into account the characteristics specific to the approached chemical engineering process. On the other hand, it benefits of a significant degree of flexibility and generality, determined by the black box nature of ANNs, so it can be easily adapted to modeling of other processes and systems.

Generally, as main steps within the ANN modeling methodology can be enumerated: (i) establishing the input–output data according to the considered process and the goal of modeling; (ii) collecting the data which will be the training data set, through experiments or simulations; (iii) selecting the topology of the neural model and training the network; (iv) testing the generalization capability of the neural model.

*Choosing the appropriate set of data* for training, as number and distribution in the investigated domain (sufficient number according to the number of inputs and outputs, and uniform coverage of the domain), is a first requirement for developing an adequate model. An important aspect is related to the correct choice of input and output measurements, in accordance with the requirements of the modeling technique.

*Processing the independent and dependent variables* is necessary as distinct step in an appropriate modeling methodology. In order to obtain better results, input and output variables should be scaled within the same range or the same variance and shifted to the general region of ANN initial conditions (Fernandes and Lona 2005).

One major problem in the development of neural network model is *determining the network architecture*, mainly the number of hidden layers and the number of neurons in each hidden layer. Due to a series of aspects such as high number of parameters, various possible combinations, multiple training algorithms (each having various drawbacks), and lack of consistent rules, determining the optimal topology and internal parameters of neural networks is a difficult task (Curteanu and Cartwright 2011).

Various methods have been applied for developing neural models, among which trial and error is frequently used. This is realized by testing several topologies and comparing the prediction errors. Low errors indicate potentially good architectures—neural network topologies with chances to train well and to output good results (Curteanu et al. 2011). Fernandes and Lona (2005) developed some rather general rules to guide a trial-and-error search, classifying networks by the ratio of the number of input variables to the number of output variables.

However, trial-and-error method does not offer the guarantee of obtaining the best, optimal models. Other methods for developing neural network topology

include: (i) empirical or statistical methods (Viswanathan et al. 2005; Sukthomya and Tannock 2005; Balestrassi et al. 2009), in which ANN's internal parameters are adjusted based on the model performance; (ii) constructive (Ma and Khorasani 2004; Firat et al. 2010; Elizondo et al. 2007) and/or pruning algorithms (Shahjahan and Murase 2006; Xing and Hu 2009; Ward and Harmarneh 2010) that add and/or remove neurons or weights from an initial architecture, respectively, based on a predefined link between architecture and ANN performance.

Evolutionary algorithms (EAs) have been used on a large scale for designing the topology of an artificial neural network and for determining the optimal set of network weights in the training phase. The advantage of this approach consists in: (1) simultaneous evolution of several defined features; (2) a flexible definition of performance criterion; (3) possibility of coupling an EA with a learning algorithm (Floreano et al. 2008).

Once trained, the network is able to make predictions, recognizing, and interpreting data not previously seen (Curteanu and Cartwright 2011). *Testing* the robustness or generalization capability of the developed models is a key issue in neural network modeling, showing how well the model performs on “unseen” data. It is important for obtaining an accurate model that can generate good predictions in agreement with the experimental testing data.

The majority of works in the open literature employs *feed-forward multiplayer perceptron* (MLP) because it has a simple structure—simple interconnected neurons organized in layers—and can be applied to approximate virtually any smooth, measurable functions. Multilayered feed-forward fully connected networks are efficient tools in process modeling. They can provide high-quality results, and they can, in principle, reproduce the behavior of any measurable function to any desired degree of accuracy, acting in this way as universal approximator. In these circumstances and using a trial-and-error method for determining the best architecture, MLP, with different number of hidden layers and neurons, is the first choice in the modeling procedure. Practical applications show that MLP provides, in the most cases, the best results compared to other types of neural networks.

Other possibilities can also be taken into consideration, especially neural networks with recurrence for long-term predictions (Jordan Elman and recurrent networks) or stacked neural networks, which aggregate different individual networks, combining their advantages.

## 2 Difficulties in Modeling of Polymerization Processes

In the chemical engineering field, there are numerous processes and systems for which chemical and physical laws controlling their behavior are missing or are limited. In such cases, phenomenological models cannot be developed or are affected by significant errors. Empirical modeling, based on experimental data, is a useful tool, with real chances to provide accurate results. Neural networks belong to this category, operating on the “black box” principle, with input–output data.

For complex chemical processes, highly nonlinear, in addition to the difficulty of obtaining a mechanistic model, one has to consider the difficulties of solving the mathematical models, often represented by systems of differential equations. Quantifying the dependence between output and input through neural networks avoids such problems.

Another major difficulty in the control of chemical product quality is the lack of “online” measurements for some variables and the delays accompanying the measurements.

Further difficulties in process modeling can be identified in the complex field of polymerization processes.

Polymeric products often contain numerous materials added to give them various useful features. Therefore, the most widely applied method for the synthesis of these materials is batch polymerization that becomes useful for obtaining polymers with different properties, by changing the initial working conditions. Discontinuous operation is a dynamic process, with the reaction conditions often carrying in a fairly wide area. Therefore, data collection for modeling is difficult, their small number assuming also difficulties of obtaining the necessary configuration of the controllers.

Unlike discontinuous processes, continuous polymerizations receive significant amounts of data and precise adjustments, corresponding to the narrow operating areas (Tian et al. 2001).

One of the most important features of polymerization is the significant increase in viscosity as the reaction progresses, especially for homogeneous systems, such as bulk and solution polymerizations. Under these conditions, the heat transfer, associated with the considerable exothermicity of the reaction, is difficult. In terms of kinetics, the viscosity changes make initiation, propagation, and especially, termination become diffusion controlled. These phenomena are the cage, glass, and gel effects, representing the most difficult part to model in a polymerization process.

The development of a kinetic model for free radical polymerization is not an easy task, especially when the process is carried out at high temperatures and pressures. These difficulties are due to the complex reactions occurring simultaneously in the reactor and to the limited understanding of the physical and chemical phenomena related to the mixtures including polymers.

Another problem related to the polymerization reactors is represented by the possibility of multiple responses. Various operating conditions (various concentrations of the feed, temperatures, pressures, addition rates of catalysts) can lead to the same type of polymer (the same molecular weight, density, composition), but with different yields.

To ensure a certain quality of products is a more difficult task for polymerization processes than for traditional reactions involving small molecules because the morphological and molecular properties of a polymer product strongly influence its physical, chemical, thermal, rheological, and mechanical properties, as well as the end-use applications of the polymer. From this point of view, the development of mathematical models to predict the polymer quality in terms of the operating

conditions in a polymerization reactor is usually the key of obtaining an efficient production and an improvement of the plant operation (Tian et al. 2001).

Many researchers performed detailed studies on the mechanistic modeling of the polymerization reactors. However, a complete mechanistic model should contain a large number of differential equations and, therefore, would require considerable time for solving them. In addition, the model contains many kinetic parameters difficult to be determined with precision. Also, the development of the model, particularly the model for diffusion controlled reactions, in batch or semi-batch operating conditions, is extremely difficult for the manufacture of polymers with different specifications in the same installation.

An alternative to the phenomenological modeling is represented by the empirical modeling because it requires fewer process-specific knowledge. Empirical modeling technique requires data (measurements) on the variables considered representative for the process behavior and for the quality or properties of the product or system. Statistical regression methods and artificial neural networks are commonly used lately for building empirical models.

### 3 Neuro-Evolutionary Techniques

Determining the optimal structure of an ANN is a difficult task, which, in a majority of cases, is treated like a trial-and-error process that depends heavily on the experience of the researcher, is time consuming (due to the high number of possible combinations) and does not ensure reaching an optimal solution (Fe et al. 2015; Vlahogianni et al. 2005). Another aspect that must be taken into consideration when efficiently using ANNs is the fact that the network topologies must be correlated with the nature of application and with the type of system being modeled (Lobato et al. 2009). As the topology of the ANN and its internal parameters play a crucial role on the model's performance, their optimal setting is based on a multitude of factors (such as type of ANN, complexity, characteristics of the system being modeled) and there are no strict rules that can be used to determine their correct values. The automatic determination of these parameters can improve the model development and eliminate or reduce some of the problems associated with the manual selection. One of the most used approaches for automatic topology and/or internal ANN parameter determination is represented by neuro-evolution.

Neuro-evolution is the process in which the learning and evolution represent two fundamental forms of artificial neural network adaptation (Xin 1999). This approach of evolving ANNs using evolutionary algorithms (EAs) that relies on the search process to build an ANN is also known as Evolutionary Artificial Neural Networks (EANNS) and represents a new way of solving reinforcement-learning problems (Kohl and Miikkulainen 2009). This evolutive approach has a series of advantages such as (i) several features can be evolved; (ii) the definition of performance criterion is flexible; (iii) there is the possibility of combining evolution with a classic learning algorithm; (iv) ability to escape local minima (Abbass 2001;

Floreano et al. 2008). The characteristics of the search space (surface that represents all potential values for the selected ANN parameters) that indicate the EAs as better search approach in comparison with the constructive and destructive variants are: (i) infinitely large (the combination neuron-connection parameters is unbounded); (ii) no differentiable (change in neurons/weights can have a discontinuous influence on performance); (iii) complex and noisy; (iv) deceptive (similar topologies can have different performances); (v) multimodal (different topologies can have the same performance) (Volna 2010).

The elements that distinguish the approaches used in neuro-evolution are (i) what parameters of the ANNs are optimized and (ii) what is the difference between solutions (Islam and Yao 2008). Regarding the parameters considered for optimization, the evolution can be applied for topology, weights, learning rules. In case of topology optimization, parameters such as number of hidden layers and neurons in each hidden layer are considered for automatic determination, while the training is performed using classical approaches. For the weight optimization (also called training), the topology is set fixed and the weights are evolved until a minimum difference between expected and predicted values is obtained. Although this approach is successfully used since the development of neuro-evolutionary methods, the fixed topology strategy has some limits related to the issue of selecting the appropriate topology (Kohl and Miikkulainen 2009). In case of learning rule evolution, this can be seen as a process of “learning to learn” (Islam and Yao 2008), where the encoding of the parameters specific to the training process represents the first step (Jung and Reggia 2008).

Along the parameters, the second aspect that must be taken into consideration is represented by encoding. When evolving only the weights, two types of encoding are usually encountered: binary (each weight is encoded using a specific number of bits) and real coding (each weight is encoded using a real number). When evolving architecture or both architecture and weights and/or learning rules, there are usually two types of encoding: direct and indirect. In the direct encoding, there is a one-to-one mapping between genotype and phenotype, while in the indirect encoding (which can produce a more compact genotype), the genome contains instructions that must be executed to determine the network (Islam and Yao 2008). Within neuro-evolution, a specific terminology is used to represent neural network structure and the individuals of the evolutionary algorithm. Therefore, EAs work with a population of genotypes and the neural network is represented by a phenotype.

As it can be observed, in order to apply neuro-evolution to solve a specific problem, different aspects must be considered. However, the application range of this class of approaches is large, and all the systems that can be solved using ANNs can benefit from EANNs. To the author’s knowledge, in the area of polymer gels, there are no applications of EANNs. However, in the polymer area, there are a few applications where neuro-evolution was used (Table 1).

**Table 1** Examples of neuro-evolution applications in polymerization

Manuscript	Type of network	Optimizer	Application
Curteanu and Leon (2008)	Feed-forward neural model	Genetic algorithm	Free radical polymerization of methyl methacrylate
Curteanu et al. (2010)	Feed-forward neural model	Genetic algorithm	Fluorescence of polydimethylsiloxane/silica composites containing lanthanum
Zhao et al. (2010)	Radial basis function neural networks	Particle swarm optimizer	Melt index of propylene polymerization processes
Hosen et al. (2014)	Artificial neural networks	Simulated annealing	Polystyrene polymerization
Cuéllar et al. (2015)	Multilayer Perceptron	Genetic algorithms (NSGA-II)	Thermochromic sensor design based on Fe (II) spin crossover/polymers hybrid materials
Khayyam et al. (2015)	Levenberg–Marquardt neural network	Genetic algorithm	Polyacrylonitrile stabilization for carbon fiber production

## 4 Neural Networks Applied for Polymer Gels

The variation of the main parameters in the synthesis of polyacrylamide-based hydrogels was modeled in correlation with reaction conditions, using direct neural network modeling (Curteanu et al. 2008).

Hydrogels based on polyacrylamide (PAAm) have multiple applications, such as gel electrophoresis, soft contact lenses, thickener and suspending agents, subdermal filler for aesthetic facial surgery, soil conditioner on farmland, construction sites for erosion control or such materials for the removal of total organic content in water treatment plants.

Concerning the synthesis of polyacrylamide gels, they are usually obtained through copolymerization of acrylamide with a bifunctional monomer or by radical polymerization of acrylamide followed by crosslinking reaction. In our study (Curteanu et al. 2008), for this complex process, “single-step” method for polymerization/crosslinking is applied.

Experimental data have been used to train different neural networks that model the yield and swelling degree as function of reaction conditions—reactant concentrations, temperature, and reaction time. The neural network representing a compromise between generalization performance and size was MLP (5:20:2), a multilayer perceptron with one hidden layer and 20 neurons in this layer. The five input neurons correspond to the input variables: concentrations of monomer ( $C_M$ ), initiator ( $C_I$ ), crosslinking agent ( $C_A$ ), temperature ( $T$ ), and time ( $t$ ), and the two outputs are polymer yield ( $\eta$ ) and maximum swelling degree ( $\alpha$ ). A neural network has a good generalization capability if it finds a correct input–output relationship for input/output patterns of testing data (so-called unseen data, not used in the training/



**Table 2** Predictions of MLP (5:20:2) on validation data in direct modeling of polyacrylamide-based hydrogels

$C_M$ (mol/l)	$C_I$ (%) weight)	$C_A$ (mol/l)	$T$ (° C)	$t$ (h)	Experim. $\eta$ (%)	Experim. $\alpha$ (%)	Network $\eta$ (%)	Network $\alpha$ (%)
1.14	0.5	12.33	50	5	21.63	4870	20.92	4750
3	0.66	12.33	50	5	43.94	1281	43.92	1190
3	0.5	6	50	5	59.74	6478	62.02	6120
3	0.5	12.33	35	5	31.81	5102	29.50	4960
3	0.5	12.33	50	1	29.27	4663	32.50	4820
3	0.5	1	50	5	92.55	1250	92.81	1153
3	0.5	12.33	50	6	44.21	6263	44.10	6262

learning phase). An example of results is represented by the predictions of MLP (5:20:2) in comparison with experimental data (Table 2).

A good agreement between simulation and experimental data can be seen in Table 2, which is a proof for the possibility of using the projected neural model to make predictions under different reaction conditions, substituting the experiments that are time and material consuming. A long time, of order of months, is necessary for swelling degree determination.

In addition, an inverse neural network modeling was applied, meaning the determination of reaction conditions that lead to the imposed final properties. This is a particular optimization, with the advantage of substituting the process model with a simple and rapid technique.

For our case study—synthesis of polyacrylamide-based hydrogels—different optimization problems were formulated and solved applying inverse neural network modeling: (1) imposing the final yield and the working conditions—temperature, time, and crosslinking agent concentration—what are the optimal values for the initiator concentration and monomer concentration? (2) Imposing the final swelling degree and the working conditions—temperature, time, initiator concentration, and crosslinking agent concentration—what are the optimal value for the monomer concentration? (3) Imposing the polymer yield, the final swelling degree, and the reaction conditions—temperature, time, crosslinking agent concentration—what are the optimal values for the monomer concentration and initiator concentration? The last problem is more complex because it tries to establish both reaction yield and swelling degree, working with the monomer and initiator concentrations as decision variables. Table 3 presents examples of results—a MLP (5:33:11:2) has as input the five variables represented by reaction conditions, two intermediate layers with 33 and 11 neurons, respectively, and two output variables: swelling degree and reaction yield. Acceptable results are obtained, with a maximum of 10% error in the validation phase (with  $E_r$  in Table 3 representing the error).

One can conclude that neural network modeling methodology gives a very good representation of the polyamide-based hydrogels synthesis. It is a general technique that can be easily applied to other polymerization processes, with a minimum effort of adaptation.

**Table 3** Predictions of MLP (5:33:11:2) on validation phase for inverse neural modeling of polyacrylamide-based hydrogels (optimization 3)

$\eta$ (%)	$\alpha$ (%)	$T$ (°C)	$t$ (h)	$C_A$ conc. (mol/l)	Exp. $C_I$ (% wt)	Exp. $C_M$ (mol/l)	Net $C_I$ (% wt)	Net $C_M$ (mol/l)	$E_r$ init	$E_r$ mon
21.63	4870	50	5	12.33	0.5	1.14	0.55	1.19	10.0000	4.3860
43.94	1281	50	5	12.33	0.66	3	0.60	3.01	9.0909	0.1691
59.74	6478	50	5	6	0.5	3	0.52	2.97	4.0000	0.9661
31.81	5102	35	5	12.33	0.5	3	0.48	2.95	4.0000	1.6173
29.27	4663	50	1	12.33	0.5	3	0.45	2.70	10.0000	9.9510
92.55	1250	50	5	1	0.5	3	0.50	3.00	0.0524	0.0053
44.21	6263	50	6	12.33	0.5	3	0.50	3.00	0.0038	0.0967

Another example of neural network modeling approached the same type of compounds, polyacrylamide-based hydrogels, but a supplementary information is introduced in the database: a biodegradable interpenetrated polymer, forming semi- and interpenetrated multicomponent networks based on polyacrylamide (Curteanu et al. 2009). The yield in crosslinked polymer, the swelling degree, and the swelling rate constant was evaluated function of reaction conditions.

The available experimental data are divided into training (a number of 157 data) and validation (20 data, approximately 10%) data sets. Seven input variables were considered:  $C_M$  (monomer concentration),  $C_I$  (initiator concentration),  $C_A$  (crosslinking agent concentration), PI (amount of inclusion polymer),  $T$  (temperature),  $t$  (reaction time), and type of included polymer codified as 1—no polymer added, 2—starch, 3—poly(vinyl alcohol) (PVA), and 4—gelatin. The outputs of the neural model were  $\eta$  (yield in crosslinked polymer) and  $\alpha$  (swelling degree).

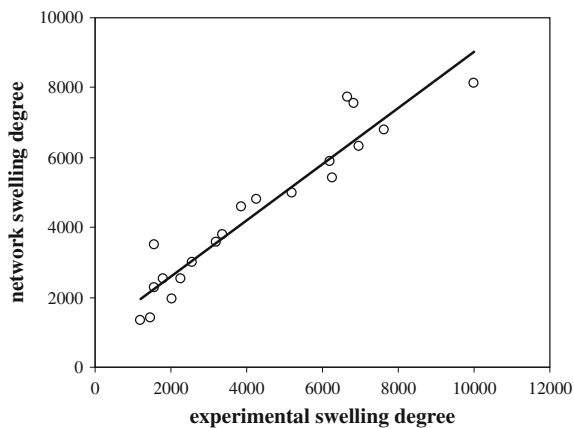
From the point of view of modeling, four types of neural networks that have as common characteristic the supervised learning control have been tested: Multilayer Perceptrons (MLPs), Generalized Feed-forward Networks (GFNs), Modular Neural Networks (MNNs) and Jordan Elman Networks (JENs). Accurate results are obtained with JEN neural network, having two hidden layers and 42 and 14 intermediate neurons, respectively, as Fig. 1 shows for swelling degree.

The study (Curteanu et al. 2009) develops a general methodology for neural network modeling which takes into account different types of neural networks, with high chances to be applied successfully to other complex polymerization processes.

An improved procedure, applied for the same database (synthesis of polyacrylamide-based multicomponent hydrogels) is represented by the development of stacked neural networks (Leon et al. 2010).

Stacked neural networks are obtained by integration of individual neural networks into an ensemble, with the goal of enhancing the model generalization capability through the possibility of using different networks, working in different domains. The idea of combining multiple networks for generating more accurate predictions than those provided by the individual neural networks alone is based on several considerations: (a) It is very difficult to obtain the optimal neural networks. (b) For an established topology, the parameters of the network can differ between

**Fig. 1** Validation phase for swelling degree predicted with neural model  
JEN (7:42:14:2)



one run of the algorithm and other. (c) Different activation functions and training algorithms can lead to different values for the neural network parameters. (d) Similarly, convergence criteria can determine different solutions for a given network architecture (Tian et al. 2001).

In our approach (Leon et al. 2010), three individual neural networks were combined, the stack output being a weighted sum of the individual network outputs. In addition, the contribution of the networks in the stack, quantified through their weights, was optimized using a method also based on neural networks. Several stacks are generated by successive trials, using different weights, and their performance was recorded for training and validation. For interpolation purposes, other two different neural networks (MLP type) are designed: one for the training and one for the validation phase.

The networks chosen for the stack were MLP (7:10:1), MLP (7:15:1), and MLP (7:12:4:1), and the Fig. 2 shows the chosen stack model for the swelling degree and yield of the hydrogels. The best results (correlation of 0.999 and error of 4.92%) in the validation phase were obtained with the stack including the above-mentioned individual networks with the contributions of 2, 40, and 58%, respectively.

Most of the characteristic properties for hydrogels are related to the phenomena of swelling/shrinkage accompanying the absorption/desorption processes. The behavior of gels in the processes of absorption/desorption is dependent on the macromolecular network features quantified through the reaction rate and process efficiency. On the other hand, these features are dependent on the synthesis conditions: nature and concentration of monomer, initiator and crosslinking agent concentrations, temperature and time of reaction. In order to obtain polyacrylamide hydrogels with appropriate features for using as pesticides, the influence of the main synthesis conditions of the crosslinked polymer on the reaction rate and swelling degree was studied by neural network modeling. Also, it was considered in the modeling methodology the conditions of “loading” of the polymer network with

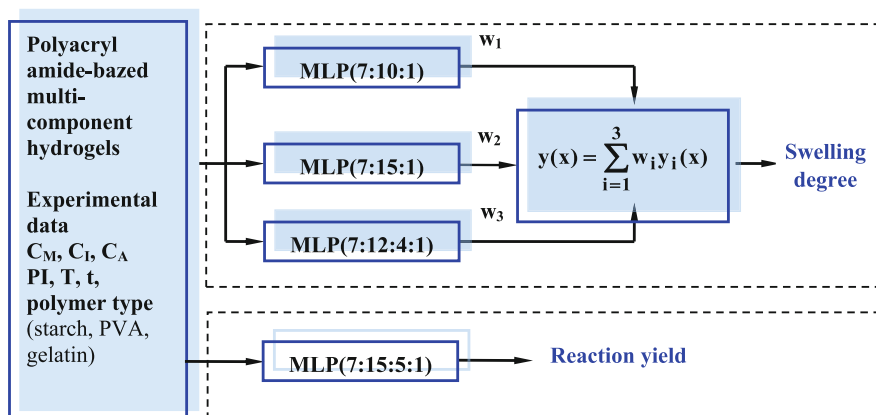


**Fig. 2** Representation of stacked modeling for swelling degree and yield of polyacrylamide-based hydrogels

copper sulfate. A radial basis function (RBF) neural network with high efficiency was designed to simulate this process (Piuleac et al. 2012).

Neural networks with radial basis functions (RBFs) are a common alternative to linear functions. They are nonlinear hybrid networks containing a single layer of processing elements (neurons). The model consists of an input layer retransmission entry without any processing, a layer of RBF neurons, and an output layer with neurons provided with linear activation function. Unlike perceptron-type networks in which neurons in a layer have connections to the next layer, the RBF network has synapses with neurons in the previous levels, achieving a local feedback, a re-entry of data principal flow. The architecture of these networks ranges from simple connection between two layers retrograde until completely connected network, each neuron receiving the input from all other neurons.

In this work (Piuleac et al. 2012), the reaction rate was evaluated as a function of synthesis conditions (time and copper sulfate concentration) using a RBF neural network. There were used 122 experimental data divided into training (90%) and validation (10%) sets and a trial-and-error method to find the best neural model. This was a RBF (2:6:1), with six hidden neurons, with a relative error of 2.7%, correlation around 0.99. Figure 3 shows the validation stage for the neural network model.

In Azzahari et al. (2016), for a gel polymer electrolyte system based on phthaloylchitosan, the process variables (lithium iodide, LiI, cesium iodide, CsI, and 1-butyl-3-methylimidazolium iodide, BMII) were investigated using a distance-based ternary mixture experimental design. A comparative approach was made between response surface methodology (RSM) and artificial neural networks (ANNs) to predict the ionic conductivity, proving better predictive results for artificial neural networks. Using experimental data, the ANN topologies were built, trained, tested, and validated, with a number of hidden layers varying from 1 to 9.

**Fig. 3** Validation results of the RBF (2:6:1) model developed for polyacrylamide hydrogels containing copper sulfate

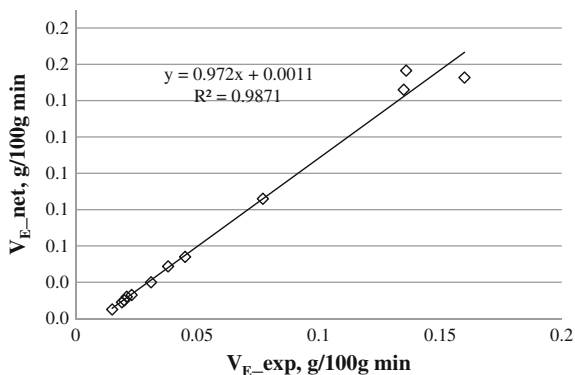
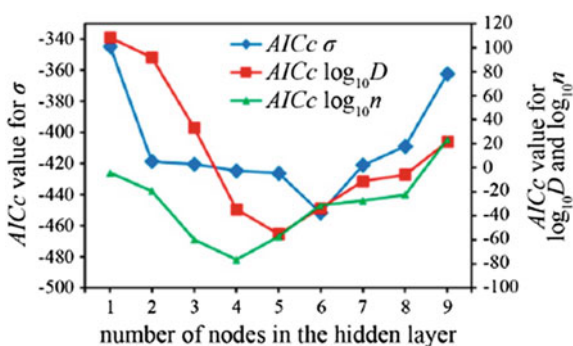


**Fig. 4** AICc for all the response outputs for a gel polymer electrolyte system based on phthaloylchitosan



Trial-and-error method was applied to develop the neural models, being conducted until minimum mean squared error was reached in the validation stage. Determination coefficient ( $R^2$ ) and Akaike Information Criterion (AIC), in a bias-corrected AIC variant (AICc), were used as indicators for the model selection. For instance, Fig. 4 shows AICc for all the response outputs: conductivity ( $\sigma$ ), diffusion coefficient ( $D$ ), and number density of charge carriers ( $n$ ).

Also, using ANN and RSM, the contribution of each of the four input variables (mixture ratio of LiI, CsI, BMII, and the sum wt% of the salt system) on the properties of prepared PhCh-(LiI:CsI:BMII) gel polymer electrolyte (GPE) was evaluated. The two methods provided different results, especially for the sum wt% of the salt system, as Fig. 5 shows. The authors argued that the ANN predictions are reliable.

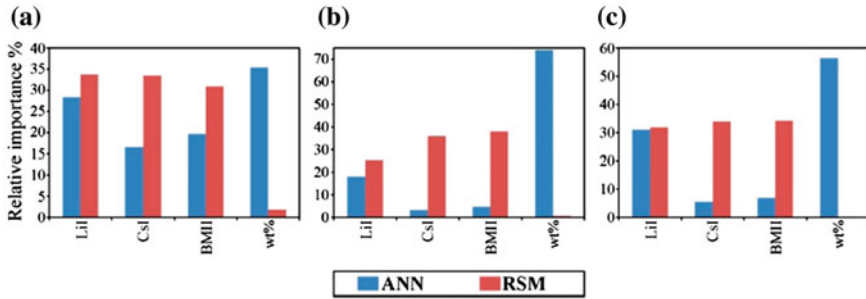


Fig. 5 Relative importance of single-input factors toward the output response properties for GPE

## 5 Case Studies

### 5.1 DE-ANN Methodology

DE is an evolutionary algorithm which has a good performance when applied to optimizations problems, indifferent of their type (linear/nonlinear, continuous, or combinatoric) (Feoktistov 2006). It is based on the Darwinian principle of evolution; its main idea consisting in evolving a population of individuals until a stop criterion is reached. In case of combining DE with ANNs and optimizing the ANNs parameters, the individuals represent encoded ANN structures. As many evolutionary algorithms, the main steps of DE are: (i) initialization; (ii) mutation; (iii) crossover, and (iv) selection.

In the initialization phase, a population of potential solutions is initialized (usually using random number generators). The closer the initial population to the solution, the faster the search procedure is.

In the mutation phase, a mutated population is created by adding a scaled differential term to a base vector. This approach is specific to DE algorithm and is the main mechanism by which more material is introduced into the population, as a mean to avoid local optimum trapping (Salman et al. 2007). Depending on the number of individuals participating in the mutation phase and the manner in which they are selected, different strategies can be encountered.

The crossover step represents a classical variant of diversity enhancement (Storn 2008), and in case of DE, two principal different types of crossover can be found: binomial and exponential. Based on the two parents, the crossover creates a child which has characteristics taken from both the parents. The difference between the two types of crossover is the manner in which the properties are selected from the parents. In the binomial case, they are randomly selected, and in the exponential crossover, they are chosen from compact sequences (Zaharie 2009). The mutation and crossover are directed by two parameters (mutation and crossover factors), their optimal values being dependent on the characteristics of the problem being solved.

In the last step, selection, the individuals from the initial population and from the one generated after crossover (also called trial population) undergo a “one-to-one” comparison, the best among them being selected to form the new generation.

The motivation for choosing DE in the detriment of other EAs is based on the fact that DE (i) is simple and straightforward to implement; (ii) has a reduced number of control parameters; (iii) has a low space complexity; (iv) is fast and robust. The three keys that ensure the DE success are based on: spontaneous self-adaptability, diversity control, and continuous improvement (Feoktistov 2006). Despite of its advantages, DE has a series of problems, mainly inherited from the EA class. In order to improve the performance and eliminate (or reduce) its disadvantages, a series of approaches can be used: (i) replacement of manual setting of control parameters with adaptive or self-adaptive procedures; (ii) hybridization with other global and/or local optimization techniques; (iii) proposal of new internal structures which can provide better individuals.

In the current work, the chosen DE-based variant uses all these directions of improvement. The variant is called SADE-NN-1 and was proposed in (Dragoi et al. 2012), where it was used to model, optimize, and control the freeze-drying process of some pharmaceutical products. The approach performs a simultaneous architectural and parametric optimization of ANNs with the scope of determining the optimal model with a reasonable amount of resources consumed. The characteristics of the SADE-NN-1 algorithm are: (i) use of opposition-based principle for improving the initialization; (ii) use of eight activation functions, where each neuron can have (at one time) one of the functions: Linear, Hard Limit, Bipolar Sigmoid, Logarithmic Sigmoid, Tangent Sigmoid, Sinus, Radial Basis with a fixed center point at 0, and Triangular Basis; (iii) a mutation scheme based on the principle of re-arranging the individuals using the fitness function; (iv) a self-adaptive procedure where the mutation and crossover factors ( $F$  and  $Cr$ , respectively) are included into the individuals and evolved as any other parameter; (v) a local search procedure, where Backpropagation is used to improve the best individual found so far. The simplified schema of SADE-NN-1 is presented in Fig. 6.

## ***5.2 DE-ANN Applied to the Synthesis of Polyacrylamide-Based Hydrogels***

For modeling the synthesis of a series of polyacrylamide-based hydrogels, a neuro-evolutive technique was applied, including differential evolution (DE) algorithm and ANNs. DE was used individually or combined with local search algorithms, obtaining improved methodologies with the role to develop optimal neural models.

In order to model the synthesis of polyacrylamide-based hydrogels, three cases were formulated. The first case is represented by the situation where a single model

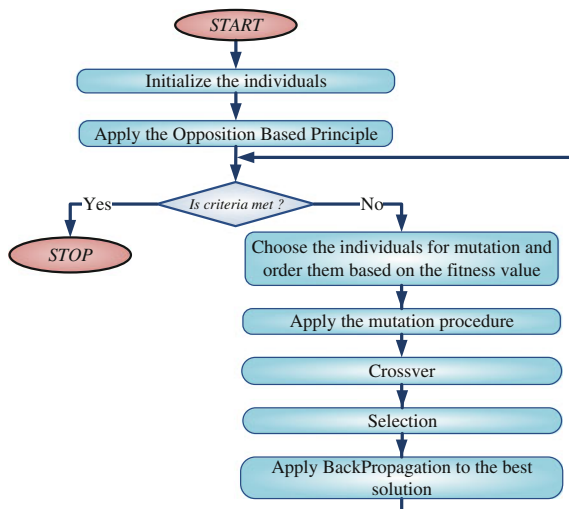


Fig. 6 SADE-NN-1 schema

Table 4 Simulation results for modeling the synthesis of polyacrylamide-based hydrogels

Output	Model	Fitness	MSE train	MSE test	Correll test 1	Correll test 2	Topology
1	Best	1.45E+04	6.89E-05	3.56E-04	9.75E-01	–	7:07:01
	Worst	4.52E+03	2.21E-04	1.17E-03	9.13E-01	–	7:07:01
	Average	7.85E+03	1.35E-04	6.79E-04	9.50E-01	–	–
2	Best	1.84E+03	5.43E-04	2.50E-03	8.51E-01	–	7:08:01
	Worst	6.42E+02	1.56E-03	2.58E-03	8.45E-01	–	7:19:01
	Average	1.15E+03	9.24E-04	2.48E-03	8.55E-01	–	–
All	Best	2.53E+03	3.95E-04	1.60E-03	9.41E-01	8.59E-01	7:19:02
	Worst	1.33E+03	7.54E-04	2.76E-03	8.07E-01	8.13E-01	7:06:02
	Average	1.85E+03	5.52E-04	1.95E-03	9.13E-01	8.36E-01	–

is determined for all the outputs. The other two cases are specific to the situation in which, for each output (yield and swelling degree), a model is determined separately. In each case, a set of 100 simulations were performed, the best, the worst, and the average data being presented in Table 4. In this table, Fitness represents the fitness function, MSE is the mean squared error, and Correll test 1 and 2 represent the correlation computed on the tested data, for the first and second output.

For the testing data, the comparison between the individual best models and the best ANN obtained when all outputs are considered is presented in Figs. 7 (for yield) and 8 (for swelling degree).



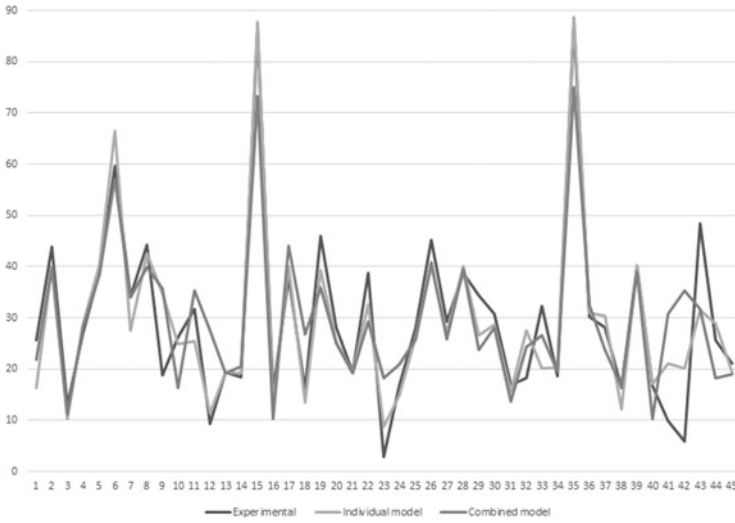


Fig. 7 Comparison between the best models obtained for yield of the reaction

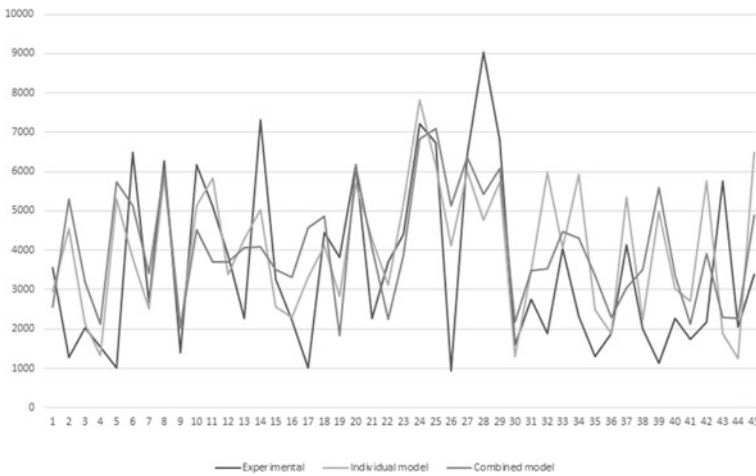


Fig. 8 Comparison between the best models obtained for swelling degree

As it can be observed from Figs. 7 and 8, the individual models are much better than the combined one. This can be explained by the fact that the two outputs are very distinct, their dynamic not having common elements.

### 5.3 *DE-ANN Technique Applied for Modeling the Release of Micromolecular Compounds from Hydrogels*

The absorption and releasing of small molecular compounds from hydrogel-type crosslinked systems are complex processes which are influenced both by factors related to the three-dimensional network as well as to the nature of the small molecular compounds incorporated into the gel. A simulation study applied to this process was carried out based on feed-forward neural networks, whose topologies were developed using an evolutionary technique, particularly differential evolution algorithm. Thus, neural network-based simulation was applied to determine the conditions of elimination/desorption of some compounds from the gels in order to assess the release rate appropriate for biomedical applications and the recovery of metal ions. At the same time, it was proven the efficiency of the DE algorithm for determining the near optimal architecture for the feed-forward neural networks.

Two multicomponent systems of hydrogel type were synthesized. Hydrogels “loaded” with small molecular compound were: (1) a physical gel based on poly(vinyl alcohol) (PVA) and the active compound hydrochloride N,N,N',N'-tetramethylthionine (CITMeTn), and (2) a permanently crosslinked gel based on polyacrylamide (PAAm), “loaded” with chromium chloride (III).

To obtain the physical gel, poly(vinyl alcohol) (PVA) and disodium tetraborate (borax) solutions were used. Biological active compound N,N,N',N'-tetramethylthionine-hydrochloride was used as aqueous solution. The syntheses were conducted at room temperature, with preset ratios of the components. The triazine derivative released from PVA–borax hydrogel was studied photocolorimetrically.

PAAm networks were used to investigate the absorption, diffusion, and release capacity of ions Cr (III) (Yanfeng et al. 2004). Chemical permanent crosslinked gels have been prepared by an original unistadial polymerization/crosslinking procedure of acrylamide (AAM). Syntheses were carried out in aqueous medium, respecting the predetermined conditions of temperature, process duration, and component concentrations (monomer, initiator, crosslinking agent) (Mihailescu et al. 2007). The obtained xerogels were loaded for 24 h with CrCl<sub>3</sub> solutions of different concentrations (4, 10, and 20%). Swelling degrees ( $\alpha_{24h}$ ) were determined by gravimetric method. Chromic ion release was followed spectrophotometrically, using a UV-1700 Pharma Spec unit (Shimadzu). The yield release of metal ions and the release rate were determined according to Eqs. (1) and (2).

$$\eta = 100 m_E/m_o \quad (1)$$

$$V_E = \eta/t \quad (2)$$

where:  $m_E$  is the mass of salt released,  $m_o$  is the mass of salt absorbed, and  $t$  is desorption time.

For the two above cases, the ANN-based modeling takes into account the evaluation of the elimination of some compounds with small molecules, respectively, (1) the elimination of the triazinic compound with biologic activity depending of the eluent volume; (2) the elimination of metallic ions as function of time and initial concentration.

Practical performances of the gels are directly correlated to the efficient control of absorption/desorption processes which are associated with swelling/collapsing phenomena. The relatively high number of factors that influence both the characteristics of the reticulated systems and the interactions that may occur between the components causes an advanced degree of complexity for the behavior of the "loaded" gels with small molecular compounds.

Synthesis of the PVA/borax gels is an opportunity to evaluate the antiseptic properties of borax. Potential disinfectant activity of such hydrogels can be achieved by "loading" the network with other biologically active compounds.

The introduction of active principles into the hydrogel three-dimensional network has a double effect: improvement for local administration by changing the architectural characteristics of the system and enhancing of the antiseptic and/or antimycotic action, as a result of synergism between borax and inclusion compound.

Complexity of diffusion phenomena requires a correlation between inflation processes and morpho-structural parameters of the polymer matrix.

In order to study the overall performance of the software application proposed for neural network architecture using DE algorithm, two case studies were performed. The first case consists in modeling the release of N,N,N',N'-tetramethylthionine chloride from PAV gels, and in the second case, the elimination of the metallic ions is studied by simulation.

### 5.3.1 N,N,N',N'-Tetramethylthionine Chloride Released from PAV Gels

The available database was split into training data set (75%) and testing data set (remaining 25%). The number of inputs and outputs of the neural network was fixed, being determined by the structure of the data. The input was the eluent volume, while the outputs were the real concentration of triazinic compound in washing water and CITMeTn (ratio between the amount of compound with biologic activity which has to be eliminated and the initial amount of compound).

Because the internal parameters of DE algorithm influence the results in a manner not yet fully understood by scientists, tests for  $F$  taking values in the interval [0.1, 0.9] and for  $Cr$  in the interval [0.91, 0.99] were performed. The fitness values and the architectures obtained are listed in Table 5. The bold cells represent the best results obtained with the two DE variants used.

**Table 5** Fitness values and architectures for the best neural networks obtained

Cr	0.1	0.2	0.3	0.4	0.5	0.6	0.7	0.8	0.9
VF									
0.91	Bin	141.07 (1:17:2)	58.76 (1:3:2)	56.63 (1:3:2)	386.05 (1:6:2)	88.89 (1:3:2)	33.38 (1:1:2)	12.57 (1:3:2)	9.82 (1:9:4:2)
	Exp	63.03 (1:13:2)	113.32 (1:11:2)	550.61 (1:3:2)	934.32 (1:1:2)	263.53 (1:2:2)	43.52 (1:8:2)	24.68 (1:1:2:2)	9.6 (1:8:2)
0.92	Bin	91.86 (1:1:2)	52.61 (1:10:2)	217.15 (1:8:2)	202.9 (1:4:2)	281.63 (1:1:2)	173.15 (1:1:2)	11.11 (1:3:2)	10.94 (1:1:2)
	Exp	34.46 (1:13:2)	154.48 (1:17:2)	516.73 (1:5:2)	478.16 (1:1:2)	190.68 (1:2:2)	63.54 (1:5:2)	22.97 (1:1:3:2)	15.9 (1:1:2)
0.93	Bin	119.96 (1:19:2)	57.77 (1:10:2)	130.199 (1:8:2)	<b>942.49</b> (1:1:2)	55.91 (1:2:2)	24.81 (1:3:2)	20.64 (1:1:2)	5.49 (1:3:2)
	Exp	61.17 (1:14:2)	73.9 (1:15:2)	259 (1:10:2)	942.48 (1:1:2)	85.89 (1:2:2)	24.62 (1:7:2)	20.46 (1:6:2)	14.93 (1:12:2)
0.94	Bin	88.64 (1:15:2)	8.55 (1:12:2)	172.72 (1:4:1:2)	793.21 (1:4:2)	942.26 (1:1:2)	45.36 (1:1:2)	15.39 (1:2:2)	10.1 (1:4:2)
	Exp	82.9 (1:20:2)	148.31 (1:4:2)	598.76 (1:3:2)	600.26 (1:2:2)	95.89 (1:11:2)	48.82 (1:10:2)	19 (1:2:2)	15.26 (1:3:2)
0.95	Bin	116.76 (1:20:2)	6.07 (1:2:4:2)	210.03 (1:4:2)	882.6 (1:3:2)	73.72 (1:8:2)	88.31 (1:1:2)	12.51 (1:1:2)	7.39 (1:7:2)
	Exp	57.51 (1:13:2)	92.89 (1:5:2)	729.97 (1:4:2)	747.77 (1:1:2)	80.84 (1:10:2)	46.87 (1:2:2)	27.44 (1:10:2)	16.19 (1:13:2)
0.96	Bin	90.61 (1:19:2)	25.06 (1:6:2)	36.4 (1:4:3:2)	464.17 (1:9:2)	83.13 (1:4:2)	158.28 (1:2:2)	11.77 (1:6:2)	12.78 (1:3:2)
	Exp	65.33 (1:15:2)	161.2 (1:14:2)	304.28 (1:5:2)	723.61 (1:1:2)	130.49 (1:5:2)	37.4 (1:3:2)	28.96 (1:4:2)	30.11 (1:7:2)
0.97	Bin	91.4 (1:18:2)	30.73 (1:7:2)	108.23 (1:2:2)	671.23 (1:6:2)	236.53 (1:7:2)	52.21 (1:2:2)	12.02 (1:8:2)	24.49 (1:2:2)
	Exp	6.42 (1:4:2)	106.13 (1:3:2)	601.77 (1:6:2)	557.42 (1:2:2)	153.57 (1:1:2)	60.4 (1:4:2)	16.67 (1:8:2)	22.34 (1:11:2)
0.98	Bin	81.06 (1:18:2)	24.82 (1:9:2)	56.57 (1:9:2)	180.57 (1:7:2)	142.35 (1:1:2)	58.28 (1:4:2)	16.08 (1:9:2)	12.38 (1:3:2)
	Exp	6.06 (1:4:3:2)	54.38 (1:16:2)	1099.61 (1:5:2)	152.64 (1:2:2)	419.94 (1:2:2)	22.63 (1:1:2)	22.92 (1:3:2)	21.58 (1:9:2)
0.99	Bin	50.66 (1:7:2)	17.58 (1:8:2)	56.86 (1:6:2)	556 (1:3:2)	180.47 (1:4:2)	69.06 (1:4:2)	8.51 (1:4:2)	14.17 (1:5:2)
	Exp	19.24 (1:6:2)	114.04 (1:17:2)	366.62 (1:3:2)	<b>1150.58</b> (1:11:2)	267.7 (1:4:2)	41.52 (1:4:2)	14.87 (1:8:2)	16.61 (1:14:2)

The fitness value is determined by using Eq. (3):

$$\text{Fitness} = \frac{1}{\text{MSE}_{\text{training}} + \text{MSE}_{\text{testing}} + \text{low}} \quad (3)$$

where  $\text{MSE}_{\text{training}}$  is the mean square error obtained in the training phase,  $\text{MSE}_{\text{testing}}$  is the mean square error in the testing phase, and  $\text{low}$  is a parameter introduced to eliminate the error  $\text{DividedBy0}$  obtained in Microsoft C# when  $\text{MSE}_{\text{training}}$  and  $\text{MSE}_{\text{testing}}$  are equal to 0. The value of the  $\text{low}$  parameter is  $e^{-10}$ .

Because the DE algorithm searched for the minimization of  $\text{MSE}_{\text{training}}$  and  $\text{MSE}_{\text{testing}}$ , and because the fitness was in inverse ratio to  $\text{MSE}_{\text{training}}$  and  $\text{MSE}_{\text{testing}}$ , the bigger value returned by the fitness functions indicated the best solution.

For each pair  $(Cr, F)$ , simulations were made using two variants of the DE algorithm. The difference between these two variants consisted in distinct crossover method: *binomial* ( $DE/\text{rand}/1/\text{bin}$ ) and *exponential* ( $DE/\text{rand}/1/\text{exp}$ ). In order to indicate the architecture, a structure coded as *inputs: neurons\_first\_hidden\_layer: neurons\_second\_hidden\_layer: outputs* was used for networks with two hidden layers. In case the network had just one hidden layer, the structure was represented as *inputs: neurons\_first\_hidden\_layer: outputs*.

As it can be noticed, for the  $DE/\text{rand}/1/\text{bin}$  variant, the best architecture was obtained with  $Cr = 0.93$  and  $F = 0.4$ , the fitness having a value of 942.49 (with a 1:1:2 topology). For the  $DE/\text{rand}/1/\text{exp}$  variant, the best architecture corresponds to  $Cr = 0.99$  and  $F = 0.4$ , the fitness value having a value of 1156.58 and a 1:11:2 topology. Although for this problem the more complex neural network had the best performance, not always this is the case because the performance is determined by the capacity of network to model the process.

The results obtained for the testing data and those expected (experimental data) are compared in Figs. 9 and 10 for the two outputs: the real concentration and the ratio between eliminated amount and initial amount of triazinic compound. The differences between simulation and experimental data were very low, proving the good generalization capabilities of the neural networks developed by DE algorithm.

The supplementary predictions performed with the best neural network, MLP (1:11:2), are listed in Table 6. The inputs correspond to arbitrarily chosen values for which no experiment was performed, so there were no means of comparing the predictions with some preexisting data. From the author's point of view, the results correspond to the specific interval in which the followed concentrations can take values.

### 5.3.2 CrCl<sub>3</sub> Released from PAAM-Based Hydrogels

The number of data used to model and simulate the release process of CrCl<sub>3</sub> (metallic ions) from synthesized gels was 106. As in the first case study, the data were split into 75% for training and 25% for testing. The selected inputs were the

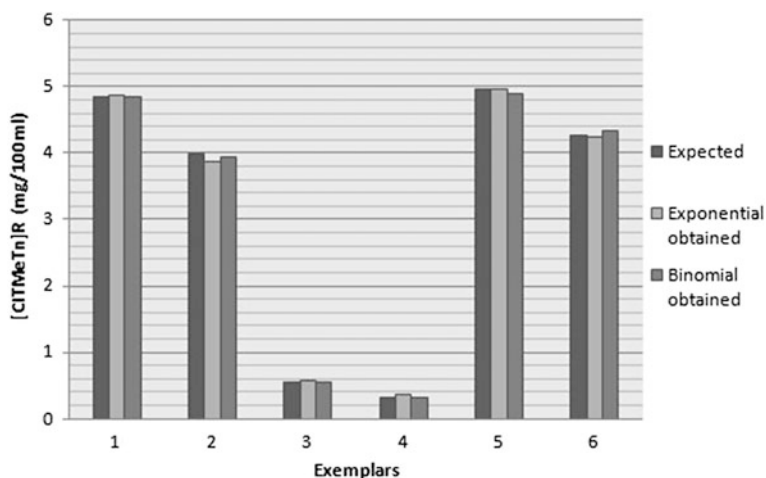


**Fig. 9** Differences between expected and obtained results for the first output (the real concentration of triazinic compound in washing water) of the neural networks MLP (1:11:2) and MLP (1:1:4), respectively

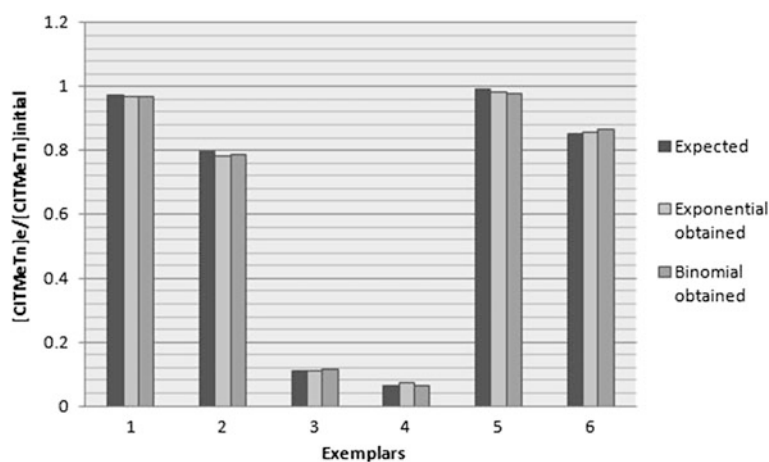


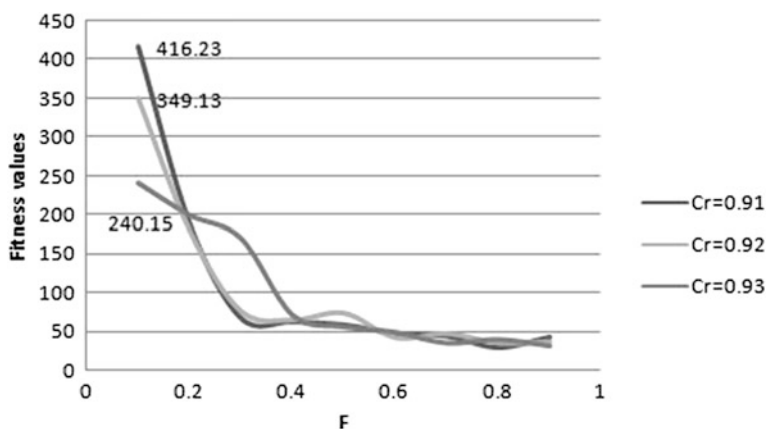
**Fig. 10** Differences between the expected and the obtained results for the second output (CITMeTn) of the neural networks, MLP (1:11:2) and MLP (1:1:4), respectively

concentration value of active compound and the time period waited from the beginning of the experiment in which the measurements were made. The output was the ratio between the concentration of active compound released and its initial concentration.

In order to determine the best neural network for the modeling of the physical-chemical process, the same variants of DE algorithm and the same parameters as

**Table 6** Predictions obtained with the best neural network MLP (1:11:2) for the N,N,N',N'-tetramethylthionine chloride release from PAV gels

Index	Input	Predictions	
	[CITMeTn] <sub>initial</sub>	[CITMeTn] <sub>R</sub> (mg/100 ml)	[CITMeTn] <sub>e</sub> /[CITMeTn] <sub>initial</sub>
1	3	0.141	0.031
2	11	0.91	0.188
3	19	2.452	0.497
4	27	3.863	0.776
5	35	4.45	0.892
6	43	4.816	0.964

**Fig. 11** Variations of the best fitness values in the DE based on binomial crossover

those in the previous case study were used. The variation of the fitness function in DE algorithm, using binomial and exponential crossover, with the control parameter,  $F$ , and for different values  $Cr$ , is presented in Figs. 11 and 12.

The best values for both DE variants were obtained when  $Cr = 0.91$  and  $F = 0.1$ , the fitness for DE/rand/1/bin being 416.23 with a 2:9:1 topology, and for DE/rand/1/exp being 311.93 with a 2:14:1 topology.

The results for the testing data and those expected for the two versions of the algorithm are compared in Fig. 13.

Although the differences between the results obtained by the two versions of the DE algorithm are higher than those in the first case, as a whole, the two neural networks gave, roughly speaking, the same results.

The predictions obtained with the best neural network, MLP (2:9:1), are listed in Table 7. The combinations of  $[CrCl_3]_0$  and time considered as inputs for prediction phase correspond to values that were not used in the training and testing steps. As a result, the values are new for the network. Because no previous experiments were

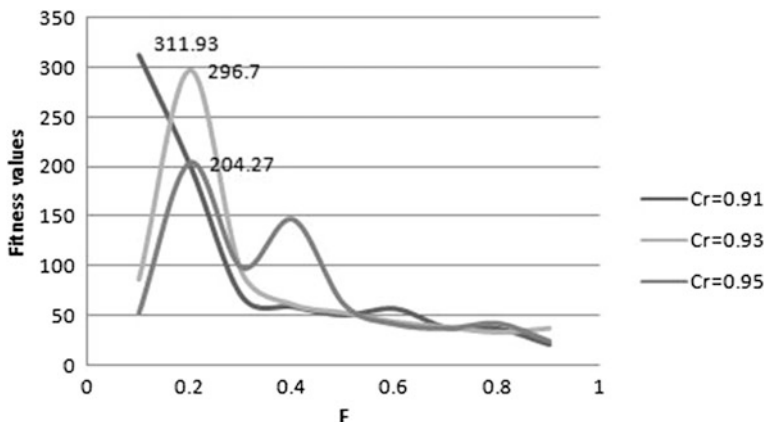


Fig. 12 Variations of the best fitness values in the DE based on exponential crossover

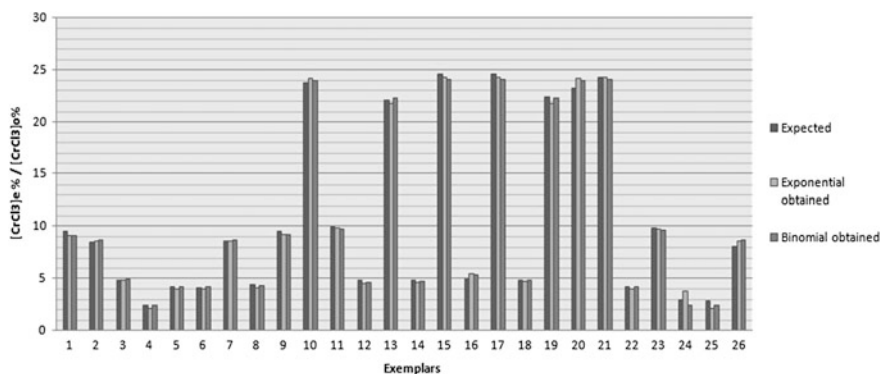


Fig. 13 Comparison between the results obtained with the two neural networks, MLP (2:14:1) and MLP (2:9:1), developed with exponential and binomial DE

performed with these input values, there is no data to compare the results, but, based on practical experience, the authors consider that they are in the correct interval.

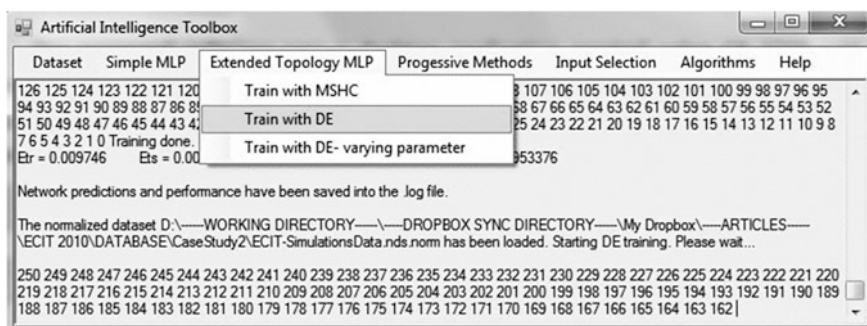
In order to obtain the two versions of the DE algorithm and, consequently, the neural networks used for modeling, a software application was created. The proposed software was a desktop application developed using C# with the target framework .NET Framework 3.5. The architecture was modular, each module being interconnected with the base module representing the neural network foundations.

The application was designed to have a simple and easy-to-use graphical interface. The targeted users were not only the IT specialists, but also the chemists who could easily perform experiments and create a neural network based on the experimental data.



**Table 7** Predictions obtained with the best neural network, MLP (2:9:1), for the CrCl<sub>3</sub> release from PAAM-based hydrogels

Index	Inputs	Time (s)	Prediction
	[CrCl <sub>3</sub> ] <sub>0</sub> %		[CrCl <sub>3</sub> ] <sub>e</sub> %/[CrCl <sub>3</sub> ] <sub>0</sub> %
1	20	19.5	3.942
2	10	39.5	9.382
3	20	99.85	5.009
4	10	14.5	8.746
5	10	59.5	9.537
6	20	4.5	2.873
7	10	1.5	4.073
8	20	1.5	2.105
9	20	139.5	5.318
10	4	1.5	19.122
11	10	19.5	9.226
12	20	69.5	4.773
13	4	4.5	22.764
14	10	4.5	7.715
15	4	14.5	24.236
16	4	19.5	24.275
17	20	29.5	4.462
18	20	14.5	3.904
19	4	9.5	22.803
20	20	49.5	4.617

**Fig. 14** User interface of the proposed software DE application

The developed neural networks could be used to model and predict new data without the necessity for new experiments. In this manner, time and expensive materials could be saved. In Fig. 14, the user interface of the proposed application is exemplified.

## 6 Conclusions

Polymer gels are important products with multiple applications in diverse areas. Simulation results bring significant contributions for experimental and industrial practice, offering the possibility to substitute or, at least, to schedule the experiments, which are time, materials, and energy consuming. Neural networks and other techniques from artificial intelligence domain, especially neuro-evolutionary methods, are recommended tools for this goal, based on the advantages of providing accurate and reliable results and of that they do not require knowledge about the processes.

Examples and case studies presented in this chapter (the majority of them belonging to the authors) emphasized different methodologies for neural network modeling, including: (i) neural models with trial-and-error or neuro-evolutionary methods; (ii) different types of neural networks, feed-forward or recurrent; (iii) individual or stacked neural networks. When using a variant of the ANN modeling methodologies, improvements are applied progressively with the goal of obtaining small errors. Also, an important aspect is the general character of the modeling procedures, which can be applied for different processes and systems with a minimum effort of adaptation.

## References

- Abbass HA (2001) A memetic pareto evolutionary approach to artificial neural networks. In: Stumptner M, Corbett D, Brooks M (eds) *AI 2001: advances in artificial intelligence*, vol 2256. Springer, Berlin, pp 113–152
- Azzahari AD, Yusuf SNF, Selvanathan V, Yahya R (2016) Artificial neural network and response surface methodology modeling in ionic conductivity predictions of phthaloylchitosan-based gel polymer electrolyte. *Polymers* 8:2–18
- Balestrassi PP, Popova E, Paiva AP, Marangon Lima JW (2009) Design of experiments on neural network's training for nonlinear time series forecasting. *Neurocomputing* 72:1160–1178
- Cuéllar MP, Lapresta-Fernández A, Herrera JM, Salinas-Castillo A, Pegalajar MDC, Titos-Padilla S, Capitán-Vallvey LF (2015) Thermochromic sensor design based on Fe(II) spin crossover/polymers hybrid materials and artificial neural networks as a tool in modelling. *Sens Actuators, B: Chem* 208:180–187
- Curteanu S, Cartwright H (2011) Neural networks applied in chemistry. I. Determination of the optimal topology of neural networks. *J Chemom* 25:527–549
- Curteanu S, Leon F (2008) Optimization strategy based on genetic algorithms and neural networks applied to a polymerization process. *Int J Quantum Chem* 108:617–630
- Curteanu S, Dumitrescu A, Mihailescu C, Simionescu B (2008) Neural network modeling applied to polyacrylamide based hydrogels synthesised by single step process. *Polym Plast Technol Eng* 47:1061–1071
- Curteanu S, Dumitrescu A, Mihailescu C, Simionescu B (2009) The synthesis of polyacrylamide-based multicomponent hydrogels. A neural network modeling. *J Macromol Sci Part A Pure Appl Chem* A46:368–380

- Curteanu S, Nistor A, Curteanu N, Airinei A, Cazacu M (2010) Applying soft computing methods to fluorescence modeling of the polydimethylsiloxane/silica composites containing lanthanum. *J Appl Polym Sci* 117:3160–3169
- Curteanu S, Piuleac CG, Godini K, Azaryan G (2011) Modeling of electrolysis process in wastewater treatment using different types of neural networks. *Chem Eng J* 172:267–276
- Dragoi EN, Curteanu S, Fissore D (2012) Freeze-drying modeling and monitoring using a new neuro-evolutive technique. *Chem Eng Sci* 72:195–204
- Elizondo D, Birkenhead R, Gongora M, Taillard E, Luyima P (2007) Analysis and test of efficient methods for building recursive deterministic perceptron neural networks. *Neural Netw* 20:1095–1108
- Fe JD, Aliaga RJ, Gadea-Girones R (2015) Evolutionary optimization of neural networks with heterogeneous computation: study and implementation. *J Supercomput* 71:2944–2962
- Feoktistov V (2006) *Differential evolution: in search of solutions*. Springer, Berlin
- Fernandes FAN, Lona LMF (2005) Neural network applications in polymerization processes. *Braz J Chem Eng* 22:323–330
- Firat M, Turan ME, Yurdusev MA (2010) Comparative analysis of neural network techniques for predicting water consumption time series. *J Hydrol* 51(384):46–51
- Floreano D, Durr P, Mattiussi C (2008) Neuroevolution: from architectures to learning. *Evol Intell* 1:47–62
- Hosen MA, Khosravi A, Nahavandi S, Creighton D (2014) Prediction interval-based neural network modelling of polystyrene polymerization reactor—A new perspective of data-based modelling. *Chem Eng Res Des* 92:2041–2051
- Islam M, Yao X (2008) Evolving artificial neural network ensembles. In: Fulcher J, Jain L (eds) *Computational intelligence: a compendium*, vol 115. Springer, Berlin, , pp 851–880 (Reprinted from: NOT IN FILE)
- Jung JY, Reggia J (2008) The automated design of artificial neural networks using evolutionary computation. In Yang A, Shan Y, Bui L (eds) *Success in evolutionary computation*, vol 92. Springer, Berlin, pp 19–41
- Khayyam H, Naebe M, Zabihi O, Zamani R, Atkiss S, Fox B (2015) Dynamic prediction models and optimization of polyacrylonitrile (PAN) stabilization processes for production of carbon fiber. *IEEE Trans Industr Inf* 11:887–896
- Kohl N, Miiikkulainen R (2009) Evolving neural networks for strategic decision-making problems. *Neural Netw* 22:326–337
- Leon F, Ciprian GC, Curteanu S (2010) Stacked neural network modeling applied to the synthesis of polyacrylamide-based multicomponent hydrogels. *Macromol React Eng* 4:537–636
- Lobato J, Canizares P, Rodrigo MA, Linares JJ, Piuleac CG, Curteanu S (2009) The neural networks based modeling of a polybenzimidazole-based polymer electrolyte membrane fuel cell: effect of temperature. *J Power Sources* 192:190–194
- Ma L, Khorasani K (2004) New training strategies for constructive neural networks with application to regression problems. *Neural Netw* 17:589–609
- Mihailescu C, Dumitrescu A, Simionescu BC, Bulacovschi V (2007) Synthesis of polyacrylamide —based hydrogels by simultaneous polymerization/crosslinking. *Rev Roum Chim* 52:1071–1076
- Piuleac CG, Curteanu S, Mihailescu C (2012) Neural network modeling applied to processes based on polyacrylamide hydrogels. In: *ModTech international conference, modern technologies, quality and innovation*, 24–26 May 2012, Sinaia, Romania
- Salman A, Engelbrecht AP, Omran MGH (2007) Empirical analysis of self-adaptive differential evolution. *Eur J Oper Res* 183:785–804
- Shahjahan M, Murase K (2006) A pruning algorithm for training cooperative neural network ensembles. *IEICE T Inf Syst* E89-D(3):1257–1269
- Storn R (2008) Differential evolution research—trends and open questions. In: Chakraborty U (ed) *Advances in differential evolution*, vol 143. Springer, Berlin, pp 1–31

- Sukthomya W, Tannock J (2005) The optimization of neural network parameters using Taguchi's design of experiments approach: an application in manufacturing process modeling. *Neural Comput Appl* 14:337–344
- Tian Y, Zhang J, Morris J (2001) Modeling and optimal control of a batch polymerization reactor using a hybrid stacked recurrent neural network model. *Ind Eng Chem Res* 40:4525–4535
- Viswanathan A, MacLeod C, Maxwell G, Kalidindi S (2005) Training neural networks using Taguchi methods: overcoming interaction problems. *ICANN* 2:103–108
- Vlahogianni EI, Karlaftis MG, Golias JC (2005) Optimized and meta-optimized neural networks for short-term traffic flow prediction: a genetic approach. *Transp Res C: Emerg Technol* 13:211–234
- Volna E (2010) Neuroevolutionary optimization. *Int J Comput Sci Issues* 7:31–37
- Ward AD, Harmarneh G (2010) The groupwise medial axis transform for fuzzy skeletonization and pruning. *IEEE Trans Pattern Anal Mach Intell* 32:1084–1096
- Xin Y (1999) Evolving artificial neural networks. *Proc IEEE* 87:1423–1447
- Xing HJ, Hu BG (2009) Two-phase construction of multilayer perceptrons using information theory. *IEEE Trans Neural Networks* 20:715–721
- Yanfeng L, Xianzhen L, Lincheng Z, Xiaoxia Z, Bonian L (2004) Study on the synthesis and application of salt-resisting polymeric hydrogels. *Polym Adv Technol* 15:34–38
- Zaharie D (2009) Influence of crossover on the behavior of differential evolution algorithms. *Appl Soft Comput* 9:1126–1138
- Zhao CY, Liu XG, Ding F (2010) Melt index prediction based on adaptive particle swarm optimization algorithm-optimized radial basis function neural networks. *Chem Eng Technol* 33:1909–1916